KLAMATH RIVER MODELING PROJECT
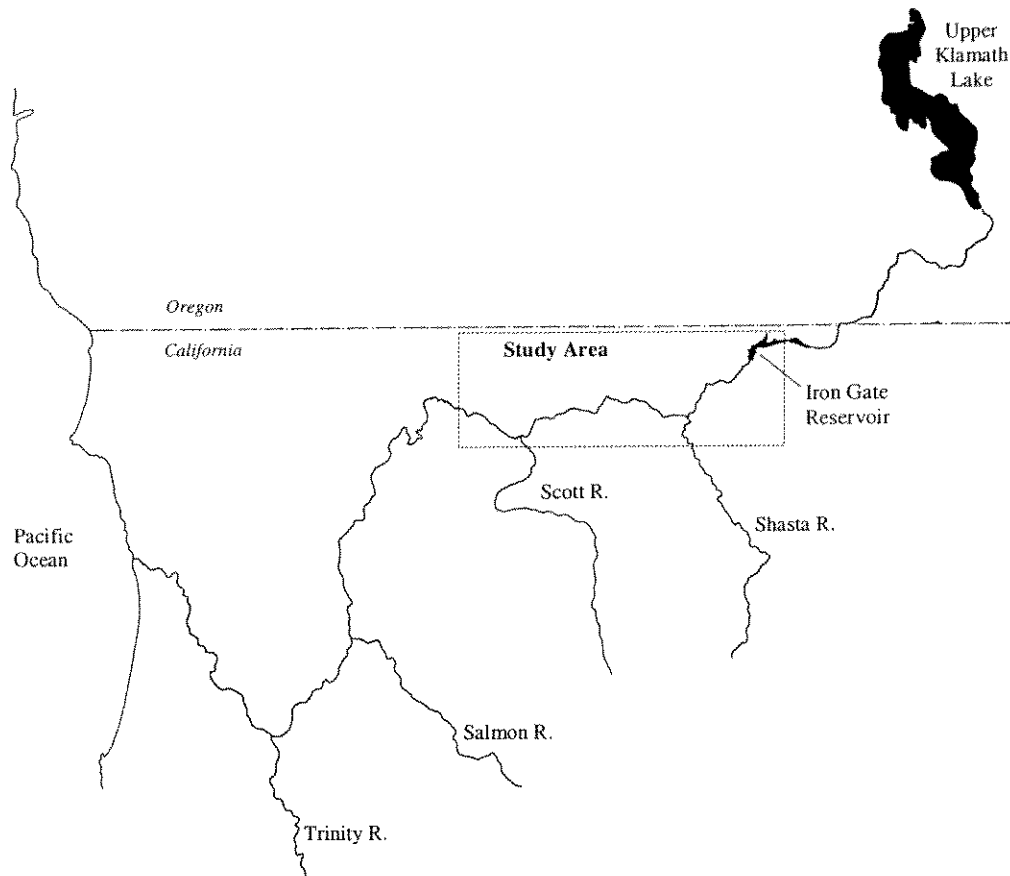
Sponsored by the United States Fish and Wildlife Service
Klamath Basin Fisheries Task Force

Upper
Klamath
Lake

Oregon

California

Study Area

Iron Gate
Reservoir

Scott R.

Shasta R.

Pacific
Ocean

Salmon R.

Trinity R.

December 1999

Report No. 99-04

KLAMATH RIVER MODELING PROJECT

by
Michael L. Deas
and
Gerald T. Orlob

Project #96-HP-01
Assessment of Alternatives for Flow and Water Quality
Control in the Klamath River below Iron Gate Dam

Center for Environmental and Water Resources Engineering
Department of Civil and Environmental Engineering
Water Resources Modeling Group
University of California, Davis

December 1999   Report No. 99-04

The University of California at Davis, under project 96-HP-01, has constructed a set of reservoir and river mathematical models capable of assessing potential water quantity and quality regulation measures for restoration and protection of anadromous fisheries in the Klamath River from Iron Gate Reservoir to Seiad Valley. The project consists of two general activities: (1) the development and implementation of a water temperature monitoring program, and (2) the implementation and application of mathematical water quality models to Iron Gate Reservoir and the Klamath River from Iron Gate Dam to Seiad Valley.

To support model application, UC Davis implemented and completed a two-year water temperature monitoring program (1996-97) in Iron Gate Reservoir and the Klamath River within the study reach. UC Davis also participated in the North Coast Regional Water Quality Control Board water quality monitoring program (1996-97) and subsequently used these observations in model calibration, validation, and application.

Iron Gate Reservoir, prone to strong thermal stratification, was modeled using Water Quality for Reservoir-River Systems (WQRRS). The models RMA-2 and RMA-11 were applied for flow and water quality, respectively, to represent the longitudinal variation and potentially dynamic nature of the Klamath River. The models were calibrated and validated for water quantity and temperature. Limited field data precluded formal calibration of water quality parameters; however, dissolved oxygen was provisionally calibrated for both the reservoir and river models.

Using available field data and model application to the historic periods May through October of 1996 and 1997, general system response under existing operational conditions were defined. Impacts of seasonal variations in flow, meteorological conditions, and operations were evaluated for both the reservoir and river systems. Definition of existing conditions provided a baseline for assessment and interpretation of alternatives

The reservoir and river models were applied to several flow, operational, and system modification alternatives. Using 1997 hydrological and meteorological conditions as a baseline, simulations were completed including (1) flows varying from 80 to 200 percent of baseline, (2) penstock intakes placed at greater depths in the Iron Gate Reservoir, (3) reduced and increased Iron Gate Reservoir storage, and (4) selective withdrawal (withdrawal

2

from multiple levels). Both reservoir release and fish hatchery intake water temperatures were assessed. A relative comparison (versus baseline) of reservoir release dissolved oxygen concentrations was completed for select alternatives.

Significant findings during the late spring, summer, and early fall period include:

- Increasing flow reduces transit time in the study reach, moderating the diurnal temperature range and providing modest temperature benefits in downstream reaches. However, increased flows increased reservoir release temperatures and adversely affected hatchery release temperature.

- Reducing storage provided little benefit to downstream temperatures, while hypothetically increasing storage illustrated increased potential for moderate temperature control well into the summer months.

- Hypothetically lowering the penstock elevation resulted in rapid evacuation (loss) of cold water supplies due to the short relatively residence time of Iron Gate Reservoir. Selective withdrawal proved to be a much more efficient use of cold water supplies stored in the reservoir.

- Combining increased reservoir storage and selective withdrawal provided the greatest degree of water temperature control in the reach below Iron Gate Dam.

In all cases, waters released from Iron Gate Reservoir during the late spring, summer, and early fall period experienced heating in transit to Seiad Valley. For the flow alternatives, flow changes directly affected transit time, thus the impacts were generally most appreciable at Seiad Valley. The storage and dam operation alternatives affected reservoir release temperature, and generally the most appreciable changes occurred in the first 30 miles downstream from the dam.

The summary, conclusion, and recommendations for future investigation are presented based on the findings of this study. Report appendices include required geometric, hydrologic, climatic, and water quality data; modeling assumptions and data analysis; together with temperature monitoring program data, computer codes, and associated files.

Table of Contents

11

14

California Department of Fish and Game	DFG
California Department of Forestry	CDF
California Department of Water Resources	DWR
Federal Energy Regulation Committee	FERC
Hydrologic Engineering Center	HEC
Klamath River Basin Fisheries Task Force	KRBFTF (Task Force)
National Marine Fisheries Service	NMFS
North Coast Regional Water Quality Control Board	NCRWQCB
State Water Resources Control Board	SWRCB
Technical Work Group	TWG
University of California, Davis	UCD
United State Environmental Protection Agency	EPA
United States Army Corps of Engineers	USCOE
United States Bureau of Reclamation	USBR
United States Fish and Wildlife Service	USFWS
United States Geological Survey	USGS
United States Geological Survey – Biological Resources Division	USGS-BRD

Class	Multiply	By	To Obtain
Area	acre	4047.0	m^2
	acre	0.4047	ha (10 000 m^2)
	ft^2	0.0929	m^2
	yd^2	0.8361	m^2
	mi^2	2.590	km^2
Length	ft	0.3048	m
	in	25.4	mm
	mi	1.6093	km
	yd	0.9144	m
Volume	ft^3	0.0283	m^3
	gal	3.785	L
	fl oz	29.575	mL
	yd^3	0.7646	m^3
	acre-feet	1233.49	m^3
Mass	oz	28.35	g
	lb	0.4536	kg
Concentration	µg/l	1.0	ppb
	µg/l	1.0	mg/m^3
	µg/l	0.001	mg/l
	mg/l	1.0	ppm
	mg/l	1.0	g/m^3
	mg/l	0.001	g/L
	g/l	1.0	ppt
	g/l	1.0	kg/m^3
Density	lb/ft^3	6894.7	kg/m^3
velocity	ft/s	0.3048	m/s
	mi/hr	0.4470	m/s
	mi/hr	1.6093	km/h
Flow Rate	cfs	0.0283	cms
Temperature	°F	$T_{°C} = (T_{°F} - 32.0)/1.8$	°C

16

Temperature Conversion Table

Temperature			Temperature	
°C	°F		°C	°F
0.0	32.0		25.0	77.0
1.0	33.8		26.0	78.8
2.0	35.6		27.0	80.6
3.0	37.4		28.0	82.4
4.0	39.2		29.0	84.2
5.0	41.0		30.0	86.0
6.0	42.8		31.0	87.8
7.0	44.6		32.0	89.6
8.0	46.4		33.0	91.4
9.0	48.2		34.0	93.2
10.0	50.0		35.0	95.0
11.0	51.8		36.0	96.8
12.0	53.6		37.0	98.6
13.0	55.4		38.0	100.4
14.0	57.2		39.0	102.2
15.0	59.0		40.0	104.0
16.0	60.8		41.0	105.8
17.0	62.6		42.0	107.6
18.0	64.4		43.0	109.4
19.0	66.2		44.0	111.2
20.0	68.0		45.0	113.0
21.0	69.8		46.0	114.8
22.0	71.6		47.0	116.6
23.0	73.4		48.0	118.4
24.0	75.2		49.0	120.2

Acre-feet	ac-ft
Cubic feet per second	cfs
Day	d
Degree Celsius	°C
Degree fahrenheit	°F
Degree Kelvin	K
Feet	ft
Fluid ounce	fl oz
Gallon	gal
Gram	g
Hectare	ha
Hour	hr
Inch	in
Joule	J
Kilogram	kg
Kilometer	km
Liter	L
Meter	m
Microgram	µg
Micromhos	µmhos
Mile	mi
Millibar	mb
Milliliter	ml
Microgram	µg
Milligram	mg
Millimeter	mm
Ounce	oz
Parts per billion	ppb
Parts per million	ppm
Parts per thousand	ppt
Pascal	Pa
Pounds per square inch	psi
Second	s
Watt	W
Yard	yd

1.1   Background

The Klamath River originates in south central Oregon and descends roughly 5000 feet over 260 miles to the Pacific Ocean south of Crescent City. Downstream of Klamath Falls, the river begins a steep descent, dropping as much as 100 to 200 feet per mile. The Klamath River carries more water than any other California River with the exception of the Sacramento River (PG&E 1962). Historically, the Klamath Basin produced more salmon than any California River except the undammed Sacramento River (Lamb and Klahn 1996). Coho salmon and steelhead also proliferated. However, shortly after the first European settlers entered the region in the early 1800's, the natural resources of the area underwent profound changes. Mining, timber practices, fishing, hydropower production and other land and water resources development have continuously altered, and continue to alter, the basin up to the present time. The cumulative effects of 150 years of impacts have had a profound effect on the Klamath River basin anadromous fisheries. Degraded habitat in the form of reduced streamflows, elevated water temperature, impaired water quality conditions, and physical blockages to migration routes have resulted in significant reductions in anadromous fish production.

In response to the diminished anadromous fish populations, Congress authorized Public Law 99-552 in 1986, stating,

> "floods, the construction of dams, diversions and hydroelectric projects, past mining, timber harvest practices, and road building have all contributed to sedimentation, reduced flows, and degraded water quality which has significantly reduced the anadromous fish habitat in the Klamath-Trinity River System" (PL 99-552, §1(3))

noting that

> "The Klamath-Trinity fall chinook salmon populations have declined 80 percent from historic levels and steelhead trout have also undergone significant reductions" (PL99-552, §1(5))

PL 99-552 created a 20-year Federal-State cooperative "Klamath River Basin Conservation Area Restoration Program" for the rebuilding of the river's fish resources. The Act created a 14-member Klamath River Basin Fisheries Task Force (Task Force), directed to assist the Secretary of Interior in creating and implementing a Restoration Program "to restore the anadromous fish populations of the [Klamath River Basin] Area to optimum levels and to maintain such levels." Members of the Task Force are appointed by the Governor of California, Hoopa Valley Tribal Council, Secretary of Interior, Secretary of Commerce, Secretary of Agriculture, Governor of Oregon, one member each representing the Boards of Supervisors of the California counties of Del Norte, Humboldt, Siskiyou, and Trinity and one member each representing the Karuk Indian Tribe and Yurok Indian Tribe.

In 1991 the Task Force produced the Long Range Plan for the Klamath River Basin Conservation Area Fishery Restoration Program (Long Range Plan). The plan identified and categorized issues concerning anadromous fish restoration. From these issues general goals and objectives were developed, and recommended policies were drafted for Task Force consideration. The Long Range Plan also developed selection criteria for restoration projects and scheduling of projects and tasks to fulfill plan objectives.

Identified in the Long Range Plan were several issues of concern with respect to water quality, including

- alteration of stream flows,
- elevated water temperatures,
- low dissolved oxygen concentrations, and
- excessive nutrient loading from Upper Klamath Basin sources.

The Long Range Plan notes that both elevated water temperature and low dissolved oxygen problems are in ranges harmful to anadromous fishes in all life stages (migration, spawning, egg incubation, and juvenile rearing). It is recognized that nutrient loading may cause excessive algal growth in system reservoirs and river reaches, affecting dissolved oxygen and other water quality parameters.

To provide the requisite modeling capability for assessment of potential water quantity and quality regulation for restoration efforts, the University of California, Davis (UC Davis), submitted the proposal "Assessment of Alternatives for Flow and Water Quality Control in the Klamath River below Iron Gate Dam" to the Klamath River Fisheries Restoration

20

Program. The project was funded in fiscal year 1996 as project number 96-HP-01. PacifiCorp supplied additional funding, and the North Coast Regional Water Quality Control Board (NCRWQCB) loaned field equipment.

This report addresses two specific activities: (1) the development and implementation of a field monitoring program, and (2) the application of water quality models to Iron Gate Reservoir and the Klamath River from Iron Gate Dam to Seiad Valley. Beyond addressing the general findings of the Long Range Plan, investigation of critical factors limiting anadromous fisheries reproduction as defined by the Task Forces' Technical Work Group (TWG) is included. The result is an improved scientific understanding of water quality conditions under existing and alternative operating conditions, as well as the technical tools to assess measures needed to restore anadromous fisheries and to evaluate potential carrying capacity in this reach of the Klamath River.

1.2   Scope and Objectives

The principal objective of this project is to provide an analytical capability (computer model) to assess consequences of water quantity and quality regulation measures designed to protect and enhance anadromous fishes of the Klamath River below Iron Gate Dam. Figure 1.1 illustrates the Klamath River basin and the UC Davis study area. This report presents overall project results and consists of several studies conducted over a three-year period.

UC Davis implemented a two-year field program to gather critical reservoir, main stem, and tributary water temperature data. Data were gathered from roughly June to October for 1996 and 1997 in the Klamath River and tributaries, while year-round temperature profile monitoring was completed in Iron Gate Reservoir. In addition, select meteorological data were gathered at several locations within the study area to assess spatial variation. UC Davis did not complete formal water quality monitoring; however, project staff assisted in the NCRWQCB water quality monitoring program that coincided with the two-year water temperature monitoring program. These water quality data proved invaluable in defining general system response, formulating model boundary conditions, and assessing model performance.
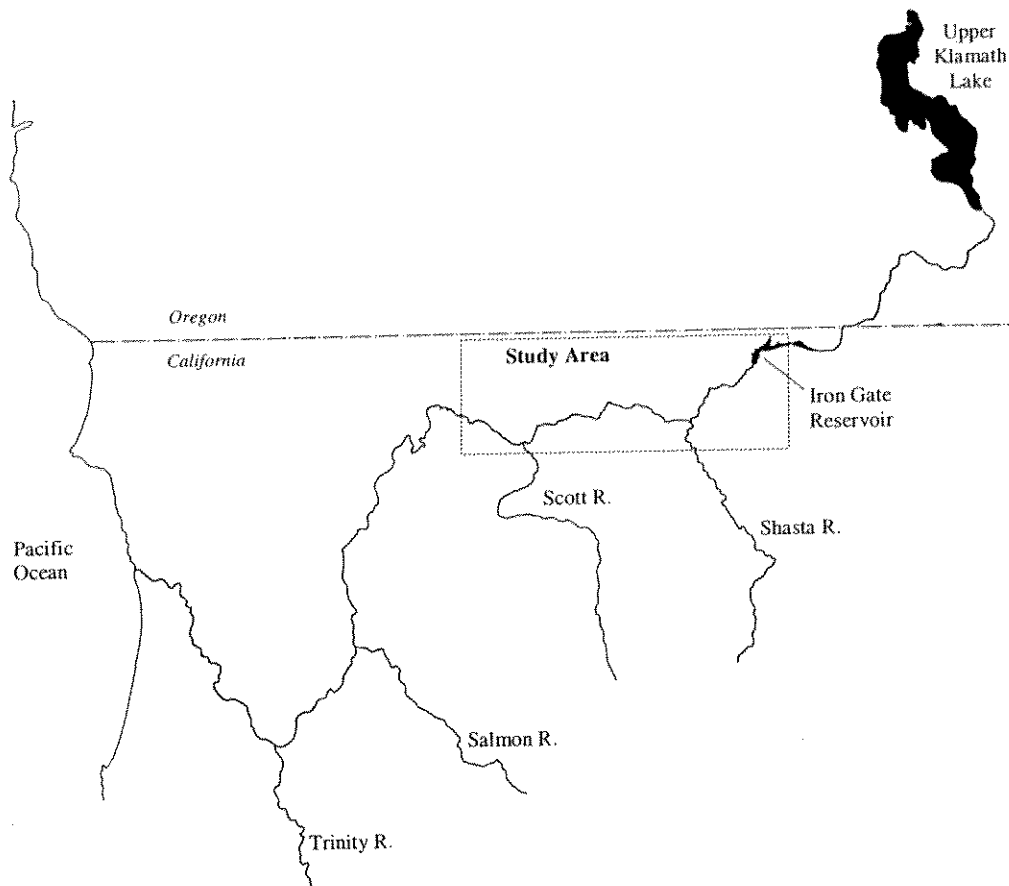
Figure 1.1   Klamath River basin and UC Davis study area

The Klamath River water quality modeling element was designed to provide two distinct modeling components: a simulation model of Iron Rate Reservoir and a model of the Klamath River from Iron Gate Dam to the USGS Gage near Seiad Valley. Each model was calibrated and validated using available hydrologic, water temperature, dissolved oxygen, and climate time series. Although there were several simulated water quality parameters, only temperature was sufficiently represented by field data to allow formal calibration and validation of the models. However, limited available dissolved oxygen data allowed preliminary calibration and validation for the reservoir and river models. In combination, the river and reservoir models are capable of assessing measures for flow and water quality regulation in the Klamath River. It is expected that the models may be extended to estimate the effects of upstream project operation on the water quality regime of the Klamath River below the study area.

1.3   Report Organization

This report includes a presentation of background information, general status of water quality in the study area, modeling approach, data requirements, field work, model calibration and validation, general system response, model application, and conclusions and recommendations. Several appendices outline data requirements, technical summaries, and supporting information. A list of acronyms, abbreviations, and a unit conversion table is included following the table of contents. Each chapter is briefly outlined below.

Chapter 1 provides a general overview of the project, its scope, objectives, acknowledgments, and organization.

Chapter 2 presents background material, including a description of the study area and project features, a brief history of the region, current conditions of anadromous fishes in the study area, and potentially limiting factors to anadromous fish reproduction.

Chapter 3 identifies and describes several key water quality parameters and their associated impacts on various life stages of anadromous fishes.

Chapter 4 describes the hydrodynamic and water quality models used in simulation of Iron Gate reservoir and the Klamath River, outlining the conceptual basis of each model and the reason for its selection. General hydrodynamic principles, heat energy budget, and water quality fate and transport are presented.

Chapter 5 addresses field monitoring programs completed by UC Davis.

Chapter 6 outlines the implementation, calibration, and validation of models for each water body. Various appendices supplement this chapter presenting calibration/validation data and results.

Chapter 7 discusses general system response. Available field data and model simulations for the historical periods 1996 and 1997 are used to discuss system performance under "existing conditions." Subject matter of chapter 7 provides an introduction to system dynamics and a background of water quality relationships necessary to interpret assessment of water quality management alternatives presented in Chapter 8.

Chapter 8 introduces and presents result of model application to various water quality management alternatives. This chapter focuses on water temperature control alternatives in the Klamath River.

Chapter 9 presents conclusions and recommendations for future model application and system monitoring.

Chapter 10 includes references and personal communications.

Several appendices attached as a separate document include geometric, hydrologic, climate, and water quality data; calibration and validation data; sample computer files; field data; model modification as well as other information.

1.4   Project Organization

The Klamath River Modeling Project was carried out under an agreement with the United States Fish and Wildlife Service (USFWS) through the Klamath River Basin Fisheries Task Force. Mr. John Hamilton and Laurie Simons provided project support for USFWS.

The Water Resources and Environmental Modeling Group of the Department of Civil and Environmental Engineering at the University of California at Davis was responsible for the development and application of water quality simulation models and execution of requisite field work. Dr. Gerald T. Orlob represented the University as Principal Investigator for the project. Dr. Ian King, who is the author of the models used to simulate river flow and quality, served as consultant advisor on model development and application. Mr. Michael Deas carried out project management, field studies, model implementation, application and assumed responsibility for editing and preparation of the final report.

Several other UCD members played key roles in the Klamath River Modeling Project including Ms. Julie Haas who assisted in deployment, collection, and data management of field devices. She also assisted Ms. Jennifer Low in data quality control and quality assurance through careful review of field data sets and determination of summary statistics. Cindy Lowney, Camilla Saviz, and Orit Kalman assisted in field trips to the Klamath Basin.

1.5   Acknowledgements

Brazie Ranch weather station, and other people and agencies that support continued data monitoring in the Klamath River basin.

Finally, we are very thankful to all UCD Department of Civil and Environmental Engineering staff personnel who helped make the production of this report possible.

2.1 Introduction

The principal focus of this study includes Iron Gate Reservoir and approximately 60 miles of the Klamath River from Iron Gate Dam to the USGS flow gage near Seiad Valley. Two major tributaries to the Klamath River in this reach are the Scott and Shasta Rivers. The Shasta River originates in the Mt Eddy region and flows northward for roughly 60 miles prior to reaching the Klamath River, roughly 15 miles downstream of Iron Gate Dam. The Scott River headwaters are located along the eastern slopes of the Salmon Mountains and northern slopes of the Scott Mountains, and the river flows over 80 miles northward to reach the Klamath roughly 47 miles downstream of Iron Gate Dam. Both the Shasta and Scott River basins are developed for agriculture.

The study area lies within two geologic regions, the Cascade Range and the Klamath Mountains. The Cascade Range geomorphic province is characterized by volcanic formations, while the Klamath Mountains geomorphic province consists of sedimentary rocks, but also include intrusive igneous formations such as granodiorite. Both regions include areas overlain by unconsolidated alluvium that are generally water bearing (DWR, 1986).

Study area hydrology is driven by regional and seasonal distribution of precipitation. Typical of Mediterranean climates, summers are warm and dry and winters are cool and wet with approximately 85% of the precipitation occurring between October and April. Mean annual runoff and associated basin areas are presented for the Klamath River and tributaries in the study area are shown in Table 2.1.

Table 2.1   Mean annual runoff and associated statistics for the Klamath River and tributary locations in the study reach: 1960-81 (DWR 1986)

Station	Mean Annual Runoff (ac-ft)	Drainage Area (mi^2)	Runoff (%)	Drainage Area (%)
Klamath River below Iron Gate	1,585,000	4,630	53	67
Shasta River near Yreka	136,000	793	5	11
Scott R. at Mouth	615,000	808	21	12
Other tributaries	615,000	709	21	10
Klamath River near Seiad Valley	2,951,000	6,940	100	100

As illustrated in Table 2.1, the Klamath River roughly doubles in annual flow volume within the study reach. Although a relatively small tributary, the Shasta River was historically one of the most productive tributaries in terms of chinook salmon runs. The bulk of the flow increase is due to the Scott River and accretions from smaller streams.

Klamath River water quality varies seasonally throughout the study reach, as well as in response to tributary contributions and upstream water resources development. The majority of the source water for the region is the 4,600 square mile drainage upstream of Iron Gate Dam. Generally, water from this area is low in mineral content and is weakly buffered, i.e., experiences low concentrations of carbonate, bicarbonate, and hydroxide. Nutrient levels are slightly elevated compared to other northern California streams, but within the range of normal background levels for natural surface waters. Dissolved oxygen levels vary seasonally strongly corresponding to seasonal variations in water temperature. Daily fluctuations in dissolved oxygen due to photosynthesizing organisms (algae) are common in the summer months, with levels reaching supersaturation during the afternoon and evening hours and dropping below saturation in the early morning hours (DWR, 1986). Water temperatures range widely over the annual period from less than 40°F in winter to over 80°F in summer.

The Shasta River has higher mineral content and is a strongly buffered system. This tributary experiences some of the highest levels of nutrients as well. Coupled with elevated summer temperatures, this stream can experience significant daily dissolved oxygen variation, especially within one of the several small impoundments used for irrigation diversions. The Scott River generally has high quality water. The high elevation headwaters and tributaries of the Scott River supply appreciable cool water inflows to the Klamath River well into spring; however, by late summer and early fall water temperatures are similar to the main stem Klamath River.

2.2   History

2.2.1   First Inhabitants

Native Americans utilized the river's resources for thousands of years and several tribal nations exist along the river corridor today. First European contact may have been by Spanish explorers who reported a river originating near Great Salt Lake and emptying into

the Pacific Ocean – Rio Buenaventura. More reliable accounts were included in the Hudson Bay Company forays into the Klamath Lake region in the 1820's (Dillon 1975). Peter Skene Ogden explored Klamath Lake and the river down to the present location of Hornbrook around 1926-27. Jedediah Smith explored the region in 1928. Fur trappers worked the region until beaver populations dwindled and in 1844 with the addition of Oregon the United States, Hudson Bay Company excursions were halted (Dillon 1975).

2.2.2   Gold Mining

Prospectors moved into the Klamath River country in 1849 following gold discoveries in the Sierra Nevada. The first mining works were located on the Trinity River. In 1850, the first party of prospectors reached Happy Camp. Within a year or two, mining operations were in place throughout much of the Klamath River and major tributaries. Once surface gold deposits were depleted, other methods were employed. Water resources were developed to support hydraulic mining and flumes and pipes several miles in length were not uncommon. By 1900 low profits had reduced the number of mining operations significantly (Jones 1971, KBRFTF 1991). However, in the early 1900's the advent of inexpensive power and motor transportation brought a resurgence of mining activity to the area. Increased gold prices and lack of work during the depression era re-kindled mining in many of the tributaries. Large dredges processed millions of cubic yards of gravels. Production decreased during World War II and never regained its former status. Today, gold mining remains an important form of recreation in the Klamath River basin (KRBFTF 1991).

2.2.3   Timber

Soon after the gold rush commenced, people became aware of the area's vast timber resources. A certain amount of timber was needed for the mining works and associated infrastructure, but not until the late 18th and early 19th century did logging become more widespread. Initially, the Klamath River was used to transport logs downstream whereupon they were towed by ship to Eureka for milling. Only after World War II did sufficient technological improvements become available to access the vast timber reserves of the area. Annual Del Norte County timber production jumped from 23.4 million board feet in 1947 to 305.7 million board feet in 1955 (KBRFTF 1991). Timber practices continue in the region albeit at levels lower than the 1950's and 1960's.

2.2.4   Commercial Fisheries

During the late 1870's people began to exploit the commercial value of salmon. At one time five canneries operated on the river (Quinn 1983). Gill netting was the primary means of fishing. Commercial ocean fisheries appeared around the turn of the century, but were fairly inefficient until motorized craft were employed. By 1920 the new ocean trolling fishery was spread along the entire coast. The commercial ocean fishery coupled with modernized gill netting technology led to declines in the salmon runs (KRBFTF 1991). Gill netting was banned on the river in 1933, the same year the canneries were closed (Quinn 1983).

2.2.5   Hydropower Development

In the early 1900's the California Oregon Power Company identified several dam sites on the Klamath River for potential hydropower production. Initial efforts to market the power failed, but in 1917 Copco Dam (Copco No. 1), located at roughly river mile 195, was completed. An additional plant, Copco No. 2, was put into production just downstream of Copco No. 1 in 1925 (KRBFTF 1991).

Power plants were operated to meet peak power demands and flow releases fluctuated with the anticipated demands. Weekly flows varied from 3,200 cfs to 200 cfs. Short-term flow changes might increase or decrease the water level several feet over a 20 minute period. Substantial and frequent flow changes adversely affected anadromous fish reproduction in downstream reaches. In the late 1950's California Oregon Power Company decided to build Iron Gate Dam (KRBFTF 1991). Iron Gate Dam was completed in 1962, to re-regulate Copco Reservoir peaking power releases and provide stable releases to the Klamath River for several months of the year.

2.2.6   Water Development

Mining activities brought the first water to lands adjacent to the main-stem and tributaries. Agriculture production in the Shasta and Scott Rivers dates back well into the 18th century. In 1905 the Secretary of the Interior authorized the Klamath Project – one of the earliest reclamation projects for the then newly formed United States Bureau of Reclamation. The Klamath Project services 230,000 acres of irrigable land, with primary storage in Upper Klamath Lake, Gerber Reservoir and Clear Lake Reservoir (DWR 1998). It is notable that shortly after daily flow records were started in 1910 near Klamathon, a change in seasonal

30

flow regime was noted by a California Oregon Power Company engineer. The shift from more uniform flows to increased spring and reduced summer flows may have been attributed to the reclamation of Lower and Middle Klamath Lakes and other associated development in the reclamation project (KRBFTF 1991). The last Klamath Project land put into production was 1949 (Lamb and Klahn 1996).

2.3   Current Conditions

Current conditions in the Klamath River today are the culmination of over a century of various impacts. Mining, timber harvest, commercial fishing, hydropower development, and water resources development have had a profound impact on the system and its anadromous fisheries. Although some of these activities are no longer in practice or play only a minor role, their impact will probably be felt on the river for decades to come. In addition, current conditions such as commercial and tribal harvest, climatic and ocean conditions, marine mammal predation, and effects of hatchery fish may adversely affect wild stocks.

Outlined herein is a brief history and current status of anadromous salmonids found in the project area. Concluding the chapter is a discussion of the potential causative factors limiting anadromous fish reproduction and their role in the water quality management analysis of this project.

2.3.1   Anadromous Salmonids

Within the Klamath River basin anadromous salmonid populations are limited to the main stem and tributaries downstream of Iron Gate Dam. Currently three species of anadromous salmonids utilize the project study area. These include chinook salmon (*Oncorhyncus tshawytscha*), coho salmon (*Oncorhyncus kisutch*), and steelhead trout (*Oncorhyncus. Mykiss irideus*). Nearly all anadromous fish runs have declined significantly in California due to loss of habitat, river impoundments, habitat alteration, and over-exploitation (Moyle 1976, Moyle et al 1995).

Chinook salmon populations consist of spring- and fall- runs. Historically, spring-run chinook are thought to have been more numerous than fall-run, but since the turn of the century their numbers have fallen dramatically. A few dozen spring chinook-run were still returning to the upper Klamath at the time that Iron Gate Hatchery was completed, roughly

31

30 years ago (KRBFTF 1991). More recently, spring-run have been occasionally sighted in the Scott River and Beaver Creek (Birk 1996). There is limited evidence that chinook salmon (fall- or spring-run) prior to the construction of Copco Dam migrated through Upper Klamath Lake and into the Williamson River. Today, it appears that spring-run chinook spawning is limited to a few tributaries of the Klamath River.

Most of the fall-run chinook spawning in the main stem Klamath River appears to be limited to a 13-mile reach from Iron Gate Dam to the mouth of the Shasta River (Leidy and Leidy 1984). However, sporadic spawning has been noted between the Scott and Shasta Rivers. Figure 2.1 illustrates the 1995 DFG assessment of optimum spawning escapement levels for adult fall-run chinook salmon in Klamath River spawning areas. A range of values is given representing the upper and lower envelope. The main stem and tributaries locateed within the study reach comprise over 50 percent of the spawning habitat in the Klamath River, excluding the Trinity Basin.
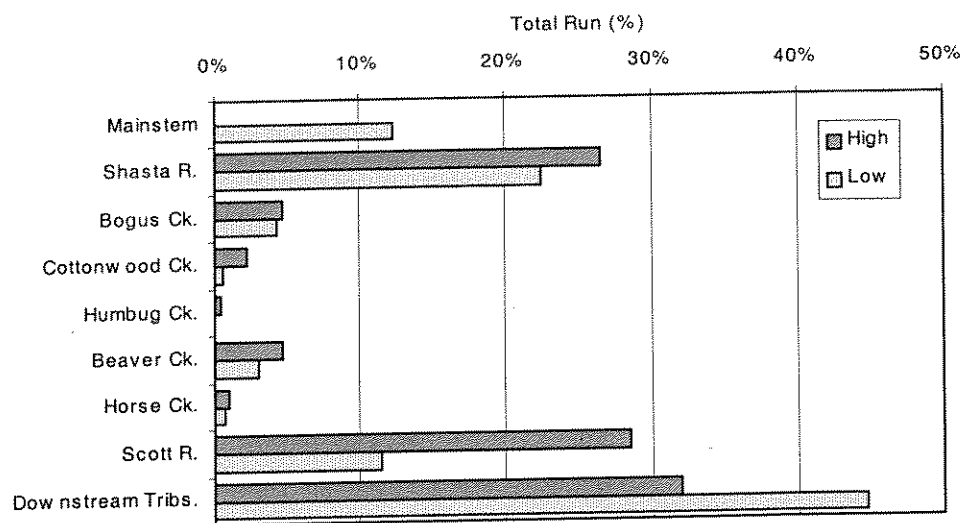
Figure 2.1   DFG optimum spawning escapement levels for adult fall-run chinook salmon in Kalmath River spawning areas (not including Trinity River Basin) (adapted from Birk 1996)

Coho salmon populations are not as well defined for the Klamath River basin. Significant runs were noted in the lower river tributaries and migrations of coho salmon were noted at Klamathon in the 1920's (KRBFTF 1991). Unfortunately, early observations focused more attention on chinook salmon. Native populations exist in the Scott River and coho have been spotted in the Shasta River basin.

Steelhead have the widest distribution of all native North American salmonids (Moyle 1976). Steelhead populations of the Klamath Basin include several distinct runs; fall-, winter-, spring-, and summer-runs have been noted. Differences between spring- and summer-run fish and fall- and winter-run fish are uncertain due to limited data. Generally, spring- and summer-run steelhead tend to migrate to upper reaches of cool water tributaries, while fall- and winter-run fish are thought to disperse widely through the system (Birk 1996). Historically steelhead were distributed throughout the basin reaching river reaches above Upper Klamath Lake. Main stem locations and tributaries above Iron Gate Dam were probably utilized by steelhead as well. Currently, winter steelhead utilize the Shasta and Scott Rivers, as well as return to the Iron Gate hatchery (Birk 1996). A few summer steelhead have been seen in the Scott River (KRBFTF 1991).

Currently the Hatchery at Iron Gate Dam raises fall-run chinook, coho and steelhead. The fall-run chinook are assumed to be relatives of the original stock that passed Iron Gate for upstream locations. Hatchery broodstock for coho are from the Columbia River, and steelhead include some native stock, but also eggs from the Trinity River Hatchery and the Cowlitz River in Washington have been imported (KRBFTF 1991).

2.3.2 Causative Factors Potentially Limiting Anadromous Fish Reproduction

In April, 1997 the Task Force directed the TWG to assess required specific studies to complete an instream flow study for the Klamath River. The purpose of a flow study was to identify the effects of water management actions on the quantity and quality of aquatic habitat as it affects anadromous fish. In response to the Task Force request, the TWG constructed a flow study plan. The process included identifying actual and potential causative factors that were or could be responsible for the decline of anadromous fisheries in the Klamath Basin. Subsequently, study questions were identified, that, if answered, would aid in understanding and addressing causative factors in relation to water management operations. The study questions were then organized by discipline so that specific study techniques could be identified. Eleven disciplines were identified, including

- Access to habitat
- Water Quality
- Watershed and upslope processes
- Microhabitat limitations
- Groundwater
- Thermal refugia

- Flow
- Geomorphology
- Biological interactions
- Stream diversions
- Harvest

33

One of the primary purposes of the Klamath River Modeling Project is to address such questions and, where possible, provide additional insight into causative factors limiting anadromous fisheries. Scoping questions formulated by the TWG that were consistent with the assessment of water quality in the Klamath River below Iron Gate Dam were reviewed for further study and are outlined below. Table 2.2 outlines identified potential causative factors referring to flow and water quality in the study area. Those shown in bold are addressed in this report.

Table 2.2   Causative factors potentially limiting anadromous fish in the main stem Klamath River Basin

Flow	Potential Causative Factor	Water Quality	Potential Causative Factor
A.	**Change in flow due to water management**	A.	**Temperature**
B.	**Timing**	B.	**Dissolved Oxygen**
C.	Duration	C.	**pH, alkalinity & conductivity**
D.	**Magnitude**	D.	Contaminants
E.	Frequency	E.	**Nutrients**
F.	**Ramping**	F.	Algal toxicity
G.	Change in natural storage	G.	Turbidity
H.	Change in groundwater storage	H.	Effects of return flows on water quality
I.	Estuarine Circulation	I.	Salinity

The general nature of the scoping questions, coupled with system complexity, precluded explicit answers to most questions. For example, temperature and water quality parameters are inextricably related – e.g., it is difficult to assess dissolved oxygen conditions without discussions of temperature, nutrients, primary production, and temporal and spatial variability of these parameters. Further, year-to-year and seasonal variations in meteorology, hydrology, and operations combine to create hundreds of potential "scenarios" to analyze. Thus, the selected water quality scoping questions, although not resolved, identified critical processes explored within the scope of this project. The following flow and water quality questions are addressed, at least in part, within the body of this report.

2.3.2.1   Flow

Flow related questions include:

What is the relationship between water travel time (velocity) and flow in the main stem below Iron Gate Dam?

How do hydroelectric operations affect flow?

Flow related questions are addressed in Chapter 8.

34

2.3.2.2 Water Quality

The TWG identified several water quality related questions. These were arranged into three general groups: process identification, system response, and water management potential. Process identification questions aim to identify or further define the spatial and temporal variation of processes or water quality variables that are underrepresented and/or poorly understood. System response questions address how different processes affect water quality variability under current conditions. Water management potential addresses measures that could possibly improve or eliminate an undesired condition. Water management could be defined as exploring system response under alternative future conditions.

Further, water quality related questions are divided into two categories: temperature and "other" water quality parameters. Unlike temperature, other water quality parameters are generally poorly understood for the Klamath River due to a lack of data and/or detailed studies. The TWG scoping questions for water quality essentially mirrored those for water temperature and they have been combined herein. Due to lack of field observations and the fact that selected modeling components of this project do not address all parameters of concern (e.g., pH), this report focuses on process identification for other water quality variables, providing baseline data for future work on system response and potential water management alternatives.

It is assumed all presented questions have spatial and temporal (e.g., seasonal and different locations) ramifications as well. Findings pertinent to process identification and system response questions are presented in Chapters 6 and 7, while water management potential questions are addressed in Chapter 8.

Process Identification

Process identification questions for water temperature include:

What is the current thermal structure (vertical profile) of Iron Gate Reservoir?
What is the current thermal structure (longitudinal profile) of the Klamath River?
What is the current water quality condition of Iron Gate Reservoir?
What is the current water quality condition of the Klamath River?

System Response

Iron Gate Reservoir and the Klamath River may respond to physical processes as well as operational processes. Physical processes include meteorology, hydrology, and other

35

processes generally beyond direct human control, while operational processes are those associated with regulation of the river. Physical process questions include:

How do meteorological conditions affect Iron Gate Reservoir and Klamath River water temperature/quality?

How do hydrologic conditions affect Iron Gate Reservoir and Klamath River water temperature/quality?

How do upstream conditions affect Iron Gate Reservoir and water temperature/quality (also an operational process)?

What influence do tributaries (and springs) have on main stem water temperature/quality?

Operational process questions include:

How do current reservoir-river operations affect water temperature/quality?

How do upper basin operations affect Iron Gate Reservoir and downstream Klamath River water temperature/quality?

How do Iron Gate Reservoir operations affect downstream river reaches?

Finally, there is a critical question that overlaps both physical and operational processes:

What processes (factors) control/govern water temperature/quality in the system (e.g., acute and chronic water temperature)?

Water Management Potential

For processes that were or could be sufficiently defined, water management potential was examined. Questions addressing potential for temperature control via water management include:

What is the potential for temperature and water quality control in the Klamath River below Iron Gate Dam by modifying:
- Upstream operations (e.g. flow quantity and timing)?
- Iron Gate release location (elevation)?
- Iron Gate depth and configuration?

Iron Gate operations with respect to flow timing are a function of upstream system operations. Though outside the study area, a brief examination of varying flow regime was completed.

36

The Klamath River is a highly regulated system. Both flow quantity and water quality have been identified as potential causative factors limiting anadromous fish reproduction. Several water quality parameters have been identified as potential limiting factors, either individually or in combination, for anadromous fish restoration and reproduction. These include:

- Temperature
- Dissolved Oxygen
- pH, alkalinity, and conductivity
- Contaminants
- Nutrients
- Algal toxicity
- Turbidity (organic and inorganic)
- Biochemical Oxygen Demand (BOD)

An additional parameter, biochemical oxygen demand, was added to the list. Each parameter will be briefly introduced below and their known impact to anadromous salmonids discussed.

3.2   Temperature

Aquatic systems experience variations in water temperature in response to normal climatic conditions. Changes vary seasonally and, in many cases, over 24 hour periods. Temperature is influenced by latitude, altitude, season, time of day, air circulation, cloud cover, flow, surface area, and depth of the water body. Typical surface water temperatures in the Klamath River basin range from 0°C (32°F) to 30°C (86°C) throughout the year.

The importance of temperature is critical to most aqueous systems because of direct effects on physical, chemical and biological processes. As water temperature rises chemical reaction rates generally increase. Increased temperature also decreases the solubility of gases such as oxygen (O_2), carbon dioxide (CO_2), and nitrogen (N_2) (Water Quality Assessments, 1996). The metabolic rate of organisms also increases with increased temperature. For example algal growth rates can increase at elevated water temperatures leading to algal blooms and associated water quality problems. However, excessive water temperatures can have adverse impacts on metabolic rate of certain organisms leading to reduced productivity and increased mortality.

The NCRWQCB Region 1 Basin Plan (1996) defines the Klamath River as "cold freshwater habitat." Cold freshwater habitat includes uses of water that support cold water ecosystems including preservation of aquatic habitats, vegetation, fish and wildlife. The general objective is that such waters cannot be increased by more than 5°F above natural receiving water temperature. Further, natural receiving water temperatures of intrastate waters shall not be altered unless it can be demonstrated to the NCRWQCB that such alteration in temperature does not adversely affect beneficial uses.

3.2.2   Impacts on Anadromous Salmonids: Temperature

Temperature has the greatest effect on fish physiology of any of the environmental variables. Salmon are poikilotherms – under most conditions the body temperature of a fish is the same as or slightly higher than the water temperature. Thus, temperature has a significant affect on respiration, food intake, digestion, assimilation, growth, and behavior.

Temperature impacts are well documented for anadromous salmonids, especially chinook salmon. Temperature requirements vary with life stage: adult (migration and spawning), egg incubation and larvae, and juvenile rearing. In general, incubating eggs and larva have the narrowest optimum temperature range, while juveniles can accommodate the widest temperature fluctuations of the three non-adult life stages. In addition, the rate of temperature change can affect thermal tolerance of salmonids (Elliott and Elliott 1995). Available information on thermal tolerances for each species is outlined below.

3.2.2.1   Chinook Salmon

Chinook salmon is the most studied anadromous salmonid. Although studies have been completed on different races of chinook, separate thermal tolerance criteria have not been developed. Little work has been completed on Klamath River stocks, but information from other Pacific river systems is available.

Adult chinook salmon thermal criteria were compiled by Marine (1992) and are reproduced in Figure 3.1. Optimum temperatures for adult chinook salmon is roughly 6°C (42.8°F) to 14°C (57.2°F), although higher temperatures for non-gravid adults or for brief periods can be tolerated (Marine 1992). Excessive temperatures may arrest fish migration, predispose adults to disease, accelerate or retard maturation, and generally provide stress to the fish. Depressed temperatures, or a sudden drop in temperature may reduce spawning activity,

38

retard maturation, as well as adversely affect other physiological processes (Marine 1992, Reiser and Bjornn 1979).

Armour (1991) studied acclimation effects in juvenile chinook salmon and found that fish subject to higher initial water temperatures could sustain higher maximum temperatures than those acclimated to cold waters. Acclimation occurs as juvenile salmon migrate downstream and are exposed to a gradually increasing temperature regime (H. Rectenwald 1996, personal communication). The importance of this phenomenon is illustrated in Table 3.1 where experimental data illustrate that juvenile fish that have spent several days in warmer water can tolerate markedly higher maximum temperatures.
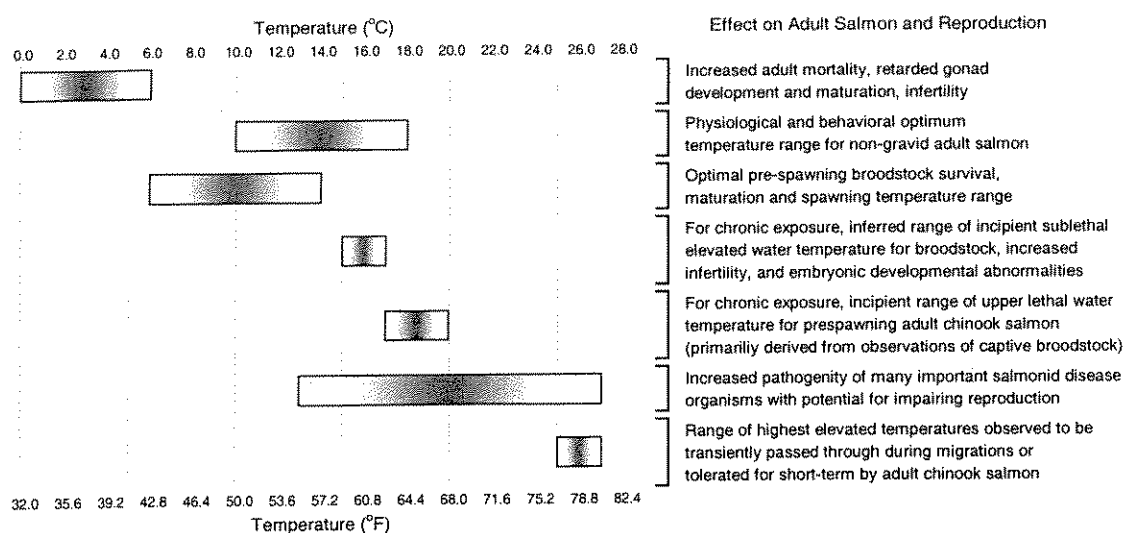
Figure 3.1   Adult thermal criteria for chinook salmon (adapted from Marine 1992)

Table 3.1   Acclimation response for juvenile chinook salmon (Armour 1991)

| Acclimation Temperature | Temperature of 50% Mortality | |
| | °C (°F) | |
°C (°F)	Lower	Upper
5.0 (41.0)	-	21.5 (68.9)
10.0 (50.0)	0.8 (33.4)	24.3 (75.7)
15.0 (59.0)	2.5 (36.5)	25.0 (77.0)
20.0 (68.0)	4.5 (40.1)	25.1 (77.2)

Acclimation assumes fish are exposed to water temperature for several days.

39

As noted, salmon at all life stages are subject to temperature stress. Table 3.2 defines recommended and tolerable temperatures for various life stages of spring-run chinook salmon. Although the values cited in the table are based on the spring-run race, the principles are applicable to other chinook salmon races (Armour 1991).

Table 3.2 Recommended and tolerance water temperature ranges for various life stages of spring-run chinook salmon (Armour 1991)

Range	Adult Migration °C (°F)	Spawning °C (°F)	Incubation °C (°F)	Juvenile Rearing °C (°F)
Recommended	3.3 - 13.3 (37.9 - 56.0)	5.6 - 13.9 (42.1 - 57.0)	5.0 - 14.4 (41.0 - 57.9)	7.9 - 13.8 (46.2 - 56.8)
Tolerance	2.0 - 16.0 (35.6 - 60.8)	5.0 - 14.0 (41.0 - 57.2)	0.0 - 16.0 (32.0 - 60.8)	2.0 - 16.0 (35.6 - 60.8)

1) Spawning adults become susceptible to lethal diseases when temperatures attain 16.0°C (60.8°F).
2) Juvenile fish cannot tolerate temperatures exceeding 25.1°C (77.2°F) for a 1 week period.
3) Adult spawning migrations are blocked at temperatures exceeding 21.0°C (69.8°F).

In addition to direct effects on salmon health and productivity, water temperature has other effects. For example, spawning adults are susceptible to lethal disease when temperatures exceed 16.0°C (60.8°F) (Armour 1991), and juvenile salmon become more susceptible to diseases, parasites and predation for temperatures above 15.5°C (59.9°F) (Boles, 1988). Water temperature can affect the types, abundance, and availability of aquatic organisms, and hence the food supply of juvenile salmon (Boles 1988). Salmon feed on drifting aquatic organisms, particularly chironomids (Chironomidae), mayflies (Ephemeroptera), stoneflies (Plecoptera) and caddisflies (Trichoptera). In areas where riparian vegetation is not present, food supplies may be reduced and near shore temperatures increased. This combines the stresses of increased metabolism and reduced food supply, and may force juvenile salmon to move into deeper waters in search of invertebrate drift, where they become more susceptible to predation and must expend more effort due to increased water velocities (USFWS 1992).

Young salmon subjected to high water temperatures may exhibit behavior that can further jeopardize their survival by increasing rates of predator discovery due to increasing erratic activity, unnatural postures, and disorientation. Survival of juvenile chinook salmon is further threatened when other species better adapted to warm water conditions out-compete them for available food supplies.

Adult upstream migrant salmon begin experiencing reductions in egg viability and increased mortality after prolonged exposure to elevated temperatures. Mortality of adults occurs

when temperatures exceed 21.1°C (70.0°F) for extended periods (USFWS 1992). Because the upstream migrant does not feed during in-migration, food reserves must support the entire journey from the ocean to spawning areas. Energy contained within food reserves may be conserved through behavioral thermoregulation. Selection of cool water refugia such as those provided by cool water tributaries or springs may prevent over-use of food reserves by maintaining lower metabolic rates. Berman and Quinn (1991) studied the habitat preference and movement of adult spring-run chinook salmon during the four months prior to spawning, finding evidence of behavioral thermoregulation. Salmon in the Yakima River, Washington, observed during their study were able to maintain body temperatures less than the temperature of the main flow through careful selection of cooler physical habitat.

3.2.2.2 Coho Salmon

Limited information is available on coho salmon thermal tolerance. Reiser and Bjornn (1979) present preferred temperature ranges for migration, spawning, egg incubation and juvenile rearing. Findings are presented in Table 3.3. Reiser and Bjornn also present an upper lethal temperature of 25.8°C (78.4°F) for juvenile coho salmon. Birk (1996) notes that Klamath River temperatures do not always fall within preferred ranges, particularly December and January, when water temperatures may fall below 7.2°C (45.0°F).

Table 3.3   Coho salmon thermal tolerance (after Reiser and Bjornn (1979), Birk (1996), and Hassler (1987))

Lifestage	Preferred °C (°F)		Upper Limit °C (°F)
		Hassler (1987)	Hassler (1987)
Migration	7.2 – 15.6 (45.0 – 60.1)	4.0 – 14.0 (39.2 – 57.2)	25.5 (77.9)
Spawning	4.4 – 9.4 (39.9 – 48.9)	6.0 – 12.0 (42.8 – 53.6)	25.8 (78.4)
Egg incubation	4.4 – 13.4 (39.9 – 56.1)	4.4 – 13.3 (39.9 – 55.9)	n/a
Juvenile rearing	11.8 – 14.6 (53.2 – 58.3)	4.4 – 9.4 (39.9 – 48.9)	25.0 (77.0)
Juvenile outmigration (Birk)	7.2 – 16.7 (45.0 – 62.1)	4.4 – 9.4 (39.9 – 48.9)	25.0 (77.0)

Studies by Konecki et al (1995) found that although juvenile coho salmon prefer 10°C to 12°C (50.0°F to 53.6°F) water, juvenile coho could tolerate temperatures in excess of 24°C (75.2°F). Further, following the eruption of Mount St. Helen's in southeastern Washington

stream temperatures where riparian vegetation had been removed reached in excess of 29°C (84.2°F), but juvenile coho were observed in the streams. Konecki et al also noted that presmolts acclimated to a significant diel cycle may have higher critical thermal maxima, but little evidence that individual coho salmon populations (e.g., those specific to a river basin) evolved levels of thermal tolerance. Additional study is required.

3.2.2.3 Steelhead

Recent work on steelhead shows that these fish may not only be able to tolerate higher temperatures, but that significant differences are expected between the various California steelhead populations (Myrick 1998). Myrick (1998) reports that critical thermal maxima (CTM) for juvenile Central Valley steelhead was significantly affected by acclimatization temperature, but only moderately influenced by ration (food), and suggests

$$CTM\ (°C) = 25.37 + 0.26T - 0.01R \tag{3.1}$$

Where T is the acclimatization temperature and R is the ration level. Note that this formula suggests critical thermal maxima on the order of 25°C (77°F) to over 30°C (86°F) (for acclimatization temperatures of 0°C to 20°C (32°F to 68°F)). Studies also showed that the preferred thermal range for juvenile steelhead from California's Central Valley was 17°C to 20° (62.6°F to 68°F). Myrick notes that caution should be used when applying lab findings to stocks of native fish due to interactive effects of other factors including predation, competition, and available habitat.

Limited thermal tolerance for steelhead is presented by Reiser and Bjornn (1979) and Birk (1996) (Table 3.4). Juvenile rearing temperature ranges do not agree with Myrick (1998), illustrating the need for additional work in the area of thermal tolerance for varying steelhead stocks.

Table 3.4   Steelhead thermal tolerance (Reiser and Bjornn 1979, Birk 1996)

Lifestage	Preferred °C (°F)
Migration	n/a
Spawning	3.9 – 9.4; 7.2 – 14.4 (Birk) (39.0 – 48.9; 45.0 – 57.9)
Egg incubation	n/a
Juvenile rearing	7.3 – 14.6 (45.1 – 58.3)

3.3   Dissolved Oxygen

Oxygen is one of several dissolved gases important to aquatic systems. Dissolved oxygen is necessary to maintain aerobic conditions in surface waters and is considered a primary indicator when assessing the suitability of surface waters to support aquatic life. The oxygen content of natural waters varies with temperature, salinity, turbulence, photosynthetic activity of algae and plants, and atmospheric pressure. Primary sources of oxygen in water bodies include diffusion of atmospheric oxygen across the air-water interface and photosynthesis of aquatic plants. For maintenance of aquatic health, dissolved oxygen concentrations should approach saturation – that concentration which is in equilibrium with the partial pressure of atmospheric oxygen. Solubility of oxygen is a function of water temperature, salinity, and atmospheric pressure; decreasing with rising temperature and salinity, and increasing with rising atmospheric pressure. Freshwater at sea level has a saturation dissolved oxygen concentration of about 14.6 mg/l at 0°C (32°F) and 8.2 mg/l at 25°C (77°F).

Generally, oxygen concentrations are below saturation due to the presence and oxidation of decaying organic matter (suspended, benthic, or sediment). In addition to the organic, or carbonaceous oxygen demand, nitrogenous materials may exert an oxygen demand through bacterial oxidation of ammonia to nitrate (Krenkel and Novotny, 1980). Other materials may likewise produce an oxygen demand on the system. Thus, variations can occur seasonally as well as over 24-hour periods in response to temperature and biological activity. Concentrations below 5 mg/l may adversely affect function and survival of biological communities, and below 2 mg/l can lead to death of most fishes (Water Quality Assessments, 1996). Dissolved oxygen distribution in reservoirs may vary substantially from river systems due to differing hydraulic regimes.

Primary production (algae) acts as both a source and sink of dissolved oxygen. During daylight hours algal photosynthesis produces oxygen in excess of algal demands (respiration), often resulting in dissolved oxygen levels in excess of saturation, i.e., supersaturation. During nighttime periods when photosynthesis is absent, algal respiration may reduce dissolved oxygen levels significantly. Another mechanism that may increase or decrease dissolved oxygen is transfer through the air-water interface. Typically the transfer is from the atmosphere into the water (re-aeration) because dissolved oxygen in most natural

waters is below saturation. However, under supersaturated conditions there is a net transfer of oxygen from the water body to the atmosphere.

Usually, dissolved oxygen levels in excess of 7.0 mg/l are desired to maintain aquatic ecosystem health. The NCRWQCB has defined water quality objectives for dissolved oxygen at several locations within the study area under the Region 1 Basin Plan (NCRWQCB 1996). Table 3.5 defines specific dissolved oxygen objectives for the Klamath, Shasta, and Scott Rivers as well as other tributaries in the middle Klamath region.

Table 3.5   North Coast Regional Water Quality Control Board Klamath River water quality objectives (NCRWQCB 1996)

System/Location	Dissolved Oxygen (mg/l)		
	Minimum	90% LowerLimit[1]	50% Lower Limit[2]
Klamath River above Iron Gate Dam[3]	7.0	n/a	10.0
Klamath River Below Iron Gate Dam	8.0	n/a	10.0
Shasta River	7.0	n/a	9.0
Scott River	7.0	n/a	9.0
Other Tributaries	7.0	n/a	9.0

[1] 90% lower limit represents the 90 percentile values for a calendar year. 90% or more of the values must greater than or equal to a lower limit.

[2] 50% lower limit represents the 50 percentile values of the monthly means for a calendar year. 50% or more of the values must be greater than or equal to a lower limit.

[3] Including Iron Gate and Copco Reservoirs

3.3.1   Impacts on Anadromous Salmonids: Dissolved Oxygen

Dissolved oxygen is one of the limiting factors for fish. In general, aquatic organisms possess highly specialized gas exchange systems that allow maximum utilization of available oxygen. Specifically, salmonids require a sufficient oxygen gradient, (oxygen tension gradient) between their bodies and surrounding waters to allow gas (i.e., dissolved oxygen) exchange through diffusion across the gills and into the blood. Further, there must be sufficient available oxygen to fulfill minimum metabolic demands – maintenance of minimum bodily functions (Davis 1975).

Theoretically, a critical oxygen level for each species exists (Colt et al, 1979); however limited data is available. Fish can resist or tolerate short-term oxygen reductions. It has been determined that certain species may acclimatize to reduced dissolved oxygen levels, as

observed in trout species, if declines are not abrupt (Vinson and Levesque 1994, Davis 1975). Behaviorally, fish may avoid low dissolved oxygen conditions by physically moving out of an area. Finally, low oxygen levels can also increase toxicity of contaminants to anadromous fish, including ammonia, zinc, lead, and copper (Colt et al 1979, Davis 1975).

Excessive oxygen levels appear to have no deleterious impact on fish. Concentration levels of 250 to 300 percent of saturation are not lethal (Wiebe and McGavock 1932). This condition should not be confused with gas bubble disease, the result of local gas supersaturation (typically nitrogen) caused by air entrainment, heating of water, and air vented into power turbines (Colt et al 1979).

3.3.1.1 Adult Salmonids: Migration and Spawning

Recommended oxygen levels for all spawning salmonids is a minimum of 80 percent saturation with temporary levels no lower than 5mg/l. While maximum sustained swimming speeds of adult coho were adversely affected when dissolved oxygen was reduced below saturation at temperatures from 10°C (50°F) to 20°C (68°F) (Reiser and Bjornn 1979).

Though different from steelhead, adult rainbow trout show negative effects at concentrations less than about 5 mg/l or 50% saturation, including elevated breathing amplitude, reduced heart rate, and reduced swimming speeds (Vinson and Levesque 1994).

Chinook, coho, and steelhead have exhibited avoidance behavior of low dissolved oxygen water (Warren et al 1973). Juvenile chinook salmon strongly avoided low DO water (1.5 mg/l to 4.5 mg/l) areas during summer periods when temperatures were high, but did not exhibit similar behavior in fall when water temperatures were cooler (Whitmore 1960). Matthews and Berg (1996) explored the relationship between temperature and dissolved oxygen for rainbow trout: when faced between high temperature and low dissolved oxygen, trout typically were distributed closest to the water with the lowest temperature despite low oxygen content. Davis (1975) categorized response of freshwater salmonids into function without impairment, exhibition of initial oxygen distress, and significant portion of population affected. The results are presented in Table 3.6.

These criteria were developed to ensure adequate oxygen tension gradient to transfer oxygen to the blood as well as sufficient oxygen to fulfill metabolic requirements. At low temperatures where solubility of oxygen is high, the criteria were set to ensure oxygen

tension gradient criteria were met. At high temperatures, higher saturation values were required to provide sufficient metabolic processes. Thus, the percent saturation values more effectively represent anadromous fish requirements than the mass per volume (mg/l) criteria. The reader is referred to Davis (1975) for additional details.

Table 3.6   Response of freshwater salmonid populations to variable dissolved oxygen levels (Davis 1975)

Response	Oxygen (mg/l)	Saturation at given temperature, °C (°F)					
		0 (32)	5 (41)	10 (50)	15 (59)	20 (68)	25 (77)
		Percent					
Function w/o impairment	7.75	76	76	76	76	85	93
Initial oxygen distress	6.00	57	57	57	59	65	72
Widespread oxygen impairment	4.25	38	38	38	42	46	51

3.3.1.2   Egg incubation and Juvenile Rearing

Reiser and Bjornn (1979) report that low dissolved oxygen concentrations during egg incubation may delay hatching, increase anomalous development, stimulate premature hatching, and ultimately lead to weaker, smaller fry. They further state that coho salmon and steelhead survival drops off dramatically when intragravel dissolved oxygen concentration falls below an average of about 8 mg/l. Although dissolved oxygen requirements for successful incubation are species and developmental stage dependent, they suggest minimum concentrations at or near saturation with temporary reductions no lower than 5 mg/l for anadromous salmonids. Similar to adult dissolved oxygen criteria, Davis (1975) categorizes dissolved oxygen criteria for salmonid larvae and mature eggs based on oxygen tension gradient and metabolic requirements, both in mg/l and as percent saturation. The results are presented in Table 3.7. As with Table 3.6, the percent saturation values account for required oxygen tension gradient and sufficient oxygen.

Maximum growth for juvenile coho occurs at about 8.3 mg/l (Colt et al 1979). Herrmann et al (1962) reported that the growth of juvenile coho salmon maintained at 20°C declined slightly when concentrations were reduced from 8 mg/l to 5 mg/l, while growth declined more rapidly at lower concentrations. Mortality was high at levels averaging 2.1 to 2.3 mg/l, and those surviving showed a reduced consumption and weight loss (Colt et al 1979).

Table 3.7   Response of freshwater salmonid larvae and mature eggs to variable dissolved oxygen levels (Davis 1975)

Response	Oxygen (mg/l)	Saturation at given temperature, °C (°F)					
		0 (32)	5 (41)	10 (50)	15 (59)	20 (68)	25 (77)
		Percent					
Function w/o impairment	7.75	98	98	98	98	100	100
Initial oxygen distress	6.00	76	76	76	79	87	95
Widespread oxygen impairment	4.25	54	54	57	64	71	78

3.4   pH, Alkalinity, and Conductivity

pH, alkalinity, and conductivity are several parameters useful in the evaluation of surface waters. The molar concentration of hydrogen ion is expressed through pH. At a given temperature, pH indicates the intensity of the acidic (pH<7) or basic characteristic (pH>7) of the system, and is controlled by dissolved chemical compounds and biochemical processes. In unpolluted surface waters, pH is principally controlled by the balance between carbon dioxide, carbonate, and bicarbonate (see "carbonate system," below). Industrial effluents, atmospheric deposition, as well as photosynthesis and respiration of algae can affect the natural acid-base balance of aquatic systems (Water Quality Analysis, 1996). Changes in pH may have a strong effect on the toxicity of metals, ammonia, and nitrite. Typical surface waters have pH ranging from 6 to 9. The NCRWQCB Basin Plan objectives for pH are outlined in Table 3.8.

Alkalinity is the base neutralizing or "buffering" capacity of water (i.e., ability to neutralize acids). Total alkalinity is a measure of the net effect of all cations and anions; however, it is typically approximated by carbon dioxide ($CO_{2(g)}$ and $CO_{2(aq)}$), carbonic acid (H_2CO_3), bicarbonate (HCO_3^-), carbonate (CO_3^{-2}), and hydrogen ion (H^+). These species make up the "carbonate system," one of the most important acid-base relationships in aquatic systems (Tchobanoglous and Schroeder, 1987). Carbonate equilibrum can be represented as equation 3.1.

$$(CO_2)_{aq} + H_2O \leftrightarrow H_2CO_3 \leftrightarrow HCO_3^- + H^+ \leftrightarrow CO_3^{-2} + 2H^+ \tag{3.1}$$
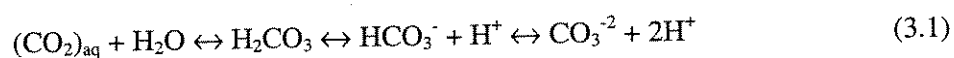
The quantity of any particular species is pH dependent: bicarbonate is the dominant species in surface waters (pH 6 to 9), while carbon dioxide and carbonate ion play increasingly important roles below pH 6 and above pH 9, respectively.

Alkalinity is expressed in a variety of units. Water quality engineers and treatment specialists typically report values in terms of calcium carbonate (mg $CaCO_3$/l), while chemists report milliequivalents or moles per liter (meq/l or mmol/l). Occasionally values are reported in terms of bicarbonate (mg HCO_3^-/l).

Waters with low alkalinity are termed weakly buffered, and are susceptible to alterations in pH due to primary production (photosynthetic activity) as well as atmospheric acid deposition (acid rain). Calcium carbonate concentrations less than 75 mg/l are termed weakly buffered systems. Incidentally, acidity is the direct counterpart of alkalinity and is controlled mainly by strong mineral acids, weak acids such as carbonic acid, and strong acids. It is not as readily applicable as alkalinity and its use is somewhat qualitative (McCutcheon et al 1993).

Conductivity or specific conductance is a measure of the ability of water to conduct electric current. Conductivity can be used as a relative measure of general quality changes within a stream in space and/or time, in response to tributary, spring, or return flow accretion. It is sensitive to variations in dissolved solids, mostly mineral salts and the degree to which these dissociate into ions. The amount of electrical charge on each ion, ion mobility, and water temperature all have an influence on conductivity. Conductivity is related to concentration of total dissolved solids plus major ions and is expressed as microsiemens per centimeter (μS cm^{-1}). The conductivity of most waters ranges from 10 to 1000 μS cm^{-1}, but may exceed 1000 μS cm^{-1} in polluted waters or those receiving large quantities of land runoff (Water Quality Assessments, 1996). The NCRWQCB Basin Plan objectives for specific conductance are outlined in Table 3.8.

3.4.1   Impact on Anadromous Salmonids: pH, Alkalinity, and Conductivity

The direct impacts of pH, alkalinty, and conductivity on anadromous salmonids are not well defined. However, indirect impacts of these parameters may be more profound. Krenkel and Novotney (1980) and EPA (1976) present a minimum alkalinity of 20 mg $CACO_3$ /l to support cold water biota in freshwater aquatic systems.

Little information is available addressing salmonid tolerance to changes in pH, although effects of rainbow trout appear to show that pH levels between 5.0 and 9.0 are acceptable. The pH range that proved lethal within 24 hours to rainbow trout, roughly 10, was independent of acclimatization pH. Extended exposure to pH above 9 or below 5 may be harmful to rainbow trout (Colt et al 1979).

Though alkalinity has few if any direct impacts on anadromous fish, a weakly buffered system is predisposed to fluctuations in pH if sufficient primary production (algae) occurs (see Section 3.7 Algae, below). As noted previously, changes in pH can lead to increased toxicity of certain constituents/contaminants.

Direct implications of conductivity on anadromous fishes are unknown.

Table 3.8   North Coast Regional Water Quality Control Board Klamath River water quality objectives (NCRWQCB 1996)

System	Specific Conductance (μmhos)[1]		Hydrogen Ion, pH	
	90% Upper Limit[2]	50% Upper Limit[3]	Minimum	Maximum
Klamath River above Iron Gate Dam[4]	425	275	7.0	8.5
Klamath River Below Iron Gate Dam	350	275	7.0	8.5
Shasta River	800	600	7.0	8.5
Scott River	350	250	7.0	8.5
Other Tributaries	300	150	7.0	8.5

[1] Specific conductance at 77°F

[2] 90% upper limit represents the 90 percentile values for a calendar year. 90% or more of the values must be less than or equal to an upper limit.

[3] 50% upper limit represents the 50 percentile values of the monthly means for a calendar year. 50% or more of the values must be less than or equal to an upper limit.

[4] Including Iron Gate and Copco Reservoirs

3.5   Pollutants (contaminants)

Pollutants can be broadly classed as chemical, physical, and biological (Krenkel and Novatny 1980). Chemical pollutants include organic and inorganic compounds (organic compounds are categorized as those containing a carbon atom). Major effects of inorganic materials include changes in pH of water and toxicity caused by contaminants (e.g., heavy metals). Conversely, organic materials potential for depleting dissolved oxygen often is the

primary concern. However, it is important to note that inorganic materials may deplete oxygen, and toxic effects may accompany organic materials (Krenkel and Novatny 1980).

Physical Pollutants include color, foam, suspended solids, turbidity, and radioactivity. These characteristics may be associated with other forms of pollutants (e.g., chemical). Color may be undesirable and may affect light transmission and thus water temperature and productivity. Foam may be anthropogenic or natural in origin and is typically aesthetically objectionable, but can affect oxygen and other gas transfer. Suspended solids may be inorganic or organic and can result in the inhibition of photosynthesis, retardation of benthic processes, reduction in waste assimilative capacity of a water body, and aesthetically unpleasing conditions. Turbidity is a measure of water clarity determined by measuring the amount of light scattered by suspended organic and inorganic particles in a water sample. Values are measured in Nephelometric Turbidity Units (NTU) with normal values ranging from 1 to 1000 NTU. Levels can be increased by the presence of organic matter, other effluents, or runoff with a high suspended matter content (Water Quality Assessments 1996) Such conditions may or may not be harmful to fish, but can affect light transmission, affecting water temperature and production (Krenkel and Novatny 1980). Radioactivity may be present as natural background levels due to radioactive minerals or anthropogenic in origin as radioactive wastes.

Biological pollutants can be classified in two categories: primary and secondary. Primary biological pollutants are those that cause disease and will not be addressed herein (but may be important in anadromous fish biology). Secondary biological pollutants are substances added to water that might result in excessive growth. Generally these include the nutrients nitrogen and phosphorus, and are discussed below (Krenkel and Novatny 1980).

General NCRWQCB Basin Plan objectives for water quality parameters that are not specifically quantified are based on impacts to beneficial uses. That is, suspended and settleable material, biostimulatory substances (e.g., nutrients), sediment, turbidity, toxicity, etc. cannot adversely impact beneficial uses of a water body. Identified or potential beneficial uses for the middle Klamath River (including Iron Gate and Copco Reservoirs) include but are not limited to municipal and industrial, agricultural, recreation, commercial and sport fishing, and warm and cold freshwater habitat uses (NCRWQCB 1996).

3.5.1   Impacts on Anadromous Fish: Pollutants

There are many contaminants that can potentially impact anadromous fish populations. A very brief discussion of chemical pollutants and physical pollutants is included. Biological pollutants in the form of nutrients are discussed in Section 3.6.

<u>Chemical Pollutants</u>

Heavy Metals are common inorganic chemical pollutants. Heavy metals found in aquatic ecosystems include, but are not limited to, lead, copper, zinc, cadmium, and mercury. The toxicity of metals varies greatly with pH, water hardness, dissolved oxygen levels, salinity, temperature and other parameters. Physiological impacts occur at small concentrations. For example, growth and mortality of rainbow trout are effected at copper levels of 17 μg/l. However, the toxicity of copper is highly dependent on water chemistry. In very soft water 32 μg/l proved lethal, but in hard water the lethal tolerance for trout ranged up to 1100 μg/l (Colt et al, 1979). (Hardness is typically represented as the sum of calcium and magnesium concentrations in milligrams per liter.)

Inorganic chemicals, such as polychlorinated biphenyl (PCB and phthalic acid (PAE), used in the plastics and electrical industry, can sometimes be found in aqueous systems. Acute toxicity is typically low, but significant levels may accumulate (i.e., bioaccumulation, bioconcentration) in body tissues when fish are exposed to low levels (Sawyer et al 1994). Colt et al (1979) reported that rainbow trout hatching from eggs containing PCB levels of 2.7 μg/g were badly deformed, experiencing 75 percent mortality after 30 days. The drinking water standard for PCBs in the United States is 0.5 μg/l.

<u>Physical Pollutants</u>

Many physical pollutants do not have direct impacts on anadromous fishes. For example, taste, color, odor may be aesthetically displeasing, and lead to public perception issues, but may be of no harm to fish. Under certain conditions color can affect light transmission and impact temperature and primary production, thus affecting other water quality parameters that ultimately could adversely affect fish.

Suspended solids and turbidity can adversely affect salmonid fish indirectly as color may affect water quality. Sight feeding is restricted above 50 NTU. Additionally, increased susceptibility to predation may result from reduced visibility. If suspended matter is organic in nature an oxygen demand may be exerted on the system, depressing DO levels. Certain

51

amounts of suspended matter may settle out. Excessive suspended material may clog fish gills, reduce feeding, and increase stress (Reiser and Bjornn 1979). In addition, indirect damage through destruction of food supply, lowered egg and alevin survival, and changes in rearing habitat would occur long before adult fish would be directly affected. Reiser and Bjornn (1979) note that several states set turbidity limits at no more than 10 NTU over background levels.

3.6 Nutrients

Certain elements are defined as nutrients because they are essential for life processes in aquatic organisms. Major nutrients include carbon, nitrogen, phosphorus, and silicon. Other potentially important nutrients include calcium, magnesium, sodium, potassium, and sulfur. Micronutrients, those required by plants and animals in very small quantities, might include manganese, copper, zinc, cobalt, and molybdenum (Horn and Goldman 1994). Nutrients are important in water quality for several reasons, but most often are associated with algal growth. Those critical to algal growth usually include phosphorus or nitrogen (though carbon, silicon or light limitations may play a role) (Bowie, et al 1985).

Nutrients are present in several forms in aquatic systems, including dissolved inorganic, dissolved organic, particulate organic, and biotic forms. Only dissolved forms are directly available for algal growth: for nitrogen and phosphorus these include ammonia, nitrate, nitrite, and orthophosphate (as well as dissolved CO_2, and dissolved silica, etc.). Nutrient forms and selected dynamics and/or processes are included in Table 3.9. Nitrogen and phosphorus species, the nitrogen-phosphorus ratio, and impacts of nutrients on anadromous fishes are outlined below.

Table 3.9   Nutrient forms and dynamics/processes

Form	Dynamics/ processes
Dissolved inorganic	photosynthetic uptake, excretion, chemical transformation, hydrolysis of dissolved organic nutrients, detritus decomposition, sediment decomposition and release, external loading
Particulate inorganic	sorbtion, complexation
Dissolved organic	excretion, hydrolysis, detritus decomposition, sediment decomposition and release, external loading
Particulate organic	particulate excretions, algal mortality, decomposition, settling, zooplankton grazing, external loading
Biotic (in living matter)	algal respiration and mortality, algal uptake, algal composition, zooplankton grazing, external loading

3.6.1   Nitrogen

Nitrogen dynamics are complex because of their substantial biogeochemical role, important oxidation-reduction reactions, and impact on other water quality variables such as oxygen. Primary forms of nitrogen include organic nitrogen (Org-N), ammonia (as ammonium ion (NH_4^+) plus unionized ammonia (NH_3); herein total ammonia is referred to as NH_4^+ unless otherwise stated), nitrite (NO_2^-), nitrate (NO_3^-), and free nitrogen (N_2). Major processes governing nitrogen dynamics include ammonification, nitrification, denitrification, nitrogen uptake, and nitrogen fixation. These are briefly outlined below.

<u>Ammonification</u>

Ammonification is the transformation of organic nitrogen to ammonia (OrgN $\rightarrow$ NH_4^+). Organic nitrogen is derived from unassimilated organic nitrogen as protein in animal wastes (urea) and the protein remaining in bodies of dead animals and plants. Ammonification takes place through decay processes such as hydrolysis (reactions that occur between material and water) and deaminization due to bacterially mediated biodegradation (Sawyer et al 1994). Organic nitrogen can be converted to ammonia by the action of heterotrophic bacteria (bacteria that can only generate energy from the oxidation of organic matter, versus autotrophic bacteria that can generate energy without organic matter), under aerobic and anaerobic conditions.

$$\text{Protein (OrgN)} \underset{\text{bacteria}}{\rightarrow} \text{Ammonia} \qquad\qquad (3.2)$$

Ammonia exists in two forms in natural waters: ammonium ion (NH_4^+) and ammonia gas (NH_3), where total ammonia is the sum of the two forms. Ammonium ion is innocuous at levels found in most natural waters, while the unionized form is toxic to fish. The equilibrium relationship is pH dependent, and to a lesser extent temperature dependent, and at high pH (>9) elevated levels of unionized ammonia can occur: $NH_4^+ \rightarrow NH_3 + H^+$ (Chapra 1997).

Some nitrogen always remains as non-digestible matter and becomes part of the non-digestible residue sink. As such, it becomes part of the detritus in water or sediments, or the humus in soils (Sawyer 1994).

Hydrolysis of organic nitrogen to ammonia does not directly exert an oxygen demand; however indirect impacts include the production of ammonia, which subsequently oxidizes to nitrite and ultimately to nitrate. Further, the hydrolysis of organic nitrogen produces

53

inorganic forms directly available for algal growth, which can subsequently impact water quality.

Nitrification

If ammonia is released in excess of plant requirements, the excess undergoes nitrification through oxidization by autotrophic nitrifying bacteria in a two-stage process to form nitrite (NO_2^-) and nitrate (NO_3^-). The Nitrosomonas group, known as the nitrite formers, converts ammonia under aerobic conditions to nitrites and derive energy from the oxidation. The nitrites are oxidized by the Nitrobacter group, known as the nitrate formers (Sawyer 1994). The process consumes oxygen and can significantly deplete aquatic system dissolved oxygen levels. Because the transformation of nitrite to nitrate is relatively fast, the process is sometimes represented as the oxidation of ammonia to nitrate directly (one-stage) (Chapra 1997). Generally, three conditions for nitrification are required: nitrifying bacteria, optimum pH and alkaline range, and aerobic conditions

Because ammonia is oxidized to nitrite relatively quickly and subsequently nitrite to nitrate, high levels of ammonia found in surface waters are normally indicative of a recent or nearby source or high rates of decomposition in the absence of oxygen. Similar to ammonia, nitrates may serve as fertilizer for plants both within the stream and under irrigation practices. Under irrigated conditions nitrates produced in excess of the needs of plant life are carried away in water percolating through the soil. Elevated concentrations of nitrates can occur in groundwater because nitrate does not have a high affinity to bind with soils.

Denitrification

Denitrification refers to the reduction of nitrate to $N_{2(g)}$ (nitrogen gas) under anaerobic conditions. Presumably, nitrates are first reduced to nitrites, and then the reduction of nitrites occurs. Though reduction of nitrites is carried all the way through to ammonia by a few bacteria, most bacterially mediated reactions produce nitrogen gas. Because free nitrogen is in a gaseous form, denitrification can result in a loss of nitrogen from the water body to the atmosphere. (Specifically, under anaerobic conditions nitrate can serve as an electron acceptor for certain bacteria, where nitrite is formed as an intermediate product with the principal end product being free nitrogen (Chapra 1997): $NO_3^- \rightarrow NO_2^- \rightarrow N_2O \rightarrow N_2$ (Wetzel 1985). Organic matter must be present and is oxidized for energy while nitrogen is being reduced (Sawyer et al 1994).)

<u>Uptake/assimilation</u>

Uptake or assimilation includes the uptake of inorganic nitrogen by algae during photosynthetic growth. Both ammonia and nitrate are accumulated, generally with preference given to ammonia over oxidized forms (Bowie et al 1985).

<u>Nitrogen Fixation</u>

Free nitrogen, e.g., atmospheric ($N_{2(g)}$), can be utilized by certain nitrogen-fixing algae and photosynthetic bacteria (e.g., blue-green algae). Nitrogen fixation is primarily light dependent, but exceptions exist. This process is an important external input of nitrogen accumulation in water bodies and can materially affect nitrogen dynamics. Fixation is suppressed if readily available sources of nitrogen (NO_3^-, NH_4^+) are available. However, because N_2 diffuses more readily than either nitrate or ammonium ions, the relationship is not always consistent (Wetzel 1985). In waters with high phosphorus loads, phytoplankton can depress nitrogen levels to the point where non-fixing algae will become nitrogen limited. The ability of nitrogen-fixing algae and bacteria to utilize free nitrogen gives them a competitive advantage under such conditions, and species such as blue-green algae can dominate resulting in objectionable water quality characteristics (foam, toxicity, recreational hazard) (Chapra 1997).

3.6.2   Phosphorus

Phosphorus is essential to all life. From a water quality perspective phosphorus is important because it is usually in short supply relative to other macro-nutrients (including carbon, oxygen, nitrogen, sulfur, silica, and iron). Scarcity is due to three primary factors:

- Phosphorus is not abundant in the earth's crust. Further, the phosphate minerals that do exist are not highly soluble.

- Phosphorus does not exist in gaseous form. Thus, in contrast to carbon and nitrogen, there is no gaseous atmospheric source.

- Under aerobic conditions phosphates tend to sorb strongly to fine-grained particles. The settling of these particles, along with sedimentation of organic particles containing phosphorus serves to remove phosphorus from the water to the bottom sediments. Anaerobic conditions or physical disturbance are required for phosphorus to be released from bottom sediments in appreciable quantities.

Though naturally scarce, human activities result in discharge of phosphorus to natural waters (Chapra 1997)

Total inorganic and organic phosphorus have been separated in various ways for chemical analysis; often, these fractions relate poorly to the metabolism of phosphorus.

The most significant form of inorganic phosphorus is soluble organic phosphorus (orthophosphate), consisting of the species $H_2PO_4^-$, HPO_4^{2-}, and PO_4^{-3} (herein referred to as PO_4^{-3}), because it is the only form of phosphorus that is readily available to most plants and microorganisms (Tchobanoglous and Schroeder, 1987). The ratio of PO_4^{-3} to the other forms of phosphorus is approximately 1:20 or 5 percent, with the percentage of total phosphorus occurring as truly ionic orthophosphate (i.e., readily available) is probably less than 5 percent in most natural waters (Wetzel, 1985). However, in nitrogen limited systems this ratio may not apply.

The phosphorus cycle involves two general steps: from organic to inorganic and from inorganic to organic, as outlined below.

- Organic phosphorus available in dead plant and animal tissue and animal waste is converted bacterially to PO_4^{-3} (orthophosphate): organic to inorganic. Similar to organic nitrogen – ammonia reaction, the conversion of organic to inorganic phosphorus does not exert an oxygen demand on the system.
- PO_4^{-3} released to the environment is incorporated into plant and animal tissue (e.g., bacteria, algae, and their predators) containing phosphorus: inorganic to organic.

3.6.3   The Nitrogen-Phosphorus Ratio (N:P)

The nitrogen-phosphorus ratio (N:P) is useful for an initial screening of the relationship between nitrogen, phosphorus, and plant biomass. Algae require both nitrogen and phosphorous for growth. Using chlorophyll a (chlr a) as a surrogate for plant biomass an approximate nutrient relationship for phytoplankton (algae) can be obtained. Noting that algal cells contain 0.5-2.0 μg/l phosphorus per μg chlr a and 7-10 μg nitrogen per μg chlr a, ratio of for nitrogen-to-phosphorus (N:P) can be formed that is roughly 7:1. Thus for an N:P less than 7, nitrogen becomes the limiting nutrient in algal growth (available nitrogen will be used up in cell growth (plant biomass) before available phosphorus). When N:P is greater than 7, phosphorus becomes limiting to algal growth. When N:P equals 7 neither nutrient is limiting. These ratios are variable based on plant stoichiometry (the determination of the proportions in which chemical elements combine or are produced and the weight relations in the chemical reaction). Generally a phosphate concentration of 0.01 mg/l will support algae species.

The N:P ratio can change between water bodies, with water temperature, season, and watershed geologic formation. Further, the N:P ratio may be based on total or inorganic forms of nitrogen and phosphorus. The argument for using total nutrient concentrations is supported by the short cycling times in aquatic systems. While others argue that only inorganic forms – those readily available to algae – should be used in calculating the ratio.

3.6.4   Impacts on Anadromous Fish: Nutrients

Direct nutrient toxicity can occur from ammonia, nitrite, and/or nitrate. Nutrient toxicity is best understood for ammonia. Indirect impacts may include eutrophication of surface waters (increasing nutrient concentrations generally associated with increasing productivity) if sufficient concentrations and conditions exist (see Section 3.7, below). Only the direct toxic effects of nutrient species to fish, and where available salmonids, is included. As with other water quality constituents, combinations of conditions or constituents can lead to increased toxicity.

<u>Ammonia</u>
Ammonia in unionized form (NH_3) is highly toxic to fish at lethal concentrations and at sub-lethal concentrations may reduce growth, damage gills and other organs, and be a predisposing factor in bacterial gill disease (Colt et al 1979). Salmonids are particularly susceptible to toxic effects (Wade et al 1998). Hofer et al (1995) report neurotoxic effects and gill damage cause mortality in rainbow trout for concentrations ranging from 160 µg/l to 800 µg/l. Recommended safe concentrations of unionized ammonia are in the 20 µg/l to 25 µg/l range (Hofer et al 1995, USEPA 1976). Magaud et al (1997) noted that variable concentrations of unionized ammonia may be more toxic than constant concentrations, the phenomenon being linked to the ability of fish to acclimate or adapt to new conditions.

The amount of unionized ammonia can be computed in freshwaters knowing the total ammonia, pH, and temperature. Table 3.10 presents percentages of total ammonia as unionized ammonia at several pH and temperature values. Table 3.11 and 3.12 illustrate chronic (4-hour) and acute (1 hour) total ammonia ($NH_4^+ + NH_3$) criteria for salmonids and their sensitivity to pH and temperature.

Table 3.10   Percentage of total ammonia as unionized ammonia in distilled water (APHS, 1995)

Temp.	Percentage unionized ammonia at given pH								
ºC (ºF)	6.0	6.5	7.0	7.5	8.0	8.5	9.0	9.5	10.0
5 (41)	0.01	0.04	0.11	0.40	1.1	3.6	10	27	54
10 (50)	0.02	0.06	0.18	0.57	1.8	5.4	15	36	64
15 (59)	0.03	0.08	0.26	0.83	2.6	7.7	21	45	72
20 (68)	0.04	0.12	0.37	1.2	3.7	11	28	55	80
25 (77)	0.06	0.17	0.51	1.8	5.1	14	35	63	84
30 (86)	0.07	0.23	0.70	2.3	7.0	19	43	70	88

Table 3.11   Chronic (4-hour) criteria for total ammonia: salmonids (EPA, 1987)

Temp.	Total ammonia (mg/l) at given pH										
ºC (ºF)	6.5	6.75	7	7.25	7.5	7.75	8	8.25	8.5	8.75	9
0 (32)	2.5	2.5	2.5	2.5	2.5	2.3	1.5	0.9	0.5	0.3	0.2
5 (41)	2.4	2.4	2.4	2.4	2.4	2.2	1.4	0.8	0.5	0.3	0.2
10 (50)	2.2	2.2	2.2	2.2	2.2	2.1	1.4	0.8	0.5	0.3	0.2
15 (59)	2.2	2.2	2.2	2.2	2.2	2.0	1.3	0.8	0.4	0.3	0.2
20 (68)	1.5	1.5	1.5	1.5	1.5	1.4	0.9	0.5	0.3	0.2	0.1
25 (77)	1.0	1.0	1.0	1.0	1.1	1.0	0.7	0.4	0.2	0.2	0.1
30 (86)	0.7	0.7	0.7	0.7	0.7	0.7	0.5	0.3	0.2	0.1	0.1

Table 3.12   Acute (1-hour) criteria for total ammonia: salmonids (EPA, 1987)

Temp.	Total ammonia (mg/l) at given pH										
ºC (ºF)	6.5	6.75	7	7.25	7.5	7.75	8	8.25	8.5	8.75	9
0 (32)	35	32	28	23	17	12	8	4.5	2.6	1.5	0.9
5 (41)	33	30	26	22	16	11	7.5	4.2	2.4	1.4	0.8
10 (50)	31	28	25	20	16	11	7.1	4.1	2.3	1.4	0.8
15 (59)	30	27	24	20	15	11	6.9	4.0	2.3	1.4	0.9
20 (68)	29	27	23	19	15	10	6.8	3.9	2.3	1.4	0.9
25 (77)	20	19	17	13	10	7.2	4.8	2.8	1.7	1.1	0.7
30 (86)	14	13	12	9.5	7.3	5.2	3.5	2.1	1.3	0.8	0.6

Nitrite

Toxicity of nitrite may be related to the concentration of nitrous acid, HNO_2 (unionized), which is a function of total nitrite, pH, temperature, and ionic strength. Nitrous acid can oxidize the ferrous ion (Fe^{+2}) of hemoglobin to ferric ion (Fe^{+3}), producing ferrihemoglobin in the bloodstream. Because ferrihemoglobin cannot transport oxygen, it displaces the ability of blood to carry oxygen and, if sufficient quantities are formed, hypoxia may result.

Lethal limits for salmonids range from 0.19 mg/l to 0.55 mg/l, and depend strongly on pH, and calcium and chloride concentrations. Colt et al (1979) further reports the 96-hour lethal concentration for 50 percent of the population (96-h LC50) for chinook salmon of 2.6 mg/l. Nitrite appears to be more toxic at increased salinity. Because levels of nitrite are typically very low in natural systems, toxicity is generally not an issue. Information concerning impacts on growth and reproduction is limited.

Nitrate

Nitrate is not very toxic. The lethal level of nitrate is on the order of 1300 mg/l for trout. The 96-h LC50 for chinook salmon is reported as 5800 mg/l. Nitrate appears to be more toxic at increased salinity. The NCRWQCB Basin Plan objective for nitrate is not to exceed 45 mg/l, but this is probably based on human consumption requirements. Above 45 mg/l nitrate may cause Methemoglobinemia (Blue Baby Syndrome) in human infants (Colt et al 1979).

3.7　　　Algae

Algae apply to a diverse group of eucaryotic (containing a nucleus enclosed within a well-defined nuclear membrane) microorganisms that share similar characteristics. They are unicellular to multi-cellular plants that occur in freshwater, marine water, and damp environments and range in size from minute phytoplankton to giant marine kelp. Algae possess chlorophyll, the green pigment essential for photosynthesis, and often contain additional pigments that mask the green color (e.g., fucoxanthin (brown) and phycoerythin (red)) (Wetzel 1983, Horn and Goldman 1994). The lifecycle of algae ranges from simple, involving cell division, to complex, involving alternation of generations. Algae are primary producers of organic matter which animals depend on either directly or indirectly through the food chain (APHA, 1995)

Typically, algae are autotrophic (derive cell carbon from inorganic carbon dioxide), photosynthetic (derive energy for cell synthesis from light), and contain chlorophyll. They are also chemotrophic in terms of nighttime respiration, e.g., metabolism of molecular oxygen (O_2). Algae utilize photosynthesis (solar energy) to convert simple inorganic nutrients into more complex organic molecules. Photosynthetic processes results in surplus oxygen and non-equilibrium conditions by producing reduced forms of organic matter, i.e., biomass containing high-energy bonds made with hydrogen and carbon, nitrogen, sulfur, and

phosphorus compounds. The organic matter produced serves as an energy source for non-photosynthetic or heterotrophic organisms (animals, including most bacteria, which subsist on organic matter). Heterotrophic organisms tend to restore equilibrium by catalytically decomposing these unstable organic products of photosynthesis, thereby obtaining a source of energy for their metabolic needs. The organisms use this energy both to synthesize new cells and to maintain old cells already formed (Stumm and Morgan, 1996). From the point of overall reactions, these heterotrophic organisms only act as reduction-oxidation catalysts – they only mediate the reaction (or more specifically the electron transfer). Oxidation may produce several intermediate reduction-oxidation states prior to reaching a fully oxidized state (e.g., inorganic state).

Respiration is the reverse process of growth in which protoplasm undergoes endogenous decay and/or cell lysis and oxidation. Through respiration and decomposition, organic matter is returned to the simpler (vs. complex and unstable) inorganic state. During breakdown oxygen is consumed and carbon dioxide is liberated (Chapra 1997). Although algae respire oxygen in the presence of sunlight, the amount produced via photosynthesis usually exceeds the amount used during daylight.

Light is the most limiting factor for algal growth, followed by nitrogen and phosphorus limitations. Algal productivity is often correlated to levels of nitrogen (N) and phosphorus (P) (See N:P ratio, above), but other nutrients are required including carbon, silica, and other micronutrients. Biomass is usually measured by the amount of chlorophyll a in the water column (measurement of gross level of algae) and/or as mass per area for attached species. Chlorophyll a is a photosynthetic pigment that serves as a measurable parameter for all algae production. Quantitative biomass estimates can be made noting that on average 1.5% of algal organic matter is chlorophyll a. Qualitative assessment of primary production on water quality can be based on chlorophyll a concentrations as noted below.

Chlr-a Concentration (µg/l)	Water discoloration
<10	no discoloration
10-15	some discoloration, some algal scum
20-30	deep discoloration, frequent algal scum
>30	very deep discoloration, algal matting

Though not true algae, certain strains of cyanobacteria (blue green-algae) can produce an active intracellular toxin, especially when phytoplankton are senescent (the growth phase

following maturity and prior to death, characterized by accumulated metabolic products, increased respiration, and loss of dry weight) and decaying.

The intensity, duration, and quality of light influence the dominance of algal species and the structure of algal communities. Likewise, water temperature influences the metabolic and reproductive rates of algae. Although algal growth rates can be relatively lower during periods of cold water conditions, the standing crop or biomass of algal communities can be comparatively large because of the absence or inactivity of grazing organisms. Discharge and velocity conditions also affect algal communities through scouring and washout. However, modest increases in current velocity may enhance rates of algal accumulation because nutrient uptake and boundary layer diffusion increases with current velocity (Stevenson 1996). During stable hydrologic conditions, algal communities can develop in streams and rivers within several weeks of colonization and reproduction. However, such communities may vary considerably within river reaches in relation to current velocity, depth, light intensity, and water chemistry factors. Further, seasonal changes in the abundance and composition of algal communities may occur (Porter et al 1993).

3.7.1   Impacts on Anadromous Fish: Algal Toxicity and Algae

Role of algal toxicity to anadromous fishes is uncertain. Although algal blooms usually pose no direct health effects, certain species produce endotoxins or exotoxins that may be harmful to aquatic life. Endotoxins are of internal origin and separable from the cell body only through disentegration (e.g., death). Exotoxins are a soluble toxin produced during growth of a mircoorganism and released into the surrounding medium. Endotoxins can be lethal if organisms are ingested by fish, while exotoxins can cause fish kills if sufficient levels exist.

Indirect algal effects, beyond toxicity, include excessive shading of the non-surface waters and subsequent reduction in photosynthetic activity, and impacts on temperature, dissolved oxygen, nutrient cycling, that may in turn affect other aspects of the ecosystem upon which salmonids may depend.

An example of indirect impacts includes the effect of primary production on system water quality. Through photosynthesis, algae produce oxygen in excess of respiratory requirements during daylight hours. Conversely, during low light or nighttime periods algae respire (consume) dissolved oxygen, sometimes depleting water column concentrations. Thus, high algae concentrations may lead to low dissolved oxygen concentrations. Further, during

61

growth, algae require carbon for cell growth. Although carbon may be present in the water column, during periods of peak growth algae may deplete readily available forms of carbon in weakly buffered systems. When dissolved forms are depleted carbon will enter the water column via the air-water interface as carbon dioxide: $CO_{2(g)} \rightarrow CO_{2(aq)}$. However, this process is often insufficient to keep up with algal demands. Under such conditions certain algae species are able to utilize (remove) CO_2 from bicarbonate ion: $HCO_3^- \rightarrow CO_2 + OH^-$. The result is an increase in hydroxyl (OH^-) concentration and an associated increase in pH. It is not uncommon to see diurnal variation in pH ranging from 0.5 to 1.5 pH units as a result of algal productivity. The increase in pH, if accompanied by elevated water temperature can cause a dramatic shift in unionized ammonia concentrations in aquatic systems. As noted previously, unionized ammonia (NH_3 vs. NH_4^+) is toxic to fish in small quantities and lethal exposure periods are on the order of hours (see Tables 3.10 through 3.12, above).

3.8   Other Parameters

3.8.1   Biochemical Oxygen Demand (BOD)

Although not identified in the causative factor matrix, biochemical oxygen demand (BOD) is an important water quality variable that should be included in water quality studies/monitoring. Most organic materials are biodegradable to various degrees. The amount of oxygen used in the metabolism of carbonaceous biodegradable soluble and non-soluble organic matter is termed biochemical oxygen demand (BOD) or carbonaceous biochemical oxygen demand (CBOD). Nearly all biodegradable material will be converted via biochemical oxidation (bacterially mediated) to CO_2, NH_3 and H_2O given enough time. Because of complications measuring this ultimate BOD (BOD_u), BOD_u is usually extrapolated from laboratory 5-day BOD bottle tests [$BOD_u = (BOD_5/(1-e^{-k1(5)})$]. BOD should be determined using nitrification inhibited samples to avoid double counting nitrogenous BOD (NBOD) (Tchobanoglous and Schroeder 1986).

Sources of BOD, in addition to direct loading, include decaying algae and macrophytes and other biota. Typically, a fraction of this matter contributes to BOD, while the remainder is assumed to oxidize immediately for energy. Background levels in natural systems range from 0.5 mg/l to 3.0 mg/l. Municipal and industrial wastes can exceed 30 mg/l (EPA 1997). Although BOD is rarely related to biota health, high BOD loads can severely depress DO. Further, it is a required parameter in most water quality simulation models.

3.8.2 Organic Detritus

Organic detritus is not a common water quality problem directly impacting anadromous fish. However, it plays a role in certain reservoir water quality models as a method to explicitly address algal mortality (versus simply adding it to BOD); thus its inclusion herein.

Wetzel (1985) defines organic detritus as consisting of organic carbon lost by nonpredatory means from any trophic level (autolysis, egestion, excretion, and secretion), or from external inputs to the ecosystem that enter and cycle in the system. Detritus includes all dead organic carbon, but generally does not include bacterial components. Heterotrophic microorganisms (e.g., bacteria) play a critical role converting organic detritus for use by higher trophic levels, thus providing a link between non-living detritus and living organisms. This "detritus food chain" provides an essential component in ecosystems. (Wetzel 1985, Seki 1982).

Total production of organic detritus in the photic zone of most natural waters exceeds degradation/utilization for most of the year. However, sedimentation (organic sediment) and advection out of the immediate environment typically compensate for excess loading. Nevertheless, nearly all organic material produced in aquatic ecosystems is decomposed at an appreciable rate. Turnover time of readily metabolized constituents range from less than a day in hypereutrophic waters (extreme productivity) to tens of days in oligotrophic water (low productivity), while moderately resistant constituents have cycling times ranging from several days to years in hypereutropohic and oligotrophic waters, respectively. It is estimated that less than one percent of organic detritus is highly resistant to biochemical decomposition, e.g., humus (Seki 1982).

Organic detritus typically increases through production of phytoplankton in spring and summer. Periodic decreases may occur after phytoplankton blooms, e.g., spring, and also in autumn and winter after summer production. Corresponding responses in bacterial densities leads to an active consumption of organic matter and the release of inorganic nutrients that become available, and may lead to the formulation of a subsequent algal bloom (Seki 1982).

4.0 Modeling Approach

To provide the required modeling capability to assess flow and water quality conditions in the Klamath River below Iron Gate Dam, several mathematical models were required. The study area encompasses Iron Gate Reservoir and roughly 60 miles of the Klamath River below Iron Gate Dam, as shown in Figure 4.1. An accompanying river mile index is included as Table 4.1
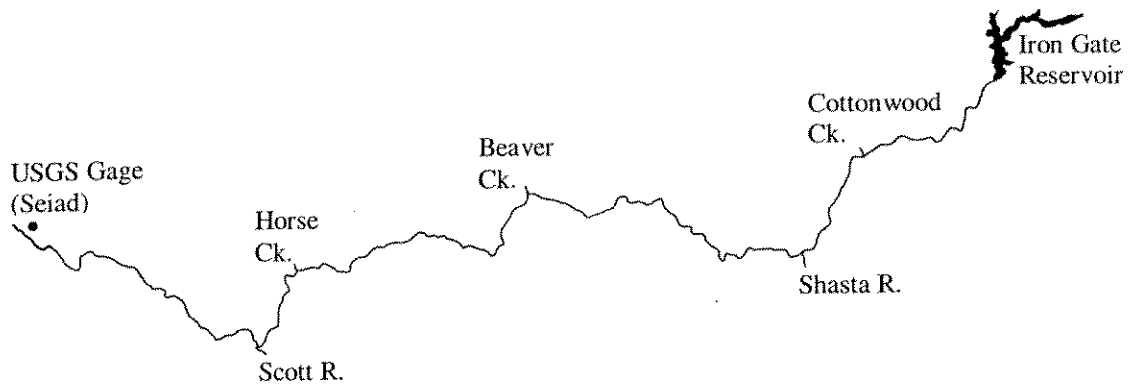
Figure 4.1   Study Area

Table 4.1   River mile index

Location	River Mile	Approximate Elevation	
		ft	m
USGS Gage	129.6	1319.7	402.3
Scott River	143.0	1528.5	465.9
Horse Creek	147.3	1594.0	485.9
Kohl Creek	151.7	1658.6	505.6
Dona Creek	152.8	1675.1	510.6
Walker Rd. Bridge	156.2	1696.6	517.1
Barkhouse Creek	157.3	1703.5	519.2
Beaver Creek	161.0	1751.9	534.0
Lime Gulch	169.7	1907.7	581.5
Badger Creek	174.4	1983.5	604.6
Shasta River	176.7	2013.6	613.8
Cottonwood Creek	182.1	2069.9	630.9
Little Bogus Creek	186.4	2153.2	656.3
Iron Gate Dam	190.1	2198.1	670.0

Three mathematical models were utilized in this project to simulate the water quality regimes of reservoirs and downstream river reaches. For Iron Gate Reservoir the one-dimensional finite difference model WQRRS (Water Quality for River-Reservoir Systems) was applied. For the Klamath River, a pair of finite element models developed by Resource Management Associates, Inc. (RMA) was employed. The model RMA-2 was utilized for hydrodynamics and the model RMA-11 was applied for water quality simulations. These models were operated in tandem to simulate the hydrologic and water quality regime in the system. Herein, RMA-2 and RMA-11 will generally be referred to as the hydrodynamic model and water quality model, respectively. Each of the models has the desirable capabilities of dynamic simulation, providing hourly descriptions of key variables. Brief descriptions of the characteristics of these models and basis for selection are presented below.

Water quality formulations for the models can be found in Appendix A. The chapter concludes with a discussion of system conceptualization and model implementation.

4.1   Iron Gate Reservoir: WQRRS

Iron Gate reservoir is prone to strong thermal stratification during summer periods. Under such conditions a one-dimensional vertical representation, such as that incorporated in WQRRS, is often practicable. WQRRS is based on the principles of conservation of mass and thermal energy. The reservoir's geometric and volumetric properties are represented conceptually by a series of one-dimensional horizontal slices, or layers. Each layer is characterized by bounding areas, a thickness, and a volume of water. Water within each layer is assumed to be fully mixed, i.e., homogeneous. Thus, properties of the system of layers are defined by discrete values identified with the vertical position of each successive layer. Internal transport of heat and mass occurs only in the vertical direction by advection and effective dispersion. Convective mixing, driven by density gradients such as occur with diurnal cooling of the reservoir surface layers or with net heat loss during the fall cooling period, may involve properties of several layers. Model results are considered representative of average conditions in the main reservoir body (away from inflowing tributaries and localized effects of outlets). It is important to note that WQRRS is not a hydrodynamic model; flows between layers in the model occur as the consequence of imbalances in the water budget in accordance with mass conservation. The reservoir's water surface rises and

falls depending on the net difference between inflow and outflow. Details concerning conceptual representation of WQRRS may be found in the model User's Manual (USCOE-HEC, 1978).

The quantity and quality of water released from a reservoir define important boundary conditions for modeling the river downstream. In the case of Iron Gate Reservoir the flows released to downstream river reaches are generally predetermined by project operating schedules designed to meet minimum instream flow requirements or demands. Temperatures and water quality, on the other hand, are governed largely by combinations of uncertain hydrologic, hydrodynamic, chemical, biological, and climatic conditions affecting the thermal energy balance and quality in the water body. An objective of this project was to select an appropriate mathematical model that can be used to reliably simulate the seasonal cycle of temperature and water quality change within the reservoir which, in combination with a specified operation schedule, will provide the needed boundary conditions for the models downstream.

Large water bodies like Iron Gate Reservoir are inherently complex in their circulation and in the distribution of internal thermal energy. In reality they are truly three-dimensional, that is, motions and properties of the water vary along all principal axes. However, with respect to temperature, such systems may become so strongly stratified that they may be modeled one-dimensionally. To determine whether the one-dimensional approach is appropriate for Iron Gate Reservoir, a criterion based on the relationship between inertial and gravitational forces developed by Water Resources Engineers, Inc. (1969) was applied. This criterion is in the form of a densimetric Froude number (Fr) and compares inertial forces, represented by an average flow-through velocity, to gravitational forces that tend to maintain stability, as given by the following expression:

$$Fr = 320 \, [LQ/HV] \qquad\qquad (4.1)$$

where Q is the average flow through the reservoir, H is the average depth of the lake, L is lake length, and V is lake volume. The coefficient 320 includes estimated gravitational and density effects and has units of time. A value of Fr greater than $1/\pi$ (approximately 0.318) indicates that inertial forces dominate the water body and complete mixing can be expected. A much lower value indicates a dominance of gravitational forces, i.e., a tendency toward stratification.

For Iron Gate Reservoir, a typical value of the densimetric Froude number can be derived from measured data for July 1996. Representative values for this month were: L= 37,000 ft, H=160 ft, Q= 1000 cfs, V= 55,000 acre-feet, which yields a densimetric Froude number of 0.029. Based on the above criterion the reservoir is classified as subject to strong stratification seasonally and could be modeled one-dimensionally. Accordingly, the well documented finite difference model WQRRS (USCOE-HEC, 1978) was selected for simulation of Iron Gate Reservoir.

WQRRS idealizes a reservoir as an assemblage of horizontal fully-mixed layers of characteristic densities determined primarily by temperature. Inflows enter this system of layers at elevations of corresponding temperature and outflows occur at temperatures identified with the level of the outlet structure(s). Within the stratified water body, flows are constrained to occur only along the vertical axis, thus redistributing thermal energy and chemical constituents advected to the reservoir with inflows. Thermal energy transferred by heat exchange at the air-water interface is likewise redistributed. Because water density is a function of temperature, a characteristic temperature profile develops in the reservoir, the form of which is governed by the seasonal changes in inflow, outflow, and surface heat exchange. One of the advantages of this model is that the heat exchange routine it uses is well documented (TVA, 1972) and has been incorporated in other widely used models like QUAL2E (Brown and Barnwell, 1987). Additionally, it is detailed enough to predict climatic impacts on the thermal regime of the reservoir at daily, even hourly, intervals. Similarly, the water quality routines have been documented and incorporated other reservoir models such as HEC-5Q (USACE-HEC 1987). The model allows withdrawals to occur from multiple outlets at different elevations which makes it especially useful for reservoir operation analysis where selective withdrawal may be an option.

Basic System Representation

Geometric, hydrologic, water quality, and meteorlogical conditions were required for simulation of Iron Gate Reservoir. The geometry of the reservoir was derived from a stage-area-volume relationship. Additional essential data included a description of outlet structure locations, design, capacities, and elevations. Hydrologic, water quality and climatic information specific to the reservoirs' geographic location was required. These included inflow hydrographs (Copco Reservoir release) and associated water temperature and quality, as well as specifics of reservoir operations, such as release schedules and outlets utilized. The analysis period extended from May through October, effectively representing the

reduced flow conditions in reservoir-river system, presumably when a one-dimensional representation of the reservoir would be most applicable. Temperature and nine water quality constituents were modeled. Water quality constituent included

- Dissolved oxygen
- Biochemical Oxygen Demand
- Ammonia (nitrogen)
- Nitrite (nitrogen)
- Nitrate (nitrogen)
- Phosphate (phosphorus)
- Organic detritus
- Organic sediment
- Algae

Data requirements and data descriptions are included in Section 4.4 and Appendix B.

4.2   Klamath River: RMA-2 and RMA-11

The Klamath River system below Iron Gate Reservoir is a dynamic system; highly variable in morphology, flow, and hydraulic characteristics - all factors that influence the thermal energy balance and fate and transport of constituent concentrations along the axes of flow. An essential requirement for modeling temperature and water quality in this system is a reasonable representation of their hydrodynamic properties, e.g., velocity, stage, discharge, hydraulic gradient, etc. Steady state hydraulics, such as for the model QUAL2E (Brown and Barnwell 1987) were not considered adequate for the complexities potentially encountered with this system. Alternatively, it was decided to adopt the model RMA-2 that has the desired capabilities. This model had been successfully applied in studies of the San Francisco Bay and Delta (Shrestha, Saviz et al 1992), Sacramento and Feather Rivers (Deas et al 1997), Shasta River (Deas and Orlob 1998), and to the Cantara Spill accident on the Upper Sacramento River (Saviz and DeGeorge 1994).

The hydrodynamic model (RMA-2) can be used to simulate either one- or two-dimensional unsteady flow systems. It was used in this project in the one-dimensional form. The model solves the fully dynamic momentum and continuity equations (shallow water equations) using the finite element method, producing time series of velocities, water levels, and discharges through a continuous system of volumetric elements approximating the actual geometry of the river. It requires specification of boundary flows at the headwaters and for tributaries and water levels at the downstream boundary. Calibration of the model is

achieved by adjustment of a boundary roughness coefficient (Manning's n), slope factor, and eddy viscosity coefficients. Eddy viscosity was not used as a calibration parameter in the Klamath River application. The calibrated and validated model provides the flow, velocity, and water surface area data needed for simulation of temperature and heat exchange along river reaches.

The water quality model (RMA-11) is a general purpose water quality model, compatible in geometry with the configuration of the hydrodynamic model. The model simulates advective heat transport and the air-water heat exchange processes, as well as fate and transport of water quality parameters, to produce dynamic descriptions of temperature and constituent concentration along the river reach. Input requirements include temperatures and quality of boundary flows, and meteorological data defining atmospheric conditions governing heat exchange at the air-water interface. Model output is in the form of synoptic longitudinal profiles of temperature and quality parameters along river reaches, or time series at fixed locations. As will be demonstrated subsequently with respect to specific model application, the hydrodynamic model and simulated temperature from the water quality model can be used interactively in calibration and validation to achieve improved results.

Basic System Representation

The Klamath River system project study area extends from Iron Gate Dam (RM 190) downstream to the USGS Gage near Seiad Valley (RM 129), a distance of approximately 60 miles. The system is composed of a main stem, two major tributaries, and minor accretions and depletions that collectively define the hydrodynamic and water quality characteristics of the river. Figure 4.1 maps the critical system components.

Similar to the reservoir model, geometric, hydrologic, water quality and climatic information specific to the river's geographic location was required. The analysis period spanned the same months as the reservoir model: May through October. Due to different model representations and formulations the water quality parameters represented in the reservoir and river models are not the same. For the Klamath River, temperature and the following water quality parameters were simulated.

- Dissolved oxygen
- Biochemical Oxygen Demand
- Organic nitrogen
- Ammonia (nitrogen)

- Nitrite (nitrogen)
- Nitrate (nitrogen)
- Organic phosphorus
- Phosphate (phosphorus)
- Algae

Unlike the reservoir where a single model was used to simulate water quality, implementation of the selected mathematical models of the Klamath River was a complex, multistage process utilizing a set of related sub-models as shown in Figure 4.2. These submodels included: 1) a pre-processor program to generate the geometry for the finite element grid (RMAGEN), 2) the hydrodynamic model (RMA-2), and 3) the water quality model (RMA-11). The process is described briefly as follows.
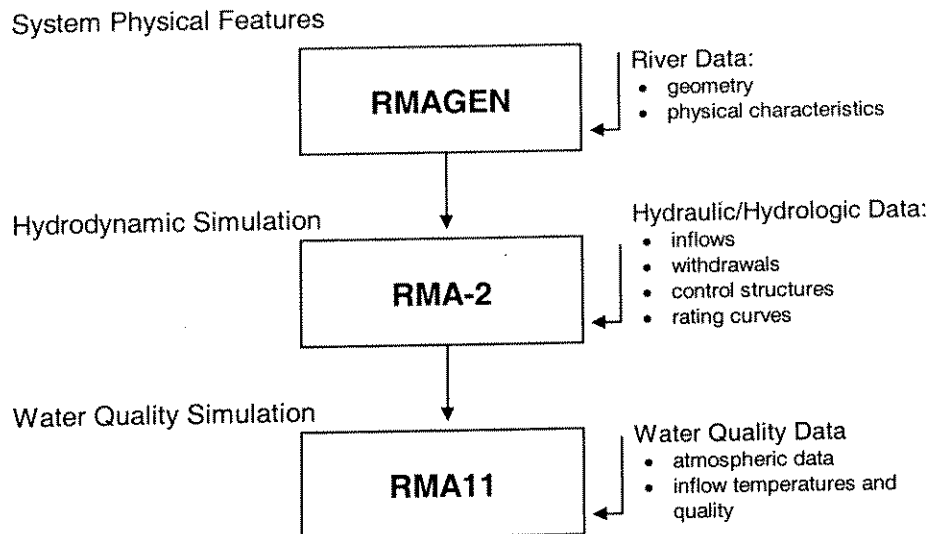
Figure 4.2   Sub-models within the Keswick Reservoir, and Sacramento and Feather Rivers temperature models

<u>Geometry: RMAGEN</u>
The pre-processor RMAGEN was used to generate a numerical description representing the geometric layout of the river including coordinate locations defining the axis of the river. This included bottom elevations and cross section data at key locations. Output also included a finite element grid of the river, represented by a series of nodes and elements. Nodes represent locations of point information such as cross sectional areas and bed elevations, and locations where boundary conditions were defined (head waters, tributaries and downstream boundary). Elements include continuous river information such as bed roughness coefficients and certain boundary flow information. Each one-dimensional element contains three nodes.

70

In this study cross-sections were adjusted to a trapezoidal form, maintaining bottom widths while assigning one-to-one (1:1) side slopes. Fixed 1:1 side slopes were assumed after field reconnaissance and discussions with habitat survey members (Jim Hendrickson, pers comm.). Appendix B contains additional information on cross-section construction.

Hydrodynamics: RMA-2

The model RMA-2 computed the hydrodynamic behavior of the system characterized by elements and nodes from the RMAGEN output. Model input included hydraulic and hydrologic boundary and initial conditions, i.e., inflows, withdrawals, control structures, and rating curves; river information such as Manning's n, turbulent exchange coefficients; and other prescribed information such as length and number of simulation time steps. Model output included velocities and depths at all nodal locations within the system.

Water Quality: RMA-11

The water quality model (RMA-11) was used to simulate river temperature and fate and transport of water quality constituents. Model input included simulated velocity and depth from the hydrodynamic model (RMA-2), as well as initial and boundary conditions (water quality), such as meteorological conditions, upstream and tributary inflow temperatures and quality for simulated constituents. Water temperatures and constituent concentrations in the river, e.g., temperatures and concentrations at all nodes in the finite element grid, were required. Other input included diffusion coefficients, values of empirical and universal constants for heat flux equations, rate constants, temperature correction constants, and other water quality relationship coefficients. Model output included water temperatures and constituent concentration at all nodal locations within the system over any selected time period. Data requirements and data descriptions are included in Section 4.4 and Appendix B.

4.3   Model Parameters: Hydrodynamics

Principal hydrodynamic properties for the river model included geometric considerations (river location, tributaries, bed slope, channel cross section), bed roughness coefficients, and viscosity coefficients. The reservoir model represents flow only through conservation of mass and will not be addressed in this section.

4.3.1   Geometric Considerations

River course, tributaries and accretions/depletions locations, bed slope and cross section geometry were required for application of RMA-2. Because RMA-2 and RMA-11 share geometric properties, all geometric considerations required for RMA-2 fulfilled requirements of RMA-11.

River course refers to the physical location of the river on the surface of the earth. Latitude and longitude or Universal Transverse Mercator (UTM) coordinates were required. A graphical information system (GIS) file for the Klamath River study reach was obtained from California Rivers Assessment at UC Davis. Bed slope was based on the USGS-BRD slope analysis completed in conjunction with the mesohabitat type and redd survey, as well as other sources including DWR (1986), USGS topographic maps, and PSIAC (1973).

River cross sections were represented as simple trapezoids. Side slopes were estimated at rise-to-run ratio of 1:1 for both right and left bank (Jim Henricksen, pers. comm.). River width was estimated from the USGS-BRD/USFWS mesohabitat type survey. Because, river widths varied widely over short distances, causing potential difficulties with the numerical model, river width was smoothed using a 7-times running average. Finally, a finite element grid was formed using this geometric information. Element lengths of 300 meter (node-to-node spacing: 150 m) was selected.

Preliminary runs showed that model results in the steep river reaches were compromised. Steep rivers are typically not uniform in slope, but consist of short cascades or riffles, combined with intermediate pools and runs. RMA-2 includes a slope factor (SF) that reduces the effective bed slope of the stream and assumes travel time through the short cascade sections is negligible compared to the transit time through the run or pool. Figure 4.3 shows a schematic of initial model application (Case 1; SF = 0) and model application with slope factor applied (Case 2: 1>SF>0). For cases 1 and 2 the stream reaches have equivalent vertical elevation change (z) and horizontal distance. But, by neglecting the short cascade reach the transit time in the river is more closely simulated.

To estimate slope factor, uniform flow was assumed and Manning equation applied.

$$Q = [1.49AR^{2/3}S^{1/2}] / n \qquad\qquad (4.2)$$

72

Where Q is flow rate, A is cross sectional area, R is hydraulic radius, S is bed slope (or water surface slope), and n is a channel roughness coefficient. Using this equation for a known cross sectional area, hydraulic radius, and an estimated value of Manning n, the slope required to deliver a known flow rate can be determined.
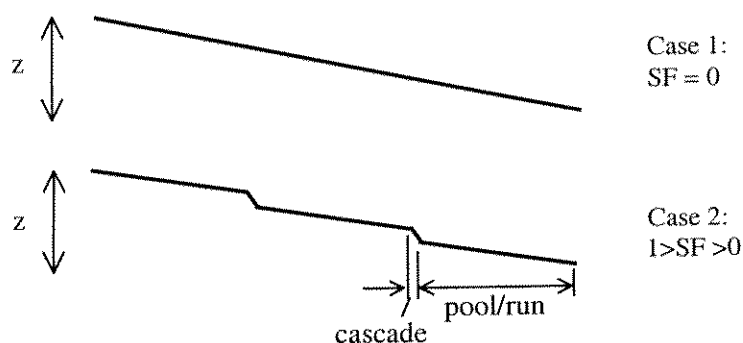
Figure 4.3 Slope factor application for a representative river reach

Elevation at Iron Gate Dam is approximately 2170 ft msl and approximately 1320 ft msl at the USGS gage near Seiad, resulting in a total drop of about 850 feet over roughly 60 miles. This translates to a slope of approximately 0.27 percent. The actual slope of the water surface is significantly less than this value. For example, assuming a representative flow of 1200 cfs, channel width of 115 feet, and an average depth of 5 feet, application of equation 4.2 would yield a Manning n value of roughly 0.10. This is an extremely high value, more appropriate for flow through extremely dense vegetation than a steep free flowing stream. However, if Manning n is estimated at a reasonable value, say 0.040, equation 4.2 can be solved for slope to yield a value of about 0.04 percent. This is roughly 15% of the gross slope, thus a slope reduction factor of 0.85 was applied in the hydrodynamic model. This value was not changed throughout calibration. The assumption is that small discrepancies in the slope factor can be accommodated in selection of an appropriate Manning coefficient. For this reason use of the Manning coefficient determined herein (see Section 6.2.1) for application in other flow models should be done with great care.

4.3.2   Hydrodynamic Coefficients

Bed roughness and viscosity coefficients were the two principal hydrodynamic variables. Viscosity coefficients were insensitive and were not varied for this project. Bed roughness,

or Manning roughness coefficient was set (calibrated) using measured stream temperature as a tracer signal and running the hydrodynamic and water quality model through several iterations until simulated and measured hourly temperatures matched in phase and amplitude. For more details see Section 6.2.1.

4.4 Model Parameters: Water Quality

Water quality modeling requires the specification of multiple constants, coefficients, and ratios to define system processes and inter-relationships. Outlined herein are descriptions, typical ranges, and selected values of key parameters used in the reservoir and river models. Parameters were selected for application in Iron Gate Reservoir and Klamath River system may not be applicable to other systems. Modeled water quality variable interrelationships are presented in Appendix A for both the reservoir and river models. Water temperature and quality data for both the reservoir and river models are addressed in Appendix B. Final selected values for model constants and coefficients are included in Appendix C.

4.4.1 Temperature Dependent Rate Constants

Temperature influences rates of many transforms. Reaction rate constants are usually provided at a standard water temperature of 20°C. These constants are adjusted to ambient water temperatures using the Van't Hoff-Arrhenius relationship.

$$A_t = A_s(\Theta)^{(T_w - T_s)} \tag{4.2}$$

Where:
- A_t = constant value at non-standard water temperature
- A_s = constant value at standard water temperature
- Θ = empirical constant, unique for each reaction constant
- T_w = non-standard water temperature
- T_s = standard water temperature: 20°C (68°F)

Temperature correction coefficients are often presented as Q_{10}. $Q_{10} = (\Theta)^{10}$, or $\Theta = (Q_{10})^{0.1}$. This formulation is based on the general rule of thumb that biologically mediated reactions in natural waters increase with temperature at a rate generally doubling for a temperature rise of 10°C (50° F) within selected range (Chapra, 1997).

4.4.1.1 Reservoir

There are two options for determining temperature correction coefficients in WQRRS: temperature limits and temperature coefficients. The temperature limit method assumes that the rate of a reaction is a function of two curves, one initially increasing exponentially then, still increasing, but exponentially approaching a maximum value and a second similar curve decreasing from the maximum value and approaching a minimum value. The result is similar to a bell curve. At low temperatures, adjustment factors are small, increasing to some peak value then, as temperatures become excessive, adjustment factors are again reduced.

The temperature coefficient method assumes that a reaction rate increases exponentially, without bound, as temperature increases. The rate constant can be adjusted for temperature using

$$R_a = R_{20} \, Q_{10}^{(T_a - 20)} \tag{4.3}$$

Where
R_a = rate constant adjusted to ambient temperature
R_{20} = rate constant at 20°C
Q_{10} = Q_{10} temperature coefficient
T_a = ambient temperature (°C)

The temperature coefficient method was used for this project. The reader is referred to USACOE-HEC (1986).

4.4.1.2 River

Temperature dependent rate constants for the river model are adjusted as per equation 4.2. Brown and Barnwell (1987) present empirical temperature correction coefficients for several rate reactions. Typical values are included in Appendix C.

4.4.2 Reaeration

Reaeration is the process of oxygen exchange between the atmosphere and a water body in contact with the atmosphere. Typically, the transfer is from the atmosphere into the water because dissolved oxygen in most natural waters is below saturation. Photosynthesis can produce supersaturated dissolved oxygen concentrations, resulting in the net transfer of oxygen into the atmosphere (Bowie, et al 1985). The reaeration process is typically modeled

75

as the product of a mass transfer coefficient multiplied by the difference between saturation and actual dissolved oxygen concentrations:

$$F_c = K_L(C_s-C) \tag{4.4}$$

Where
F_c = flux of dissolved oxygen across the air-water interface (mass/volume/area)
K_L = surface transfer coefficient (length/time)
C_s = saturation dissolved oxygen concentration (mass/volume)
C = dissolved oxygen concentration (mass/volume)

Pollutants (e.g., surfactants), suspended particles, wind, hydraulic structures, and water temperature influence reaeration. Hydraulic structures and water temperature are the dominant factors in rivers, while wind and water temperature are often important in lakes and reservoirs.

4.4.2.1 Reservoir

Because lakes and reservoirs are often deep and not well mixed like rivers, reaeration is usually modeled using the transfer coefficient rather than a depth averaged reaeration coefficient. The surface transfer coefficient is often based on wind speed and in WQRRS is calculated as

$$K_L = (a+bV^2) \tag{4.5}$$

Where:
K_L = transfer coefficient (m/d)
a, b = empirical coefficients (i.e., 0.50 and 0.025, respectively)
V = wind speed (m/s)

A reaeration coefficient is then produced for the surface layer by averaging the transfer coefficient over the surface layer thickness

$$K_2 = K_L/(\Delta z) \tag{4.6}$$

Where:
Δz = surface element thickness (m)

WQRRS (1986) simulates the reservoir in multiple layers, but atmospheric re-aeration only occurs in the surface layer. Dissolved oxygen is subsequently diffused/dispersed and advected to layers lower in the reservoir. See Appendix F for details on effective vertical diffusion.

76

4.4.2.2 River

Typical river formulations combine the surface transfer coefficient and depth, called the reaeration rate

$$K_2 = K_l/d \tag{4.7}$$

Where:
K_2 = reaeration rate (1/d)
d = depth (m)

Stream reaeration formulations are generally based on theory and empirical relationships, and are a function of stream velocity and depth. A popular formula presented by O'Conner and Dobbins (1958) is

$$K_2 = [(12.9\ u)^{0.5}]/(d^{1.5}) \tag{4.8}$$

Where:
u = mean stream velocity (m/s)

The river model, RMA-11, has two options: a user specified value, or calculating the transfer coefficient based on O'Conner and Dobbins formula. The O'Conner and Dobbins formulation is used herein.

4.4.3 Biochemical Oxygen Demand (BOD_u)

Two processes are modeled with regard to BOD: oxidation (decay) and settling. Temperature affects on BOD oxidation and settling are addressed using the Van't Hoff-Arrhenius relationship. Model parameters are summarized in Table 4.2.

4.4.3.1 Oxidation

The oxidation of carbonaceous organic material is modeled by a first order reaction in both the stream and reservoir models. Insufficient field data were available to determine the deoxygenation rate constant, K_1 explicitly. However, K_1 can be estimated using

$$K_1 = 0.3(H/8)^{-0.434} \qquad \text{for } 0<H<8 \tag{4.9}$$

$$K_1 = 0.3 \qquad \text{for } H>8 \tag{4.10}$$

after Hydroscience (1971), where H equals depth in feet. Further, Wright and McDonald (1979) present K_1 values from thirty-six United States river reaches plus flume experiments that range from 0.08/day to 4.24/day (at 20°C). Bowie et al (1985) presents values for decay of carbonaceous BOD that are typically less than 0.5/day.

In many natural rivers, the reaction rate constant for stream water is usually less than that of an undiluted wastewater sample (typical values range from 0.25/day for treated effluent, 0.35/day for raw sewage, and 0.4/day for settled sewage) and usually decreases with distance downstream. Decreasing values indicate the progressive resistance to the oxidation of the more stable (refractory) end products (EPA, 1997). A value of 0.3/day was used for both stream and reservoir models.

4.4.3.2 Settling

Because BOD addresses non-soluble as well as soluble organic matter, there may be a component that settles from the water column and is no longer available to exert an oxygen demand.

Both WQRRS and RMA-11 use a first order rate reaction to represent BOD decay. Though the reservoir model does not include a term for BOD settling, there is an organic detritus settling term included. The river model did include a BOD settling rate. King (1997) presents a range from 0 to 0.75 m/d, noting the term incorporates loss rate due to flocculation converted to an effective settling rate. Settling rate was set to zero in the river system due to low background levels and turbulent environment. Model parameters for BOD are included in Table 4.2.

Table 4.2   Model parameters for BOD

Parameter	Reservoir: WQRRS	River: RMA-11
BOD rate constant	0.3 /d	0.3 /d
Settling	n/a	0.0 m/d

4.4.4   Organic Detritus

Organic detritus is modeled in the reservoir application to explicitly account for algal respiration and mortality, and their variable effects throughout the eplimnion, metalimnion, and hypolimnion. Specifically, algal photosynthesis and respiration directly impact epiliminetic dissolved oxygen levels, while death and decay often impart significant oxygen demand on the hypolimnion. Although external sources of organic detritus often occur, e.g., waste discharges and allochthonous material (leaf litter and eroded organically rich soil), detritus is included herein to track primarily autochthonous sources (internal sources, i.e., primary production).

78

To properly represent organic detritus, organic sediment is modeled to observe remaining oxygen demand of settled detritus. Organic sediments in direct contact with the water column typically undergo aerobic decomposition, albeit at a slower rate than suspended organic detritus due to lower organic fraction and their limited access (Thomann and Meuller 1987). Anaerobic processes in the bed are not included. Both organic detritus and organic sediment are modeled as first order rate reactions. Explicit modeling of organic detritus is not included in the river model, and is of lesser importance in the well-mixed stream environment.

Settling rates for organic detritus are on the order of algae settling rates for fine particulate matter, up to an order of magnitude greater for larger matter (Thomann 1987) – 0.2 to 2.3 m/d. Settling rates typically range from zero to two meters per day. Decay rate organic detritus range from 0.005 to 0.05 per day.

Oxidation of organic matter utilizes available dissolved oxygen. Decay rates for organic matter in sediment are significantly less than the detritus ranging from 0.001 to 0.01 per day, reflecting a lower organic fraction than suspended matter (Seki 1982, USACOE 1987). Model parameters for associated with organic detritus are included in Table 4.3

Table 4.3   Model parameters for organic detritus

Parameter	Reservoir: WQRRS	River: RMA-11
Organic detritus rate constant	0.05 /d	n/a
Organic detritus settling	0.15 m/d	n/a
Organic sediment decay rate constant	0.005 /d	n/a

4.4.5   Nutrients: Nitrogen

The most common approach to modeling nitrogen transforms is to use first-order kinetics where the rate of accumulation or depletion is dependent on the amount of nitrogen available. Factors affecting transformation rates include temperature, pH, nitrogen concentrations, dissolved oxygen, suspended solids, and organic and inorganic compounds.

WQRRS models only nitrification and uptake. RMA-11 includes ammonification of organic nitrogen, nitrification, uptake, and a benthos source rate for ammonia. Stoichiometric equivalences with regard to oxygen demand via oxidation are applied consistently in both

the reservoir and river models. Algal uptake is addressed in Section 4.4.8. Model parameters associated with nitrogen representation are shown in Table 4.4.

4.4.5.1 Ammonification:

All nitrogen present in organic compounds may be considered organic nitrogen. In addition, organic nitrogen is created by respiration of algae and is lost through deposition (settling). Ammonification is assumed to occur primarily through hydrolysis. Rate constants for the decay of organic nitrogen to ammonia nitrogen presented by Bowie (1985) range from 0.001 to 0.14 per day. Brown and Barnwell (1987) present a range of 0.02 to 0.4 per day for application of the model QUAL2E. A value of 0.1 /day was selected for stream modeling. Transformation of organic nitrogen to ammonia was not explicitly included in reservoir modeling.

4.4.5.2 Nitrification:

All rate constants that involve nitrification assume that a sufficient population of nitrifying bacteria is present and that conditions for nitrification are suitable. Minimum dissolved oxygen levels required range from 1 to 2 mg/l (Thomman and Mueller, 1987). Wetzel (1983) reports that nitrification processes continue to about 0.3 mg/l, but reaction rate impacts are not presented.

Rate constants for the initial step of nitrification, oxidation of ammonia nitrogen to nitrite, range from 0.1 to 1.0 per day. Rate constants for the second step, oxidation of nitrite to nitrate, range from 0.2 to 2.0 per day (Bowie, 1985). Rate constants are higher for shallow streams with rocky bottoms that favor the growth of nitrifying bacteria (nitrifiers). Deep rivers composed of sand, silts, or clays generally have fewer attached nitrifiers and lower rate constants, although suspended particles in the water column can provide surfaces for nitrifier attachment (EPA, 1997). Temperature effects on nitrification rate can be represented with the Van't hoff-Arrhenius relationship for temperatures ranging from 10°C (50°F) to 30°C (86° F). Below 10°C (50°F) nitrifying bacteria growth is significantly reduced and application of the Van't hoff-Arrhenius relationship would over estimate the rate constants. Rate constants are usually set equal to zero for water temperatures in the range 5°C (41°F) to 10°C (50°F) (Thomann and Mueller, 1987), i.e., seasonal adjustments may be necessary.

For the stream model, rate constants for biological oxidation of ammonia to nitrite and nitrite to nitrate were set to 1.0/day and 2.0/day, respectively. Lower values were selected for the reservoir due to limited substrate for nitrifying organisms. Rate constnats of 0.2/day and 0.5/day were applied for ammonia to nitrite and nitrite to nitrate transformations, respectively.

4.4.5.3   Benthos source rate for ammonia:

No data was available for ammonia source rate from the benthos. The rate was set equal to zero.

4.4.5.4   Settled algae transforming directly to ammonia:

Algal decay can occur during settling time. Brown and Barnwell (1987) present a rate constant for the transformation form settling average directly to ammonia ranging from 0.002 – 0.200 m/d. No settling rate was applied for the river model.

4.4.5.5   Preference factor for ammonia:

Because nitrate (NO_3^-) must be reduced to ammonia (NH_4^+) before it can be assimilated into plants, ammonia is a preferred energy efficient source of nitrogen for plants. Preference among nitrate and ammonia is included in the stream model through an ammonia preference factor. Brown and Barnwell (1987) present a range of 0.0 to 1.0, with 1.0 corresponding to all nitrogen requirements obtained from ammonia. WQRRS does not include a preference factor, but partitions uptake according to relative proportions of ammonia and nitrate. RMA-11 requires a user-specified value for ammonia preference or sets the value to default at 1.0. A value of 0.6 was applied for this project.

4.4.5.6   Nitrification inhibition:

Denitrification was not modeled; however, inhibition of nitrification, which occurs at low dissolved oxygen concentrations, was included in the stream analysis. Nitrification rates are multiplied by an inhibition factor

$$f_{nit} = 1\text{-}e^{-knit(DO)} \qquad\qquad (4.11)$$

Where k_{nit} is the first order nitrification inhibition coefficient, set to 0.6 l/mg. The factor, f_{nit}, is close to 1.0 for dissolved oxygen concentrations greater than about 3 mg/l (Chapra, 1997). No such factor is included in WQRRS.

4.4.5.7 Modeling Nitrogen Transformations – Stoichiometric Equivalence

Stoichiometric equivalence is the ratio of the amount of two constituents needed for a given chemical or biological reaction. In many cases nitrogen transforms are modeled with fixed stoichiometry (e.g., Michaelis-Menton or Monod relationships).

Four relationships were required for stream and reservoir model application: Oxygen consumed with ammonia decay, nitrite decay, algal respiration, and algal photosynthesis (growth). Oxygen consumption associated with ammonia and nitrite decay are discussed below.

Ammonia-Nitrite

The oxidation of ammonia to nitrite can be represented as

$$NH_4^+ + 1.5O_2 \rightarrow NO_2^- + H_2O + 2H^+ \qquad (4.12)$$

(Stumm and Morgan 1986, Bowie 1985). The reaction is bacterially mediated by Nitrosomonas. The stoichiometric equivalent is calculated as the ratio of grams of oxygen consumed to grams of ammonia nitrogen oxidized. Examining the left hand side of equation 4.12,

        Oxygen:Nitrogen
        1.5 mols (2*16 g/mols):1.0 mols (14 g/mols)
        48:14
        3.43:1.0

Thus, oxidation of ammonia to nitrite requires 3.43 g O_2

Nitrite-Nitrate

Similarly, the stoichiometric equivalence of the second stage of nitrification, mediated by nitrobacter, given by

$$NO_2^- + 0.5\ O_2 \rightarrow NO_3^- \qquad (4.13)$$

Examining the left hand side of equation 4.13,

        Oxygen:Nitrogen
        0.5(2*16): 14
        16:14
        1.14:1.0

Thus, oxidation of nitrite to nitrate requires 1.14 g O_2.

The total oxidation associated with nitrification can be examined by combining equations 4.12 and 4.13,

$$NH_3 + 2.0O_2 \rightarrow NO_3^- + H_2O + 2H^+ \tag{4.14}$$

Repeating the process outlined above 4.57 g O_2 are required to oxidize a gram of N from ammonia to nitrate. Though the sum of the two processes is 4.57 g O_2 per g N (3.43 + 1.14), the stoichiometric coefficients for the above transforms are actually higher than total oxygen requirements because of cell synthesis, i.e, a certain amount of ammonia is used for bacterial cell production. Some researchers have suggested stoichiometric equivalence values of 3.22, 1.11, and 4.33 for ammonia-nitrite, nitrite-nitrate, and ammonia-nitrate, respectively (Bowie, et al 1985). Table 4.5 includes values applied in the reservoir and river models.

Table 4.4   Model parameters for nitrogen

Parameter	Reservoir: WQRRS	River: RMA-11
Organic nitrogen hydrolysis rate	n/a	0.3 /d
Ammonia decay	0.3 /d	0.3 /d
Nitrite Decay	0.5 /d	0.5 /d
Benthos source rate	n/a	0.0
Transfer settled algae to ammonia	n/a	0.0
Ammonia preference factor	n/a	0.0
Nitrification inhibition, KNIT	n/a	0.6
Stoichimetry: Ammonia oxidation	3.43 gO_2/gN	3.43 gO_2/gN
Stoichimetry: Nitrite oxidation	1.14 gO_2/gN	1.14 gO_2/gN

4.4.6   Nutrients: Phosphorus

Transforms typically include the decay of particulate organic phosphorus, removal of dissolved inorganic phosphate to sediment, benthos source rate for dissolved organic phosphorus, and settled algae transforming directly to dissolved inorganic phosphorus. Reported decay rates illustrate a broad range of values indicating uncertainty in quantifying these processes (Bowie, et al, 1985).

The river model includes logic to address the four processes outlined above, but due to lack of field data only organic phosphorus decay was included in these analyses. Moreover, the reservoir model does not include any of the processes outlined above. User specified inorganic phosphorus (orthophosphate) concentrations are input directly.

4.4.6.1   Organic phosphorus to dissolved inorganic phosphorus:

Wide ranges of rate reaction constants for the transformation of phosphorus (organic) to orthophosphate (inorganic) are presented in the literature. However, it is often unclear if the reported rates include the transform from particulate organic to dissolved organic phosphorus or if the particulate form transforms directly to dissolved orthophosphate.

Bowie et al (1985) present rate constants for particulate organic phosphorus to dissolved inorganic P, incorporating the intermediate stage of dissolved organic phosphorus, ranging from 0.001 to 0.8 per day). Brown and Barnwell (1987), et al presents rate constants for this simplified transformation ranging from 0.1 to 0.7 per day. A value of 0.3 was selected for application in the stream model.

4.4.7   Algae

Modeling algal growth requires several parameters related to concentration, growth and respiration, settling, nutrient uptake and algal composition, production of oxygen through photosynthesis, and utilization of oxygen through respiration and death. Model parameters corresponding to modeled algal processes are presented in Table 4.5.

4.4.7.1   Algal Concentration

Algae were represented by phytoplankton in the reservoir model, but as attached algae in the river. Algal concentrations are usually related to observed chlorophyll *a* levels. Chlorophyll *a* is considered to be directly proportional to the concentration of algal biomass by

$$\text{Chlr } a = \alpha_o (A) \tag{4.15}$$

Where:
Chlr *a* = Chlorophyll a concentration (μg/l)
A   = Algal biomass (mg/L)
α_o = conversion factor (μg-Chl *a*/mg A)

The conversion factor, α_o is assumed to be independent of temperature. Brown and Barnwell (1987) present at range for the conversion factor of 10 to 100 μg-Chl *a*/mg A. A conversion factor of 67 μg-Chl *a*/mg A was presented by APHA (1995) and was adopted for this project.

4.4.7.2 Algal Growth and Respiration

The limiting nutrient concept, originally developed by Liebig, is known as the "Law of the Minimum," and states that yield of any organism will be determined by the abundance of the substance that, in relation to the needs of the organism, is least abundant in the environment. Since yield is a result of growth, rate of growth has been substituted for yield in many subsequent analyses, the most important of which is the well-known Monod model for a single nutrient limitation in the growth of microorganisms (Wetzel 1983).

Brown and Barnwell (1987) present a range of maximum algal growth rates ranging from 1.0 to 3.0 per day. In both the reservoir and river model limiting factors include light, nitrogen, and phosphorus. Parameters associated with light limitation include light extinction coefficients and a Monod (Michaelis-Menton) half-saturation coefficient for light. Reservoir and river values range from 0.002 to 0.004 kcal/m^2/s (0.00873 to 0.01675 kJ/m^2/s) (USACOE-HEC 1986) and 0.0037-0.0185 kJ/m^2/s (00088 to 0.0044 kcal/m^2/s) (King (1997), respectively. The reservoir and river models utilize different units. The reservoir and the river models represent light extinction coefficient as a composite of multiple shading coefficients. Only the non-algal water extinction coefficients were used in each case.

The nutrient limiting parameters include Monod half-saturation constants for algae utilizing nitrogen (ammonia and or nitrate) and phosphate. Ranges vary for reservoir and river representations. USACOE-HEC presents 0.04 to 0.10 mg N/l and 0.02 to 0.05 mg P/l for half-saturation constants for algae utilizing nitrogen and phosphorus, respectively. Values for river systems range from 0.01 to 0.3 mg N/l and 0.001-0.05 mg P/l for half-saturation constants for algae utilizing nitrogen and phosphorus, respectively (Brown and Barnwell 1987, Bowie et al 1985).

Algal respiration ranges from 0.05 to 0.5 per day for river and reservoir applications (Bowie et al 1985, Brown and Barnwell 1987, Thomann and Mueller 1987, USACOE-HEC 1986), but higher values were employed for attached algae in the river application. All values are included in Table 4.6.

4.4.7.3 Algal Settling

Algal settling is a function of species or population composition. Values range from 0 to 6 ft/d or greater (Wetzel 1983, Bowie et al 1985, Thomann and Mueller 1987). Reservoir

algal settling rates were set to 0.3 ft/d. Settling was set to zero for the river model because attached algae were modeled.

4.4.7.4   Algal Biomass Fraction and Stoichiometry

Algae utilize photosynthesis (solar energy) to convert simple inorganic nutrients into more complex organic molecules for cell growth. Respiration is the reverse process in which biomass undergoes decay and/or cell lysis and oxidation. Nitrogen and phosphorus, as well as carbon and other elements, are utilized during algal cell synthesis. Algal biomass fraction consists of that portion of algal cells consisting of a particular element, e.g., carbon, nitrogen or phosphorus. Similar to oxygen consumption during nitrification, stoichiometric relationships are used to relate algal biomass and oxygen production and consumption for photosynthesis and respiration, respectively.

Algal Biomass Fraction

The composition of organic matter in plankton can be approximated as $C_{106}H_{263}O_{110}N_{16}P_1$. Nitrogen and phosphorus fractions of algal biomass are approximately 7.2 and 1.0 percent, based on dry weight (Chapra 1997). Estimates may vary with algal species. Nitrogen content of algae ranges from 7 to 10 percent by weight (Foree and McCarty 1968, McKenthum and Ingram 1967), while nitrogen content of attached algae ranges from 2 to 4 percent by weight (McKenthum and Ingram 1967, Gerloff, 1969).

Algal Stoichiometry

Several models are available for cell synthesis. Thomann and Mueller (1987), Chapra (1997), and Horne and Goldman (1994) use glucose as a simplified model for photosynthesis and respiration, but it is insufficient for purposes of this report. More complex representations of cell structure and synthesis are required to form the necessary relationships between algal biomass and oxygen consumption and respiration. Cell synthesis can vary depending on nitrogen source (Chapra 1997). When ammonia is the primary source of nitrogen cell synthesis may be represented by

$$106CO_2 + 16NH_4^+ + HPO_4^{2-} + 108H_2O \rightarrow$$
$$C_{106}H_{263}O_{110}N_{16}P_1 + 107O_2 + 14H^+ \qquad (4.16.a)$$
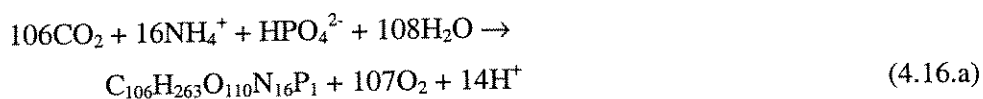
and for nitrate as the primary nitrogen source

$$106CO_2 + 16NO_3^- + HPO_4^{2-} + 122H_2O + 18H^+ \rightarrow$$
$$C_{106}H_{263}O_{110}N_{16}P_1 + 138O_2 \qquad (4.16.b)$$
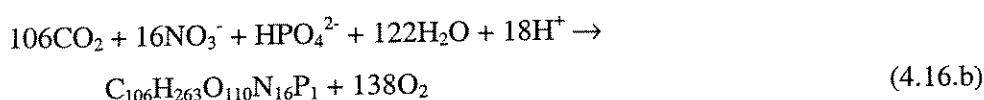
Environmental Lab (1995) presents different formulations when ammonia and nitrate are the primary nitrogen species as represented in equations 4.17.a, and 4.17.b, respectively.

$$132CO_2 + 16\ NH_4^+ + H_3PO_4 + (177/2)H_2O\ \rightarrow$$
$$C_{132}H_{228}O_{58}N_{16}P_1 + (597/4)O_2 + 16H^+ \tag{4.17.a}$$

$$132CO_2 + 16\ HNO_3 + H_3PO_4 + (209/2)H_2O\ \rightarrow$$
$$C_{132}H_{228}O_{58}N_{16}P_1 + (725/4)O_2 \tag{4.17.b}$$
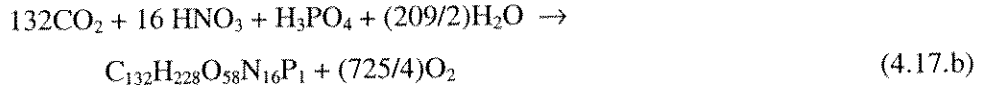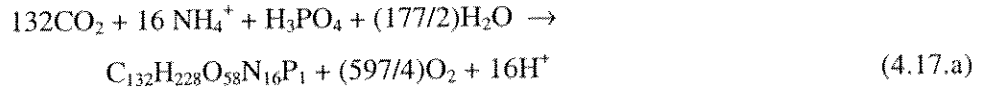
All models illustrate the importance of phosphate in aquatic systems. For example, equation 4.16a illustrates that each atom of phosphorus (as phosphate) added to an aquatic system can result in the fixation of about 106 atoms of carbon in organic matter. Further, when the organic matter produced from one atom of phosphorus decays, as per equation 4.16b, it has the potential to consume 138 molecules of oxygen (Drever, 1988).

As long as free oxygen is available, the net result of respiration and decay are essentially the reverse of photosynthesis. Respiration yields carbon as CO_2, organically combined nitrogen as NO_3^-, and organically combined phosphorus as HPO_4^{-2}. The models represented by Chapra (1997) and Environmental Lab (1995), equation 4.16.b and 4.17.b, respectively are used to represent respiration because they yield nitrate as the appropriate end product versus ammonia. Thus, respiration is represented as

$$C_{106}H_{263}O_{110}N_{16}P_1 + 138O_2 \rightarrow$$
$$106CO_2 + 16NO_3^- + HPO_4^{2-} + 122H_2O + 18H^+ \tag{4.18}$$

$$C_{132}H_{228}O_{58}N_{16}P_1 + (725/4)O_2 \rightarrow$$
$$132CO_2 + 16\ HNO_3 + H_3PO_4 + (209/2)H_2O \tag{4.19}$$
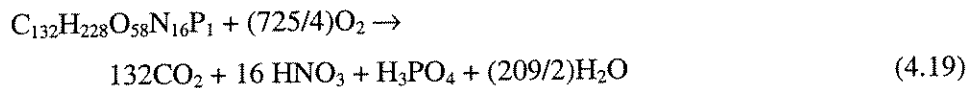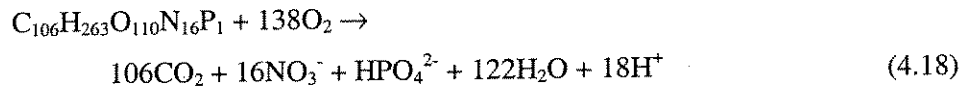
These inorganic forms of nitrogen and phosphorus are readily available for plant uptake. The release of CO_2 increases its partial pressure and hence can decrease pH (i.e., $CO_2 + H_2O \rightarrow H_2CO_3 \rightarrow H^+ + HCO_3^-$). When molecular oxygen is not available, or when it has been depleted, decay of organic matter can continue under anoxic conditions (reduction). Some of the most important reactions are denitrification, deaminization of amino acids, sulfate reduction, and fermentation reactions (Drever 1988, Snoeyink and Jenkins 1980).

Using equation 4.16.a where ammonia is the nitrogen source, the stoichiometric relationship for oxygen produced during photosynthesis is

Algal biomass (A): $C_{106}H_{263}O_{110}N_{16}P_1 = 3550$ g

Oxygen produced: $107(2*16) = 3424$ g

Stoichiometric ratio of oxygen produced to algal biomass: $3424/3550 = 0.96$ g O/g A

Similarly, stoichiometric ratios for equations 4.16.b, 4.17.a, and 4.17.b are 1.24, 1.59, and 1.94 grams of oxygen produced per gram of algal biomass, respectively. Stoichiometric ratios for respiration represented in equations 4.18 and 4.19 are 0.96 and 1.59 grams of oxygen consumed per gram of algal biomass, respectively. Stoichiometric ratios for growth and respiration were each set equal to 1.6 mg O per mg A in both the reservoir and river model.

Table 4.5   Model parameters for algae

Parameter	Reservoir: WQRRS	River: RMA-11
Chlr a to algae conversion	67 µg Chlr a/mg A	n/a
Maximum specific growth rate	2.0 /d	2.0 /d
Local respiration rate	0.15 /d	1.0 /d
Non-algal light extinction coefficient	n/a	1.0 /m
Monod half-saturation for light	0.0023 kcal/m^2/s	0.01 kJ/m^2/s
Monod half-saturation: N	0.1 mg N/l	0.01 mg N/l
Monod half-saturation: P	0.01 mg P/l	0.001 mg P/l
Settling rate	0.10 m/d	n/a
Fraction of algal biomass: N	0.072 mg N/mg A	0.072 mg N/mg A
Fraction of algal biomass: P	0.01 mg N/mg A	0.01 mg N/mg A
Stoichiometry: O$_2$ production	1.6 mg O$_2$/mg A	1.6 mg O$_2$/mg A
Stoichiometry: O$_2$ respiration	1.6 mg O$_2$/mg A	1.6 mg O$_2$/mg A
Preference factor for ammonia*	n/a	0.60

Data requirements for the river and reservoir models included geometric, hydrologic, water quality, and climatic parameters. Much of the project data were derived from readily available sources including, but not limited to USGS, DWR, PacifiCorp, and the NCRWQCB. To secure additional required field data, UC Davis, in cooperation with several of the above agencies undertook a field monitoring program to systematically measure water temperature in Iron Gate Reservoir and the Klamath River. In addition, meteorological studies and limited water quality sampling was completed. No additional geometric or flow data were compiled. For detailed description of all project data, the reader is referred to Appendix B.

5.1   Water Temperature Monitoring Program

Water temperature monitoring programs were developed for Iron Gate Reservoir and the Klamath River systems. Onset Corporation stowaway temperature devices were used to record water temperatures year-round in the reservoir and seasonally in the river. The field programs for the reservoir and river are outlined below.

5.1.1   Reservoir

Working in cooperation with PacifiCorp, UC Davis deployed up to seven temperature loggers in Iron Gate Reservoir to measure hourly temperature at various depths. Loggers were initially deployed in June 1996 and the last loggers were removed in November 1997. Throughout that period several loggers failed and data at selected elevations were lost. Further, the loss of loggers reduced the total number of depths where temperature was recorded from a maximum of seven to three during the winter of 1996-97. Figure 5.1 illustrates the depths and approximate periods when hourly temperatures monitoring occurred in Iron Gate Reservoir.
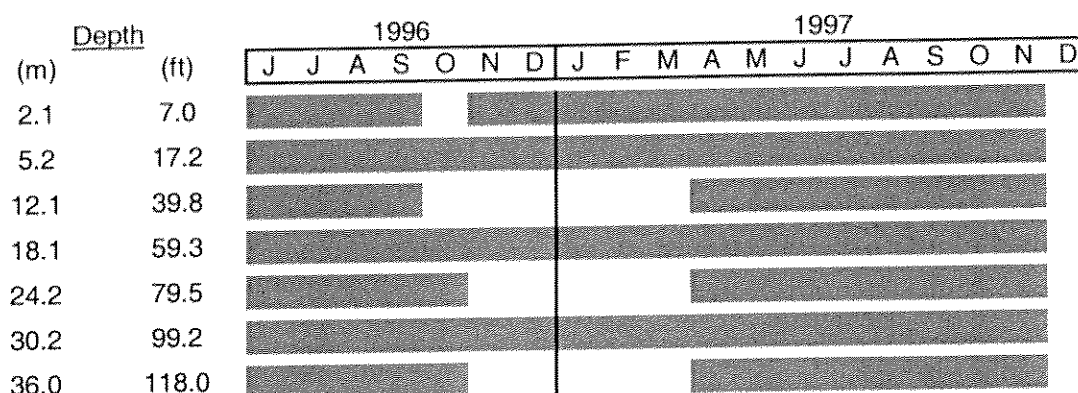
Figure 5.1 Temperature monitoring depths and periods of deployment in Iron Gate Reservoir

Regardless of lost data or limited deployment during portions of the year, the temperature profile provided critical system thermal definition and invaluable data for initial conditions, and calibration and validation of the reservoir model. Results of the reservoir monitoring program are discussed in detail in Chapter 7.

5.1.2   River

River water temperature monitoring was carried out in the reach from Iron Gate Dam to the USGS gage at Seiad Valley. Temperature loggers were deployed in May and June and removed in October in both 1996 and 1997 (October 7, 1996 and October 12, 1997). The period May through October allowed reasonable access to the river for logger deployment. High flows and elevated water levels limited deployment and retrieval options during other portions of the year due.

Temperature loggers were placed at multiple main stem and tributary locations. Loggers were added at intermediate locations when possible. Figure 5.2 illustrates monitoring locations, approximate river mile, and period of deployment. Additional loggers were deployed in 1997 to further define the thermal profile of the river. Chapter 7 addresses detailed interpretation of these data in conjunction with model simulation results.

Location	River Mile	1996 J J A S O	1997 J J A S O
Below Iron Gate Dam	190.1	▓▓▓▓▓	▓▓▓▓▓
Below Little Bogus Ck.	186.4		▓▓▓▓▓
Above Cottonwood Ck.	182.1	▓ ▓▓▓	▓▓▓▓▓
Above Shasta River	176.7	▓▓▓▓▓	▓▓▓▓▓
Shasta River	0.5	▓▓ ▓▓	▓▓▓▓▓
Below Shasta River	176.6	▓▓▓▓▓	▓▓▓▓▓
Near Lime Gulch	169.7		▓▓▓▓▓
Below Lumgrey Ck.	163.0		▓▓▓▓▓
Near Walker Road Bridge	156.2	▓▓▓▓	▓▓▓▓▓
Below Kohl Ck.	151.7		▓▓▓▓▓
Below Horse Ck.	147.2		▓▓▓▓▓
Above Scott River	143.5		▓▓▓▓▓
Scott River	1.0		▓▓▓▓▓
Below Scott River	142.5	▓▓▓▓▓	▓▓▓▓▓
USGS Gage, Seiad	128.9	▓▓▓▓▓	▓▓▓▓▓

Figure 5.2   Klamath River temperature monitoring locations and periods of deployment.

5.2   Meteorological Monitoring

There are no complete meteorological monitoring stations within the immediate study area. With the exception of limited air temperature observations, the closest meterological station was located in the Shasta Valley, just south of Yreka. To address potential meteorological variability between this meteorological station (CDF, Brazie Ranch) and conditions within the study area, limited meteorological monitoring was completed during the 1996 and 1997 field seasons at the reservoir and several river locations.

5.2.1   Reservoir

To ascertain similarities and differences in local climate between Iron Gate Reservoir and a meteorological station located at Brazie Ranch, a meteorological station was deployed at Iron Gate Reservoir during September and early October 1996. The weather station was mounted on the intake tower at Iron Gate Dam, and air temperature, relative humidity, wind speed and direction, barometric pressure, and solar radiation were measured.   Air temperature, wind speed, and relative humidity were then compared with Brazie Ranch data

91

to determine limitations, if any, of using climate data from the Shasta Valley for Klamath River studies.

Review of the data and comparisons illustrate that the location of the meterological station at Iron Gate – over the water – possibly impacted relative humidity and air temperature measurements. Maximum air temperature, relative humidity, and wind speed were often higher at Iron Gate Reservoir. Although differences were apparent in the comparison of Brazie Ranch and Iron Gate data, overall similarities between the data sets warranted adoption of the Brazie Ranch observations.

5.2.2   River

During the design phase of the study there were concerns of climatic variability within the study area. Namely, it was postulated that meteorological conditions may differ between Iron Gate Dam and the Seiad Valley. To explore such potential variations, air temperature and relative humidity were recorded adjacent to the river at three locations during the 1996 and 1997 field seasons. Hourly data was measured below Iron Gate Dam, below the mouth of the Shasta River, and below the mouth of the Scott River.

Findings illustrate that relative humidity is fairly consistent in these near-river areas, but slight variations in air temperature were apparent. It appears that air temperatures remain slightly elevated after sundown at the Shasta River location compared to the Scott River location. Overall differences were not deemed sufficient to warrant use of spatially variable air temperature in the model. Extension of the study area downstream of Seiad Valley should include further study of the potential impacts of variable meteorological conditions.

5.3   Water Quality

UC Davis did not complete any formal water quality monitoring in the Klamath River. However, two hydrolabs were deployed in the Klamath River during the 1997 field season from June 28 – 30. The instruments were deployed below the mouth of the Shasta River (RM 176.6) and near Walker Road Bridge (156.6). Although this record spanned only two days, it illustrates critical water quality processes occurring in the Klamath River. UC Davis also participated in the NCRWQCB 1996-97 water quality monitoring effort, both in various scoping meetings and in fieldwork.

This chapter addresses calibration and validation of the reservoir and river models. Steps in calibration and validation include selecting fundamental hydrologic and water quality model parameters, defining boundary and initial condition data sets, and selecting appropriate periods for calibration and validation. Calibration typically includes running the model over a selected period and adjusting coefficients and constants within reasonable ranges until simulated values agree, under some predetermined criteria, with measured field data. Validation entails applying the model, using the selected calibration parameters, over an independent period and determining if simulated results again agree with field observations.

The overall objective of model application is to assess water quality control alternatives in the Klamath River downstream of Iron Gate Dam. To meet this objective, models must be calibrated and validated to provide sufficient confidence in simulation results to meet these ends. As such, this effort was a quantification of model uncertainty where calibration defined model accuracy, and validation supported the model performance at the same level of accuracy for an independent set of hydrologic, meteorologic, and water quality conditions. Calibration criteria were developed for the reservoir and river separately because the dynamics of the two systems and the method of simulation differ dramatically. For example, reservoir hydrology is addressed with a simple mass balance, thus there were no parameters to calibrate.

Calibration criteria, methods, and findings are presented for the reservoir and river models. Formal calibration was performed for two water quality variables: temperature and dissolved oxygen. Insufficient data were available to provide a complete calibration of all model variables. Other parameter values and coefficients (e.g., nitrification rates) were fixed during calibration. Nonetheless, where data were available model output was compared with measured data to ensure reasonable system representation.

6.1   Iron Gate Reservoir Calibration and Validation

WQRRS was calibrated and validated for Iron Gate Reservoir over the periods May 15, 1996 through October 31, 1996, and May 13, 1997 through October 31, 1997, respectively. Calibration and validation periods, data, selection of model coefficients and constants, and results for Iron Gate Reservoir are discussed herein.

6.1.1 Data

Initial reservoir water temperature and dissolved oxygen profiles were derived from NCRWQCB limnological surveys. Calibration and validation observations employed both UC Davis field studies and NCRWQCB surveys. Although there were sufficient temperature observations for complete calibration and validation, only two dissolved oxygen profiles were available: 8/20/96 and 8/18/97. In addition, ammonia, nitrate, phosphorus and chlorophyll a samples from the August 1996 and 1997 surveys were compared with simulated values to ensure reasonable system representation. Further information concerning calibration and validation data is included in Appendix B.

6.1.2 Calibration Parameters

Temperature related calibration parameters include secchi depth, water column stability and diffusion parameters, and evaporation coefficients. Descriptions and details of these parameters, including final values, are presented in Appendix F.

Dissolved oxygen is directly dependent upon several water quality variables. Thus effective representation of dissolved oxygen for reservoirs requires inclusion of temperature, nitrogen and phosphorus transforms, BOD and/or organic detritus, and algae. Multiple parameters were used in model calibration including, but not limited to, the following rates and coefficients,

- ammonia decay rate
- BOD decay rate
- organic sediment decay rate
- algal respiration
- algal settling rate

- nitrite decay rate
- organic detritus decay rate
- organic detritus settling rate
- algal maximum growth rate
- algal shading coefficient

Several other parameters were explored, as well as the impact of varying boundary and initial conditions. However, the model was either insensitive or insufficient data was available to support selection of a different parameter. Final values were selected that fell within ranges typically found in literature sources. Appendix C includes all final parameter values for WQRRS calibration.

6.1.3 Results

The general seasonal thermal response of Iron Gate Reservoir includes development of stratification in the spring; strongly stratified conditions during the summer months; and

94

weakening stratification during the fall, leading to turn-over (isothermal conditions) sometime in the late fall or early winter. Thermal stratification plays an important role in many reservoir water quality processes. Algal productivity and gas exchange at the air-water interface characterize the surface zone, or epilimnion. The thermocline acts as a barrier between the epilimnion and the deeper portion of the reservoir, called the hypolimnion. The hypolimnion experiences very little exchange with epilimnion and is characterized by a lack of productivity, and little or no dissolved oxygen. Thus, thermal stratification directly affects dissolved oxygen distribution, as well as other water quality variables, in Iron Gate Reservoir.

Because temperature is generally independent of other water quality variables, separate calibration criteria were developed for each of the two constituents. Iron Gate Reservoir temperature was more completely represented by field observations than dissolved oxygen conditions. A degree of professional judgement was used to assess overall results. Though numerical or statistical criteria are necessary, some degree of judgement, accounting for the various limitations and/or uncertainty of data, models, assumptions, and numerical representations is vital to any assessment.

6.1.3.1 Water Temperature

Calibration criteria for temperature were developed to reflect processes deemed important to assessment of historical and alternative operations. These included effective representations of the thermocline, evolution of stratification through the spring and summer, as well as proper representation of water temperatures in the vicinity of the penstock, and in deeper hypolimnetic waters. Specific criteria were developed to assess water temperatures at three key locations: a representative epilimnion location (elevation 2310 ft msl), turbine intake (2299 ft msl), and hatchery intake (2254 ft msl). Model error (measured minus simulated) at each elevation were compared to assess model performance. A calibration objective of $\pm$ 2°C (3.8°F) was selected. Simulated and measured data from near the dam were compared on the 1st, 10th, and 20th of each month, subject to data availability. Figure 6.1 illustrates calibration period model error for the selected Iron Gate Reservoir elevations, at approximately 10-day intervals throughout the study period. Simulated temperatures were within $\pm$2.0°C (3.6°F) for all dates and usually within $\pm$1.0°C (1.8°F) at selected elevations.

95
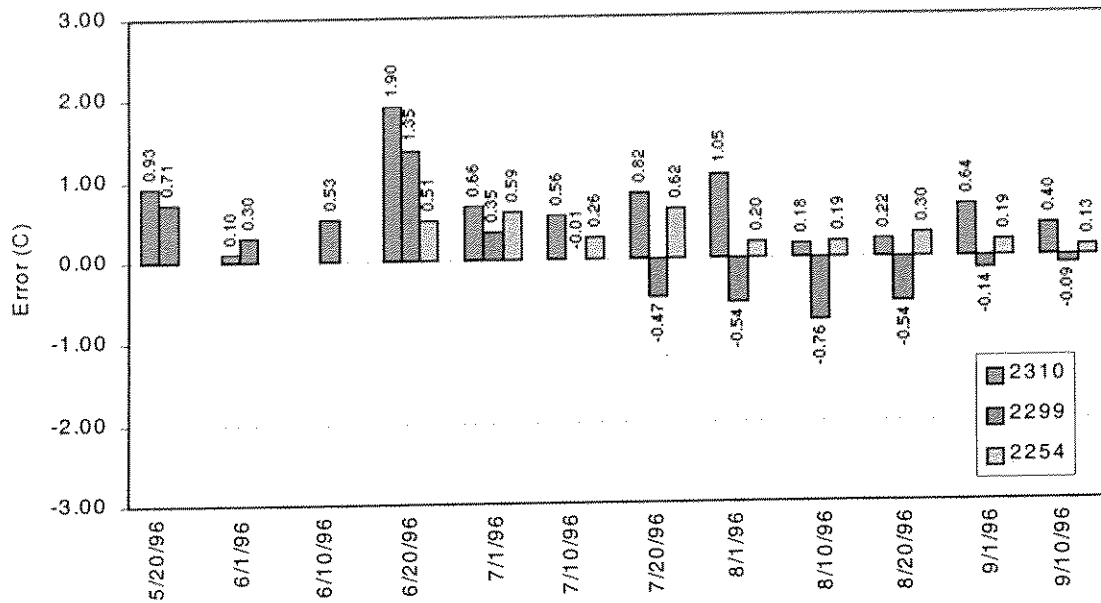
Figure 6.1   1996 Iron Gate Reservoir temperature calibration model error at elevation
2310, 2299, and 2254 ft msl.

Validation required applying the model to 1997 data using the model parameter values from
the 1996 calibration. Validation results at the same elevations for 1997 are shown in Figure
6.2. Additional measured temperature data were available during the 1997 field season; thus
comparisons extend through the end of October. Validation results illustrate that the model
was within ±2.0°C (3.8°F) of measured values at all selected elevations.
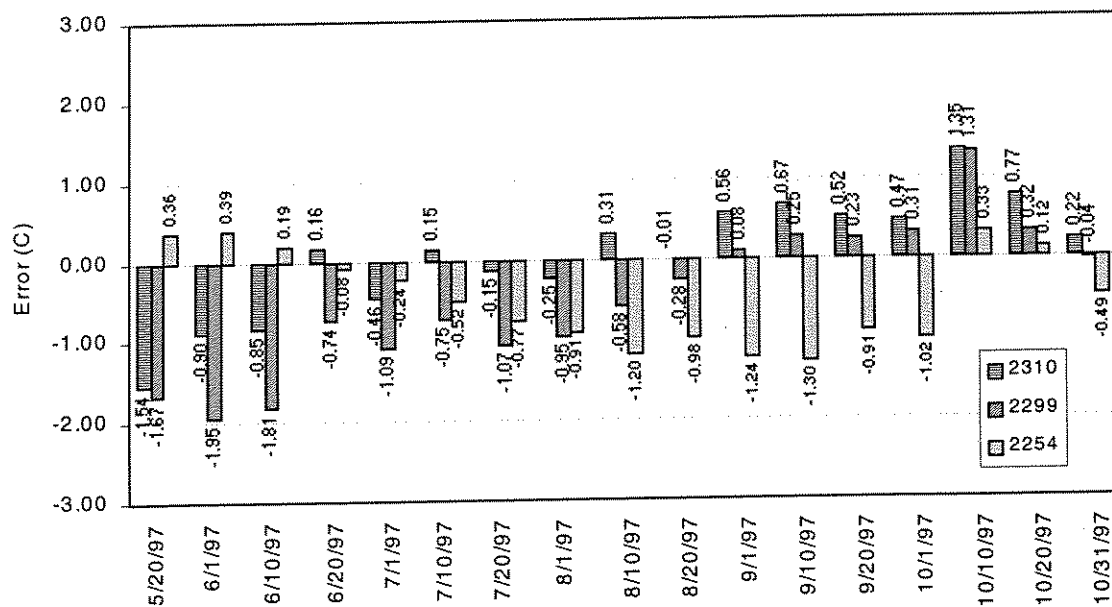
Figure 6.2   1997 Iron Gate Reservoir temperature validation model error at elevation 2310,
2299, and 2254 ft msl.

96

In addition to examining model performance at individual elevations, more general criteria were applied to assess overall thermal profile representation. In this case, an envelope of simulated profile temperatures was developed that ranged from ± 2°C (3.8°F), which translates to an error of roughly 10% at 20°C (68°F). Model performance was assessed according to the number of temperature observations that fell within the envelope.

Figure 6.3 illustrates profiles on the first of each month for simulated versus measured data, with the ± 2°C (3.8°F) criteria included as dashed lines. The results show that the Iron Gate Reservoir model not only reproduced temperatures within the calibration objective throughout the reservoir depth, but also the onset of stratification in the late spring (June-July), strongly stratified conditions of mid-summer (August-September), fall cooling (October), and approaching isothermal conditions at the end of October.
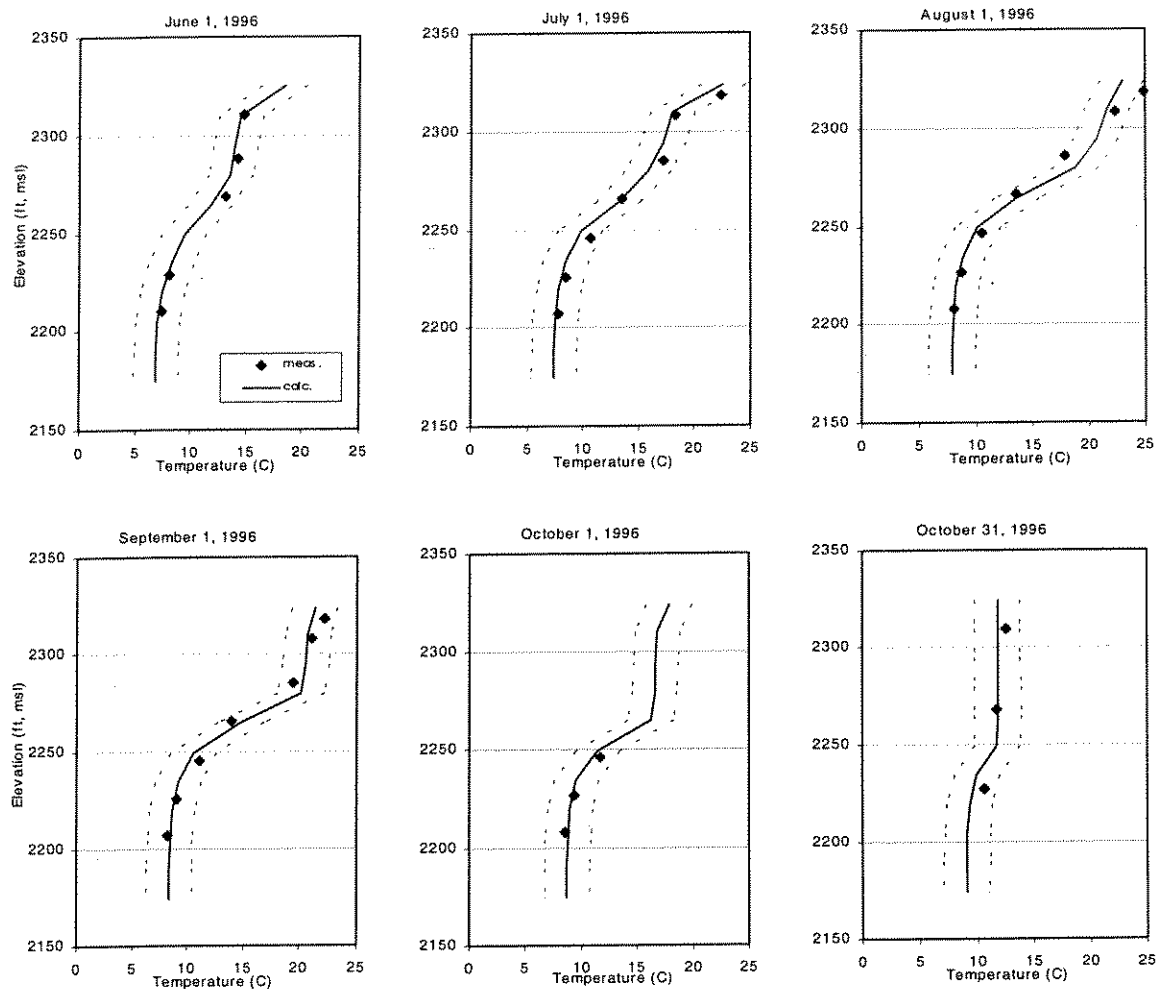
Figure 6.3   1996 Iron Gate Reservoir profile temperature calibration, measured versus simulated data with ±2°C (3.6°F) envelope

Simulation results for the 1997 validation period proved representative of field conditions as well. Figure 6.4 illustrates that the reservoir model simulated thermal conditions in Iron Gate Reservoir within the calibration objective for nearly all locations. The profiles were well represented through the seasons, effectively reproducing thermal variations in space and time. Both the calibration and validation temperature simulations include impacts of algal self shading.
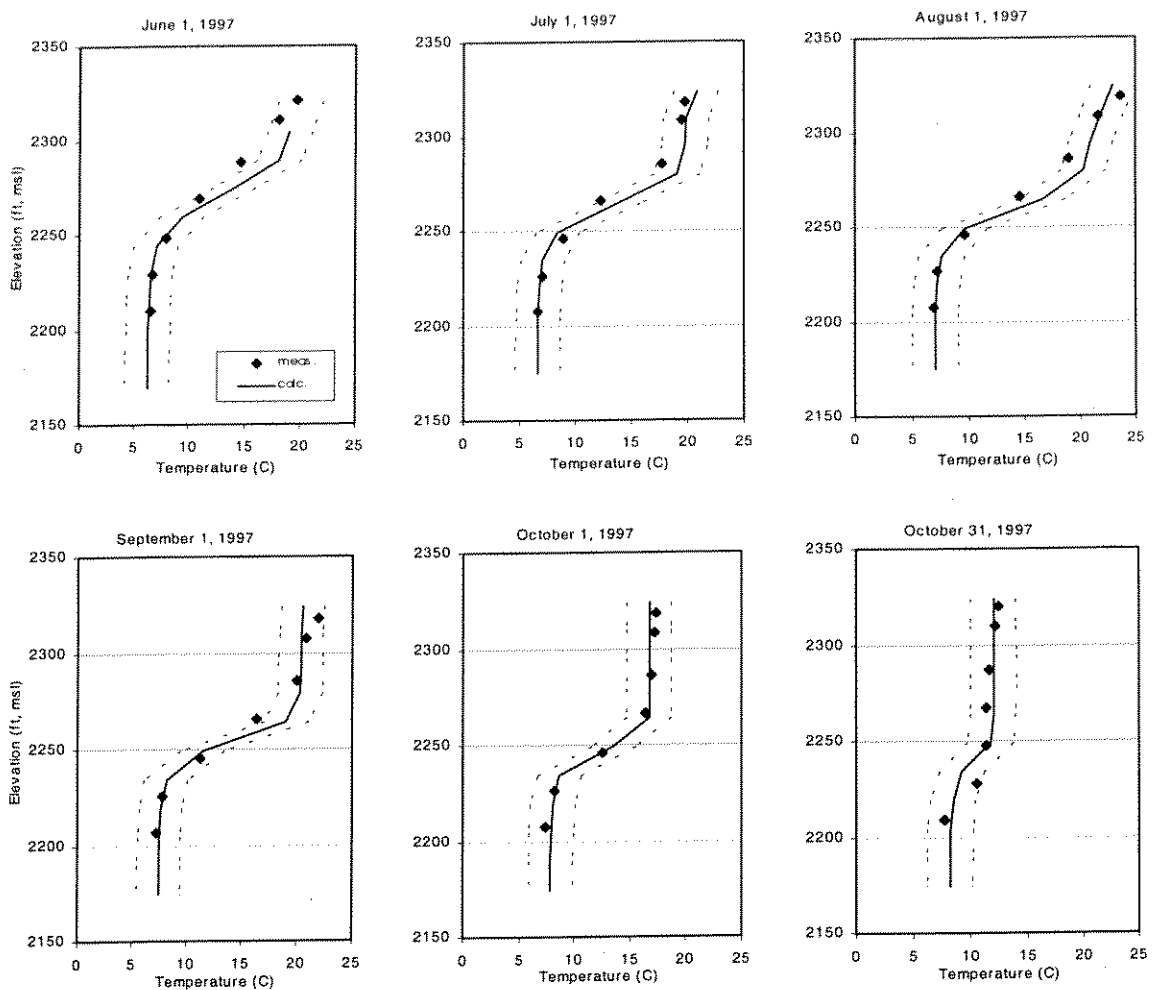
Figure 6.4   1997 Iron Gate Reservoir profile temperature validation, measured versus simulated data with ±2°C (3.6°F) envelope

Model calibration and validation procedures focused on reproduction of the reservoir thermal structure or profile. However, simulated reservoir outflow temperature was analyzed to ensure proper representation. Simulated reservoir outflow temperatures are representative of conditions immediately inside the penstock intake, prior to entering the turbines. Because the closest temperature observations were approximately 0.75 miles downstream in the main stem Klamath River, comparisons may not be definitive, but do

98

represent a general measure of model performance. Figure 6.5 (a) and (b) present simulated reservoir outflow temperature and measured temperature below Iron Gate Dam on the 1st, 10th and 20th of each month for 1996 and 1997, respectively.
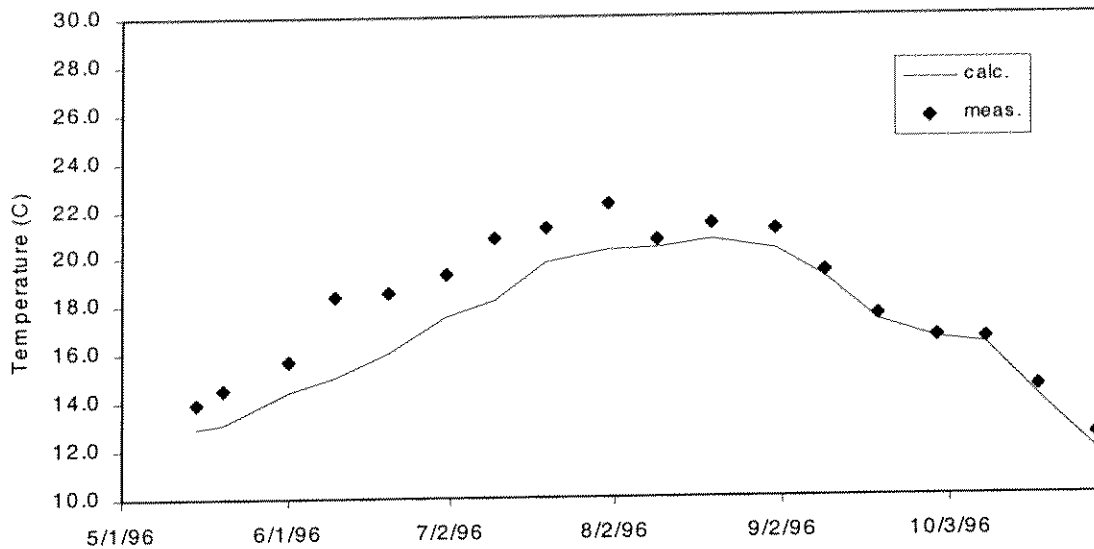
(a)
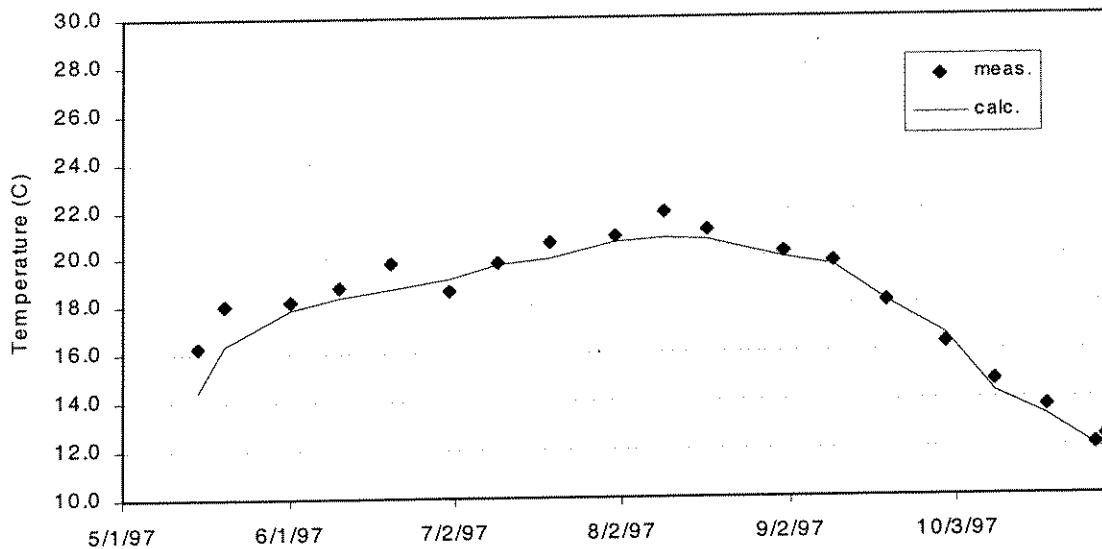
(b)

Figure 6.5   Simulated Iron Gate Reservoir Outflow water temperature and measured water temperature below Iron Gate Dam on the 1st, 10th and 20th of each month for (a) 1996 and (b) 1997

99

The model underpredicted temperature for the first half of the 1996 period by about 2°C (3.6°F); however, from August through October performance was significantly improved with simulated temperatures within 1°C (1.8°F) of observed values. During the 1997 simulation period model performance was within approximately ±1°C (1.8°F) for all but the month of May (which may be a function of initial conditions). Similar to 1996 results, August through October 1997 model performance improved over the first half of the year. Table 6.1 provides summary statistics for outflow water temperature simulation and downstream measured temperature for 1996 and 1997.

Table 6.1   Summary statistics for outflow water temperature simulation and downstream measured temperature for May – October 1996 and 1997

Statistic	Year (May – October)	
	1996	1997
Mean error (°C)	1.17	0.47
Maximum overprediction (°C)	3.40	1.90
Maximum underprediction (°C)	0.10	-0.50
Mean absolute error (°C)	1.17	0.56
Root mean squared error (°C)	1.49	0.75
Standard deviation (°C)	0.96	0.60
See Table 6.3 for description of summary error statistics		

6.1.3.2   Dissolved Oxygen

Dissolved oxygen concentration in reservoirs is influenced by many factors: thermal stratification, hydrodynamic and water quality influences of reservoir inflows and withdrawals, nutrient concentrations, and primary production all play pivotal roles. Due to the complex inter-relationships of the many parameters, dissolved oxygen simulation is often less predictable than temperature. This inherent complexity, coupled with limited available dissolved oxygen profiles for Iron Gate Reservoir, resulted in qualitative or provisional calibration.

The qualitative calibration objective for dissolved oxygen was to reproduce dissolved oxygen concentration dynamics in space and time for Iron Gate Reservoir and to quantify uncertainty associated with simulated dissolved oxygen concentrations. As with temperature, mid-May through October 1996 and mid-May through October 1997 formed the calibration and validation periods, respectively.

Simulations were completed for 1996, and output was compared to measured profiles near Iron Gate Dam for August 21. Figure 6.6 illustrates simulated versus measured data with and without a ±2.0 mg/l envelope. Several points require consideration. First, it is apparent that the hypolimnion of Iron Gate Reservoir experiences severe anoxia, i.e., zero dissolved oxygen. Second, an examination of the measured field data indicates a "pocket" of dissolved oxygen below the thermocline. This is a relic of spring conditions when oxygen concentrations were appreciable throughout depth in the reservoir. The onset of stratification with seasonal warming "trapped" available dissolved oxygen below the thermocline, which was subsequently subjected to the various oxygen demands of the hypolimnion (e.g., BOD, detrital decay). It is assumed that by sometime in late August or September this pocket was depleted as well. The model does not reproduce this condition during the calibration period.

Finally, the envelope shown in Figure 6.6 provides insight to the uncertainty in simulated DO concentrations. Surface waters can be difficult to model effectively because of the high potential for primary production and exchange across the air-water interface. Nonetheless, the model does a fair job simulating near-surface concentrations. Model values are roughly 2 mg/l high throughout most of the epilimnion. Though the model does not simulate the small pocket of dissolved oxygen below the thermocline, it does represent anoxic conditions below the thermocline effectively.

To further assess dissolved oxygen response in Iron Gate Reservoir, simulated reservoir profiles were examined throughout the calibration period; however, no measured data were available for comparison. Figure 6.7 illustrates simulated first of month dissolved oxygen profiles for the 1996 period. Simulated reservoir dissolved oxygen indicates the reservoir has oxygen throughout its full depth in late spring, but following the onset of thermal stratification experiences increasingly severe dissolved oxygen deficit in the hypolimnion. By mid-summer only the top 60 ft (18.2 m) of the reservoir has any appreciable dissolved oxygen. Though fall cooling produces near isothermal conditions (see Figure 6.4), the reservoir has yet to turn over and still experiences an anoxic hypolimnion.
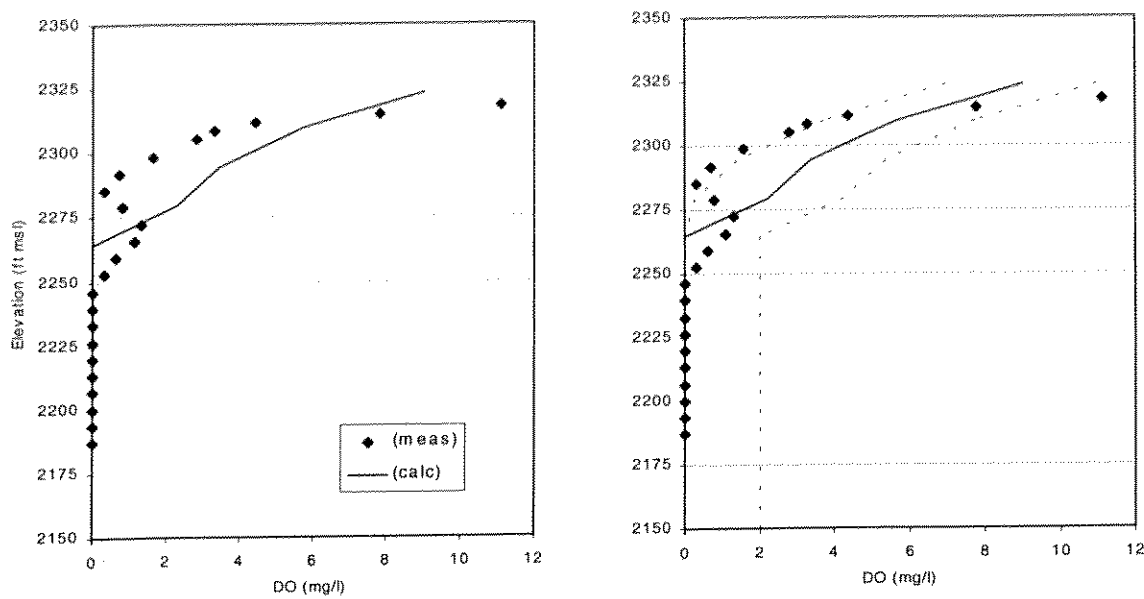
Figure 6.6   1996 Iron Gate Reservoir profile dissolved oxygen calibration, measured versus simulated data without (left) and with (right) ±2.0 mg/l envelope: August 21, 1996.

Validation was completed using 1997 data with the calibration parameters defined for the 1996 period. Figure 6.8 illustrates simulates versus measured values near Iron Gate Dam; included are profiles with a 2.0 mg/l and 4.0 mg/l envelope. Simulation results for epilmnetic dissolved oxygen content were less accurately represented in the validation year. Surface epilmnion concentrations were understated, while simulated concentrations of deeper epilimnetic waters were overstated. Few measured data points fell within the 2.0 mg/l envelope, but all fell within the 4.0 mg/l envelope. It appears that primary production in the photic zone substantially impacts dissolved oxygen concentrations in the epilmnion. Secchi depth for August 1997 was about 2 meters (6.5 ft), corresponding to a photic zone of about 6 meters (19.7 ft). A sharp reduction in dissolved oxygen concentration from roughly 10 mg/l to less than 3 mg/l is illustrated in measured data at a depth of approximately 5 meters (16.4 feet). The measured data may reflect short-term variations in primary production, meteorological events, or operations; however, such estimations are limited by available field data.

Hypolimnetic waters were well represented. Seasonal variations of simulated dissolved oxygen with depth in Iron Gate Reservoir are shown in Figure 6.9. Conditions are similar to 1996. Note, that in the August 1 profile a small oxygen pocket below the thermocline was

102

effectively reproduced by the reservoir model, similar to that illustrated in the 1996 measured data. It is assumed that by August 21, 1997 the pocket was depleted.

The reservoir model also provides simulated dissolved oxygen concentration for reservoir releases, but unlike water temperature, insufficient field data were available to fully assess model performance. However, comparison with limited NCRWQCB grab samples completed in 1996 and 1997 suggest that the model under predicts dissolved oxygen concentration in reservoir releases. Additional study is required to address this issue.
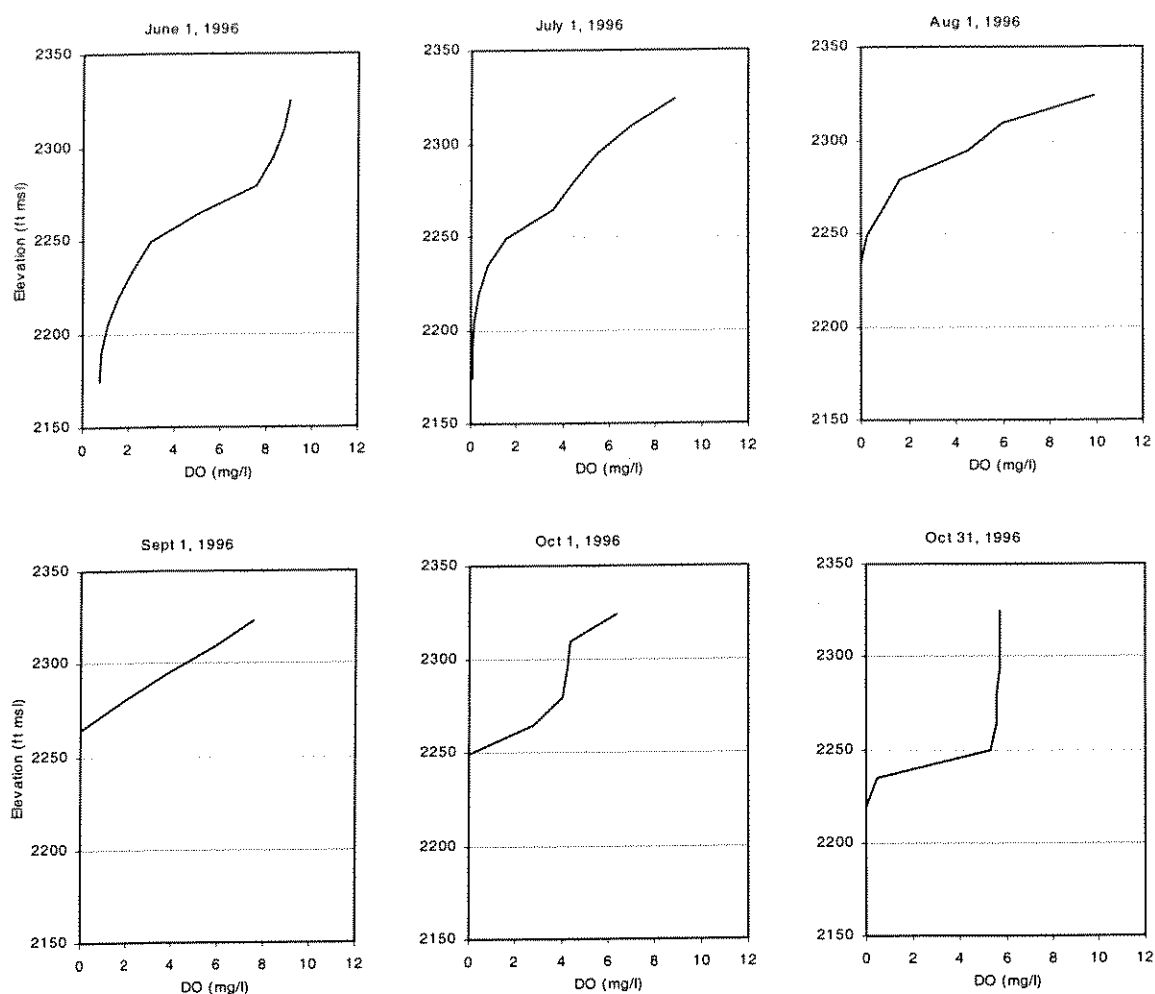
Figure 6.7   Iron Gate Reservoir simulated dissolved oxygen profiles, calibration period 1996 (measured data unavailable)
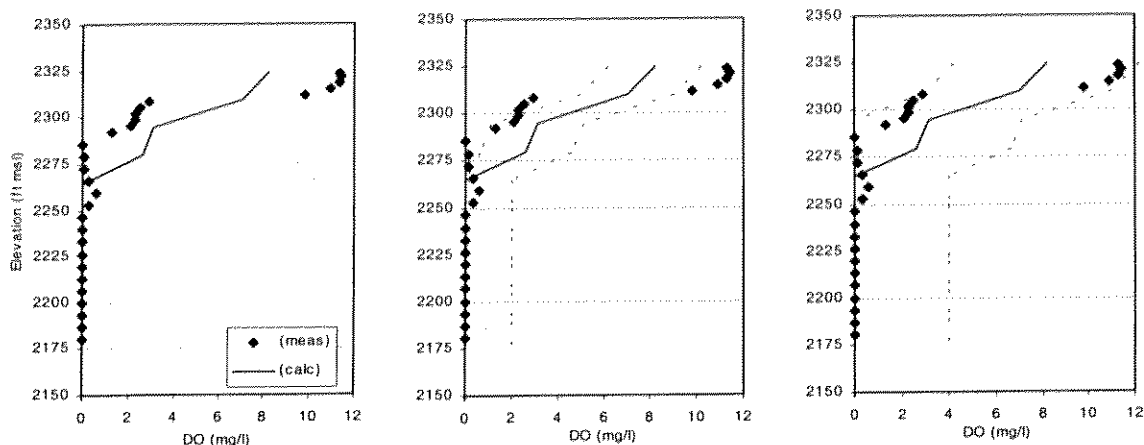
Figure 6.8   1997 Iron Gate Reservoir profile dissolved oxygen validation, measured versus simulated data (left), ±2.0 mg/l (center) and ±4.0 mg/l (right) envelope
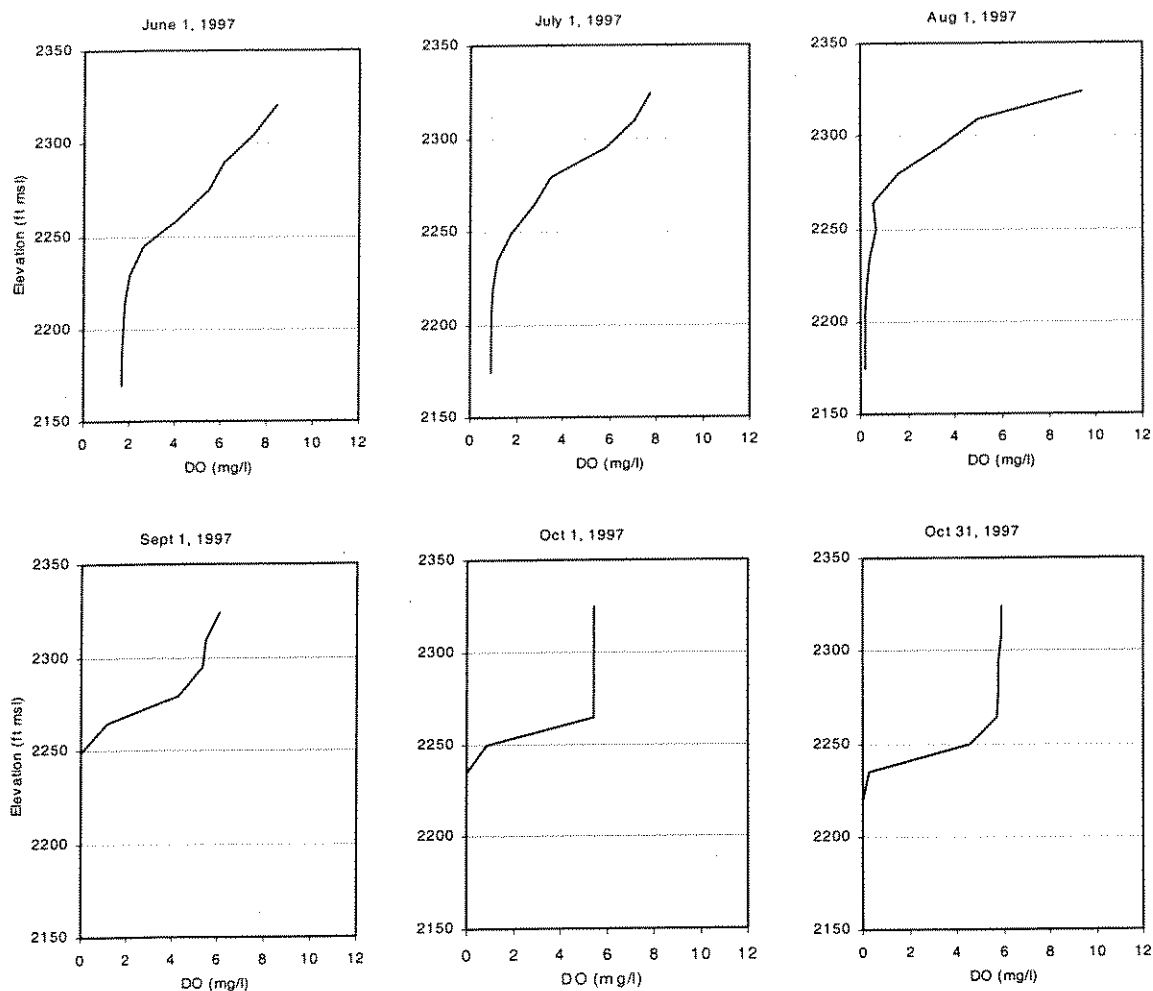
Figure 6.9   Iron Gate Reservoir simulated dissolved oxygen profiles, validation period 1997 (measured data unavailable)

6.1.3.3   Other Water Quality Variables

Though not formally calibrated, simulated and measured values of ammonia, nitrate, orthophosphate and algae were examined to ensure model produced reasonable values. These values were selected from the NCRWQCB 1996 and 1997 limnological studies of Iron Gate Reservoir based on availability. Comparisons are tabulated in Table 6.2. With the exception of algae in August 1997 the model reproduced reasonable nutrient concentrations.

Table 6.2   Comparison of simulated and measured values for selected parameters.

Constituent	Date	Measured (mg/l)	Date	Simulated (mg/l)
Ammonia	8/21/96	0.025	8/20/96	0.061
Nitrate	8/21/96	0.047	8/20/96	0.047
Orthophosphate	8/21/96	0.25[1]	8/20/96	0.11
Algae[2]	8/21/96	4.96	8/20/96	4.00
Ammonia	8/18/97	0.060	8/18/97	0.073
Nitrate	8/18/97	0.040	8/18/97	0.077
Orthophosphate	8/18/97	0.20	8/18/97	0.115
Algae[2]	8/18/97	0.13	8/18/97	3.47

[1] In 1996 only total dissolved phosphate was sampled. Simulated value of orthophosphate is consistent with assumption that PO_4^{-3} is roughly 50% of P-D.

[2] Measured algal concentrations derived from chlorophyll a concentrations.

6.1.3.4   Conclusion

Temperature calibration and validation for Iron Gate Reservoir was successful and the model can be applied with a considerable degree of confidence. Dissolved oxygen proved to be more elusive. Additional data would allow an improved calibration. Further, during model application it was found that the model was sensitive to hatchery withdrawals. Hatchery data was unavailable during the 1997 validation period and a value of 40 cfs constant withdrawal was assumed. Finally, Iron Gate Reservoir inflow quality data was limited. Improved representation could aid calibration of the model.

Overall, the performance of the reservoir model was deemed acceptable for analysis of water quality control alternatives in the Klamath River below Iron Gate Dam. Application of the calibrated and validated model to alternative water quality control operations is addressed in Section 8.

6.2   Klamath River

The Klamath River models, RMA-2 and RMA-11, were calibrated and validated over the period June through September 1996 and 1997, respectively. A primary difference between the river and reservoir simulations was that the river hydrodynamic model required calibration. Effective calibration of the hydrodynamic model is critical because transit time directly impacts water temperature, dissolved oxygen, and nutrient dynamics. Similar to the reservoir model, temperature and dissolved oxygen were the water quality variables subject to calibration; however, other variables were examined to ensure realistic representation.

Hydrodynamic calibration was done in tandem with the water quality model, using measured flow and temperature data to assess model performance. Upon completion of flow and temperature calibration, dissolved oxygen and other constituents were addressed.

6.2.1   Hydrodynamic and Water Temperature Calibration

Hydrodynamic calibration typically requires varying channel roughness (e.g., Manning coefficient, n) through a range of values while comparing simulated transit time and river stage with measured data. Transit time can be estimated from stream velocity measurements or tracking changes in river stage under varying flow conditions. Though UC Davis took several velocity measurements in the Klamath River in the reach between Iron Gate Dam and the Shasta River, insufficient data were available for a complete calibration. Further, although a USGS gage is located 60 miles downstream near Seiad Valley, travel time was difficult to ascertain accurately due to the long distance and uncertainty in tributary flows and accretions.

To overcome limitations of independent calibration of hydrodynamic and water quality models, Deas and Orlob (1997) present a method for iterative calibration wherein the models were used jointly. Application requires modeling on a sub-daily time step and availability of associated sub-daily water temperature data (e.g., hourly). Both criteria were fulfilled for this project. The method is outlined below in the context of the Klamath River.

6.2.1.1   Iterative Calibration: Background
Iron Gate Dam generally provides steady releases to the Klamath River. In addition, reservoir release water temperatures vary seasonally, but over short periods of time are

106

roughly constant. Because the heat budget is driven primarily by solar energy, river temperature downstream of the reservoir responds to daily cycles of heating and cooling. In response to this cycle, a characteristic diurnal temperature pattern is produced, the advective transport of which serves as a "tracer" of the flow. Thus, diurnal variations in water temperature provide a signal similar to that of a conservative tracer that is superimposed on the mean daily thermal profile. This signal is effectively reproduced in model results, and can be "fit" to measured data in the process of model calibration.

Calibration parameters for the hydrodynamic model include bed roughness (Manning coefficient) and turbulent exchange coefficients, although in this exercise longitudinal mixing was assumed minimal (i.e., turbulent exchange coefficients were not varied). In the water quality model, temperature calibration parameters include evaporative cooling coefficients, where evaporation, E, is represented by

$$E = (a+b\mathrm{W})(\mathrm{e_s}-\mathrm{e_a}) \tag{6.1}$$

where a and b are empirical evaporation coefficients, W is wind velocity, $\mathrm{e_s}$ is saturation vapor pressure, and $\mathrm{e_a}$ is actual atmospheric vapor pressure.

The calibration technique requires that the hydrodynamic model initially be applied to simulate a flow field that is then used as input to the water quality model. Computed hourly water temperature data are then compared to measured field data. Three possible relationships between phase and amplitude of computed and measured values may occur: both phase and amplitude are correct; phase is correct, but amplitude is incorrect; and, phase is incorrect. The calibration technique is represented schematically in Figure 6.10. Pre-selection of calibration criteria is required to compare simulation results and measured data.

Phase of the diurnal temperature variation is directly related to travel time. Travel time, in turn, is determined by water velocity, and is thus a function of bed roughness. The amplitude of diurnal temperature variations is affected by two processes: travel time (i.e., exposure time), and evaporation coefficients. The possible outcomes of the calibration process are described below.

Case 1: Phase correct, amplitude correct - If the simulated phase and amplitude of the diurnal variation in water temperature match measured data, the calibration is complete.
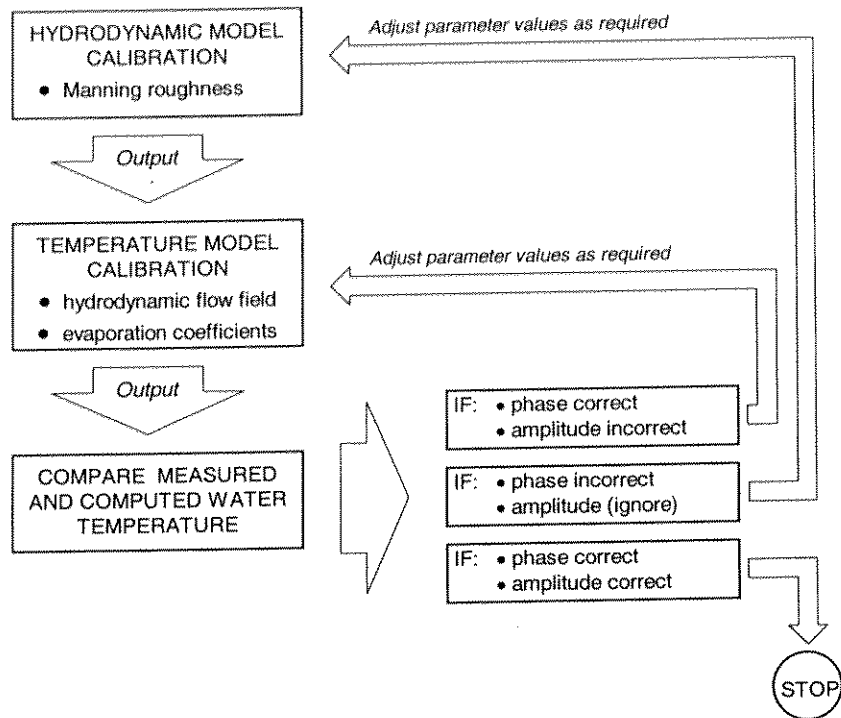
Figure 6.10 Schematic of iterative hydrodynamic and water temperature model calibration process

Case 2: Phase correct, amplitude incorrect - If the phase of simulated diurnal temperature variation matches measured data, but amplitude is incorrect, the applied Manning roughness coefficient is representative and hydrodynamic calibration is complete. Subsequently, evaporation coefficients (*a* and *b*) may be adjusted to improve/calibrate diurnal temperature amplitude.

Case 3: Phase incorrect - If the phase of simulated diurnal temperature variation does not coincide with measured field data, transit time in the river has been compromised. For excessive roughness values, average river velocities are reduced and transit time is increased; the converse is true for roughness values that are too small. The result is a temperature tracer signal that is displaced upstream or downstream, respectively. Amplitude of the signal is ignored because replication of the phase is necessary prior to assessing the amplitude, i.e., increased or decreased travel time will lead to greater or lessor heating of river water, directly affecting amplitude. Under these conditions, the Manning coefficient must be modified appropriately and both the hydrodynamic and water quality models re-run. Water quality model calibration coefficients remain unchanged because amplitude calibration cannot be completed until the phase of the tracer signal is correctly determined.

The steps of calibrating for phase and subsequently calibrating for amplitude are illustrated for an idealized example in Figure 6.11. The initial simulated temperatures illustrate both a phase shift and amplitude error. Calibration of channel roughness corrects for phase and, because travel time has been changed, also affects amplitude error. Subsequently, the amplitude is calibrated with evaporation coefficients. In practice, simulated phase and amplitude may not consistently match measured data due to short-term variations in upstream operations, local meteorology, and tributary influences.
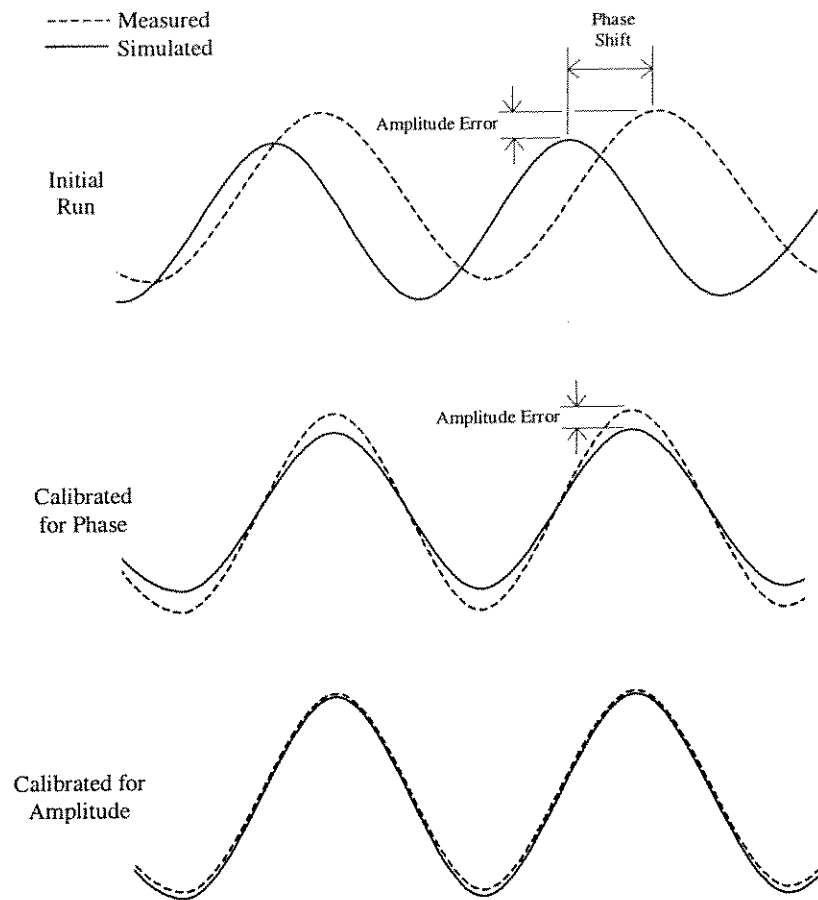
Figure 6.11 Example calibration of phase and amplitude for diurnal temperature trace

6.2.1.2 Results Calibration Measures and Methods

Calibration required comparison of several alternative parameter sets. Selecting final parameter values may include professional judgement, graphical comparisons of simulated versus measured data, and statistical analysis of simulated and measured data, to name a few.

Though each measure has merits and demerits, statistical analyses were used as the primary method to select final calibration parameters for the flow and temperature models. Graphical comparisons and professional judgement were used to assess general model performance and provided significant insight, but proved difficult to quantify differences over long time periods and at multiple locations along the river. Thus, several basic statistics were applied to the simulated data and associated error to provide additional insight into model performance and to quantify model uncertainty.

Sample statistics included daily average (mean), maximum, and minimum. The error was calculated as measured minus simulated values. Statistics applied to the error include bias, relative bias, maximum and minimum error, mean absolute error, relative mean absolute error, root mean squared error, variance, and standard deviation. Each term is briefly described in Table 6.3.

Table 6.3   Sample and error statistics

Data	Statistic	Description
Sample	Mean	Average simulated temperature
	Maximum/minimum	Maximum and minimum simulated temperature
Error	Bias	Average error calculated as measured minus simulated. A negative value translates to the model systematically over predicting temperature, a positive value means the inverse
	Relative bias	Average error divided by sample mean. Relates bias to magnitude of parameter
	Maximum overprediction/ underprediction	Maximum and minimum error
	Mean absolute error (MAE)	Average of the absolute value of all errors. Positive and negative values do not cancel, providing a measure of model uncertainty. Outliers (large errors) may be difficult to identify.
	Relative mean absolute error	Mean absolute error divided by sample mean. Relates bias to magnitude of parameter
	Root mean square error (RMSE)	Square root of the sum of the squared errors divided by the sample mean. Similar to mean absolute error, but outliers (large errors) can more easily be identified, especially when compared to MAE
	Variance	Measure of the spread of the data
	Standard deviation	Square root of the variance. Roughly 66% of the data are within plus or minus one standard deviation and 95% within plus or minus two standard deviations

Bias and relative bias describe systematic errors, while variance and standard deviation, assuming a normal distribution, represent random errors. All other statistics are a combination of systematic and random errors.

110

Three locations were selected for comparison: above Cottonwood Creek (RM 182.2), below Shasta River (RM 176.2), and below Scott River (RM 142.5). The months of June, July, August and September were used for calibration of flow and water temperature parameters. Hourly and daily data analyses were completed for each month.

An important distinction of hourly simulation is the reproduction of diurnal variation in water temperature. Ideally, model performance should be based upon the ability to reproduce proper magnitude and timing of maximum and minimum water temperature, as well as replicate the ascending and descending limbs of the daily trace of temperature. To assess model performance, iterative calibration of the hydrodynamic and water quality (temperature) models was completed.

Phase Assessment

As noted in the previous section, reproduction of the correct temperature trace phase is determined through multiple application of the flow and water quality (temperature) models under different Manning roughness coefficients. Once phase is effectively represented, flow model calibration is complete and the water quality model alone is used to calibrate temperature trace amplitude. Thus, for any particular flow-water quality simulation, the first step in comparing measured and simulated data was the identification of maximum and minimum water temperatures and their associated magnitude and timing.

For this project, such identification required visual examination of data sets because sometimes water temperature would persist at a maximum or minimum for more than one hour. In addition, resolution of the field measuring devices (loggers) often resulted in temperatures oscillating when the rate of change of temperature was small, resulting in multiple maximum or minimum over the span of a few hours. To address logger resolution, which was ±0.2°C (±0.4°F), all field data points that were within 0.2°C of the measured minimum or maximum temperature were assumed to be at the minimum or maximum, respectively. Thus, the impact of field data uncertainty was that a daily maximum or minimum temperature typically spanned more than a single hour, presenting a period of time that the maximum or minimum probably occurred within. Model data was taken as absolute, i.e., with no adjustment for uncertainty.

Assessing successful simulation of the measured temperature trace required formulating criteria to quantify error in phase or "phase shift." It was predetermined that if a simulated maximum or minimum temperature fell within the time frame of the maximum and

minimum defined for the measured data, phase shift would be set to zero. If simulated data overlapped measured data, a phase shift of 0.5 hours was assigned. If simulated data was offset by an hour, a phase shift of 1.0 hours was assigned; if offset by 2.0 hours a shift of 2.0 hours was assigned; and so on. In all cases the positive or negative sign was preserved to denote the direction of the shift, with lagging being represented as a positive number. Figure 6.12 illustrates the application of this methodology to phase shift determination over a representative day for three locations in along the Klamath River. For this example, simulated temperatures at Cottonwood Creek fell within the envelope of measured temperatures (plus 0.2°C (0.4°F) uncertainty), as did the maximum at the Shasta River, and a phase shift of zero hours was assigned. The envelope of simulated maximum temperature at the Scott River overlapped with measured data and was assigned a phase shift of 0.5 hours. Similarly, minimum simulated temperatures at the Shasta and Scott rivers were assigned phase shifts of one and two hours, respectively. Root mean squared error was used to aggregate the phase error both daily maximum and minimum temperature at the three locations for comparison. (Note, if measured data illustrated a persistent value, yet the model produced only a single maximum or minimum, the lag phase shift was still set to zero. That is, persistence of a peak was not a calibration criterion.)

	nr. Cottonwood Ck. Temperature			bel. Shasta River Temperature			bel. Scott River Temperature		
	(simul)	(field)		(simul)	(field)		(simul)	(field)	
12:00 AM	21.4	22.1		23.6	23.7		25.1	25.4	
1:00 AM	21.3	21.9		22.8	23.1		24.8	25.1	
2:00 AM	21.2	21.9		22.1	22.6		24.6	24.5	
3:00 AM	21.2	21.6		21.5	22.1		24.3	24.2	
4:00 AM	21.0	21.4	X	21.1	21.9		24.1	23.8	
5:00 AM	20.9	21.2	Min X	20.8	21.7		23.9	23.7	
6:00 AM	20.9	21.2	Min X	20.6	21.6	Min	23.6	23.3	Min
7:00 AM	21.2	21.2	X	20.7	21.4	X	23.5	23.2	
8:00 AM	21.6	21.4	X	21.0	21.2	X	23.6	23.0	
9:00 AM	22.3	21.9	Shift: 0.0 hrs	21.4	21.4	X	23.8	22.7	X
10:00 AM	23.0	22.6		21.9	21.7	Shift: 1.0 hrs	24.3	22.8	X
11:00 AM	24.0	23.4		22.6	22.2		24.9	23.3	Shift: 2.0 hrs
12:00 PM	24.9	24.3		23.5	22.9		25.6	23.8	
1:00 PM	25.6	25.3		24.5	23.7		26.3	24.5	
2:00 PM	26.2	26.0		25.4	24.4		26.9	25.4	
3:00 PM	26.4	26.5	Max X	26.2	25.3		27.4	26.2	X
4:00 PM	26.4	26.5	Max X	26.8	25.8		27.5	26.4	X
5:00 PM	26.1	26.5	X	27.3	26.4	X	27.6	26.4	Max X
6:00 PM	25.5	26.2	Shift: 0.0 hrs	27.4	26.5	Max X	27.6	26.1	Max
7:00 PM	24.8	25.5		27.2	26.4	X	27.0	25.8	Shift: -0.5 hrs
8:00 PM	23.9	24.4		26.7	26.0	Shift: 0.0 hrs	26.5	25.4	
9:00 PM	23.0	23.6		26.1	25.5		25.9	25.1	
10:00 PM	22.3	22.7		25.3	25.0		25.5	24.8	
11:00 PM	21.7	22.1		24.5	24.3		25.0	24.4	

Figure 6.12   Sample phase shift assignment procedure

112

Because the process was somewhat time intensive, the last week of June, July, August, and September were used to compare simulated and measured phase in the diurnal temperature trace. End of the month values were used to avoid first of month flow changes at Iron Gate Reservoir. The objective was to find a value of Manning n that produced the smallest aggregate phase error.

Phase assessment was carried out using values of Manning n that ranged from 0.025 to 0.055. These values spanned channel types ranging from sandy streams to cobbles and boulders (Chow 1959). The flow model was applied with little regard to evaporative heat flux coefficients (*a* and *b*) because hydrodynamic calibration required only matching the diurnal temperature trace phase. Average phase error for each month at the various Manning n values is shown in Figure 6.13. The circled data points represent the minimum average phase error for each month, showing phase error is minimized for Manning n in the range of 0.035 to 0.045. Figure 6.14 presents phase error averaged over the four months. Though a minimum is shown a Manning n value of 0.040, total average error at 0.035 and 0.045 is not significantly greater. For the purposes of this study a value of 0.040 was used. It should be noted that phase assessment findings may change slightly with calibration of *a* and *b* coefficients because peaks may persist for slightly longer or shorter periods. However, these changes would have a negligible effect, and phase analysis was not revisited after selection of the final roughness coefficient.
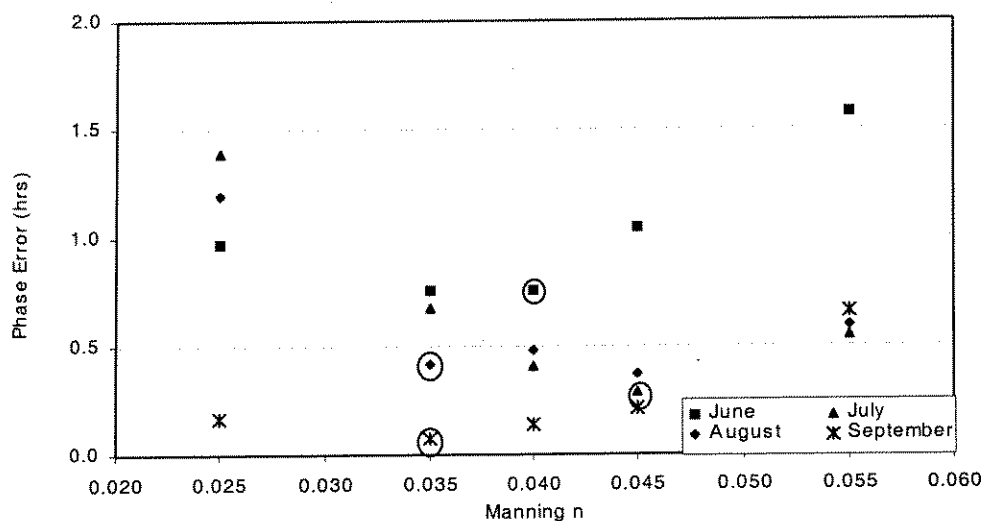
Figure 6.13   Average monthly phase error for Manning n values ranging from 0.025 – 0.055
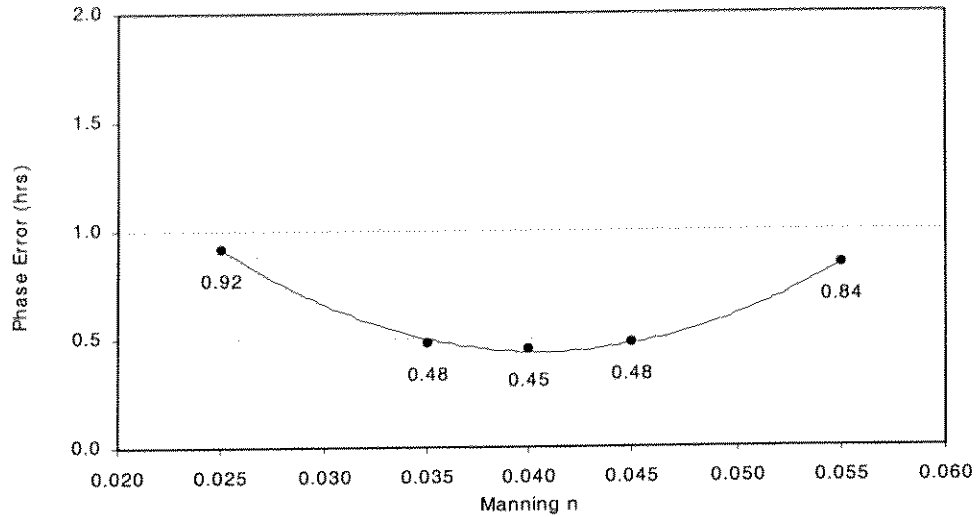
Figure 6.14 Four month average phase error for Manning n values ranging from 0.025 – 0.055

Final Calibration: Amplitude Assessment

With phase effectively reproduced, the final step in calibration was to adjust evaporation coefficients in the water quality model to reproduce amplitude. Initial investigation illustrated that if phase and amplitude were realistically simulated the ascending and descending portions of the daily temperature trace were generally well represented. To assess amplitude, summary statistics including bias, mean absolute error (MAE), root mean squared error (RMSE), and standard deviation were calculated for both hourly and aggregated daily data at the same locations defined for the phase analysis. Emphasis was given to the months of July, August and September, a stable flow period with minimum accretions, in order to reduce model uncertainty associated with accretion quantity, quality, and location (see Appendix B for details concerning accretions).

At this point in the process only the water quality model was required. There were no straightforward methods to assess parameter values for evaporative heat flux coefficients a and b because there is not a unique solution set. That is, there are multiple pairs of values that may reproduce acceptable simulated water temperature. TVA (1972) provides a wide range of values for a and b, ranging from 7.0×10^{-4} to 5.5×10^{-6} m hr^{-1} mb^{-1} and 1.9×10^{-3} to 5.9×10^{-6} m hr^{-1} mb^{-1} per m s^{-1}, respectively. Initial simulations were completed with estimates of parameter a, while b set to zero. This provided a rough estimate for one coefficient. Subsequently, the b coefficient was approximated and several iterations completed modifying both a and b to arrive at a final set of values.

114

Final values for the evaporative heat flux coefficients a and b were 1.7×10^{-5} m hr^{-1} mb^{-1} and 2.3×10^{-6} m hr^{-1} mb^{-1} per m s^{-1}, respectively. Table 6.4 includes monthly sample statistics for the four months of analysis: mean simulated water temperature and maximum positive and negative error. Although in certain months simulated water temperature deviated more than $\pm 2^\circ$C (3.8°F) from field values, examination of MAE, RMSE, and standard deviation illustrates that large errors were the exception rather than the rule. Table 6.5 defines hourly summary statistics for each month at the three calibration locations.

Table 6.4   Monthly sample statistics at three calibration locations: calibration period, June – September 1996

Statistic	Month	Location °C (°F)		
		Klamath River at Cottonwood Creek	Klamath River bel. Shasta River	Klamath River bel. Scott River
Sample Mean	June[1]	18.87 (66.0)	18.99 (66.2)	19.06 (66.3)
	July[2]	22.41 (72.3)	22.35 (72.2)	23.29 (73.9)
	August	21.72 (71.1)	21.86 (71.3)	22.23 (72.0)
	September	18.32 (65.0)	18.22 (64.8)	18.20 (64.8)
Maximum Underprediction				
	June[1]	1.06 (1.9)	1.40 (2.5)	0.81(1.5)
	July[2]	0.86 (1.5)	2.12 (3.8)	0.64 (1.2)
	August	0.89 (1.6)	1.38 (2.8)	1.77 (3.2)
	September	1.08 (1.9)	1.56 (2.8)	1.40 (2.5)
Maximum Overprediction				
	June[1]	-1.82 (-3.3)	-2.03 (-3.7)	-2.18 (-3.9)
	July[2]	-1.37 (-2.5)	-2.55 (-4.6)	-2.07 (-3.7)
	August	-0.75 (-1.3)	-0.91 (-1.6)	-1.16 (-2.1)
	September	-0.64 (-1.2)	-0.95 (-1.7)	-1.27 (-2.3)

[1] Partial month: system-wide (6/19-6/30)

[2] Partial month: Klamath River near Cottonwood Creek (7/17-7/31)

MAE at all locations was less than 0.60°C (1.08°F) with the exception of June at the Scott River. It is notable that RMSE at all locations is not only less than 0.75°C (1.4°F), but that it is not much larger than MAE, illustrating that if large errors (outliers) do exist, they are few in number. The standard deviation in all cases is less than 0.70°C (1.3°F), and usually considerably smaller, supporting the finding that large errors are few in number. Recall, that roughly two-thirds of the data in a sample population reside within one standard deviation of the mean and roughly 95% reside within two standard deviations of the mean. Because bias in general is small, on average roughly 95% of the simulated values fall within $\pm 1.0^\circ$C

(1.8°F) of field data. Exceptions being June and July at the Shasta River where simulated values generally fall within ±1.4°C (2.5°F).

Table 6.5   Hourly error statistics at three calibration locations, including season averages: calibration period, June – September 1996,

Statistic	Month	Location (all values °C)		
		Klamath River at Cottonwood Creek	Klamath River bel. Shasta River	Klamath River bel. Scott River
BIAS	June[1]	0.140 (0.252)	0.001 (0.002)	-0.892 (-1.61)
	July[2]	0.096 (0.173)	-0.155 (-0.279)	-0.518 (-.932)
	August	0.123 (0.221)	0.168 (0.302)	0.007 (0.013)
	September	0.259 (0.466)	0.471 (0.848)	0.235 (0.423)
	Average:	0.154 (0.277)	0.122 (0.220)	-0.292 (0.526)
MAE	June[1]	0.395 (0.711)	0.488 (0.878)	0.928 (1.67)
	July[2]	0.275 (0.495)	0.549 (0.988)	0.566 (1.02)
	August	0.249 (.448)	0.329 (0.592)	0.277 (0.499)
	September	0.329 (0.592)	0.521 (0.938)	0.215 (0.387)
	Average:	0.312 (0.562)	0.472 (0.850)	0.496 (0.893)
RMSE	June[1]	0.501 (0.902)	0.614 (1.11)	1.046 (1.88)
	July[2]	0.370 (0.666)	0.713 (1.28)	0.721 (1.30)
	August	0.313 (0.563)	0.421 (0.758)	0.526 (0.947)
	September	0.402 (0.724)	0.623 (1.12)	0.464 (0.835)
	Average:	0.397 (0.715)	0.593 (1.07)	0.689 (1.24)
Standard Dev.	June[1]	0.482 (0.868)	0.614 (1.11)	0.546 (0.983)
	July[2]	0.357 (0.643)	0.696 (1.25)	0.501 (0.902)
	August	0.288 (0.518)	0.393 (0.707)	0.526 (0.947)
	September	0.307 (0.553)	0.412 (0.742)	0.393 (0.707)
	Average:	0.358 (0.644)	0.529 (0.952)	0.492 (0.886)

[1] Partial month: system-wide (6/19-6/30)

[2] Partial month: Klamath River near Cottonwood Creek (7/17-7/31)

Aggregating hourly data to a daily time step led to significant improvement in system representation. Table 6.6 and 6.7 show daily sample and error statistics, respectively. Table 6.6 illustrated that maximum underprediction and maximum overprediction are less than 1.0°C (1.8°F) with the exception of the Scott River where one maximum underprediction and two maximum overpredictions were larger. Table 6.7 shows that MAE was less than 0.5°C (0.9°F) in all cases except the Scott River in June and was generally below 0.25°C (0.45°F). Daily RMSE followed a similar pattern with values generally less than 0.60°C (1.1°F) and usually below 0.35°C (0.63°F). Finally, standard deviation of daily error was below 0.36°C (0.65°F) and often less than 0.20°C (0.36°F) – the resolution of the field

116

temperature loggers. Thus, daily average simulated temperature fell within approximately ±0.7°C (1.3°F) roughly 95 percent of the simulation period (June – September).

Table 6.6   Daily sample statistics at three calibration locations: calibration period, June – September 1996

Statistic	Month	Location °C (°F)		
		Klamath River at Cottonwood Creek	Klamath River bel. Shasta River	Klamath River bel. Scott River
Sample Mean	June[1]	18.87 (66.0)	18.99 (66.2)	19.06 (66.3)
	July[2]	22.41 (72.3)	22.35 (72.2)	23.29 (73.9)
	August	21.72 (71.1)	21.86 (71.3)	22.23 (72.0)
	September	18.32 (65.0)	18.22 (64.8)	18.20 (64.8)
Maximum Underprediction				
	June[1]	0.48 (0.86)	0.44 (0.79)	-0.29 (-0.52)
	July[2]	0.26 (0.47)	0.54 (0.97)	0.00 (0.00)
	August	0.51 (0.92)	0.58 (1.0)	1.31 (2.3)
	September	0.58 (1.0)	0.90 (1.6)	0.84 (1.5)
Maximum Overprediction				
	June[1]	-0.18 (-0.32)	-0.45 (-0.81)	-1.40 (-2.5)
	July[2]	-0.13 (-0.23)	-0.91 (-1.6)	-1.44 (-2.6)
	August	-0.12 (-0.22)	-0.22 (-0.40)	-0.41 (-0.73)
	September	-0.06 (-0.11)	-0.11 (-0.20)	-0.39 (-0.70)

[1] Partial month: system-wide (6/19-6/30)

[2] Partial month: Klamath River near Cottonwood Creek (7/17-7/31)

In addition to these statistical measures, simulated data were regressed against field measurements. In each case, simulated data was the dependent variable and field data the independent variable. The adjusted r^2, and slope and intercept coefficients are tabulated for each month at the three calibration locations in Appendix D. These analyses provided additional insight not readily ascertained from the summary statistics alone. For example, the small sample size for daily statistics during certain months where field data were unavailable (e.g., June) occasionally identified non-normally distributed data. Overall, the results of the regression analysis directly supported the findings of the statistical analysis addressed above.

Figure 6.15 compares simulated and measured hourly water temperature at the selected locations for the August 1996. Model results track field data with a high degree of accuracy. The reader is referred to Appendix D for a complete set of figures comparing both hourly and daily average water temperature for all months at all calibration locations.

117

Table 6.7   Daily error statistics at three calibration locations, including season averages: validation period, June – September 1997

Statistic	Month	Location (all values °C)		
		Klamath River at Cottonwood Creek	Klamath River bel. Shasta River	Klamath River bel. Scott River
BIAS	June[1]	0.139 (0.250)	0.000 (0.000)	-0.892 (-1.61)
	July[2]	0.100 (0.180)	-0.154 (-0.277)	-0.518 (-0.932)
	August	0.129 (0.232)	0.166 (0.299)	0.036 (0.065)
	September	0.256 (0.461)	0.457 (0.823)	0.257 (0.463)
	Average:	0.156 (0.281)	0.117 (0.319)	-0.279 (-.502)
MAE	June[1]	0.213 (0.383)	0.222 (0.400)	0.892 (1.61)
	July[2]	0.145 (0.261)	0.271 (0.488)	0.518 (0.932)
	August	0.147 (0.265)	0.194 (0.349)	0.208 (0.374)
	September	0.251 (0.452)	0.449 (0.808)	0.266 (0.479)
	Average:	0.189 (0.340)	0.284 (0.511)	0.471 (0.849)
RMSE	June[1]	0.250 (0.450)	0.266 (0.479)	0.961 (1.73)
	July[2]	0.158 (0.284)	0.334 (0.601)	0.621 (1.12)
	August	0.177 (0.319)	0.236 (0.425)	0.335 (0.603)
	September	0.303 (0.545)	0.509 (0.916)	0.328 (0.590)
	Average:	0.222 (0.400)	0.336 (0.605)	0.561 (1.01)
Standard Dev.	June[1]	0.209 (0.376)	0.266 (0.479)	0.358 (0.644)
	July[2]	0.123 (0.221)	0.296 (0.533)	0.343 (0.617)
	August	0.121 (0.218)	0.168 (0.302)	0.333 (0.599)
	September	0.162 (0.292)	0.223 (0.401)	0.202 (0.364)
	Average:	0.154 (0.277)	0.238 (0.428)	0.309 (0.556)

[1] Partial month: system-wide (6/19-6/30)
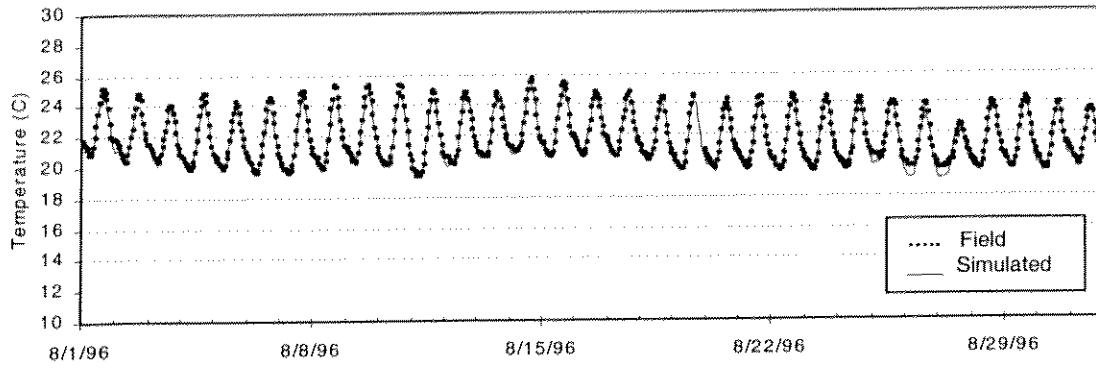
[2] Partial month: Klamath River near Cottonwood Creek

118

(a) Klamath River near Cottonwood Creek
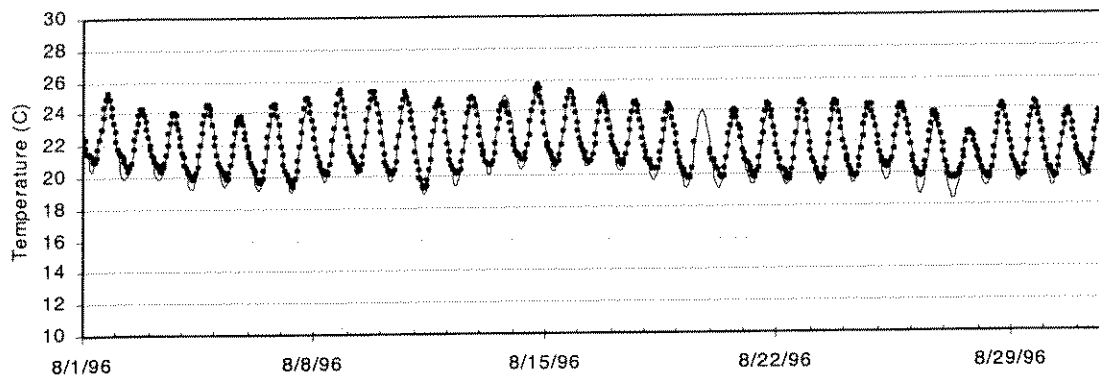
(b) Klamath River below Shasta River
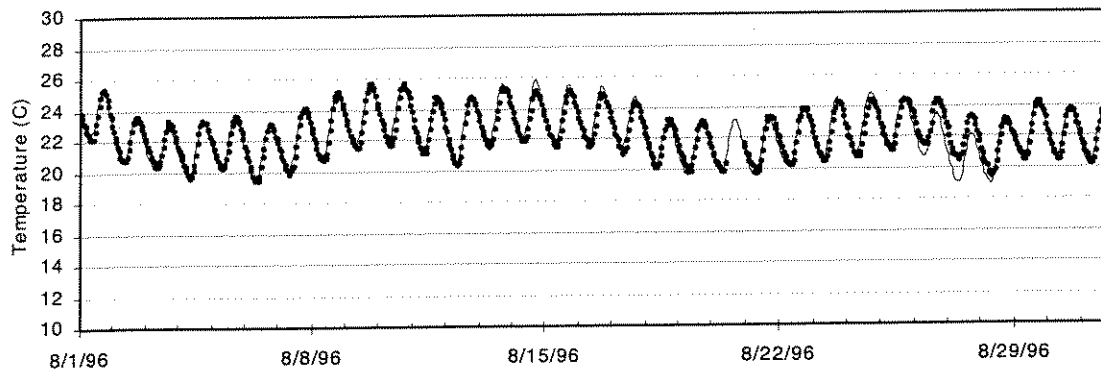
(c) Klamath River below Scott River

Figure 6.15   Calibration results at three Klamath River locations, August 1996

6.2.2   Hydrodynamic and Water Temperature Validation

The hydrodynamic and water quality parameters selected in the calibration phase were applied to an independent period, namely June through September 1997. The three calibration locations were retained and the same statistics analyzed.

Phase error was examined for the last week of each month and averaged 0.62, 0.95, 0.21 and 0.73 hours for the months of June through September, respectively. The aggregate average phase error for validation was 0.63 hours compared with 0.45 hours for the calibration period. Thus, the model predicted phase within the resolution of the model time step, i.e., ± 1 hour.

Comparing the calibration and validation sample statistics illustrates the validation period produced maximum overprediction and underprediction that were larger at Cottonwood Creek, but smaller at the Shasta and Scott River. The magnitude of the differences in all cases (larger and smaller) was roughly 0.5°C (0.9°F). For aggregated daily sample statistics, the validation period was roughly equivalent to the calibration period. Comparing monthly averages of hourly statistics of bias, MAE, RMSE, and standard deviation, validation results were within ±0.2°C (0.36°F) of measured field data. For monthly average daily statistics the validation period values were essentially equivalent to the calibration period. All tables are included in Appendix D.

As with the calibration exercise, simulated data were regressed against field measurements. In each case, simulated data was the dependent variable and field data the independent variable. As with calibration, these analyses directly supported the findings of the summary statistics. The adjusted r^2, and slope and intercept coefficients are tabulated for each month at the three validation locations in Appendix D.

Comparison of simulated and measured water temperature for August 1997 is illustrated in Figure 6.16. Simulations effectively reproduced measured temperatures and diurnal variation at multiple locations in the Klamath River study reach. The reader is referred to Appendix D for a complete set of figures comparing both hourly and daily average water temperatures for all months at all calibration/validation locations.

Validation illustrated no significant degradation in model forecasting ability under different operations, tributary accretion quality and quantity, and meteorological conditions. Upon completion of the flow and temperature calibration and validation, dissolved oxygen was explored.
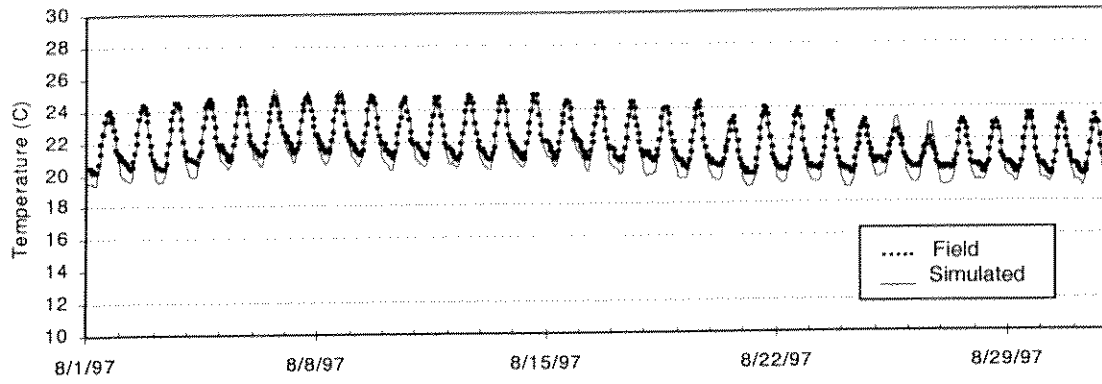
(a) Klamath River near Cottonwood Creek
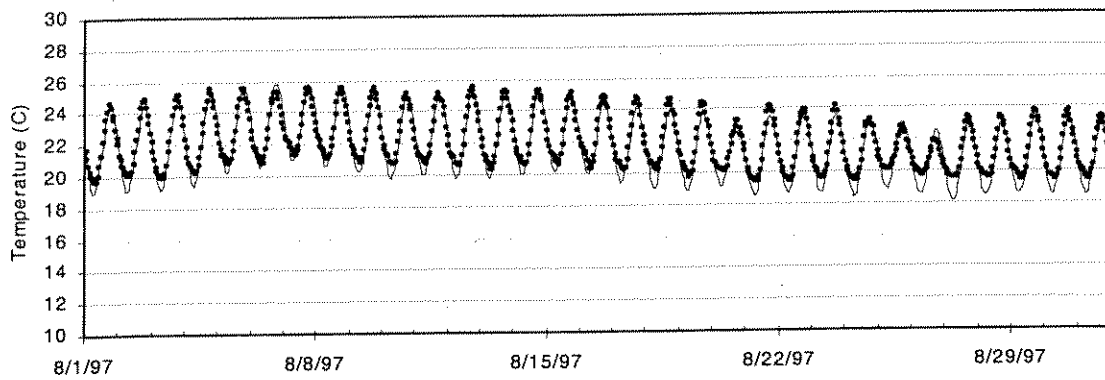
(b) Klamath River below Shasta River
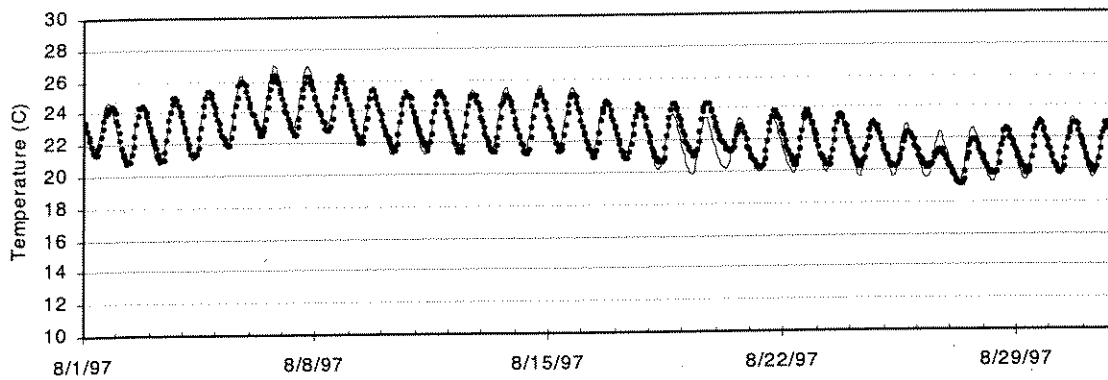
(c) Klamath River below Scott River

Figure 6.16   Validation results at three Klamath River locations, August 1997

121

6.2.3 Dissolved Oxygen

6.2.3.1 Introduction

Dissolved oxygen is a function of water temperature, reaeration, primary production, and oxizable constituents such as organic matter or certain nitrogen compounds. Critical in the role of modeling dissolved oxygen variation over the diurnal period is the role of primary production. Generally, stream velocities in excess of about one foot per second preclude effective colonization by phytoplankton – free floating or suspended species. Thus, unlike Iron Gate Reservoir, where primary production was predominately represented by phytoplankton, macrophytes and periphyton (attached algae) most likely dominate primary production in the downstream study reach. Such attached plants may be rooted in the substrate, attached to the bed, found growing on debris or other plants, or growing in biofilm on solid media. Oxygen and nutrient requirements may be derived from the bed or directly from the water column, and certain species may be able to fix nitrogen from the atmosphere. During summer low flow conditions, attached algae may gain considerable biomass, potentially leading to oxygen depletion due to plant respiration, pH elevation caused by high rates of photosynthesis, restriction of intragravel water flow and oxygen replenishment, degradation of benthic invertebrate habitat, as well as aesthetic concerns (River Ecology and Management 1998).

The original RMA-11 model formulation included only algae as phytoplankton. This was deemed unacceptable for the highly advective environment in the Klamath River below Iron Gate Dam. A critical limitation of this representation was that simulated algal concentrations experienced advection, i.e., physical transport, in the downstream direction. Thus, processes associated with algal production such as photosynthesis, respiration, nutrient uptake, and death and decay were transported through the system. Though general seasonal trends could be assessed with this approach, short-term and diurnal variations could not be reproduced.

To more effectively assess dissolved oxygen conditions in the study reach the RMA-11 model was modified to include an attached algae component. Appendix E outlines modifications made to the water quality model to incorporate attached algae. The model was tested through a set of trial cases by the model's author, Dr. Ian King. Further, repetitive application of the model to the Klamath River provided further opportunity to test the model, as well as to determine sensitivity to initial conditions, boundary conditions, and associated coefficient values.

6.2.3.2 Model Results: Calibration

Available system-wide dissolved oxygen field data were limited to several grab samples collected at various locations from April through October 1996 and 1997. Hourly data were available for the period July 28-30, 1997 at two location: below the mouth of the Shasta River (RM 176) and near Walker Road Bridge (RM 156.2). As noted above, algal dynamics have a direct impact on diurnal dissolved oxygen concentrations. However, little information was available for attached algae growth rates, respiration rates, existing algal species present, seasonal changes in community, densities, or other factors addressing algal function.

Due to limited field data and information, the river water quality model was calibrated, but not validated for dissolved oxygen. Calibration for dissolved oxygen relied primarily on estimating background BOD concentrations and varying the algal growth and respiration rates. Background BOD levels were set at 2.0 mg/l. Algal growth and respiration rates ranged from 1.0 – 2.0 per day and from 0.1 to 1.5 per day, respectively. Ultimately, growth and respiration rates were set at 2.0 per day and 1.0 per day respectively. The respiration rate is higher than literature values, but provided acceptable model performance. Further data collection is recommended to improve these values.

Figure 6.17 shows simulated versus measured hourly dissolved oxygen below the Shasta River (RM 176.0) and at Walker Road Bridge (RM 156.2) for July 28-30, 1997. Simulated values are within 2 mg/l below the mouth of the Shasta River and within about 1 mg/l near Walker Road Bridge. The diurnal response of the system was effectively represented at both locations. Daily average values were within 1.0 mg/l at both locations through the sampling period as outlined in Table 6.8.

Table 6.8   Daily average dissolved oxygen simulation results

Location	Data Value	Daily Average Dissolved Oxygen Concentration (mg/l)	
		July 28-29, 1997	July 29-30, 1997
Below Shasta River	RMA-11	7.8	8.0
	Meas.	7.6	7.2
	Δ =	-0.2	-0.8
Near Walker Rd. Br.	RMA-11	7.6	7.8
	Meas.	7.2	7.3
	Δ =	-0.4	-0.5

Daily average was calculated mid-day to mid-day to fully utilize limited data

Additional model performance assessment was completed using 1997 NCRWQCB grab samples for dissolved oxygen at several locations within the study reach. Figures 6.18, 6.19, and 6.20, show simulated values versus infrequent grab sample data for June, July, and August 1997, respectively. The model effectively brackets the grab samples collected during June through August. Although model results are good, there are two findings that merit discussion. First, simulated dissolved oxygen is underestimated above Cottonwood Creek in July and August (Figures 6.19 and 6.20). Measured dissolved oxygen concentrations at this location reached 180 percent of saturation, while simulated values do not approach this level. The authors have discussed these findings with field personnel responsible for gathering the data and were assured that protocols were consistent throughout data collection efforts. With limited available information, interpretation of these findings is tenuous; however, model results may shed light on this issue as discussed in Section 7.3.3

Second, in late August, simulated values fall below measured data and the amplitude of the dissolved oxygen daily variation is appreciably diminished. Further, grab samples from September suggest that diurnal variation in dissolved oxygen is appreciable into the fall season. It is believed that the single set of algal growth and respiration rates applied over the simulation period may not effectively capture seasonal variations in algal dynamics.

Because of limited data, validation was not feasible for hourly simulation. Moreover, because only a few days of hourly observations and infrequent grab samples were used, calibration is termed "preliminary." Further, although the modified version of the model allowing simulation of attached algae versus phytoplankton represents an improvement in modeling dissolved oxygen, additional algae data are required to properly represent this important process. As such, simulated dissolved oxygen values should be used with care. Aggregation of hourly data to daily or weekly values may be more representative than calculated hourly values.
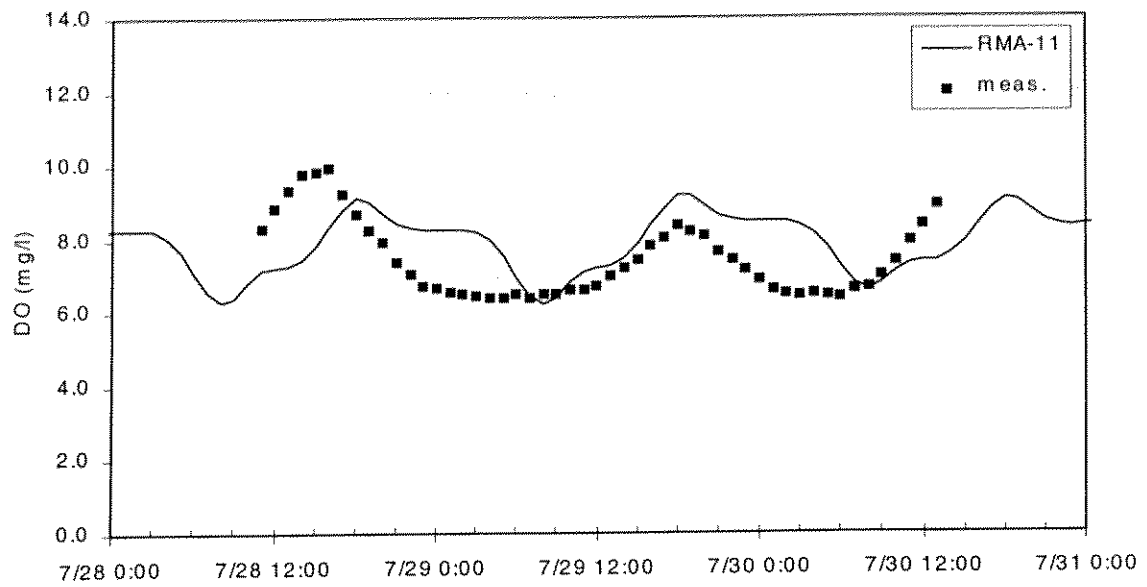
(a) below Shasta River
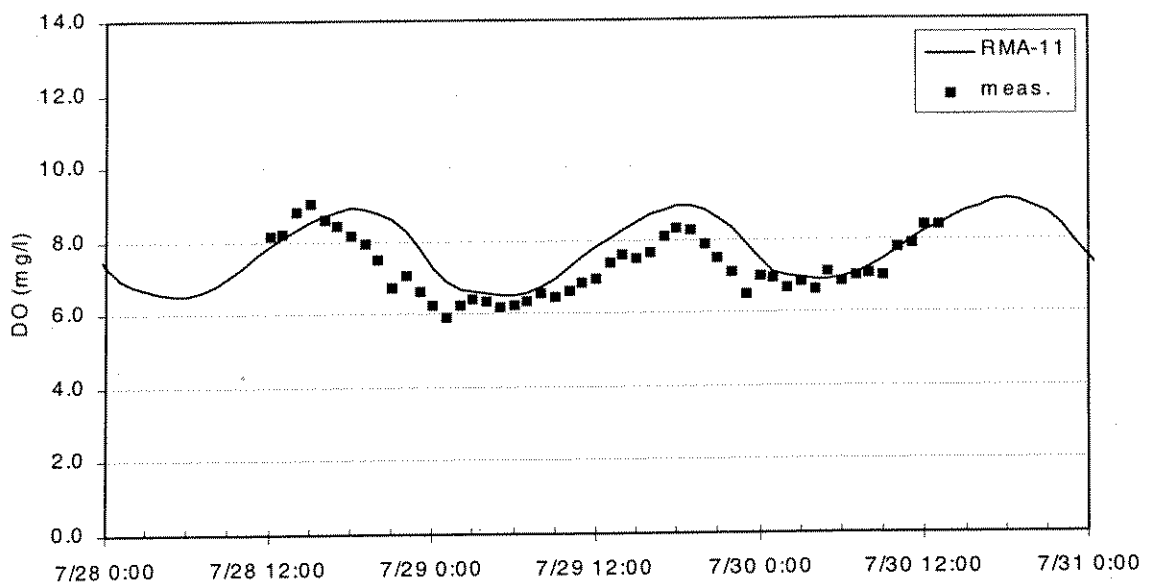
(b) near Walker Road Bridge

Figure 6.17   Simulated versus measured dissolved oxygen (a) below the mouth of the Shasta River and (b) near Walker Road Bridge: July 28-30, 1997
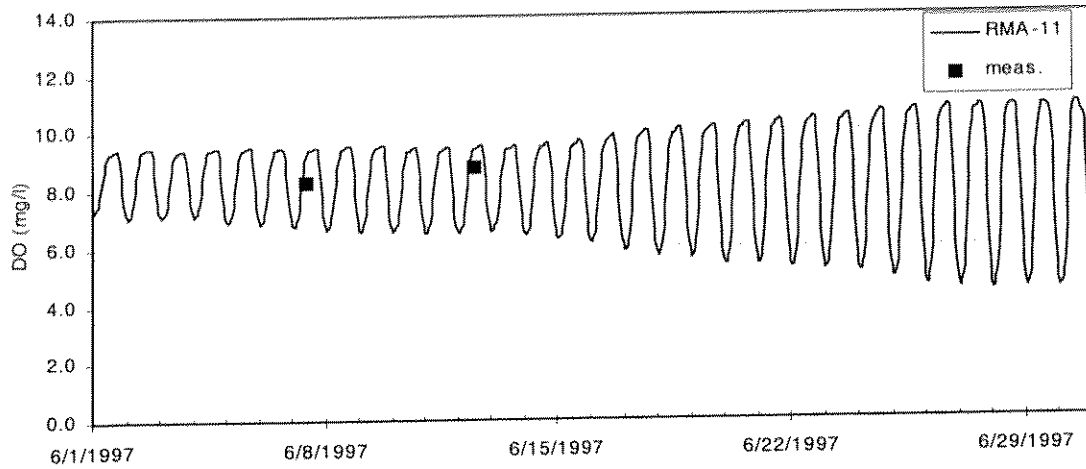
(a) above Cottonwood Creek: RM 182.1
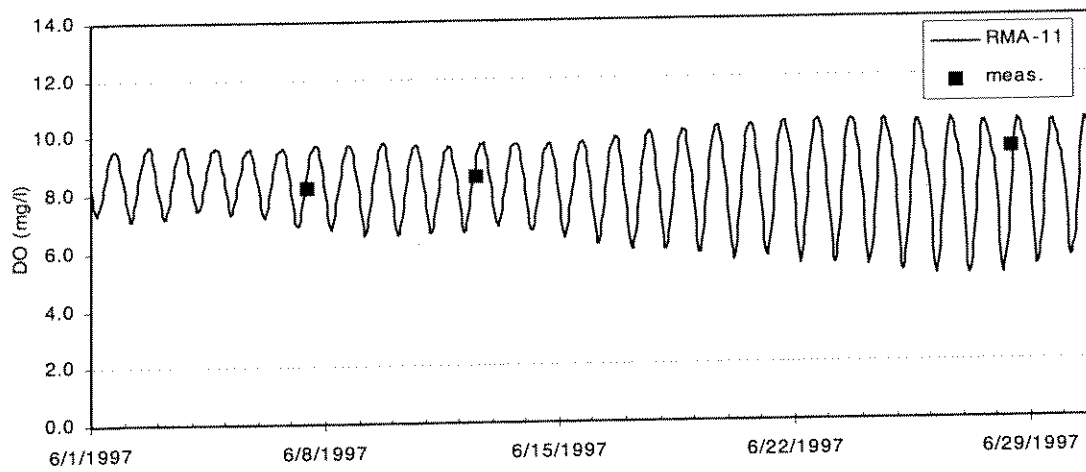
(b) below Shasta River: RM 176.0
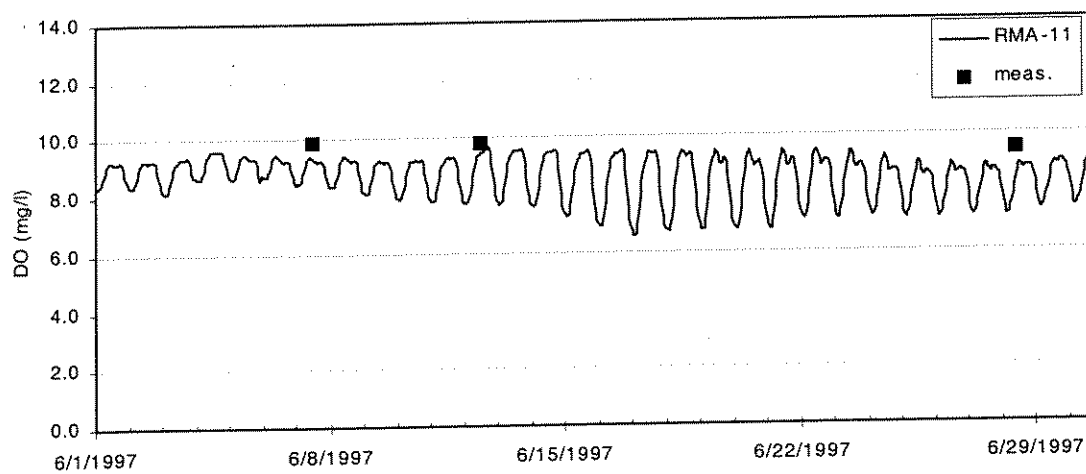
(c) below Scott River: RM 142.5

Figure 6.18   Simulated versus measured dissolved oxygen (a) above Cottonwood Creek, (b) below the Shasta River, and (c) below the Scott River: June 1997.

126
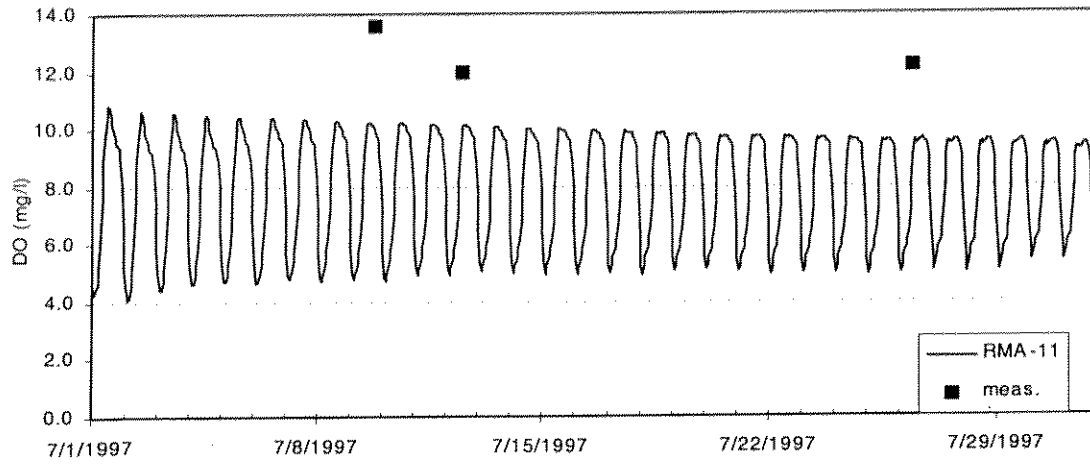
(a) above Cottonwood Creek: RM 182.1
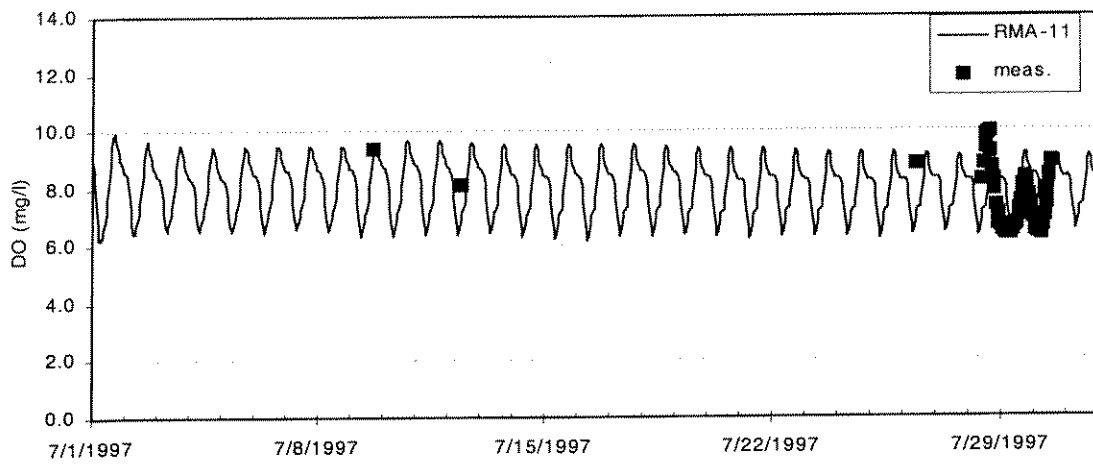
(b) below Shasta River: RM 176.0
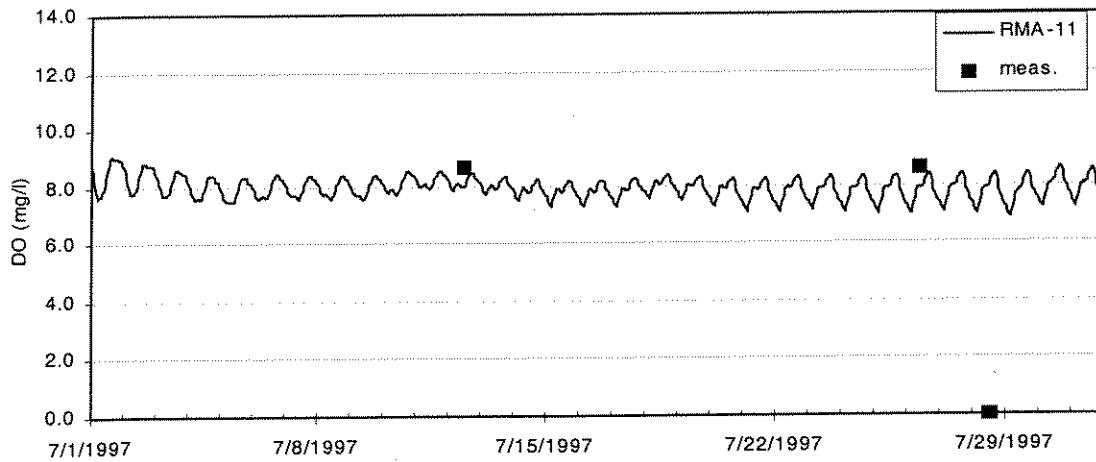
(c) below Scott River: RM 142.5

Figure 6.19   Simulated versus measured dissolved oxygen (a) above Cottonwood Creek, (b) below the Shasta River, and (c) below the Scott River: July 1997.
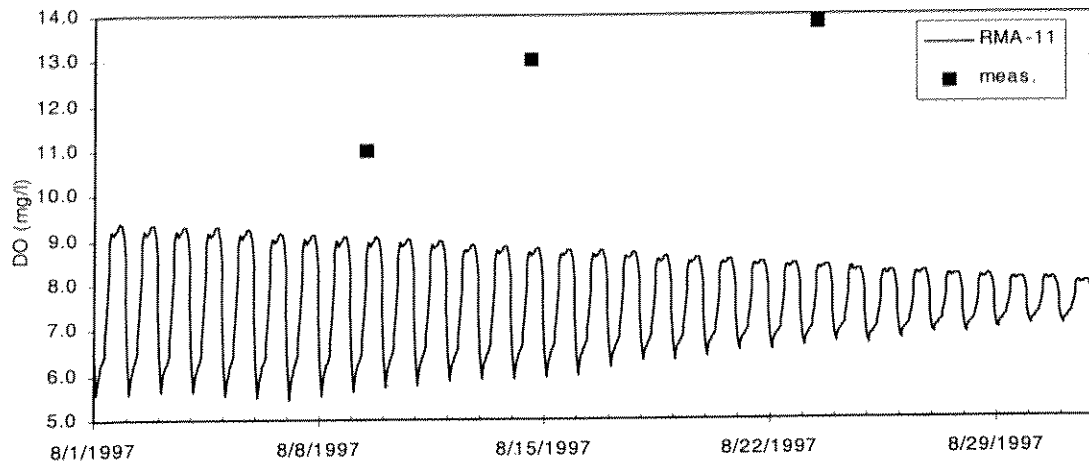
(a) above Cottonwood Creek: RM 182.1
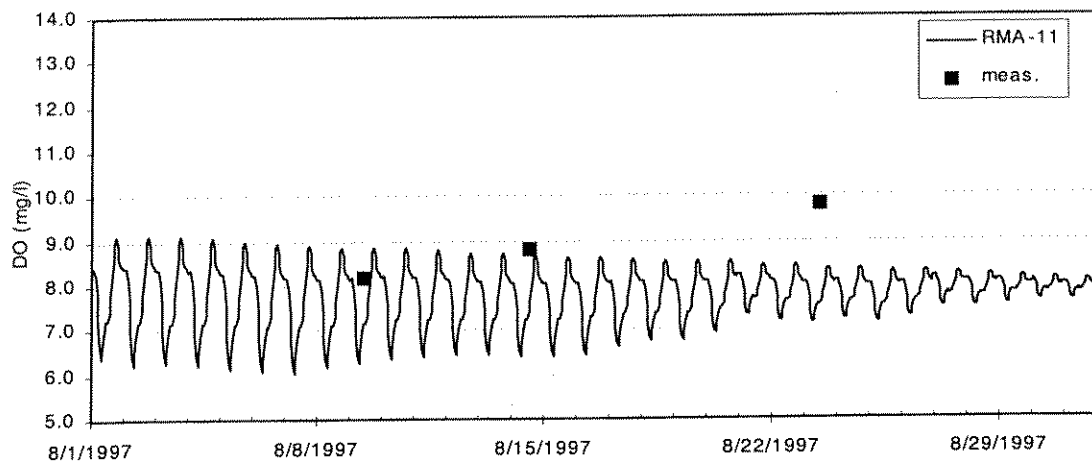
(b) below Shasta River: RM 176.0
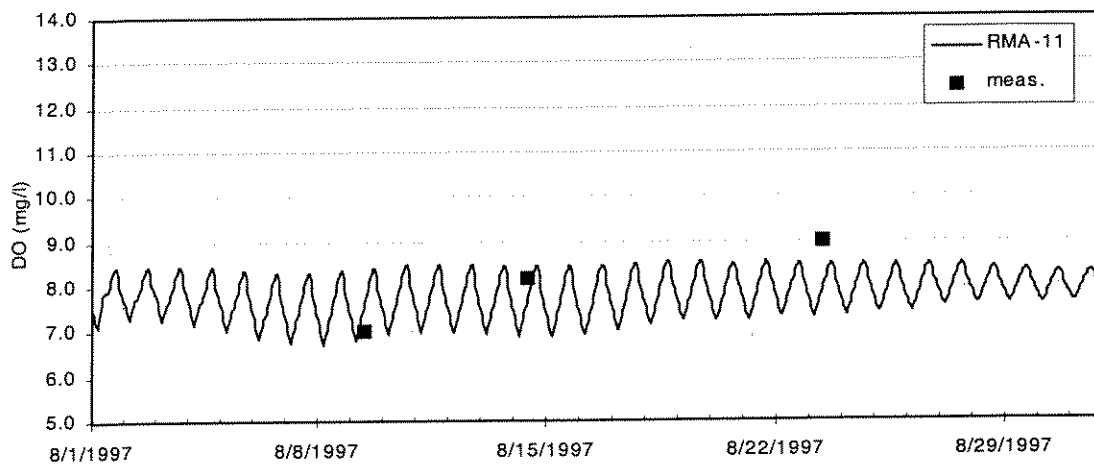
(c) below Scott River: RM 142.5

Figure 6.20   Simulated versus measured dissolved oxygen (a) above Cottonwood Creek, (b) below the Shasta River, and (c) below the Scott River: August 1997.

6.2.4   Other Water Quality Variables

Though other water quality parameters were not formally calibrated, simulated values were compared with the limited available field data to ensure outputs were reasonable.

Nitrogen Species

Available data included ammonia (herein, $NH_3 = NH_3 + NH_4^+$), nitrate (NO_3^-), and organic nitrogen (OrgN). Nitrite (NO_2^-) was not examined, but concentrations are typically negligible in the river system. Measured field data were available for June and August of 1997. Figures 6.21 and 6.22 are simulated hourly results with grab samples plotted. The general trend in the field data is low concentrations of ammonia and nitrate, and larger concentrations of organic nitrogen. The model reproduces this trend, representing ammonia and nitrate concentrations closely. Simulated organic nitrogen is overestimated in June and underestimated in August, with the exception of below the Scott River where field measured values of organic nitrogen drop considerably. A diurnal cycle in response to algal uptake is clearly evident for the inorganic forms of nitrogen (NH_3 and NO_3^-) in Figures 6.21 and 6.22. Simulated values show depression of ammonia to near zero concentrations during periods of intense algal growth, i.e., the system is nitrogen limited. Measured data support this finding. Given the paucity of data these results show good promise for modeling nutrients in the study reach.

Phosphorus Species

Although limited NCRWQCB phosphorus data were available, the measured field data were inconsistent with model output. That is, total phosphorus was reported by the NCRWQCB, but the model works with sub-sets of total phosphorus: organic phosphorus and orthophosphate. Thus model results could not be directly compared with field data. This was of minor consequence because the system was nitrogen limited throughout the study periods.

Algae: Chlorophyll a

Likewise, limited NCRWQCB chlorophyll *a* data were available, but the measured field data were inconsistent with model representation of attached algae. Chlorophyll *a* field measurements were based on free water column algal concentrations versus attached forms. These measured river samples probably represented a diverse assemblage of phytoplankton released into the river from Iron Gate Reservoir, as well as attached algal species that were dislodged by biological or physical processes, or were undergoing reproductive processes.
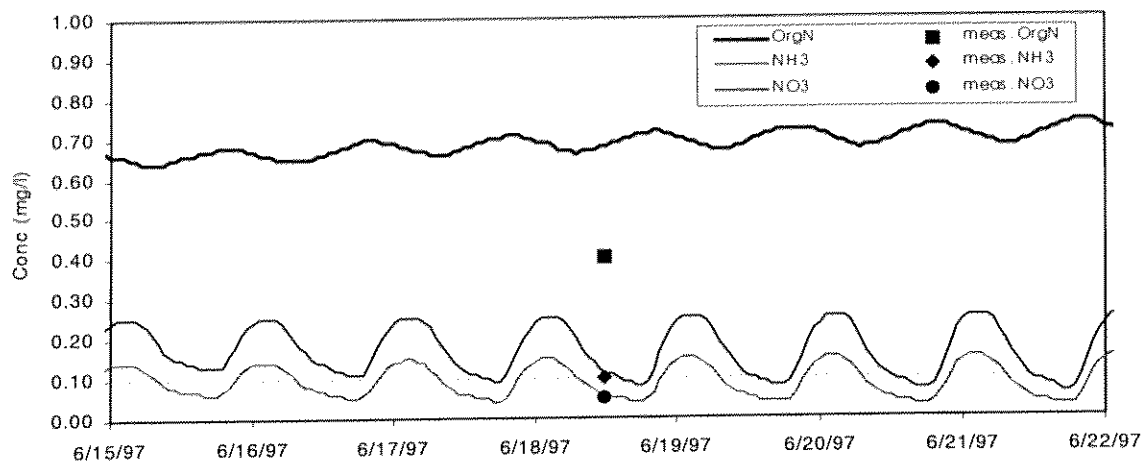
(a) above Cottonwood Creek: RM 182.1
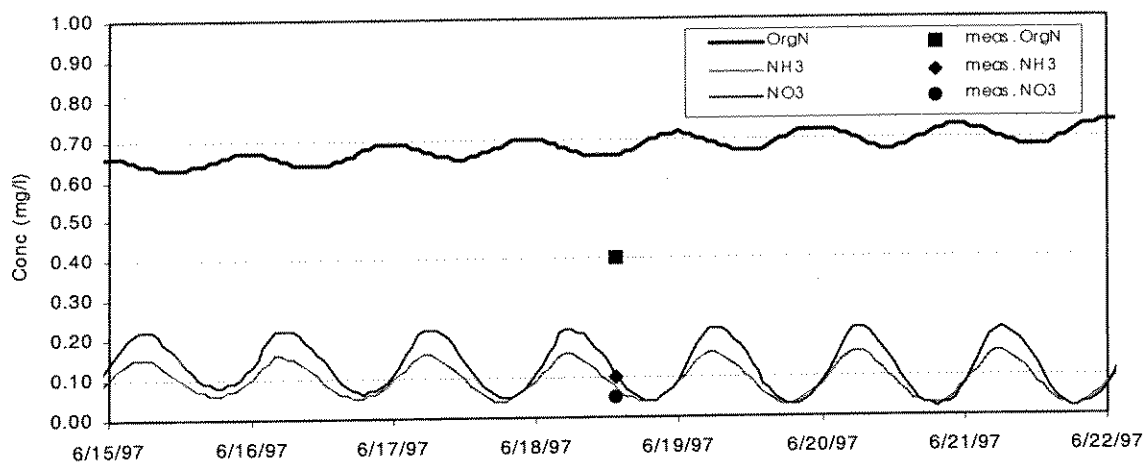
(b) below Shasta River: RM 176.0
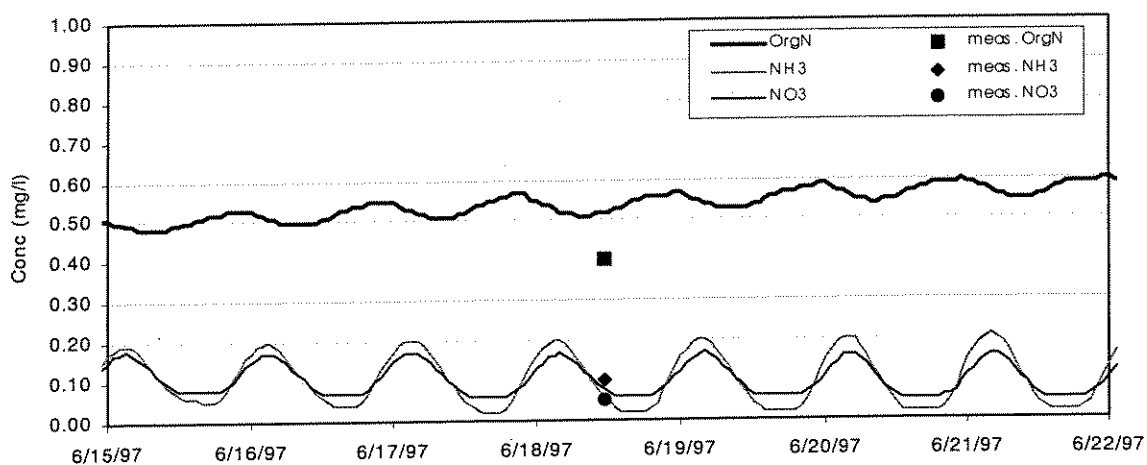
(c) below Scott River: RM 142.5

Figure 6.21   Simulated versus measured nitrogen species (a) above Cottonwood Creek, (b) below the Shasta River, and (c) below the Scott River: June 1997.
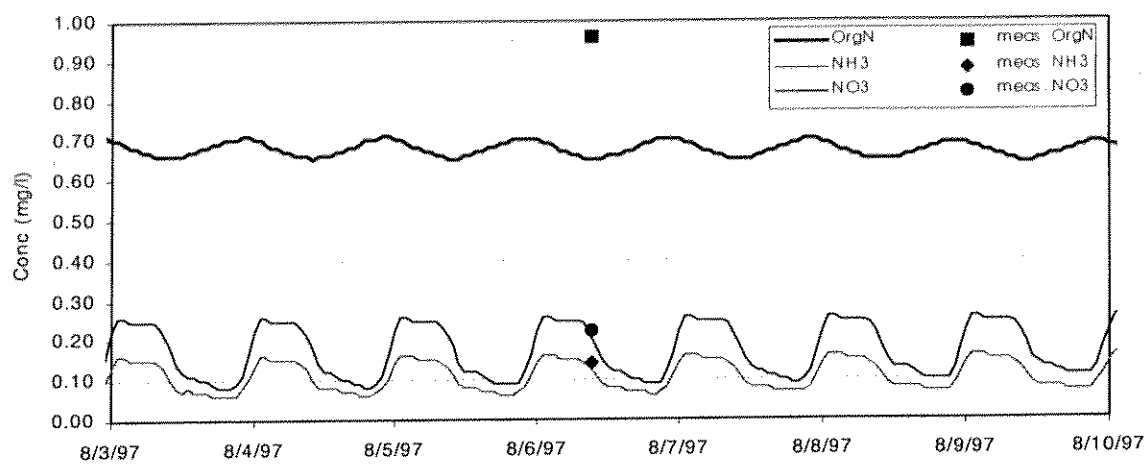
(a) above Cottonwood Creek: RM 182.1
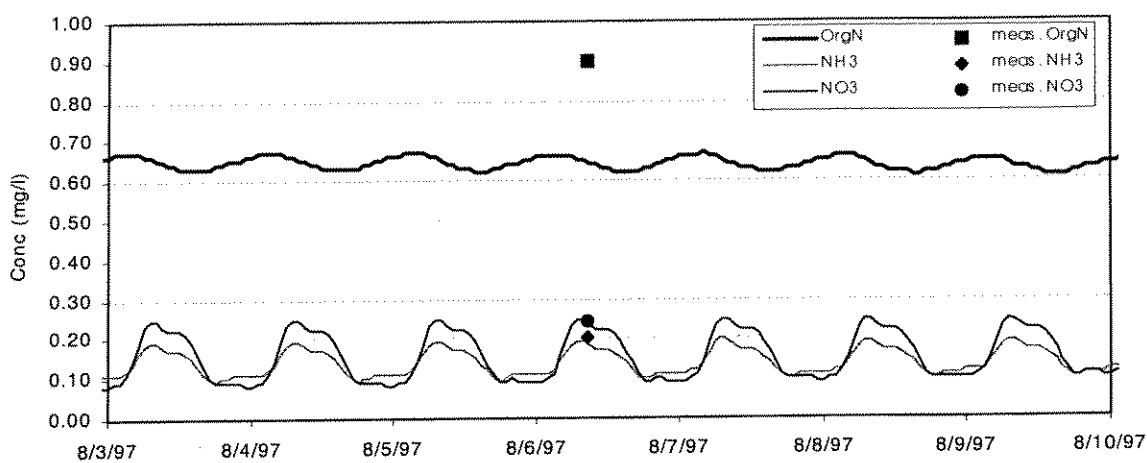
(b) below Shasta River: RM 176.0
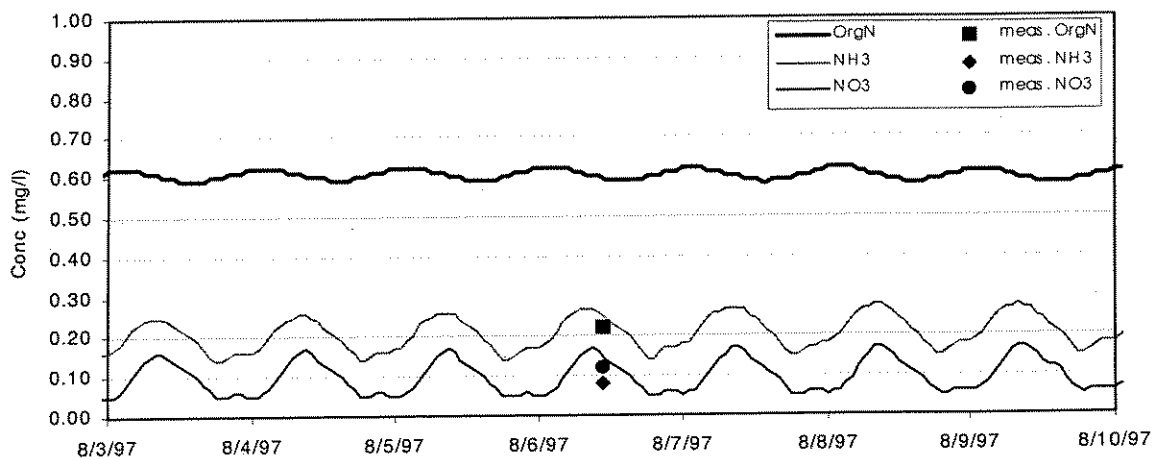
(c) below Scott River: RM 142.5

Figure 6.22   Simulated versus measured nitrogen species (a) above Cottonwood Creek, (b) below the Shasta River, and (c) below the Scott River: August 1997.

131

7.1 Introduction

Water temperature and water quality response of the reservoir and river system to historic hydrological conditions, meteorological conditions, and operations was assessed using available field data and model simulations from the calibration/validation period (1996 and 1997). Through definition of general system response a baseline condition was formed from which alternative management options (Section 8) could be compared. Because sufficiently detailed water quality field observations were typically unavailable, discussions focus on temperature and dissolved oxygen. Both Iron Gate Reservoir and Klamath River responses are addressed herein. Descriptions of temperature and water quality responses of Iron Gate Reservoir are addressed first, followed by Klamath River response, including impacts of Iron Gate reservoir operations on river conditions.

7.2 Iron Gate Reservoir

Iron Gate Reservoir water quality is a function of hydrology, operating conditions, inflow water quality, and meteorological conditions. Variations in water quality occur seasonally and, at certain locations, on time scales as short as hours or days. Reservoir residence time and water temperatures play key roles in reservoir water quality. Herein, the concept of reservoir residence time is introduced, and temperature, dissolved oxygen, and other water quality responses presented. Upper basin characteristics and operations, although potentially significant, are not addressed.

7.2.1 Residence Time

The primary hydrologic issue for Iron Gate Reservoir is residence time – roughly defined as the time it takes a parcel of water to pass through the reservoir. A gross estimate of residence time is represented in equation 7.1.

$$\Psi = V/Q \tag{7.1}$$

Where Ψ is residence time, V is reservoir volume and Q is flow through rate. Because Iron Gate Reservoir is operated within a small range of elevations Q can be represented as either

132

mean reservoir inflow or release. Table 7.1 outlines Iron Gate Reservoir residence times for a range of flow rates as per equation 7.1. For the purpose of residence time calculations reservoir volume was assumed to be controlled at 58,800 acre-feet (surface elevation 2328 ft msl) to accommodate spills at higher flow rates.

Table 7.1   Iron Gate Reservoir residence times at various flow rates

Flow	Residence Time	
(cfs)	(hrs)	(days)
600	1185.8	49.4
800	889.4	37.1
1000	711.5	29.6
1200	592.9	24.7
1400	508.2	21.2
1600	444.7	18.5
1800	395.3	16.5
2000	355.7	14.8
4000	177.9	7.4
6000	118.6	4.9
8000	88.9	3.7
10000	71.1	3.0

Assumed Iron Gate Reservoir Volume: 58,800 AF (elevation 2328 ft msl)

At low flow rates (<1500 cfs) residence time is appreciable, on the order of weeks or months. At high flow rates (>6000 cfs) residence time is reduced to several days. Flows in excess of 10,000 cfs probably produce conditions more like a slow river than a static reservoir. For example, at a flow rate of 20,000 cfs the mean velocity through the reservoir is roughly 0.3 ft per second.

7.2.2   Water Temperature

Water temperature is a function of meteorology, hydrology, inflow quantity and temperature, and operations. The general response of these factors can be considered through examination of measured water temperature profiles completed during 1996 and 1997 field monitoring program.

Figure 7.1 illustrates average daily water temperatures at several depths in Iron Gate Reservoir for the period January through November 1997. All depths were in reference to the water surface elevation, which varied from roughly 2324 ft msl to 2331 ft msl. Careful

133

review of these data illustrates multiple processes occur in Iron Gate Reservoir throughout the year. Thus, the seasonal thermal response of the reservoir associated with meteorologic conditions, hydrologic conditions, inflow water temperature, and operation will be discussed in roughly chronological order starting in January and ending in December.
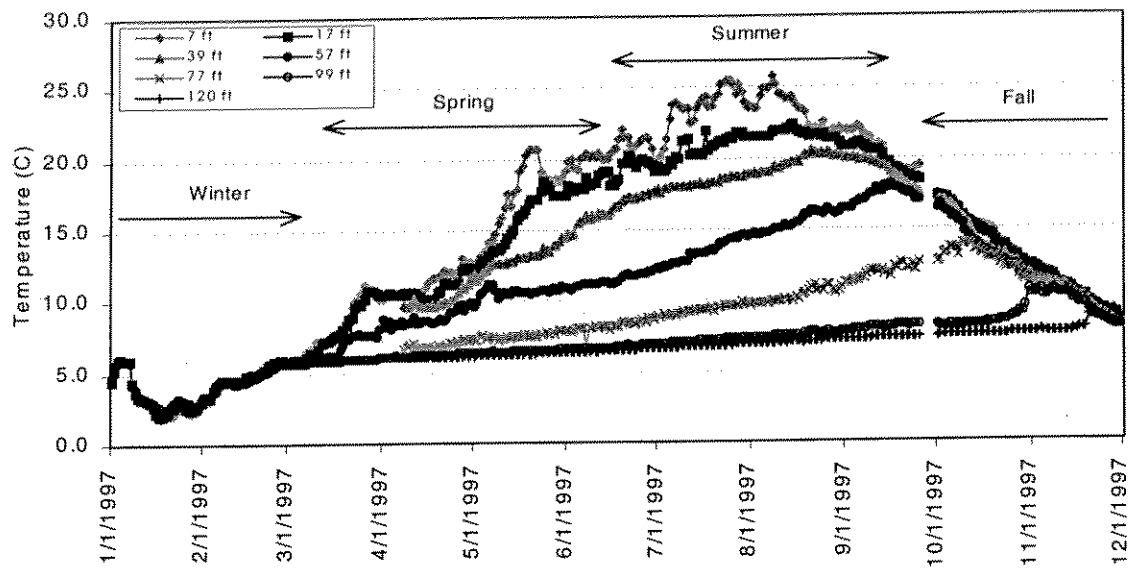
Figure 7.1   Mean daily measured profile temperature for Iron Gate Reservoir, January – December 1997
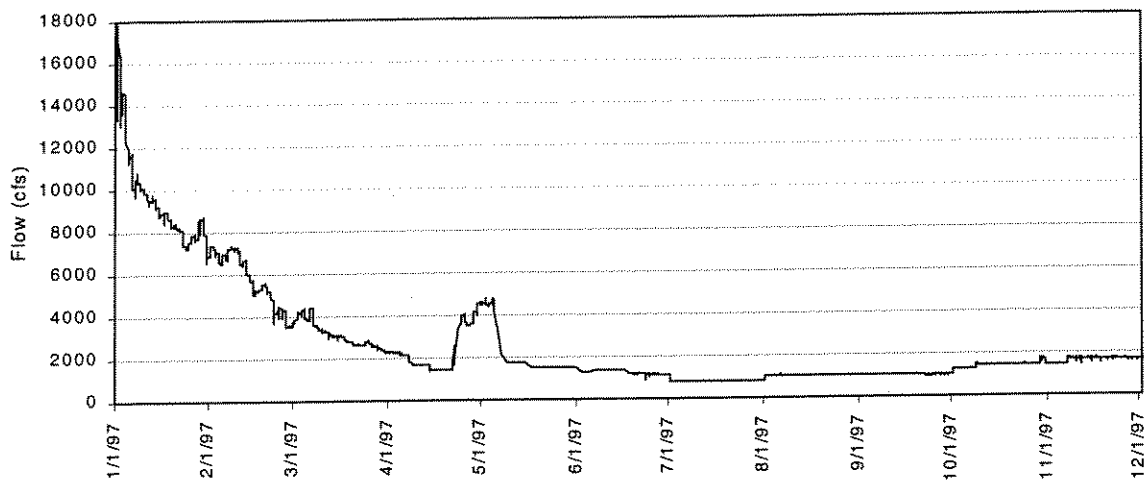
Figure 7.2   Iron Gate inflow (Copco Release), January –December 1997

7.2.2.1 Seasonal Response

Winter

During the winter months the reservoir experiences isothermal conditions, i.e., temperature is approximately constant throughout depth. Reservoir temperature responds to meteorological conditions in the basin and generally reflects river inflow temperature. As illustrated in Figure 7.1, the large rainfall driven event in early January (the New Years Eve Flood) produced water temperatures in excess of 5°C (9°F), while colder meteorological conditions later in the month lowered water temperature in the basin and reservoir to less than 3°C (5.4°F). The influence of appreciable river inflows and a corresponding lack of thermal stratification kept the reservoir well mixed.

Spring.

The onset of thermal stratification occurred in March 1997, as depicted by diverging temperature traces at the various depths. The onset of stratification is a function of inflow rate and seasonal meteorological conditions (rate of thermal loading). As stratification strengthens, it provides appreciable resistance to mixing, as evidenced by the roughly 5000 cfs event that passed through the reservoir in early May with minimal impact on thermal regime (Figures 7.1 and 7.2).

The bulk of the reservoir volume is typically resistant to sudden changes in water temperature due to its large thermal mass. As spring proceeds, day length increases (solar altitude), base flows recede to a regulated regime, and the reservoir begins to heat throughout its volume. Surface waters heat rapidly. However, a steadily increasing degree of thermal stratification impedes vertical mixing and deeper waters heat much more slowly. For example, the rate of heating in the surface layer of the reservoir is roughly 2.5°C (4.5°F) and 6.3°C (11.3°F) per month for April and May, respectively, while at depths of 120 feet the rate is approximately 0.2°C (0.4°F) per month for the same time period. By the end of the spring period surface waters exceed 20°C (68°F) while bottom waters remain below 7°C (44.6°F).

Summer

Peak thermal loading to the reservoir occurs in the summer period and sufficient time has passed to allow heat to diffuse to deeper waters. Examining Figure 7.1, reveals that waters at depths of 80 feet show appreciable heating. Hydropower penstock withdrawals also affect

the thermal structure of the reservoir. The nine-foot diameter penstock has a centerline elevation of roughly 2295 ft msl, but has an envelope of influence that is considerably larger. An approximation for the size of the withdrawal envelope can be made using the relationships formulated by Bohan and Grace (1973) for density stratified impoundments

$$Z = [V_o A_o / ((\Delta\rho'/\rho_o)g)^{0.5}]^{0.4} \qquad\qquad (7.2)$$

Where:

Z = vertical distance from the centerline of the withdrawal orifice to the upper or lower limit of the zone of withdrawal (ft)

V_o = average velocity through orifice (ft s^{-1})

A_o = orifice area (ft^2)

$\Delta\rho'$ = density difference of fluid between elevation of orifice centerline and upper or lower limit of zone of withdrawal (slug ft^{-3})

ρ_o = fluid density at elevation of orifice centerline (slug ft^{-3})

g = acceleration of gravity (ft s^{-2})

Assuming the water surface forms an upper limit to the zone of withdrawal and using data typical to August the withdrawal zone depth can be estimated, namely

V_o = 15.7 ft s^{-1} (based on a flow rate of 1000 cfs)

A_o = 63.6 ft^2

$\Delta\rho'$ = 0.002 slug ft^{-3} (based on 20°C (50°F) at the orifice centerline and 25°C (59°F) at the reservoir surface)

ρ_o = 1.937 slug ft^{-3} (based on 20°C (50°F) at the orifice centerline)

g = 32.2 ft s^{-2}

the zone of withdrawal is estimated as roughly 60 feet (Z = 30 feet). This translates to a withdrawal envelope extending from the water surface to elevations in the neighborhood of 2260 ft msl to 2265 ft msl, roughly 60 feet deep. Late in the summer, as the epilimnion deepens and the thermocline becomes well developed the withdrawal zone increases due to reduced density gradients in the region of penstock intake.

This estimate explains the increased heating rate for depths less than approximately 60 feet, as shown in Figure 7.1. However, as noted earlier there is appreciable heating at the 77-foot depth during the summer period. This heating is due to fish hatchery releases from the low level outlet at elevation 2252 ft, msl – about 75 feet deep. Fish hatchery withdrawal also has an envelope of influence that seasonally varies in size. In the late spring and early summer when density gradients in the region are small, the withdrawal zone is disproportionately large compared to its size: roughly 30 feet (Z = 15 feet) for the 40 cfs withdrawal through the 2-foot diameter orifice. As the thermocline descends through the summer season into the

region of the low level intake, both as a function of thermal loading and due to fish hatchery withdrawal of cool bottom waters, the density gradient can become appreciable. Rough estimates using equation 7.2 suggest withdrawal envelope is reduced roughly 30 percent during late summer periods.

Another important process that occurs during the summer period is the onset of cooling. As illustrated in Figure 7.1, surface water temperatures peak around the first of August and begin a varied, but steady descent. Though air temperatures can remain high during the mid- to late-summer period, reduced day length limits the reservoir thermal loading (this is actually a system-wide phenomenon based on seasonal meteorology). Also notable is the lag in peak temperature for measured temperature at successively greater depths. While surface temperatures peak around August 1, maximum water temperatures at 17 feet, 39 feet, 57 feet, and 77 feet are lagged by about 2-, 4-, 6-, and 8-weeks, respectively. The convergence of the temperature traces through September at depths less than 60 feet illustrate deepening of the epilimnion, probably through a combination of convective cooling and reduced inflow temperatures.

Fall

Fall brings significant changes to the reservoir thermal structure. Reduced day length and overall cooler climatic conditions depress surface water temperatures. These cool water "parcels" are denser than underlying waters and "sink" into the reservoir, mixing with neighboring water until they reach depths of similar density. This process is called convective cooling. During this period inflow water temperature is also decreasing due to seasonal changes in meteorological conditions. These cooler inflow waters will seek a depth within the reservoir of similar density.

As with the onset of thermal stratification, isothermal conditions, i.e., fall turnover, is a function of hydrologic and meterologic conditions. In certain cases, high flow events or sustained winds can cause a lake or reservoir to turn over in a short period of time. Although reservoir turnover for 1997 was a gradual process, this may not always be the case. Data were not gathered below 120 feet, but isothermal conditions existed to this depth by late November. Finally, it should be noted that bottom waters continued to heat well into November, illustrating the slow response of the reservoir's large thermal mass.

7.2.2.2 Year-To-Year Variability

In addition to seasonal response, Iron Gate Reservoir experiences year-to-year variations in thermal response due to annual variability in meteorology, hydrology, inflow water temperature, and system operations. Sufficient field observations were available for the 1996-97 period to compare late spring through early fall thermal conditions in Iron Gate Reservoir. Further, model simulation for calibration and validation substantiated field observations and provided additional insight into reservoir response. Field observations and simulation results are presented below.

Field Observations

Field observations of flow and temperature conditions were used to define the thermal conditions in Iron Gate Reservoir. Flow patterns for the two years differed in the winter and spring months (Figures 7.3 and 7.4). Significant differences in the winter period hydrograph are evident. From June through October the reservoir flows were regulated, but notable differences occurred in July and September where flows were 1000 cfs and 1300 cfs, respectively, in 1996; and 800cfs and 1000 cfs, respectively, in 1997. For all cases under regulated flow, the residence times were sufficiently long that impacts on thermal regime were probably minor.
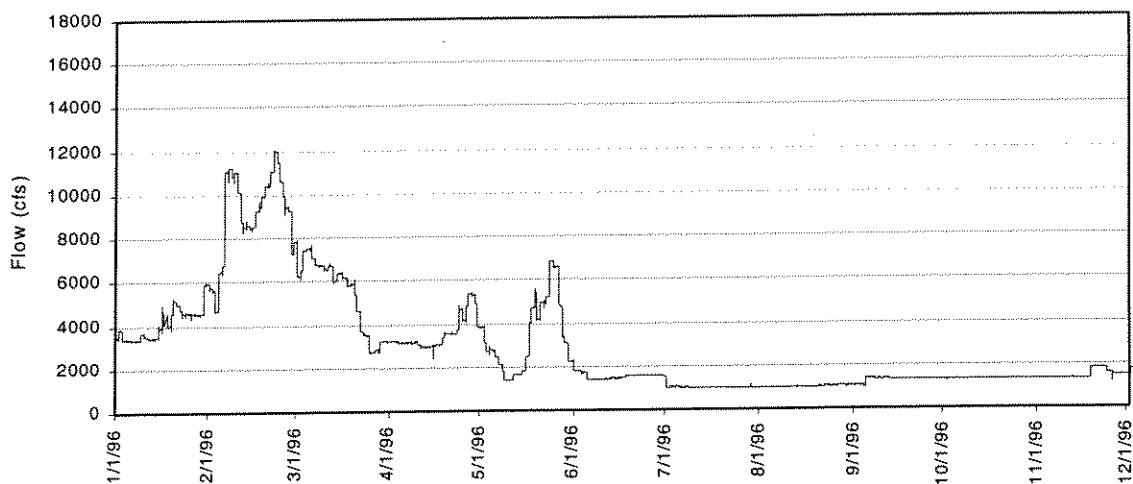
Figure 7.3   Iron Gate inflow (Copco Release), January –December 1996
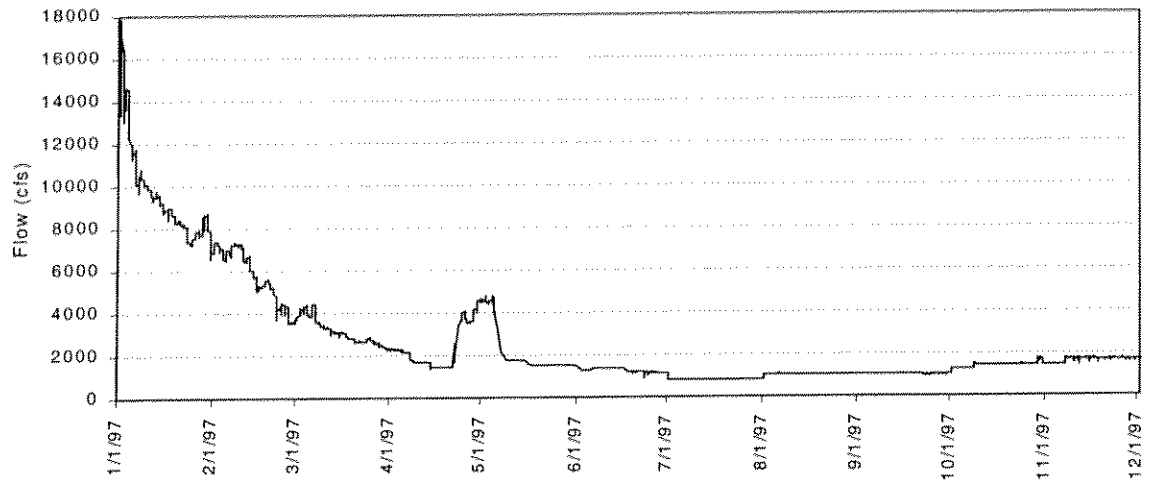
Figure 7.4   Iron Gate inflow (Copco Release), January –December 1997

Comparison of measured profile water temperatures from mid-May into October for the 1996 and 1997 periods illustrate market differences in thermal structure. One difference is that initial water temperature deep within the reservoir was about 1°C (1.8°F) warmer in mid-May 1996 than for the same period in 1997. Reasons for this are unknown, but may be attributable to both meteorology and hydrology. The January 1, 1997 flood may have contributed to mixing cold waters deep within the reservoir.

Another difference is that peak temperature of surface water occurred on July 15 (25.9°C (78.6°F)) in 1996, but not until August 8 (25.8°C (78.4°F)) in 1997; probably attributable to meteorological variability between the two periods. For example, using air temperature as a parameter for comparison it was determined that from June through August 1996 there were 31 days when air temperature was greater than or equal to 35°C (95°F), while for the same period during 1997 there were only 12 such days. Overall, 1996 experienced a warmer summer.

Although meteorological conditions contributed to different reservoir thermal regimes between 1996 and 1997, variable fish hatchery operations at Iron Gate Dam had a larger impact. Specifically, for much of the 1996 summer season there were no appreciable low level withdrawals for fish hatchery supplies due to work at the hatchery. Though the withdrawal is relatively small, roughly 40 cfs, the result was a remarkable difference between the temperature traces for depths at 57 ft and 77 ft. A comparison of the slopes of these traces in Figures 7.5 and 7.6 illustrates more rapid heating in 1997. Heating rates in

139

August 1996 were roughly 0.4°C (0.7°F) per month at both depths, while rates for the same period in 1997 were 1.8°C (3.2°F) and 1.2°C (2.2°F) per month for depths of 57 ft and 77 ft, respectively. It should be noted that Iron Gate Reservoir storage was not significantly different between the 1996 and 1997 seasons, varying within ±3 feet, equating to about 2500 AF of storage, or about ±4 percent of capacity
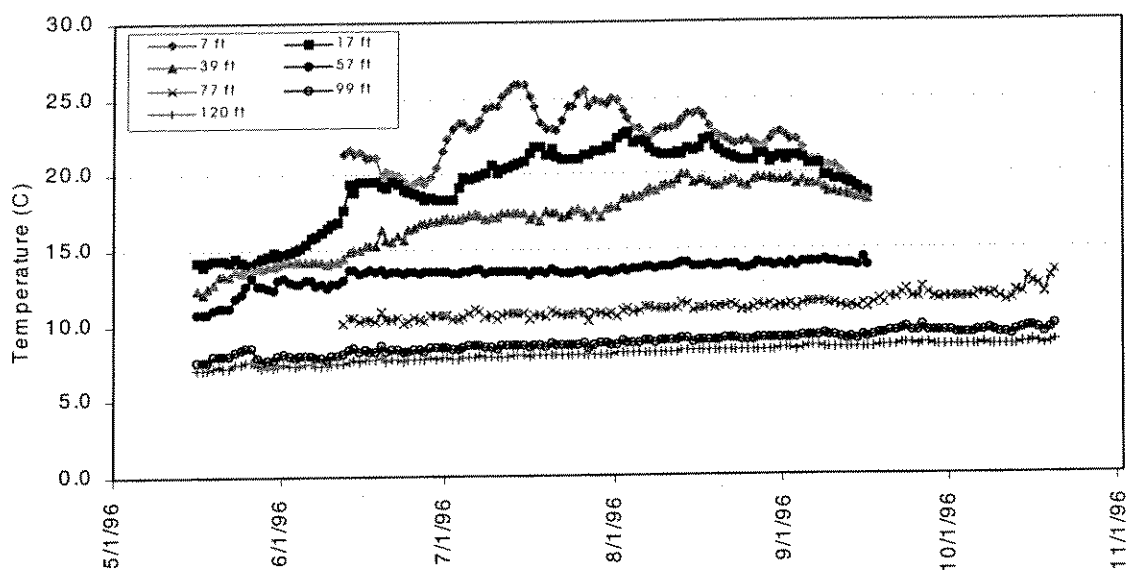
Figure 7.5   Iron Gate Reservoir measured profile water temperature, 1996
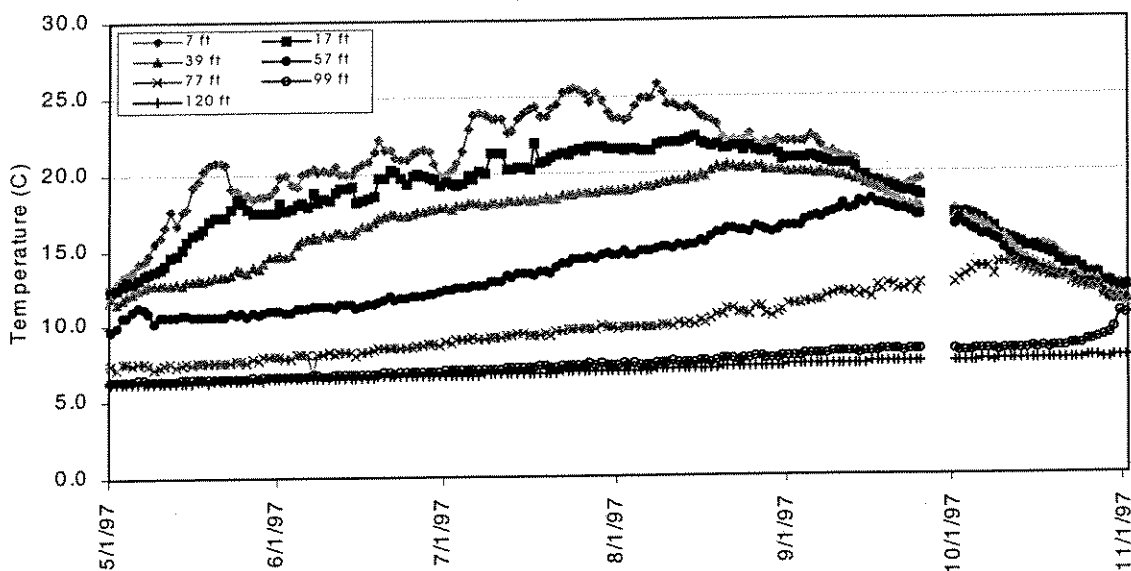
Figure 7.6   Iron Gate Reservoir measured profile water temperature, 1997

Application of WQRRS to Iron Gate Reservoir substantiated the field obsevations, as illustrated in calibration and validation (Section 6.1). Using simulated temperature results from 1996 and 1997, the variable thermal structure between the two years can be readily compared. Figure 7.7 illustrates the temperature difference (1996 minus 1997 profile temperatures). Several previously discussed issues are illustrated in the figure.

First, the cooler waters reported in field data for 1996 are apparent as the dark band (negative values) running from left to right through the figure, where temperatures up to 4°C (7.2°F) cooler occurred in 1996. Second, recall that temperatures of deeper waters (i.e., elevation 2200 ft msl) were roughly 1°C (1.8°F) warmer in 1996 than 1997: the simulation results support these field observations. Third, the warmer surface waters of 1996 are apparent by the positive isotherm values in the near-surface zone. Finally, not readily observable in the field measurements due to missing data in the fall of 1996 is the finding that the epilimnion remained warm well into fall for the 1996 period, appreciably warmer than 1997, possibly due to the relatively large number of warm days (<35°C (95°F)) during 1996 compared to 1997.
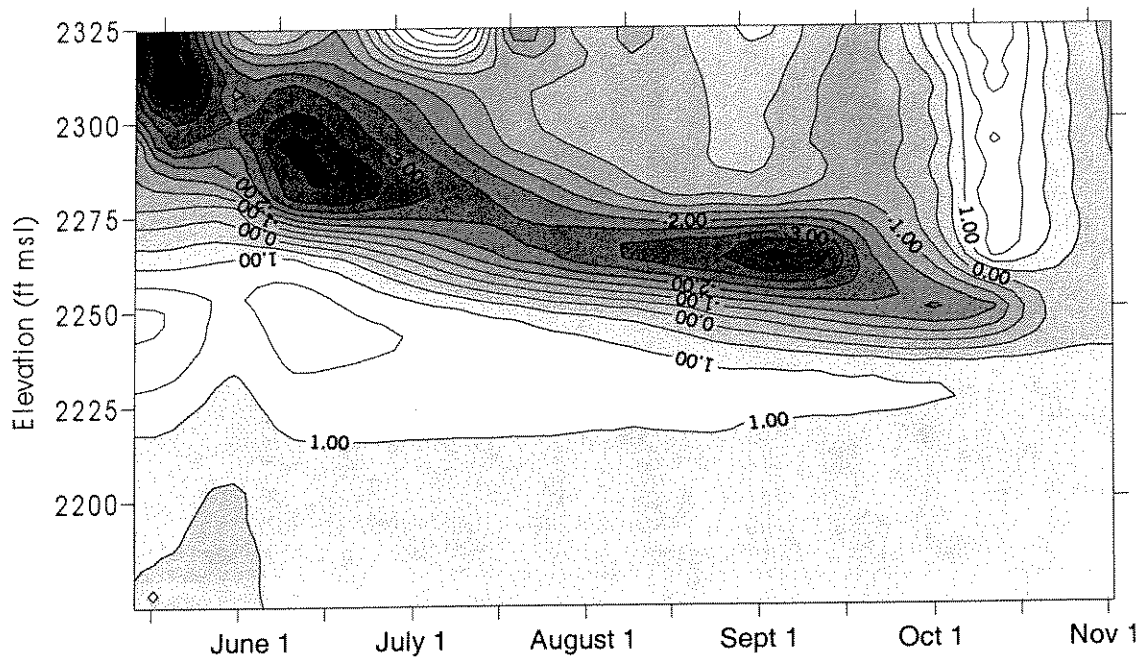
Figure 7.7   Iron Gate profile simulated temperature differences (°C) between 1996 and 1997 (1996 minus 1997)

Quantifying individual impacts of hydrology, meteorology, and operations using available field and simulated data is difficult. However, it is apparent that all three processes have

potential impacts on the year-to-year thermal structure of Iron Gate Reservoir. Of particular interest is the sensitivity of the thermal regime to relatively small fish hatchery withdrawals. These withdrawals are generally on the order of 10,000 acre-feet from June through September (roughly 120 days at 40 cfs), and during this period the hatchery uses the bulk of the accessible cool water stored in Iron Gate Reservoir.

7.2.2.3   Short-Term Response

Beyond year-to-year and seasonal variations, Iron Gate Reservoir exhibited short-term thermal response, on the order of hours, as determined by field observations. Field monitoring of Iron Gate Reservoir consisted of deploying temperature loggers at various depths (thermistor string) to record water temperatures at hourly intervals. As expected the temperature logger near the surface recorded diurnal variations in temperature. However, analysis of data gathered at greater depths produced unanticipated results. Namely, sub-daily temperature fluctuations were identified as occurring at depths up to 100 feet. Further, investigation of these fluctuations determined that they did not follow the diurnal pattern found in the near surface data.

Hourly measured data for the month of June 1997 are shown in Figure 7.8. Apparent in the data at the 57-, 77-, and 99-foot level are fluctuations that range over roughly 2°C, 3°C, and 1°C, (3.6°F, 5.4°F, and 1.8°F) respectively. Close examination shows that there are often two peaks during a single 24-hour period. The largest fluctuations occur in the vicinity of the 57- and 77-foot depths because the temperature gradient is greatest in that region during this month, i.e., in the vicinity of the thermocline (refer to Figure 6.3, July and August profiles).

Inspection of Copco Reservoir hydropower operations provided insight as to the potential mechanisms causing short-term variations at depth in Iron Gate Reservoir. Figure 7.9 illustrates hourly Copco Reservoir release for July 1997. Peaking power operations are clearly evident. Power production typically starts in the morning hours, with flow abruptly increasing to approximately 1300 cfs. Releases are terminated in the evening to conserve water for subsequent power production.

It is postulated that the impact of the abrupt onset and cessation of Iron Gate Reservoir inflow perturbs the thermocline and subsequently alters the thermal structure of the reservoir. This perturbation is most likely in the form of an internal wave or seiche. As the

142

wave passes through the reservoir it may be subject to reflection from system boundaries, e.g., reservoir walls and the dam. Variable water temperatures at deeper locations in Iron Gate Reservoir are in response to such a wave "washing" past the thermistor string.

The deepest recorded temperatures (120 ft, approximately elevation 2200) did not show appreciable response to such seiching. It is assumed that volumes stored at the extreme low levels of Iron Gate Reservoir, far downstream from the inflow location and below any outlet structures (i.e., in the vicinity of the dam), do not materially participate in such processes due to the relatively small volumes of water and the solid boundaries of the reservoir bottom.

The mechanics (e.g., amplitude, speed, and period) of internal waves were not examined in detail. Measured water temperatures below Iron Gate Dam did not exhibit the apparent strong characteristics of loggers deployed in the reservoir, but instead demonstrated only slight diurnal variations. Thus, the downstream temperature effects appear to be relatively negligible. This is probably due to the large withdrawal envelope for the power penstock intake. Impacts on fish hatchery flows may be more appreciable due of the location of the hatchery intake and its smaller withdrawal envelope. Insufficient fish hatchery data were available to ascertain potential impacts. Potential water quality impacts are discussed below.
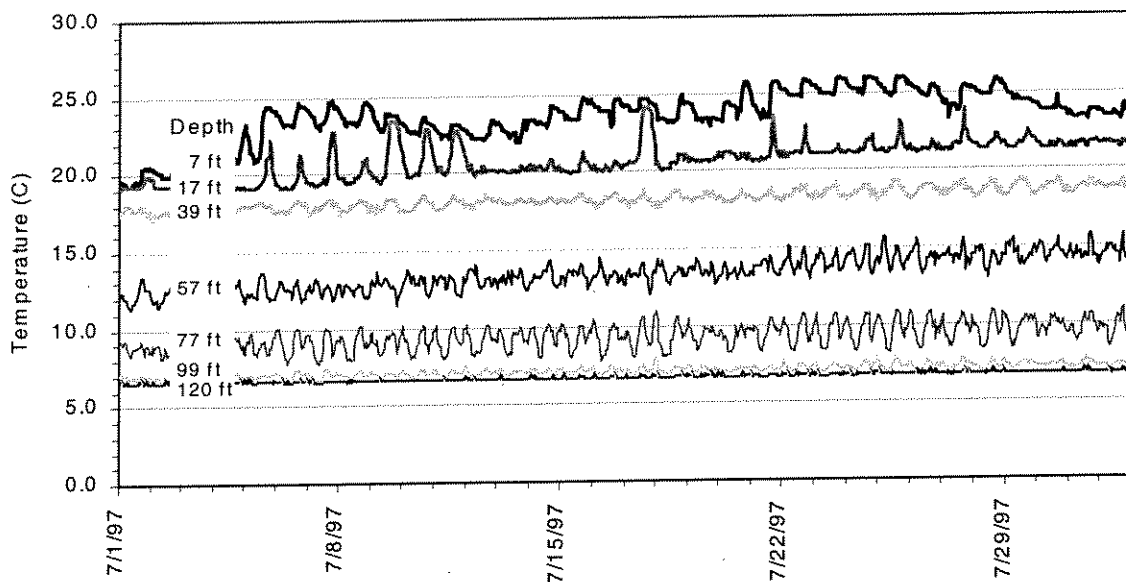
Figure 7.8   Hourly measured Iron Gate Reservoir water temperature at seven monitoring depths, July 1997
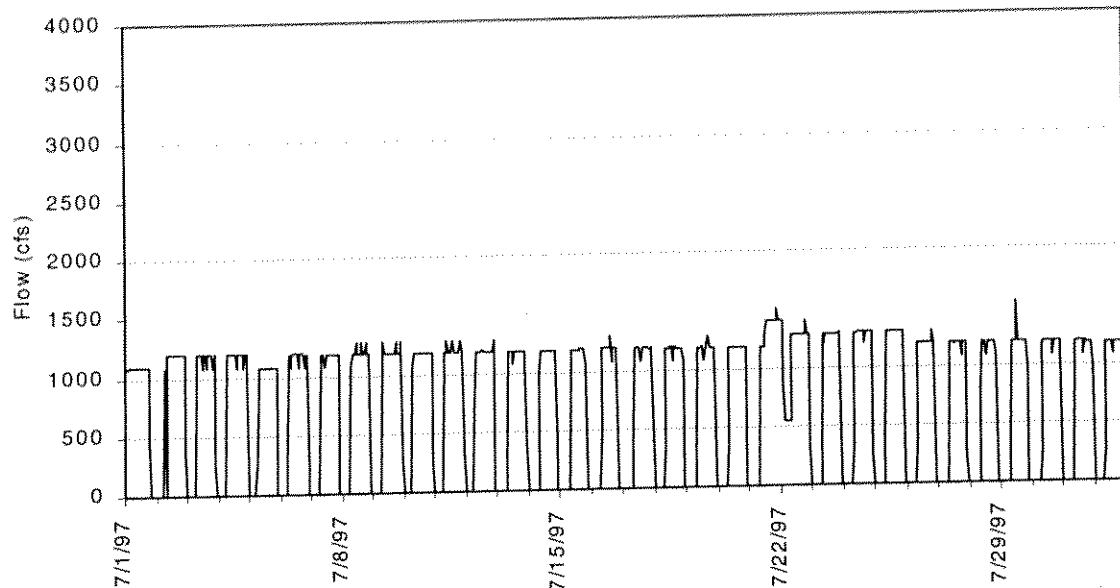
Figure 7.9   Hourly Copco Reservoir release, July 1997

7.2.3   Dissolved Oxygen

Similar to temperature, dissolved oxygen concentration is a function of meteorology, hydrology, inflow water quality, and reservoir operations.   However, temperature stratification, primary production, available organic matter, and nutrient cycling also play fundamental roles in the fate of this water quality variable.

7.2.3.1   The Role of Thermal Stratification

As noted previously, during winter periods when flows are often significant and thermal loading rate is low, Iron Gate Reservoir is in an isothermal condition.   Under these conditions there exists the opportunity for exchange of oxygen-rich waters from near surface layers to deeper layers, and appreciable dissolved oxygen may be present throughout the water column.   It is typically greater in the near surface layers because organic sediment in bottom deposits, even during cool winter periods, can exert oxygen demands on bottom waters.   With the onset of thermal stratification, mixing between surface and deeper layers (below the thermocline) is impeded and dissolved oxygen dynamics change dramatically.

In Iron Gate Reservoir, the thermocline is located below the photic zone, thus no primary production takes place in hypolimnion and the principal method of transfer for dissolved oxygen is vertical diffusion through the thermocline – a slow and inefficient process. Though cold water has a higher saturation level for dissolved oxygen, if appreciable

144

unoxidized organic matter is present, stratification will lead to depressed dissolved oxygen concentrations in the hypolimnion. Dissolved oxygen could enter deeper waters through cold water tributaries; however, no significant sources are available at Iron Gate Reservoir. Fall turnover returns the system to isothermal conditions and allows surface and bottom waters to commingle.

7.2.3.2 *Primary Production, Organic Matter, and Nutrient Cycling*

Primary production, organic matter, and nutrient cycling all play important roles in the dissolved oxygen dynamic of Iron Gate Reservoir. A general introduction to these processes as they may occur in Iron Gate Reservoir is outlined below, followed by more detailed examples of Iron Gate Reservoir responses

<u>General</u>

Primary production in Iron Gate Reservoir consists of free-floating phytoplankton and near-shore attached algae. Attached algae production is usually limited due to a narrow band of shallow, shoreline portions of the reservoir, thus it is assumed that phytoplankton (algae) dominate primary production processes. In the winter, algae populations are generally depressed due to reduced photo-periods and lower water temperatures. With increasing day length and an associated rise in water temperature, algal concentrations increase rapidly. Algal photosynthesis and respiration produces dissolved oxygen concentrations in surface waters that vary diurnally, with maximum values occurring in the afternoon and minimum values in the pre-dawn hours. In general, dissolved oxygen concentration in Iron Gate Reservoir during summer periods is greatest in the surface layers where sufficient light is available, but decreases markedly below the photic zone.

The byproduct of algal growth is death and decay. Upon death algae break down and sink in the reservoir. This algal detritus (organic) consists of oxidizeable material, and thus exerts an immediate oxygen demand on the system. Because of its physical mass, algal detritus settles through the thermocline into the hypolimnion, delivering a continuing stream of oxygen demanding material throughout the summer and fall months. Dissolved oxygen trapped beneath the thermocline is thus consumed by both organic sediment and detritus. When light is limited, a considerable oxygen demand can be exerted in the epilimnion. Settling algae can exert an oxygen demand and thereby depress dissolved concentrations above the thermocline in these cases. Other organic material may enter the system from external sources or from tributary inflow.

145

Finally, nutrient cycling can affect dissolved oxygen concentrations throughout the water column. Examples include the oxidation of ammonia to nitrite and subsequently to nitrate. This process is often referred to as nitrification and is addressed in detail in Section 4.4.6.

Iron Gate Reservoir Response
There are many aspects of dissolved oxygen conditions in Iron Gate Reservoir; however, the focus will be on three principal issues:

- Iron Gate Reservoir experiences severe anoxia during summer periods
- Dissolved oxygen concentration of reservoir releases reflects reservoir conditions
- Oxygen concentrations as modeled do not reflect spatial variations in dissolved oxygen distribution longitudinally in the reservoir

Under current operating conditions, Iron Gate Reservoir experiences anoxic conditions, i.e., no dissolved oxygen, through a considerable portion of its depth for an appreciable period of time. Figures 7.10 and 7.11 show simulated dissolved oxygen concentrations from mid-May through October for 1996 and 1997, respectively. Simulated dissolved oxygen for 1996 shows that by mid-August all but the top 70 feet of the reservoir was anoxic. This corresponds to a volume of roughly 17,000 AF, or about 30 percent of storage, of anoxic water. Further, all but the top 35 to 40 feet of the reservoir experienced dissolved oxygen less than 3 mg/l, roughly 30,000 AF, or about 50 percent of the reservoir volume. 1997 faired moderately better; the deeper thermocline due to utilization of cool bottom water for hatchery flows appears to have lead to greater oxygen concentrations deeper in the reservoir.

Reservoir withdrawal water quality is directly affected by the distribution of dissolved oxygen. Because the power penstock has a large withdrawal envelope, depressed dissolved oxygen concentration in release waters although depressed somewhat are generally acceptable. However, low dissolved oxygen content waters are not uncommon just below Iron Gate Dam, especially in the later summer months. Flow, meteorological conditions, algal dynamics, and possibly internal seiching contribute to episodic dissolved oxygen problems. On the other hand, fish hatchery releases are from depths that commonly reach extremely low or zero dissolved oxygen concentrations. To overcome this problem, an aerator is employed by the hatchery to effectively bring concentrations close to saturation prior to use.
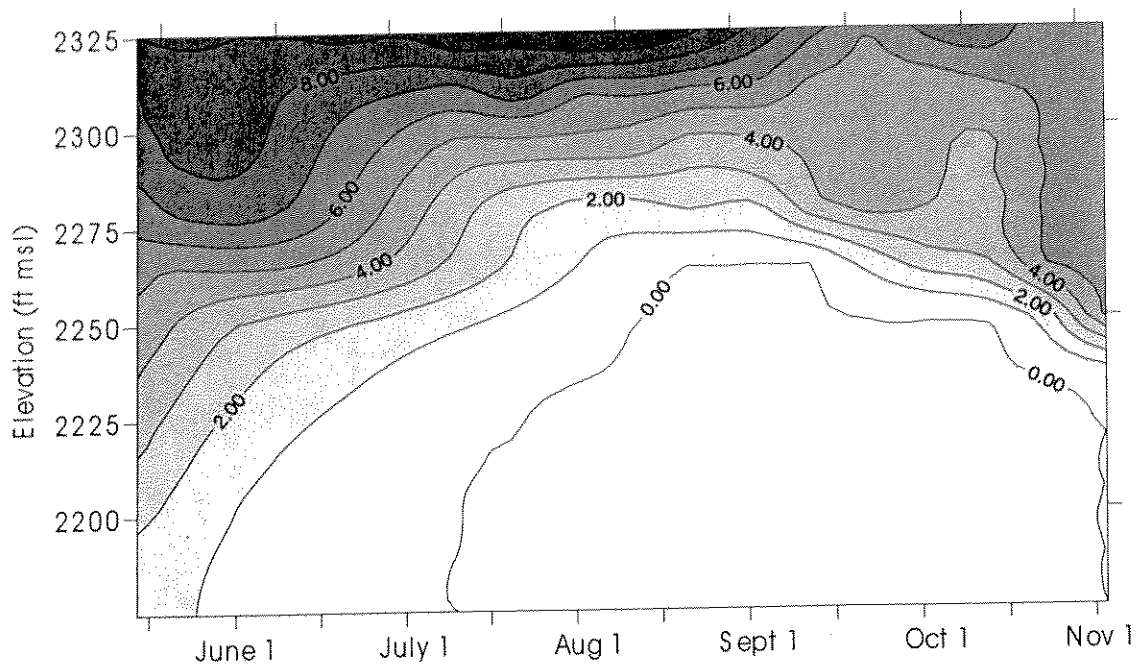
Figure 7.10 Simulated mean daily dissolved oxygen (mg/l) for Iron Gate Reservoir, May-
October 1996
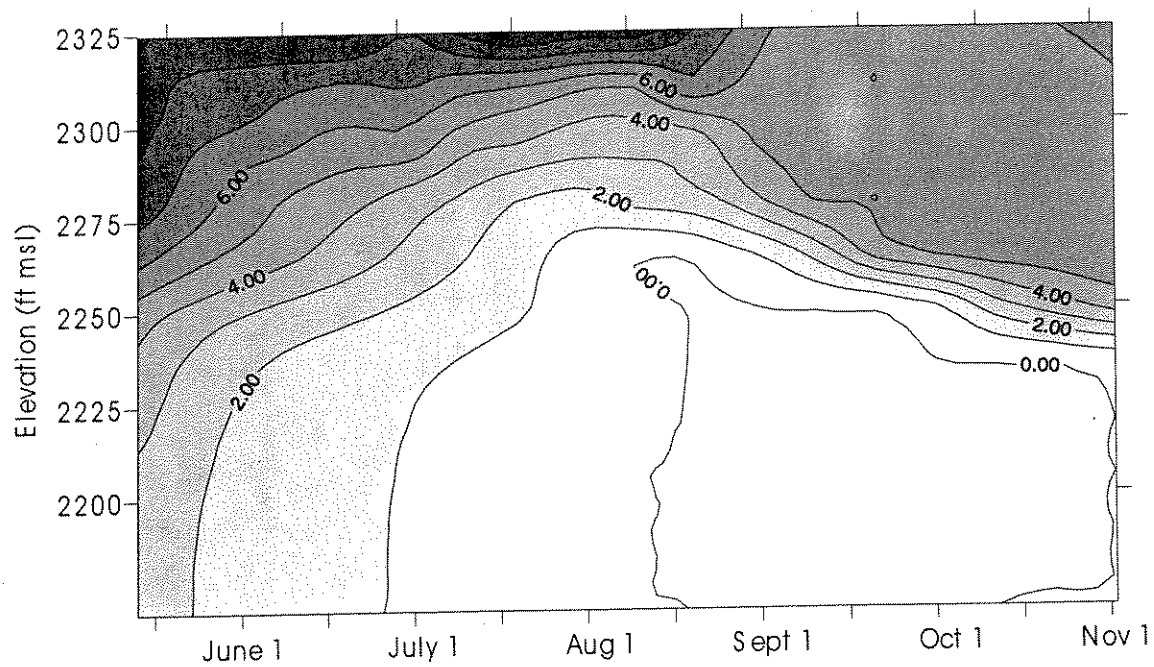
Figure 7.11 Simulated mean daily dissolved oxygen (mg/l) for Iron Gate Reservoir, May-
October 1997

147

Finally, review of NCRWQCB data for the 1996 and 1997 field seasons illustrates that dissolved oxygen concentrations may vary spatially in the reservoir. Figure 7.12 shows NCRWQCB measured profiles for May 15, 1996 at four locations; in the vicinity of the dam and at three locations spaced at approximately 2 mile increments upstream. It is clear that even at significant depth the profiles are not coincident. The profile at roughly 6 miles upstream is approximately homogeneous, 8 mg/l from surface to bottom. This location, near the shallow, upper end of the reservoir, is most likely affected by Copco Reservoir releases, which provide waters of near constant temperature and uniform dissolved oxygen concentration. Further, it is likely that the turbulent mixing in the reach just below Copco Reservoir locally prevents the development of stratification.
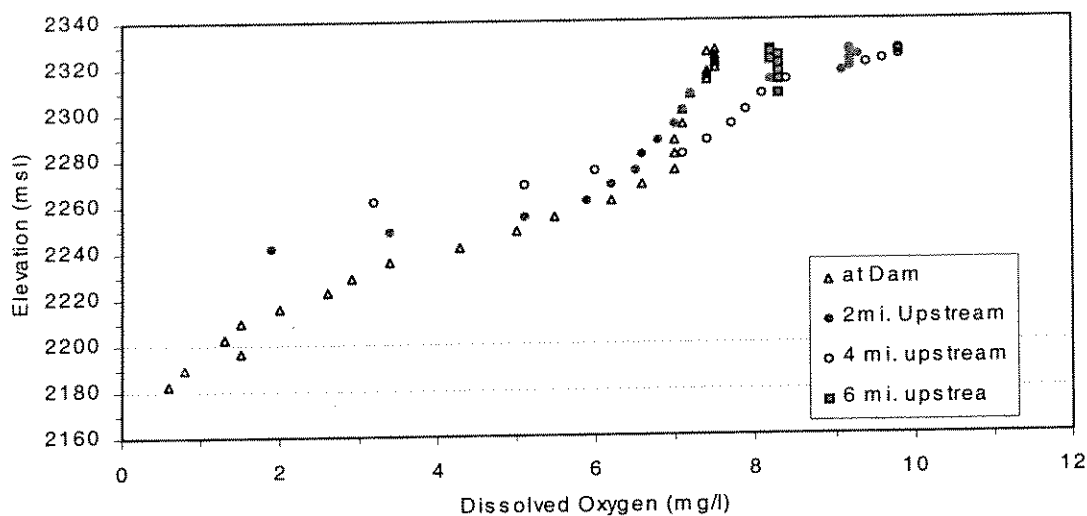
Figure 7.12 NCRWQCB measured dissolved oxygen profiles at four locations in Iron Gate Reservoir: May 15, 1996

Figure 7.13 shows dissolved oxygen profiles at the same locations on August 21, 1996. Apparently primary production in surface waters elevated dissolved oxygen concentrations up to nearly 140 percent of saturation. However, at the upstream end of the reservoir, dissolved oxygen concentration is approximately 6 mg/l from surface to bottom, reflecting the influence of Copco Reservoir releases.

Anoxic conditions extend well above elevation 2300 ft msl during August 1996. However, there was a pocket of dissolved oxygen trapped beneath the thermocline near the dam that extends from elevation 2270 to 2310 ft msl – a thickness of approximately 40 feet. Moving two miles up the reservoir the thickness of this pocket decreased significantly to about 10 or 15 feet, and it was not detected at locations further upstream. Unlike thermal stratification,

148

which is generally consistent in the horizontal direction throughout all but the shallow areas of the reservoir, dissolved oxygen exhibits variability in the horizontal plane. As noted in Section 6.1.4, this pocket of dissolved oxygen is a relic of spring time conditions when oxygen concentrations were appreciable throughout much of the reservoir profile. The model WQRRS does not represent these lateral variations in dissolved oxygen (or temperature for that matter), but only provides a general description of laterally averaged conditions.
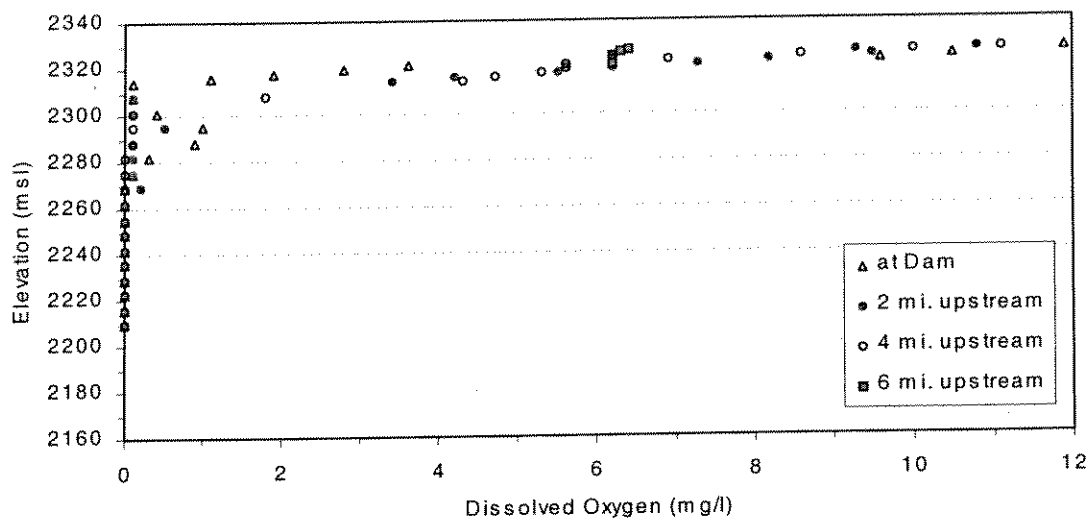
Figure 7.13   NCRWQCB measured dissolved oxygen profiles at four locations in Iron Gate Reservoir: August 21, 1996

Conditions in 1997 followed similar trends. It appears that the impact of fish hatchery withdrawals during summer 1997 resulted in a deeper thermocline, maintaining the maximum extent of anoxic conditions to elevations below 2290 ft msl. Additional data collection and analysis is necessary to further define the response of dissolved oxygen to operations, meteorological conditions, primary production, and other pertinent processes.

7.2.4   Other Water Quality Variables: Algal Dynamics

As noted above, primary production, organic matter, and nutrient cycling play important roles in reservoir water quality. Although little measured data were available for analyses, model simulations provided insight into system processes. These responses are presented herein with respect to algal dynamics, because primary production directly influences dissolved oxygen in surface waters, is a source of organic matter (death and decay), and affects nutrient concentrations.

149

Using simulation results from 1996, the relationships between algae, dissolved oxygen, ammonia nitrogen and nitrate nitrogen were explored. Figure 7.14 illustrates reservoir profile concentrations for the four constituents of interest in descending order (top-to-bottom). Starting with algae, it can be seen that algal concentrations are modest in the early summer months and peak in early July. Concentrations are limited to the photic zone and are maximum in the near surface waters. Concentrations begin to decrease in late August, primarily in response to reduced day length. By October algal concentrations have dropped to the point that they no longer significantly impact water quality, except for localized, short-term events.

Comparing algal production with dissolved oxygen concentrations in the reservoir, it is apparent that primary production maintains dissolved oxygen concentrations in the range of 8 mg/l to 9 mg/l in near surface waters throughout the summer period. When algal populations begin to decline in late summer to early fall, dissolved oxygen concentration in near surface waters drop to below 6 mg/l. Settling of material through the water column depresses dissolved oxygen concentrations in deeper waters. As illustrated in Figure 7.14, simulated hypolimnetic anoxic conditions in response to this seasonal influx of organic material first appear in early July and extend through October.

Both ammonia and nitrate nitrogen are available for uptake by algae. The response of these two nutrients in the near surface waters directly related to primary production. Specifically, as algal concentration and corresponding uptake increase, surface waters become depleted of both ammonia and nitrate. When algal populations diminish in the fall, concentrations of these nutrients return to higher levels. Nitrate is diminished to the point that for certain summer periods it may be limiting; however, with ammonia available it appears such conditions are probably short-lived and local. Deeper reservoir waters experience different processes due to lack of primary production and anoxic conditions. Under such conditions, the conversion of ammonia to nitrate is suspended. Thus, hypolimnetic ammonia concentrations increase from zero, when oxygen is present, to positive values through the summer and into the fall months when anoxic conditions dominate, as illustrated in Figure 7.14. If released, these waters would exert a nitrogeneous oxygen demand in downstream river reaches. Because nitrate is the end product of nitrification, it is expected that concentrations are expected to increase hypolimnetic waters through the summer and fall period; however, proceeding more slowly later in the season due to reduced contributions from ammonia under anoxic conditions. Simulation results support these assertions.

150

Though not discussed here, phosphorus (orthophosphate) responds similarly to nitrate. During peak algal production months, surface water concentrations of orthophosphate are reduced, while hypolimnetic concentrations slowly increase through the summer period.

Finally, nutrient concentrations will be elevated in the lower level of the epilimnion and thermocline because this region is below the photic zone available nutrients are not utilized by algae. Further, because effective diffusion is suppressed in the region of maximum density gradient (i.e., the thermocline), transfer of these dissolved constituents into the hypolimnion is slow. (Simulated results from 1997 illustrate similar system response for Iron Gate Reservoir.)

7.2.5   Copco Reservoir

Copco Reservoir is located just under two miles upstream of Iron Gate Reservoir. Copco Reservoir is smaller than Iron Gate, with maximum storage and depth of roughly 47,000 acre-feet and 107 feet, respectively. Full pool elevation is 2607.5 ft msl and turbine intake elevation is 2571 ft msl.

Iron Gate Reservoir water quality is directly related to Copco Reservoir water quality. Review of NCRWQCB data reveals that Copco Reservoir responds similarly to Iron Gate Reservoir: experiencing strongly stratified conditions and anoxia in the hypolimnion during the summer months. Unlike Iron Gate Reservoir, there are no low level withdrawals (e.g., fish hatchery) from Copco Reservoir. As such, releases are moderated in temperature and experience dissolved oxygen concentrations below saturation. Moreover, penstock elevation is such that release temperatures are comparable to Iron Gate Dam release temperatures: on the order of 21 to 22°C (69.8 to 71.6°F). The reach between Copco Dam and Iron Gate Reservoir is sufficiently short that heating is probably modest and recovery of dissolved oxygen concentrations incomplete. Thus, Copco Reservoir, in terms of water quality, does not supply appreciable benefit to Iron Gate Reservoir under current operations. The impact of hydropower operations at Copco Reservoir, and the role of Copco #2, on Iron Gate Reservoir inflow water quality is unknown. Additional water quality monitoring and study of Copco Reservoir, as well as reservoir inflow and outflow, are required to more completely characterize the impact on downstream releases. Additional details on Copco Reservoir release water quality can be found in Appendices B.5.4 and B.9.5.
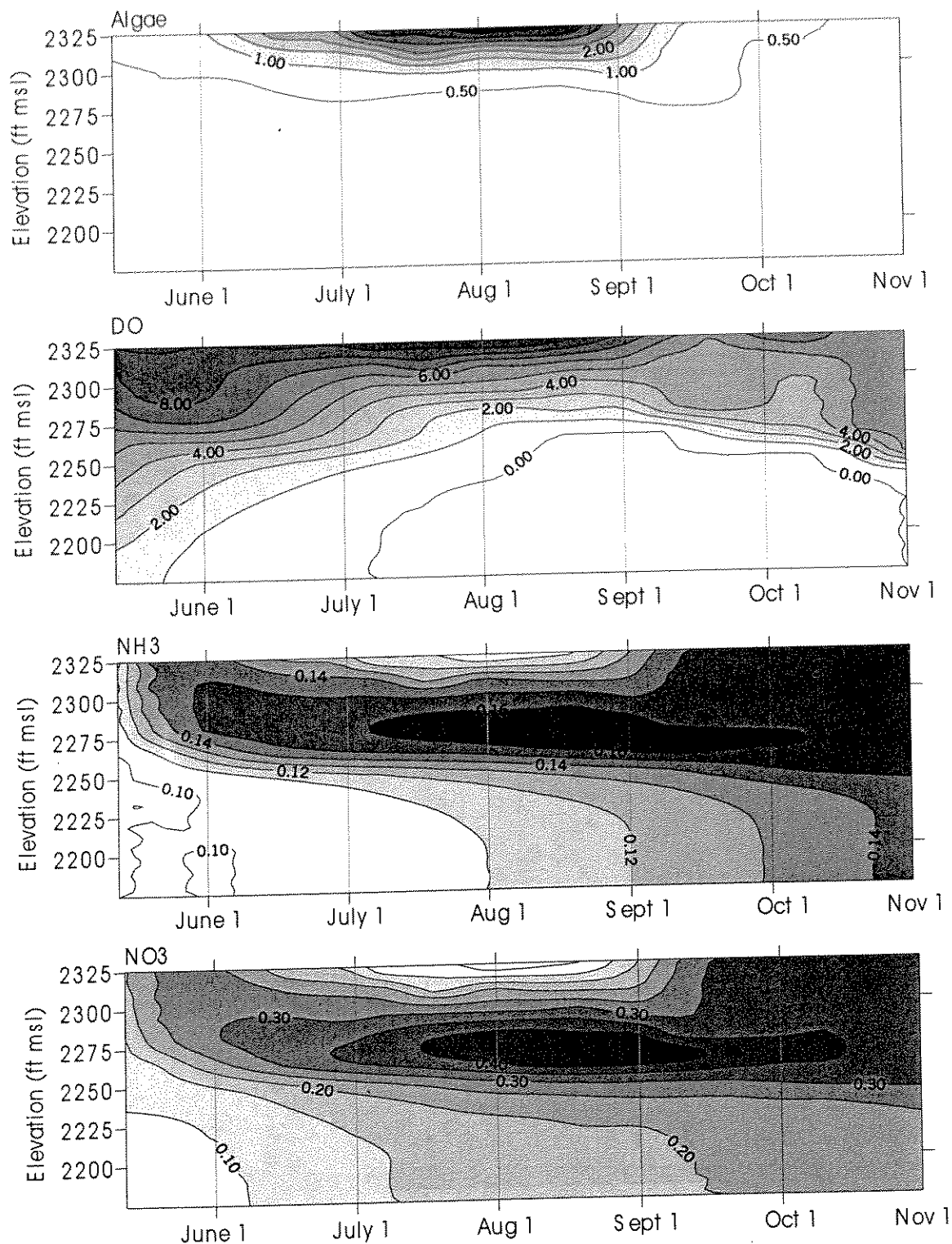
Figure 7.14 Iron Gate Reservoir algae, dissolved oxygen, ammonia (NH3), and nitrate (NO3⁻) concentrations, June-October 1996. All values in mg/l.

7.3 Klamath River

Klamath River water quality is a function of hydrology, upstream operations, tributary inflows, and meteorological conditions. Variations in water quality range from sub-daily cycle to long-term seasonal response. Unlike Iron Gate Reservoir, residence time in the river study reach is significantly shorter, on the order a day or two depending on flow conditions. Further, the relatively shallow depth and turbulent nature of the river precludes appreciable thermal stratification. In the following discussion, flow and travel time issues are introduced, and water temperature and quality issues are outlined with respect to flow, upstream operations and tributary influence.

7.3.1 Travel Time

Travel time can be thought of as residence time, thus it affects water temperature and other quality parameters. Flow directly affects travel time in the Klamath River below Iron Gate Dam. For example, a cool water release from Iron Gate Dam at a low flow rate (e.g., 800 cfs) may experience two days of net thermal loading enroute to Seiad Valley. At higher flow rates (e.g., 4000 cfs) the release would experience roughly one day of net thermal loading.

Travel time is affected by tributaries and other accretions that incrementally increase base flow in the downstream direction. Seasonally, tributaries and accretions vary dramatically, providing significant base flow additions in the winter and spring, while contributing relatively minor quantities in the summer and fall.

River geometric considerations can affect travel time as well. Slope and cross-section may affect travel time at various flow rates. Bed slope within the study reach is nearly constant so the river experiences a fairly steep, but uniform descent from Iron Gate Dam to Seiad Valley. Further, channel cross-sections vary slightly and flood plains are either absent or small, and much of the river is constrained by paralleling roads, confined canyons, or narrow valleys. Thus, at the range of flows experienced from late spring through fall, geometric considerations are considered to be of minor importance.

In the following discussion of water temperature and other water quality variables, travel time will be revealed as a major factor governing the fate of non-conservative constituents (e.g., those that undergo transforms from one species to another).

153

7.3.2   Water Temperature

Water temperature in the study reach is a function of meteorological conditions, reservoir operations, and tributary contributions of heat. Other factors, either directly or indirectly influencing water temperature, include river depth and surface width, accretions, bed conduction, and riparian and topographic shading. Changes in depth and width over the range of flows analyzed will be discussed under operations in terms of flow ramping effects. Because information on accretion quantity, temperature and quality are unknown, these impacts were not specifically examined. Further, it was assumed that the riverbed was in thermal equilibrium with overlying water, so bed conduction could be considered negligible. Finally, Although identified as a potentially important form of water temperature control in the original proposal, riparian shading was not assessed in this project. The impact of riparian vegetation shading on Klamath River main stem water temperatures is unknown. Appreciable river width, limited restoration opportunities, and over-riding effects of topographic shading may limit its effectiveness as a sole source of main stem temperature control.

7.3.2.1   Meteorological conditions

Meteorological conditions affect river temperatures seasonally, over short periods (e.g., "cold" or "hot" spells), as well as over the daily cycle. Unlike Iron Gate Reservoir, the Klamath River responds relatively quickly to changes in meteorological conditions, especially under low flow rates and long transit times. To illustrate the impacts of seasonal and short-term changes, measured mean daily Klamath River water temperatures at three locations are shown in Figure 7.15: below Iron Gate Dam (RM 190.1), below the Shasta River (RM 176.4), and below the Scott River (RM 142.5).

Seasonal variations are apparent as river temperatures rise from 16°C (60.8°F) to 18°C (64.4°F) in the spring to 22°C (71.6°F) to 24°C (75.2 °F) by mid-summer, and then decline below 16°C (60.8°F) by early October. The overall rise and decline in water temperature through the spring, summer, and fall months is subject to short-term fluctuations on the order of several days. Under regulated flows these fluctuations may be due to meteorological conditions, tributary influences, or combinations of the two. Periods of cool weather can depress water temperatures, while warm weather may increase water temperatures. In some cases, warm weather may result in locally decreased water temperature as increased rates of snowmelt water enter the system, e.g., the Scott River basin.
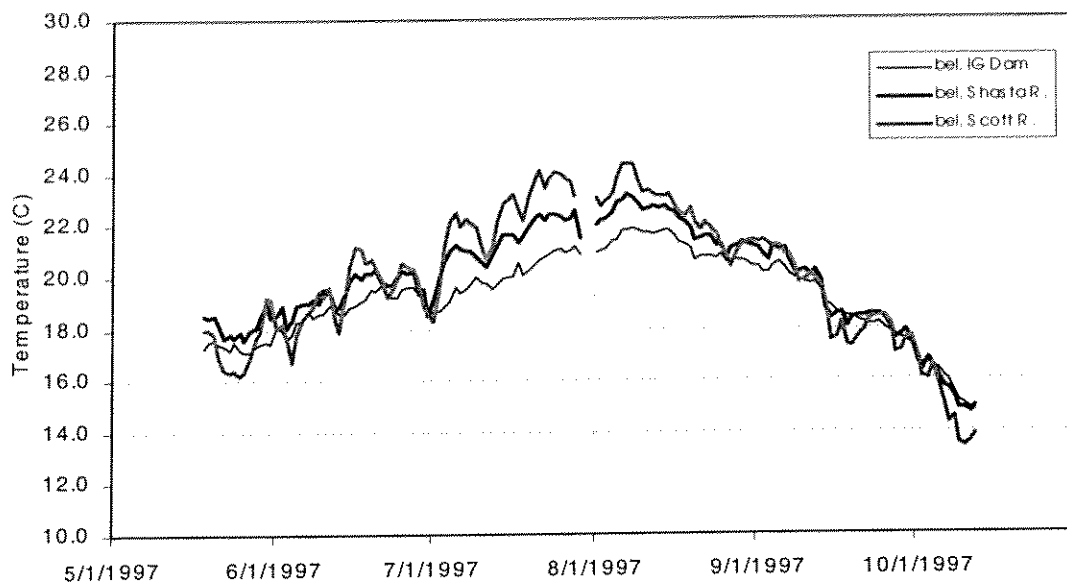
Figure 7.15 Measured mean daily water temperature below Iron Gate Dam, Shasta River, and Scott River, 1997

Comparing water temperature at the three locations, it is noted that Scott River temperatures are lowest in the late spring. During this period, the Scott River has flows on par with the main stem, derived primarily from snowmelt, thus maintaining cool temperatures in downstream reaches. During summer, releases from Iron Gate Dam are the coolest. The moderating effect of Iron Gate Reservoir provides a near-constant temperature release to the Klamath River, which subsequently begins to heat (or cool) as waters move downstream. The result is successively higher and more variable mean daily temperatures in the downstream direction, as depicted in Figure 7.15. Variability increases with distance from Iron Gate Dam as increased travel time assures longer exposure of river waters to meteorological conditions.

During early fall, mean daily measured water temperatures are fairly uniform throughout the river system. However, by late fall it is apparent that temperatures are decreasing in the downstream direction by late fall, i.e., after October 1. During this period, releases from Iron Gate Dam are generally at temperatures above equilibrium and the reservoir is acting as a heat source to the river (see also Figure 7.21).

Meteorological conditions also affect the diurnal temperature response of the river. Seasonally, the diurnal range in water temperature is smallest in winter and largest in

155

summer. Figure 7.16 shows the measured mean, maximum, and minimum daily water temperature for the Klamath River below the Shasta River. The difference between the maximum and minimum daily temperatures steadily increases to about 5°C (9°F) by late summer, then decreases to about 2°C (3.6°F) by mid-October. The impact of short-term meteorological conditions on the diurnal range of temperature is depicted as transient expansions and contractions of the maximum/minimum envelope.
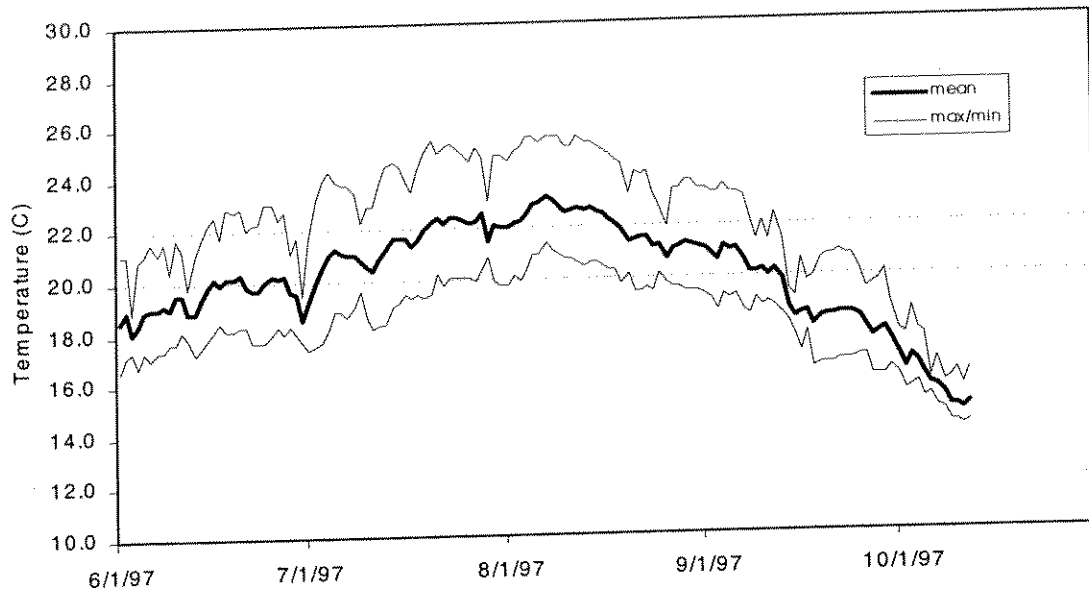
Figure 7.16 Measured Klamath River daily mean, maximum, and minimum measured temperature below the Shasta River, 1997

Finally, meteorological changes from year-to-year affect Klamath River water temperature. Examining Figure 7.17 (a) it appears that meteorological conditions during July and August 1996 resulted in warmer water temperatures below Iron Gate Dam. However, examination of Figure 17.17 (b), a comparison of measured mean daily measured Klamath River water temperatures below the Scott River, suggest that the relationship between the annual experiences is less clear. It appears that 1996 experienced more extreme water temperatures, but perhaps was more meteorologically diverse than 1997. In addition, flow conditions through the river differed for the two years: mean flow rate for the months of July through September was 1230 cfs in 1996 and 1035 cfs in 1997. Perhaps a lower flow regime in 1997 somewhat offset meteorological conditions through reduced depths and longer transit times to the Scott River confluence (i.e., increased heating).

156
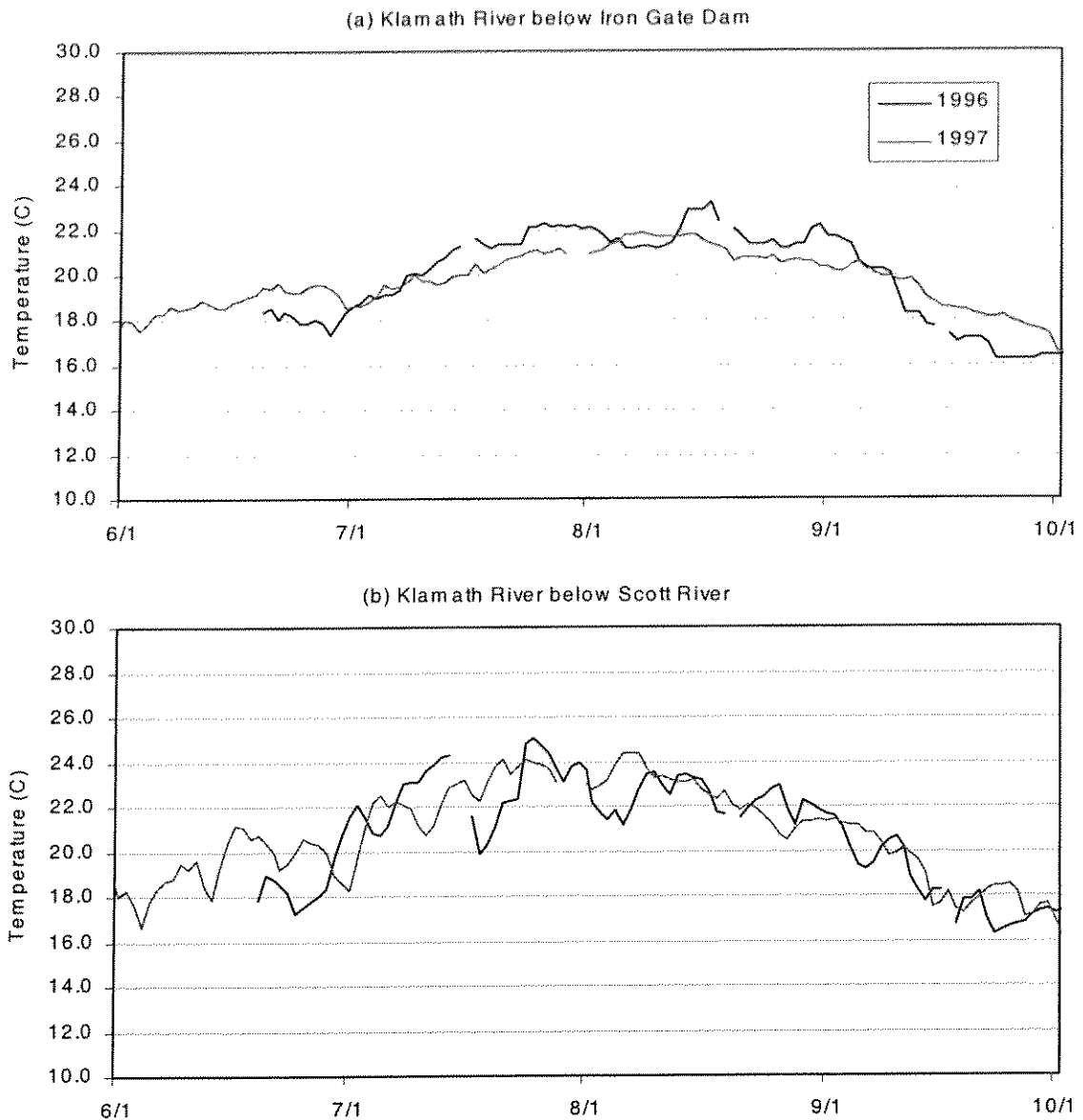
Figure 7.17 Comparison of 1996 and 1997 Klamath River mean daily measured water temperature: (a) below Iron Gate Dam, (b) below Scott River

7.3.2.2 Operations

Operations govern release quantities and temperatures from Iron Gate Reservoir. Releases are regulated throughout the year to the extent consistent with power production objectives. When high flow events occur in the basin, the spillway at Iron Gate dam is used to bypass flows in excess of desired penstock withdrawals. From late spring through fall, spills are rare and flows follow a highly regulated structure. Table 7.2 presents approximate monthly reservoir releases for June through September 1996 and 1997.

157

Table 7.2   Iron Gate Reservoir releases

Year	Flow (cfs)			
	June	July	August	September
1996	1530	1040	1060	1320
1997	1240	820	1060	1035

Due to the size and outlet structure of Iron Gate Reservoir, releases during the late spring through fall are at nearly constant temperature from day-to-day. Figure 7.18 illustrates measured daily mean, maximum, and minimum measured water temperature below Iron Gate Dam for June through September 1997. Comparing Figure 7.18 with Figure 7.16, it is apparent that Iron Gate Dam provides significant water temperature moderation, with daily variations on the order of ±1°C (1.8°F). The impact of this regulated, nearly constant temperature release is two-fold. First, because there is no appreciable diurnal signal in the release it is of interest to know how far downstream these conditions persist, i.e., at what point does a "normal" diurnal signal occur? Second, such conditions predispose the river to zones of minimum diurnal temperature variation. Actually, the two issues are directly related.
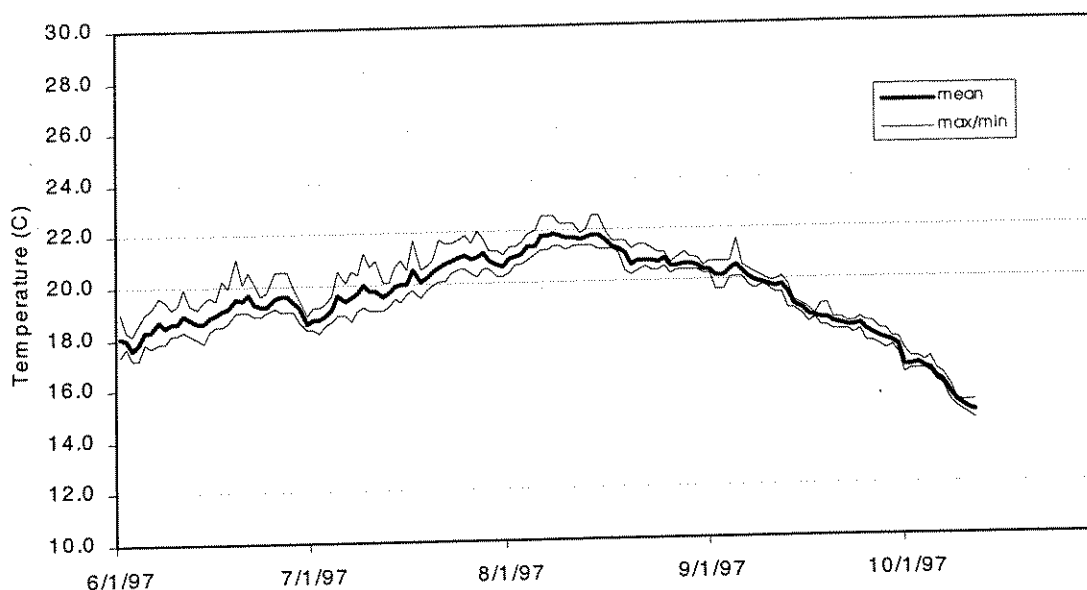
Figure 7.18   Klamath River daily mean, maximum, and minimum measured temperature below Iron Gate Dam, 1997

Zones of minimum diurnal temperature variation are defined as locations along the river where the range in diurnal temperature variation is notably less than locations upstream and downstream. To support the observations of such zones, consider a constant discharge and discharge temperature from Iron Gate Dam during a representative week of the summer season. A parcel of water released at sunrise that travels downstream a distance corresponding to one day's travel time, would be warmed (and cooled) over one diurnal cycle. Similarly, a parcel released in the evening would first experience nighttime cooling, then warming the following day. Because meteorological conditions in the region are nearly uniform from day to day during the summer season, subsequent parcels released from Iron Gate Dam would experience approximately the same net heat gain or loss over a one-day travel time. Therefore, all parcels of water arriving at a location one-day's travel downstream would have approximately the same temperature throughout the diurnal period. The result is a zone of minimum diurnal temperature variation, a "node," one day's travel time downstream. However, at one-half days travel there would be a maximum difference in temperature between parcels released at one-half day intervals; an "anti-node." Under ideal conditions, these zones would repeat at one-day intervals downstream. Under more typical conditions, the pattern is degraded through distance by tributary influences, accretions, variable meteorological conditions, and release temperature and/or quantity changes.

The locations of such zones of minimum and maximum temperature range, nodes and anti-nodes, are a function of travel time at the mean velocity of river flow. Longer transit times lead to increased exposure to atmospheric conditions and subsequent increases in overall heat gain in the Klamath River between Iron Gate Dam and Seiad Valley. A zone of minimum diurnal temperature variation was apparent in model results and measured data.

Figure 7.19 shows a longitudinal profile of daily mean, maximum, and minimum simulated water temperature for August 7, 1997 from Iron Gate Dam to Seiad Valley. A node of minimum diurnal variation is evident at approximately river mile 160, denoting the one-day travel time downstream of Iron Gate Dam. Correspondingly, offset from the zone of minimum diurnal fluctuation (node) by roughly 12 hours (a half day's travel time) are zones of maximum diurnal variation (anti-node), one of which lies in the vicinity of the Shasta River, while the other lies downstream near the Scott River. Thus, under typical summer flow conditions a full diurnal pattern is imposed in the river by the time the release waters reach the mouth of the Shasta River, or soon thereafter. Under higher flow conditions, the zone of minimum diurnal temperature variation would be shifted downstream to correspond

159

with the decreased travel time at mean river velocity. Accordingly, the zone of maximum diurnal variation would be shifted downstream. The location of the zone of maximum diurnal variation is a function of day length (season) and other factors, and is thus only approximately located plus or minus 12 hours from nodes of minimum temperature variation.
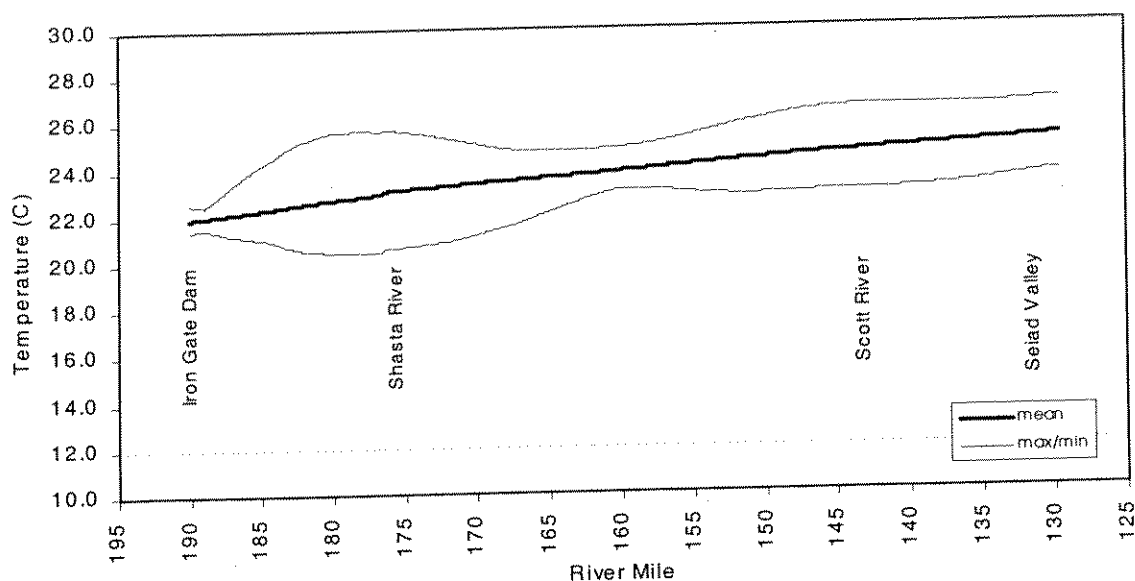
Figure 7.19 Simulated mean, maximum, and minimum daily longitudinal temperature profile for the Klamath River from Iron Gate Dam to Seiad Valley: August 1, 1997

Field observations support the simulation results. Figure 7.20 shows measured daily mean, maximum, and minimum water temperature at five locations for August 1, 1997 from Iron Gate Dam to below the Shasta River. While intermediate locations such as Little Bogus Creek show a suppressed diurnal cycle (i.e., small range in the daily maximum-minimum temperature envelope), diurnal range continues to grow in the downstream direction, reaching a maximum at roughly the Shasta River. Near Lime Gulch, downstream of the Shasta River, the daily maximum-minimum temperature envelope begins to contract. These field observations coupled with those from downstream locations effectively reproduce the node and anti-node of minimum and maximum diurnal temperature variation represented in Figure 7.19. Also evident in Figure 7.19 is that releases from Iron Gate Dam in early August 1997 were below equilibrium temperature. The rise toward equilibrium temperature through distance shows a net gain in river temperature of over 3°C (5.4°F) over the 60-mile study reach.

160
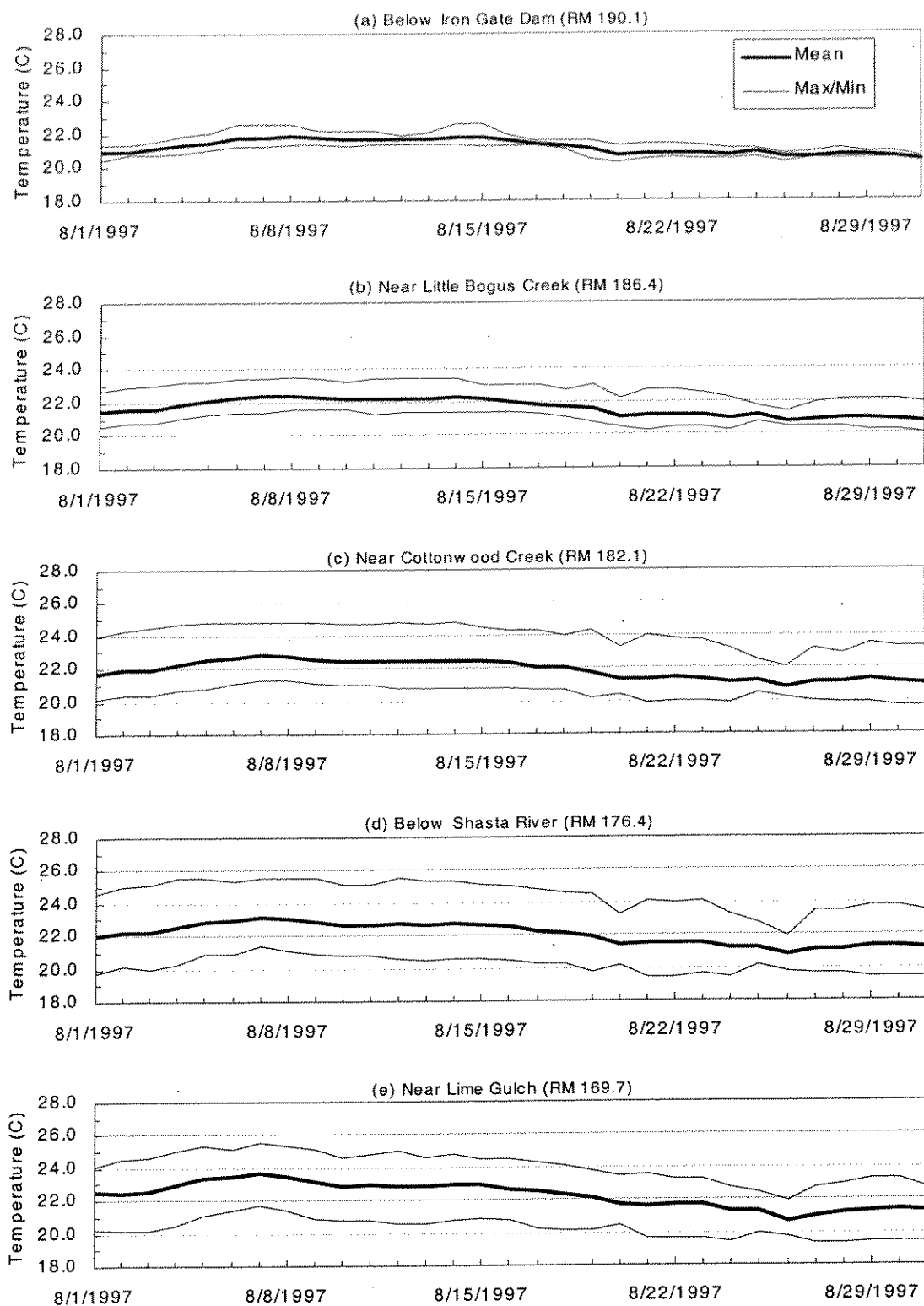
Figure 7.20 Klamath River measured daily mean, maximum, and minimum temperature (a) below Iron Gate Dam, 1997, (b) near little Bogus Creek, (c) near Cottonwood Creek, (d) below the Shasta River: August 1997, and (e) near Lime Gulch.

7.3.2.3   Tributaries

Tributary influences on main stem temperatures are seasonally important. During much of the summer and fall, tributaries and ungaged accretions are small in relation to the main stem flow. Locally, these tributaries may have an impact, but generally they contribute neither substantial cool nor warm waters to the system. However, in spring certain tributaries contribute significant inflow. For example, Scott River flows are appreciable and cool, derived from snowmelt runoff in the Marble mountains, and have a notable impact on the Klamath River downstream of the confluence. Conversely, the Shasta River is regulated by Dwinnell Reservoir, is heavily utilized for agriculture, and experiences a smaller, more moderate snowmelt runoff hydrograph. By mid- to late spring, the river base flow drops appreciably in response to irrigation demand and contributions to the main stem are minor. However, the termination of irrigation season in late fall results in increased inflow from both the Shasta and Scott Rivers. These modest rivers have small thermal mass compared to the Klamath River (and Iron Gate Reservoir), and thus can cool quickly to provide local thermal relief to the main stem. For example, during fall periods it is common for daily mean water temperature of the Shasta and Scott Rivers to be colder than the main stem Klamath. Figure 7.21 illustrates a longitudinal profile of simulated mean daily temperature for October 10, 1999. The Shasta River reduced main stem temperatures by roughly 1°C (1.8°F), while the impact of the Scott River is smaller because it is roughly 30 miles downstream from the Shasta River and the main stem has cooled appreciably in the interim. It is notable that in the summer period (see Figure 7.19) the impact of tributaries is imperceptible. In contrast, during the fall period in 1997, Iron Gate Reservoir was acting as a heat source to the river (Figure 7.19): meteorological conditions were such that releases from the dam cooled with distance downstream.
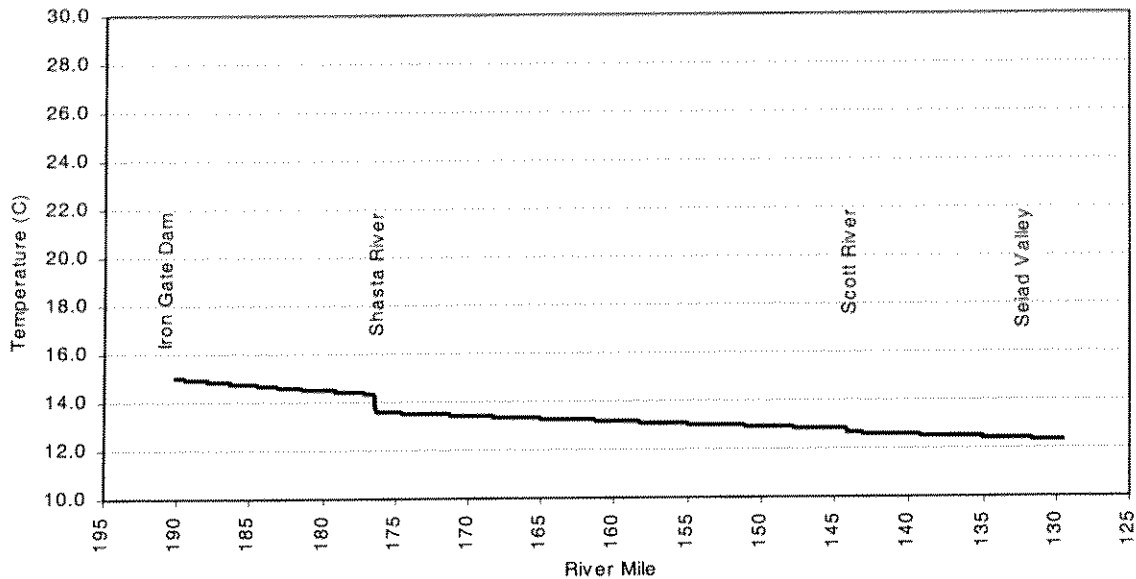
Figure 7.21 Simulated mean daily longitudinal temperature profile for the Klamath River from Iron Gate Dam to Seiad Valley: October 10, 1997

7.3.3 Dissolved Oxygen

Dissolved oxygen concentration in the study reach is primarily a function of reservoir release, tributary quality and quantity, and primary production. Other factors either directly or indirectly influencing dissolved oxygen include river depth and width, meteorological conditions, and accretions. Depth and width affect re-aeration but do not appreciably change under the reasonable range of flows expected during critical summer and fall months. Both seasonal and short-term meteorological conditions may affect primary production, thus impacting dissolved oxygen concentrations. These conditions, other than general consideration of day length and cooler or warmer water temperatures, are not addressed. Finally, because information on accretion quality was unknown these impacts were not examined. This discussion focuses on the impacts of upstream releases, tributary influences, and the impact of primary production on dissolved oxygen.

7.3.3.1 Reservoir Releases

Iron Gate Reservoir releases can impact downstream reaches in several ways. First, releases of water that is significantly below saturation concentration may adversely affect downstream aquatic habitats. Second, release of unoxidized organic material can impose an oxygen demand on the downstream system. Finally, release of available nutrients can lead to increased algal growth downstream, which in turn may impact dissolved oxygen. The

163

impact of unoxidized organic matter on downstream dissolved oxygen concentrations is not discussed due to lack of field observations, while primary production will be addressed in Section 7.3.3.3, below.

NCRWQCB dissolved oxygen data indicate that Iron Gate Reservoir releases experience increasingly depressed dissolved oxygen concentration throughout the summer and fall months below Iron Gate Dam. Figure 7.22 shows both saturation and dissolved oxygen concentration in mg/l for 1996 and 1997. A trendline has been added to the percent saturation data to illustrate the decrease from roughly 100 to 80 percent saturation over the spring-summer-fall period. The two years indicate consistent responses to sub-saturation releases from Iron Gate Dam, with absolute dissolved oxygen concentrations falling as low as 6 mg/l in fall months.

Depressed dissolved oxygen concentrations are a function of reservoir water quality dynamics. As noted previously, as the summer progresses, thermal stratification and primary production in Iron Gate Reservoir lead to increasingly anoxic conditions. Penstock withdrawals from deeper waters (i.e., non-surface) of Iron Gate Reservoir incorporate ever increasing amounts of anoxic or low dissolved oxygen waters, resulting in the trend illustrated in Figure 7.22. It is presumed that breakdown of thermal stratification, i.e., fall turnover, results in a more completely mixed reservoir condition, leading to increased dissolved oxygen concentrations at greater depths and resulting in increased concentrations in releases.

7.3.3.2   Tributary Influences

Dissolved oxygen concentrations of tributaries are not well characterized. Long- and short-term dissolved oxygen response of tributaries may differ dramatically from the main stem Klamath River. Generally the flow contributions of the major tributaries are relatively small, and when flows are appreciable dissolved oxygen concentrations are usually not of concern (i.e., winter or spring high flow events). Thus, the widespread impact of the tributaries on main stem conditions is probably modest during much of the summer and fall period. However, transient, local impacts have not been studied and may be appreciable.
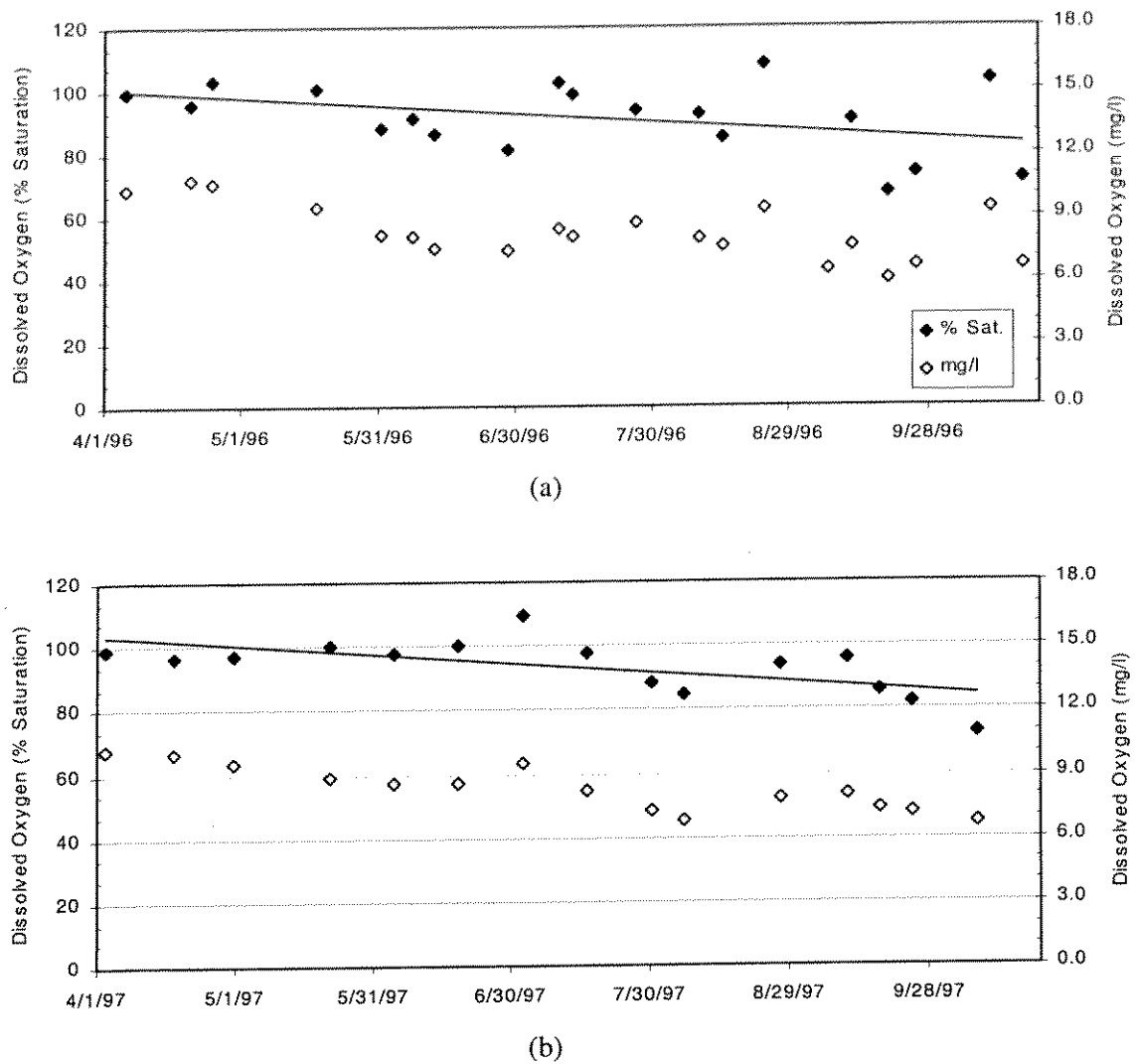
Figure 7.22 Dissolved oxygen concentration as percent saturation below Iron Gate Dam,
(a) 1996 and (b) 1997 NCRWQCB grab samples

7.3.3.3   Primary Production

Unlike water temperature, limited field data were available for dissolved oxygen. Figure 7.23 shows measured temperatures and dissolved oxygen concentrations over a 48-hour period in the main stem Klamath River below the Shasta River.

Dissolved oxygen ranges from a high of over 10 mg/l, roughly 120 to 130 percent of saturation, to a low of just above 6 mg/l, or 70 to 80 percent of saturation. Temperature ranges from roughly 20°C (68.0°F) to 25°C (77°F) over the same period. Thus, diurnal changes in water temperature account for less than 1 mg/l of the associated change in

165

dissolved oxygen. These measured data illustrate that primary production has an appreciable impact on diurnal dissolved oxygen concentration. Incidentally, July 29 was a cloudy day and dissolved oxygen and temperature remained depressed throughout the day and into the night-time period.
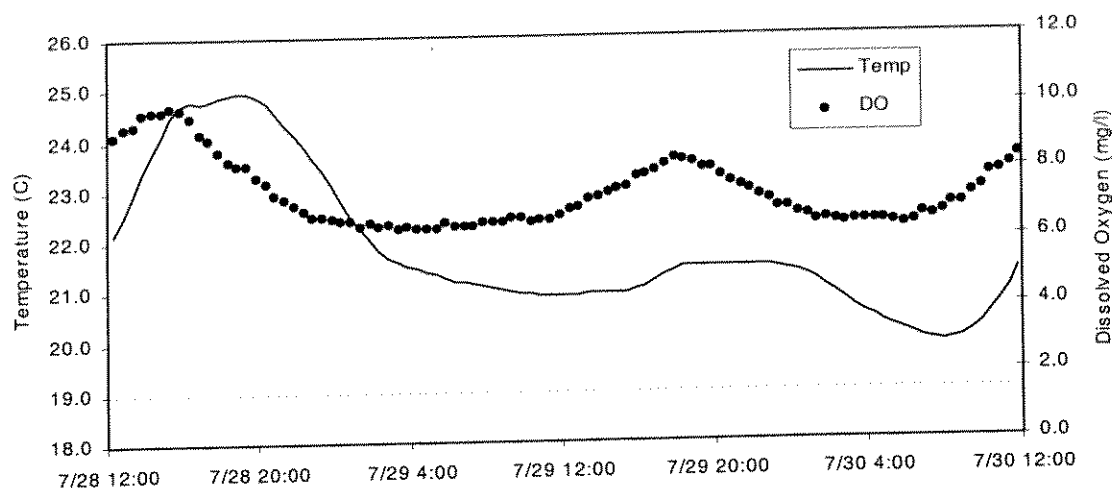
Figure 7.23 Temperature and dissolved oxygen: Klamath River below Shasta River, June 28, 12:00 – June 30, 12:00

Grab samples from the NCRWQCB water quality survey provided further insight. A most remarkable characteristic of these data was the super saturation dissolved oxygen concentrations that appear to persist in the region of Cottonwood Creek (RM 182.1). Recall that dissolved oxygen concentrations up to 180 percent of saturation were recorded in July and August of 1997. Dissolved oxygen below Iron Gate Dam (RM 190.1) was consistently below saturation, while the three locations downstream of Cottonwood Creek (Below Shasta River, RM 176.7; below Beaver Creek, RM 160; and below Scott River, RM 143) generally fell within ±10 to 15 percent of saturation. This anomalous spike near Cottonwood Creek may be due to locally excessive primary production, i.e., algal growth in response to nutrient laden water released from Iron Gate Reservoir.

Using the RMA-11 model, a hypothetical response was derived for attached algal biomass along the longitudinal profile of the river for a representative mid-summer day. Figure 7.23 illustrate this profile. The vertical axis represents relative mean daily algal biomass (only a relative scale is presented because lack of field data precluded validation of the model for attached algae), and the horizontal axis represents river mile with downstream progressing

166

from left to right: Iron Gate Dam to Seiad Valley. There are three notable features shown in Figure 7.24. First, there is a marked peak in algal biomass in the vicinity of RM 185 due to readily available nutrients from Iron Gate Reservoir releases. Assuming reservoir releases supply a relatively constant source of nutrients to the river, by mid-summer, algal biomass in the immediate downstream reach would approach equilibrium with available nutrients. That is, biomass could potentially increase up to the point of effectively capturing the bulk of the nutrients. Thus, immediately downstream of this peak is a depression in algal biomass due to lack of available nutrients, labeled point A in Figure 7.24. The condition of marked primary production in the reach below Iron Gate Dam may explain the supersaturated conditions in the vicinity of Cottonwood Creek (RM 182), while at other downstream locations algal biomass densities, and thus diurnal variation in dissolved oxygen concentrations, are more modest.

A second feature is the tributary contribution of nutrients. Although the Shasta and Scott Rivers are minor contributors of flow, Klamath River attached algae quickly utilize their nutrient loads. Two peaks in algal biomass are readily visible downstream of tributary locations in Figure 7.24.

The third feature of interest is a broad peak in algal biomass around RM 155 (point B in Figure 7.24). It is theorized that this peak is a related to the initial large peak below Iron Gate Dam. As algal biomass increases below Iron Gate Dam, mortality (respiration) likewise increases. Associated with death and decay are the release of organic forms of nitrogen and phosphorus. These forms undergo hydrolysis to inorganic forms that are readily available for use by algae. It is notable that the peak at point B roughly coincides with one-day's travel time downstream from the initial peak. One would expect the second peak to be reduced in magnitude and broader due to the small quantity of available nutrients, the transformation time (decay rate) from organic to inorganic species, and processes of natural dispersion. As with the peak below Iron Gate Dam, the second peak is likewise followed by a depression in algal biomass.

A further consideration is that algal response varies seasonally in the study reach. Spring time conditions typically consist of cooler water temperatures and higher flow rates. The long days of summer, warm water temperatures, and steady flow conditions favor algal colonization during this period. As day length decreases in late summer and early fall, light limitations and lower water temperatures create conditions that are insufficient to support

spring and summer biomass accumulations, and biomass begins to decline throughout the river system.

These findings, although preliminary, illustrate the potential for a spatially and temporally diverse attached algae population. Nutrient laden releases from Iron Gate Reservoir may not only increase algal biomass in the reach immediately below the dam, but also at one-day's travel distance downstream. Likewise, tributary contributions have the potential to increase algal densities immediately downstream of their confluence with the Klamath River. In all cases, increased algal biomass may lead to larger diurnal variations in dissolved oxygen concentrations and associated water quality concerns (e.g., elevated pH). Below Iron Gate Dam, low dissolved oxygen concentrations during nighttime periods may be exacerbated by depressed dissolved oxygen concentrations in reservoir release waters.
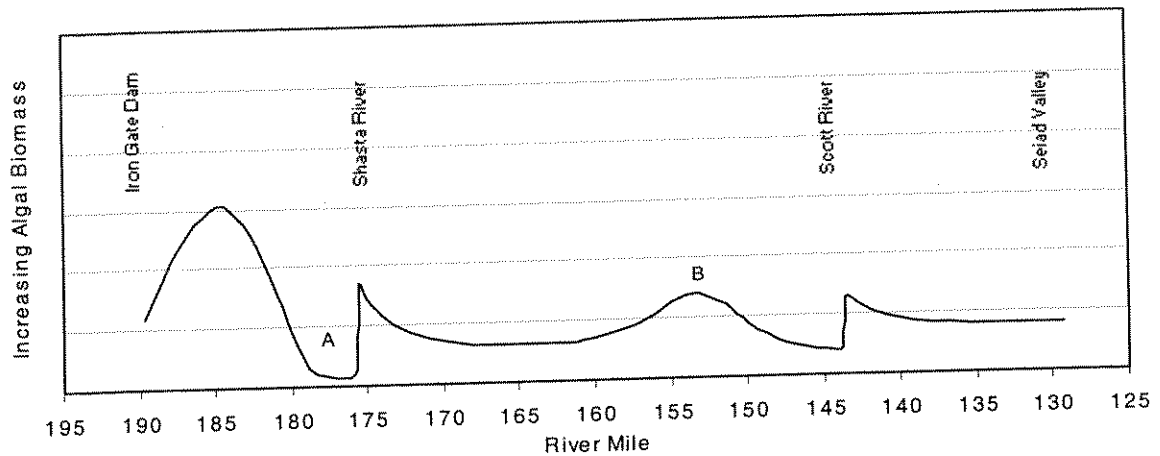
Figure 7.24 Hypothetical longitudinal profile of mean daily algal biomass in midsummer

7.3.4   Other Water Quality Variables

Measured field data and model simulation provided insight into other constituent processes. Probably of most importance is the effect of primary production on pH. Though pH is not a modeled parameter, hourly data were collected during dissolved oxygen monitoring in July of 1997. Figure 7.25 shows pH ranging from a high of about 9.2 to a low of about 7.7 over the period July 28-30, 1997. These data illustrate that primary production has a significant impact on system water quality. Because alkalinity of the Klamath River ranges from 50 to 120 mg CACO₃/l, and is thus a weakly or moderately buffered system, the river is subject to elevated pH. As noted previously, an increase in pH can have a direct impact on the toxicity

168

of certain constituents such as ammonia, especially at elevated temperature (see Sections 3.4 and 3.7).

Recall that the Klamath River during the study period was nitrogen limited. NCRWQCB samples show that the maximum concentration of ammonia and nitrate were on the order of 0.2 and 0.5 mg/l. (Observed phosphorus concentrations were on the order of 0.2 mg/l, leading to a N:P ratio of roughly 1.0 (<< 7).) Measured unionized ammonia concentrations typically ranged from 0.001 to 0.01 mg/l, well below critical limits. Further, simulation results (see Figures 6.20 and 6.21) showed that the nitrogen species of ammonia and nitrate are depressed during peak periods of algal photosynthesis (growth). Thus, when pH is elevated, ammonia concentrations may be depressed, abating ammonia toxicity concerns. However, these are preliminary findings, and it is difficult to assess the impact of system response with limited field data that were possibly not gathered during critical periods of the day. Additional field monitoring is recommended to better understand these complex processes.

Other constituents of interest include nutrient and algae, both of which have been discussed in previous sections.
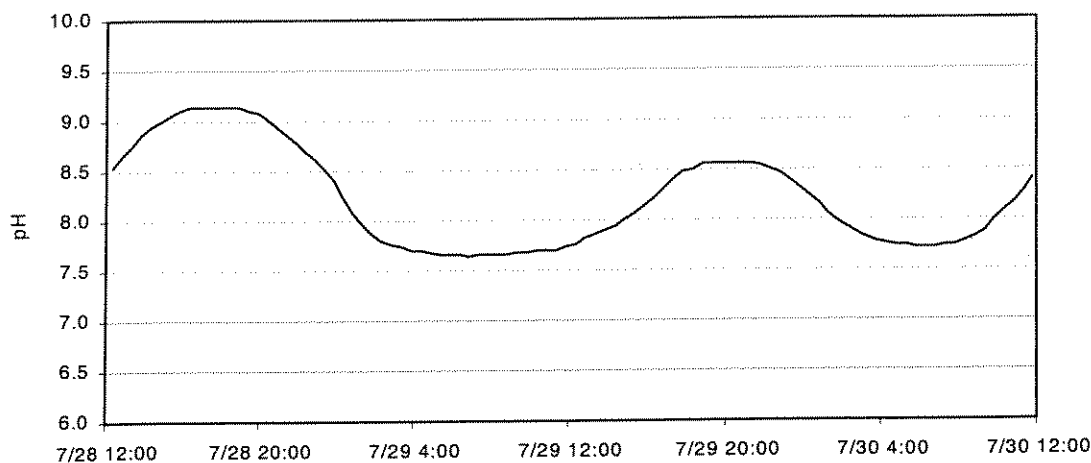
Figure 7.25 Measured pH in the Klamath River below Shasta River, June 28, 12:00 – June 29, 12:00

8.0   Model Application to Reservoir-River System

8.1   Introduction

Model application consisted of applying the calibrated and validated river and reservoir models to define current system conditions and assess water management alternatives. Required conditions for model application and model capability are presented, followed by model application and alternatives. Application generally refers to analysis of existing conditions, while alternatives represent deviations from existing conditions, e.g., change in system operations and/or change in reservoir storage. Finally, the concept of a water quality index is introduced

8.2   Model Conditions and Capabilities

By their nature, models are simplifications of physical, chemical, and biological processes. Outlined below are some conditions for appropriate model application based on physical system representation of the reservoir and river system. Further, the capability of the model to reproduce water temperature and dissolved oxygen concentrations is estimated from calibration and validation results.

8.2.1   Reservoir Model: WQRRS

The one-dimensional, vertical representation of Iron Gate Reservoir with WQRRS assumes that the reservoir is prone to strong thermal stratification and that simulation results are representative of average conditions in the main body of the reservoir away from inflowing tributaries and localized effects of outlets. Recall that the criterion for a one-dimensional representation was based on the densimetric Froude number (F_D = f(volume, depth, length and flow)) with values less than $1/\pi$ prone to stratification. Further, F_D values on the order of $1/\pi$ are prone to weak stratification, while $F_D \ll 1/\pi$ are prone to strong stratification. Application of the one-dimensional approximation (WQRRS) generally requires a $F_D \ll 1/\pi$ for summer period conditions. Development of alternative flow and reservoir configuration options developed for this project considered this limitation in the application of WQRRS. Table 8.1 illustrates F_D values for a variety of flow rates at various levels of Iron Gate Reservoir storage. Those values denoted in bold (lower right corner of Table 8.1) illustrate

weakly stratified conditions. Thus, model limitations constrain analysis with WQRRS to storage elevations greater than approximately 2300 ft msl and flow rates less than 2500 cfs.

Table 8.1 Densimetric Froude Number for various stage and flow conditions at Iron Gate Reservoir: **bold** denotes weakly stratified conditions

Reservoir Properties				Densimetric Froude Number (F_D)				
				Flow Rate (cfs)				
Stage (ft msl)	Volume (AF)	Depth (ft)	Length* (ft)	1000	1500	2000	2500	3000
2325	56000	155	37000	0.031	0.047	0.063	0.078	0.094
2300	36200	130	31000	0.048	0.073	0.097	**0.121**	**0.145**
2290	29850	120	28600	0.059	0.088	**0.117**	**0.147**	**0.176**
2280	24200	110	26200	0.072	**0.108**	**0.145**	**0.181**	**0.217**
2270	19200	100	23800	0.091	**0.137**	**0.182**	**0.228**	**0.273**
2260	15000	90	21400	**0.116**	**0.175**	**0.233**	**0.291**	**0.349**
2250	11300	80	19000	**0.154**	**0.232**	**0.309**	**0.386**	**0.463**

*Estimated

8.2.2 River Models: RMA-2 and RMA-11

Recall that RMA-2 is a hydrodynamic model producing mean stream velocity, flow depth, and water surface area. Results from RMA-2 are used in RMA-11, the water quality model, to assess fate and transport of thermal energy and constituent concentrations. Geometric representation of river cross sections was approximated using a trapezoidal form; however, at low flows this approximation can produce excessively high simulated water temperatures. Figure 8.1 shows a set of representative cross sections for (1) a natural channel and (2) a trapezoidal channel under (a) normal and (b) low flow conditions. Average depth for both the natural and trapezoidal sections are comparable under normal flows. However, at low flows the river most likely seeks a low flow channel that, when compared with the trapezoidal approximation, experiences reduced surface width and greater depth. Thus, for low flow conditions the trapezoidal approximation results in a wide shallow flow (large simulated surface area and small depth), and simulated water temperatures are probably in excess of actual conditions. For this project, minimum flows for effective temperature simulation were found to be 500 cfs or greater.

171
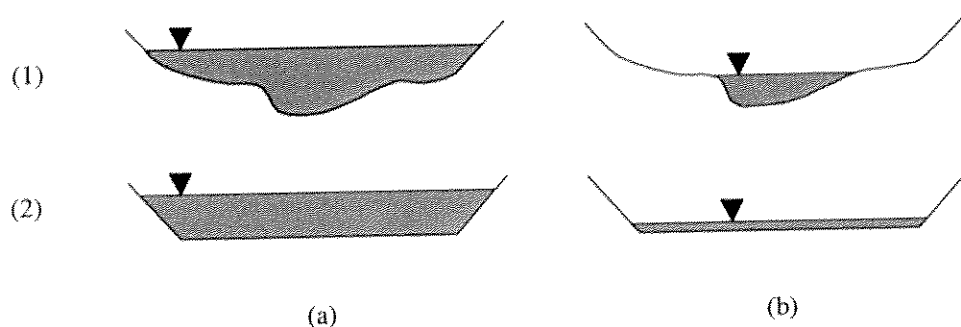
Figure 8.1 Representative cross-section for (1) natural and (2) trapezoidal channels under (a) normal, and (b) low flow condtions.

8.2.3 Model Capability

For purposes of these applications, it is estimated that the reservoir model can predict hourly (and daily) temperatures throughout the water column within ±2°C (3.6°F,) and hourly dissolved oxygen within ± 4 mg/l. Spill events, if they occur, take place early in the season, are small, and have little impact on considered alternatives. Daily aggregation does little to improve model representation due to the slow response/change in reservoir water quality (e.g., weekly versus daily or hourly).

Simulated river water temperature is estimated to be within ±1°C (1.8°F) on an hourly basis and within ±0.5°C (0.9°F) for daily average values. Dissolved oxygen values are assumed to be within ±4 mg/l on an hourly basis and ±2 mg/l on a daily average basis.

Although explicit values for model accuracy are presented, comparative analysis was used to assess alternatives, i.e., a relative comparison between simulated baseline and simulated alternative results. This approach reduces uncertainty due to model capability, and the efficacy of alternatives can be more readily assessed. The assumption being that model error will be consistent within each simulation: an assumption that is sometimes questionable.

8.3 Model Applications and Alternatives

Two levels of simulation were completed. First, several model applications were completed to further assess system response to physical conditions. Second, alternative operations for water quality control in the Klamath River below Iron Gate Dam were formulated. Each application and alternative is described below.

8.3.1   Model Applications

Several applications were completed to further define system processes, or response of system processes, to variable flow, meteorological, and operational conditions. These include travel time determination, ramping flow changes at Iron Gate, and impacts of flow rate on main stem water temperature. Potential meteorological impacts on water temperature, although not addressed with the models, are briefly discussed.

8.3.1.1   Travel Time Determination

To assess travel time in the Klamath River below Iron Gate Dam, the calibrated models were applied over a range of flow rates, from 600 cfs to 4000 cfs in 200 cfs increments. Figure 8.2 illustrates travel time versus distance in the Klamath River between Iron Gate Dam (RM 190.1) and the USGS gage near Seiad Valley (RM 129.6) for various flow rates. At flow rates below 1000 cfs travel times through the reach are greater than 2 days, while successively higher flows lead to reduced travel time. At 4000 cfs the travel time is just over one-day – about 28 hours.
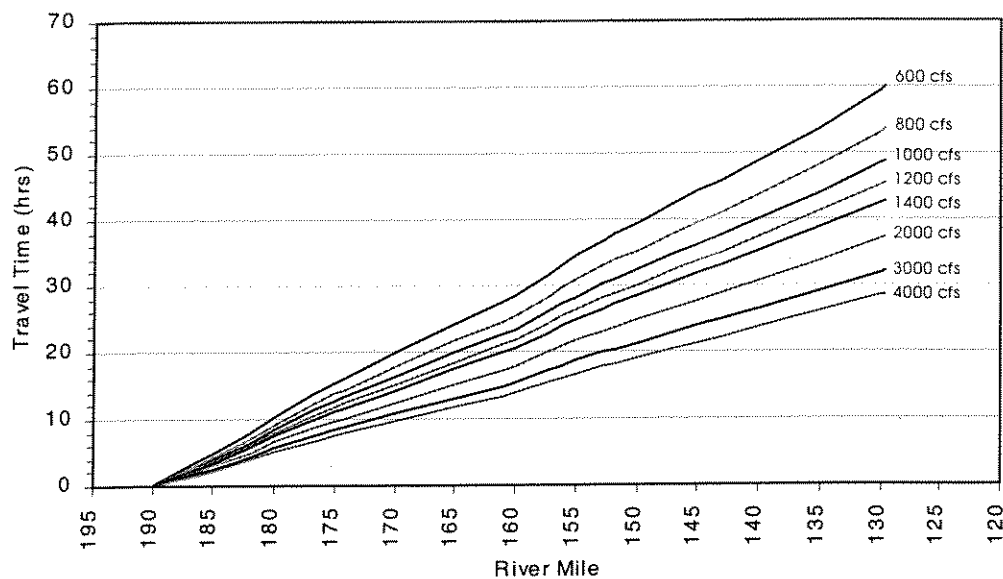
Figure 8.2   Travel time versus distance at various flow rates for the Klamath River between Iron Gate Dam and Seiad Valley

Travel times were produced under steady state conditions; that is, Iron Gate Dam releases were set at a single value and the models applied without tributary inflow or accretions. The results were travel times independent of tributary conditions, which can then be used to determine travel times accounting for variable tributary flow conditions. Table 8.2 outlines travel times for flow rates from 600 to 4000 cfs at 5-mile increments, as well as locations of

173

several tributaries through the study reach. The table is divided into three general areas: less than one-day transit time, one- to two- day transit time and greater than two-day transit time.

Using the table to determine approximate travel time when tributary flows are included is best illustrated by example. Assume a release from Iron Gate Dam of 1000 cfs, and Shasta and Scott River inflows were 200 cfs each with negligible accretions. Table 8.2 shows that travel time from Iron Gate Dam to the Shasta River at 1000 cfs is 11.5 hours. Downstream of the Shasta River the flow is 1200 cfs due to tributary contributions. Tabulations shows that travel time between the Shasta River and Scott River at 1200 cfs to be 24.3 hours (35.0 hours minus 10.7 hours). Subsequently, the Scott River increases flows to 1400 cfs between its confluence with the Klamath River and the USGS Gage at Seiad Valley with an associated travel time of 9.8 hours (42.8 hours minus 33.0 hours). Summing the individual reach travel times yields 45.6 hours. This process can be used to determine approximate travel times between other locations with various accretion quantities. For intermediate values of space, time, and flow rate, linear interpolation between values can be applied with only minor error.

Section 7.3.2.2 introduced the concept of zones of minimum and maximum diurnal variations. It was noted that the location of a node of minimum diurnal variation was a function of flow rate (travel time) and occurred at one-day's travel time downstream. Using Table 8.2, the one- and two-day travel times (delimited in the table) can be used to locate such nodes. Zones of maximum diurnal variation (antinodes) are located approximately 12 hours from nodes of minimum diurnal variation. For example, at 1200 cfs a node of minimum diurnal variation occurs in the area of Barkhouse Creek (RM 157.3), while an antinode of maximum diurnal variation occurs near Badger Creek (RM 174.4). At 2400 cfs, twice the flow rate, the node and antinode are shifted downstream to locations near Horse Creek (RM 147) and below Beaver Creek (RM 170), respectively.

8.3.1.2 Ramping

Currently, managed flow changes at Iron Gate Reservoir occur over periods as short as several hours. The FERC imposed ramping schedule below Iron Gate specifies a maximum of 250 cfs per hour, or a maximum change in stage of 3 inches per hour (measured at the USGS gage below Iron Gate Dam), whichever is less (J. Kelly, pers. comm.). To assess the impact of changes in stage below Iron Gate Dam, as well as at various distances downstream, the hydrodynamic model RMA-2 was applied.

174

Table 8.2 Travel time in the Klamath River between Iron Gate Dam and Seiad Valley for flowrates from 600 to 4000 cfs (one- and two-day travel times delimited)

River Mile	Location	600	800	1000	1200	1400	1600	1800	2000	2200	2400	2600	2800	3000	3200	3400	3600	3800	4000
								Travel Time (hrs)											
190.1	IGDam	0.0	0.0	0.0	0.0	0.0	0.0	0.0	0.0	0.0	0.0	0.0	0.0	0.0	0.0	0.0	0.0	0.0	0.0
186.4	L. Bogus	3.5	3.1	2.8	2.6	2.5	2.4	2.2	2.2	2.1	2.0	1.9	1.9	1.8	1.8	1.7	1.7	1.7	1.6
185.0		4.7	4.2	3.9	3.6	3.4	3.2	3.0	2.9	2.8	2.7	2.6	2.6	2.5	2.4	2.4	2.3	2.3	2.2
182.1	Cottonwood	7.8	7.0	6.4	6.0	5.7	5.4	5.2	5.0	4.8	4.7	4.5	4.4	4.3	4.2	4.1	4.0	3.9	3.9
180.0		10.3	9.2	8.5	7.9	7.4	7.1	6.8	6.5	6.3	6.1	5.9	5.8	5.6	5.5	5.4	5.3	5.2	5.1
176.7	Shasta R.	14.0	12.5	11.5	10.7	10.1	9.6	9.2	8.8	8.5	8.3	8.0	7.8	7.6	7.4	7.2	7.1	6.9	6.8
175.0		15.5	13.9	12.7	11.9	11.2	10.7	10.2	9.8	9.4	9.2	8.9	8.6	8.4	8.2	8.0	7.9	7.7	7.6
174.4	Badger Ck.	16.1	14.4	13.2	12.3	11.6	11.0	10.5	10.1	9.8	9.5	9.2	8.9	8.7	8.5	8.3	8.1	8.0	7.8
170.0		19.9	17.8	16.3	15.2	14.3	13.6	13.0	12.5	12.1	11.7	11.4	11.1	10.8	10.5	10.3	10.0	9.8	9.7
165.0		24.2	21.7	19.9	18.5	17.5	16.6	15.9	15.3	14.7	14.3	13.9	13.5	13.1	12.8	12.5	12.2	12.0	11.8
161.0	Beaver Ck.	27.6	24.7	22.6	21.1	19.9	18.9	18.1	17.4	16.8	16.3	15.8	15.3	15.0	14.6	14.2	13.9	13.7	13.4
160.0		28.6	25.5	23.4	21.9	20.6	19.6	18.7	18.0	17.4	16.9	16.4	15.9	15.5	15.1	14.8	14.5	14.2	13.9
157.3	Barkhouse Ck.	31.6	28.3	26.0	24.2	22.9	21.7	20.8	20.0	19.3	18.7	18.2	17.7	17.2	16.8	16.4	16.0	15.7	15.4
156.2	Walker Rd.	33.1	29.6	27.1	25.3	23.9	22.7	21.7	20.8	20.1	19.5	18.9	18.4	17.9	17.5	17.1	16.7	16.4	16.1
155.0		34.5	30.8	28.3	26.4	24.8	23.6	22.6	21.7	20.9	20.3	19.7	19.1	18.7	18.2	17.8	17.4	17.0	16.7
152.8	Dona Ck.	36.8	32.9	30.2	28.1	26.5	25.2	24.1	23.1	22.3	21.6	21.0	20.4	19.9	19.4	18.9	18.5	18.2	17.8
151.7	Kohl	37.8	33.8	31.0	28.9	27.2	25.9	24.7	23.8	22.9	22.2	21.6	21.0	20.4	19.9	19.5	19.0	18.7	18.3
150.0		39.4	35.3	32.3	30.1	28.4	27.0	25.8	24.8	23.9	23.2	22.5	21.9	21.3	20.7	20.3	19.8	19.4	19.1
147.3	Horse Ck.	42.0	37.6	34.4	32.1	30.2	28.7	27.5	26.4	25.4	24.7	23.9	23.3	22.7	22.1	21.6	21.1	20.7	20.3
145.0		44.1	39.4	36.2	33.7	31.8	30.2	28.9	27.7	26.7	25.9	25.2	24.5	23.8	23.2	22.7	22.2	21.8	21.4
143.0	Scott R.	45.8	40.9	37.5	35.0	33.0	31.3	29.9	28.8	27.7	26.9	26.1	25.4	24.7	24.1	23.5	23.0	22.6	22.1
140.0		48.8	43.7	40.0	37.3	35.1	33.4	31.9	30.7	29.6	28.7	27.8	27.1	26.4	25.7	25.1	24.6	24.1	23.6
135.0		53.8	48.1	44.1	41.1	38.7	36.8	35.2	33.8	32.6	31.6	30.7	29.8	29.0	28.3	27.6	27.0	26.5	26.0
130.0		59.5	53.0	48.6	45.2	42.6	40.4	38.6	37.1	35.7	34.7	33.6	32.7	31.8	31.0	30.3	29.6	29.0	28.5
129.6	USGS Gage	60.1	53.5	48.9	45.5	42.8	40.6	38.8	37.3	35.9	34.8	33.8	32.8	32.0	31.1	30.4	29.8	29.2	28.6
	Mean velocity (mph)	1.01	1.13	1.24	1.33	1.41	1.49	1.56	1.62	1.68	1.74	1.79	1.84	1.89	1.94	1.99	2.03	2.08	2.12
	Mean velocity (fps)	1.48	1.66	1.81	1.95	2.07	2.18	2.29	2.38	2.47	2.55	2.63	2.70	2.77	2.85	2.92	2.98	3.04	3.10

Recall, for this project RMA-2 was applied in the one-dimensional mode with trapezoidal cross-sections approximating actual measured cross sections (see Figure 8.1). Simulated depth for this geometry is representative of an average depth and cannot be directly compared with measured data; however, comparative analysis of the rate of change in water surface under a normal range of flow conditions (see Section 8.2.2) provided valuable insight into this dynamic process.

To illustrate the impact of current operations and to assess the potential of variable ramping rate, historic flow changes were examined with RMA-2, as well as for two- and four-day ramping periods. The selected historic conditions were those of June-July and July-August, 1997. On July 1, 1997 the release to the Klamath River from Iron Gate Dam was ramped down from approximately 1130 cfs to 810 cfs (28 percent change in base flow) over a period of five hours. On August 1, 1997 the release was ramped up from roughly 890 cfs to 1040 cfs (17 percent change in base flow) over a period of four hours. Typically, minor adjustments in flow were made after ramping was complete. Figure 8.3 illustrates the historic Iron Gate Dam hourly release flow rates and the corresponding rate of change in flow rate for the July and August periods, respectively. For these modest flow changes the ramping rates are well within the 250 cfs limiting criteria provided by FERC.

The hydrodynamic model was used to examine local and downstream impacts on water surface level rate of change for July 1, 1997. The July 1 flow change was selected because it is the larger (320 cfs or a 28 percent change in base flow) of the two changes addressed above and theoretically would have a larger impact. The model was applied to the historic event, and the rates of change of water surface levels were examined immediately below Iron Gate Dam (RM 190.1) and at 10-mile increments downstream to RM 140.

Figure 8.4 illustrates simulated water depths below Iron Gate Dam and at 10-mile increments downstream. Because cross-section geometries at the various locations are different, and due to tributary contributions of the Shasta and Scott Rivers, as well as ungaged accretions, depths are variable, so the figure is difficult to interpret. Further, due to the trapezoidal approximation this simulated depth is only a cross-section "average." To compare locations more readily, changes in depth and rates of change in depth were used. Figure 8.5 shows the changes in depth at each location, and illustrates how flow changes affect stage at different locations downstream. Although cross-section geometry plays a role, it is clear that changes in depth are largest immediately downstream of Iron Gate Dam where a depth change of 0.9 feet takes place within a matter of hours. As expected, the impacts diminish with distance downstream from Iron Gate Dam. By RM 140 the depth change is roughly 0.45 feet and occurs over a much longer period of time. In sum, the flow change can be viewed as a wave (a disturbance) propagated downstream, the magnitude of which will diminish, while the wave is attenuated through time and distance. The propagation of these waves are more clearly illustrated by examining the rate of change of water surface level.
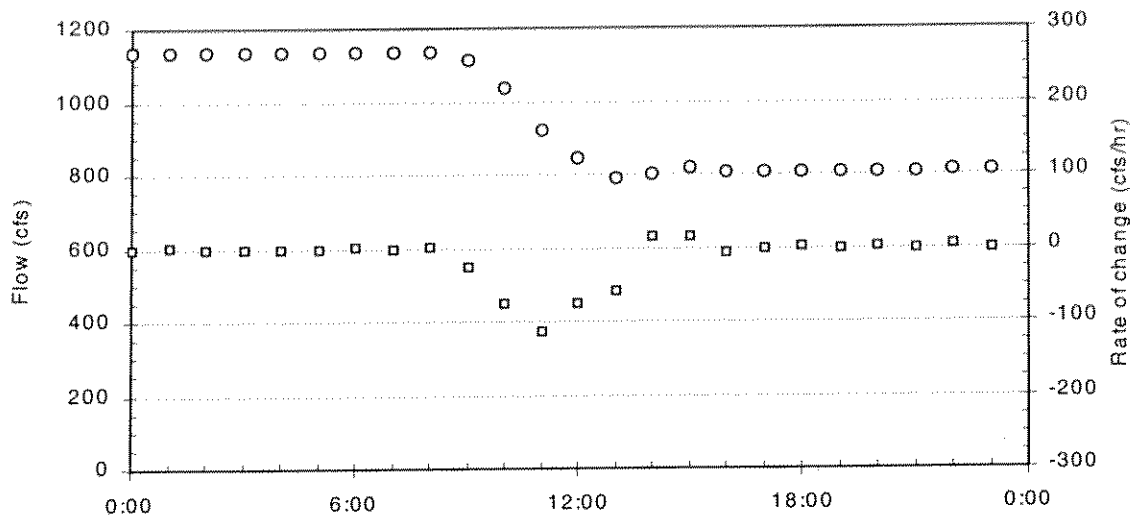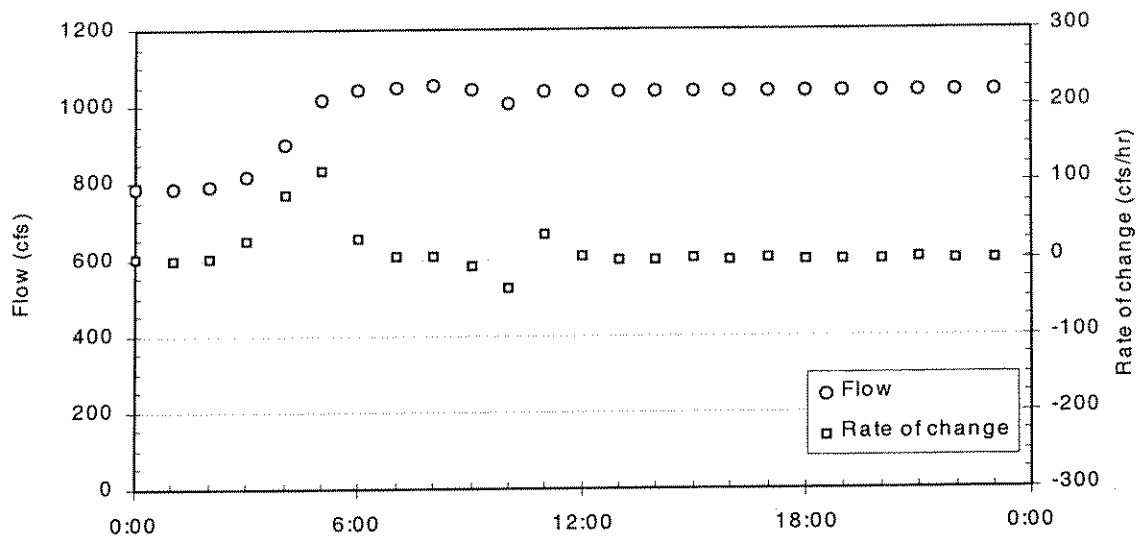
Figure 8.3   Iron Gate Dam releases and rate of change of flow rate for (a) July 1, 1997 and
(b) August 1, 1997

Figure 8.6 shows that immediately below Iron Gate Dam the maximum rate of change is approximately 3 inches per hour – very close to the FERC limits. Negative values denote a decreasing river stage. At RM 170 the maximum rate of change is less than 2 inches per hour and this rate decreases exponentially with distance downstream to about 0.5 inches per hour at RM 140. Notice the traces are diminishing in height and attenuating (spreading out) with increasing distance downstream from Iron Gate Dam

177
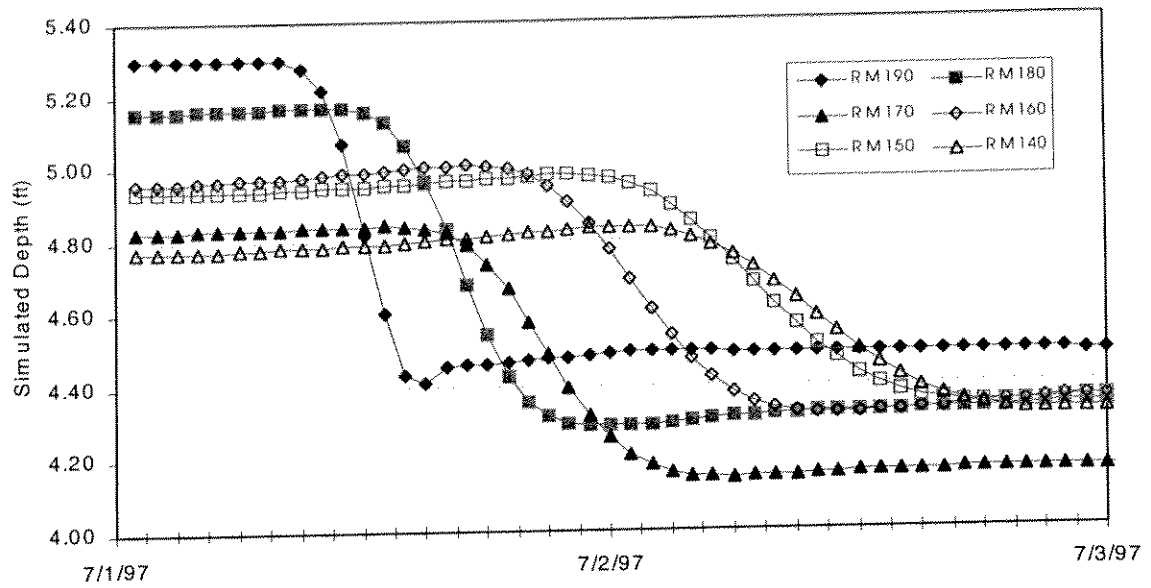
Figure 8.4   Simulated depth below Iron Gate Dam and at 10-mile increments downstream
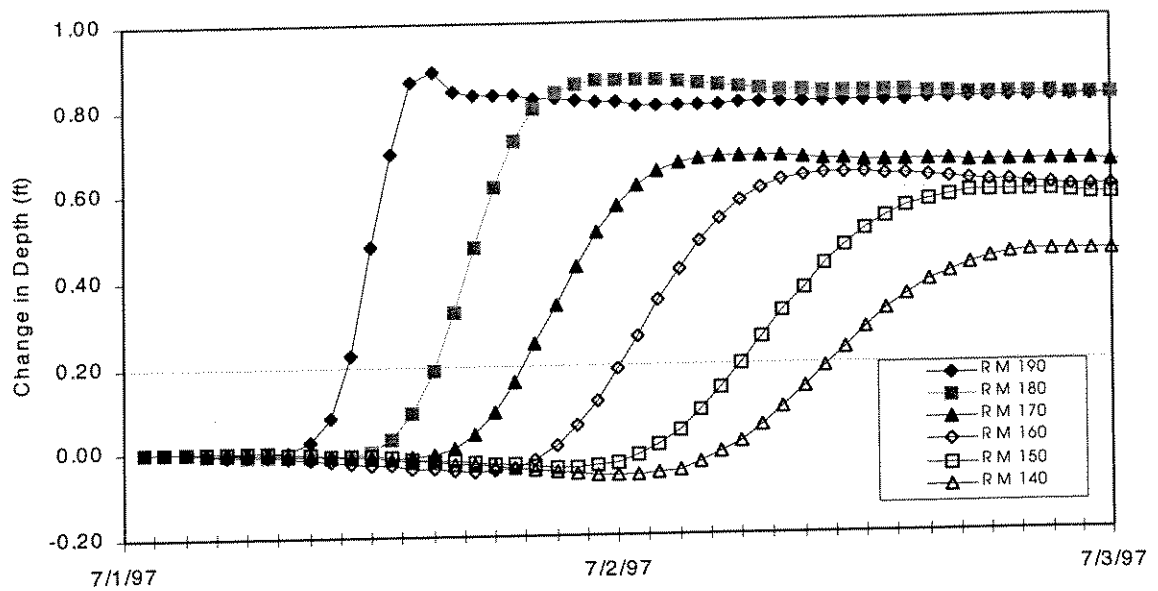
Figure 8.5   Simulated change in depth below Iron Gate Dam and at 10-mile increments downstream (change equals initial depth (7/1/97 7:00) minus simulated depth at a subsequent future time)
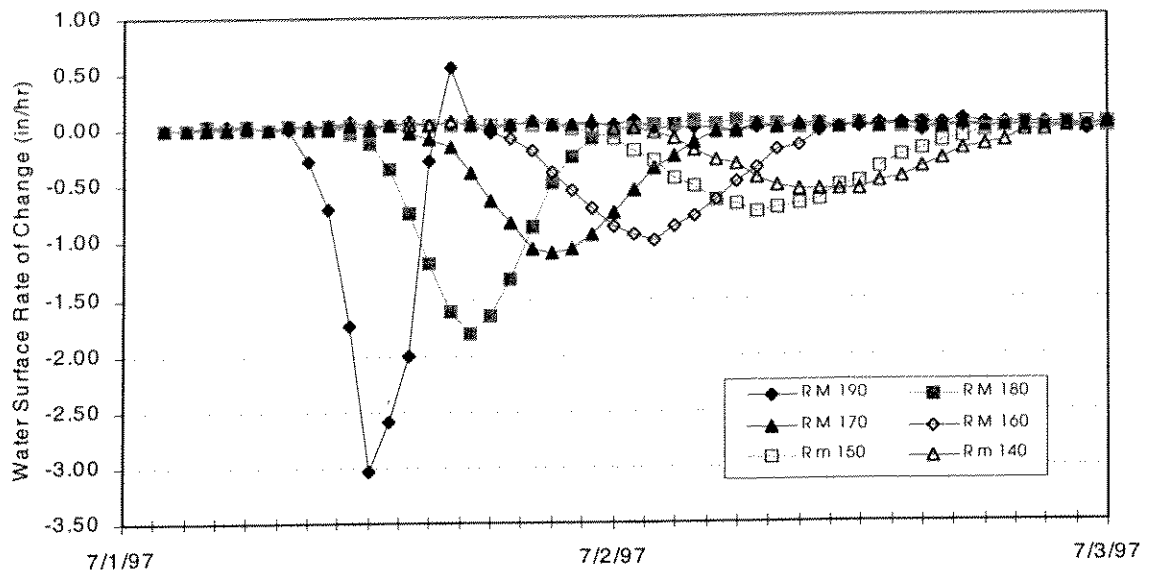
Figure 8.6   Simulated rate of change of water surface level below Iron Gate Dam and at
             10-mile increments downstream

To examine impacts of increased ramping periods, RMA-2 was used to simulate the 320 cfs flow rate change over 48 and 96 hour periods (i.e., two-day and four-day ramping periods). Flow changes were varied linearly over the extended ramping periods. Figure 8.7 and 8.8 illustrate the two- and four-day ramping results, respectively. For clarity, only the results from RM 190 to RM 170 are presented: rates of change in downstream impact are less than or equal to results at RM 170. Two-day ramping reduces the maximum water surface rate of change below Iron Gate Dam to about 0.4 inches per hour, while downstream locations experience rates of change on the order of 0.2 inches per hour or less. The four-day ramping provides modest improvement over the two-day ramping scenario, with maximum water surface rates of change below Iron Gate Dam of roughly 0.3 inches per hour, and 0.1 inches per hour or less at downstream locations.

Although these analyses are preliminary and limited to modest flow changes, the findings show that flow rate changes that are an appreciable proportion of the base flow may have a considerable impact on the rate of change of water level, especially immediately below Iron Gate Dam. Further, under short ramping periods (e.g., historical), impacts of a flow change are evident at appreciable distances downstream, although the disturbances diminished with distance from Iron Gate Dam. Even modest increases in ramping periods significantly reduced the rates of change of water levels below Iron Gate Dam and at downstream locations. However, longer ramping periods (i.e., four-day versus two-day) provided little improvement in decreasing rate of water surface level change.

179
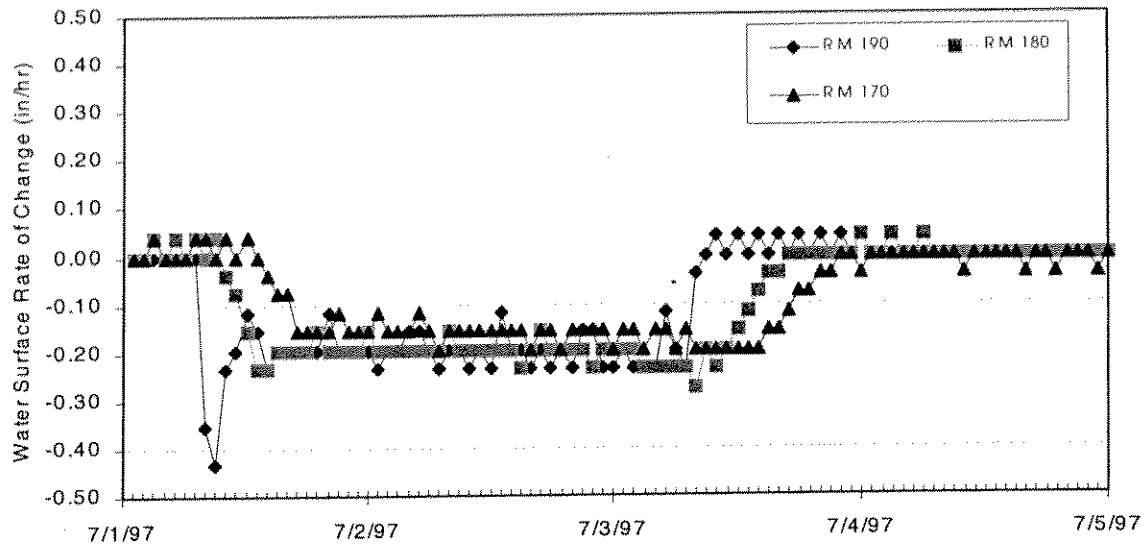
Figure 8.7   Two-day ramping rate of change of water surface level below Iron Gate Dam and at 10-mile increments downstream
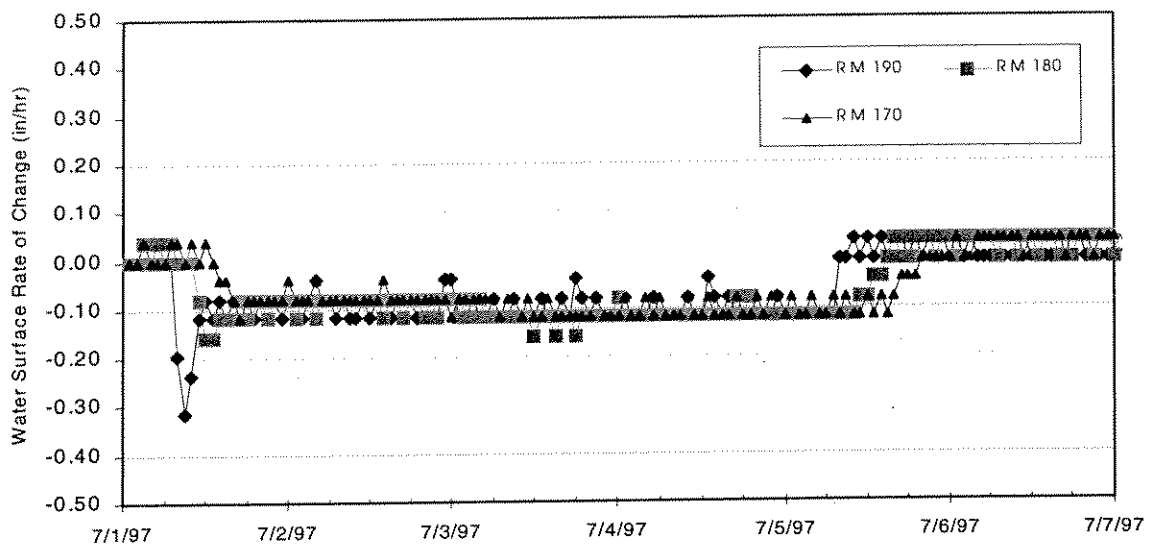
Figure 8.8   Four-day ramping rate of change of water surface level below Iron Gate Dam and at 10-mile increments downstream

8.3.1.3   Flow and Water Temperature

Flow has a direct impact on water temperature. At low flows, mean stream velocity is reduced and transit times through the study reach are increased, and conversely for high flows, as illustrated in Table 8.2. In general, increased transit times lead to increased opportunity for heat exchange through the air-water interface. During summer periods this translates to a greater thermal loading potential. To examine the relationship between flow and water temperature, simulations were completed for a representative summer day for flow rates between 500 and 3000 cfs.

Meteorological and flow boundary conditions for August 14, 1996 were selected as representative of a summer day. Tributary and accretion influences are typically small during this period and meteorological conditions are generally stable. Observed water temperatures for the Iron Gate Dam release on the selected day were assumed. Figure 8.9 illustrates longitudinal water temperature profiles for the Klamath River under 500, 1000, 2000, and 3000 cfs releases from Iron Gate Dam. At 500 cfs, the transit time through the study reach is on the order of 2.5 days. While at 1000, 2000, and 3000 cfs, transit times are roughly 2 days, 1.5 days, and 1.25 days, respectively. At 500 cfs the rate of heating is appreciable, increasing daily mean water temperature by 2.7 °C (4.9°F) over the 60-mile study reach, or an average of 0.045°C per mile (0.08°F per mile). For the 1000, 2000, and 3000 cfs flow releases from Iron Gate Dam heating rates are approximately 0.035, 0.022, and 0.013°C per mile (0.063, 0.040, 0.024°F per mile), respectively. In addition to reduced transit times, reduction in thermal loading at higher flow rates is related to increased stream depth and greater thermal mass. Although the surface area of the river also increases at higher flow rates, the increase is relatively small – on the order of a few percent – and is deemed to have a small impact.

It is interesting to note that the influence of the Shasta River is practically insignificant throughout the range of specified flows. Minor contributions of heat to the main stem Klamath evident at the 1000 cfs flow rate. However, at lower flow rates the main stem has heated sufficiently to cancel the impact of the tributary. At higher flow rates the effect of tributary inflow quantity is insignificant. Conversely, Scott River (RM 143) contributions provide a thermal benefit to the main stem Klamath River for low flows (<1000 cfs). As with the Shasta River, at high flows Scott River contributions are relatively small and do not impact Klamath main stem water temperature.

Diurnal water temperature range is also affected by flow regime. Maximum and minimum daily temperatures are similarly affected by travel time. At low flow rates and increased transit times daily maximum temperatures increase and daily minimum water temperatures decrease compared to conditions with higher flow rates. Figure 8.10 (a) and (b) shows the envelope of maximum and minimum water temperatures for releases of 1000 cfs and 3000 cfs, respectively. The maximum diurnal range in water temperature for the 1000 cfs release is about 6°C (10.8°F) and occurs near RM 175, while the maximum diurnal range for the 3000 cfs release is a greater than 3°C (5.4°F), occurring near RM 165. Thus, higher flow

rates and decreased transit times result in moderated diurnal temperature ranges. Higher flow rates lead to lower daily mean water temperatures and reduced daily maximum temperatures, but minimum temperatures are not as low as those occurring at lower flow rates.
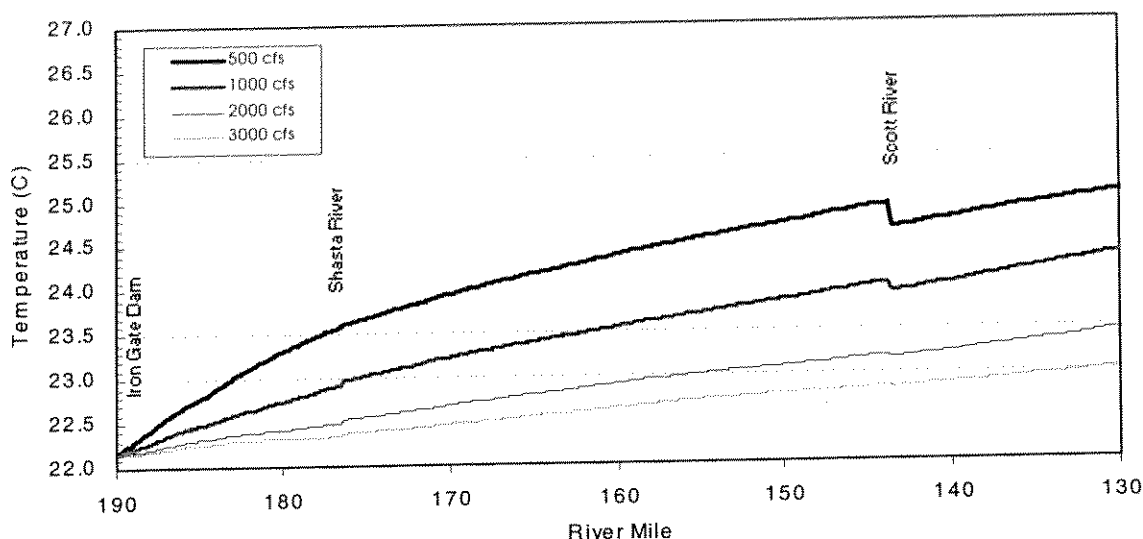
Figure 8.9   Simulated longitudinal daily mean water temperature profile, Klamath River from Iron Gate Dam to Seiad Valley for Iron Gate Dam releases ranging from 500 to 3000 cfs: August

The thermal response of the river will vary during different periods of the year due to release water temperature from Iron Gate Reservoir, tributary and accretion contributions (both quantity and temperature), and seasonal variations in meteorology.

8.3.1.4   Meteorological Conditions

Water temperature is governed primarily by heat exchange through the air-water interface. The net rate of heat transfer is a function of atmospheric short wave (solar) radiation flux, net atmospheric long wave radiation flux, long wave radiation flux from the water body, evaporative heat flux, and sensible heat flux. Although these radiation terms can be measured directly, it is typically uneconomical, except for solar radiation. As a result, these terms are usually estimated using common meteorological parameters as proxy variables. These common meteorological parameters include dry bulb (air) temperature; wet bulb temperature (or relative humidity, or dew point), wind speed; and atmospheric pressure. The formulation of the individual fluxes of the heat budget using these parameters is outlined in Appendix A.2.2.1.

182
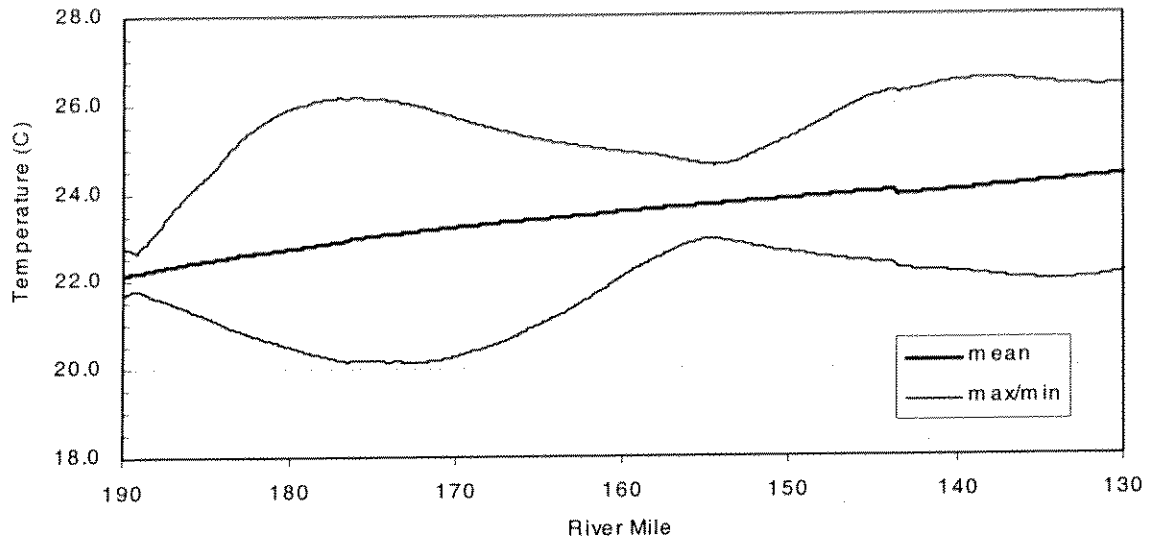
(a)
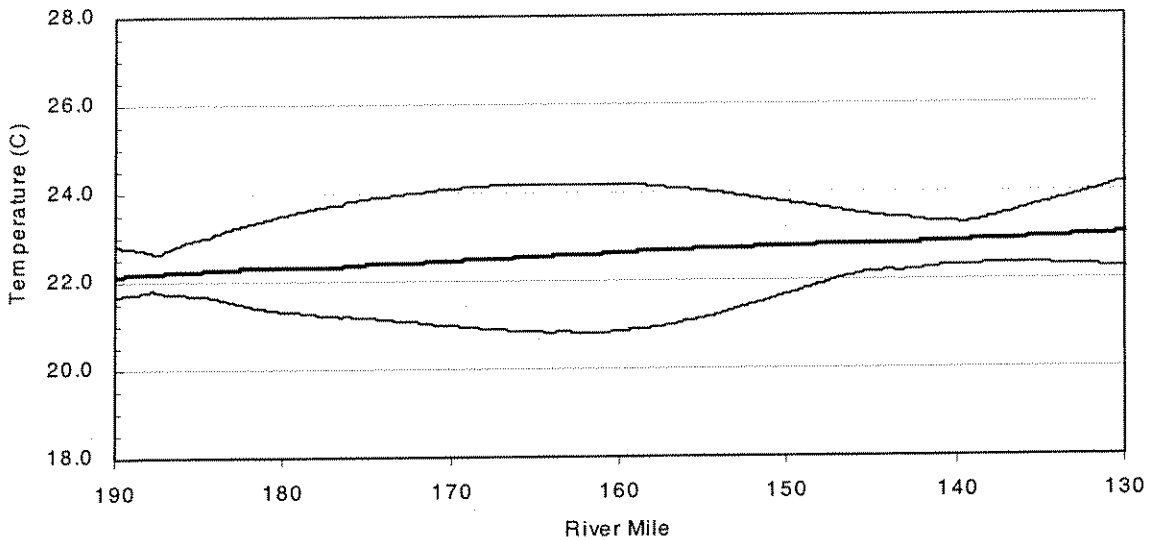
(b)

Figure 8.10 Simulated daily maximum, mean, and minimum longitudinal water temperature, Klamath River from Iron Gate Dam to Seiad Valley for Iron Gate Dam releases (a) 1000 cfs and (b) 3000 cfs

Solar radiation flux is by far the most important component of the heat budget, while other flux terms play varying roles depending on season, time of day, climate, and water temperature. The reader is cautioned about interpreting water temperature in light of proxy variable values (e.g., dry bulb and wet bulb temperature, wind speed and atmospheric pressure). The magnitudes of the individual heat budget terms and the role they play in the total heat budget are more appropriate means of interpreting water temperature responses.

183

Although the TWG identified a need to determine the impact of meteorological conditions on water temperature and water quality, the initial inquiry was general and thus too broad a topic for this report. It is recommended that specific questions be developed in regard to system response prior to model application. For example, if there is a concern about potential impacts of global warming in long-term operations planning, an appropriate analysis could be designed and completed.

8.3.2   Alternatives

Alternative operations for water quality control in the Klamath River below Iron Gate Dam included flow modification, varied reservoir storage, and/or modified reservoir intake configuration. Hydrologic, climatic and operations conditions from 1997 were selected as baseline conditions for comparison of alternatives. For all alternatives, meteorological conditions, tributary inflow quantity and quality (including Klamath River inflow to Iron Gate Reservoir, see Section 7.2.5), and accretions for 1997 were assumed. Water temperature control by means of Iron Gate Reservoir operations is emphasized throughout this section for two principal reasons. First, simulated dissolved oxygen concentrations include uncertainty due to limited calibration and validation data for both the reservoir and river models. Second, depressed dissolved oxygen, unlike elevated water temperature, is a condition that can be remedied by mechanical means, e.g., hypolimnetic oxygenation or direct oxygen injection into penstock releases. Though these are clearly capital intensive measures, most of the alternatives examined herein would require improvement of system facilities for successful implementation.

Baseline conditions, and alternatives for flow modification, varied reservoir storage, and/or outlet modification are described herein, followed by modeling results and interpretation.

8.3.2.1   Baseline Conditions and Alternative Descriptions
Baseline Conditions
Baseline conditions were defined for the river and reservoir as the period using data from mid-May through October 1997. During this period average monthly Iron Gate Dam releases ranged from 820 to 1500 cfs. The baseline thermal and dissolved oxygen conditions for Iron Gate Reservoir and the Klamath River are defined for model calibration and validation as described in Chapter 6. Additional system characterization for 1997 reservoir and river conditions can be found in Chapter 7.

Flow Modification Alternatives

Four flow alternatives were developed to assess system water temperature and water quality response. Baseline and the four alternative flow regimes are presented in Table 8.3. Average monthly flows for May were maintained for all cases at the baseline level: 1500 cfs. The High Flow-One (HF-1) case maintained a constant 2500 cfs release from Iron Gate Dam from June through October, and resulted in a total release of 849,400 acre-feet: over a 100 percent increase above baseline conditions. The HF-2 case maintained a constant 1700 cfs flow rate throughout the study period and resulted in a total release of 607,100 acre-feet: approximately a 50 percent increase over the baseline condition. The low flow (LF) case reduced Iron Gate Dam releases to 800 cfs from July through September and maintained flows of 1000 cfs during June and October. The total LF release was 358,600 acre-feet, or roughly a 12 percent reduction from the baseline case. The modified flow (MF) alternative was designed to release the same quantity as the baseline case (approximately 406,000 acre-feet), but with varied timing. None of the proposed flow regimes conflict with model limitations.

Table 8.3   Baseline, high, low and modified flow alternatives

Month	Baseline	High-1 (HF1)	High-2 (HF-2)	Low (LF)	Modified (MF)
			(cfs)		
May	1500	1500	1500	1500	1500
June	1240	2500	1700	1000	1400
July	820	2500	1700	800	800
August	1050	2500	1700	800	800
September	1050	2500	1700	800	800
October	1035	2500	1700	1000	1400
Total (TAF):	406.4	849.4	607.1	258.6	406.9

Flow changes between months assumed to occur linearly over one day

Reservoir Storage Modification Alternatives

To assess the impact of modifying Iron Gate Reservoir storage on downstream river reaches two reservoir storage alternatives were analyzed: reduced storage and increased storage. The reduced storage (RS) alternative included decreasing maximum capacity of Iron Gate Reservoir to elevation 2305 ft msl, or to about 39,700 acre-feet (about 68 percent of maximum storage). The increased storage (IS) alternative included raising Iron Gate Dam to allow storage to elevation 2360 msl, thereby increasing storage to roughly 90,000 acre-feet (a 50 percent increase in existing storage). All runs were completed using baseline

hydrologic conditions. The engineering, economic, social, and political feasibility of these alternatives was not explored in this study, although they may be appropriate topics for future investigation.

For the RS alternative it was assumed that all flows in excess of fish hatchery requirements were released through the power penstock (2299 msl). Realistically, it is unlikely that designated flows could be passed through the penstock at this decreased reservoir surface elevation due to lack of static head. Nonetheless, this alternative illustrates the impact of reduced storage while utilizing existing facilities. The IS alternative assumes that the dam would be raised without changing to fish hatchery or power penstock intake elevations.

Modified Outlet Configuration Alternatives

Additional water management options analyzed for water temperature control in downstream river reaches included modified outlet configurations. Two general scenarios were examined: lowering the penstock and/or fish hatchery intakes, and selective withdrawal.

Three low level intake configurations were analyzed. Reservoir operation was simulated for penstock elevations at 2270 ft msl (LL1) and 2240 ft msl (LL2), while maintaining the current fish hatchery intake elevation. A third simulation was completed for the penstock elevation at 2240 ft msl and a fish hatchery intake lowered to 2200 ft msl (LL3).

Two selective withdrawal alternatives were examined: selective withdrawal under current storage conditions and under increased storage. To simulate selective withdrawal from multiple levels at current storage conditions, two hypothetical outlets were added at elevations 2285 and 2270 ft msl, in addition to the existing outlet at 2299 ft msl. Further, the fish hatchery intake was lowered to 2200 ft msl to assure cool water supplies. Selective withdrawal from lower level intakes (2285 and 2270 ft msl) was assumed to start on June 1, because May water temperatures at the penstock elevation (2299 ft msl) remained cool. Although utilization of cold water from lower outlets would result in even cooler May releases, conserving cold water for use later in the year could provide more substantial benefit. Note: this application of selective withdrawal did not utilize the optimization logic available in WQRRS to meet release temperature objectives, though optimal operation may be a topic for future investigation.

Because both selective withdrawal (SW) and increased storage (IS) alternatives showed promise for temperature control in reservoir releases to the Klamath River, a combined alternative examining both modifications (SW-IS) was simulated analyzed. Iron Gate Reservoir capacity was represented as in the IS alternative and three withdrawal intake elevations were set at 2330, 2300, and 2370 ft msl. The fish hatchery intake was set at 2200 ft msl. Baseline hydrologic conditions were assumed. Table 8.4 outlines alternative outlet configurations. All runs were completed using baseline hydrologic conditions.

Table 8.4   Intake configuration alternatives

Alternative	Penstock Intake (ft msl)	Hatchery Intake (ft msl)
Baseline	2299	2254
Low Level 1 (LL1)	2270	2254
Low Level 2 (LL2)	2240	2254
Low Level 3 (LL3)	2240	2200
Selective Withdrawal 1 (SW)	2299/2285/2270	2200
Selective Withdrawal 2 (SW-IS)	2330/2300/2270	2200

8.3.2.2   Results

Reservoir operation simulations were completed first, and simulated reservoir release quantities and qualities were subsequently used as input to the river models. Herein, reservoir outflow temperature refers to the combined temperatures of the penstock and fish hatchery releases, and does not account for minor heating during hydropower production. Due to the small magnitude of hatchery flows, penstock water temperature was assumed equivalent to reservoir outflow temperatures. Reservoir and river responses are outlined below.

Reservoir Response

Few of the alternatives resulted in appreciable impacts on reservoir outflow temperatures. Table 8.5 illustrates water temperature deviation from baseline conditions for each alternative on the first day of each month. Baseline outflow temperature is provided for relative comparison.

Although the system was fairly insensitive to alternative operations, storage modification and outlet configuration, this was in part due to the selected upstream boundary condition. Recall that during the summer period, Copco Reservoir release temperatures are generally comparable to Iron Gate Reservoir release temperatures, i.e., providing little temperature

187

benefit. However, the impacts of hydropower operations on Iron Gate Inflow water temperature are unknown. If Copco Reservoir operations/modifications were examined in tandem with Iron Gate Reservoir, additional system flexibility could be realized.

Table 8.5   Simulated deviation (alternative minus baseline) in Iron Gate Dam release water temperature for all alternatives

Date	Base T_w^1 °C	Deviation from Baseline Iron Gate Release Temperature (°C)										
		HF-1	HF-2	LF	MF	RS[2]	IS[2]	LL1[2]	LL2[2]	LL3[2]	SW[2]	SW-IS[2]
		(1)	(2)	(3)	(4)	(5)	(6)	(7)	(8)	(9)	(10)	(11)
6/1	17.9	-0.1	-0.2	-0.2	-0.2	0.7	-0.9	-0.1	-0.1	0.1	-0.1	-0.6
7/1	19.1	0.4	0.3	-0.1	0.2	0.5	-0.7	0.3	0.2	0.1	-0.4	-1.3
8/1	20.6	0.4	0.3	0.0	0.0	0.8	-1.0	0.0	-0.1	-0.1	0.3	-1.9
9/1	20.0	0.2	0.1	-0.1	0.0	0.0	0.2	0.5	0.6	0.7	0.0	-0.3
10/1	16.7	-0.2	-0.2	0.0	0.0	-0.4	0.5	0.1	0.5	0.6	-0.1	0.3

[1] Base T_w refers to the Iron Gate Dam release temperature under baseline conditions
[2] All storage and outlet modification alternatives were run for baseline conditions

Flow Alternatives: HF, LF, and MF

The high flow alternatives (HF-1 and HF-2) resulted in modest outflow temperature increases, up to 0.4°C (0.72°F). The high flow alternatives produce a deeper thermocline, which adversely affected water temperature at the penstock intake, as well as at the fish hatchery intake (increases up to 2°C (3.6°F)). Deviation from baseline conditions was insignificant for the low flow (LF) and modified flow (MF) alternatives.

Modified Storage Alternatives: RS and IS

The reduced storage alternative (RS) essentially changed the penstock intake depth from approximately 25 feet below the water surface (baseline) to about 5 feet. Thus, reservoir releases were comprised principally of surface or near surface waters. During summer periods, release temperatures were increased by up to 0.8° C (1.4°F) above baseline conditions. Conversely, fall period release temperatures were slightly lower than baseline conditions, as surface waters cool more rapidly than deeper waters. Additionally, reduced reservoir storage led to increased temperatures throughout the reservoir depth. Water temperatures at the fish hatchery elevation increased roughly 4°C (7.2°F) above baseline conditions.

188

Increased storage (IS) provided a significant benefit, with reduction in release water temperatures of as much as 1°C (1.8°F) through August 1. Much of the benefit was due to the deeper location of the penstock intake (roughly 55 feet versus 25 feet). Late fall water temperatures are slightly greater than baseline values. Figure 8.11 illustrates release water temperatures for the IS alternative. Under this alternative fish hatchery intake temperatures decreased appreciably from the baseline case and may prove to be too cold for optimum hatchery use.

For both the reduced and increased storage alternative, thermal response of the reservoir was a complex function of volume; surface area; heat energy entering and leaving the reservoir via inflow and outflow, respectively; and operational assumptions (e.g., location of penstock intake).
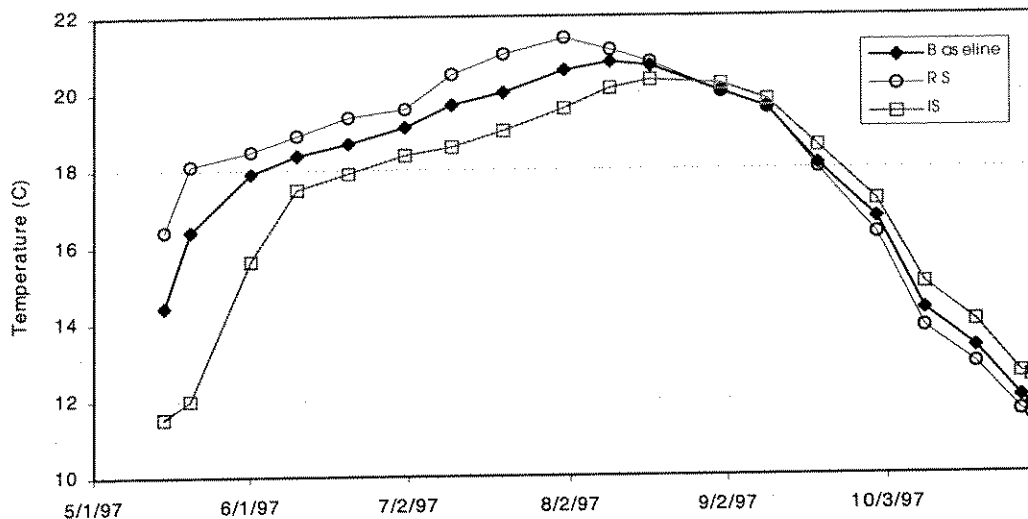
Figure 8.11 Simulated Iron Gate Reservoir release water temperatures for baseline, reduced storage, and increased storage alternatives.

Modified Outlet Configuration Alternatives

All low level intake alternatives shared a common disadvantage: lowering the single penstock intake did not allow sufficiently flexible operation to take advantage of cold water supplies. Lowering the penstock intake elevation lead to appreciably lower reservoir release temperatures in May, but effectively evacuated much of the cold water prior to June 1. No temperature benefits occurred after June 1. Moreover, due to loss of cold water early in the season, fall reservoir release temperatures were increased for all low level intake alternatives. Likewise, hatchery intake temperatures were compromised for all alternatives.

189

Examining these trials in more detail showed that during the period May 15 to 31 the release rate was roughly 1500 cfs, or a total volume of about 47,500 acre-feet – about 80 percent of Iron Gate Reservoir total storage. Removing such a large volume of water through a single intake can quickly exhaust the reservoir cold water supply in and above the region of the intake. A more flexible operating approach is to withdraw water from several levels, utilizing cold water supplies only when they are required: selective withdrawal

To illustrate temperature control potential under the selective withdrawal alternatives (SW and SW-IS), a target release temperature of 18°C (64.4°F) was assumed. Figure 8.12 illustrates the release schedule for the SW alternative. Early in the season, when surface waters were still relatively cool, water was withdrawn from the upper intake. By early June both the upper and mid-elevation intakes (2285 ft msl) were utilized, and by late June all water was drawn from the low elevation intake (2270 ft msl). The 18°C (64.4°F) temperature target could be maintained only through June 20. Further, although July temperatures were slightly cooler than baseline conditions, cold water supplies were exhausted by August 1 (Table 8.6). Lowering of the fish hatchery intake provided sufficient cold water supplies to meet demands through the summer period. Overall, selective withdrawal under current reservoir geometry provided only modest operational flexibility. Limited cold water storage in Iron Gate Reservoir precluded temperature control through the summer months.
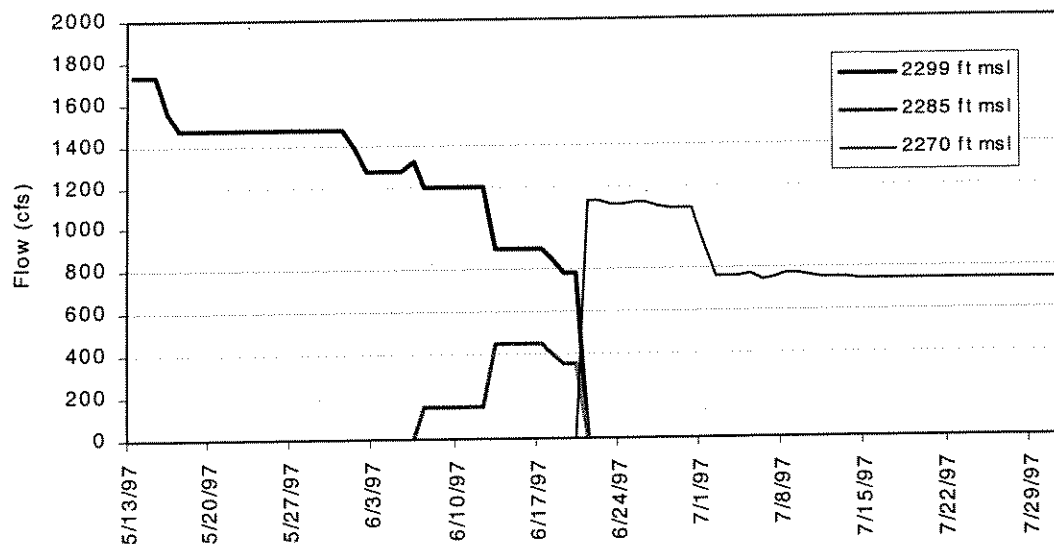
Figure 8.12 Iron Gate Reservoir Reservoir intake schedule for the selective withdrawal alternative (SW)

Observing that some measure of temperature control was possible through increased storage and selective withdrawal, the combined SW-IS alternative was assessed using the same release temperature objective of 18°C (64.4°F). Figure 8.13 illustrates the allocation of reservoir release between the three intakes. Iron Gate Reservoir release temperatures are shown in Figure 8.14. With increased storage and selective withdrawal, the 18°C (64.4°F) objective was met through mid-July. Release temperatures under this alternative were reduced through August, such that overall release temperatures never exceeded 20°C (68°F). Fall release temperatures were elevated only slightly above baseline conditions; however, not until much later in the season, when release temperatures dropped off dramatically. Temperatures in the region of the fish hatchery intake remained less than 10°C (50°F) throughout the simulation. Similar to the SW alternative, fish hatchery intake temperatures under the SW-IS alternative may be too cold, requiring mixing with waters from higher elevations within the reservoir.

River Response

Water temperature response in the Klamath River downstream of Iron Gate Dam is a function of flow rate (transit time) and reservoir release temperature (upstream boundary condition). Because reservoir release temperatures for all but a few alternatives did not deviate significantly from baseline conditions, a reduced number of alternatives were employed to assess river response. Seven alternatives were analyzed using the river flow and water quality models including: HF-1, HF-2, LF, MF, RS, IS, and SW-IS.
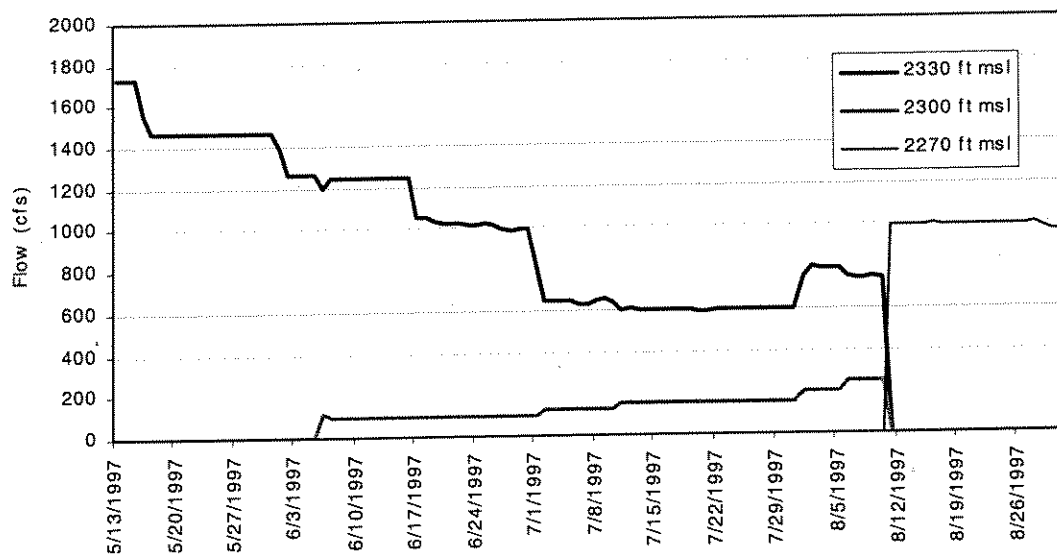
Figure 8.13 Iron Gate Reservoir Reservoir intake schedule for the selective withdrawal – increased storage alternative (SW-IS)
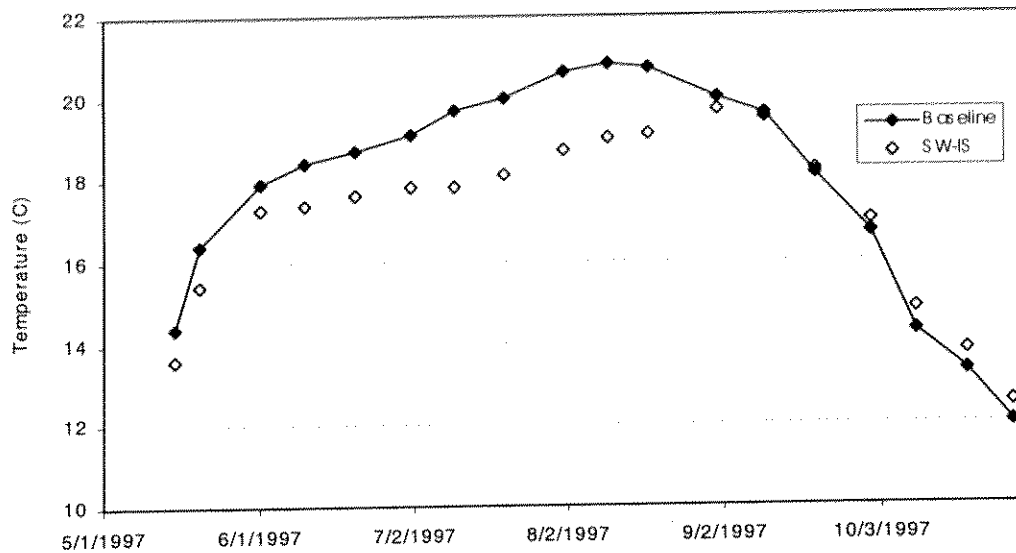
Figure 8.14 Simulated Iron Gate Reservoir release water temperatures for baseline and selective withdrawal with increased storage.

Flow Alternatives

The HF-1, HF-2, LF, and MF alternatives were examined with the river models. The variable flow rates affect transit time through the study reach, potentially affecting water quality. Longer transit times result in increased exposure to meteorological conditions, thus increasing the potential for temperature change. Transit time through the study reach for the various flows employed in the alternatives are outlined in Table 8.6. At flow rates corresponding to the HF-1 alternative, a parcel of water released from Iron Gate Dam reaches Seiad Valley in about 1.4 days. At the lowest flow rates for the LF and MF alternatives, transit time exceeds two days. Actual transit times may be slightly less due to tributary and accretion contributions.

Table 8.6 Transit times between Iron Gate Dam and Seiad Valley for various release rates from Iron Gate Dam (tributary contributions neglected)

Flow Rate (cfs)	Travel Time (hrs)	(days)
800	53.5	2.2
1000	48.9	2.0
1400	42.8	1.8
1700	39.5	1.6
2500	34.3	1.4

Increased flow rates resulted in two benefits: an overall reduced temperature increase between Iron Gate Dam and Seiad Valley and a moderated diurnal variation in downstream reaches. Because upstream boundary conditions (Iron Gate release temperature) may vary for each alternative, the differences between the rates of increase for each run are compared. Overall temperature increases for the HF-1 alternative, between Iron Gate Dam and Seiad Valley, were reduced by 0.2 to 1.3°C (0.36 to 2.3°F) during the summer months, as shown in Table 8.7. However, recall that high flow conditions generally resulted in Iron Gate Reservoir release temperatures up to 0.4°C (0.72°F) warmer than baseline conditions during the summer months. Thus, for high flow rates, increased reservoir release temperatures offset some of the benefit obtained in downstream river reaches.

Increased flow rates resulted in reduction in diurnal range of about 30 percent for the HF-1 alternative. As shown in Figure 8.15, the maximum diurnal range for June 15 is about 3.9°C (7.0°F), compared to the baseline case of 5.7°C (10.3°F). In this case, the maximum daily temperature is decreased and the minimum daily temperature is increased. Other noteworthy features of the HF-1 alternative are illustrated in Figure 8.15. First, the general rate of increase in temperature in the downstream direction, represented by the slope of the daily mean temperature trace, is less for the HF-1 alternative. Second, under high flow conditions the tributaries have a smaller impact on main stem temperature, most noticeable as the lesser cool water benefit from Scott River inflows near RM 143. Finally, the node of minimum diurnal variation is shifted downstream from approximately RM 157 to RM 149 under the HF-1 alternative.

Table 8.7   Simulated temperature below Iron Gate Dam and at Seiad Valley and rate of temperature change for the baseline and HF-1 alternative

Alternative	Simulated Temperature									
	June 1		June 15		July 1		Aug. 1		Sep. 1	
	IG Dam	Seiad USGS	IG Dam	Seiad USGS	IG Dam	Seiad USGS	IG Dam	Seiad USGS	IG Dam	Seiad USGS
Baseline	17.8	18.6	18.5	21.0	19.1	19.2	20.6	23.3	20.0	21.1
ΔTw IG→Seiad		0.8		2.5		0.1		2.7		1.1
HF-1	17.7	18.6	18.7	20.6	19.5	19.4	21.0	22.4	20.2	20.8
ΔTw IG→Seiad		0.9		1.9		-0.1		1.4		0.6
Difference:		0.1		-0.6		-0.2		-1.3		-0.5

IG Dam: Iron Gate Dam release temperature (RM (190.1)

Seiad USGS: USGS Gage at Seiad Valley (RM 128.9)

Difference = ΔTw (HF-1) − ΔTw (baseline)
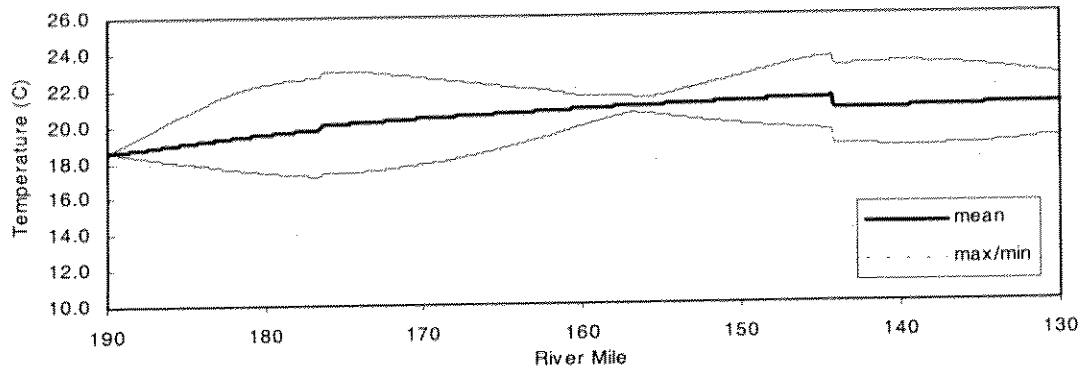
(a)
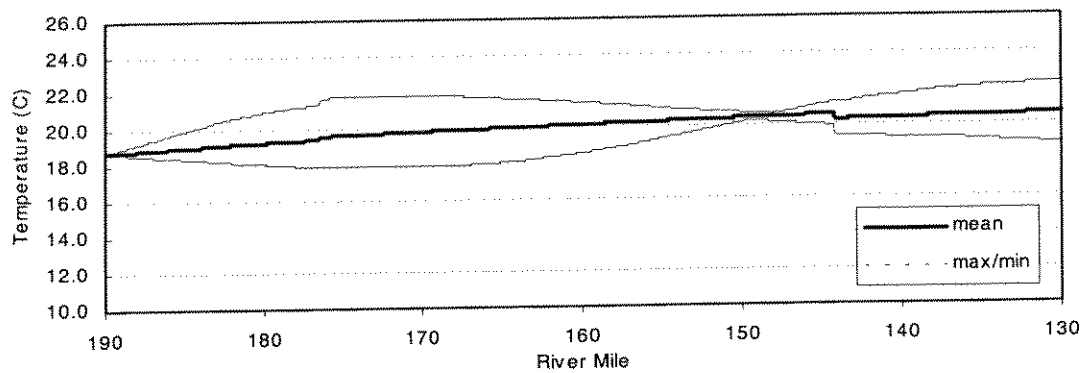
(b)

Figure 8.15 Longitudinal maximum, mean, and minimum water temperature profiles for the Klamath River from Iron Gate Dam to Seiad Valley on June 15 for (a) baseline and (b) HF-1

In contrast, the LF alternative led to a larger diurnal range, a greater degree of heating between Iron Gate Dam and Seiad Valley, and an increased tributary influence. Overall, the HF-2, LF, and MF alternatives provided little or no temperature benefit over baseline conditions. Longitudinal daily mean temperature profiles for each flow alternative, compared to baseline conditions, are included in Appendix H for May 15, June 1, June 15, July 1, August 1, September 1, October 1 and October 31.

Modified Storage Alternatives

The modified storage alternatives – reduced (RS) and increased storage (IS) – utilized baseline flow conditions. Thus, the principal difference between these alternatives was in the Iron Gate Dam release temperature. Because the RS alternative resulted in generally warmer reservoir release temperatures during summer periods, downstream temperature

194

control was infeasible. However, the IS alternative resulted in cooler reservoir releases to the river, which, in turn, reduced temperatures throughout the study reach from June through August. Although downstream temperatures were reduced, the overall temperature increase from Iron Gate to Seiad was greater than for the HF-1 alternative (see Tables 8.7 and 8.8). This is due to decreased flow rates for the IS alternative and the fact that the cooler release is further from equilibrium temperature, and thus heating occurs at a greater rate during transit to Seiad. Longitudinal daily mean temperature profiles for each the RS and IS alternatives, compared to baseline conditions, are included in Appendix H for May through October.

Table 8.8   Simulated temperature below Iron Gate Dam and at Seiad Valley and rate of temperature change for the baseline and IS alternative

Alternative	Simulated Temperature									
	June 1		June 15		July 1		Aug. 1		Sep. 1	
	IG Dam	Seiad USGS	IG Dam	Seiad USGS	IG Dam	Seiad USGS	IG Dam	Seiad USGS	IG Dam	Seiad USGS
Baseline	17.8	18.6	18.5	21.0	19.1	19.2	20.6	23.3	20.0	21.1
$\Delta T_{w\ IG\rightarrow Seiad}$		0.8		2.5		0.1		2.7		1.1
IS	15.5	18.4	17.7	20.8	18.4	19.0	19.6	23.0	20.2	21.1
$\Delta T_{w\ IG\rightarrow Seiad}$		2.3		3.1		0.6		3.4		0.9
Difference:		1.5		0.6		0.5		0.7		-0.2

IG Dam: Iron Gate Dam release temperature (RM (190.1)

Seiad USGS: USGS Gage at Seiad Valley (RM 128.9)

Difference = $\Delta T_{w\ (IS)} - \Delta T_{w\ (baseline)}$

Modified Outlet Configuration

To assess the potential temperature for control using modified outlet configurations, the selective withdrawal-increased storage alternative (SW-IS) was evaluated using the river models. Selective withdrawal allowed more efficient use of cool water supplies under increased storage conditions. Release temperatures were below baseline conditions well into summer months, as shown in Table 8.9. Comparison of SW-IS results with IS results (Table 8.8) shows that for the SW-IS alternative Iron Gate Dam release temperatures were 0.3 to 1.9°C (0.54 to 3.4°F) cooler than the baseline case, and 0.2 to 0.9°C (0.36 to 1.6°F) cooler than the IS alternative. However, water temperatures at Seiad Valley were comparable to those of the IS alternative – differing by less than 0.2°C (0.36°F). Although reservoir release temperatures were cooler, the benefit was less significant at Seiad Valley, due to a more rapid rise towards equilibrium temperature. River reaches closer to Iron Gate Dam

experienced a greater benefit from cold water releases, as shown in the longitudinal mean daily temperature profiles (Figure 8.16).

As noted above, no attempts were made in this study to optimize intake elevation or withdrawal schedule. WQRRS has the capability to optimize reservoir withdrawals to meet specified downstream objectives for a given set of intake elevations and capacities. More efficient selective withdrawal operations could be determined using WQRRS through varying the number of intakes, intake elevation, and intake capacity. This remains a topic for future investigation.

Table 8.9   Simulated temperature below Iron Gate Dam and at Seiad Valley and rate of temperature change for the baseline and SW-IS alternative

Alternative	Simulated Temperature									
	June 1		June 15		July 1		Aug. 1		Sep. 1	
	IG Dam	Seiad USGS	IG Dam	Seiad USGS	IG Dam	Seiad USGS	IG Dam	Seiad USGS	IG Dam	Seiad USGS
Baseline	17.8	18.6	18.5	21.0	19.1	19.2	20.6	23.3	20.0	21.1
ΔT_w IG→Seiad		0.8		2.5		0.1		2.7		1.1
SW-IS	17.2	18.4	17.5	20.7	17.8	18.8	18.7	22.8	19.7	21.0
ΔT_w IG→Seiad		1.2		3.2		1.0		4.1		1.3
Difference:		0.4		0.7		0.9		1.4		0.2

IG Dam: Iron Gate Dam release temperature (RM (190.1)

Seiad USGS: USGS Gage at Seiad Valley (RM 128.9)

Difference = ΔT_w (SW-IS) − ΔT_w (baseline)

Summary

Principal findings of these river and reservoir analyses illustrate that temperature control options may be feasible during spring, but are limited during the summer and early fall period. Under the existing dam and outlet works configurations, increased flow rates generally result in increased reservoir release temperatures, but decreased overall heating between Iron Gate Dam and Seiad Valley. Conversely, low flow rates do not significantly increase reservoir release temperature, but subsequent releases to downstream reaches are subject to larger thermal gains due to longer transit times to Seiad Valley. Further, colder reservoir releases are prone to more rapid rates of heating in downstream reaches. Spring and fall periods are usually not as critical because temperatures are generally within acceptable ranges. Modifying outlet works and storage capability provides th emost promise for water temperature control in downstream reaches, especially just below the dam. However, as distance from Iron Gate Dam increases, water temperature control capability

decreases. Significant temperature findings for the late spring, summer, and early fall period include:

- Increasing flow reduces transit time in the study reach, moderating the diurnal temperature range and providing modest temperature benefits in downstream reaches. However, increased flows increased reservoir release temperatures and adversely affected hatchery release temperature.

- Reducing storage provided little benefit to downstream temperatures, while hypothetically increasing storage illustrated increased potential for moderate temperature control well into the summer months.

- Hypothetically lowering the penstock elevation resulted in rapid evacuation (loss) of cold water supplies due to the short relatively residence time of Iron Gate Reservoir. Selective withdrawal proved to be a much more efficient use of cold water supplies stored in the reservoir.

- Combining increased reservoir storage and selective withdrawal provided the greatest degree of water temperatures in the reach below Iron Gate Dam.
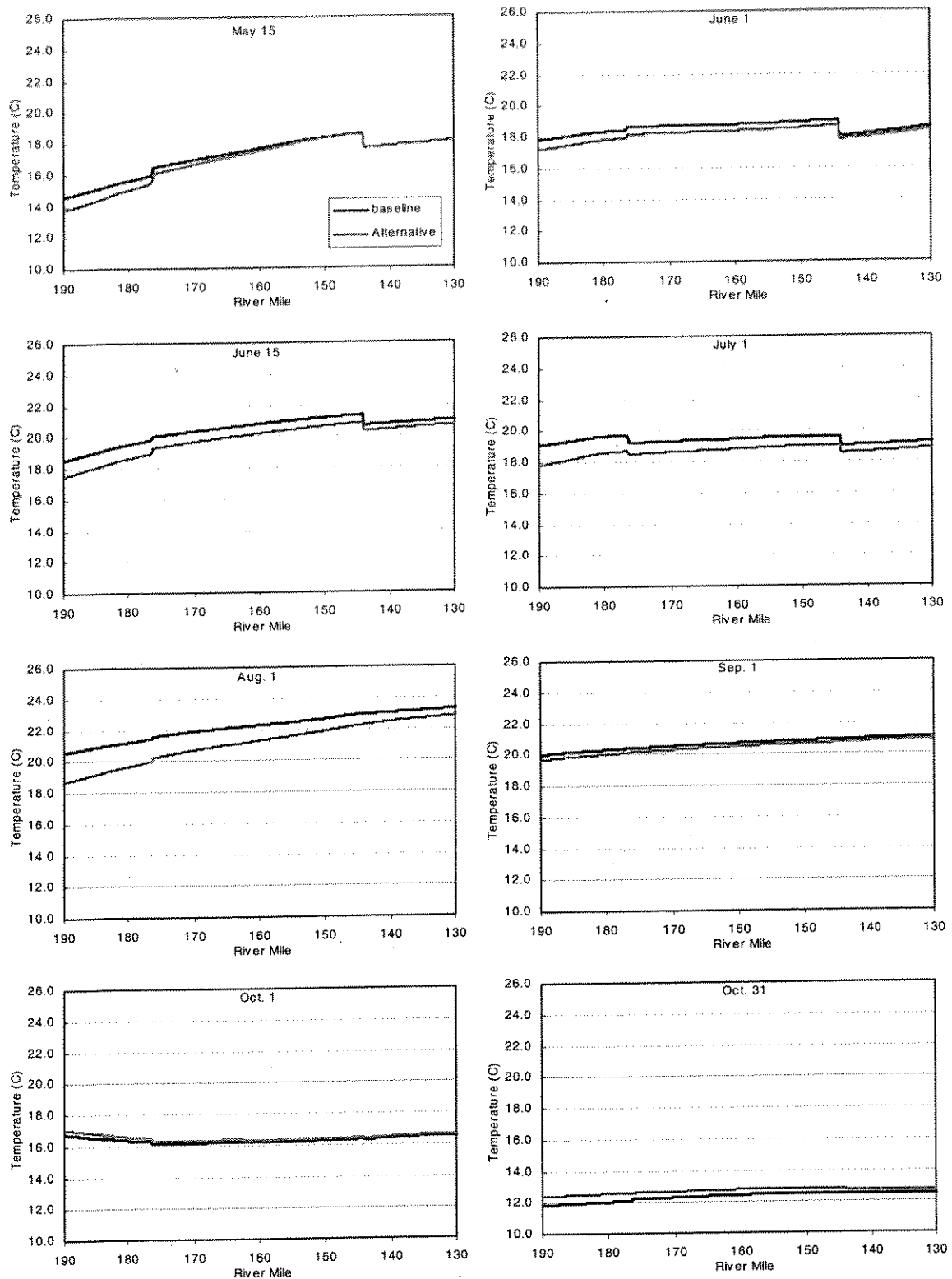
Figure 8.16   Alternative SW-IS: Klamath River mean daily water temperature profiles from
Iron Gate Dam to Seiad Valley, May through October

198

8.3.3　Dissolved Oxygen – General Findings

Although simulated dissolved oxygen values were not formally used in the assessment of alternatives, review of model results in downstream river reaches did provide additional insight into system processes. General findings are outlined below.

8.3.3.1　Iron Gate Reservoir

Current reservoir configuration and operation results in depressed dissolved oxygen concentrations throughout much of the water column by mid-summer. Anoxic conditions are evident in the reservoir from late spring through mid-fall of most years. Under alternative flow, outlet, and storage conditions, dissolved oxygen concentrations do not improve appreciably. The impact of Copco Reservoir operations and release quality on Iron Gate dissolved oxygen concentration was not assessed. Improved definition of this upstream boundary condition would aid in overall system characterization and assessment.

Under simulated high flow conditions, dissolved oxygen concentration in Iron Gate Dam release increased slightly during mid-summer. These results are most likely attributable to a deeper thermocline and a more thermally uniform epilimnion. Probably the most important result of these predicted conditions is that under high flow conditions anoxic hypolimnetic waters are less accessible to penstock withdrawal. All other flow alternatives showed little or no impact on dissolved oxygen concentration in reservoir releases.

Varying the intake elevation, e.g., lowering the penstock intake, generally resulted in lower dissolved oxygen concentrations of reservoir releases throughout the season. That is, a greater proportion of oxygen deficient water is entrained in the discharge. Likewise, selective withdrawal, while providing cooler water, further depressed dissolved oxygen in releases. Withdrawing water from deeper elevations in the reservoir increases the opportunity to access anoxic hypolimnetic water.

Modifying storage had the most profound effects on dissolved oxygen. The reduced storage alternative resulted in the penstock entraining near-surface waters that were higher in dissolved oxygen content. Thus, dissolved oxygen concentrations were appreciably increased under these operations. Conversely, increased storage resulted in decreased dissolved concentration in reservoir releases in this option because the penstock was located at a much deeper depth in the reservoir where oxygen deficits were greater.

Overall, only the reduced storage alternative significantly improved dissolved oxygen concentrations above baseline conditions. In all cases, releases were at or below saturation concentration.

8.3.3.2 Klamath River

Dissolved oxygen concentrations in the Klamath River below Iron Gate Dam varied primarily with the quantity and quality of release water. Reservoir releases varied in concentration from about 100 percent saturation to less than 50 percent saturation for the range of alternatives examined. In all cases, dissolved oxygen concentrations increased in the river downstream of Iron Gate Dam, due primarily to stream reaeration and primary production. Responses varied seasonally, with sharpest increases in dissolved oxygen concentrations occurring in summer months when primary production was most prevalent. For nearly all cases mean daily concentrations approached 100 percent saturation within the first 10 to 15 miles downstream of Iron Gate Dam. For those cases where dissolved oxygen concentrations were initially extremely depressed, deficit conditions persisted several miles further downstream

Longitudinal responses of dissolved oxygen, i.e. variations with distance below the dam, were not examined beyond approximating distances for stream concentrations to approach saturation. Additional field data are required to assess the impact of primary production on dissolved oxygen and to effectively characterize these processes in the water quality model.

8.3.4 Application of a Water Quality Index

Assessment of alternative water management options is often difficult without a quantitative measure of comparison. To assess trends, identify river reaches where conditions have changed, detect seasonal variations, and to compare alternative management actions it is feasible to rate conditions on a numerical scale, i.e., to devise an index. The risks of employing a numerical index include over-simplification of complex processes, improper application, and lack of transferability. However, in the proper context, the advantages of quick assessment may offset these limitations and make an index a useful tool.

Three numerical indices have been developed specifically for comparison of alternative water quality management options for the Klamath River below Iron Gate Dam: a temperature index, a dissolved oxygen index, and a combined temperature-dissolved oxygen

index. The temperature index is based on daily maximum, mean, and minimum water temperatures, thus accounting for sub-daily variations in water temperature. The dissolved oxygen index is based only on daily mean dissolved oxygen concentration due to a lack of available validated model output; however, the index is designed to accommodate sub-daily data when it becomes available. The combined index employs the discrete temperature and dissolved oxygen index values to identify locations and periods where both temperature and dissolved oxygen are of concern.

8.3.4.1   Index Development

The indices are based on predetermined threshold values for water temperature and dissolved oxygen. Two values for each parameter are defined: a no-effect/chronic (NC) threshold and chronic/acute (CA) threshold. These thresholds define three "condition levels:"

(1) desirable range: index below NC threshold,
(2) degraded range: index between NC and CA thresholds
(3) undesirable range: index above CA threshold

Theoretically, threshold criteria may vary for each species of anadromous fish, as well as for various life stages. For this project, species differentiation was not considered. Temperature threshold criteria were estimated for two life stages: adult migration and spawning, and juvenile rearing and emigration, as stipulated in Table 8.10. Dissolved oxygen threshold criteria were not differentiated for life stage due to lack of available information. The dissolved oxygen index was examined in terms of both absolute concentration and percent saturation. For absolute concentrations, the no-effect/chronic threshold was set at 7 mg/l and the chronic/acute threshold was set at 5 mg/l. Percent saturation criteria are not fixed, but vary with water temperature. Complete index description, development, and water quality criteria are defined in Appendix I.

Table 8.10   Temperature criteria to define condition levels for adult and juvenile salmonids

Life stage	Temperature Criteria (°C (°F))	
	No-Effect/Chronic Temperature Threshold T_{NC}	Chronic/acute Temperature Threshold T_{CA}
Adult Migration/Spawning	18.0 (64.4)	22.0 (71.6)
Juvenile Rearing and Emigration	16.0 (60.8)	20.0 (68.0)

201

The temperature, dissolved oxygen, and combined indices are shown in equations 8.1, 8.2, and 8.3, respectively.

$$I_T = \sum_i \omega_i / 3, \quad i = max, mean, min \tag{8.1}$$

Where
    I_T = temperature index
    ω_i = index weighting coefficient for max, mean, or min daily water temperature

$$I_{DO} = \alpha_i, \quad i = mean \tag{8.2}$$

Where
    I_{DO} = dissolved oxygen index
    α_i = index weighting coefficient for mean daily dissolved oxygen

$$I_{T\text{-}DO} = \gamma \, I_T \, \beta + (1 - \gamma) \, I_{DO} \, \beta \tag{8.3}$$

Where
    $I_{T\text{-}DO}$ = combined effect index for temperature and dissolved oxygen
    I_T = temperature index value
    I_{DO} = dissolved oxygen index value
    γ = relative parameter bias $(0 < \gamma < 1.0)$
    β = combined effect factor for temperature-dissolved oxygen interaction $(\beta \geq 1.0)$

Identical index weighting coefficients (ω and α) were applied for both temperature and dissolved oxygen. The index weighting coefficients for the three condition levels (desirable, degraded, and undesirable) were set to 0, 0.5, and 2, respectively. That is, as conditions progressed from no-effect, to degraded, to undesirable, index values increased geometrically, weighing undesirable conditions disproportionately more than degraded conditions.

For the combined index, adverse dissolved oxygen and temperature conditions were assumed to be equally responsible for impacts on salmon (i.e., γ was set equal to 0.5). The combined effect factor, β, was set at 2.0 to assure that combined index values equaled or exceeded individual index values. Figure 8.17 shows the scale of each index for the selected parameter values. The reader is referred to Appendix I for descriptions of index development and definition of all variables and coefficients.
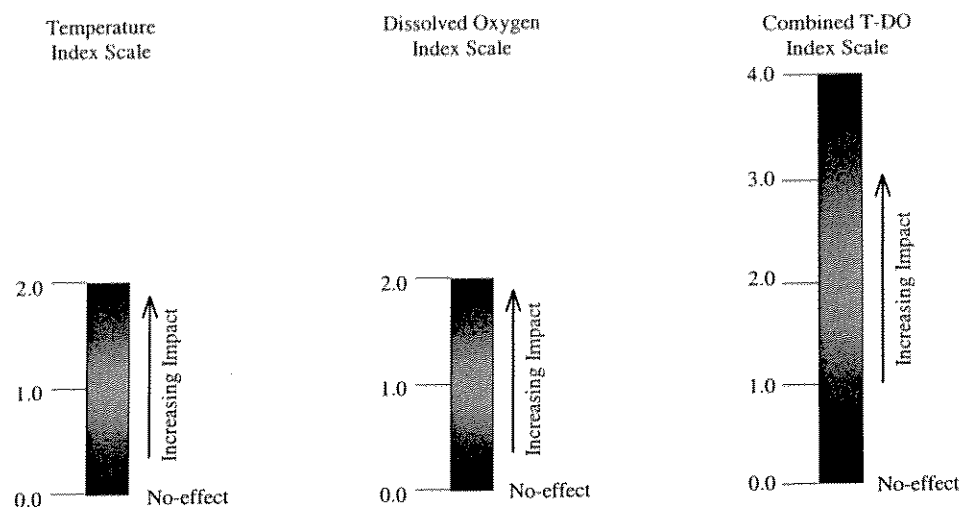
Figure 8.17 Temperature, dissolved oxygen, and combined T-DO index scales for selected parameters

8.3.4.2 Index Application

Baseline conditions and the selective withdrawal-increased storage (SW-IS) alternative are used to illustrate the application of the three water quality indices. Each index is discussed below, starting with dissolved oxygen. The state of the system on June 15 and August 1, as derived from model simulations, is used to illustrate application of the index scheme.

<u>Dissolved Oxygen Index</u>

The dissolved oxygen index was based on daily mean concentration, i.e., weighting coefficient values were assigned only according to mean values. Longitudinal profiles of simulated daily mean dissolved oxygen concentrations in milligrams per liter (absolute concentration) and percent saturation for June 15 are shown in Figure 8.18. As noted previously, dissolved oxygen levels for Iron Gate Dam releases are generally below saturation concentration. When absolute concentration is utilized, dissolved oxygen levels progressively increase with distance downstream. However, when represented as percent saturation, dissolved oxygen concentrations illustrate more variability throughout the river reach. A portion of this variation is due to water temperature, as addressed in Appendix I, while a certain degree of variability is a function of primary production. These differences are apparent in the dissolved oxygen indices for June 15, shown in Figure 8.19. The index based on absolute concentration (Figure 8.19(a)) implies the river experiences degraded conditions (I_{DO} = 0.5) from the dam, at RM 190, to RM 182, about 8 miles. The index based on percent saturation (Figure 8.19(b)) indicates that less than 2 miles experience degraded

conditions. Downstream locations illustrate no-effect and are assigned an index value of zero (undesirable conditions (I_{DO} = 2.0) do not occur in the system on June 15). For purposes of this example, the index based on absolute concentration is applied; however, these findings suggest this criteria, although easy to apply from a regulatory standpoint, may be conservative when compared to the percent saturation criteria.

The dissolved oxygen index was applied for comparison of baseline conditions to the SW-IS alternative. Figure 8.20 depicts index values throughout the study reach for each case on June 15 and August 1. As noted above, Iron Gate Reservoir releases typically exhibit some degree of depressed dissolved oxygen concentration, affecting downstream river reaches. The dissolved oxygen index suggests that approximately three additional miles of river will experience degraded conditions under the SW-IS alternative on June 15, but by August 1 dissolved oxygen concentrations are nearly equivalent to baseline conditions. It is notable that on June 15 only about 8 miles of river are degraded (I_{DO} = 0.5), but by August 1 roughly 6 miles experience undesirable conditions (I_{DO} = 2.0), and approximately 16 miles are degraded (I_{DO} = 0.5). The river recovers, i.e., shows no deleterious dissolved oxygen conditions for juvenile salmon (I_{DO} = 0.0), by RM 178 and RM 168 for June 15 and August 1, respectively.
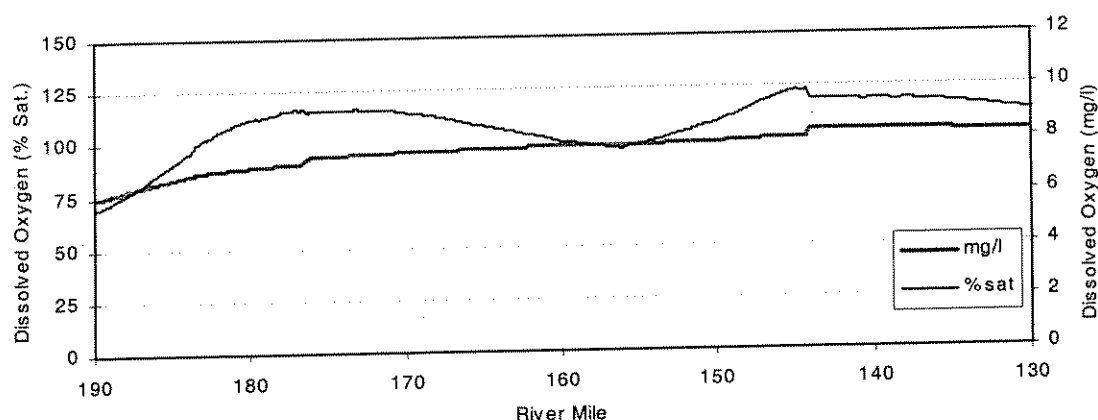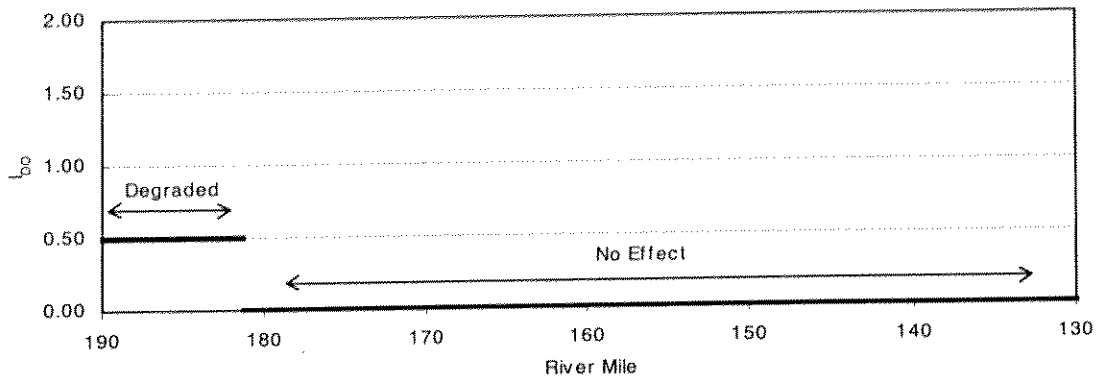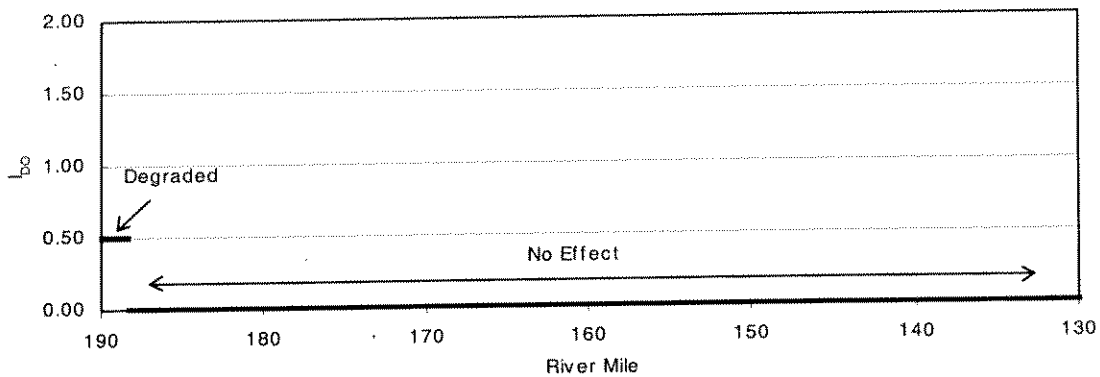

Figure 8.18   Simulated mean daily dissolved oxygen for the Klamath River from Iron Gate Dam to Seiad Valley – baseline: June 15 as percent saturation and mg/l

(a)

(b)

Figure 8.19 Dissolved Oxygen index (mean) for the Klamath River from Iron Gate Dam to Seiad Valley – baseline: June 15: (a) mg/l criteria and (b) percent saturation criteria)

Temperature Index

The temperature index utilized simulated daily mean, maximum, and minimum water temperatures. Consequently, it is not as readily interpreted as the dissolved oxygen index, wherein index values were equivalent to the weighting coefficients for the no-effect, degraded, or undesirable ranges, i.e., the dissolved oxygen index could only take on values of 0.0, 0.5, or 2.0, respectively. Thus, river thermal conditions for juvenile salmon can not be simply designated as no-effect, degraded, or undesirable

As per equation 8.1, the temperature index utilizes the three daily temperature statistics (T_{max}, T_{min}, and T_{mean}) to assign appropriate weighting coefficients. The index value is calculated as the average of the three the weighting coefficients. Because T_{max}, T_{min}, and T_{mean} may fall into different condition levels, the temperature index may assume one of several values between 0.0 and 2.0.
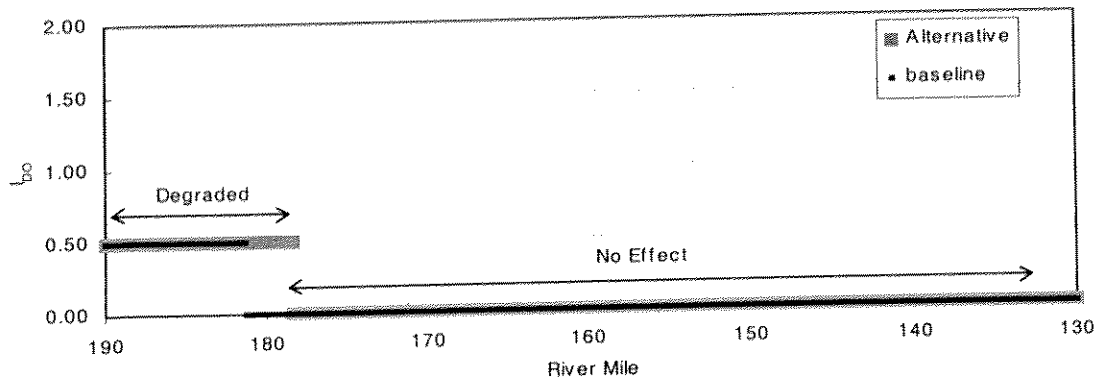
(a)
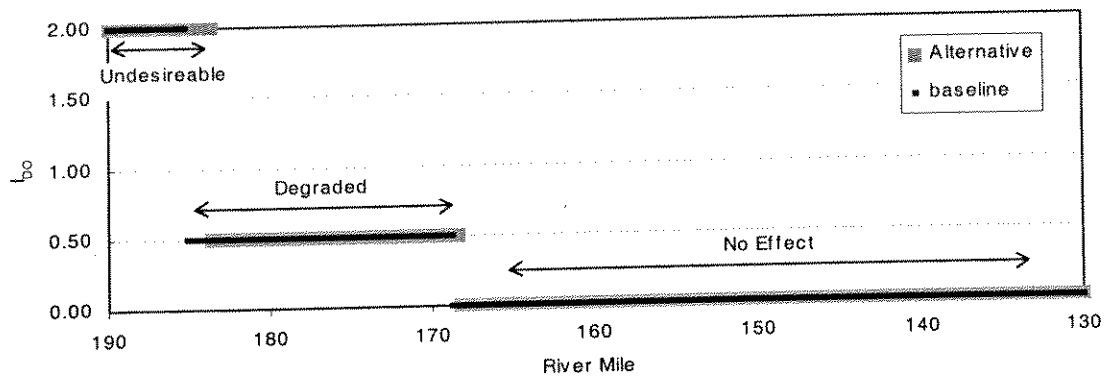
(b)

Figure 8.20 Dissolved oxygen index (mean: mg/l) for the Klamath River from Iron Gate
Dam to Seiad Valley – SW-IS vs. baseline: (a) June 15 and (b) August 1

For this application, temperature index values of 0.0 illustrate no-effect throughout a 24-hour period. Index values between 0.0 and 0.5 indicate some level of degradation during the day (24-hour period). An index value of 0.5 denotes that average conditions over the day are degraded. Values between 0.5 and 2.0 illustrate that conditions are progressively becoming undesirable throughout a greater portion of the day. An index of 2.0 represents undesirable conditions throughout a 24-hour period. The application of the sub-daily temperature index is best described by way of an example.

Figure 8.21 shows a longitudinal profile of simulated daily mean, maximum, and minimum water temperature for the Klamath River between Iron Gate Dam and Seiad Valley on June 15. (Recall there is a node of minimum diurnal temperature variation in the vicinity of RM 156.) Using the no-effect/chronic (T_{NC}) and chronic/acute (T_{CA}) thresholds of 16°C and 20°C (60.8°F and 68°F), respectively, for the juvenile life stage, the index for June 15 was

206

calculated from simulation results (Figure 8.21) and is shown in Figure 8.22. At this time, releases from Iron Gate Dam are in excess of the T_{NC} and less than the T_{CA} thresholds, and an index value of 0.5 is assigned at the dam (RM 190). At roughly RM 188 maximum daily temperatures exceed the T_{CA} threshold, so the index increases to 1.00, illustrating that a portion of the day experiences increasingly undesirable temperatures. The index increases to 1.5 near RM 177 where the daily mean temperature surpasses the T_{CA} threshold. Between RM 160 and RM152 the daily maximum, mean and minimum temperature all exceed the T_{CA} threshold, denoting undesirable conditions 100 percent of the day – a thermal barrier (I_T = 2.0). Below RM 152 minimum temperatures fall into the degraded range, and the index is reduced to 1.5. Under the conditions of June 15 it is apparent that the node of minimum temperature variation, occurring about RM 156, is detrimental to juvenile salmon, forming what is essentially a thermal barrier to downstream migration. By August 1, much of the river experiences highly degraded or undesirable conditions throughout the 24-hour period, providing little or no relief for juvenile salmon, as shown in Figure 8.23.

Utilizing sub-daily data, as depicted graphically in Figure 8.22, provides a fairly detailed representation of the system. In contrast, Figure 8.24 illustrates a temperature index based solely on daily mean temperature for June 15. Comparison with Figure 8.22 shows that the daily mean index does not account for deleterious maximum temperatures experienced between RM 188 and RM 177. Further, the benefits of minimum temperatures below the T_{CA} threshold are not included downstream of RM 177.

For further comparison, the temperature index (using sub-daily data, i.e., (T_{max}, T_{min}, and T_{mean})) was calculated for the selective withdrawal-increased storage (SW-IS) alternative. Longitudinal profiles of simulated daily mean, maximum, minimum water temperature and the corresponding calculated index for the SW-IS alternative (June 15) are shown in Figures 8.25 and 8.26, respectively. Comparison with baseline conditions indicates that more miles of river are amenable to juvenile salmon under alternative water management conditions, i.e., lower index values are computed for the SW-IS alternative throughout most of the reach below Iron Gate Dam. Further, the extent of the thermal barrier between RM 160 and 152 (I_T = 2.0) is significantly reduced. The SW-IS alternative also provides significant benefit later in the summer, especially in the reaches immediately below Iron Gate Dam, as illustrated in Figure 8.27 for August 1 simulated temperatures.

Figure 8.21   Simulated maximum, mean, and minimum temperature for the Klamath River from Iron Gate Dam to Seiad Valley – baseline: June 15

Figure 8.22   Temperature index (max-mean-min) for the Klamath River from Iron Gate Dam to Seiad Valley – baseline: June 15.

Figure 8.23   Temperature index (max-mean-min) for the Klamath River from Iron Gate Dam to Seiad Valley – baseline: August 1

208

Figure 8.24   Temperature index (mean) for the Klamath River from Iron Gate Dam to Seiad
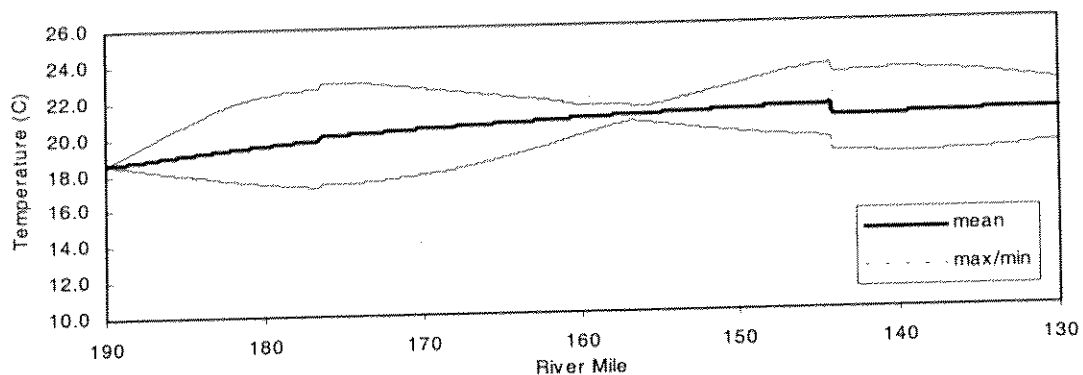   Valley – baseline: June 15
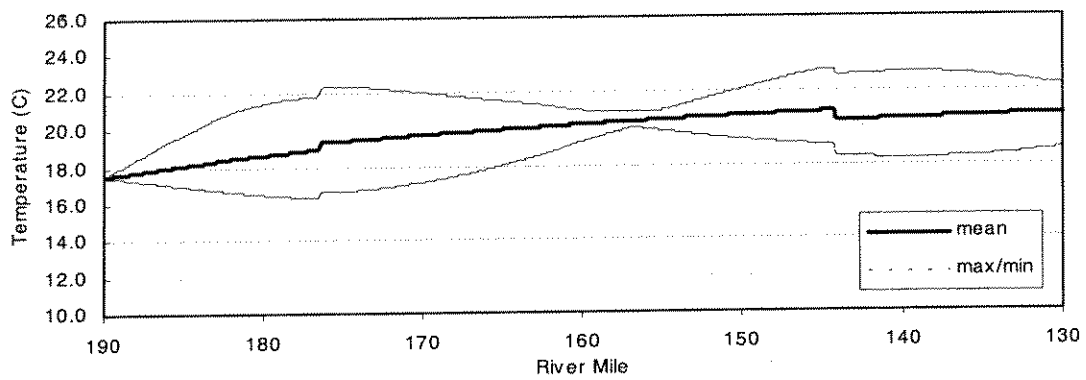
Figure 8.25   Simulated maximum, mean, and minimum temperature for the Klamath River
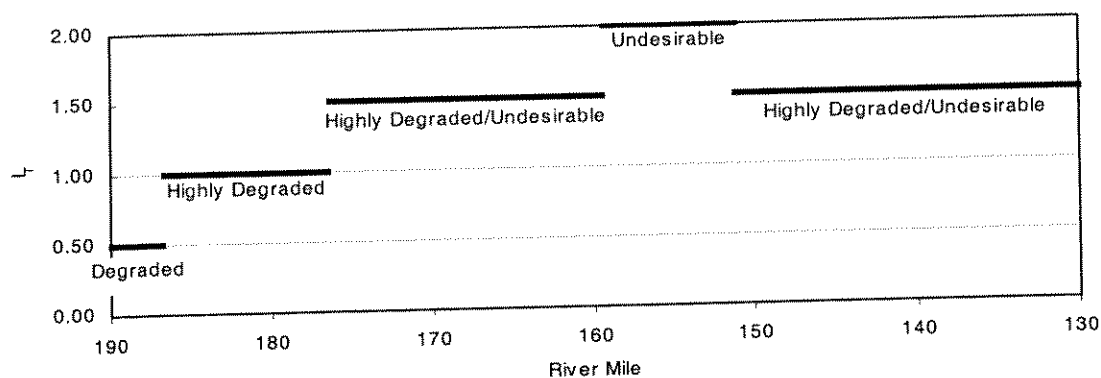   from Iron Gate Dam to Seiad Valley – SW-IS: June 15
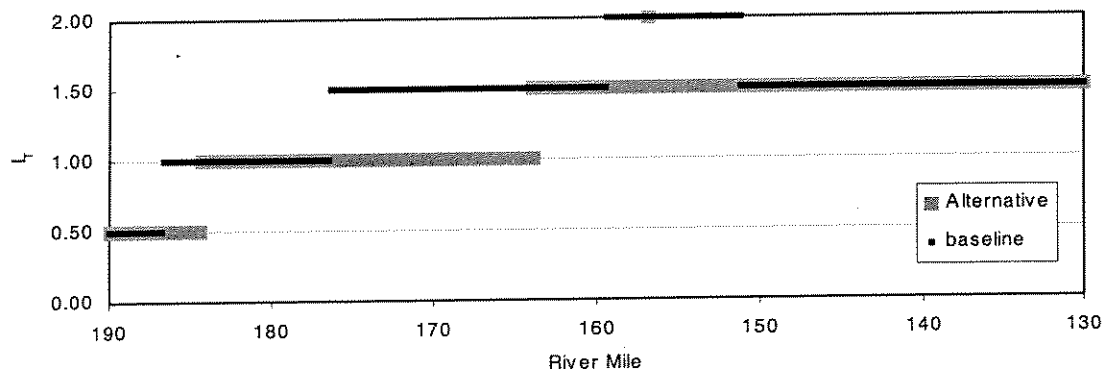
Figure 8.26   Temperature index (max-mean-min) for the Klamath River from Iron Gate
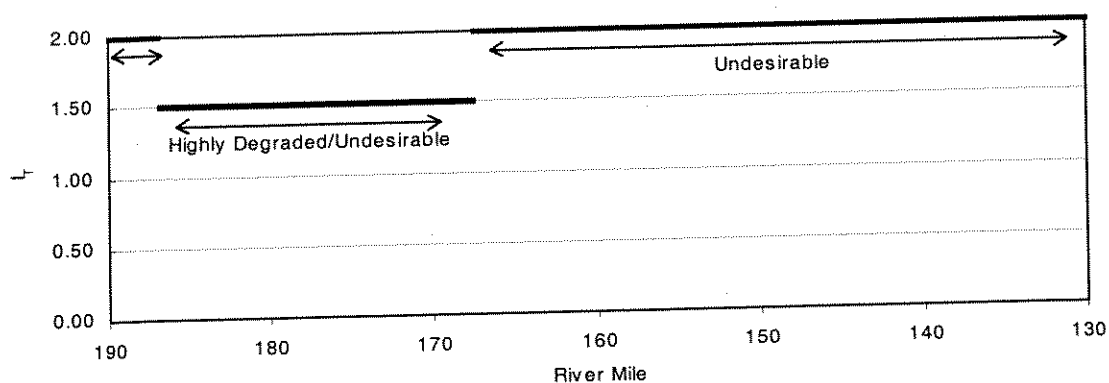   Dam to Seiad Valley – SW-IS vs. baseline: June 15
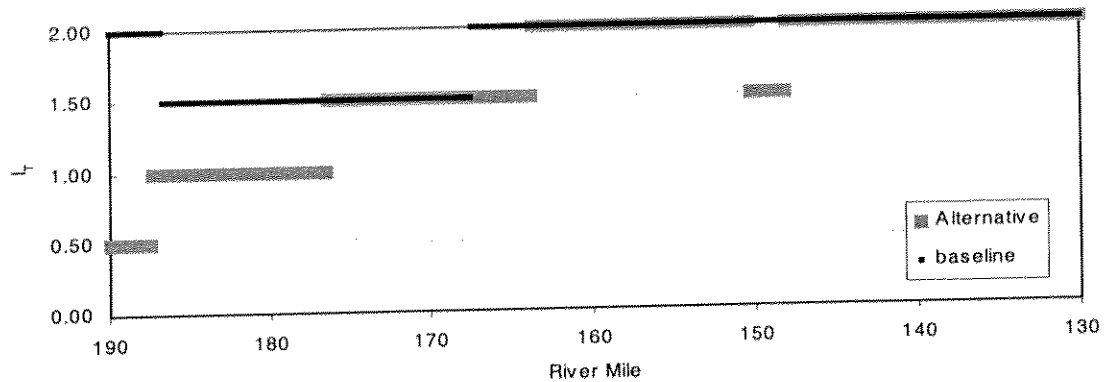
Figure 8.27 Temperature index (max-mean-min) for the Klamath River from Iron Gate Dam to Seiad Valley – SW-IS vs. baseline: August 1
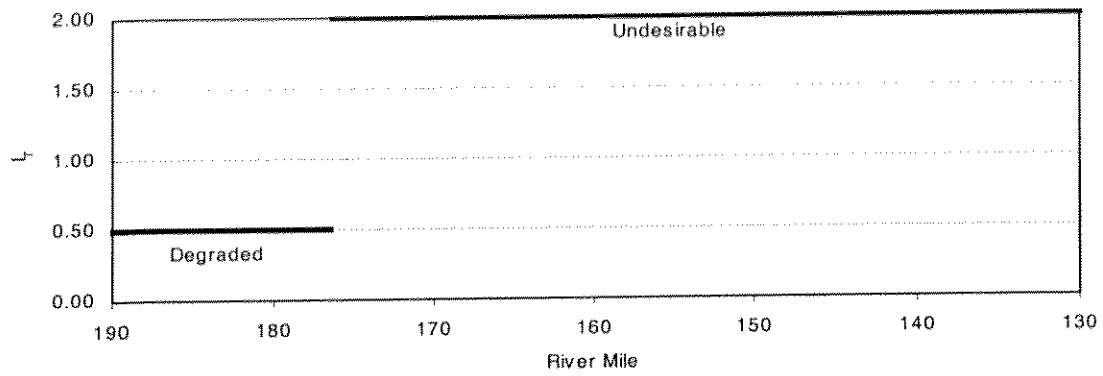
Combined Index

To address concurrent dissolved oxygen and temperature conditions throughout the study reach, the combined index was calculated as per equation 8.3. For the selected parameters, the combined index ranges from 0 to 4, with zero representing no-effect and 4 representing undesirable conditions throughout the 24-hour period. The combined index values for baseline conditions within the study reach on June 15 are reproduced in Figure 8.28. Unlike the individual parameter indices, where certain portions of the river faired better than others, the entire system experiences some level of degraded conditions under baseline conditions. In the reach immediately downstream of Iron Gate Dam, where temperature problems are only moderate, dissolved oxygen deficits increase index values to degraded levels. As oxygen levels progressively improve in downstream reaches, higher water temperatures are responsible for increases in the combined index value, reaching values of 2.0 between RM 152 and RM 160. Thus, when accounting for the combined effects of temperature and dissolved oxygen, the entire river reach is affected.
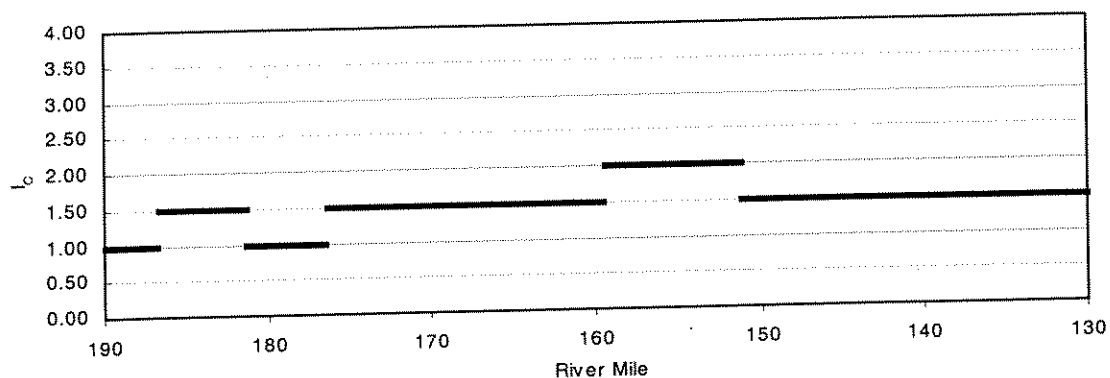
Figure 8.28 Combined Temperature (max-mean-min) and dissolved oxygen (mean: mg/l) index for the Klamath River from Iron Gate Dam to Seiad Valley – baseline: June 15

210

The combined index comparing baseline conditions with the SW-IS alternative for June 15 and August 1 are shown in Figures 8.29 and 8.30, respectively. The SW-IS alternative reduces the index value over more than 25 miles of river on June 15, and about 20 miles on August 1. Significant improvement over baseline conditions is evident later in the summer (August), as index values of 4 (undesirable) are reduced appreciably.
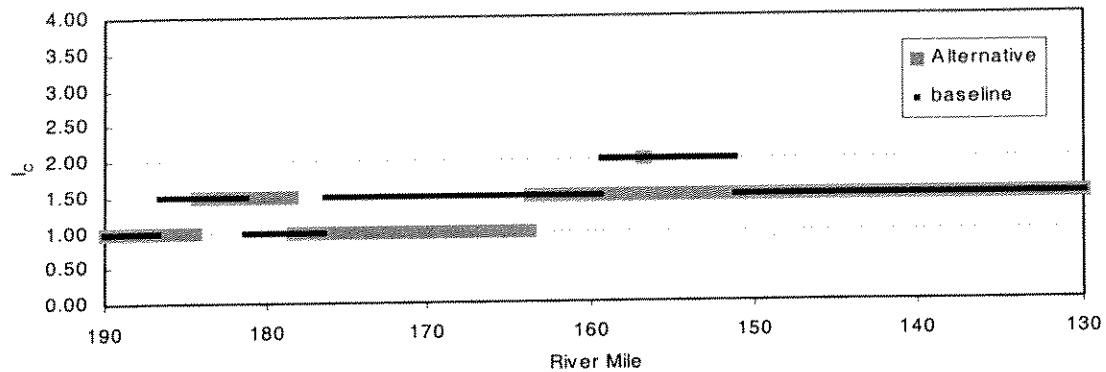
Figure 8.29 Combined temperature (max-mean-min) and dissolved oxygen (mean: mg/l) index for the Klamath River from Iron Gate Dam to Seiad Valley – SW-IS vs. baseline: June 15
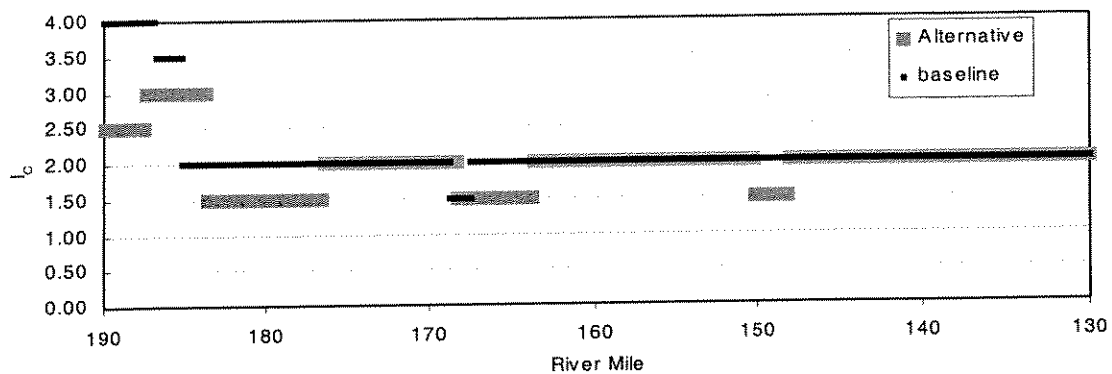
Figure 8.30 Combined temperature (max-mean-min) and dissolved oxygen (mean: mg/l) index for the Klamath River from Iron Gate Dam to Seiad Valley – SW-IS vs. baseline: August 1

Summary

Application of numerical index to assess water quality requirements for salmon at various life stages, based on no-effect/chronic and chronic/acute thresholds, can provide a means to compare alternative management scenarios. Further, the use of sub-daily data can provide insight into system response not available in an index based on daily mean values. Finally,

the ability to examine combined effects of multiple parameters, e.g., temperature and dissolved oxygen, provides a more comprehensive measure of system response.

Although June 15 and August 1 were selected for this example, other periods could be examined, and temperature and dissolved oxygen criteria modified to accommodate the appropriate life stage(s).

9.0 Summary, Conclusions, and Recommendations

The primary objectives of the Klamath River Modeling Project were to develop and implement a set of mathematical models capable of simulating the water temperature and quality regime of the Klamath River below Iron Gate Dam, and demonstrate their application in assessment of alternative measures to enhance water quality in the reservoir and river. These objectives have been achieved through a series of interrelated analyses described in the preceding sections of this report. A brief summary of project accomplishments, the principal conclusions derived from this study, and recommendations for future investigations are presented below.

9.1   Iron Gate Reservoir

Seasonal changes in temperature and water quality of Iron Gate Reservoir releases define the upstream boundary condition for downstream reaches of the Klamath River. The model WQRRS was used to simulate reservoir temperature and water quality during the critical period from May through October. Calibration and validation of water temperature and dissolved oxygen were completed using 1996 and 1997 data, respectively. Temperature calibration and validation provided confidence in model forecasting ability, with simulated outflow temperatures falling within about 1°C (1.8°F) of measured values. However, limited available field observations for reservoir dissolved oxygen concentrations compromised the model's capability to accurately forecast dissolved oxygen in downstream reaches. Typically, seasonal variations were correctly represented, but simulated outflow dissolved oxygen concentrations were under predicted in mid-summer periods (i.e., the model produces a lower concentration). In assessment of alternatives, temperature values were compared directly, while variations in dissolved oxygen were compared on a relative basis. Other water quality parameters (e.g., nutrients and phytoplankton) were also modeled. Where data were available, simulated values were compared with field observations, and overall model performance was favorable.

9.2   Klamath River Models

The Klamath River from Iron Gate Dam to the USGS Gage below Seiad Valley was modeled using RMA-2 for hydrodynamics and RMA-11 for water quality. Because the

system is treated one-dimensionally, changes are simulated only along the major axis of the river. In addition to the headwater conditions set by Iron Gate Dam, tributaries and accretions and depletions affect the system's hydrodynamics. Certain quantities are not measured or measurable. Accretions and depletions were estimated from available data. An overall water balance for the river from Iron Gate Dam to Seiad Valley was achieved using a combination of direct measurements and estimates based on tributary basin areas.

Hydrodynamic and water temperature calibration and validation were completed utilizing the two models interactively, and using data for the period June through September 1996 and 1997 periods, respectively. Adjustment of the Manning roughness coefficient in the flow model influences the hydraulic gradient of the stream, and consequently its velocity and transit time through reaches. This adjustment, in turn, affects the position and magnitude of the daily temperature cycle imposed upon the system by meteorological conditions as simulated with the water quality model. Using the models in tandem, the two models were calibrated to reproduce observed hourly temperature traces (diurnal cycle). Simulated hourly temperatures typically fell within 1°C (1.8°F) of measured values. Aggregating hourly data to daily averages produced simulated values within about 0.5°C (0.9°F) of observed daily average values.

Dissolved oxygen was calibrated separately. The water quality model was modified to include attached algae, rather than phytoplankton, to represent primary production in the steep, swift Klamath River environment. Primary production, as well as available nutrients, plays a critical role in dissolved oxygen dynamics. Because of the scarcity of reliable field data, the model could not be validated for dissolved oxygen. When used for comparative analysis hourly dissolved oxygen data were aggregated to daily average values with satisfactory results.

9.3   Field Work

Hourly water temperature data were collected at 17 stations along the Klamath River and in Iron Gate Reservoir during the 1996 and 1997 field campaigns. Hourly air temperature and relative humidity were recorded at 3 locations along the Klamath River to assess meteorological variability within the study reach. A meteorological station was installed at Iron Gate Dam in the fall of 1997 to ensure that the more extensive available observations for a station near Yreka could be considered representative of the Klamath River area. UC

214

Davis also assisted the North Coast Regional Water Quality Control Board in its water quality monitoring program during the 1996 and 1997 field seasons. These field data provided critical insight into system dynamics and were essential to successful model calibration/validation, and application.

9.4 General System Response

Prior to analyzing alternatives, the Iron Gate Reservoir and Klamath River system response was summarized using historical data, field observations from the study, and calibration and validation simulations for the reservoir and river models. Principal characteristics of the system are briefly described as follows.

Iron Gate Reservoir

Iron Gate Reservoir is subject to strong thermal stratification during the late spring through early fall period. Flow conditions during this period result in a residence time of two weeks to slightly longer than one month. Stratification and appreciable residence time, coupled with significant primary production within the reservoir, lead to low dissolved oxygen or anoxic conditions throughout much of the water column by mid-summer. Penstock release temperatures approach 22 to 23°C (71.6 to 73.4°F) during this period, while hatchery temperatures are usually below 15°C (59°F). Typically, sufficient cool water reserves are available for the fish hatchery, but anoxic water delivered to the hatchery must be aerated prior to use. Currently, normal fish hatchery operations utilize nearly all of Iron Gate Reservoir cold water supplies.

Reservoir releases to the river are generally cool, and well below equilibrium temperature in the spring period. By early summer, the epilimnion of the reservoir has heated to a sufficient depth that release temperatures do not provide appreciable thermal benefits, with the exception of a moderated diurnal cycle. In the reach immediately below the dam, maximum water temperatures are usually 2 to 4°C (3.6 to 7.2°F) lower than at downstream locations in this period. However, minimum temperatures are 1 to 2°C (1.8 to 3.6°F) warmer than at downstream locations. Dissolved oxygen concentrations in release waters are generally below saturation.

Klamath River

River water quality is a complex function of channel hydrodynamics and transit time. Inflow conditions include Iron Gate Dam releases, as well as contributions from the Shasta and Scott Rivers, the two major tributaries in the study reach. From mid-May through September, Shasta River flows are generally on the order of 100 cfs, or less, as much of the water is diverted for agricultural use upstream. Consequently, the Shasta is a minor contributor to flow in the Klamath River, usually accounting for less than 10 percent of the total below the confluence of the two rivers. Nonetheless, under low flow in the Klamath main stem, the Shasta River can significantly affect Klamath River quality. The Scott River's hydrology is substantially different than that of the Shasta. Driven largely by snowmelt runoff from the Marble Mountains, the Scott can contribute appreciable, cool temperature flows well into early summer. However, by late summer flows are typically less than 50 cfs, insufficient to appreciably influence the main stem. Later in the fall months, these small tributaries cool quickly, so despite their relatively small volumes they provide cool water to the main stem Klamath River.

Transit time through the study reach, a primary water quality factor, can range from less than a day to over two days for the range of flows experienced from May through October. During the spring and summer period, longer transit times typically translate to more heat gain because exposure time to extreme climatic conditions is increased. The results are higher mean daily water temperatures and greater diurnal variations. Generally, cool releases from Iron Gate Dam heat rapidly as they progress downstream in response to the warmer climatic conditions experienced in spring and summer. In the fall, Iron Gate Reservoir may release waters above the river's equilibrium temperature, acting as a heat source for the river. Another result of flow regulation at Iron Gate Dam is the occurrence of nodes of minimum diurnal temperature variation: locations where diurnal temperature fluctuation is suppressed. Located at intervals corresponding to one-day's travel time downstream, these nodes are direct responses of several factors: stable day-to-day meteorological conditions, near constant release temperatures, and steady release from the reservoir. Offset by roughly 12 hours from the nodes of minimum diurnal temperature variation are antinodes of maximum diurnal temperature variation.

Finally, dissolved oxygen concentrations vary in space and time throughout the study reach. Initial findings suggest that nutrients released from Iron Gate Reservoir may be enriching

algal populations immediately downstream, especially attached species. Spatial variation in attached algal populations may significantly affect the spatial variation in dissolved oxygen.

9.5   Model Applications

After being calibrated and validated, the models were applied for preliminary analysis of alternative water management scenarios. Several cases were developed, including variable flow, variable storage capacity, modification of intake elevation, and selective withdrawal. The flow alternatives were compared to a baseline case, defined as the May through October 1997 period. Flow rates for the flow alternatives considered flows that ranged from 80 to 200 percent of baseline conditions. A modified flow alternative considered releasing the same total amount of water over the May through October period, but with variable timing.

Several potential modifications in the structure and operation of Iron Gate Dam were examined. These included reducing storage capacity, increasing storage capacity, lowering the penstock intake, selective withdrawal, and combinations of increased storage and selective withdrawal. All analyses used baseline flow conditions. River release and fish hatchery temperatures were compared. Because formal calibration was only achieved for temperature, dissolved oxygen was only considered in relative terms.

For comparison of alternatives, baseline conditions were selected to correspond to historic 1997 hydrology, meteorology, and operations. The reservoir model was applied initially, with release quantity and quality passed to the river model for subsequent downstream simulation. When compared to baseline conditions, several alternatives were shown to affect water temperature control for downstream river reaches. These included scenarios that considered increased flow, selective withdrawal, or increased storage.

Flow Alternatives
Increased flow, although resulting in slightly elevated release temperatures, resulted in sufficiently reduced transit times through the river reach to provide a modest benefit, less than 1°C (1.8°F). Further, the increased volume and reduced river transit time resulted in a moderated diurnal range, i.e., maximum daily temperatures were cooler and minimum daily temperatures were warmer. However, fish hatchery temperatures were compromised under the high flow alternatives. Low and modified flow alternatives had little impact on downstream water temperatures.

217

Reduced and Increased Storage Alternatives

Reducing storage caused near-surface waters, those most prone to excessive heating, to be entrained in the penstock discharge. Overall, reservoir water temperatures throughout depth were elevated for this alternative. Reducing storage compromised fish hatchery operations: raising intake temperatures up to 2°C (3.6°F) over baseline conditions.

For the increased storage alternative, Iron Gate Dam was simulated with a hypothetical capacity of roughly 90,000 acre-feet – roughly a 50 percent increase in volume (equivalent to raising the water level approximately 25 to 30 feet). Under these assumptions, simulated release temperatures were decreased through August 1 by roughly 0.5 to 1.0°C (0.9 to 1.8°F). Fish hatchery intake temperatures were colder than baseline conditions in the mid- and late summer.

Lowering the Penstock Intake Alternatives

Lowering the penstock intake resulted in rapid evacuation of cool bottom waters (providing a short-term benefit) generally prior to June 1, followed by elevated reservoir release temperatures. Lowering the penstock compromised fish hatchery operations: raising intake temperatures up to 4°C (7.2°F) over baseline conditions.

Selective Withdrawal Alternative

Selective withdrawal, the withdrawal of water from different elevations within the reservoir at varying times, overcame the inflexibility of simply lowering the penstock. Three intakes were hypothetically positioned at successively deeper locations in the reservoir, and cool waters were accessed only as conditions warranted. Conservation of cool water supplies allowed release temperatures to be maintained roughly 0.5°C to 1°C (0.9°F to 1.8°F) cooler than baseline conditions through June. By lowering the fish hatchery intake by roughly 60 feet (2254 ft msl to 2200 ft msl), intake temperatures remained close to baseline levels.

Combined Selective Withdrawal and Increased Storage Alternative

Using the findings of the previous alternatives, a combined selective withdrawal – increased storage alternative was simulated. This alternative assumed 90,000 acre-feet of storage with three reservoir withdrawal elevations. Appreciable temperature control was available under this alternative. Reservoir release water temperatures were maintained 1 to 2°C (1.8 to 3.6°F) lower than baseline conditions through August 1, with more modest decreases thereafter.

Dissolved Oxygen Response

In general, reservoir releases for all the water management alternatives experienced dissolved oxygen concentrations that were lower than baseline conditions. This was due to the fact that, for temperature control, most alternatives either indirectly affected or directly accessed deeper, cooler reservoir waters. Because the hypolimnion of Iron Gate Reservoir is typically anoxic by mid-summer, entrainment of bottom waters can lead to depressed dissolved oxygen concentrations in reservoir releases. Once released to the river, the dissolved oxygen levels typically rise toward, or above, saturation due to reaeration and primary production. The river generally recovered within 5 to 15 miles of Iron Gate Dam.

Water Quality Index

Finally, the concept of a water quality index was introduced as a potential tool to assist in assessing baseline conditions and comparison of alternatives. Individual indices for temperature and dissolved oxygen and a combined index addressing both parameters were demonstrated. The indices are designed to use daily maximum, minimum, and mean data, thus including sub-daily information in alternative assessment. Index values are calculated based on user-specified chronic and acute threshold criteria. Sub-daily information was used in temperature index determination; however, mean daily data were used for dissolved oxygen index calculation. Such indices ease interpretation of results and provide a mechanism to examine the impact of multiple environmental stressors.

9.6   Recommendations

Development and application of the models for the simulation of temperature and water quality in the Klamath River system, although generally successful, has identified areas of additional needs, analyses, and future research. Recommendations addressing these issues are presented, first as they apply to all phases of the project, and then as they apply to specific computer models.

9.6.1   General Recommendations

Based on experience in developing, calibrating, validating, and applying the models, the following general recommendations are made:

1. That the models developed in this project be applied in the further assessment of specific options for flow and water quality control to preserve and enhance anadromous fisheries supported within the Klamath River system, including modifications to Iron Gate Dam (e.g., selective withdrawal); operational modifications (e.g., flow changes); assessing the impacts of tributary restoration; and other identified water management alternatives.

2. That modeling be extended to Copco Reservoir to further characterize the thermal and water quality regime of Iron Gate Reservoir inflow, as well as to assess coordinated management alternatives using the two reservoirs.

3. That reaches upstream of the reservoirs be investigated to determine if conditions are amenable to anadromous fishes.

4. That data gathering stations required to support flow and water quality assessment be established and a data base constructed to support sub-daily model application. Critical parameters include time series of:

   - Klamath River and tributary stream flows

   - local meteorological observations (dry and wet bulb temperature, dew point, wind speed, solar radiation, and atmospheric pressure, or equivalent parameters)

   - water temperatures at selected locations

   - water quality parameters at selected locations, see below

5. That a water quality monitoring program be implemented to assist in system characterization/assessment and to support application of the developed models. Critical parameters include, but are not limited to, dissolved oxygen, nitrogen and phosphorous species, electrical conductivity, pH, BOD, and algae. An investigative study to define economically viable and effective long-term sampling program is recommended.

6. That the scoping questions addressing potential limiting factors for anadromous fishes, as developed by the Technical Working Group, be revisited in light of the findings presented herein. Identify new questions and/or reformulate original questions as specific problem statements, with identified study tasks, for assessment with flow and water quality models.

9.6.2   Model-Specific Recommendations

Based on experience with the specific models and their respective systems, the following recommendations are made:

Iron Gate Reservoir

1. That a fully equipped meteorological station be established at Iron Gate Reservoir.

2. That water temperature and dissolved oxygen profiles be measured in the reservoir at monthly intervals during the year and at selected locations along the axis of the reservoir.

3. That water quality samples be taken at selected depths at least four times per year.

4. That upstream boundary conditions for temperature and water quality be monitored (i.e., Copco Reservoir release).

5. That WQRRS be recalibrated and validated for a wider range of water quality parameters using the data developed from items 1) through 4), above.

6. That the recalibrated and validated model be applied to assess a wider range of water quality control alternatives for Iron Gate Reservoir and downstream releases and their associated impacts on salmon production in the Klamath River. Applications should consider utilizing the optimization logic available in WQRRS to determine selective withdrawal release schedules for downstream temperature control.

Klamath River

1. That boundary conditions, specifically water temperature and quality, be improved by increased monitoring below Iron Gate Dam and at downstream locations.

2. That contributions of the Shasta and Scott Rivers be characterized in terms of water temperature and quality.

3. That a study be undertaken to more completely quantify accretions.

4. That an investigation be conducted to characterize the distribution of macrophytes in the main stem Klamath River between Iron Gate Dam and Seiad Valley.

5. That the water quality model, RMA-11, be recalibrated and validated for dissolved oxygen and a wider range of water quality parameters using the data developed from items 1) through 4), above.

6. That the model be extended to downstream reaches to assess flow, temperature, and water quality issues downstream of Seiad Valley.

7. That the recalibrated and validated model be applied to assess a wider range of water quality control alternatives for Iron Gate Reservoir releases and their associated impacts on salmon production in the Klamath River (including dam removal).

9.7   Concluding Comment

The Klamath River Modeling Project has produced a set of operating mathematical models, calibrated and validated for flow and water temperature, and preliminarily calibrated for dissolved oxygen. These models have been applied in the investigation of alternative measures to regulate and enhance salmon habitat in downstream reaches of the Klamath River where water quality may be a limiting environmental factor. They represent the state-of-the-art in mathematical modeling of hydrodynamics and water quality of riverine systems, providing a framework for future investigation of measures to preserve and enhance the habitat for anadromous fishes dependent on the water resources of the Klamath River basin.

Adams, S.M., K.D. Ham, and R.F. LeHew. 1998. A framework for evaluating organism response to multiple stressors: mechanisms of effect and importance of modifying ecological factors. In *Multiple stresses in Ecosystems.* Ed. J.J. Cech, Jr., B.W. Wilson, and D.G. Crosby. CRC Press, Lewis Publishers, New York.

Algal Ecology: freshwater benthic ecosystems. 1996. Ed. R.J. Stevenson, M.L. Bothwell, and R.L. Low. Academic Press.

American Public Health Assc., American Water Works Assc., and Water Environment Federation (APHA). 1995. *Standard Methods for the examination of water and wastewater,* 19th Ed. Editors. A.E. Eaton, L.S. Clesceri, and A.E. Greenberg. Washington D.C.

Anderson, D. A. 1998. Evaluation and impact of multiple stressors on ecosystems: four classic case histories. In *Multiple stresses in Ecosystems.* Ed. J.J. Cech, Jr., B.W. Wilson, and D.G. Crosby. CRC Press, Lewis Publishers, New York.

Armour, C.L. 1991. *Guidance for Evaluating and Recommending Temperature Regimes to Protect Fish.* USFWS, Biological Report 90(22), Instream Flow Paper 27. December.

Ayers Associates. 1998. Geomorphic and Sediment Evaluation of the Klamath River below Iron Gate Dam. Prepared for USFWS, Klamath River Restoration Office. Project 96-FLOW-03.

Belchik, M. 1997. *Summer locations and salmonid use of cool water areas in the Klamath River: Iron Gate Dam to Seiad Creek, 1996.* Yurok Tribal Fisheries Program. Funded by National Biological Service. August.

Berman, C.H. and T.P. Quinn. 1989. *The effects of holding temperatures on adult spring chinook reproductive success.* Center for Streamside Studies/Fisheries Research. University of Washington, Seattle, WA. June.

Birk, S. 1996. *General biology of anadromous salmonids affected by the Klamath Reclamation Project.* March.

Bohan, J.P. and J.L. Grace, Jr. 1973. *Selective Withdrawal from Man-Made Lakes; Hydraulic Laboratory Investigation.* Technical Report H-73-4, U.S. Army Engineer Waterways Experiment Stations, CE, Vicksburg, MS, March/

223

Boles, G.L. 1988. *Water Temperature Effects on Chinook Salmon with Emphasis on the Sacramento River - Literature Review.* California Department of Water Resources, Northern District, Red Bluff, CA. January.

Bowie, G.L., W.B. Mills, D.B. Porcella, C.L. Campbell, J.R. Pagenkopf, G.L. Rupp, K.M. Johnson, P.W. Chan, and S.A. Gherini. 1985. *Rates, constants and kinetics formulations in surface water quality modeling.* 2nd Ed. EPA/600/3-85/040 U.S. Environmental Protection Agency, Environmental Research Laboratory, Athens GA.

Breithaupt, S.A. 1997. *Modeling Benthic* Processes. Ph.D. Dissertation. University of California, Davis.

Brown, L.C. and T.O. Barnwell, Jr. 1987. *The enhanced stream water quality models QUAL2E and QUAL2E-UNCAS: documentation and user's manual.* EPA/600/3-87/700. U.S. Environmental Protection Agency, Environmental Research Laboratory, Athens GA. May.

Brown, R.L., S. Greene. 1992. Biological Assessment: Effects of Central Valley Project and State Water Project Delta Operations on Winter-Run Chinook Salmon. California Department of Water Resources (DWR). October.

California Department of Fish and Game (DFG). 1992. *Water Quality and Water Quantity Needs for Chinook Salmon Production in the Upper Sacramento River.* Prepared by DFG for the 1992 Hearing Process on the San Francisco/Sacramento-San Joaquin Delta Estuary. WRINT-DFG Exhibit No. 14.

California Department of Fish and Game (DFG). 1993. *Restoring Central Valley Streams: A Plan for Action.* Compiled by Reynolds, F.L., T. J. Mills, R. Benthin and A. Low. November.

California Department of Fish and Game (DFG). 1993b. *Central Valley Anadromous Sport Fish Annual Run-Size, Harvest, and Population Estimates, 1967-1991.* Compiled by T.J. Mills, F. Fisher. Inland Fisheries Technical Report, August.

California Department of Fish and Game (DFG). 1995. *Klamath River Basin Fall Chinook Salmon Run-Size, In-River Harvest Escapement - 1995 Season.* Klamath Trinity Program.

California Department of Water Resources (DWR). 1998. *California Water Plan Update, Bulletin 160-98.* Department of Water Resources, Sacramento. November.

California Department of Water Resources (DWR). 1991. *Shasta Rivers Valley Water Quality Literature Review.* Prepared by D. Boegner, Northern District.

California Department of Water Resources (DWR). 1986. *Klamath and Shasta Rivers Water Qulaity Study.* Northern District, February.

Campbell, E.A. and P.B. Moyle. (1990). *Effects of temperature flow and disturbance on adult spring-run chinook salmon.* University of California, Water Resources Center Technical Completion Report, Project No. W-764. August.

Chapra, S.C. 1997. *Surface water quality modeling.* McGraw-Hill, NewYork, NY.

Cech, J.J., S.J. Mitchell, D.T. Castleberry, and M. McEnroe. (1990) Distribution of California stream fishes: influence of environmental temperature and hypoxia. *Environmental biology of Fishes.* 29 95-105.

Chow, V.T. 1959. *Open Channel Hydraulics.* McGraw Hill, New York.

Colt, J., S. Mitchell, G. Tchobanoglous, and A. Knight. 1979. *The use and potential for aquatic species for wastewater treatment: Appendix B, the environmental requirements of fish.* Publication No. 65, California State Water Resources Control Cboard, Sacramento, CA.

Davis, J.C. 1975. Minimal dissolved oxygen requirements of aquatic life with emphasis on Canadian species: a review. *Journal of Fisheries Research Board Canada.* 32(12), 2295-2332.

Deas, M.L., G.K. Meyer, C.L. Lowney, G.T. Orlob, and I.P. King. 1997. *Sacramento River Temperature Modeling Project.* Center for Environmental and Water Resources Engineering. Report No. 97-01. Sponsored by the State Water Resources Control Board 205(j) Clean Water Act Grant Program, Trinity County Planning Department, and California Department of Fish and Game Proposition 70 Salmon Stream Restoration Fund. January.

Deas, M.L. and G.T. Orlob. 1998. *Shasta River Hydrodynamic and Water Temperature Modeling Project.* Center for Environmental and Water Resources Engineering. Report No. 97-01. Sponsored by the State Water Resources Control Board 205(j) Clean Water Act Grant Program. May.

Deas, M.L. and G.T. Orlob (1997) Iterative calibration of hydrodynamic and water temperature models – application to the Sacramento River." *Proceedings Water for a Changing Global Community.* 27th Congress of the International Association for Hydraulic Research and hosted by the American Society of Civil Engineers Water Resources Division, August 10-15, San Francisco, CA, 1997.

225

DeHaven, R.W. 1989. Shaded Riverine Aquatic Cover of the Sacramento River System, 1987-88 Study Results and Recommendations. Unites States Fish and Wildlife Service, Sacramento CA. May.

Dillon, R. 1975. *Siskiyou Trail*. McGraw-Hill, New York. 318 p.

Domenico, P.A. and F.W. Schwartz. 1990. *Physical and chemical hydrogeology*. John Wiley and Sons, Inc. New York, NY.

Donigan, A.S. and N.H. Crawford. 1979. Water quality model for agricultural runoff, *Modeling of Rivers*. H.W. Shen, ed., John Wilet and Sons, New York, pp12-1 – 12-82.

Drever, J.I. 1988. *The geochemistry of natural waters, 2nd Ed.* Prentice Hall. Englewood Cliffs, New Jersey.

Droste, R.L. 1997. Theory and Practice of Water and Wastewater Treatment. John Wiley and Sons, Inc. New York.

Earthinfo Inc. 1995. USGS Quality of Water: West 1, Surface, 1996.

Eckenfelder W.W. and D.J. O'Conner 1961. *Biological waste*. Pergamon Press, New York.

Elliott, J.M. and J.A. Elliot. 1995. The effect of the rate of temperature increase on the critical thermal maximum for parr of Atlantic salmon and brown trout. *The Fisheries Society of the British Isles.* 47: 917-919.

Elwood, J.W., J.D. Newbold, R.V. O'Neill, and W. Van Winkle. 1983. Resource spiraling, an operational paradigm for analyzing lotic ecosystems. In *Dynamics of Lotic Systems*. Ed. T.D. Fontaine III, and S.M. Bartell. Ann Arbor Science, Michigan USA.

Environmental Laboratory. 1995. *CE-QUAL-RIV1: A dynamic, one-dimensional (longitudinal) water quality model for streams: User's Manual*, Instructional report EL-95-2, U.S. Army Corps of Engineer Waterways Experiment Station, Vicksburg, MS.

Federal Water Pollution Control Administration (FWPCA). 1968. *Water Quality Criteria.* Report to the National Technical Advisory Committee to the Secretary of the Interior. Washington D.C.

Fisher, H.B., E.J. List, R.C.Y. Koh, J. Imberger, and N.H. Brooks. 1979. *Mixing in inland and coastal waters.* Academic Press, New York, NY.

226

Foree E.G., and P.L. McCarty. 1968. *The decomposition of algae in anaerobic waters*, Technical Report No. 95, Department of Civil Engineering, Stanford University, Stanford, CA.

Foote, J.S. and R.L. Walker. 1992. Disease Survey of Trinity River Salmonid Smolt Populations. USFWS, California-Nevada Health Center, Anderson CA. 31 pp + Appendix. November.

Forsberg O.I., and A. Bergheim. The impact of constant and fluctuating oxygen concentrations and two water consumption rates on post-smolt Atlantic salmon production parameters. *Aquacultural Engineering*. 15(5): 327-347.

Fredricksen, Kamine and Associates. 1980. Proposed Trinity River Basin Fish and Wildlife Management Program, "Main Report - Final: Volumes 1 and 2, Fish and Wildlife Analysis, Appendix C." Prepared by the Water and Power Resources Service, Sacramento CA.

Garland, J.H.N. 1978 Nitrification in the River Trent, *Mathematical Models in Water Pollution Control*. A. James, ed., John Wiley and Sons, New York.

Gerloff, G.C. 1969. Evaluating nutrient supplies for the growth of aquatic plants in natural waters. *Nitrification: Causes, consequences, correctives*. National Academy of Sciences, Washington DC, pp 537-555.

Hassler, T.J. 1987. *Species Profiles: Coho Salmon*. Biological Report 82(11.70). U.S. Fish and Wildlife Service. U.S. Gov. Print. Office, Washington, D.C.

Herrmann, R.B., C.E. Warren, and P. Doudoroff. 1962. Influence of oxygen concentration on the growth of Juvenile coho salmon. *Transaction of Amer. Fisheries Soc.* 91(2):155-167.

Hofer, R., Z. Jeney, and F. Bucher. 1995. Chronic effectsof linear alkylbenzene sulfonate (LAS) and ammonia on rainbow trout (Oncorhynchus mykiss) fry at water criteria limits. *Water Res.* 29(12): 2725-2729.

Holmberg, J.J. 1972. *Salmon in California*. USBR, Sacramento, CA. 73 pp.

Hoover, S.R. and N. Porges. 1952. Assimilation of dairy wastes by activated sludge—II. The equation of synthesis and rate of oxygen utilization, *Sewage and Industrial Wastes*, Vol 24, pp 306-312.

Hydroscience, Inc. 1971. *Simplified mathematical modeling of water quality*. 444-368/392. U.S. Environmental Protection Agency, Office of Water Programs, Washington D.C.

Jewell, W.J. and P.O. McCarty. 1968. *Aerobic decomposition of algae and nutrient regeneration,* Technical report No. 91. Department of Civil Engineering, Stanford University, Stanford, CA.

Jones, J.R. 1971. *The Land of Remember.* Naturegraph Publishers, Inc. Happy Camp, CA.

King, I.P. 1994. *RMA-2; A Two-Dimensional Finite Element Model for Flow in Estuaries and Streams, Version 5.1.* Department of Civil and Environmental Engineering, University of California, Davis.

King, I.P. 1997. *RMA-11 A Three Dimensional Finite Element Model for Water Quality in Estuaries and Streams – Documentation Version 2.5.* Department of Civil and Environmental Engineering, University of California, Davis.

Klamath River Basin Fisheries Task Force (KRBFTF). 1991. *Long Range Plan for the Klamath River Basin Conservation Area Fishery Restoration Program.* Prepared for the Klamath Basin Task Force with Assistance from William M. Kier and Associates. January.

Konecki, J.T., C.A. Woody, and T.P. Quinn. 1995. Critical thermal maxima of coho salmon (*Oncorhynchus kisutch*) fry under field and laboratory acclimation regimes. *Canadian Journal of Zoology.* 73: 993-996.

Krenkel, P.A. and V. Novotney. 1980. *Water Quality Management.* Academic Press, New York.

LaFaunce, D.A. 1965. *King (Chinook) Salmon Spawning Escapement in the Upper Trinity River, 1963.* Marine Resources Administrative Report No. 65-3. Region 1, Inland Fisheries Branch. 10 pp.

Lamb, B.L, and S. Klahn. 1996 Klamath River Institutional Analysis. Draft report to the Klamath River Fisheries Task Force. National Biological Service, Midcontinental Ecological Science Center, Ft. Collins, CO. May.

Leidy, R.A. and G.R. Leidy. 1984. Life stage periodicities of anadromous salmonids in the Klamath River basin, northwest California. U.S. Fish and Wildlife Service. Division of Ecological Services, Sacramento CA. April.

Levin, S.A. 1998. Extrapolating and scaling in ecotoxicology. In *Multiple stresses in Ecosystems.* Ed. J.J. Cech, Jr., B.W. Wilson, and D.G. Crosby. CRC Press, Lewis Publishers, New York.

Lloyd, R. 1961. Effect of dissolved oxygen concentrations on the toxicity of several poisons to rainbow trout (*Salmo gairdnerii richardson*). *Journal of Exp. Biol.* 38: 447-455.

MacKenthum K.M. and W.M. Ingram. 1967. *Biological associated problems in freshwater environments.* Federal Pollution Control Admin., U.S. Dept. of the Interior, Washington, DC.

Magaude, H., B. Migeon, P. Morfin, J. Garric, and E. Vindimian. 1997. *Water Resources,* 31:(2): 211-218.

Marine, K.R. 1992. *A background investigation and review of the effects of elevated water temperature on reproductive performance of adult chinook salmon (Oncorhynchus tshawytscha).* Department of Wildlife Fishereis Biology, Univ. of Calif., Davis. October.

Matthews, K.R. and N.H. Berg. 1997. Rainbow trout responses to water temperature and dissolved oxygen stress in two southern California stream pools. Journal of Fish Biology. 50: 50-67.

McCuthcheon, S.C., J.L. Martin, and T.O. Barnwell, Jr. 1994. Water Quality. In *Handbook of Hydrology.* Ed. D.R. Maidment . McGraw-Hill, New York.

Michny, F., and M. Hampton (1984) *Sacramento River, Chico Landing to Red Bluff Project, 1984 Juvenile Salmon Study.* U.S. Fish and Wildlife, Division of Ecological Services, Sacramento CA, October. Prepared for the U.S. Army Corps of Engineers.

Miller, J.E., and M.E. Jennings. 1979. Modeling nitrogen and Oxygen, Chattahoochee River, Ga. *Journal of Environmental Engineering Division,* American Society of Civil Engineers, Vol 105, pp641-653.

Moyle, P.B. 1976. Inland fishes of California. University of Calif. Press, Berkeley, CA.

Moyle, P.B., J.E. Williams, and E.D. Wikramanayake. 1995. *Fish Species of Special Concern.* Department of Wildlife Fisheries Biology, U.C. Davis, October. Prepared for the State of California, The Resources Agency under the Department of Fish and Game Inland Fisheries Division, Rancho Cordova, Contract #7337.

Myrick, C.A. 1988. *Temperature, genetic, and ration effects on juvenile rainbow trout (Oncorhynchus mykiss) bioenergetics.* Doctoral Dissertation, University of California, Davis.

North Coast Regional Water Quality Control Board (NCRWQCB) 1997. Water Quality Sampling, Clean Water Act 104(b) grant project data set. Preliminary: December 14.

North Coast Regional Water Quality Control Board (NCRWQCB) 1993. *Investigations of Water Quality in the Shasta River, Siskiyou County.* Prepared by B. Gwynne. Santa Rosa, CA. September.

O'Conner, D.J. and W.E. Dobbins. 1958. Mechanism for reaeration is natural streams. *Transaction of American Society of Civil Engineers.* Vol 123, pp 641-684.

Pacific Salmon Life Histories. 1991. Editors: C. Groot, L. Margolis. Department of Fisheries and Oceans, Biological Science Branch, Pacific Biological Station, Nanaimo, British Colombia, Canada. University of British Colombia Press.

Pacific Southwest Inter-Agency Committee (PSIAC) 1973. *River Mile Index; Klamath River Basin.* Report to the Water Management Subcommittee. July.

Parker, D.S., R.W. Stone, R.J. Stenquist, and G. Culp. 1975. *Process design manual for nitrogen control.* Office of Technology Transfer. US Environmental Protection Agency, Washington D.C.

Pacific Gas and Electric (PG&E). 1962. *Rivers of California.* San Francisco.

Pacific Southwest Inter-Agency Committee (PSIAC) 1973. *River Mile Index; Klamath River Basin.* Report to the Water Management Subcommittee. July.

PacifiCorp. 1995. *Available Water Supply Estimates for Iron Gate Fish Hatchery: Klamath River, California.* Portland Oregon, March.

Peterson, N.P., A. Hendry, and T.P. Quinn. 1992. *Assessment of cumulative effects on salmonid habitat: some suggested parameters and target conditions.* Center for Streamside Studies. University of Washington, Seattle, WA. March.

Porter, S.D., T.F. Cuffney, M.E. Gurtz, and M.R. Meador. 1993. *Methods for Collecting Algal Samples as Part of the National Water-Quality Assessment Program.* U.S. Geological Survey Open-File Report 93-409.

Quinn, J.W. and J.M. Quinn. 1983. *Handbook to the Klamath River Canyon.* 180 p.

Quinn, T.P. 1991. *Patterns of flow, temperature, and migration of adult Yakima River spring-run chinook salmon.* Fisheries Research Institute and Center for Streamside Studies. University of Washington, Seattle, WA. June.

Reiser, D. W., and T.C. Bjornn. 1979. *Influence of Forest and Rangeland Management on Anadromous Fish Habitat in Western North America: Habitat Requirements of Anadromous Salmonids.* U.S. Department of Agriculture Forest Service Pacific Northwest Forest and Range Experiment Station. General Technical Report PNW-96. October.

River Ecology and Management – Lessons from the Pacific Coastal Ecoregion. 1998. Ed. R.J. Naiman and R.E. Bilby. Springer, New York.

Ruane R.J. and P.A. Krenkel. 1977. Nitrification and other factors affecting nitrogen in the Holston River. *Progress in water technology*, Vol 8, No. 4-5, pp209-224.

Saviz, C.M., J.F. DeGeorgr, G.T. Orlob, and I.P. King. 1995. *Modeling the Fate of Metamsodium and MITC in the Upper Sacramento River: The Cantara Southern Pacific Spill.* Department of Civil and Environmental Engineering. Center for Environmental and Water Resources Engineering, University of California, Davis. Report 95-2.

Sawyer, C.N., P.L. McCarty, G.F. Parkin. 1994. *Chemistry for Environmental Engineering.* McGraw-Hill, Inc. San Francisco.

Seki, H. 1982. *Organic materials in aquatic ecosystems.* CRC Press, Boca Raton, FL.

Shresthat, P.L., C.M. Saviz, G.T. Orlob, and I.P. King. 1993. *Hydrodynamic Simulation of San Francisco Bayand Delta for Oil Spill Fate Studies.* Department of Civil and Environmental Engineering. Center for Environmental and Water Resources Engineering, University of California, Davis. Report 93-1. Prepared for Environmental Impact Statement – Unocal, San Francisco Marine Terminal, Contra Costa County. Agreement # C9167.

Snoeyink V.L. and D. Jenkins. 1980. *Water Chemistry* John Wiley and Sons. NY..

Stumm, W. and J.J. Morgan. 1996. *Aquatic Chemistry, Chemical equilibria and rates in natural waters, 3rd Ed.* John Wiley and Sons, Inc. New York.

Stumm, W. and J.J. Morgan. 1986. *Aquatic Chemistry, Chemical equilibria and rates in natural waters, 2nd Ed.* John Wiley and Sons, Inc. New York.

Tchobanoglous, G. and E.D. Schroeder. 1985. *Water quality.* Addison-Wesley, Menlo Park, CA.

Tennessee Valley Authority (TVA). 1972. *Heat and mass transfer between a water surface and the atmosphere.* Report No. 14. April.

The Resources Agency of California (RAC). 1989. *Upper Sacramento River Fisheries and Riparian Habitat Management Plan.* Prepared by an Advisory Council established under SB 1086, authored by Senator Jim Nielsen. January.

Thomann, R.V. and J.A. Mueller. 1987. *Principles in surface water quality modeling.* Harper and Row, New York, NY.

United States Army Corps of Engineers, Hydrologic Engineering Center (USACE -HEC). 1987. *Water Quality Modeling of Reservoir System Operations Using HEC-5.* Training Document No. 24. September.

United States Army Corp of Engineers – Hydrologic Engineering Center (USACE-HEC). 1986. *WQRRS Water Quality for River-Reservoir Systems, User's manual.* Hydrologic Engineering Center. October 1978, revised 1986.

United States Fish and Wildlife Service, California Department of Fish and Game (USFWS, DFG). 1987. *Water Quality and Water Quantity Needs for Chinook Salmon Production in the Upper Sacramento River.* Prepared by the USFWS and DFG for the 1987 Hearing Process on the San Francisco/Sacramento-San Joaquin Delta Estuary.

United States Environmental Protection Agency (EPA). 1997. *Technical guidance manual for developing total maximum daily loads.* Book 2: Streams and rivers, Part 1: Biochemical oxygen demand/dissolved oxygen and nutrients/eutrophication. 823-B-97-002. March.

United States Environmental Protection Agency (EPA). 1978. *National Eutrophication Survey Report on Iron Gate Reservoir, Siskiyou County, CA.* EPA Region IX, Working Paper No. 749.

United States Environmental Protection Agency (EPA). 1973. *Development of Dissolved Oxygen Criteria for Freshwater Fish.* Ecological Research Series EPA-R3-73-019. February.

United States Geologic Survey – Biological Resources Division (USGS-BRD). 1995. *Compilation of Phase I Reports for the Klamath River Basin.* Prepared for the Technical Work Group of the Klamath River Basin Fisheries Task Force. River Management Section. Mid-continent Ecological Science Center. Ft. Collins, CO, May.

Vinson, M. and S. Levesque. 1994. Redband trout response to hypoxia in a natural environment. *Great Basin Naturalist.* 54(2): 150-55.

Wade, A., B. Maher, I. Lawrence, N. Davis, C. Zoppou, and C. Bell. 1998. Estimating the allowable ammonia concentration in wastewater treatment plant discharge to ensure protection of aquatic biota. *Environmental Technology,* 19: 749-754.

Ward, J.V. and J.A. Stanford. 1983. The serial discontinuity concept of lotic ecosystems. In *Dynamics of Lotic Systems.* Ed. T.D. Fontaine III, and S.M. Bartell. Ann Arbor Science, Michigan USA.

Warren, C.E., P. Doudoroff, and D.L. Shumway. 1973. *Development of dissolved oxygen criteria for freshwater fishes.* Ecological Research Series, EPA-R3-73-019, U.S. Environmental Protection Agency, U.S. Government Printing Office, Washington D.C.

Water Quality Assessments. 1996. Water Quality assessments: A guide to the use of biota, sediments and water in environmental modeling. Ed. D. Chapman. Published on behalf of UNESCO United Nations Education, Scientific, and Cultural Organization; WHO World Health Organization; UNEP United Nations Environmental Programme. Chapman & Hall, London.

Water Resources Engineers. (WRE) 1969. Mathematical Models for the Prediction of Thermal Energy Changes in Impoundments. Report to the U.S. Environmental Protection Agency, Project # 16130 EXT. December.

Westin, D.T 1974. Nitrate and nitrite toxicity to salmonid fishes. *Prog Fish-Cult.* (absorbed by *Fish Culture*). 36(2): 86-89.

Wetzel, R.G. 1983. *Limnology,* 2nd Ed. Harcourt Brace College Publishers, New York, NY.

Wheatland, A.B. M.J. Barrett, and A.M. Bruce. 1959. Some observations of denitrification in rivers and estuaries. *Journal and Proceedings of the Institute of Sewage Purification,* pp 149-162.

Whitmore, C.M., C.E. Warren, and P.Doudoroff. 1960. Avoidance reactions of salmonids and centrachid fishes to low dissolved oxygen concentrations. *Trans of Americ. Fisheries Soc.* 89(1): 17-26.

Wiebe, A.H. and A.M. McGavock. 1932. The ability of several species of fish to survive on prolonged exposure to abnormally high concentrations of dissolved oxygen. *Transactions of Americ. Fisheries Soc.* 63: 267-274.

Williams, R.E. and M.S. Lewis. 1986. Stream model of benthic nitrification-denitrification. *Journal of Environmental Engineering,* Amer. Soc. Civil Eng., Vol 112, No. 2 pp 367-386.

Wood, R. and D.W. Rogers. 1991. *Shasta River Fisheries Water Quality Project.* Prepared by Ouzal Enterprises for the Shasta Resources Conservation District.

Wright, R.M. and A,J, McDonnell. 1979. In-stream deoxygenation rate prediction. ASCE *Journal of Environmental Engineering.* Vol. 105, pp 323-335.

Yen, T.F. 1999. *Environmental Chemistry: essentials of chemistry for engineering practice.* Prentice Hall. New Jersey.
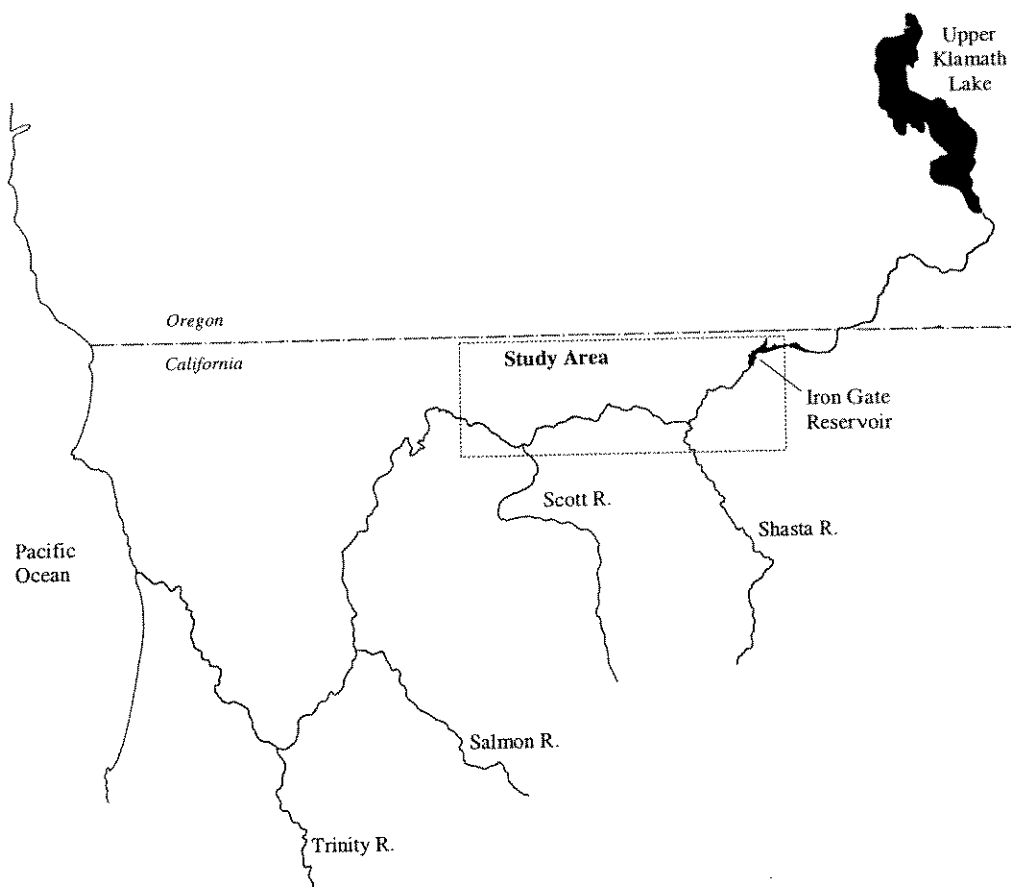
Personal Communications

Jennifer Kelly   PacifiCorp

Bruce Gwynne   NCRWQCB

Bill Winchester   NCRWQCB

Jim Henricksen   USGS

KLAMATH RIVER MODELING PROJECT

- APPENDICES -

Sponsored by the United States Fish and Wildlife Service
Klamath Basin Fisheries Task Force

Center for Environmental and Water Resources Engineering
Department of Civil and Environmental Engineering
Water Resources Modeling Group
University of California, Davis
Project #96-HP-01

December 1999

Report No. 99-04

KLAMATH RIVER MODELING PROJECT

- APPENDICES -

by
Michael L. Deas
and
Gerald T. Orlob

Project #96-HP-01
Assessment of Alternatives for Flow and Water Quality
Control in the Klamath River below Iron Gate Dam

Center for Environmental and Water Resources Engineering
Department of Civil and Environmental Engineering
Water Resources Modeling Group
University of California, Davis

Table of Contents

6

California Department of Fish and Game	DFG
California Department of Forestry	CDF
California Department of Water Resources	DWR
Federal Energy Regulation Committee	FERC
Hydrologic Engineering Center	HEC
Klamath River Basin Fisheries Task Force	KRBFTF (Task Force)
National Marine Fisheries Service	NMFS
North Coast Regional Water Quality Control Board	NCRWQCB
State Water Resources Control Board	SWRCB
Technical Work Group	TWG
University of California, Davis	UCD
United State Environmental Protection Agency	EPA
United States Army Corps of Engineers .	USCOE
United States Bureau of Reclamation	USBR
United States Fish and Wildlife Service	USFWS
United States Geological Survey	USGS
United States Geological Survey – Biological Resources Division	USGS-BRD

Unit Conversion Factors

Class	Multiply	By	To Obtain
Area	acre	4047.0	m^2
	acre	0.4047	ha (10 000 m^2)
	ft^2	0.0929	m^2
	yd^2	0.8361	m^2
	mi^2	2.590	km^2
Length	ft	0.3048	m
	in	25.4	mm
	mi	1.6093	km
	yd	0.9144	m
Volume	ft^3	0.0283	m^3
	gal	3.785	L
	fl oz	29.575	mL
	yd^3	0.7646	m^3
	acre-feet	1233.49	m^3
Mass	oz	28.35	g
	lb	0.4536	kg
Concentration	µg/l	1.0	ppb
	µg/l	1.0	mg/m^3
	µg/l	0.001	mg/l
	mg/l	1.0	ppm
	mg/l	1.0	g/m^3
	mg/l	0.001	g/L
	g/l	1.0	ppt
	g/l	1.0	kg/m^3
Density	lb/ft^3	6894.7	kg/m^3
velocity	ft/s	0.3048	m/s
	mi/hr	0.4470	m/s
	mi/hr	1.6093	km/h
Flow Rate	cfs	0.0283	cms
Temperature	°F	$T_{°C} = (T_{°F} - 32.0)/1.8$	°C

Temperature			Temperature	
°C	°F		°C	°F
0.0	32.0		25.0	77.0
1.0	33.8		26.0	78.8
2.0	35.6		27.0	80.6
3.0	37.4		28.0	82.4
4.0	39.2		29.0	84.2
5.0	41.0		30.0	86.0
6.0	42.8		31.0	87.8
7.0	44.6		32.0	89.6
8.0	46.4		33.0	91.4
9.0	48.2		34.0	93.2
10.0	50.0		35.0	95.0
11.0	51.8		36.0	96.8
12.0	53.6		37.0	98.6
13.0	55.4		38.0	100.4
14.0	57.2		39.0	102.2
15.0	59.0		40.0	104.0
16.0	60.8		41.0	105.8
17.0	62.6		42.0	107.6
18.0	64.4		43.0	109.4
19.0	66.2		44.0	111.2
20.0	68.0		45.0	113.0
21.0	69.8		46.0	114.8
22.0	71.6		47.0	116.6
23.0	73.4		48.0	118.4
24.0	75.2		49.0	120.2

Acre-feet	ac-ft
Cubic feet per second	cfs
Day	d
Degree Celsius	°C
Degree fahrenheit	°F
Degree Kelvin	K
Feet	ft
Fluid ounce	fl oz
Gallon	gal
Gram	g
Hectare	ha
Hour	hr
Inch	in
Joule	J
Kilogram	kg
Kilometer	km
Liter	L
Meter	m
Microgram	μg
Micromhos	μmhos
Mile	mi
Millibar	mb
Milliliter	ml
Microgram	μg
Milligram	mg
Millimeter	mm
Ounce	oz
Parts per billion	ppb
Parts per million	ppm
Parts per thousand	ppt
Pascal	Pa
Pounds per square inch	psi
Second	s
Watt	W
Yard	yd

A.1   WQRRS

A.1.1   Modeling Water Quality

Fate and transport of water quality constituents in WQRRS are modeled based on the principles of conservation of heat energy and conservation of mass. The reservoir is discretized into a series of layers or elements. Each element is assumed to be completely mixed. For the typical element, mass may enter or leave via advection or diffusion from adjacent elements (vertical), may enter via inflow from tributary contributions to the reservoir (lateral), and/or may be removed through reservoir withdrawal (lateral). Exceptions occur at the surface and bottom elements where air-water interface and sediment–water interfaces, respectively, may play a role.

Applying a mass balance to an element of volume V and thickness z

$$V\, \partial C/\partial t = \Delta z\, Q_z\, \partial C/\partial z + \Delta z\, A_z\, D_c\, \partial^2 C/\partial t^2 + Q_i\, C_i - Q_o C \pm VS \tag{A.1}$$

where:
C   = constituent concentration $[M\,L^{-3}]$
V   = volume $[L^3]$
z   = depth $[L]$
Q_z = vertical advection $[L^3\,T^{-1}]$
Q_o = lateral outflow $[L^3\,T^{-1}]$
Q_i = lateral inflow $[L^3\,T^{-1}]$
C_i = constituent concentration of lateral inflow $[M\,L^{-3}]$
A_z = element surface area normal to direction of flow $[L^2]$
D_c = effective diffusion coefficient $[L^2\,T^{-1}]$
S   = all sources and sink (including rate reactions) $[M\,L^{-3}\,T^{-1}]$
t   = time $[T]$

Equation (A-1) represents the advection-diffusion equation written in the vertical direction. Dividing Equation (A.1) by element volume results in

$$\partial C/\partial t = u\, \partial C/\partial z + D_c\, \partial^2 C/\partial t^2 + (u_i\, C_i)/\Delta z - (u_o\, C)/\Delta z \pm S \tag{A.2}$$
or
$$\partial C/\partial t = u\, \partial C/\partial z + D_c\, \partial^2 C/\partial t^2 \pm S' \tag{A.3}$$

where:
$S' = S + (u_i\, C_i)/\Delta z - (u_o\, C)/\Delta z$

13

Equation (A.1) holds for constituents passively transported with the movement of water or through diffusion. For temperature, concentration takes the role of thermal energy. Finally, certain constituents, such as organic sediment, are assumed fixed to the bed and modeled without advection or diffusion as

$$V\, \partial C / \partial t = \pm\, VS \qquad\qquad\qquad (A.4)$$

A.1.2   Source and Sink Equations for Water Quality Constituents

The source and sink term for temperature is limited to external heat fluxes. Sources and sinks for water quality constituents may include settling, first order decay, re-aeration, chemical transformations, biological uptake and release, and respiration and mortality. Each process is introduced below. Only those processes modeled in this project are presented (e.g., upper trophic dynamics are not included), as per Figure A.1.
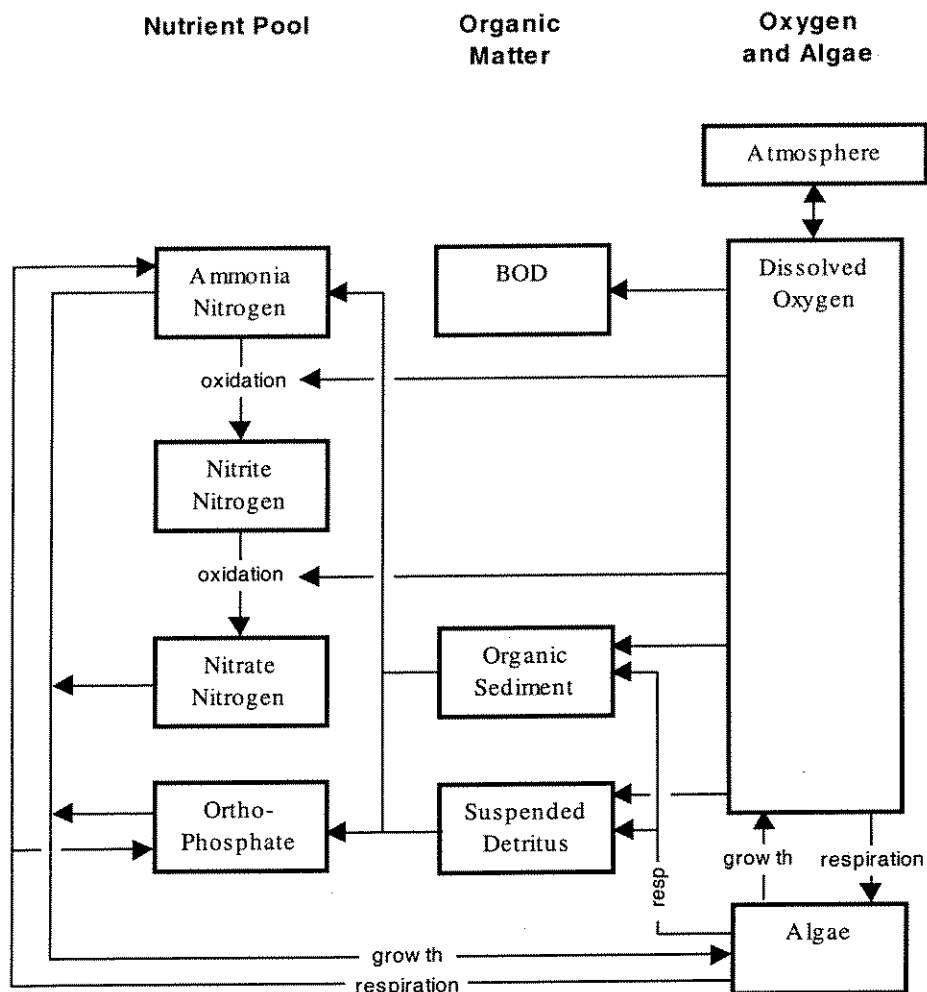
Figure A.1   Major nutrient/quality interactions modeled with WQRRS

14

A.1.2.1 Temperature

The external source and sink for thermal energy is heat exchange at the air-water interface. The net rate of heat transfer per unit surface area can be expressed as

$$H_n = q_{ns} + q_{na} - q_w - q_e - q_c \tag{A.5}$$

Where

H_n = net rate of heat transfer (kcal m^{-2} s^{-1})

q_{ns} = net rate of short wave solar radiation across the air-water interface after losses by adsorption and scattering in the atmosphere and by reflection at the water surface

q_{na} = net rate of atmospheric long-wave radiation across the air-water interface after losses by reflection at the water surface

q_w = rate of long-wave radiation from the water surface

q_e = rate of heat loss by evaporation

q_c = rate of convective heat exchange between the water surface and the overlying air mass.

The basic formulation for each term is reported in TVA (1972).

Application of the heat budget method is simplified by linearizing the water temperature dependent terms (i.e., q_w, q_e, and q_c) resulting in

$$H = \mu - \lambda T \tag{A.6}$$

Where

μ = $q_{ns} + q_{na} - 7.36 \times 10^{-2} - \rho L(a+bW)(\alpha_j - e_a - 6.1 \times 10^{-4} p T_a)$

λ = $1.17 \times 10^{-3} + \rho L(a+bW)(\beta_j + 6.1 \times 10^{-4} p)$

T = water temperature (°C)

ρ = water density (kg m^{-3})

a, b = evaporation coefficients

W = wind speed (m s^{-1})

α_j, β_j = temperature dependent empirical coefficients (linearized)

e_a = vapor pressure (mb)

p = atmospheric pressure (mb)

T_a = dry bulb temperature (°C)

L = latent heat of vaporization (kcal kg^{-1})

Short-wave radiation is the only component that penetrates the water column to appreciable depth. Energy penetrating beyond the surface element must be properly assigned to subsequently "deeper" elements. The light energy or intensity at any depth is determined by Beer's Law

$$I = I_o e^{-kz} \tag{A.7}$$

Where

I = light intensity at any depth (kcal m^{-2} s^{-1})

15

I_o = surface intensity at any depth (kcal m^{-2} s^{-1})
k = light extinction coefficient (m^{-1})
z = depth (m)

The light extinction coefficient reflects light transmissibility, and is dependent on the light attenuation characteristics of the water, e.g., suspended particulate matter such as inorganic suspended solids, detritus, and plankton. It is assumed the effects of particulate material on light transmissibility are additive, thus

$$k = k_o + \Sigma S\ C' \tag{A.8}$$

Where
k = composite light extinction coefficient (m^{-1})
k_o = extinction coefficient in pure water (m^{-1})
S = shade/light attenuation constant for each particulate material (m^{-1} per mg l^{-1})
C' = particulate material concentration (mg l^{-1})

The source term for temperature in Equation (A-1) is thus

$$S = (\mu - \lambda T)/(\rho C_p \Delta z) \tag{A.9a}$$

or

$$S = H/((\rho C_p \Delta z)) \tag{A.9b}$$

Where
C_p = specific heat of water (kcal kg^{-1} °C^{-1})

A.1.2.2   Temperature Dependent Rate Constant Adjustment

Two approaches are used in WQRRS to adjust chemical and biological processes that are a function of temperature: temperature limits and temperature coefficients.

The temperature limit method assumes that the rate at which a reaction takes place initially increases exponentially from a low temperature. This exponential increase cannot continue unabated. Thus as temperatures increase the rate reaction, though still increasing, slows exponentially to some maximum value. Temperature limits for decay, growth, mortality, and respiration can be selected for the various constituents and processes modeled. For growth, additional temperature limits can be employed to model suppressed growth (beyond maximum) at high temperatures.

16

Rate constants can also be adjusted using the Van't Hoff-Arrehnius equation.

$$k = k_{20}\theta^{(T-20)} \tag{A.10}$$

where
- k = reaction rate at ambient water temperature
- k_{20} = reaction rate at 20°C
- θ = temperature coefficient
- T = ambient water temperature

A.1.2.3   Biochemical Oxygen Demand (BOD)

Biochemical oxygen demand is modeled as a first order reaction,

$$\partial L/\partial t = -k_L L \tag{A.11}$$

where
- L = ultimate carbonaceous BOD concentration (mg/l)
- k_L = BOD decay rate (d^{-1})

Sources of BOD include tributary contributions and initial water quality conditions. Decay of BOD ceases when dissolved oxygen is depleted. Algal death and decay do not contribute to BOD, but are modeled separately under organic detritus and organic sediment.

A.1.2.4   Organic Detritus (DET)

Organic detritus is primarily composed of particulate zooplankton excrement, and concentration is a function of tributary contribution, settling rate, zooplankton production, and benthic algae scour. Zooplankton and benthic algae were not included in this study, but organic detritus was included to incorporate oxygen demand due to algal respiration and mortality, and to address organic detritus inputs from an upstream reservoir. Organic detritus decay is modeled with a first order rate reaction, with gains/losses due to settling incorporated using a gradient of detrital concentration with depth.

$$\partial(DET)/\partial t = (DS)\,\partial(DET)/\partial z - k_{DET}\,(DET) \tag{A.12}$$

where
- (DET) = detritus concentration (mg l^{-1})
- (DS) = detritus settling velocity (m d^{-1})
- k_{DET} = detritus decay rate (d^{-1})
- z = depth (m)

17

A.1.2.5 Organic Sediment (OS)

Organic sediment is modeled assuming first order decay using the same rate constant as was applied for organic detritus. Organic sediment exerts an oxygen demand on the system based on algae (phytoplankton) concentration and sediment rate (source), detritus concentration and settling rate (source), as well as predatory excrement (source) and sediment grazed fish, benthic animals, and aquatic insects (sink). Only algae and detritus are included in this analysis. Note, organic sediment does not undergo advection or diffusion in the reservoir model, i.e., application of Equation A.4.

$$\partial(S)/\partial t = -K_{(DET)} (S) + P (PS) + (DET) (DS) \tag{A.13}$$

where
- (S) = organic sediment concentration (mg l^{-1})
- (P) = algal concentration (mg l^{-1})
- (PS) = algal settling velocity (m d^{-1})

A.1.2.6 Nitrogen Species

Three nitrogen species are included in the reservoir model: ammonia (NH_3), nitrite (NO_2^-) and nitrate (NO_3^-). Organic nitrogen sources are not included.

Ammonia(NH_3)

Ammonia decay is modeled as first order rate reaction. Sources include ammonia fraction of detritus (e.g., fraction of biomass that is nitrogen), while sinks include loss due to decay and consumption (growth) by algae. Note, algal respiration (algal death and decay) typically produces organic forms of nitrogen; however, the model assumes respiration a source of inorganic ammonia. (Herein, total ammonia = $NH_3 + NH_4^+$)

$$\partial(NH3)/\partial t = -k_{NH3}(NH3) + k_{DET}(DET+S) - \Sigma A(AN)[(AG)(FNN) - (AR)] \tag{A.14}$$

where
- NH3 = ammonia concentration (mg l^{-1})
- k_{NH3} = ammonia decay rate (d^{-1})
- A = algae concentration (mg l^{-1})
- AN = nitrogen fraction of algae
- AG = algal growth rate (d^{-1})
- AR = algal respiration rate (d^{-1})
- FNN = ammonia fraction of available nitrogen (NH3 and NO3 pool only)

Nitrite (NO_2^-)

Nitrite decay is modeled as first order rate reaction. Sources include ammonia decay and sinks are nitrite decay.

18

$$\partial(NO2)/\partial t = k_{NH3}(NH3) - k_{NO2}(NO2) \qquad (A.15)$$

where
    NO2   = nitrite concentration (mg l^{-1})
    k_{NO2} = nitrite decay rate (d^{-1})

Nitrate (NO$_3$)

Nitrate is the terminal state of nitrification. Sources include nitrite decay and the sink is loss due consumption (growth) by algae. Denitrification is not included in the model.

$$\partial(NO3)/\partial t = k_{NO2}(NO2) - \Sigma A(AN)[(AG)(1\text{-}FNN)] \qquad (A.16)$$

where
    NO3 = nitrate concentration (mg l^{-1})

A.1.2.7 Phosphorous Species (PO$_4^{-3}$)

Only orthophosphate is included in the reservoir model. Sources of phosphorous include organic detritus and sediment, and losses occur due to algal growth. Note, the model assumes that releases of phosphorous due to algal respiration are in the form of orthophosphate versus organic phosphate.

$$\partial(PO4)/\partial t = k_{DET}(DET+S) - \Sigma A(AP)[(AG - (AR)] \qquad (A.17)$$

where
    PO4 = phosphate concentration (mg l^{-1})
    AP   = phosphorous fraction of algae

A.1.2.8 Dissolved Oxygen

Dissolved oxygen is a function of dissolved oxygen concentration and saturation dissolved oxygen concentration, as well as oxygen demands of BOD, NBOD, sediment/detritus oxidation and algal respiration. Sources of oxygen include atmospheric exchange and as a byproduct of algal growth. Oxygen exchange across the air water interface is positive (into the water column) if dissolved oxygen concentrations are less than saturation and negative for the inverse condition.

$$\partial(O_2)/\partial t = k_o(O_{2sat}\text{-}O_2) - k_L\,L - k_{NH3}\,(NH3)(O_2NH3) \qquad (A.18)$$
$$- k_{NO2}\,(NO2)(O_2NO2)$$
$$- k_{(DET)}\,(DET+S)(O_2\,DET)$$
$$- \Sigma A[(O_2G)(AG) - (O_2R)(AR)]$$

where

O_2 = concentration dissolved oxygen (mg l^{-1})
O_{2sat} = concentration dissolved oxygen at saturation (mg l^{-1})
k_o = surface exchange coefficient for dissolved oxygen (d^{-1})

$$k_o = (a' + b'V_w^2)(1/\Delta z) \qquad (A.18a)$$

where:
a', b' = empirical coefficients (0.50 and 0.025, respectively)[units]
V_w = wind speed (m/s)

O_2NH3 = stoichiometric equivalence: oxygen consumption and ammonia decay
O_2NO2 = stoichiometric equivalence: oxygen consumption and nitrite decay
O_2DET = stoichiometric equivalence: oxygen consumption and detritus decay
O_2R = stoichiometric equivalence: oxygen consumption and algal respiration
O_2G = stoichiometric equivalence: oxygen production and algal growth

A.1.2.9 Algae (Phytoplankton)

Algae concentrations are governed by growth, respiration, and settling. The reservoir model lumps respiration and mortality into a single term, algal respiration rate. Algal growth is represented via Michaelis-Menton or Monod kinetics. The limiting (critical) nutrient and/or light govern growth rate. The limiting nutrient concept is implemented using the Liebigs law of the minimum.

$$\partial(A)/\partial t = A[(AG) - (AR)] + (AS)\,\partial(A)/\partial z \qquad (A.19)$$

where

A = algae concentration (mg l^{-1})
AG = algal growth rate (d^{-1})

$$= AMAX\,|\,[N/(k_{NPOOL}+N)],[P_c/(k_{PO4}+P_c)],[L_I/(L_2+L_I)]\,|_{min} \qquad (A.19a)$$

where
AMAX = maximum phytoplankton growth rate (d^{-1})
N = available nitrogen pool concentration.
Available nitrogen includes $NH_3^+ + NO_3^-$ (mg l^{-1})
P_c = available phosphorous concentration as PO_4^{2+} (mg l^{-1})
k_N = half saturation constant for algae utilizing nitrogen as NH_3^+ or NO_3^- (mg l^{-1}).
k_{PO4} = half saturation constant for algae utilizing phosphorous (mg l^{-1})
L_I = available light energy (kcal)
L_2 = half saturation constant for algae utilizing light energy (kcal)
AR = algal respiration rate (d^{-1})
AS = algal settling velocity (m d^{-1})

A.2   RMA-11

A.2.1   Modeling Water Quality

RMA11 is a finite element model capable of simulating one-, two-, and three-dimensional systems. For this application, the one-dimensional simulation was applied. The model is designed to use the same geometry as well as accept input velocities and depths produced from the hydrodynamic model RMA-2. RMA-2 was used to simulate hydrodynamic response of the system for this project. These velocities and depths are used in the solution of the advection-diffusion constituent transport equation. Additional terms for each constituent represent sources or sinks, and growth or decay.

The equations for one-dimensional transport can be assumed to represented laterally and vertically averaged transport. The three dimensional equations are integrated in both the vertical and horizontal direction, normal to the desired flow direction. The basic equations are constructed to permit trapezoidal cross sections and off channel storage. The equations include,

Continuity

$$\partial A_s/\partial t + A\ \partial u/\partial x + u\ \partial A/\partial x - q = 0 \tag{A.20}$$

where
    A = flowing cross-sectional area of one-dimensional element
    A_s = storage cross-sectional area of one-dimensional element
    u = velocity
    q = lateral inflow per unit length
    x = distance
    t = time

Constituent Transport

$$\partial(A_sC)/\partial t + \partial(AuC)/\partial x - \partial(D_xA\ \partial C/\partial x)/\partial x - KA_sC - A_s\theta_s = 0 \tag{A.21}$$

where
    C = constituent concentration
    D_x = diffusion coefficient
    K = first order rate constant

Substituting continuity into constituent transport (non-conservation form) results in

21

$$A_s \partial C/\partial t + Au \, \partial C/\partial x - \partial(D_x A \, \partial C/\partial x)/\partial x + (q - KA_s) \, C - A_s \theta_s = 0 \qquad \text{(A.22)}$$

Successive solution of the governing equations is applied. Temperature is solved first to update all rate reaction coefficients.

A.2.2   Source and Sink Equations for Water Quality Constituents

The source and sink term for temperature is limited to external heat fluxes. Sources and sinks for water quality constituents may include settling, first order decay, re-aeration, chemical transformations, biological uptake and release, and respiration and mortality. Each process is introduced below (Figure A.2). Only those processes modeled are presented.
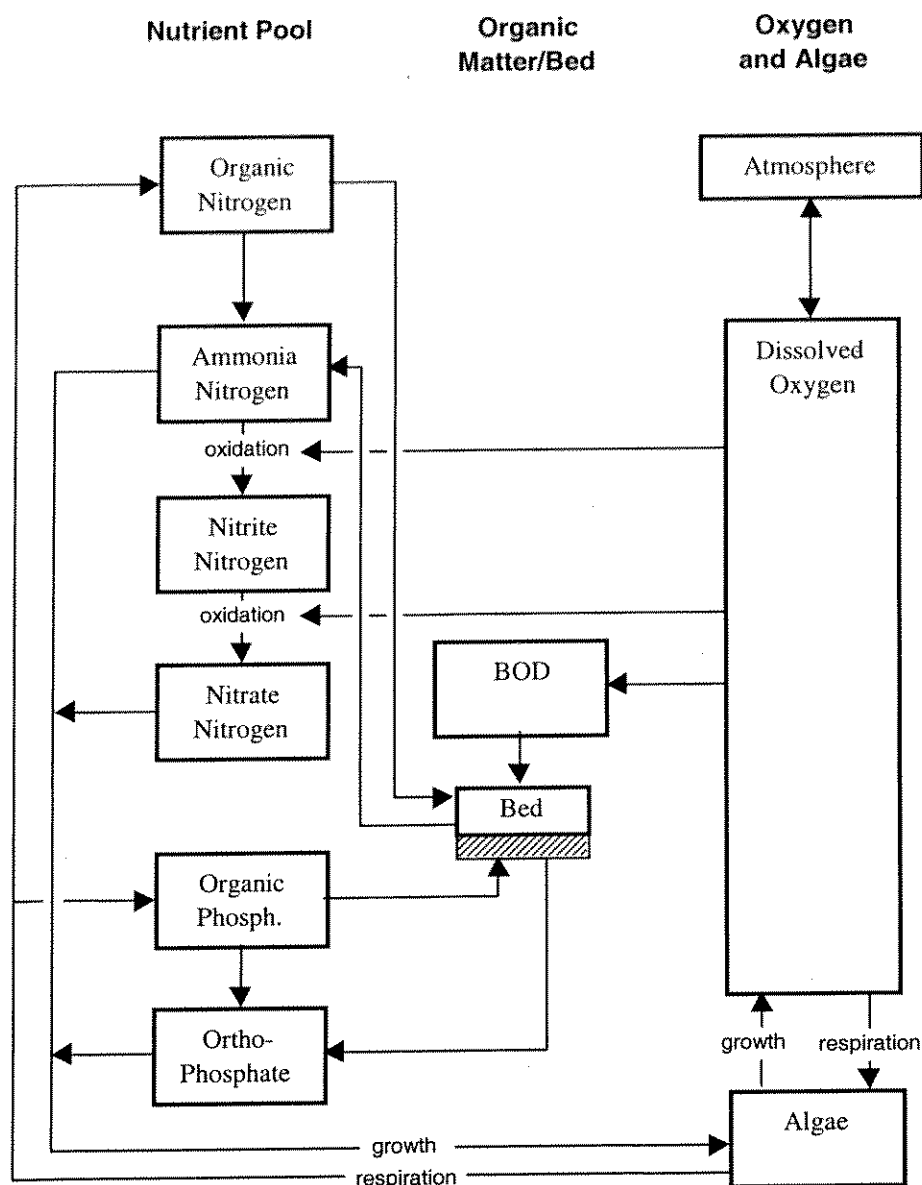
Figure A.2   Major nutrient/quality interactions modeled with RMA11

A.2.2.1   Temperature

As with WQRRS, the external source and sink for thermal energy is heat exchange at the air-water interface. The net rate of heat transfer per unit surface area can be expressed as per equation A.5, reproduced below as equation A.23. Note, heat flux is expressed in KJ m^{-2} hr^{-1} in RMA11.

$$H_n = q_{ns} + q_{na} - q_w - q_e - q_c \tag{A.23}$$

Where
   H_n = net rate of heat transfer (kJ m^{-2} hr^{-1})

23

q_{ns} = net rate of short wave solar radiation across the air-water interface after losses by adsorption and scattering in the atmosphere and by reflection at the water surface

q_{na} = net rate of atmospheric long-wave radiation across the air-water interface after losses by reflection a the water surface

q_w = rate of long-wave radiation from the water surface

q_e = rate of heat loss by evaporation

q_c = rate of convective heat exchange between the water surface and the overlying air mass.

The basic formulation for each term is outlined below

Net Short-wave Radiation Flux

Incoming short-wave radiation is that which passes directly from the sun to the earth's surface. The magnitude is a function of the solar altitude, reduction due to scattering and adsorption in the atmosphere due to cloud cover, and reflection from the water surface.

$$q_{sn} = q_o \, a_\tau \, (1 - R_s) \, (1.0 - 0.65C_L^2)$$ (A.24)

where
  q_o = incoming solar short-wave radiation to the earth's atmosphere
  a_τ = atmospheric transmissivity
  R_s = albedo or reflection coefficient
  C_L = cloudiness (expressed as a fraction, range 0 to 1.0)

Net Long-wave Atmospheric Radiation Flux

The atmosphere is heated by short-wave radiation, and in turn re-radiates long-wave radiation in all directions, including downward toward the water surface. Net long-wave radiation is dependent on air-temperature, cloudiness, and reflection from the water surface. Air temperature is the most important variable, while reflection is the least important. The amount of radiation reflected is assumed to be approximately three percent of the incoming radiation.

$$q_{na} = C_{at} \, \sigma \, T_a^6 \, (1 + 0.17C_L^2)(1-R_S)$$ (A.25)

where
  C_{at} = Swinbank's coefficient ($9.37 \times 10^{-6} \, K^{-2}$)
  σ = Stephan Boltzman constant ($2.0412 \times 10^{-7} \, kJ \, m^{-2} \, hr^{-1} \, K^{-1}$)
  T_a = air temperature (K)

Net Long-wave Water Surface Radiation Flux

Water surface long-wave radiation is that heat lost by radiation of the water surface body at the air-water interface. Using black-body radiation (Kirchoff's Law) as an approximation, back radiation can be expressed as

$$q_{sw} = \epsilon \, \sigma \, T_w^{\,4} \qquad (A.26)$$

where
ϵ = emissivity, the ratio of actual long-wave radiation of the mass to that of an ideal black body, on the order of 0.97
T_w = surface water temperature (K)

Evaporative Heat Flux

Evaporation is a significant process governing heat loss from the water body to the atmosphere. The evaporative heat flux is a function of latent heat of vaporization and the rate of evaporation. The evaporation rate may be expressed as a function of the difference between the saturation vapor pressure and the actual vapor pressure of the air, and the local wind speed.

$$q_e = \rho_w \, L_v \, E \qquad (A.27)$$

where
ρ_w = water density (kg m^{-3})
L_v = latent heat of vaporization (kJ kg^{-1})
E = evaporation (m hr^{-1}), expressed as
$E = (a+bW)(e_s - e_a)$
Where
a, b = coefficients (units: a: m hr^{-1} mb^{-1}
b: m hr^{-1} mb^{-1} (m/h)$^{-1}$)
W = wind speed (m s^{-1})
e_s = saturation vapor pressure at the surface water temperature (mb)
e_a = actual atmospheric vapor pressure (mb)
$= e_{wb} - 6.606 \times 10^{-4} \, P_a (T_a - T_{wb})[1 + (T_{wb}/872.78)]$
where
e_{wb} = saturation vapor pressure at the wet bulb temperature (mb)
$= 8.8534 \times 10^{(0.054 T_{wb})} - 2.8345$
P_a = actual atmospheric pressure (mb)
T_{wb} = wet bulb temperature (°C)

Sensible Heat Flux

Heat transfer between the water and atmosphere, due to mixing of surface heat with surrounding ambient air by wind and turbulence (not related to water vapor exchange), is called conduction and is represented by the sensible heat flux. It is usually expressed using a proportionality constant known as Bowen's ratio.

25

$$B = q_h/q_e \qquad \text{(A.28a)}$$

$$= C_B [(T_w - T_a)/(e_s - e_a)](P/P_o) \qquad \text{(A.28b)}$$

where
  C_B = coefficient (0.6096 (metric units))
  P_o = standard atmospheric pressure at sea level (1013.25 mb)

Solving for q_h

$$q_h = C_B L (a + bW) (P - P_o) (T_w - T_a) \qquad \text{(A.29)}$$

Source Term

The source term for heat in Equation (A.22) is thus

$$S = H_n/(3600 \, \rho \, C_p) \qquad \text{(A.30)}$$

where
  C_p = specific heat of water (kJ kg^{-1} °C^{-1})

A.2.2.2 Temperature Dependent Rate Constant Adjustment

Rate constants are adjusted using the Van't Hoff-Arrehnius equation.

$$k = k_{20}\theta^{(T-20)} \qquad \text{(A.31)}$$

where
  k = reaction rate at ambient water temperature (d^{-1})
  k_{20} = reaction rate at 20°C (d^{-1})
  θ = temperature coefficient
  T = ambient water temperature (°C)

A.2.2.3 Biochemical Oxygen Demand (BOD)

Biochemical oxygen demand loss due to reaction and settling are modeled as a first order reaction,

$$\partial L/\partial t = -(k_L + \sigma_1) L \qquad \text{(A.32)}$$

where
  L = ultimate carbonaceous BOD concentration (mg/l)
  k_L = BOD decay rate (d^{-1})
  σ_1 = BOD settling rate (m/d^{-1}): note, for depth averaged formulation the rate constant is divided by depth in the model

Decay of BOD ceases when dissolved oxygen is depleted, but settling can continue. Both rate costants are temperature dependent.

26

A.2.2.4 Organic Detritus

Not modeled in RMA11

A.2.2.5 Organic Sediment

Not modeled in RMA11.

A.2.2.6 Nitrogen Species

Four nitrogen species are included in the reservoir model: organic nitrogen (OrgN), ammonia (NH_3), nitrite (NO_2^-) and nitrate (NO_3^-). See Appendix E for modifications to RMA-11 concerning bed (attached) algae uptake and decay with regard to nitrogen species.

Organic Nitrogen (OrgN)

Organic nitrogen losses are due to settling and hydrolysis to ammonia. Sources include algal respiration. All processes are modeled with first order rate reactions, with the exception of settling, which is represented as a zero order rate reaction. Algal contributions to organic nitrogen are a function of algal concentration, respiration, and biomass nitrogen fraction.

$$\partial(OrgN)/\partial t = (AN)(AR) A - k_{OrgN}(OrgN) - \sigma_2(OrgN) \qquad (A.33)$$

where
  OrgN = organic nitrogen concentration (mg l^{-1})
  A   = algae concentration (mg l^{-1})
  AN   = nitrogen fraction of algae (mg-N/mg A)
  AR   = algal respiration rate (d^{-1})
  k_{OrgN} = organic nitrogen hydrolysis (decay) rate (d^{-1})
  σ_2 = organic nitrogen settling rate (m/d): note, for depth averaged formulation the rate constant is divided by depth in the model

Hydrolysis rate constant and settling coefficients are temperature dependent.

Ammonia (NH_3)

Sources include ammonia created by hydrolysis of organic nitrogen and by releases from benthic sources, while sinks include loss due to oxidation and consumption (growth) by algae. All processes are represented with first order rate kinetics, while all other processes are represented as a zero order rate reactions. Algal uptake of ammonia is a function of algal concentration, growth rate, and ammonia fraction of available nitrogen. (Herein, total ammonia = $NH_3 + NH_4^+$.)

$$\partial(NH3)/\partial t = k_{OrgN}(OrgN) + k_1 - k_{NH3}(NH3) - F_1(AN) (AG) A \qquad (A.34)$$

27

where
NH3 = ammonia concentration (mg l^{-1})
k_1 = benthos source rate for ammonia (mg-N m^{-2} d^{-1}): note, for depth averaged formulation the rate constant is divided by depth in the model
k_{NH3} = ammonia decay rate (d^{-1})
F_1 = ammonia fraction of available nitrogen (NH3 and NO3 pool only)
$F_1 = P_N(NH3)/[P_N(NH3) + (1-P_N)(NO3)]$
Where P_N is a preference factor for ammonia. The ammonia preference factor is equivalent to the fraction of algal nitrogen uptake from the ammonia pool when the concentrations of ammonia and nitrate (NO3) nitrogen are equal (range: 0-1)
AG = local specific growth rate of algae (d^{-1})

The biological oxidation rate constant, settling rate, and growth rate of algae are temperature dependent.

Nitrite (NO$_2$)
Sources of nitrite include ammonia decay and sinks are oxidation of nitrite to nitrate.

$$\partial(NO2)/\partial t = k_{NH3}(NH3) - k_{NO2}(NO2) \qquad (A.35)$$

where
N02 = nitrite concentration (mg l^{-1})
K_{NO2} = nitrite decay rate (d^{-1})

Processes are modeled with first order rate reactions and all rate constant are temperature dependent.

Nitrate (NO$_3$)
Nitrate is the terminal state of nitrification. Sources include nitrite decay and the sink is loss due consumption (growth) by algae. Denitrification is not included in the model. Algal uptake of ammonia is a function of algal concentration, growth rate, and nitrate fraction of available nitrogen.

$$\partial(NO3)/\partial t = k_{NO2}(NO2) - (1-F_1)(FN)(AG) A \qquad (A.36)$$

where
NO3 = nitrate concentration (mg l^{-1})

Inhibition of Nitrification at low Dissolved Oxygen
Though denitrification is not included in the model, RMA11 includes logic to simulate an inhibited rate of nitrification at low dissolved oxygen concentrations. Nitrification rates are modified (reduced) by computing the inhibition coefficient and then applying this factor to the rate constants for ammonia and nitrite.

28

$$CO = 1.0 - 1 \times 10^{-[(KNITR)(DO)]} \qquad (A.37)$$

where
    CO = nitrification rate correction factor
    KNITR = first order nitrification inhibition coefficient (range: 0.6-0.7 l mg^{-1})
    DO   = dissolved oxygen concentration (mg l^{-1})

A.2.2.7 Phosphorous Species

Organic and inorganic (orthophosphate) are included in the river model. Sources of organic phosphorous include algal respiration, while losses are hydrolysis and settling. Modeled orthophosphate sources are benthic uptake, hydrolysis of organic phosphorous. The phosphorous cycle is completed via algal uptake of orthophosphate. See Appendix E for modifications to RMA-11 concerning bed (attached) algae uptake and decay with regard to phosphorous species.

<u>Organic Phosphorous</u>

Sources of organic phosphorous include gains from algal respiration. Losses include hydrolysis to orthophosphate and loss to settling.

$$\partial(OrgP)/\partial t = (AP)(AR) A - k_{OrgP}(OrgP) - \sigma_3 \qquad (A.38)$$

where
    $OrgP$ = organic phosphorous concentration (mg l^{-1})
    k_{OrgP} = ammonia decay rate (d^{-1})
    AP = phosphorous fraction of algae (mg-P/mg-A)
    σ_3 = organic phosphorous settling rate (m/d): note, for depth averaged formulation the rate constant is divided by depth in the model

Hydrolysis and settling are modeled as a first-order and zero order reactions, respectively. Algal contributions to organic phosphorous are a function of algal concentration, respiration, and biomass phosphorous fraction. All rate reactions are temperature dependent.

<u>Inorganic Phosphorous (Orthophosphate)</u>

Sources of orthophosphate include hydrolysis of organic phosphorous and desorption from the benthos. Losses include algal uptake and loss to suspended sediments. Suspended sediment was not included in this analysis.

$$\partial(PO4)/\partial t = k_{OrgP}(OrgP) + k_2 - (AP)(AG) A \qquad (A.39)$$

where
    $PO4$ = orthophosphate concentration (mg l^{-1})

29

$$AP \quad = \text{phosphorous fraction of algae (mg-P/mg-A)}$$

k_2 = benthos orthophosphate source rate (mg-P m^{-2} d^{-1}): note, for depth averaged formulation the rate constant is divided by depth in the model

The benthic source is modeled as a zero order reaction. Algal uptake is a function of algal concentration, respiration, and biomass phosphorous fraction. All rate reactions are temperature dependent.

A.2.2.8   Dissolved Oxygen

Dissolved oxygen is a function of dissolved oxygen concentration and saturation dissolved oxygen concentration, as well as oxygen demands of BOD, NBOD, sediment, and algal respiration. Sources of oxygen include reaeration and as a photosynthetic byproduct during algal growth (see Appendix E for bed algae dissolved oxygen interactions). Oxygen exchange across the air–water interface is positive (into the water column) if dissolved oxygen concentrations are less than saturation, and negative for the inverse condition.

$$\partial(O_2)/\partial t = k_r(O_{2sat}-O_2) - k_L L + [(AG)(\alpha_3) - (AR)(\alpha_4)] A$$
$$- k_{NH3} \, \alpha_5 \, (NH_3)$$
$$- k_{NO2} \, \alpha_6 \, (NO2)$$
$$- k_3 \qquad\qquad (A.40)$$

where

O_2 = concentration dissolved oxygen (mg l^{-1})

O_{2sat} = concentration dissolved oxygen at saturation (mg l^{-1})

k_r = surface exchange coefficient for dissolved oxygen (d^{-1})

    $k_r = 5.026 \, u_s^{0.969} \, d^{-0.673}$

    where:

      u_s = surface water velocity (m s^{-1})

      d = mean stream depth (m)

      (after Churchill et al (1962)

α_3 = stoichiometric equivalence: oxygen production: algal photosynthesis (mg-O/mg A)

α_4 = stoichiometric equivalence: oxygen consumption: algal respiration

α_5 = stoichiometric equivalence: oxygen consumption: ammonia decay

α_6 = stoichiometric equivalence: oxygen consumption: nitrite decay

k_3 = sediment oxygen demand rate (mg m^{-2} d^{-1})

Dissolved oxygen saturation concentration is a function of water temperature, atmospheric pressure, and concentration of dissolved solids. RMA-11 incorporates the APHA (1985) formulation, namely

$$\ln (O_{sn}) = -139.34411 + (1.575701 \times 10^5/T) - (6.642308 \times 10^7/T^2)$$
$$+ (1.243800 \times 10^{10}/T^3) - (8.621949 \times 10^{11}/T^4) \qquad (A.41)$$

where
  O_{sn} = saturation dissolved oxygen at 1 atmosphere (mg l^{-1})
  T = water temperature (K)
To correct for atmospheric pressure

$$O_s = O_{sn} P [(1-(P_{wv}/P)](1- \phi P) / [(1-P_{wv}) (1-\phi)] \qquad (A.42)$$

where
  O_s = equilibrium dissolved oxygen concentration at non-standard pressure
    (mg $^{l-1}$)
  P = atmospheric pressure (atm)
  P_{wv} = partial pressure of water vapor (atm) computed from,
    $\ln (P_{wv}) = 11.8571 - 3840.70/(T_{a'}) - 216961/(T_{a'})^2$
      where $T_{a'}$ is air temperature (K), and
    $\phi = 0.000975 - 1.425 \times 10^{-5} (T_a) + 6.436 \times 10^{-8}(T_a)^2$
      where T_a is air temperature (°C)
Salinity (dissolved solids) can be incorporated in the above formulation, but was not addressed in this analysis.

A.2.2.9   Algae (Phytoplankton)

Algae concentrations are governed by growth and respiration and settling. Similar to the reservoir model, respiration and mortality are lumped into a single term, algal respiration rate. Algal growth is represented via Michaelis-Menton or Monod kinetics. The limiting (critical) nutrient and/or light govern growth rate. The limiting nutrient concept is implemented using the Liebig's law of the minimum. For this model, algal biomass is assumed directly proportional to chlorophyll a (i.e., Chl a = α_o A, where Chl a is chlorophyll concentration (mg l^{-1}), and α_o is a conversion factor (µg Chl a/mg A))

$$\partial(A)/\partial t = A[(AG) - (AR)] + (AS) \qquad (A.43)$$

where
  A = algae concentration (mg l^{-1})
  AG = algal growth rate (d^{-1})
    = AMAX [FL] | FN, FP |$_{min}$
    where
      AMAX = maximum phytoplankton growth rate (d^{-1})
      FL   = algal growth rate limitation factor for light. For depth
         averaged modeling, the light intensity is averaged over depth
         thus
          FL   = $(\lambda d)^{-1} [(L_2+I_0)/(L_2 + I e^{-\lambda d})]$ $\qquad$ (A.43a)
          and
          λ = light extinction coefficient (m^{-1})

31

L_2 = half saturation coefficient for light (kJ m^{-2} s^{-1})

d = depth (m)

I_0 = light intensity at surface (kJ m^{-2} s^{-1})

Algal self shading is incorporated into the light extinction coefficient as

$$\lambda = \lambda_0 + \lambda_1 + \lambda_2 \qquad \text{(A.43b)}$$

where

λ_0 = non-algal portion of light extinction coefficient (m^{-1})

λ_1 = linear algal self shading coefficient (m^{-1} (mg Chl a/l)$^{-1}$)

λ_2 = non- linear algal self shading coefficient(m^{-1} (mg Chl a/l)$^{-2/3}$)

FN = algal growth rate limitation factor for nitrogen

where

$$FN = [N_e/(k_N+N_e)] \qquad \text{(A.43c)}$$

and

N_e = effective local concentration for available inorganic nitrogen (mg l^{-1})

N_e = (NH3) + (NO3)

k_N = half saturation coefficient for algae utilizing inorganic nitrogen (i.e., NH$_3^+$ or NO$_3^-$) (mg l^{-1}).

FP = algal growth rate limitation factor for phosphorous

where

$$FP = [(PO4)/(k_{PO4}+(PO4))] \qquad \text{(A.43d)}$$

and

PO4 = effective local concentration for available inorganic phosphorous (mg l^{-1})

k_{PO4} = half saturation coefficient for algae utilizing inorganic phosphorous (mg l^{-1})

AR = algal respiration rate (d^{-1})

AS = algal settling velocity (m d^{-1}): note, for depth averaged formulation the rate constant is divided by depth in the model

For modifications to the code incorporating attached (bed) algae, the reader is referred to Appendix E.

Computer simulation modeling is a primary component for project 96-HP-01, Assessment of Alternatives for Flow and Water Quality Control in the Klamath River below Iron Gate Dam. The project area includes Iron Gate Reservoir and the Klamath River from Iron Gate Dam (river mile (RM) 190) to the USGS gage near Seiad Valley (RM 129). Model calibration, validation, and application required a significant quantity of data, including geometric information, meteorological observations, initial flow and water quality conditions, time series of flow and water quality parameters defining boundary conditions for the period of analysis, and calibration/validation water quality data. Geometric data defined reservoir and river morphology, and reservoir outlet works configuration at Iron Gate Dam. Meteorological conditions were necessary to model heat exchange at the air-water interface. Initial conditions were specified to start model simulations. For the Klamath River, water quality boundary conditions were applied over several days of simulation to produce an initial condition used in future model runs. Boundary conditions were required throughout simulations, defining the quantity and quality of reservoir inflow. Calibration and validation data included field observations, to which model output was compared for calibrating model parameters and verifying that selected parameters were representative.

B.1   Data Appendix Format

The data appendix includes a presentation of data sets required for modeling Iron Gate Reservoir and the Klamath River downstream to Seiad Valley. Data sources are outlined in Appendix B.2. Appendices B.3 and B.4 address geometric data and meteorological data, respectively. Initial conditions and boundary conditions for Iron Gate Reservoir and the Klamath River for flow and water quality constituents are included in Appendix B.5 and B.6, respectively. Appendix B.7 includes calibration and validation data for the reservoir and river. Appendix B.8 is a presentation on determination of saturation dissolved oxygen concentration. Appendix B.9 includes various attachments related to data and estimated data.

Throughout this section, stream model refers to the application of RMA-2 (hydrodynamics) and/or RMA-11 (water quality). The reservoir model refers to the application of WQRRS.

B.2   Data Sources

Project data were derived from multiple sources. State and federal agencies provided the bulk of the data. Other sources of data included the PacifiCorp and University of California, Davis. Because data were not uniformly available throughout the 1996 and 1997 analysis periods, particularly for water quality constituents, historic records were used to estimate representative values. Table B.1 outlines sources of data for Iron Gate Reservoir and Klamath River data. Additional data details are included in sections addressing individual data types.

With the exception of geometric data, all data sets consisted of time-series observations. For example, flow data generally consisted of daily flow rates, available at the various gages throughout the system. Likewise, water temperature data was recorded at hourly intervals in the river as well as Iron Gate Reservoir, thus providing a detailed thermal history of the system. In contrast, water quality data were measured at infrequent intervals, at different times of day, and at relatively few locations in the basin. These data formed weak time series, and the result was a level of detail significantly less than that found in the meteorological, flow, or water temperature data.

The bulk of the water quality data developed for this project was derived from the North Coast Regional Water Quality Control Board (NCRWQCB) Clean Water Act 104(b) grant project completed during the 1996 and 1997 field seasons. (Field seasons typically run from late spring through early fall.) A total of eight sampling stations fell within the UC Davis study area

- Copco Dam outflow
- Iron Gate Reservoir
- Iron Gate Dam outflow
- Klamath River upstream of Cottonwood Creek
- Klamath River below Shasta River
- Klamath River below Badger Creek
- Klamath River below Scott River
- Shasta River at mouth

Sites were visited two to four timed per month between April and October. Shasta River monitoring locations were less frequently sampled. Also, reservoir sampling and monitoring was less frequent, occurring twice per year in the months of May and August.

Table B.1.   Data sources for the Klamath River water quality modeling project

Data Type	System	Source(s)
Geometry	Iron Gate Reservoir	PacifiCorp
	Klamath River	California Rivers Assessment, UC Davis
		USGS (topographic maps)
		USGS-BRD (habitat studies)
		DWR (1986)
Meteorology	Iron Gate Reservoir	CDF, Brazie Ranch
		CIMIS, Tule Lake
		UC Davis studies
		NOAA
	Klamath River	CDF, Brazie Ranch
		CIMIS, Tule Lake
		UC Davis studies
		Medford Airport
Hydrology	Iron Gate Reservoir	PacifiCorp
		USGS
	Klamath River	USGS
		USGS-BRD
Water Temperature	Iron Gate Reservoir	PacifiCorp
		UC Davis studies
		NCRWQCB (1997)
	Klamath River	UC Davis Studies
		NCRWQCB (1997)
		USGS-BRD
Water Quality	Iron Gate Reservoir	NCRWQCB (1997)
		EPA (1978)
	Klamath River	NCRWQCB (1997)
	(including tributaries)	USGS-BRD
		DWR (1986)
		Earthinfo Inc. (1995)
		EPA (1978)
		UC Davis studies

Notes:

CDF – California Department of Forestry

CIMIS – California Irrigation Management Information System

DWR – California Department of Water Resources

EPA – United States Environmental Protection Agency

NCRWQCB – North Coast Regional Water Quality Control Board

USGS – United States Geological Survey

USGS-BRD - United States Geological Survey, Biological Resources Division

Because water quality sampling was infrequent and complete analysis cost prohibitive, historic data were reviewed in many cases to estimate seasonal variations and typical background levels of several constituents. Historical data were obtained from DWR (1986), EPA (1978), NCRWQCB (1993), and Earthinfo, Inc. CD ROMS (1995). DWR (1986) data consisted of EPA STORET water quality summaries and coupled with the USGS data (Earthinfo, Inc., 1995) spaned from the late 1950's to the mid-1980's. EPA (1978) included Iron Gate Reservoir in the national eutrophication survey. And the NCRWQCB (1993) did extensive monitoring on the Shasta River in the late 1980's and early 1990's.

Other available water quality data includes observations recorded by USGS-BRD during 1996 and 1997. USGS-BRD deployed Hydrolabs® to record water temperature, dissolved oxygen, electrical conductivity, pH at several locations in the Klamath River system, including below Iron Gate Dam. Mechanical problems associated with the dissolved oxygen probes rendered the hourly data questionable; however, monthly and seasonal variations were discernible. UC Davis deployed Hydrolab® water quality probes in the Klamath River near the mouth of the Shasta River (River Mile (RM) 176.3) and at RM 156.2 for approximately for two days in August 1997. These data provided insight into the potential diel range of dissolved oxygen. When water quality data were unavailable or measured data too infrequent, reference was often made to typical background levels cited in the available literature.

B.3   Geometry

Geometric data was required for both river and reservoir models. Reservoir geometry included length, stage-area-capacity relationships, and outlet works configuration. River geometry consisted of description of river course (e.g., latitude/longitude), slope, cross section data, and tributary locations.

B.3.1   Reservoir Geometry

Iron Gate Dam is located on the Klamath River at approximately RM 190 (41.55 N, 122.26 W), and is approximately 7 miles in length (11.3 km). Maximum reservoir depth is 167 feet (50.9 m) at full pool elevation of 2328 feet msl (709.6 m) and an associated storage of 58,794 acre-feet (72.5×10^6 m^3).

Stage-volume relationships for Iron Gate and Copco Reservoirs were supplied by PacifiCorp (See section B.9.1 and B.9.2), and used to create the necessary physical parameters in WQRRS (See section B.9.3). Iron Gate Dam outlet elevations, capacities, and diameters are defined in Table B2. Capacities for the upper and lower fish hatchery intakes were estimated at 100 cfs for modeling purposes; however, hatchery flows seldom exceed 60 cfs.

Table B.2. Iron Gate Dam outlet work features

Facility	Invert Elevation [ft (m)]	Capacity [cfs (cms)]	Diameter [ft (m)]	Area [ft² (m²)]
Spillway	2328 (709.6)	100,000 (2832)	n/a	n/a
Power Penstock	2293 (698.9)	1825 (51.7)	12.0 (3.66)	113.1 (10.5)
Upper Hatchery	2309 (703.8)	100 (2.83)	2.0 (0.61)	3.14 (0.3)
Lower Hatchery	2253 (686.7)	100 (2.83)	2.0 (0.61)	3.14 (0.3)

B.3.2 River Geometry

Klamath River geometry was derived from several sources of information. A base map of the river course and tributary locations were derived from a GIS layer supplied by California Rivers Assessment. Bed slope was based on the USGS-BRD slope analysis completed in conjunction with the mesohabitat type and redd survey. Other sources reviewed include DWR (1986), USGS topographic maps, and PSIAC (1973). The elevation of the Klamath River at Iron Gate is approximately 2170 ft msl (661.4 m) and elevation at the end of the study reach at the USGS gage near Seiad Valley is 1320 ft msl (402.3 m). For purposes of solar calculations a representative study area latitude and longitude of 41.50N – 122.45W was designated, in the approximate area of Beaver Creek.

River cross sections were represented as simple trapezoids. Side slopes were estimated at rise-to-run ratio of 1:1 for both right and left bank (Jim Henricksen, pers. comm.). River width was estimated from the USGS-BRD mesohabitat type survey. Because, river widths varied widely over short distances, causing potential numerical difficulties for the models, river width was smoothed using a 7-times running average. Ultimately, 100 cross sections were used. Actual measured river widths versus the 7-times running average is illustrated in Figure B.1.

River geometry was used to create a finite element grid for the river system. Element lengths were 300 meters, for a total of 631 nodes and 315 elements. Original measured cross

sections, averaged cross sections, and those created using RMAGEN for application the river models are included in the electronic data, Appendix J.
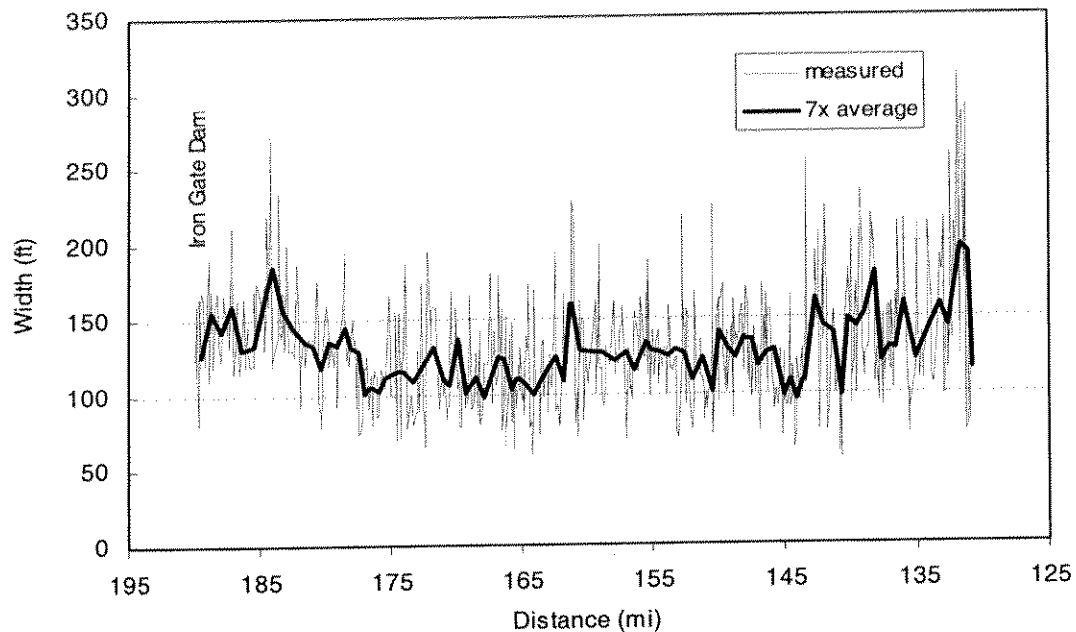
Figure B.1   Measured Klamath River width and 7-times running average, Iron Gate Dam to Seiad Valley

B.4   Meteorological Data

B.4.1   Introduction

A representative meteorological data set was assembled using data from several locations. Hourly air temperature, relative humidity, and wind speed were available from the California Department of Forestry (CDF) weather station at Brazie Ranch near Yreka. Brazie Ranch is located 20 miles (32.2 km) southeast of Iron Gate Reservoir. Daily cloud cover was derived from solar radiation measurements made at Tule Lake in eastern Siskiyou County, roughly 45 miles (72.5 km) due east from Iron Gate Reservoir. Daily mean atmospheric pressure was assumed constant throughout the study period.

Additional meteorological data were available from UC Davis field studies. Air temperature and relative humidity were monitored at three locations during the 1996 and 1997 field seasons (June – October): below Iron Gate dam, below the confluence of the Shasta and Klamath Rivers, and below the confluence of the Scott and Klamath Rivers. In addition, a

meteorological station (air temperature, wind speed, relative humidity, atmospheric pressure, and solar intensity) was deployed at Iron Gate Reservoir in 1996 from early September to early October.

Comparison of the Klamath River sites (below Iron Gate Dam, and near the Shasta and Scott Rivers) illustrated minor differences in air temperature and relative humidity throughout the monitoring period. However, these differences were typically small over this relatively short river reach (roughly 60 miles (80.5 km)). Air temperature, relative humidity, and wind speed from Brazie Ranch were compared with similar parameters monitored at the Iron Gate Dam meteorological station deployed by UC Davis. Climate conditions were roughly equivalent, though the Iron Gate Dam station recorded higher air temperatures, higher relative humidity, and experienced more frequent wind. The location of the Iron Gate Dam meteorological station probably contributed to these discrepancies: the station, mounted on the reservoir outlet tower for security and power accessibility, was located over water, at a non-standard elevation, and partially sheltered by the outlet tower and dam. Nonetheless, local observations lent confidence to the use of Brazie Ranch data for model simulation.

B.4.2   Data Reconstruction

Meteorological data from Brazie Ranch in the Shasta Valley near Yreka was used to drive the water temperature models for both Iron Gate Reservoir and the Klamath River. Data is available for 1996 and 1997. Available data included air temperature, relative humidity and wind speed. Relative humidity was converted to wet bulb temperatures for use in RMA-11.

Several missing records were estimated to complete this hourly data set. When 6 hours or less of data were missing, simple linear interpolation was used to fill the record. Where data were missing for periods of more than 6 hours, data were estimated from previous or subsequent periods. Extended periods of missing data occurred 16 times through the record (see below). Shorter periods of missing data (six hours or less) are not explicitly addressed herein.

Cloud Cover
Cloud cover was estimated from daily solar radiation measurements at Tule Lake in eastern Siskiyou County. Initially, records from Montague Airport were to be employed. However, monitoring at Montague is completed with an Automated Weather Observation Station (AWOS) and is not equipped with a solar pyranometer or other cloud cover monitoring

39

instrumentation. The only available records that could possibly represent cloud cover and/or incoming solar radiation was daily visibility. However, daily visibility does not effectively represent cloud cover. Thus, daily solar radiation was compared to theoretical maximum daily solar radiation for latitude 42N for calendar years 1996 and 1997 (Figure B.2). The maximum theoretical was fit with a sine function of the form S = AsinB + C, where S is solar radiation, and A, b, and C represent amplitude, period, and phase shift. Values for A, B, and C were 142, the day number (converted to radians: $2\pi*day/365$), and 247, respectively.

If measured solar radiation exceeded 80 percent of theoretical maximum, clear sky conditions were assumed (cloudiness = 0.0); between 60 and 80 percent, cloudiness was assumed equal to 0.25; between 40 and 60 percent, cloudiness was set to 0.5; between 20 and 40 percent, cloudiness was set to 0.75; and between 0 and 20 percent, cloudiness was set to 1.0 (Figure B.3).

Atmospheric Pressure

Daily atmospheric pressure was assumed constant at 1013 mb, but corrected for elevation using

$$P = 1013 - 3.436(E/100) - 0.0029(E/100)^2 + 0.0001(E/100)^3 \tag{B.1}$$

Where E is elevation in feet and P is barometric pressure in millibars (University of California. Converting humidity expressions with computers and calculators, Leaflet 21372. Cooperative Extension.)

Wet Bulb

During the months of May and October, air temperatures (dry bulb) can approach or fall below freezing. Under such conditions, wet bulb temperatures, which are always less than air temperature, may become negative. The frequency of such events is rare, short term, and the air temperature rarely produce wet bulb temperatures more than a degree or so below zero. Impact on model results is minimal, but if winter-period modeling should be undertaken, the role of below freezing temperatures on heat budget formulations should be reviewed.

40
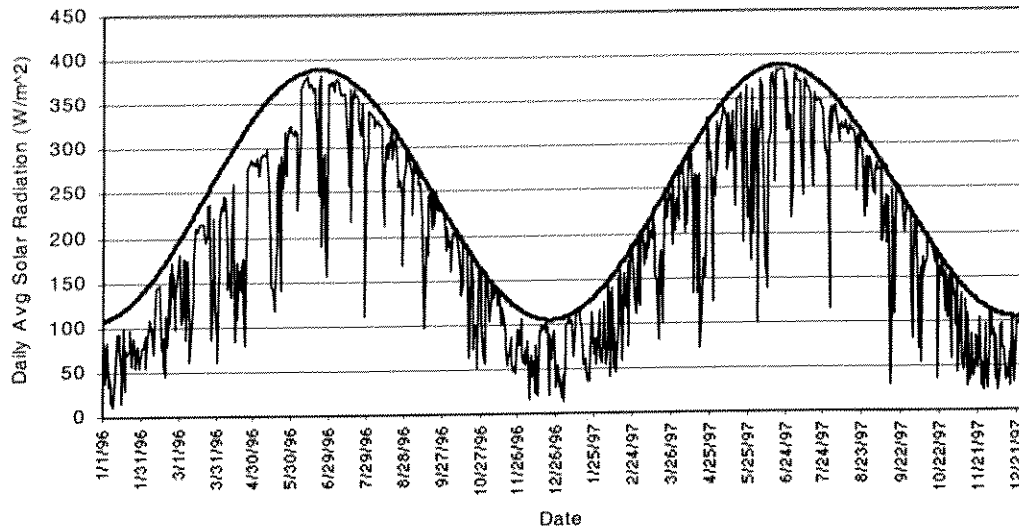
Figure B.2   Theoretical maximum (bold line) and measured solar radiation at Tule Lake, calendar years 1996-97
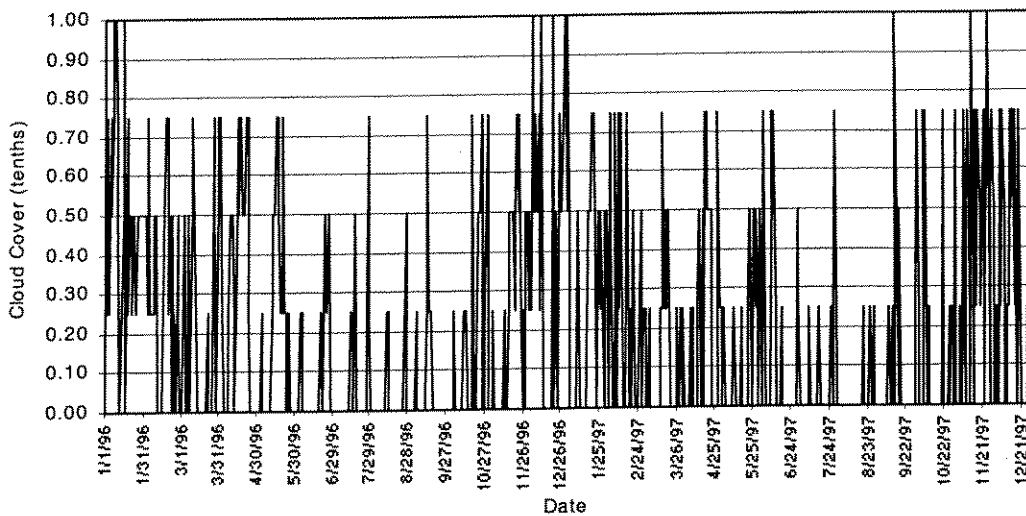
Figure B.3   Estimated cloud cover from Tule Lake solar radiation

B.4.3   Data Inventory

Missing meteorological data occurred throughout the 1996 and 1997 data. Most data gaps were limited to a few hours, but more extensive station downtime occurred. Outlined below are the periods, as well as the methodologies used to fill data gaps. The 1996 and 1997 meteorological data used in the project is included in the electronic data, Appendix J.

1996

Data availability: January 1 - December 31

Estimated data for periods longer than 6 hours and methodology/assumptions

    2/1 (12:45) - 2/2 (10:45) - previous day

    2/21 (11:45-20:44) - following day

    3/5 (23:44) - 3/6 (9:44) - previous day

    3/11 (16:44) - 3/12 (8:44) - 3/10 and 3/11 (previous), did not smooth transition (few degrees)

    3/12 (10:44) - 3/13 (11:44) - 3/10 and 3/11 (previous), did not smooth transition (few degrees)

    5/21 (5:44 - 16:44) - previous (5/16)

    6/24 (13:44 - 23:44) - following day

    9/11 (15:43 - 23:43) - previous day

    9/24 (18:43) - 9/25 (6:43) - following day

    12/12 (15:42) - 12/13 (2:42) - previous day

    12/13 (10:42) - 12/14 (1:42) - used 12/19 and 12/20 (following)

    12/14 (10:42) - 12/15 (19:42) - used (12/19 and 12/20 data (following)

    12/16 (3:42 - 18:42) - used 12/19 data (following)

    12/17 (2:42) - 12/19 (1:42) - following (12/19 to 12/21) did not smooth transition (few degrees)

    12/21 (12:42) - 12/23 (7:42) - used 12/23 to 12/25 (following)

    12:30 (7:42) - 12/31 (23:42) - used 12/29 data (previous)

1997

Data availability: Jan 1 - Dec 31

Estimated data were less than or equal to six hours in length for this data set with the exception of February 12,13 and 14 through 21, data from neighboring days was used.

B.5   Iron Gate Reservoir

B.5.1   Initial Conditions: Reservoir Water Quantity (Reservoir Stage)

Initial conditions for reservoir water quantity consists of reservoir stage at the start of simulation. Reservoir stage for Iron Gate reservoir was provided in the hydrology data supplied by PacifiCorp. Initial reservoir stage for 1996 and 1997 simulations were assumed 2327.4 ft msl and 2326.0 ft msl for May 15 and May 13, respectively.

B.5.2   Initial Conditions: Reservoir Water Quality

Initial conditions for water temperature and all other water quality constituents were necessary to start model simulation. Temperature, dissolved oxygen, biochemical oxygen demand (BOD), chlorophyll *a* (surrogate for algae), nutrients and electrical conductivity are outlined below. Model simulations for 1996 and 1997 started on May 15 and May 13, respectively (to coincide with available data from NCRWQCB sampling).

B.5.2.1 Water Temperature - Profile

UC Davis collected water temperature profile data in cooperation with PacifiCorp. Data was collected at seven depths for much of the 1996 and 1997 field seasons. Several loggers were left in the reservoir during the winter of 1996-97. In addition, NCRWQCB completed May and August limnological surveys in 1996 and 1997.

Initial temperature profiles for 1996 and 1997 simulations were based on NCRWQCB data. Model analyses commenced in May and extended through October. Initial temperature profiles could be estimated for other starting periods. It is common to assume isothermal reservoir conditions during winter as an initial condition. Caution should be used when estimating initial water temperature profiles, and a sufficient simulation period should be selected to ensure uncertainty associated with such estimations is minimized.

B.5.2.2 Dissolved Oxygen – Profile

Unlike rivers, saturation dissolved oxygen conditions cannot be assumed constant throughout the water column of the reservoir because bottom waters do not have free exchange with the atmosphere. Though reservoirs may undergo periods of complete mixing due to wind events, large reservoir inflows or outflows, or meteorological processes (e.g., seasonal cooling), the events are typically short-lived or transitory. Once these events abate, bottom waters are typically exposed to recurring oxygen demand (e.g., sediment oxygen demand). Even during winter periods, when biological productivity is low, dissolved oxygen of bottom waters may fall well below saturation.

Initial conditions were based on NCRWQCB dissolved oxygen profiles competed in May 1996 and May 1997. These data illustrated an approximately linear relationship between dissolved oxygen and depth, with surface dissolved oxygen concentrations of roughly 10 mg/l and bottom concentrations less than 1 mg/l.

B.5.2.3 Biochemical Oxygen Demand (BOD) – Profile

Profile BOD data were unavailable. Background levels of 2.0 mg/l were assumed constant with depth for both 1996 and 1997. Values of 1.0 to 3.0 mg/l are typical in samples collected below Iron Gate Dam (NCRWQCB, 1997; DWR, 1986). EPA (1997) provides a range of 0.5 to 3.0 mg/l for background levels in natural streams.

B.5.2.4 Organic Detritus – Profile

Organic detritus data were unavailable. Initial profile concentrations were not required.

B.5.2.5 Chlorophyll a – Profile

Limited chlorophyll *a* data were available from the NCRWQCB. Initial conditions for May 1996 were estimated at 15 μg/l (1.0 mg algae/l) from the surface to a depth of 5 m (16.4 ft), and 1 μg/l (0.067 mg algae/l) from 5 m to the bottom of the reservoir. Initial concentrations of chlorophyll *a* for May 1997 were estimated at 40 μg/l (2.68 mg algae/l) from the surface to a depth of 5 m (16.4 ft), and 1 μg/l (0.067 mg algae/l) from 5 m to the bottom of the reservoir. Secchi depth typically ranged from 2.6 ft to 5.7 ft (0.8m to 1.75 m) during 1996 and 1997 monitoring, and a value of 5 ft (1.5 m) was selected for simulation.

B.5.2.6 Nitrogen and Phosphorous – Profile

Initial conditions for May 1996 and 1997 were estimated from the limited nitrogen and phosphorous data available from the NCRWQCB. Due to limited data availability and small variation in samples, identical initial conditions for 1996 and 1997 were assumed. Additional information for nutrient concentration profiles for Iron Gate Reservoir was derived from EPA (1978), especially with regards to orthophosphate. Table B.3 outlines profile approximations.

B.5.2.7 Electrical Conductivity – Profile

Electrical conductivity profiles typically varied between 180 and 200 μS/cm (TDS: 115 and 128 mg/l) in May, 1996 and 160 to 180 μS/cm (TDS: 102 to 128 mg/l) in May, 1997 (NCRWQCB, 1997). Electrical conductivity was assumed constant at 180 μS/cm (TDS: 128 mg/l) for Iron Gate reservoir from surface to bottom in both 1996 and 1997.

B.5.3 Boundary Conditions: Reservoir Water Quantity

Boundary conditions for Iron Gate Reservoir included reservoir inflow, reservoir releases, plus accretions and depletions. Hourly water quantity data for Iron Gate Reservoir were compiled from data supplied by PacifiCorp. A significant amount of the flow data had to be reconstructed. Model data are available for calendar years 1996 and 1997

Table B.3. Estimated initial profile water quality concentrations for nitrogen and phosphorous species, 1996 and 1997

Parameter	Variability	Surface (mg/l)	Bottom (mg/l)
ORG N – T_a	constant	0.6	0.6
ORG N – D_a	constant	0.42	0.42
NH3-T	linearly	0.1	0.1
NH3-D	linearly	0.08	0.02
NO3-T	n/a	n/a	n/a
NO3-D	linearly	0.04	0.20
TKN-T	constant	0.7	0.7
TKN-D	constant	0.5	0.5
P-T	constant	0.2	0.2
P-D_b	constant	0.1	0.1
OP$_b$	constant	0.1	0.1

[a] Org N is calculated as TKN – NH3
[b] P-D only sampled in 1996, OP estimated based on EPA (1978)

<u>Nitrogen and Phosphorous Species</u>

ORG N – organic nitrogen
NO3 – nitrate
P – phosphorous (phosphate)
T – total
D - dissolved

NH3 – ammonia
TKN – Kjeldahl nitrogen
OP – orthophosphate

Hourly reservoir inflow consisted of the Copco Dam total release (spill plus power penstock), and included accretions and depletions. Hourly Iron Gate Reservoir release was calculated as the sum of reservoir spill, penstock and fish hatchery releases. Hourly Iron Gate Reservoir accretions and depletions were calculated as the difference between Copco Reservoir releases and total Iron Gate Dam releases (spill, penstock, and hatchery), while accounting for changes in storage. Thus, accretions include reservoir evaporation. The distance from Copco Dam to the headwaters of Iron Gate Reservoir is small enough to accommodate such an approximation. As noted above, total reservoir inflow was calculated as inflow plus accretion/depletion. All required Iron Gate flow data is summarized below.

B.5.3.1 Data and Data Reconstruction

The flow data necessary to represent Iron Gate Reservoir in the reservoir model include system inflow, outflow, and stage. Inflow, for the purposes of this study, consists predominately of releases from Copco Reservoir. Outflow includes all releases from Iron Gate Reservoir: spill, power penstock, and fish hatchery. Other reservoir inflows and

outflows include evaporation, precipitation, local drainage, leakage, and Jenny and Fall Creeks. These components are typically small values and are represented through a lumped accretions and depletions (A/D) term.

Data for JC Boyle, Copco and Iron Gate Reservoirs was supplied from PacifiCorp. In addition, USGS supplied Klamath River flow data for the gage located below Iron Gate Reservoir (Sta. No. 11516530). PacifiCorp data include hourly discharge, inflow, and staff gage readings, while all USGS data were daily average values. Table B.4 defines data supplied by PacifiCorp by station numeric code and name.

Table B.4.   Hourly data supplied by PacifiCorp for calendar years 1996 and 1997

Number	Numeric Code	Name
1	1420200	COPCO INFLOW (CFS)
2	1420216	IRON GATE INFLOW (CFS)
3	1420220	JC BOYLE INFLOW(CFS)
4	1420230	BOYLE STOR CHG(DSF)
5	1420231	COPCO STOR CHG(DSF)
6	14420200	IRON GATE GAGE-FT
7	14420201	IRON GATE PLANT-CFS
8	14420202	IRON GATE GAGE-CFS
9	14420203	JC BOYLE GAGE-CFS
10	14420205	**IRON GATE HATCH-CFS**
11	14420215	JC BOYLE GAGE-FT
12	4420200	JC BOYLE TURBINE
13	4420201	**COPCO #1 TURBINE**
14	4420202	**IRON GATE TURBINE**
15	5420219	JC BOYLE SPILL (CFS)
16	5420225	**COPCO #1 SPILL (CFS)**
17	5420232	**IRON GATE SPILL (CFS)**
18	6420218	JC BOYLE LAKE ELEV
19	6420224	**COPCO#1 LAKE ELEV**
20	6420230	**IRON GATE LAKE ELEV**

Data Review
Both Copco and Iron Gate Reservoir data were reviewed to determine periods and extent of missing data. Initial review of the hourly PacifiCorp data illustrated that the data sets were for the most part complete. However, several missing and/or erroneous data points were discovered. In addition, method of the determination for reservoir inflows and storage changes were uncertain. To provide a consistent data set, the stage-storage tables were used to determine storage and storage change from staff gage data (Copco: 6420224, Iron Gate:

6420230 – i.e., it was easier to locate and correct or to estimate errors in staff gage than to work with the storage change values). As a result, only those Table B.4 data sets defined in **BOLD** were used (No. 10, 13, 14, 16, 17, 19, and 20).

All of the utilized data sets had missing data. These data were interpolated (linear or first differences) or estimated to fill in the record. Corrections are too numerous to note individually, but typical data problems included

- Missing Data: a value given as -1, 0 or 1

- Transcription/Interpretation Error: incorrect entries were common in the gage data. For example, Copco Reservoir would exhibit a slowly falling stage as shown in the following series of readings: 193.1, 193.06, 193.01, **193.98**, 192.94. Note that the fourth number should read 192.98. These errors were easily spotted due to abrupt increase in stage over the period of an hour and decrease in the subsequent hour. Because storage change can change appreciably, storage changes less than 8000 day-second-feet (dsf) (660 acre-feet, or 8000 cfs release for one-hour) in an hour were not corrected unless a transcription error appeared obvious. Though an inflow rate of 8000 cfs is in excess of penstock capacity, such a value provided a general rule that would account for spill and other accretions.

Most of the missing data was limited to a single reading or two, the most appreciable data gap being on the order of two days (an exception was Iron Gate Hatchery, see below). It was found that the most effective method to reproduce missing or unavailable records, was to use the daily flow from the USGS Gage below Iron Gate Dam and work upstream using Iron Gate releases, spill and fish hatchery flows. Though the discrepancy between total Iron Gate Dam releases (power plant, hatchery and spill) and USGS records was often appreciable, such instances were restricted to high flow events during winter months (December - February). During the remainder of the year it was found that USGS daily records typically matched PacifiCorp records within ±10% - the rating of the USGS Gage. By comparing total Iron Gate release, and reservoir storage change, penstock releases and reservoir spill were estimated. All releases were assigned to the penstock unless high flow conditions prevailed, at which time the missing data point(s) was estimated after reviewing neighboring data points. Transcription errors in staff gage readings were corrected separately.

47

Using Iron Gate Reservoir stage, coupled with Copco Reservoir stage (staff gage), missing values for Copco power releases and spills were estimated. The combination of these values form total Iron Gate Reservoir inflow.

Estimation, Interpolation, and First Differences

To fill data gaps several methods were used. Some values were estimated based on the trend of neighboring data points, especially if the record in question remained constant for long periods of time. For example, occasional missing Iron Gate hatchery flows were denoted with a value of -1. Because all nearby values for days at a time were zero, it was assumed that the missing value was zero, as it is unlikely that the hatchery would open the gate for a single hour throughout the course of a week. Oftentimes values were estimated to balance (approximately) flows at the USGS Gage.

Many missing data points were filled with linear interpolation, especially if several data points were absent. Interpolation by first differences was often used when a single data point was missing in a series that showed a rising or falling trend.

Iron Gate Hatchery Releases

Iron Gate hatchery releases are an important component of reservoir operation, as these releases utilize cold hypolimnetic water from Iron Gate Reservoir. In 1996 the raceways at Iron Gate hatchery were refurbished. During this period (specifically, 6/10/96 to 7/30/96 and 8/13/96 to 9/11/96) there were minimal or no hatchery releases from Iron Gate Reservoir. The 1997, data were missing from 4/15/97 through 12/31/97. These data were estimated using available water temperature records for this period. It was assumed that if water temperature was recorded at the head box to the hatchery, hatchery releases were taking place. Flow volume was estimated as 40 cfs from 4/11/97 9:00 to 12/31/97 23:00, based on PacifiCorp (1995).

Accretions and Depletions

When completing a water balance on Iron Gate Reservoir, the measured inflows minus the measured outflows do not equal the measured storage change. To close the water balance an additional term called "accretions and depletions" (A/D) was added or subtracted to storage change. Accretions and depletions represent inflows and outflows to the system that are not explicitly quantified. For example, precipitation, evaporation, groundwater inflow and outflow, dam seepage, overland flow, and ungaged tributaries. Furthermore, gage error related to flow measurement incorporates additional uncertainty into the water balance. An

A/D term was determined for Iron Gate Reservoir, Copco Reservoir, and the short reach of river between Iron Gate Dam and the USGS Gage. The A/D term calculated for Iron Gate reservoir closely matches the station 1420216, Iron Gate Inflow; however, the Copco A/D term does not match station 1420200, Copco inflow. The A/D term was included in each time step, i.e., hourly.

Because Iron Gate Dam is located directly downstream of Copco, the hourly data effectively captures flow changes out of Copco Reservoir. Because JC Boyle is located several miles above Copco Reservoir, the hourly data cannot be applied directly to a water balance to calculate Copco Inflow.

Other Information
Iron Gate spill was assigned to penstock (412 cfs), on 10/20/97. It appears there may have been operational spill on 10/20, but available data do not illustrate that reservoir elevation was sufficient to support a spill without a several foot change in elevation on the order of a few hours. Impact on thermal structure of reservoir is negligible. Short-term-impact on releases to river probably minimal as well due to fully mixed epilimnion to depths well below penstock.

Iron Gate Spillway rating equation is

$$Q_{spill} = 2664H^{1.5} \tag{B.2}$$

Where H is water depth (capacity: 100,000 cfs)

B.5.4   Boundary Conditions: Reservoir Inflow Water Quality

Iron Gate Reservoir inflow water temperature and quality boundary conditions consisted of total inflow from Copco Reservoir. Total inflow includes accretions and depletions, and although accretions from creeks tributary to Iron Gate may differ substantially in quality, the contributions were typically a small percentage main stem flows during the primary months of simulation.

B.5.4.1   Water Temperature
Water temperature data for Copco Dam release (Copco tailrace #2) were available for portions of 1996 and 1997, but were reconstructed for each calendar year. It was assumed

that spill and penstock releases commingle completely by the time they reach Copco #2 tailrace, and can thus be represented by a single water temperature. Further, it was assumed that measured temperatures at Copco #2 tailrace were representative of Iron Gate Reservoir inflow, i.e., minimal heating is assumed to occur in the short reach between Copco #2 tailrace and Iron Gate Reservoir.

B.5.4.2 Dissolved Oxygen

Dissolved oxygen data were estimated using Copco Dam release grab samples from the NCRWQCB, and estimated saturation dissolved oxygen values based on water temperature and corrected for elevation (APHA, 1985). Based on available water temperature records, releases from Copco Reservoir originate from sufficient depth to moderate diurnal fluctuations. Review of NCRWQCB further illustrates that Copco Reservoir becomes strongly stratified in the late spring, summer and fall months leading to depressed dissolved oxygen levels in the hypolimnion. Reservoir releases in the winter and early spring appear to be near or slightly below saturation concentration. As the spring transitions to summer, water temperatures increase, algal productivity increases, and dissolved oxygen levels in the hypolimnion decrease. Subsequent releases from Copco Dam exhibit decreasing dissolved oxygen concentration, 70 to 90 percent of saturation, through the summer and into fall (NCRWQCB, 1997). Dissolved oxygen levels most likely remain suppressed well into fall, due to remaining oxygen demand in the hypolimnion of Copco Reservoir prior to fall turnover (and slow cooling of the reservoir at depth).

Using this information and NCRWQCB water quality samples, monthly concentrations for dissolved oxygen were estimated for calendar years 1996 and 1997, and a third data set was estimated for forecasting applications. 1996 and 1997 data were used for calibration and validation, respectively. The forecasting data set was a compilation of the dissolved oxygen data from 1996 and 1997, and could be applied to examine other years using the calibrated and validated model.

Because penstock withdrawals at Copco Dam originate from significant depth (roughly 30 feet) within the reservoir, it was assumed there were no marked diurnal dissolved oxygen variations. This assumption can be supported by Copco Reservoir secchi depth measurements. The photic zone, where primary production occurs, can be estimated as 3 times secchi depth. Copco Reservoir secchi depth measurements range from roughly 1 to 3 m, corresponding to a maximum photic depth of about 10 to 30 feet.

Table B.5 outlines the monthly dissolved oxygen concentrations for the periods described above. Dissolved oxygen concentrations were assumed to vary linearly, assuming tabulated values represent average monthly conditions, i.e., each value was assumed to represent the conditions on the 15th of any particular month and linear interpolation was used to determine intermediate values.

B.5.4.3   Biochemical Oxygen Demand

Biochemical oxygen demand (BOD) data were estimated using Copco Dam release grab samples from the NCRWQCB. Values ranged from 1.5 mg/l to 8 mg/l with typical values ranging from 1.5 to 3.0 mg/L. Only two measurements (12 total measurements: 1996:8, 1997:4) exceeded 3 mg/l: 5 mg/l in September 11, 1996 and 8 mg/l in August 6, 1997. Background levels in natural systems typically range from 0.5 to 3.0 mg/l (EPA, 1997) and Thomann and Mueller (1987) report 8 mg/l input from forest regions. Measured values for the Klamath River system within the study generally fell within this range.

Because BOD levels were low with the exception of two measurements BOD of Iron Gate inflow was assumed 2 mg/l constant for calendar years 1996 and 1997.

B.5.4.4   Organic Detritus

Organic detritus data were unavailable. Wetzel (1983) reports that phytoplankton dry weight ranged from 5 to 25 percent of organic particulate detritus and rarely exceeded 40 to 50 percent. Seasonal variations were accommodated by varying inflow concentrations from 2 mg/l on May 15, ramping to 5 mg/l on June 1 and maintaining 5 mg/l through August, then ramping down to 2 mg/l on September 30 and maintaining 2 mg/l through October 31. These estimates produced simulated organic detritus numbers consistent with the values presented by Wetzel (1985). Also, assumed values were consistent with sample applications included in USACE-HEC (1987). (Note: Though organic detritus was loaded in the Iron Gate Reservoir inflow as a release from Copco Reservoir, it actually represents an estimate of all sources of organic detritus entering Iron Gate Reservoir.)

Table B.5. Estimated monthly Copco Reservoir release dissolved oxygen concentrations (values in bold used in model)

Month	Estimated DO[1] 1996	Saturation DO[2] 1996	Estimated DO[1] 1997	Saturation DO[2] 1997	Forecast DO[3]
January	10.5	12.0	10.5	12.0	DO_{sat} - 1.0 mg/l
February	10.5	11.5	10.5	11.5	DO_{sat} - 1.0 mg/l
March	10.5	10.7	10.5	10.7	DO_{sat}
April	10.0	10.2	9.4	10.0	DO_{sat}
May	**9.7**	9.5	**8.6**	8.7	DO_{sat}
June	**7.7**	8.7	**8.0**	8.6	DO_{sat} - 1.0 mg/l
July	**8.7**	8.6	**8.1**	8.3	DO_{sat} - 1.0 mg/l
August	**6.7**	8.7	**7.9**	8.1	DO_{sat} - 2.0 mg/l
September	**6.3**	8.9	**7.0**	8.6	DO_{sat} - 2.0 mg/l
October	**7.2**	9.2	**6.8**	9.5	DO_{sat} - 2.0 mg/l
November	**7.5**	10.4	**7.5**	10.4	DO_{sat} - 3.0 mg/l
December	8.0	11.5	8.0	11.5	DO_{sat} - 3.0 mg/l

[1]Estimated DO based on RWQCB average DO for April through October. January through March and November and December based on review of USGS DO data 1996 and 1997.
[2]Saturation DO based on average monthly water temperature
[3]Forecasts of DO require calculating saturated DO values and subtracting tabulated quantity to address depressed DO values due to BOD.

B.5.4.5 Chlorophyll a

Copco Reservoir release chlorophyll *a* concentrations reported by the NCRWQCB (1997) differed slightly between 1996 and 1997, with 1996 values ranging from roughly 3 to 11 µg/l (0.20 to 0.74 mg algae/l) and 1997 values ranging from 2 to 7 µg/l (0.13 to 0.47 mg algae/l). Though 1996 concentrations were slightly higher than 1997, both show a seasonal trend of increasing in the spring and then falling off in the late summer and fall (Figure B.4). Using the limited available data an Iron Gate Reservoir inflow concentration of 8 µg/l (0.54 mg algae/l) was estimated for the period May through September, and 4 µg/l (0.27 mg algae/l) for all other months during 1996 and 1997.

B.5.4.6 Nitrogen and Phosphorous

Nitrogen and phosphorous parameters were estimated based on NCRWQCB (1997) data and other references. Typical background levels of nitrogen species in surface waters in surface waters given by EPA (1997) are

Org-N: 0.05 – 0.50 mg/l
NH_3: 0.05 – 0.27 mg/l
NO3: 0.07 – 0.37 mg/l

52
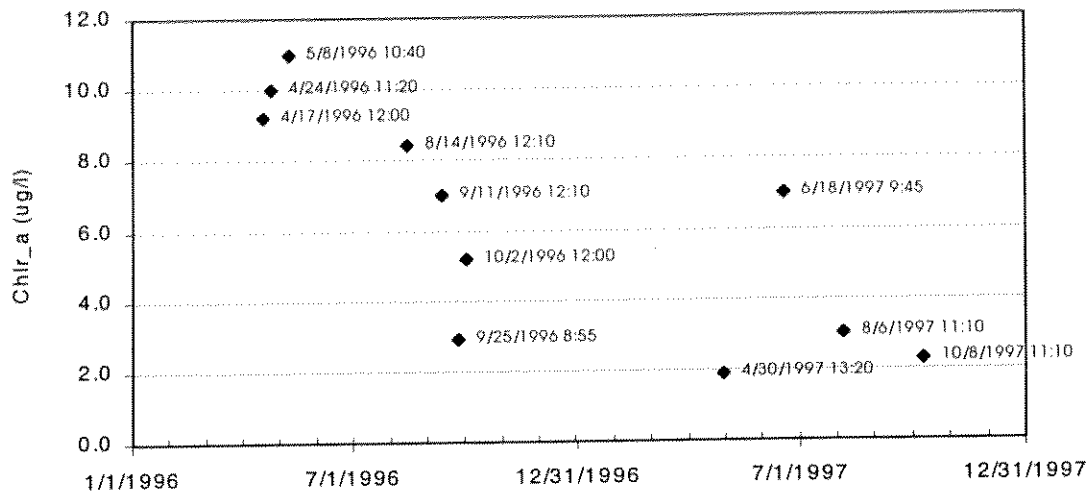
Figure B.4   Copco reservoir release chlorophyll a concentrations, 1996-1997

Because available data was sparse, and both the 1996 and 1997 NCRWQCB field data fell within the approximate range of background levels expected for nitrogen species, the field data were combined and average values applied as boundary conditions in both years. NCRWQCB data and estimated values are presented in Table B.6. Nitrite concentrations are assumed zero.

Interpretation of phosphorous, specifically orthophosphate concentrations was more complex. Orthophosphate data was scant throughout the system. Wetzel (1985) states that inorganic phosphate phosphorous totals about five percent of other forms of phosphorous, and that this percentage is remarkably constant in a large variety of lakes within the temperate zone. It is further stated that the percentage of total phosphorous occurring as truly ionic orthophosphate is probably considerably less than five percent. Historic data available for the Klamath River waters in the study area do not support this finding. Source waters apparently derive a certain level of phosphorous from geologic formations and possibly anthropogenic sources. DWR (1986) notes that orthophosphate concentrations in the Klamath River are higher than normally found in northern California rivers. Further, EPA (1978) concluded that Iron Gate Reservoir was nitrogen limited, further supporting reports of elevated phosphorous concentrations. Additional data reported by EPA support a ratio of orthophosphate to total phosphorous of approximately 0.4 to 0.8 (40 to 80 percent). Orthophosphate concentrations were estimated as roughly 0.15 mg/l. Because phosphorous is typically not limiting in Iron Gate Reservoir exact specification of concentrations was not deemed critical. NCRWQCB data and estimated values are presented in Table B.6.

53

Table B.6   Iron Gate Reservoir inflow (Copco Dam release) water quality concentrations for nitrogen and phosphorous species, 1996 and 1997

Parameter	1996 Range (mg/l)	1997 Range (mg/l)	1996 Average (mg/l)	1997 Average (mg/l)	Estimated Value (mg/l)
Org N-T$_a$	0.51 – 1.32	0.50 – 1.00	0.88	0.77	0.83
Org N-D$_a$	0.32 – 1.13	0.50 – 1.07	0.71	0.80	0.75
NH3-T	0.025 – 0.20	0.10 – 0.29	0.13	0.20	0.16
NH3-D	0.025 – 0.22	0.16 – 0.23	0.14	0.19	0.15
NO3-T	n/a	n/a	n/a	n/a	n/a
NO3-D	0.04 – 0.53	0.10 – 0.55	0.29	0.27	0.28
TKN-T	0.65 – 1.35	0.68 – 1.10	1.01	0.97	0.99
TKN-D	0.54 – 1.18	0.66 – 1.30	0.85	0.99	0.92
P-T	0.07 – 0.71	0.27 – 0.46	0.33	0.32	0.33
P-D	0.08 – 0.60	0.15 – 0.46	0.26	0.30	0.28
OP$_b$	n/a	n/a	n/a	n/a	0.15

[a] Org N calculated as TKN – NH3

[b] Orthophosphate concentrations estimated as 0.15 mg/l; DWR (1986) presents a range form 0 – 0.24 mg/l below IG Dam

B.5.4.7   Electrical Conductivity

Electrical conductivity of NCRWQCB grab samples ranged from 118 to 220 μS/cm (TDS: 76 to 141 mg/l) and from 150 to 220 μS/cm (TDS: 96 to 141 mg/l) for 1996 and 1997, respectively (field data). Mean values were approximately 180 μS/cm (TDS: 115 mg/l) for each field season. No clear trend was observable for available data, thus electrical conductivity was assumed to be 180 μS/cm (TDS: 115 mg/l) for Iron Gate reservoir inflow for all analyses. (Conversion: 1μ mho/cm = 1 μS/cm = 0.1 μS/m) (Conversion: TDS: 1 μS/cm x 0.64 (mg/l)/(μS/cm))

B.6   Klamath River

B.6.1   Initial Conditions: River Water Quantity

Initial conditions for Klamath River water quantity required system wide definition of the water surface for the hydrodynamic model. This was completed by running the model at steady state for a period of time that exceeded travel time in the study reach. For example, at 1000 cfs (28.3 cms) travel time from Iron Gate Dam to Siead Valley is approximately 1.5 days (neglecting excessive tributary inflow). Thus, steady-state simulations were completed for a period of three to four days to define initial water surface elevations used in subsequent model applications. Note, the initial conditions generally varied from actual field boundary

54

conditions. To ensure subsequent analyses were not influenced by initial conditions the results from the first few days of analysis were typically discarded.

B.6.2   Initial Conditions: River Water Quality

The stream model does not require system wide specification of initial conditions for water quality parameters, though the user may specify such conditions. More typically the user applies a set of boundary conditions and lets the system attain equilibrium over several simulation steps. As with flow, a period sufficiently longer than the reach travel time was required to attain an initial water quality profile for the river. Diurnal variations and specific aquatic processes may require a longer "wash out" period. For these analyses the model was run with fixed boundary conditions for several days to form an initial longitudinal profile of water quality throughout the study reach.

B.6.3   Boundary Conditions: Water Quantity

The Klamath River receives inflow from Iron Gate Dam releases, Shasta River, Scott River, and various smaller creeks, springs, and return flow, as well as groundwater accretions and precipitation. Depletions include diversion, groundwater depletion, evapotranspiration, and other losses. For simulation modeling, the major tributaries (Shasta and Scott Rivers) were explicitly included; all other inflows and outflows were combined into accretions and depletions and distributed throughout the system.

Boundary conditions were derived from available daily flow records. Records for Klamath River below Iron Gate Dam (RM 190.1), Shasta River near Yreka (RM 0.5), Scott River near Ft. Jones (RM 23.4), and Klamath River near Seiad Valley (RM 128.9) were obtained for calendar years 1996 and 1997. Within the study reach, accretions and depletions were assigned in a manner similar to the USGS MODSIM project (USGS/BRD MESC 1995). The total accretion was calculated between Iron Gate Dam and Seiad Valley as the sum of flow at Iron Gate Dam, Shasta and Scott Rivers minus flow at Seiad Valley. This value was subsequently partitioned into four sub-reaches and assigned percentages based on tributary basin areas:

- Iron Gate Dam to Shasta River (24.4%)
- Shasta River to Scott River (38.2%)
- Scott River from Ft. Jones to confluence with Klamath River (29.0%)
- Scott River to Seiad Valley (8.6 %)

Though further reduction of reach accretions and depletions were assigned to smaller tributaries (e.g., Bogus, Willow, Cottonwood, Humbug, Beaver, Dona, and Horse Creeks) by USGS, such detail was not included in this study. The Scott River accretion accounted for inflow to the system between the gage at Ft. Jones and the confluence with the Klamath River. The accretions and depletions were assigned to selected locations in the study reach. Each accretion/depletion location is outlined below and discussed further in Appendix B.9.6.

Accretion 1 (RM 181): Iron Gate to Shasta River

The Iron Gate to Shasta River accretion and depletion was located below Cottonwood Creek. This location was selected because it is the furthest downstream creek of any significant size in the study reach. Further, any groundwater accretion within this reach would most likely be limited to the alluvial deposits that extend from near Klamathon to just downstream of Cottonwood Creek, where the Klamath River turns southward and enters a canyon section.

Accretion 2 (RM 161): Shasta River to Scott River

The accretion point within the second sub-reach was located at Beaver Creek. Upstream of this point there is little flow contribution, especially during the summer months. Downstream of Beaver Creek small creeks become more common. For example, Horse Creek contributes appreciable flow throughout the summer.

Accretion 3 (RM 43): Scott River at Ft Jones to Confluence with Klamath River

This accretion/depletion was added to the Ft. Jones record and applied at the confluence of the Scott and Klamath Rivers

Accretion 4 (RM 139): Scott River to Seiad Valley

The accretion depletion point for the most downstream reach was applied at approximately river mile 139. Though the bulk of this contribution probably occurs downstream of this point (Seiad and Grider Creeks), the accretion/depletion point was located here so as not to interfere with the downstream boundary condition at Seiad Valley (i.e., for modeling purposes).

Accretions and depletions could not be determined through a simple water balance using the available daily data because transit time in the study reach is greater typically than one day (during the low flow periods). Steady-state simulations determined that one day travel time through the study reach occurs for flows of approximately 4000 cfs and two day travel time occurs for flows under 800 cfs. Ideally, the model would be used to route flows and

accretions at each point. This process would require multiple iterations because adding or subtracting water from the system would change the travel time in the downstream reach. Because accretions and depletions are generally a small percentage of the total main stem flow during the June through October period, accretions and depletions were calculated using a water balance, with releases from Iron Gate reservoir lagged a day for downstream calculations. Effective representation was obtained for the majority of flow conditions using this method. Additional details are included in section B.9.6.

B.6.4   Boundary Conditions: Water Quality

Klamath River receives inflow from Iron Gate Dam releases, Shasta River, Scott River, and accretions and depletions. Water quality for these inflows were determined from measured temperature data (UC Davis monitoring program), NCRWQCB (1997) sampling, DWR (1986) and other sources of available data. These sources are outlined below.

Calibration and validation of the river and reservoir models were carried out separately. However, for assessment of certain reservoir-river alternatives, Iron Gate Reservoir model results formed the upstream boundary conditions for the Klamath River hydrodynamic and water quality models.

B.6.4.1   Iron Gate Dam Release

Boundary conditions for water temperature, dissolved oxygen, BOD, chlorophyll *a*, nitrogen and phosphorous and electrical conductivity are defined for Iron Gate Dam releases.

<u>Water Temperature</u>

Hourly water temperature data was available for June 1996 – October 1996 and May 1997 – October 1997 (UCD monitoring program), May 1996 through November 1997 (USGS monitoring program), and from grab samples between April and October 1996 and 1997 (NCRWQCB sampling program). In addition, DFG had temperature loggers in the mouth of the Shasta River throughout much of the study period. Preliminary review illustrated that UCD and USGS hourly measured water temperature data were in general agreement. The UCD record was used as the primary water temperature boundary condition, with USGS and DFG data applied where UCD data were unavailable. Scott River water temperatures were unavailable early and late in the season (May and October). A comparison of Shasta and Scott River water temperatures illustrated that the Scott River runs much cooler in the spring

due to snowmelt runoff, but approximately equal to the Shasta River in the fall when base flow is generally at a minimum. Scott River temperatures were estimated from May 15 through June 15 as 2.5°C cooler than the Shasta River, and 1.5°C cooler from June 15 through July 15. October Scott River temperatures were estimated to be equal to the Shasta River. The Scott River typically has a reduced diurnal range when compared to the Shasta River, but this was not included in data synthesis. Section 10.7 includes notes on data availability and estimation. All data are included as electronic files, Appendix J.

Dissolved Oxygen

NCRWQCB data were used to describe the dissolved oxygen concentration of Iron Gate Dam release. Because the bulk of Iron Gate reservoir releases are via the penstock, which is located at a centerline depth of approximately 29 feet (8.84 m) at full pool, diurnal fluctuations in dissolved oxygen due to temperature and plant photosynthetic processes are moderated. Thus, grab samples supplied by the NCRWQCB are most likely representative of daily average conditions. However, review of hourly temperature profile data indicated that peaking power operations at Copco Powerhouse may disturb the quiescent nature of Iron Gate Reservoir, allowing hypolimnetic water (i.e., low dissolved oxygen) to be entrained by the penstock intake. Such short-term events were not addressed in this project.

Comparison of NCRWQCB dissolved oxygen data to other data illustrated a wide range of measurements. USGS-BRD hourly dissolved oxygen data generally did not agree with the NCRWQCB data, which typically ranged between 1 and 3 mg/l lower. DWR (1986) grab samples from 1962 to 1984 (43 samples, all months except July represented) illustrated a range in dissolved oxygen from 7.2 to 15.8 mg/l. Examination of saturation dissolved oxygen provided insight into selection of an appropriate boundary condition.

Dissolved oxygen concentrations in Iron Gate reservoir releases were estimated using NCRWQCB grab sample data. Three dissolved oxygen values were dropped from the analysis as outliers. These data points occurred in July (1997), August (1996) and September (1996) and were significantly above saturation concentration. Though primary production can elevate dissolved oxygen concentrations above saturation, immediately below Iron Gate Dam there appears to be little opportunity to attain values significantly in excess of saturation. The upstream boundary conditions for dissolved oxygen were estimated as mean monthly values based on combined 1996 and 1997 data. Table B.7 defines the final values. As with monthly estimated dissolved oxygen for Iron Gate

58

Reservoir inflow, values are assumed for the 15th of the month and linear interpolation is used to determine intermediate values.

Table B.7.   Mean monthly dissolved oxygen concentration below Iron Gate Dam, derived from 1996 and 1997 NCRWQCB data (Values in bold derived from USGS grab sample data, 1967-80)

Month	DO (mg/l)	Month	DO (mg/l)
January	12.1	July	8.1 (11.2)
February	12.1	August	7.6 (8.9)
March	12.6	September	7.1 (8.8)
April	10.2 (11.7)	October	6.7 (7.5)
May	8.9 (11.1)	November	8.6
June	8.0 (10.2)	December	10.7

Chlorophyll a

Limited chlorophyll *a* data were available for 1996 and 1997, and all data was derived from NCRWQCB sampling. Data from 1996 consisted of three grab (April 24, August 14, and October 2) samples yielding 5.0, 10.0, and 7.6 µg/l (0.34, 0.67, and 0.51 mg algae/l, respectively)). Data from 1997 consisted of four grab samples (April 30, June 18, August 6, and October 8) with values of 1.7, 6.0, 2.9, and 5.2 µg/l (0.11, 0.40, 0.19, and 0.35 mg algae/l), respectively. Data are shown in Figure B.5. Though seasonal variations most likely affect concentrations of algal species, growth and death rate, and settling rate, a fixed value of 5.0 µg/l (0.34 mg/algae/l) was assumed constant for both years. No attached algae data were available for the study reach. See Appendix E for additional details.

BOD

Limited BOD data were available, but values were consistent with background levels for natural systems of about 0.5 to 3.0 mg/l (EPA, 1997). NCRWQCB data for 1996 report values of 2.5, 1.5, 3.0, and 6.0 mg/l between April and October, and 1997 values of 1.5, 1.5, 2.5, and 1.5 mg/l over the same 7 month period.

DWR (1986) included EPA STORET summaries of 15 grab samples below Iron Gate Dam from 1977 through 1982. Samples were collected in the months of March (1), April (4), May (1), June (3), September (4), and November (2). BOD values ranged from 0.8 to 3.3 mg/l with a mean of 2.0 mg/l. A constant value of 2.0 mg/l was used for all analyses.

59
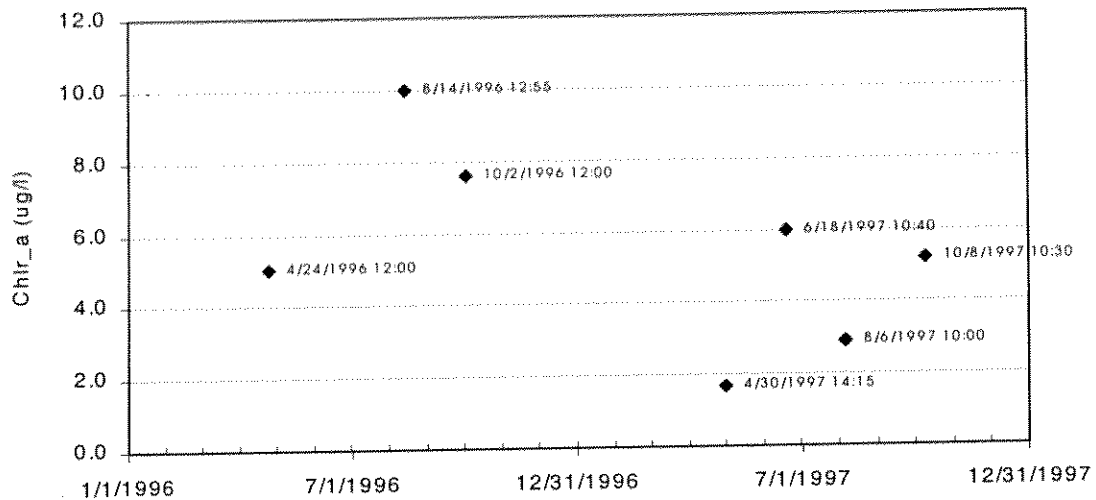
Figure B.5   Chlorophyll a concentrations below Iron Gate Dam, 1996 and 1997

Nitrogen and Phosphorous

Nitrogen and phosphorous parameters were estimated based on NCRWQCB data (1997) and other references. Because values were typical of background levels in surface waters (see Thomann and Mueller, 1987 and EPA, 1997) and the range of values was limited, average values for 1996 and 1997 were used as boundary conditions in both years. NCRWQCB data and estimated values are presented in Table B.8. Nitrite concentrations are assumed zero. Values are similar to Iron Gate Reservoir inflow (Copco Dam release), refer to Table B.6 for comparison.

Electrical Conductivity

Electrical conductivity of NCRWQCB grab samples ranged from 105 to 286 μS/cm (TDS: 67 to 183 mg/l) and from 157 to 214 μS/cm (TDS: 100 to 137 mg/l) for 1996 and 1997, respectively (field data). Mean values were approximately 180 μS/cm (TDS: 115 mg/l) for each field season. A brief comparison between Iron Gate inflow and Iron Gate Dam releases illustrated that in 1996 conductivity varied over a wider range than 1997, but during both years averaged nearly the same value. No clear trend was observable for available data, thus electrical conductivity was assumed to be 180 μS/cm (TDS: 115 mg/l) for Iron Gate reservoir release. (Not modeled)

60

Table B.8.   Iron Gate Dam release water quality concentrations for nitrogen and phosphorous species, 1996 and 1997

Parameter	1996 Range (mg/l)	1997 Range (mg/l)	1996 Average (mg/l)	1997 Average (mg/l)	Estimated Value (mg/l)
Org N-T[a]	0.47 – 1.54	0.40 – 0.64	0.92	0.48	0.70
Org N-D[a]	0.32 – 1.13	0.40 – 0.66	0.68	0.49	0.60
NH3-T	0.08 – 0.12	0.10 – 0.28	0.10	0.19	0.15
NH3-D	0.07 – 0.10	0.10 – 0.24	0.08	0.17	0.10
NO3-T	n/a	n/a	n/a	n/a	n/a
NO3-D	0.04 – 0.52	0.13 – 0.46	0.26	0.23	0.25
TKN-T	0.58 – 1.66	0.50 – 0.80	1.02	0.67	0.85
TKN-D	0.41 – 1.20	0.50 – 0.80	0.77	0.65	0.70
P-T	0.03 – 0.44	0.16 – 0.39	0.20	0.27	0.25
P-D	0.03 – 0.32	0.03 – 0.24	0.17	0.16	0.15
OP[b]	n/a	n/a	n/a	n/a	0.10

[a] Org N calculated as TKN – NH3

[b] Orthophosphate concentrations estimated as 0.1 mg/l; DWR (1986) presents a range form 0 – 0.24 mg/l below IG Dam

B.6.4.2   Shasta River

The waters of the Shasta River are used for agriculture upstream from the confluence with the Klamath River. Further, the river traverses a long valley section with mild slope. Significant transit time, low flows, shallow depths, and agricultural return flow contribute to water quality that differs significantly from other tributaries.

Water Temperature

Shasta River water temperature data were derived from the UCD temperature monitoring program completed during the 1996 and 1997 field season. Hourly data were available for the 1996 and 1997 field seasons. Additional data was available from California Department of Fish and Game (DFG).

Dissolved Oxygen

Dissolved oxygen values presented by NCRWQCB (1997) grab samples during the 1996 and 1997 field seasons were examined to estimate the dissolved oxygen boundary condition of the Shasta River. Only four samples were available from 1996 (April, June, August, and October), while 14 samples were taken in 1997. All samples were taken mid-day with the exception of June 1996 (5:30 a.m.). Values ranged from 8.2 to 12.3 mg/l. All values except 10/8/97 exceeded theoretical saturation concentration (a function of water temperature and atmospheric pressure (elevation), see Section B.9). Further examination of 26 grab samples

61

from 1961 to 1984 (DWR, 1986) found dissolved oxygen ranged from 8 to 12.4 mg/l – all but seven exceeded theoretical saturation. Approximately half of these samples were collected before 9:00 a.m. Similar findings occurred in USGS data reviewed for the period 1967-79 (Earthinfo, Inc., 1996).

Low dissolved oxygen concentrations have been reported in the Shasta River by NCRWQCB (1993), Wood and Rogers (1991), DWR (1991), DWR (1986) and others. However, most studies have focused in the Shasta Valley region well upstream from the confluence with the Klamath River. As the river leaves the Shasta Valley, it traverses a steep canyon where slopes reach 0.015. While fine sediments dominate in the valley reaches and are postulated to exert potentially significant sediment oxygen demands (NCRWQCB 1993), the Canyon reach has sufficient slope and water velocities to minimize significant fine sediment deposition. Coupled with re-aeration through the riffle-run environment typical of the canyon dissolved oxygen levels should remain close to saturation; a hypothesis supported by current and historic data.

Given the above examination of available data, hourly dissolved oxygen concentration for Shasta River inflows was estimated as the saturation concentration corresponding to water temperature, and corrected for elevation above sea level (2000 ft (610 m)) using standard atmospheric pressure.

Chlorophyll a

Chlorophyll a measurements for the mouth of the Shasta River were available for the NCRWQCB (1997). Two samples from 1996 (5.3 and 5.5 µg/l; 0.36 and 0.37 mg algae/l)) and four samples from 1997 (4.9, 2.5, 1.2, and 2.4 µg/l; 0.33, 0.17, 0.08, and 0.16 mg algae/l)). Though seasonal variations most likely affect concentrations of algal species, growth and death rate, due to lack of available data a value of 5.0 µg/l (0.34 mg algae/l) was assumed constant for all analyses.

BOD

Limited BOD data were available, but values were consistent with background levels for natural systems of about 0.5 to 3.0 mg/l (EPA, 1997). NCRWQCB data for 1996 report values of 2.5, 1.5, 1.5, and 1.5 mg/l between April and October, and 1997 values of 1.5, 2.5, 3.0, and 1.5 mg/l over the same 7 month period. A constant value of 2.0 mg/l was used for all analyses.

<u>Nitrogen and Phosphorous</u>

Nitrogen and phosphorous parameters were estimated based on NCRWQCB data (1997) and other references. Because values were typical of background levels in surface waters (see Thomann and Mueller, 1987 and EPA, 1997), and the range of values was limited, average values for 1996 and 1997 were used as boundary conditions in both years. NCRWQCB data and estimated Shasta River values are presented in Table B.9. Values are similar to Iron Gate Reservoir inflow (Copco Dam release) and Iron Gate Dam release, see Table B.6 and B.8 for comparison. Shasta River phosphorous levels were elevated and ammonia and nitrate levels were slightly lower compared to Iron Gate Reservoir inflow and release. Nitrite concentrations were assumed zero.

Table B.9   Shasta River water quality concentrations for nitrogen and phosphorous species, 1996 and 1997

Parameter	1996 Range (mg/l)	1997 Range (mg/l)	1996 Average (mg/l)	1997 Average (mg/l)	Estimated Value (mg/l)
Org N_a	0.47 – 0.65	0.36 – 0.90	0.55	0.63	0.90
Org N_a	0.37 – 0.61	0.38 – 0.72	0.47	0.48	0.50
NH3-T	0.03 – 0.15	0.05 – 0.14	0.10	0.11	0.10
NH3-D	0.03 – 0.11	0.03 – 0.12	0.08	0.08	0.05
NO3-T	n/a	n/a	n/a	n/a	n/a
NO3-D	0.04 – 0.26	0.04 – 0.11	0.09	0.07	0.10
TKN-T	0.62 – 0.67	0.50 – 1.00	0.65	0.73	0.70
TKN-D	0.47 – 0.63	0.50 – 0.74	0.55	0.56	0.55
P-T	0.14 – 0.57	0.26 – 0.54	0.37	0.41	0.40
P-D	0.15 – 0.65	0.24 – 0.42	0.39c	0.34	0.35
OP_b					0.20

[a] Org N calculated as TKN – NH3

[b] Orthophosphate concentrations estimated as 0.2 mg/l; DWR (1986) presents a range form 0 – 0.24 mg/l below IG Dam

[c] Dissolved phosphorous exceeds total phosphorous: accuracy acceptable within laboratory analysis range of uncertainty

<u>Electrical Conductivity</u>

Electrical conductivity values for the Shasta River were considerably higher than for the Klamath River. Electrical conductivity values were estimated based on NCRWQCB data (1997) and other sources. Two samples were available from 1996: 375 and 588 µS/cm (TDS: 240 and 376 mg/l) for an average of 480 µS/cm. Fourteen samples were available from 1997: minimum, maximum and average values were 503, 649, and 580 µS/cm, respectively (TDS: 322, 415, and 371 mg/l). DWR (1986) reported 15 values between 1982

and 1984 with a range of 409 to 587 µS/cm (TDS: 212 to 376 mg/l) and a mean of approximately 500 µS/cm (TDS: 320 mg/l). NCRWQCB (1993) presents similar values for upstream locations along the Shasta River. A constant value of 500 µS/cm (TDS: 320 mg/l) was assumed. (Not modeled.)

B.6.4.3 Scott River

The waters of the Scott River enter the Klamath River at RM 143.2. Though waters of the Scott River are used for agriculture and other uses upstream, significant contributions from the Marble Mountains, coupled with steep canyon reaches upstream of the confluence with the Klamath River, lead to water quality conditions appreciably better than the Shasta River. For all water quality parameters except temperature there were no available data for the 1996 and 1997 field seasons. Historical data was used to estimate boundary values for these constituents. However, this method was further limited because historical data was typically available only at Ft. Jones, located roughly 24 miles upstream from the confluence with the Klamath River.

Water Temperature

UC Davis collected hourly water temperature data approximately 0.5 miles upstream from the confluence with the Klamath River for the 1996 and 1997 field seasons. See Section B.9 for additional details on the Scott River temperature record.

Dissolved Oxygen

Dissolved oxygen data were available from 1967 to 1979 at Ft. Jones (Earthinfo Inc., 1995) and from 1961 to 1967 and 1984 (DWR, 1986). A single sample was available at the mouth of the Scott River in 1983 (DWR, 1986). Dissolved oxygen data available from Earthinfo Inc. (78 observations) ranged from 9.0 to 13.9 mg/l (one reading was 7.4 mg/l, 9/5/68, time not specified). The STORET data presented by DWR (1986) (12 observations) ranged from 9.0 to 13.8 mg/l. The single observation available at the mouth was 11.7 mg/l. All observations (with the exception of the 9/5/98 sample) were at or above saturation, and time of observation ranged from 7:30 a.m. to 5:00 p.m.

As with the Shasta River, the Scott traverses a steep canyon prior to confluence with the Klamath River. Further, the Scott River is not as heavily developed for agriculture, receives tributary contributions from the Marble Mountains, and is typically slightly cooler than the Shasta River in its canyon reach.

Given these conditions, hourly concentrations for Scott River inflow were estimated as the saturation concentration corresponding to water temperature, corrected for elevation from sea level 1525 ft (465 m)).

Chlorophyll *a*

No chlorophyll *a* data was available for the Scott River. Due to the limited quantity of attached algae and general water clarity an estimated value of 2.0 μg/l (0.13 mg algae/l) was assumed constant for all analyses.

BOD

No BOD data was available. A background level of 2 mg/l was assumed constant for all analyses.

Nitrogen and Phosphorous

A limited amount of historical data existed for nutrients both at Ft Jones and at the mouth of the Scott River. Combining all nutrient monitoring, DWR (1986) and USGS (Earthinfo Inc., 1995) reported data for only a few dozen samples between 1959 and 1984. Table B.10 outlines the estimated concentration of the various nitrogen and phosphorous species used as boundary conditions at the Scott River. Nitrite concentrations are assumed zero.

Table B.10. Scott River water quality concentrations for nitrogen and phosphorous species, historical data

Parameter	Estimated Value (mg/l)
Org N-T$_a$	0.10
Org N-D$_b$	0.10
NH3-T	0.05
NH3-D$_c$	0.05
NO3-T	0.35
NO3-D	0.20
TKN-T	0.15
TKN-D$_d$	0.10
P-T	0.10
P-D	0.05
OP$_e$	0.05

[a] OrgN calculated as TKN – NH3
[b] OrgN-D estimated as 0.8(OrgN-T)
[c] NH3-D estimated as 0.8(NH3-T)
[d] TKN-D calculated as OrgN-D + NH3-D
[e] Orthophosphate concentrations estimated as 0.5(P-T)

<u>Electrical Conductivity</u>
Similar to other water quality parameters, there was limited available data for electrical conductivity. A constant value of 180 µS/cm (TDS: 115 mg/l) was applied to all analyses based on a review of DWR (1986) and USGS (Earthinfo, Inc., 1995). Values ranged from less than 100 µS/cm to over 200 µS/cm (TDS: 64 to 128 mg/l). (Not modeled.)

B.6.4.4 Accretions/Depletions
Accretions and depletions are dispersed along the length of the river and vary in quantity and quality, are affected by seasonal conditions, and are not assigned water quality attributes. The exception is the Scott River where flow at Ft. Jones is combined with the estimated accretion and water quality parameters are assigned to the sum.

B.7 Calibration and Validation Data: Water Quality

Calibration and validation data is typically independent of initial or boundary condition data that is used to assess model performance. The reservoir and stream models were calibrated for the 1996 and 1997 seasons for water temperature and dissolved oxygen. The models were not formally calibrated to other water quality parameters, including BOD, chlorophyll a, and nutrients. General lack of available data limit the usefulness of such an exercise; however, model results were reviewed to ensure simulation results were within the range of acceptable values.

B.7.1 Iron Gate Reservoir

Calibration and validation water temperature and quality data were derived primarily from the UC Davis temperature monitoring program and the NCRWQCB limnological surveys of Iron Gate Reservoir. Because Iron Gate Reservoir hydrology is represented by conservation of mass (e.g., water budget), there is no quantity data required for calibration.

B.7.1.1 Water Temperature
Hourly water temperature was monitored at seven depths (7, 17.2, 39.8, 59.3, 79.5, 99.2, and 118 feet) for the 1996 and 1997 field seasons, plus limited 1996-97 winter monitoring. This record provides a complete data set for temperature calibration and validation. Section B.9.8

includes a discussion of Iron Gate Reservoir profile temperature data used for calibration and validation purposes.

B.7.1.2 Water Quality
Dissolved oxygen profiles from May and August 1996 and 1997 were used to calibrate and validate the model. Measurements were taken at 3.2 ft (1.0 m) increments near the surface and 6.5 ft (2.0 m) at depths greater than one and a half times the measured secchi depth. Nutrient and chlorophyll a concentrations were limited to a few grab samples labeled as "surface" and "below thermocline."

Secchi depths at Iron Gate Reservoir ranged from approximately 0.8 to 2.7 meters during the 1996 and 1997 field seasons. Secchi depth varied spatially in the reservoir as well. At NCRWQCB station 5, near the reservoir inflow (below Copco Dam), secchi depths exceeded 3 meters on occasion. These measurements were assumed not to be representative of the transparency of the main reservoir body.

B.7.2 Klamath River
Water temperature and quality data were derived from the UC Davis temperature monitoring program, limited dissolved oxygen data gathered by UC Davis, and NCRWQCB (1997) main stem grab samples.

B.7.2.1 Water Temperature
Hourly water temperature data was available at several main stem locations. Temperature monitoring studies varied from year-to-year, but ten sites were monitored consistently for both the 1996 and 1997 field season. These sites are listed in Table B.11. Data from additional locations was also used in calibration and validation.

B.7.2.2 Water Quality
Water quality sampling was completed by the NCRWQCB at four locations within the study reach. Table B.12 outlines the locations, delineates approximate river mile, elevation of site, and number of samples for each site. Dissolved oxygen was sampled with a YSI field probe. Lab analyses for nutrients, BOD, and chlorophyll a were completed approximately four times per season at each site.

Table B.11. UC Davis temperature monitoring program: logger locations

Location	River Mile
Klamath River below Iron Gate Dam	190.1
Klamath River above Cottonwood Creek	182.1
Klamath River above Shasta River	176.7
Shasta River	0.5
Klamath River below Shasta River	176.3
Klamath River near Walker Road Bridge	156.2
Klamath River above Scott River	143.5
Scott River	1.0
Klamath River below Scott River	142.5
Klamath River at USGS Gage near Seiad Valley	128.9

Other monitoring locations:
  Klamath River below Little Bogus Creek (RM 186.4): fall 1996, 1997
  Klamath River at Klamathon (RM 182.1): fall 1996
  Klamath River near Carson Gulch (RM 180.0): fall 1996
  Klamath River near Lime Gulch (RM 169.7): 1997
  Klamath River below Lumgrey Creek (RM 165.9): fall 1996, 1997
  Klamath River below Kohl Creek (RM 151.7): fall 1996, 1997
  Klamath River below Horse Creek (RM 147.2: fall 1996, 1997

Table B.12. NCRWQCB sampling locations between Iron Gate Dam and Seiad Valley, including river mile, elevation, and number of samples

Location	River Mile	Elevation (ft msl)	# DO Samples 1996/1997	# Nutrient Samples 1996/1997
Above Cottonwood Ck.	182	2050	19/14	3/4
Below Shasta R.	176	2000	20/14	4/4
Below Beaver Ck.	161	1740	17/15	4/4
Below Scott R.	142	1525	18/15	4/4

Limited diurnal data are available from a short deployment completed by UC Davis from June 28-30, 1997. Two field probes were deployed, one below the Shasta River (RM 176) and one at Walker Road Bridge (RM 156). Dissolved oxygen, water temperature, EC, and pH were monitored at 30-minute intervals.

B.8   Determination of Saturation Dissolved Oxygen Concentration

Saturation dissolved oxygen concentration was estimated using the following formulation (Bowie 1985):

$$C_s = \exp[-139.34411 + (1.575701 \times 10^5/T)$$

$$- (6.672308 \times 10^7/T^2)$$

$$+ (1.243800 \times 10^{10}/T^3)$$

$$- (8.621949 \times 10^{11}/T^4) \tag{B.3}$$

Where:
C_s = saturation dissolved oxygen (mg/l)
T   = temperature (K)

Dissolved oxygen correction for Non-Standard Pressure (elevation)

$$C_s' = C_s P \tag{B.4}$$

Where:
C_s' = saturation dissolved oxygen (mg/l)
C_s = saturation dissolved oxygen (mg/l)
p   = pressure, (atm)

Equation B.4 applies for elevations less than 4000 feet and pressures between 0.00 and 2.00 atmospheres.

B.9 Attachments

B.9.1 Iron Gate Reservoir stage-volume data (PacifiCorp 1995)

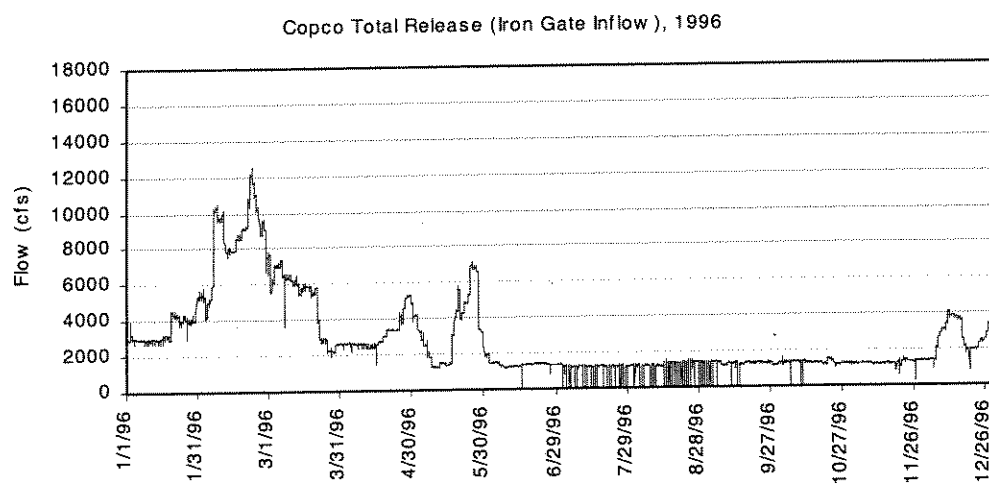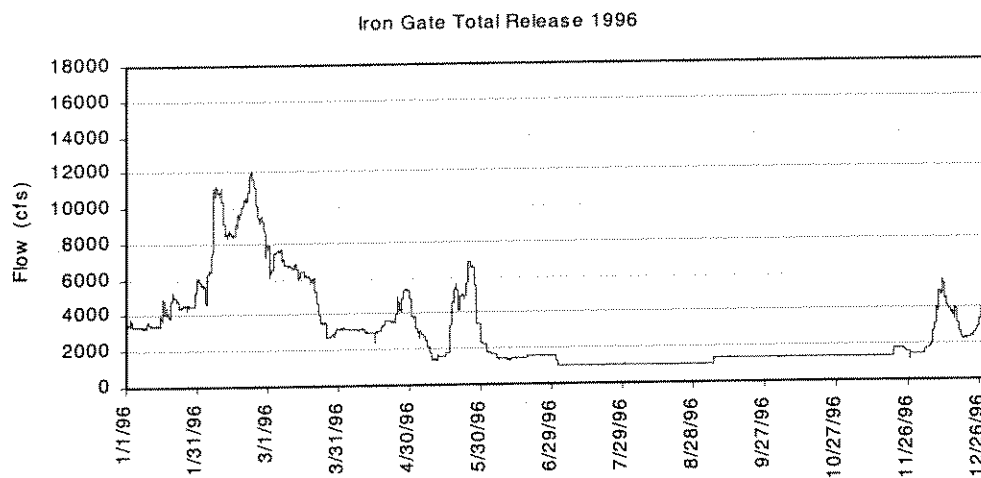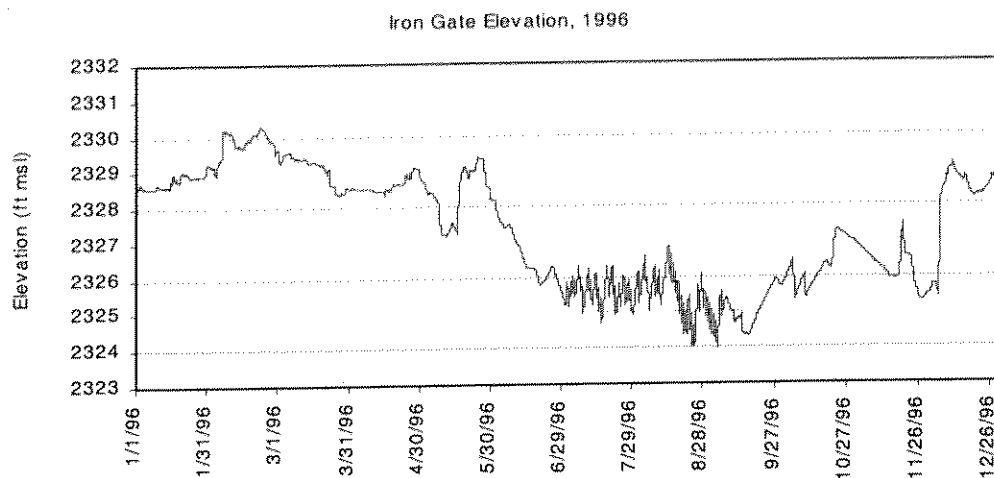| Elev (ft msl)	Storage (AF)	Elev (ft msl)	Storage (AF)	Elev (ft msl)	Storage (AF)	Elev (ft msl)	Storage (AF)
2328	58794	2285	26935	2245	9766	2202	1440
2327	57822	2284	26370	2244	9462	2201	1352
2326	56867	2283	25819	2243	9169	2200	1264
2325	55928	2282	25268	2242	8876	2199	1184
2324	55004	2281	24731	2241	8594	2198	1104
2323	54094	2280	24194	2240	8312	2197	1031
2322	53198	2279	23670	2239	8041	2196	958
2321	52314	2278	23146	2238	7770	2195	892
2320	51442	2277	22636	2237	7510	2194	826
2319	50582	2276	22126	2236	7250	2193	767
2318	49734	2275	21630	2235	7001	2192	708
2317	48898	2274	21134	2234	6752	2191	655
2316	48073	2273	20652	2233	6514	2190	602
2315	47259	2272	20170	2232	6276	2189	555
2314	46453	2271	19703	2231	6049	2188	508
2313	45661	2270	19236	2230	5822	2187	466
2312	44877	2269	18783	2229	5606	2186	424
2311	44103	2268	18330	2228	5390	2185	387
2310	43339	2267	17891	2227	5185	2184	350
2309	42585	2266	17452	2226	4980	2183	318
2308	41841	2265	17026	2225	4784	2182	286
2307	41106	2264	16600	2224	4588	2181	258
2306	40380	2263	16187	2223	4400	2180	230
2305	39663	2262	15774	2222	4212	2179	206
2304	38954	2261	15374	2221	4032	2178	182
2303	38253	2260	14974	2220	3852	2177	161
2302	37560	2259	14586	2219	3681	2176	140
2301	36875	2258	14198	2218	3510	2175	122
2300	36198	2257	13823	2217	3348	2174	104
2299	35533	2256	13448	2216	3186	2173	89
2298	34868	2255	13086	2215	3033	2172	72
2297	34219	2254	12724	2214	2880	2171	62
2296	33570	2253	12375	2213	2736	2170	50
2295	32935	2252	12026	2212	2592	2169	41
2294	32300	2251	11689	2211	2457	2168	32
2293	31679	2250	11352	2210	2322	2167	25
2292	31058	2249	11026	2209	2197	2166	18
2291	30451	2248	10700	2208	2072	2165	13
2290	29844	2247	10385	2207	1957	2164	8
2289	29521	2246	10070	2206	1842	2163	5
2288	28658			2205	1737	2162	2
2287	28079			2204	1632	2161	1
2286	27500			2203	1536		

B.9.2 Copco Reservoir Stage-Volume Relationship (PacifiCorp 1995)

Elev (ft msl)	Storage (AF)	Elev (ft msl)	Storage (AF)	Elev (ft msl)	Storage (AF)
2607.5	46867	2570	16795	2530	1855
2607	46382	2569	16254	2529	1736
2606	45390	2568	15714	2528	1616
2605	44419	2567	15173	2527	1497
2604	43458	2566	14633	2526	1377
2603	42507	2565	14092	2525	1258
2602	41565	2564	13552	2524	1138
2601	40632	2563	13011	2523	1019
2600	39708	2562	12471	2522	899
2599	38792	2561	11930	2521	780
2598	37884	2560	11390	2520	660
2597	36986	2559	10962	2519	607
2596	36098	2558	10534	2518	554
2595	35220	2557	10106	2517	501
2594	34352	2556	9678	2516	448
2593	33922	2555	9250	2515	395
2592	33494	2554	8822	2514	342
2591	32646	2553	8394	2513	289
2590	31808	2552	7966	2512	236
2589	30981	2551	7538	2511	183
2588	30164	2550	7110	2510	130
2587	29263	2549	6794	2509	117
2586	28415	2548	6478	2508	104
2585	27010	2547	6162	2507	91
2584	26718	2546	5846	2506	78
2583	25870	2545	5530	2505	65
2582	25021	2544	5214	2504	52
2581	24173	2543	4898	2503	39
2580	23325	2542	4582	2502	26
2579	22672	2541	4266	2501	13
2578	22019	2540	3950	2500	0
2577	21366	2539	3741		
2576	20713	2538	3531		
2575	20060	2537	3321		
2574	19407	2536	3112		
2573	18754	2535	2903		
2572	18101	2534	2693		
2571	17448	2533	2484		
		2532	2274		
		2531	2065		

B.9.3 WQRRS Stage-Dam Width Relationship

Elev	Reservoir Width @ Dam	Spillway Width	Elev	Reservoir Width @ Dam	Spillway Width
(ft msl)	(ft)	(ft)	(ft msl)	(ft)	(ft)
2162	18	-	2255	450	-
2165	97	-	2260	476	-
2170	217	-	2265	507	-
2175	228	-	2270	527	-
2180	237	-	2275	533	-
2185	250	-	2280	547	-
2190	258	-	2285	560	54
2195	268	-	2290	590	54
2200	278	-	2295	614	55
2205	293	-	2300	629	58
2210	305	-	2305	645	63
2215	318	-	2310	655	64
2220	333	-	2315	665	66
2225	348	-	2320	677	69
2230	364	-	2325	686	73
2235	377	-	2328	692	74
2240	393	-	2330	700	-
2245	410	-	2335	710	-
2250	427	-	2338	713	-

B.9.4   Iron Gate Flow Data – Graphs (Elevation, Inflow, Release)

Iron Gate Elevation, 1996

Iron Gate Total Release 1996

Copco Total Release (Iron Gate Inflow), 1996

Iron Gate Elevation, 1997

Iron GateTotal Release, 1997

Copco Total Release (Iron Gate Inflow), 1997
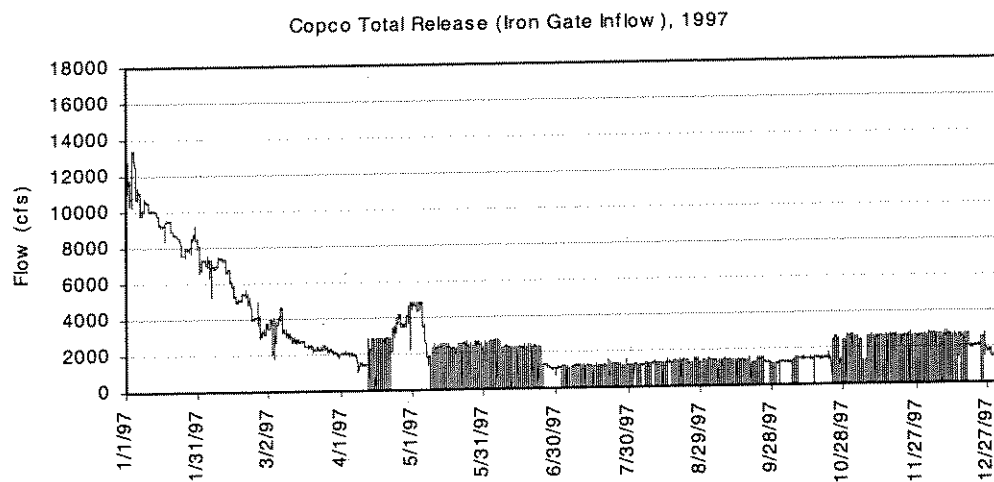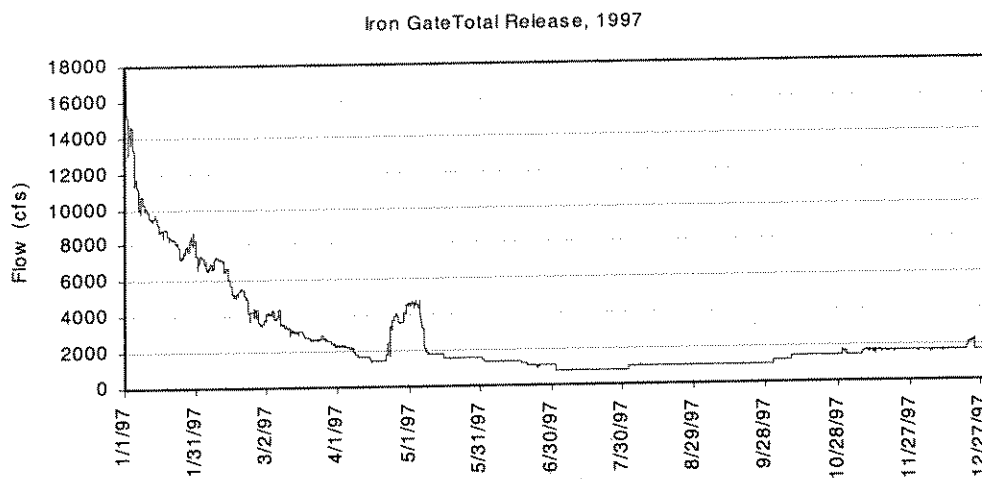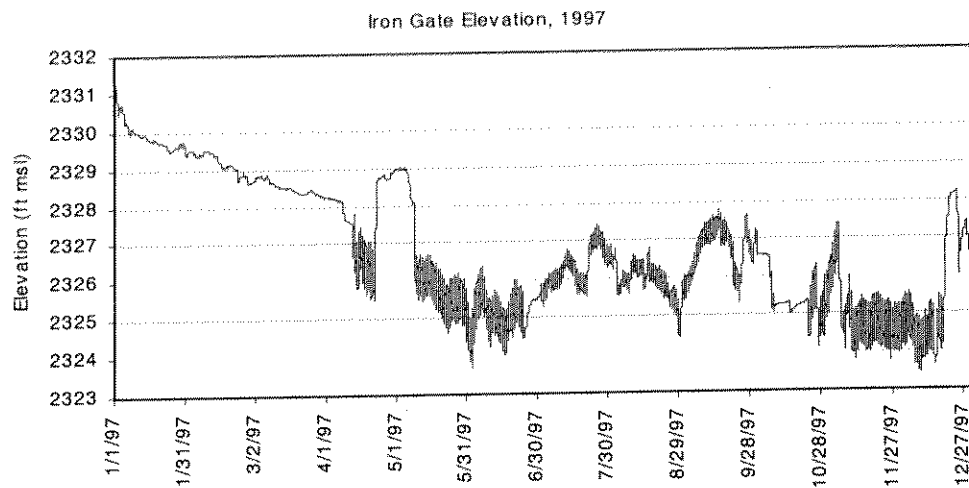
B.9.5   Iron Gate Reservoir Water Temperature: Inflow Temperature

<u>Copco Reservoir Release Temperature (Iron Gate Reservoir Inflow)</u>

Copco Reservoir release temperature records were obtained from PPL, and represent Copco #2 tailrace. Significant data gaps existed in records for both 1996 and 1997. 1996 was missing data from June 12 through September 16, while 1997 was missing data from June 18 through August 20. In addition, the April through October 1997 deployment was subject to dewatering (exposure to the atmosphere) in response to Copco operations/release. Much of this record was recreated from limited measurements. Daily average temperature for 1996 and 1997 are shown in Figure B.6.

1996

After careful review, data recorded for May and the first half of June, as well as the last half of September through December were deemed acceptable. July 12 through September 16 were missing completely. The records were estimated based on 1997 data trace and water temperatures in Iron Gate Reservoir for 1996 and 1997. It was noted that the descending (October) limbs on the seasonal temperature plots were nearly coincident. Moreover, the Iron Gate profile loggers (IG0, IG1, and IG2) were of similar temperature in both 1996 and 1997. Using this information it was assumed that Copco Reservoir, though cooler in the spring of 1996, heated to similar late summertime levels as 1997. Point estimates in time were made to approximate thermal loading of the reservoir and thus release temperatures. Briefly,

> 5/15/96 - 6/12/96: recorded field data used
> 6/12/96 - 9/16/96: estimated thermal loading rate as 7/1 (18.0), 7/15 (20.0), 8/1 (20.6),
>   8/15 (20.75), 9/1 (20.0) and used linear interpolation to determine
>   intermediate values
> 9/16/96 - 12/31/96: recorded field data used

All data were averaged over the day at the end of reconstruction. Daily records were deemed sufficient for input into the hourly Iron Gate Reservoir model because diurnal fluctuations in Copco Reservoir release temperatures are moderated due to depth of penstock intake. However, seasonal trends are clearly seen in the temperature records

1997

January - March data were deemed acceptable as recorded, but April through October data had to be reconstructed from partial records due to dewatering of loggers. Briefly,

75

1/1/97 - 3/29/97: smoothed with 24 hour running average

3/29/97 - 4/15/97: smoothed with a 92 hour running average. It appears that the logger was completely exposed to air (for the most part) during this period and the assumption that mean air temperature approximates mean water temperature was applied.

4/19/97 - 4/23/97: linear interpolation

4/23/97 - 5/6/97: smoothed with 24 hour running average

5/6/97 - 6/17/97: estimated using periods of record where logger was recording water temperature (air temperature portion of record dropped, as were transitional readings where logger may have been partially submerged or equilibrating - examined Shasta Valley meteorological data to determine if air temperatures were of correct magnitude and estimate this recreated record is fairly representative of inflow temperature)

6/17/97 - 8/21/97: estimated thermal loading rate as 7/1 (20.25), 7/15 (20.5), 8/1 (20.75) and used linear interpolation to determine intermediate values

8/21/97 - 9/25/97: see explanation for 5/6/97 - 6/17/97.

9/25/97 - 10/8/97: linear interpolation

10/8/97 - 10/14/97: smoothed with 24 hour running average

10/15/97 - 10/31/97: linear interpolate from 10/14 to 11C (similar to 1996)

All data are averaged over the day at the end of reconstruction.
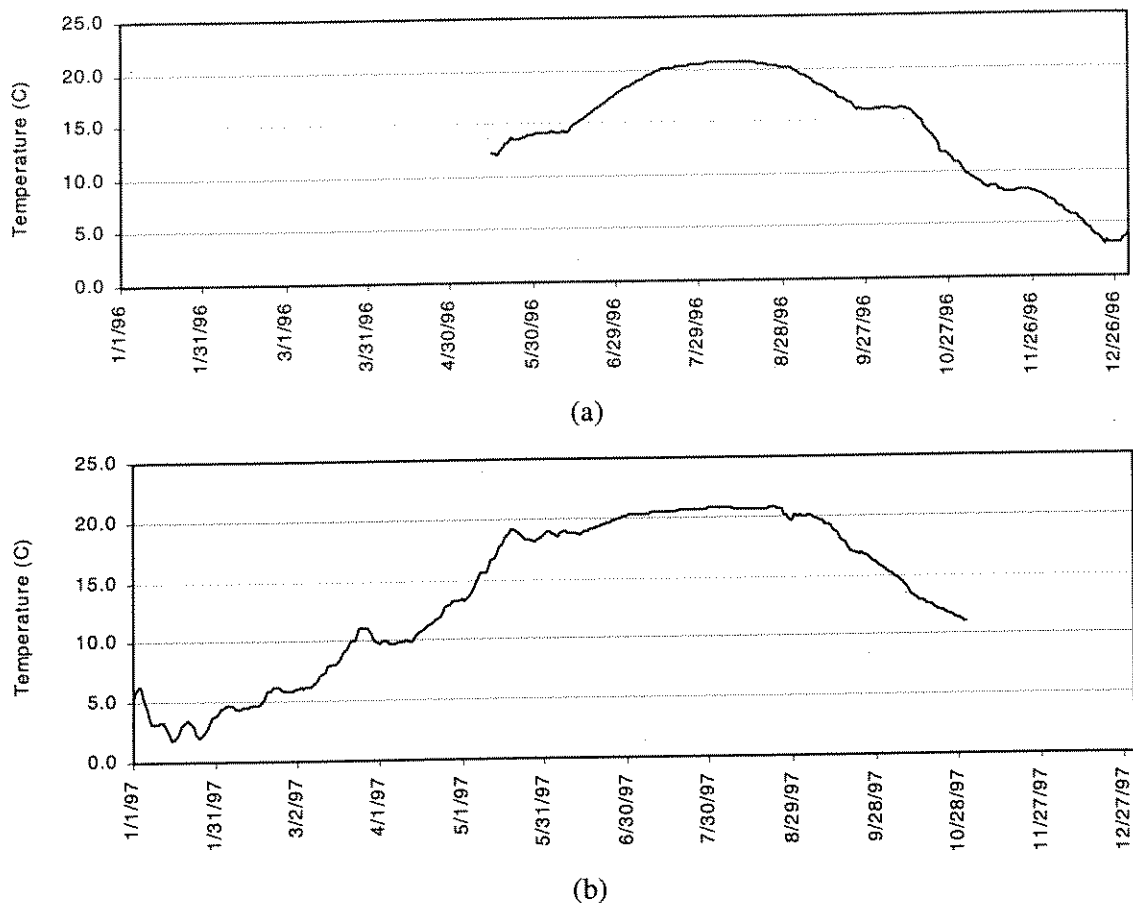

(a)

(b)

Figure B.6   Copco #2 tailrace daily average temperature, (a) 1996 and (b) 1997

B.9.6　Klamath River Accretion/Depletion Estimation

Determination of accretions and depletions for the Klamath River from Iron Gate Dam to Seiad Valley were estimated based on flow rate. An overall accretion/depletion was determined between Iron Gate Dam and the USGS gage near Seiad Valley. Flow at Seiad Valley was always greater than the flow below Iron Gate Dam, thus the study reach was gaining throughout the study period. This total accretion was then divided into four accretions,

- between Iron Gate Dam and the Shasta River (Accretion #1),
- between the Shasta River and the Scott River (Accretion #2),
- between the Scott River and the USGS gage near Seiad Valley (Accretion #3), and
- between the Scott River flow reported at Ft. Jones and the confluence of the Scott River with the Klamath River (Scott River Accretions).

Figure B.7 shows a schematic for the Klamath River system in the study reach with accretions is shown below. The total accretion was apportioned as

> Accretion #1: 24.2%
> Accretion #2: 38.2%
> Accretion #3: 8.6%
> Scott River Accretions: 29.0%

Contributions are based on basin areas. Though USGS-BRD (1995) further reduced accretions to smaller reaches, because accretions are relatively minor during the lower flow periods, this estimate was assumed representative.

Estimation of Total Accretion/Depletion

Because travel time between Iron Gate Dam and Seiad Valley is greater than one day at flow rates less than approximately 4000 cfs, simply completing a water balance using USGS daily gage data was inappropriate.

Flow was typically well below 4000 cfs for the majority of the analysis period. Exceptions were periods in May when flows were transitioning from rainfall events or system operations. Sustained flows in the neighborhood of 4000 cfs were rare. To estimate accretions and depletions for preliminary analysis, when flows were less than 4000 cfs, a water balance was completed using following day data at Seiad Valley. This method applied

well in the summer and fall low flow periods. Spring periods and flow changes experienced poorer results.

This approach results in increasing uncertainty with distance downstream. However, the approach is deemed acceptable because accretions for the most part are minor as illustrated in Figure B.8. A finding supported by model simulations, which showed only moderate sensitivity to accretions and depletions during the late spring through fall periods. Total accretion was apportioned in previously defined percentages and located as shown in Figure B.7. Accretions are calculated daily, and are thus constant for each hour of each day.
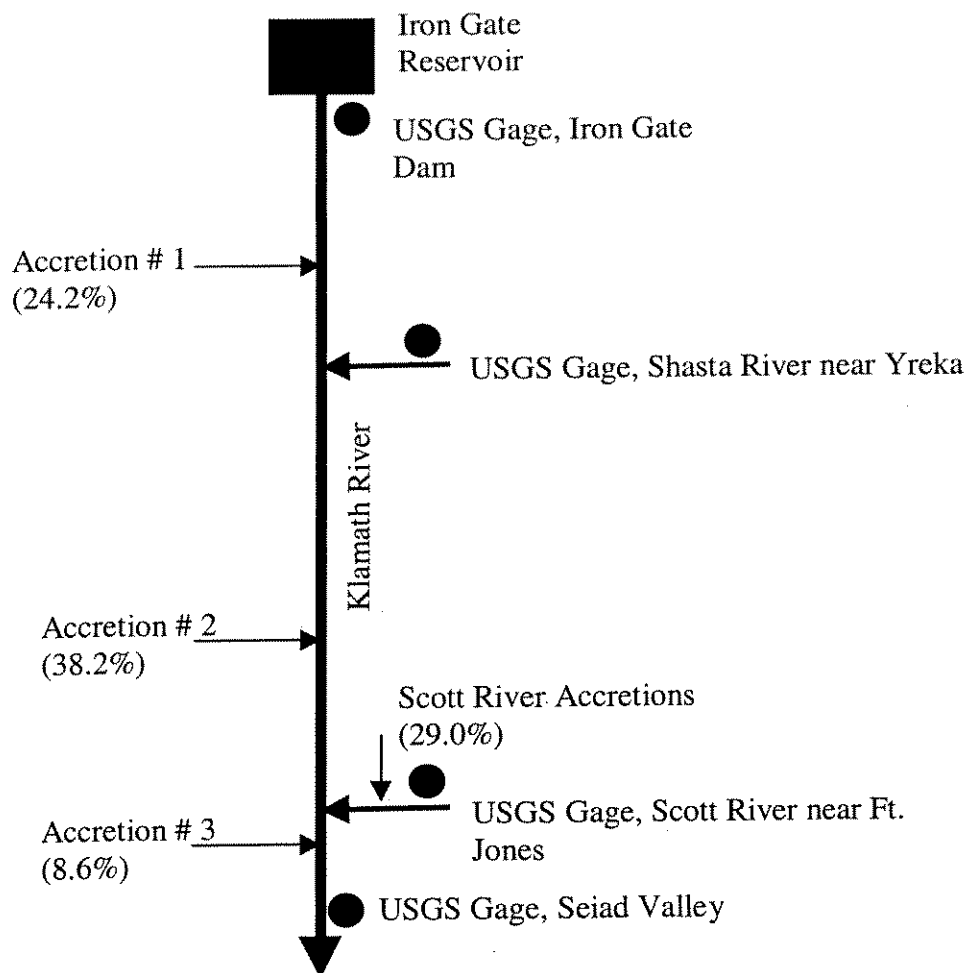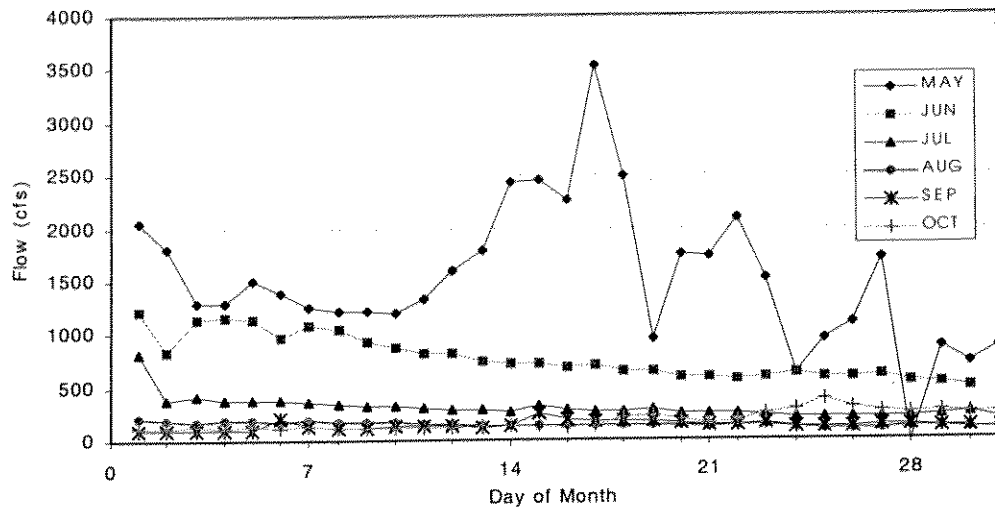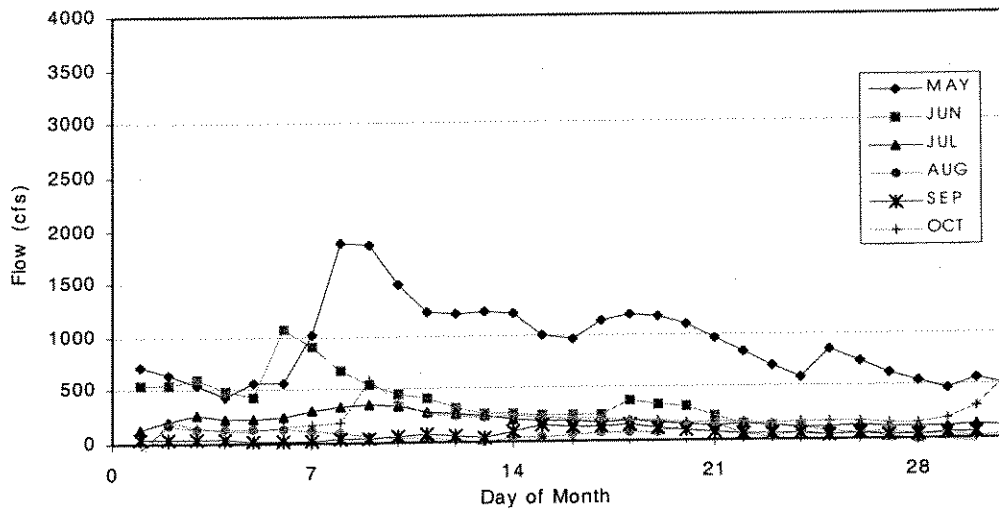

Figure B.7   Klamath River accretions, locations, and relative magnitude

<u>Additional Notes</u>

- The reduction of accretions by basin introduces a measure of uncertainty. Tributary hydrographs are not coincident in the basin and thus seasonal variations are not incorporated into the analysis. For example, during winter period rainfall events, basin areas may (or may not) contribute proportionately to the Klamath River. However, during spring and summer, higher elevation tributaries may sustain base flow due to snowmelt runoff, while lower elevation tributaries run dry. Other basin characteristics such as geographic location, vegetation, slope, aspect, soil type, and land use further define the uniqueness of individual watersheds and their hydrographs.

- The model could be used to explicitly define the travel times and to produce a set of accretion and depletion values for a chosen set of accretion/depletion locations. However, these calculated accretion/depletion values would be unique to the particular hydrologic data set chosen and to the accretion/depletion locations selected. As a result, different accretion depletion definition (either more numerous or at different locations) would result in a different set of accretion/depletion values. If detailed model results are required, such an exercise could be completed. Careful thought as to accretion/depletion locations and their individual contributions should be defined prior to such an exercise.

(a)

(b)

Figure B.8   Klamath River total accretion, (a) 1996, and (b) 1997

B.9.7   Klamath River Water Temperature Boundary Conditions

To provide desired resolution for stream simulation, hourly temperature boundary conditions for the Klamath River simulation model were required at Iron Gate Dam, Shasta River and Scott River. Data were derived from three sources: the UC Davis temperature monitoring study, USGS temperature monitoring below Iron Gate Dam, and Department of Fish and Game in the Shasta River. Accretions and depletions were not assigned water temperature or water quality attributes.

Summarized herein are available data sources for each location and how missing data was synthesized. Also included are plots of water temperature below Iron gate Dam, and for Shasta River and Scott River inflows during 1996 and 1997 (May – Oct).

1996
All gaps less than 12 hours filled with linear interpolation

KR bel IG Dam:
    5/14/96 - 6/18/96: USGS
    5/22/96 - 5/23/96 and 5/30/96 - 6/5/96: linear interpolated 15-17C
    6/19/96 - 10/8/96: UCD
    10/9/96 - 10/31/96: USGS

Shasta R.:
    5/14/96 - 5/20/96: estimated w/ Shasta River at Anderson Grade (4 hr)
    5/21/96 - 6/18/96: DFG
    6/18/96 - 7/15/96: UCD
    7/16/96 - 8/20/96: DFG
    8/20/96 - 10/7/96: UCD
    10/9/96 - 10/21/96: estimate w/ Shasta River at Anderson Grade (6 hr)
    10/21-96-10/31-96: estimated as trend 7.5 to 6.0C

Scott River:
    5/14/96 - 6/15/96: estimated as Shasta - 2.5C (cool snowmelt RO)
    6/16/96 - 7/16/96: estimated as Shasta - 1.5C (cool snowmelt RO)
    6/19/96 - 10/8/96: UCD
    10/8/96 - 10/31/96: estimated as Shasta
    (Scott R is cooler in spring but similar to the Shasta in fall)

1997
KR bel IG Dam:
    5/15/97 - 5/31/97: USGS
    6/1/97 - 10/12/97: UCD
    10/12/97 - 10/17/97: USGS
    10/17/97 - 10/28/97: estimate linear interpolation
    10/29/97 - 10/31/97: USGS

Shasta R.:
    5/15/97 - 5/20/97: Estimated as 5/21 temp repeated
    5/20/97 - 5/31/97 DFG
    6/1/97 - 10/12/97: UCD
    10/12/97 - 10/31/97: DFG

Scott River.:
    5/15/97 - 5/20/97: Estimated as Shasta -2.5C
    5/20/97 - 5/31/97 Estimate as Shasta - 2.5C
    6/1/97 - 10/12/97: UCD
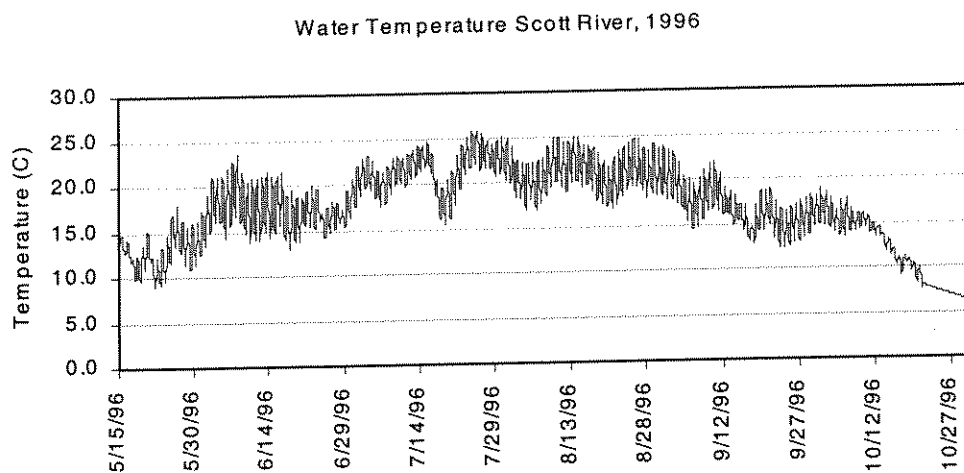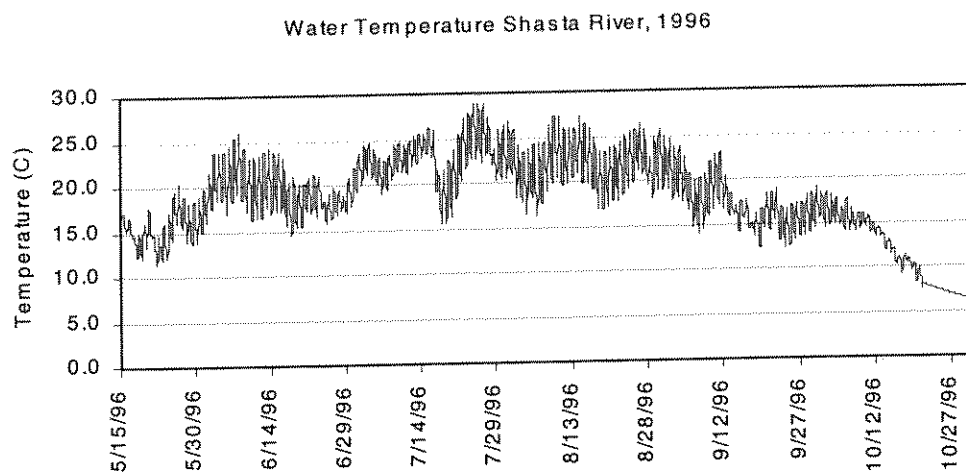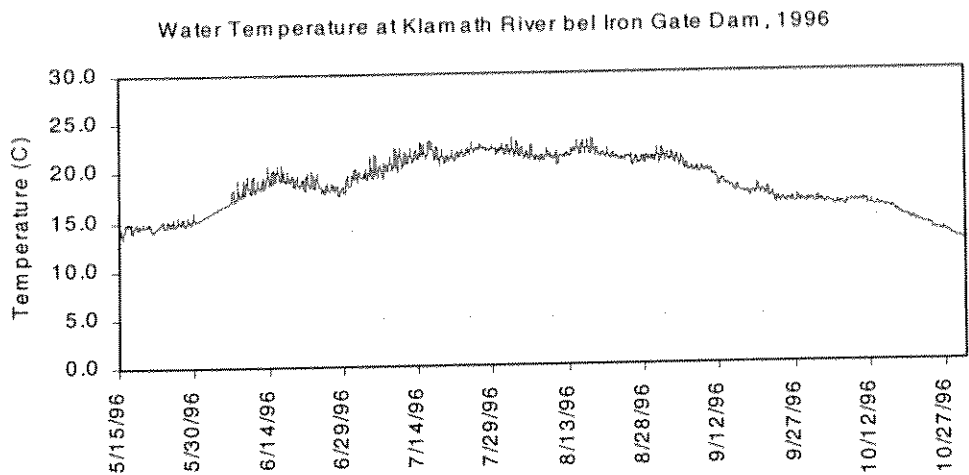   10/12/97 - 10/31/97: Estimate equal to Shasta

Figure B.9 1996 observed hourly water temperature below Iron Gate Dam, and Shasta and Scott River inflows
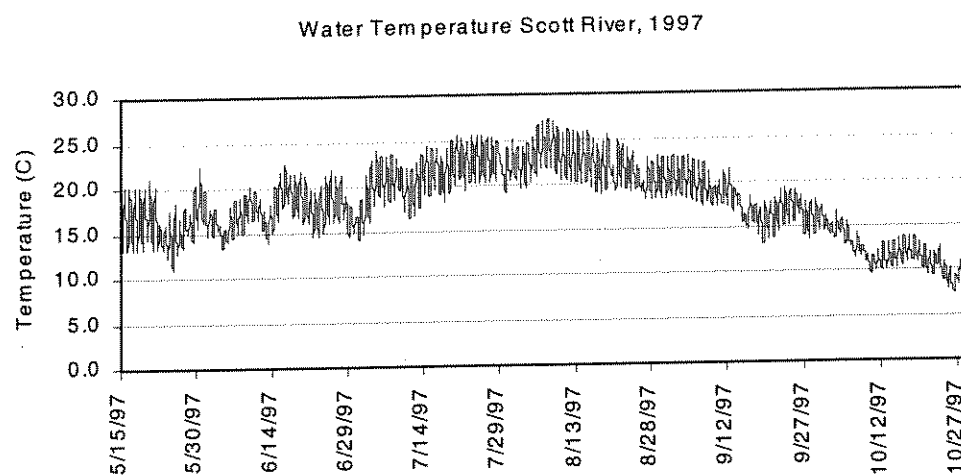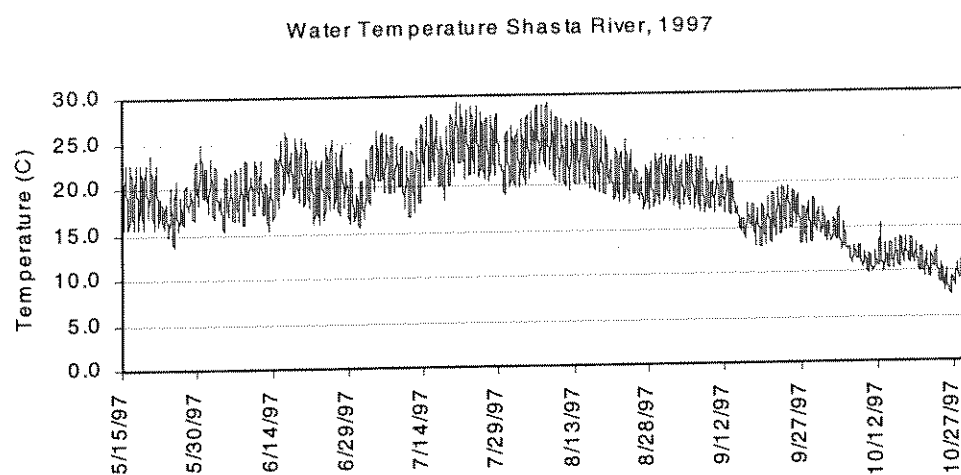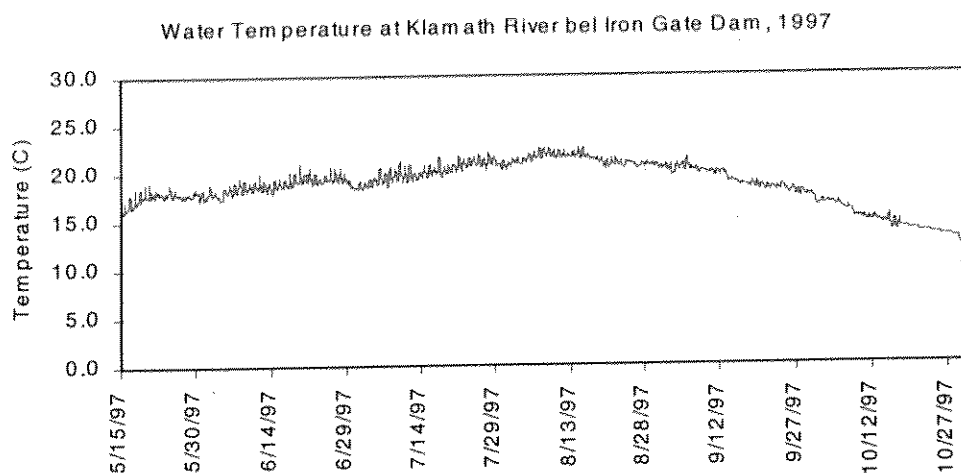
Figure B.10   1997 observed hourly water temperature below Iron Gate Dam, and Shasta and Scott River inflows

B.9.8   Iron Gate Reservoir Profile Temperature Data

Profile water temperatures were recorded in Iron Gate reservoir from May 1996 to November 1997. Loggers were suspended from the log boom, located approximately 1500 feet upstream of the dam. Logger deployment depths are outlined in Table B.13.

Table B.13   Iron Gate temperature logger deployment depths

Logger Number	Deployment Depth (ft)	Initial Deployment Date
IG0	7.0	June 1996
IG1	17.2	May 1996
IG2	39.8	May 1996
IG3	59.3	May 1996
IG4	79.5	May 1996
IG5	99.2	May 1996
IG6	118.0	May 1996

Notes:
Deployment depth measured August 1996
For details of data availability see discussion in text, below

The logger nearest the surface (IG0) was deployed in June 1996, approximately one month after the logger cable was deployed. Review of water temperature data revealed that the deployment depth was unknowingly changed slightly during the June 1996 deployment. Data prior to this date are subject to uncertainty because actual deployment depths were measured after this time. In the fall of 1996 (September 16) loggers IG0 through IG4 were replaced with optical stowaways. On October 22, it was found that these loggers had filled with water and data were irrecoverable. At this time, PPL personnel re-deployed the remaining three devices (IG4, IG5, and IG6) at depths of 17.2, 59.3, and 99.2 feet to provide a range of depths through the winter months. During the November data retrieval visit, a fourth thermistor was added at the 7.0 ft depth. In the spring of 1997 (April), the cable was re-deployed with seven loggers in place. All loggers were Onset Corporation Stowaway® loggers with resolution of ±0.2°C. Recording intervals were set for one hour. Outlined below are the files containing the data and data coverage.

<u>Data Coverage:</u>

1996:
(filled values completed using linear interpolation except and/or estimated values (especially when hourly differences were on the order of the resolution of instrument (±0.2°C); in such cases an adjacent measured value was used).

<u>IGO:</u>
  availability: 6/12/96 - 9/16/96, 11/20/96 - 12/31/96
  filled: 7/17/96 (10:51, 11:51)
  missing: 9/16/96 - 11/20/96
<u>IG1:</u>
  availability: 6/12/96 - 9/16/96, 10/22/96 - 12/31/96
  filled: 7/17/96 (11:12)
  missing: 5/15/96 - 6/12/96, 9/16/96 - 10/22/96
<u>IG2:</u>
  availability: 6/12/96 - 9/16/96
  filled: 7/17/96 (11:06), 7/31/96 (12:06 through 23:01 - used previous day's data)
  missing: 5/15/96 - 6/12/96, 9/16/96 - 12/31/96
<u>IG3:</u>
  availability: 6/12/96 - 9/16/96, 10/22/96 - 12/31/96
  filled: 7/17/96 (11:01)
  missing: 5/15/96 - 6/12/96, 9/16/96 - 10/22/96
<u>IG4:</u>
  availability: 6/12/96 - 10/22/96
  filled: 7/17/96 (11:42), 9/16/96 (13:56)
  missing: 5/15/96 - 6/12/96, 10/22/96 - 12/31/96
<u>IG5</u>
  availability: 5/15/96 - 12/31/96
  filled: 6/12/96 (9:12, 10:12), 7/17/96   (9:54, 10:54), 9/16 (12:45, 13:45), 10/22/96 (12:45, 13:45)
  missing: none
<u>IG6:</u>
  availability: 5/15/96 - 10/22/96
  filled: 6/12/96 (9:08, 10:08), 7/17/96   (9:08, 10:08), 9/16 (13:49)
  missing: 10/22/96 - 12/31/96

1997
(filled values completed using linear interpolation except and/or estimated values (especially when hourly differences were on the order of the resolution of instrument (±0.2°C); in such cases an adjacent measured value was used).

<u>IGO:</u>
  availability: 1/1/97 - 12/1/97
  filled: 4/8/97 (10:00, 11:00, 12:00), 6/19/97 (9:03), 8/18/97 (11:39, 12:39, 13:39, 14:39, 15:43)

missing: 12/1/97 - 12/31/97

IG1:

availability: 1/1/97 - 12/1/97

filled: 4/8/97 (11:03, 12:03), 6/19/97 (9:03), 8/18/97 (11:42, 12:42, 13:42, 14:42, 15:46)

missing: 12/1/97 - 12/31/97

IG2:

availability: 4/8/97 - 12/1/97

filled: 6/19/97 (9:06), 8/18/97 (11:43, 12:43, 13:43, 14:43, 15:49)

missing: 1/1/97 - 4/8/97, 12/1/97 - 12/31/97

IG3:

availability: 1/1/97 - 12/1/97

filled: 4/8/97 (11:10), 6/19/97 (9:03), 8/18/97 (12:46, 13:46, 14:46, 15:50)

missing: 12/1/97 - 12/31/97

IG4:

availability: 4/8/97 - 12/1/97

filled: 6/19/97 (9:00), 8/18/97 (12:49, 13:49, 14:49, 15:50)

missing: 1/1/97 - 4/8/97, 12/1/97 - 12/31/97

IG5:

availability: 1/1/97 - 12/1/97

filled: 4/8/97 (11:59), 6/19/97 (8:59, 9:59), 8/18/97 (12:51, 13:51, 14:51, 15:53)

missing: 12/1/97 - 12/31/97

IG6:

availability: 4/8/97 - 12/1/97

filled: 6/19/97 (8:58), 8/18/97 (12:55, 13:55, 14:55, 15:54)

missing: 1/1/97 - 4/8/97, 12/1/97 - 12/31/97

Table C.1 Empirical temperature correction coefficients for rate constants (adapted from Brown and Barnwell, 1987, Bowie et al, 1985, Thomann 1987)

Table C.2 Parameters values for WQRRS

Table C.3 Parameters values for RMA-11

Table C.1   Empirical temperature correction coefficients for rate constants (adapted from Brown and Barnwell, 1987, Bowie et al, 1985, Thomann 1987)

Rate constant	Symbol	Empirical Constant, Θ	
		Range	Value
BOD Decay		1.03 – 1.075	1.047
BOD Settling	K_3	1.024	1.024
Reaeration	K_2	1.008 – 1.047	1.024
SOD Uptake	K_4	1.02 – 1.13	1.060
Organic Nitrogen Decay	β_3	1.02 – 1.08	1.047
Organic Nitrogen Settling	K_1	1.024	1.024
Ammonia Decay	β_1	1.0548 – 1.0997	1.083
Ammonia Source	σ_3	1.074	1.074
Nitrite Decay	β_2	1.0470 – 1.0689	1.047
Organic Phosphorus Decay	β_4	1.02 – 1.08	1.047
Organic Phosphorus Settling	σ_5	1.024	1.024
Diss. Phosphorus Source	σ_2	1.074	1.074
Algal Growth	μ	1.01 – 1.20	1.047
Algal Respiration	ρ	1.01 – 1.20	1.047
Algal Settling	σ_1	1.047	1.047

87

Table C.2   Parameter values for WQRRS

Parameter Description	Units	Range	Value
Chl a to algal biomass conversion factor	µg-Chl a/mg-A	10 – 100	n/a
Fraction of algal biomass that is nitrogen	mg-N/mg-A	0.07 – 0.09	0.072
Fraction of algal biomass that is phosphorous	mg-P/mg-A	0.01 – 0.02	0.010
Rate O_2 production per unit of algal photosynthesis	mg-O/mg-A	1.4 – 1.8	1.6
Rate O_2 uptake per unit of algae respired	mg-O/mg-A	1.6 – 2.3	1.6
Rate O_2 uptake per unit NH3-N oxidation	mg-O/mg-A	3.0 – 4.0	3.43
Rate O_2 uptake per unit NO2-N oxidation	mg-O/mg-A	1.00 – 1.14	1.14
Rate constant: biological oxidation NH3-N (T adjusted)	day^{-1}	0.05 – 0.30	0.30
Rate constant: biological oxidation NO2-N (T adjusted)	day^{-1}	0.20 – 0.50	0.50
Rate constant: hydrolysis Org N to NH3-N (T adjusted)	day^{-1}	0.02 – 0.40	n/a
Rate constant: transformation Org P to P-D (T adjusted)	day^{-1}	0.01 – 0.70	n/a
Rate constant: removal PO_4 by adhesion to sediment	day^{-1}	0.00 – 0.10	n/a
Non-algal portion of light extinction coefficient	m^{-1}	Variable	n/a
Linear algal self-shading coefficient	1/m/mg/l	0.15 – 0.2	0.15
Non-linear algal self shading coefficient	m^{-1} (µg-Chl a/L)$^{-2/3}$	0.05	n/a
Maximum specific growth rate	day^{-1}	1.0 – 2.0	1.35
Local respiration rate of algae (T adjusted)	day^{-1}	0.05 – 0.20	0.20
Settling rate of algae (T adjusted)	m/day	0.00 – 2.00	0.10
Benthos source rate of P-D (T adjusted)	mg-P/m^2-day	Variable	n/a
Benthos source rate of NH3-N (T adjusted)	mg-NH^3-N/m^2-day	Variable	n/a
Org N settling rate constant (T adjusted)	m/day	0.002 – 0.200	n/a
Org P settling rate constant (T adjusted)	m/day	0.002 – 0.200	n/a
Empirical temperature constant for each reaction coefficient	(see Table C.1)		
Deoxygenation rate constant: BOD (T adjusted)	day^{-1}	0.10 – 0.30	0.5
Reaeration rate constant (T adjusted)	day^{-1}	0.0 – 100	calc
BOD settling rate constant (T adjusted)*	m/day	0.00 – 0.75	n/a
First order nitrification inhibition coefficient	L/mg	0.6 – 0.7	n/a
Half saturation coefficient for light	Kcal/m^2-s	0.002 – 0.006	0.0023
Michaelis-Menton half saturation constant: NH$_3$+N0$_3^-$ as N	mg-N/L	0.04 – 0.10	0.10
Michaelis-Menton half saturation constant: phosphate	mg-P/L	0.01 – 0.05	0.01
Preference factor for NH3-N		0.0 – 1.0	n/a
Detritus decay rate	day^{-1}	0.005 – 0.05	0.05
Detritus settling rate	m/day	0.0 – 2.0	0.7
Organic sediment decay rate	day^{-1}	0.001 – 0.01	0.005

Notes:
* term incorporates loss rate due to flocculation converted to an effective settling rate

Abbreviations:

Chl a – chlorophyll a
Org N – organic nitrogen
NO3-N – nitrate nitrogen
PO_4 – orthophosphate
T adjusted – temperature adjusted

O_2 – oxygen
NH3-N – ammonia nitrogen
P-D – dissolved phosphorous
BOD – biochemical oxygen demand

Table C.3   Parameters values for RMA-11

Parameter Description	Units	Range	Value
Chl a to algal biomass conversion factor	µg-Chl a/mg-A	10 – 100	67
Fraction of algal biomass that is nitrogen	mg-N/mg-A	0.07 – 0.09	0.072
Fraction of algal biomass that is phosphorous	mg-P/mg-A	0.01 – 0.02	0.010
Rate O_2 production per unit of algal photosynthesis	mg-O/mg-A	1.4 – 1.8	1.6
Rate O_2 uptake per unit of algae respired	mg-O/mg-A	1.6 – 2.3	1.6
Rate O_2 uptake per unit NH3-N oxidation	mg-O/mg-A	3.0 – 4.0	3.43
Rate O_2 uptake per unit NO2-N oxidation	mg-O/mg-A	1.00 – 1.14	1.14
Rate constant: biological oxidation NH3-N (T adjusted)	day^{-1}	0.1 – 1.0	0.30
Rate constant: biological oxidation NO2-N (T adjusted)	day^{-1}	0.2 – 1.0	0.50
Rate constant: hydrolysis Org N to NH3-N (T adjusted)	day^{-1}	0.02 – 0.40	0.30
Rate constant: transf. Org P to P-D (T adjusted)	day^{-1}	0.01 – 0.70	0.30
Rate constant: removal PO4 by adhesion to sediment	day^{-1}	0.00 – 0.10	0.0
Non-algal portion of light extinction coefficient	m^{-1}	Variable	1.0
Linear algal self-shading coefficient	m^{-1} (µg-Chl a/L)$^{-1}$	0.006 - 0.060	0.0
Non-linear algal self shading coefficient	m^{-1} (µg-Chl a/L)$^{-2/3}$	0.05	0.0
Maximum specific growth rate (bed algae)	day^{-1}	1.0 – 3.0	2.0
Local respiration rate of algae (T adjusted, bed algae)	day^{-1}	0.05 – 0.50	1.0
Settling rate of algae (T adjusted)	m/day	0.15 – 1.82	n/a
Benthos source rate of P-D (T adjusted)	mg-P/m^2-day	Variable	0.0
Benthos source rate of NH3-N (T adjusted)	mg-NH^3-N/m^2-day	Variable	0.0
Org N settling rate constant (T adjusted)	m/day	0.002 – 0.200	0.0
Org P settling rate constant (T adjusted)	m/day	0.002 – 0.200	0.0
Empirical constant for each reaction coefficient	(see Table C.1)		
Deoxygenation rate constant: BOD (T adjusted)	day^{-1}	0.02 – 3.5	0.30
Reaeration rate constant (T adjusted)	day^{-1}	0.0 – 100	Calc
BOD settling rate constant (T adjusted)*	m/day	0.00 – 0.75	0.0
First order nitrification inhibition coefficient	L/mg	0.6 – 0.7	0.0
Half saturation coefficient for light	KJ/m^2-s	0.0037 – 0.0185	0.01
Michaelis-Menton half saturation constant: nitrogen	mg-N/L	0.01 – 0.30	0.01
Michaelis-Menton half saturation constant: phosphorous	mg-P/L	0.001 – 0.050	0.001
Preference factor for NH3-N	•	0.0 – 1.0	0.60
Detritus decay rate	day^{-1}	0.005 – 0.05	n/a
Detritus settling rate	m/day	0.0 – 2.0	n/a
Organic sediment decay rate	day^{-1}	0.001 – 0.01	n/a

Notes:
* term incorporates loss rate due to flocculation converted to an effective settling rate

Abbreviations:

Chl a – chlorophyll a

Org N – organic nitrogen

NO3-N – nitrate nitrogen

PO4 – orthophosphate

T adjusted – temperature adjusted

O_2 – oxygen

NH3-N – ammonia nitrogen

P-D – dissolved phosphorous

BOD – biochemical oxygen demand

This appendix includes calibration and validation data. Summary statistics, regression statistics, as well as figures of simulated hourly and daily average water temperature versus field measured values are included. Outlined below is a list of tables and figures included in the appendix. Calibration and validation locations are coincident. Temperature data are presented in °C only.

Table D.1 Aggregate hourly and daily error statistics: calibration period, June – September 1996

Statistic	Period	Location (all values °C)		
		Klamath River at Cottonwood Creek	Klamath River bel. Shasta River	Klamath River bel. Scott River
Bias	Hourly	0.154	0.122	-0.292
	Daily	0.156	0.117	-0.279
MAE	Hourly	0.312	0.472	0.496
	Daily	0.189	0.284	0.471
RMSE	Hourly	0.397	0.593	0.689
	Daily	0.222	0.336	0.561
Standard Deviation	Hourly	0.358	0.529	0.492
	Daily	0.154	0.238	0.309

Table D.2 Aggregate hourly and daily error statistics: validation period, June – September 1997

Statistic	Period	Location (all values °C)		
		Klamath River at Cottonwood Creek	Klamath River bel. Shasta River	Klamath River bel. Scott River
Bias	Hourly	0.236	0.152	-0.030
	Daily	0.236	0.151	-0.048
MAE	Hourly	0.417	0.442	0.415
	Daily	0.248	0.302	0.266
RMSE	Hourly	0.520	0.542	0.512
	Daily	0.278	0.347	0.329
Standard Deviation	Hourly	0.460	0.462	0.480
	Daily	0.140	0.226	0.261

92

Table D.3 Hourly simulated (dependent) versus field water temperature regression statistics: calibration period, July – September 1996

Statistic	Month	Location (all values °C)		
		Klamath River at Cottonwood Creek	Klamath River bel. Shasta River	Klamath River bel. Scott River
r^2 (adj)	June[1]	0.838	0.801	0.744
	July[2]	0.960	0.920	0.936
	August	0.967	0.958	0.886
	September	0.977	0.961	0.942
α (Coeff/Std Err)	June[1]	-0.871 / 0.513	1.30 / 0.522	1.68 / 0.603
	July[2]	1.07 / 0.232	-2.78 / 0.274	0.687 / 0.218
	August	0.560 / 0.139	-1.68 / 0.182	-0.131 / 0.295
	September	-1.48 / 0.116	-1.69 / 0.151	-0.544 / 0.174
β (Coeff/Std Err)	June[1]	1.04 / 0.027	0.931 / 0.027	0.957 / 0.033
	July[2]	0.948 / 0.010	1.13 / 0.012	0.993 / 0.010
	August	0.968 / 0.006	1.07 / 0.008	1.01 / 0.013
	September	1.07 / 0.006	1.07 / 0.008	1.01 / 0.009

[1] Partial month: system-wide (6/19-6/30)

[2] Partial month: Klamath River near Cottonwood Creek (7/17-7/31)

Table D.4 Daily simulated (dependent) versus field water temperature regression statistics: calibration period, July – September 1996

Statistic	Month	Location (all values °C)		
		Klamath River at Cottonwood Creek	Klamath River bel. Shasta River	Klamath River bel. Scott River
r^2 (adj)	June[1]	0.684	0.622	0.694
	July[2]	0.964	0.908	0.944
	August	0.932	0.929	0.870
	September	0.990	0.979	0.967
α (Coeff/Std Err)	June[1]	1.58 / 3.48	3.29 / 3.59	5.77 / 2.61
	July[2]	0.046 / 1.16	0.288 / 1.28	1.98 / 0.946
	August	-1.40 / 1.16	-4.51 / 1.36	-3.19 / 1.83
	September	-1.26 / 0.381	-1.70 / 0.549	0.234 / 0.626
β (Coeff/Std Err)	June[1]	0.910 / 0.183	0.827 / 0.189	0.732 / 0.144
	July[2]	0.994 / 0.051	0.994 / 0.058	0.936 / 0.042
	August	1.06 / 0.053	1.20 / 0.062	1.14 / 0.082
	September	1.05 / 0.020	1.07 / 0.029	0.973 / 0.034

[1] Partial month: system-wide (6/19-6/30)

[2] Partial month: Klamath River near Cottonwood Creek (7/17-7/31)

Table D.5 Hourly sample statistics at three validation locations: validation period, June – September 1997

Statistic	Month	Location (all values °C)		
		Klamath River at Cottonwood Creek	Klamath River bel. Shasta River	Klamath River bel. Scott River
Sample Mean	June	19.22	19.50	19.37
	July	20.96	21.58	22.73
	August	21.55	21.76	22.52
	September	19.01	18.75	18.89
Maximum Underprediction	June	1.62	1.11	0.89
	July	1.38	1.19	0.63
	August	1.45	1.50	0.14
	September	1.09	1.55	1.06
Maximum Overprediction	June	-1.85	-1.81	-1.42
	July	-1.67	-1.41	-1.40
	August	-1.20	-1.02	-1.14
	September	-1.51	-0.91	-1.48

Table D.6 Hourly error statistics at three validation locations, including season averages: validation period, June – September 1997

Statistic	Month	Location (all values °C)		
		Klamath River at Cottonwood Creek	Klamath River bel. Shasta River	Klamath River bel. Scott River
BIAS	June	0.235	-0.065	-0.048
	July	0.192	-0.100	-0.255
	August	0.320	0.292	0.026
	September	0.196	0.482	0.155
	Average:	0.236	0.152	-0.030
MAE	June	0.379	0.412	0.379
	July	0.468	0.385	0.453
	August	0.429	0.433	0.413
	September	0.391	0.537	0.415
	Average:	0.417	0.442	0.415
RMSE	June	0.481	0.524	0.469
	July	0.580	0.463	0.547
	August	0.543	0.539	0.519
	September	0.475	0.642	0.513
	Average:	0.520	0.542	0.512
Standard Dev.	June	0.419	0.520	0.466
	July	0.548	0.450	0.448
	August	0.439	0.452	0.518
	September	0.433	0.424	0.489
	Average:	0.460	0.462	0.480

94

Table D.7 Daily sample statistics at three validation locations: validation period, June – September 1997

Statistic	Month	Location (all values °C)		
		Klamath River at Cottonwood Creek	Klamath River bel. Shasta River	Klamath River bel. Scott River
Sample Mean	June	19.22	19.50	19.37
	July	20.96	21.58	22.73
	August	21.55	21.76	22.52
	September	19.01	18.75	18.89
Maximum Underprediction				
	June	0.67	0.45	0.63
	July	0.44	0.36	0.14
	August	0.61	0.63	1.06
	September	0.42	1.00	0.72
Maximum Overprediction				
	June	-0.14	-0.73	-0.70
	July	0.00	-0.43	-0.61
	August	0.10	-0.20	-0.53
	September	-0.13	0.03	-0.43

Table D.8 Daily error statistics at three validation locations, including season averages: validation period, June – September 1997

Statistic	Month	Location (all values °C)		
		Klamath River at Cottonwood Creek	Klamath River bel. Shasta River	Klamath River bel. Scott River
BIAS	June	0.235	-0.065	-0.048
	July	0.192	-0.104	-0.326
	August	0.320	0.292	0.026
	September	0.196	0.482	0.155
	Average:	0.236	0.151	-0.048
MAE	June	0.256	0.192	0.256
	July	0.192	0.222	0.280
	August	0.320	0.312	0.239
	September	0.225	0.482	0.291
	Average:	0.248	0.302	0.266
RMSE	June	0.301	0.255	0.307
	July	0.223	0.244	0.345
	August	0.335	0.352	0.314
	September	0.252	0.539	0.351
	Average:	0.278	0.347	0.329
Standard Dev.	June	0.189	0.247	0.303
	July	0.114	0.221	0.113
	August	0.099	0.196	0.313
	September	0.158	0.241	0.315
	Average:	0.140	0.226	0.261

95

Table D.9   Hourly simulated (dependent) versus field water temperature regression statistics: validation period, July – September 1997

Statistic	Month	Location (all values °C)		
		Klamath River at Cottonwood Creek	Klamath River bel. Shasta River	Klamath River bel. Scott River
r^2 (adj)	June[1]	0.918	0.921	0.939
	July[2]	0.961	0.973	0.936
	August	0.959	0.957	0.914
	September	0.968	0.962	0.938
α (Coeff/Std Err)	June[1]	-1.18 / 1.05	-2.15 / 1.11	-2.41 / 1.13
	July[2]	-4.46 / 1.20	-2.72 / 1.13	0.459 / 0.991
	August	-4.60 / 1.20	-3.03 / 1.12	-1.18 / 1.05
	September	-0.429 / 1.012	-2.49 / 1.10	-1.37 / 1.06
β (Coeff/Std Err)	June[1]	0.228 / 0.012	0.237 / 0.012	0.208 / 0.011
	July[2]	0.190 / 0.009	0.151 / 0.007	0.219 / 0.010
	August	0.198 / 0.009	0.193 / 0.009	0.267 / 0.012
	September	0.188 / 0.010	0.158 / 0.008	0.194 / 0.010

Table D.10   Daily simulated (dependent) versus field water temperature regression statistics: validation period, July – September 1997

Statistic	Month	Location (all values °C)		
		Klamath River at Cottonwood Creek	Klamath River bel. Shasta River	Klamath River bel. Scott River
r^2 (adj)	June[1]	0.903	0.883	0.943
	July[2]	0.976	0.949	0.969
	August	0.976	0.965	0.934
	September	0.984	0.971	0.959
α (Coeff/Std Err)	June[1]	-1.28 / 1.05	-1.49 / 1.08	-1.49 / 1.08
	July[2]	-0.408 / 1.01	-2.02 / 1.10	1.21 / 0.958
	August	-0.868 / 1.03	-4.08 / 1.17	-1.76 / 1.17
	September	1.12 / 0.931	-2.00 / 1.08	-1.26 / 1.06
β (Coeff/Std Err)	June[1]	1.27 / 0.065	1.41 / 0.073	0.953 / 0.050
	July[2]	0.601 / 0.029	1.02 / 0.048	0.725 / 0.032
	August	0.645 / 0.029	0.901 / 0.041	1.08 / 0.052
	September	0.425 / 0.022	0.673 / 0.035	0.790 / 0.042

Figure D.1 Klamath River near Cottonwood Creek, July-Sept 1996
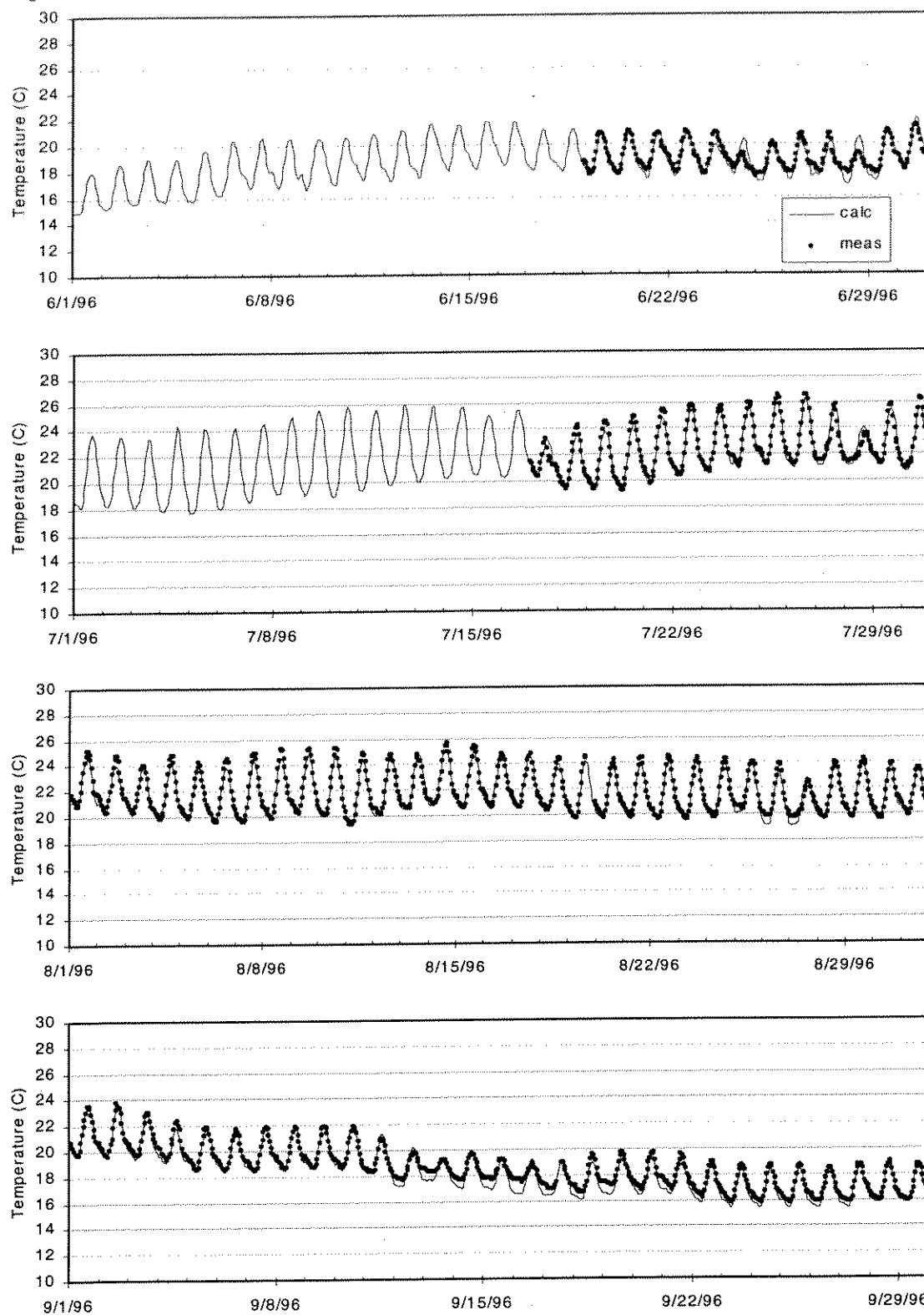
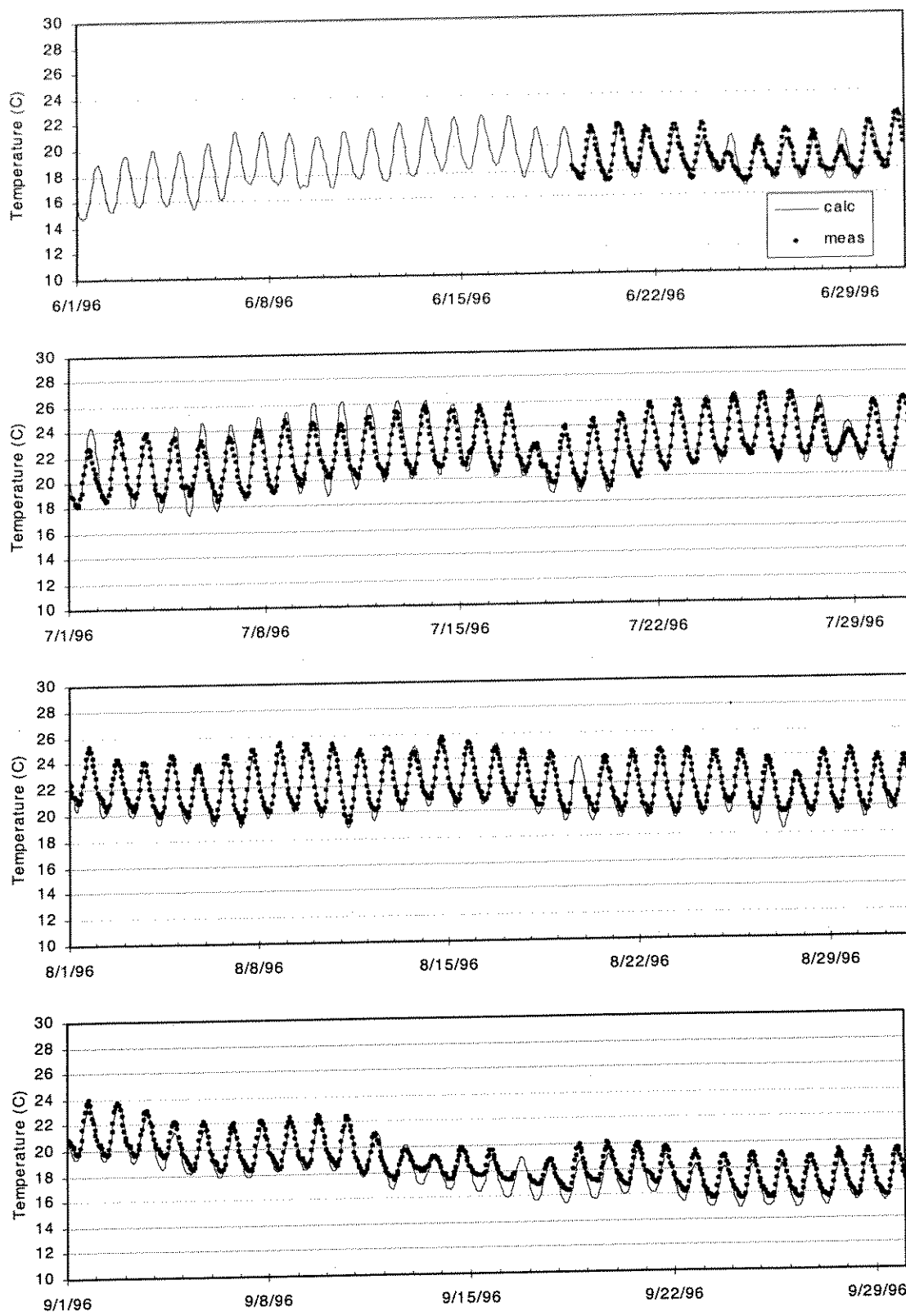Figure D.2 Klamath River below Shasta River, June - Sept, 1996

Figure D.3 Klamath River below Scott River, June - Sept. 1996

Figure D.4 Klamath River near Cottonwood Creek, Daily - June-Sept. 1996

Figure D.5 Klamath River below Shasta River, Daily - June-Sept. 1996

Figure D.6 Klamath River below Scott River, Daily - June-Sept. 1996

Figure D.7 Klamath River near Cottonwood Creek, Hourly - June-Sept. 1997

Figure D.8 Klamath River below Shasta River, Hourly - June-Sept. 1997

104

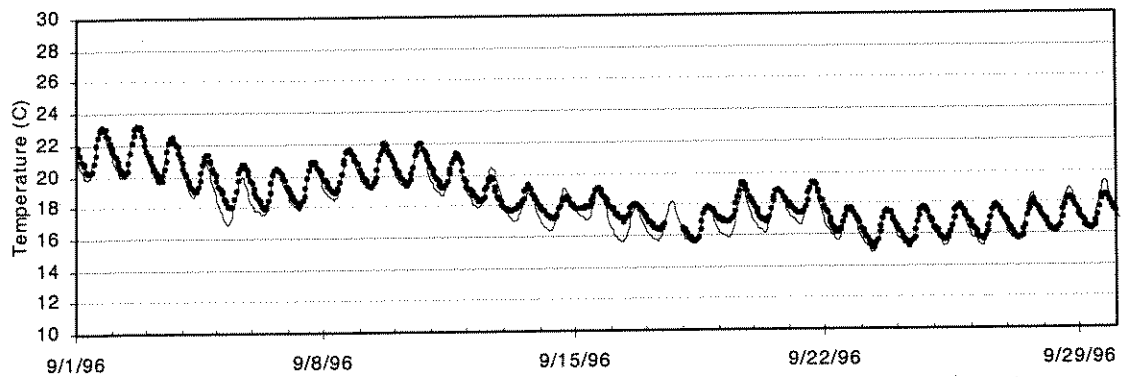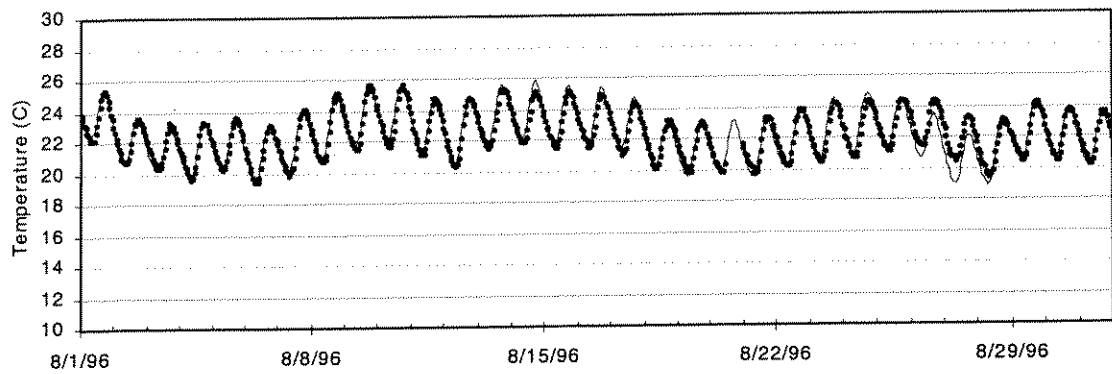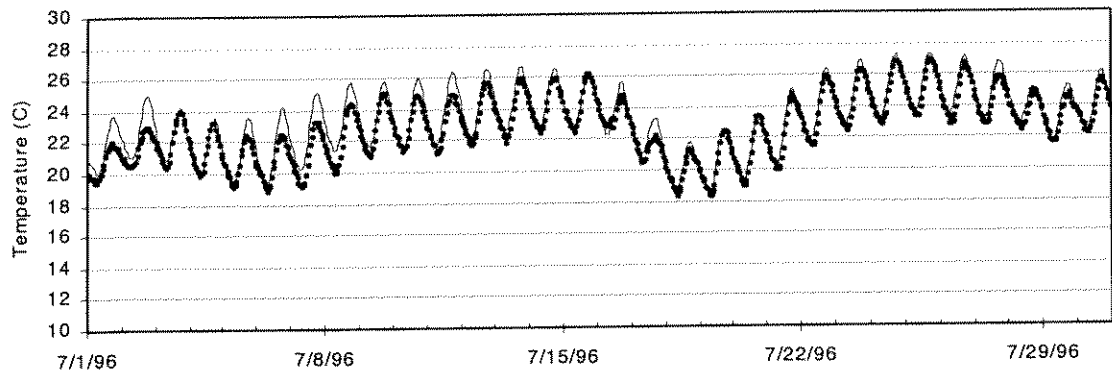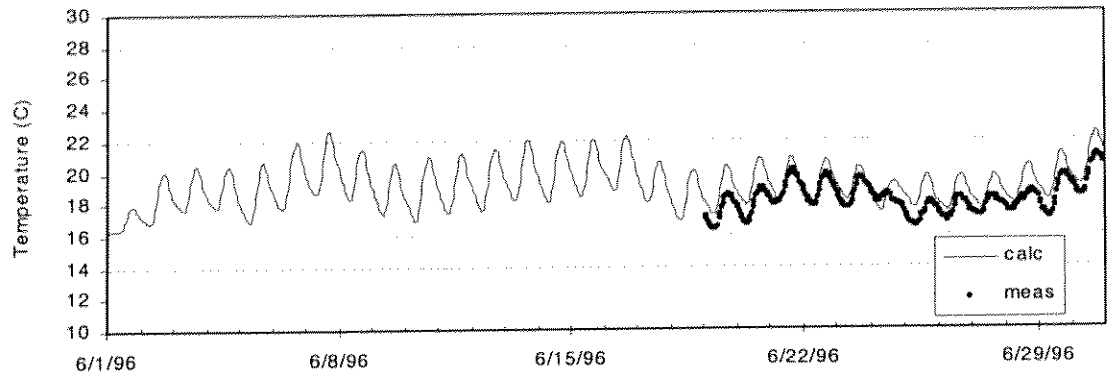Figure D.9 Klamath River below Scott River, Hourly - June-Sept. 1997

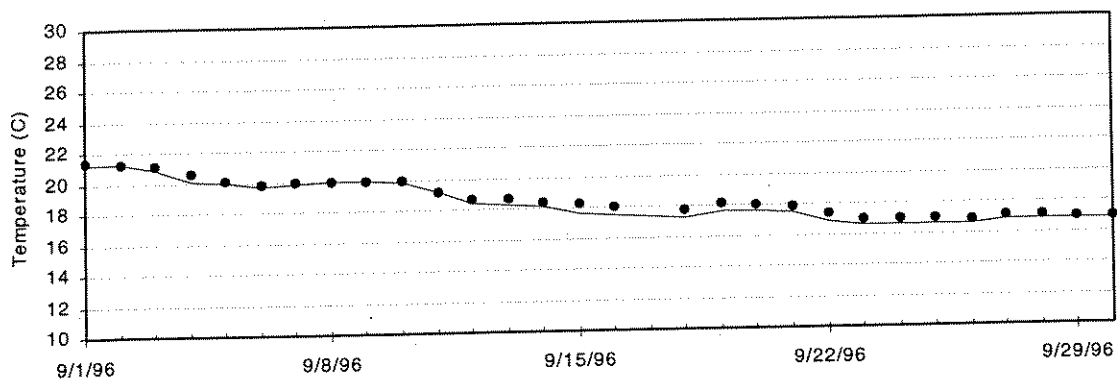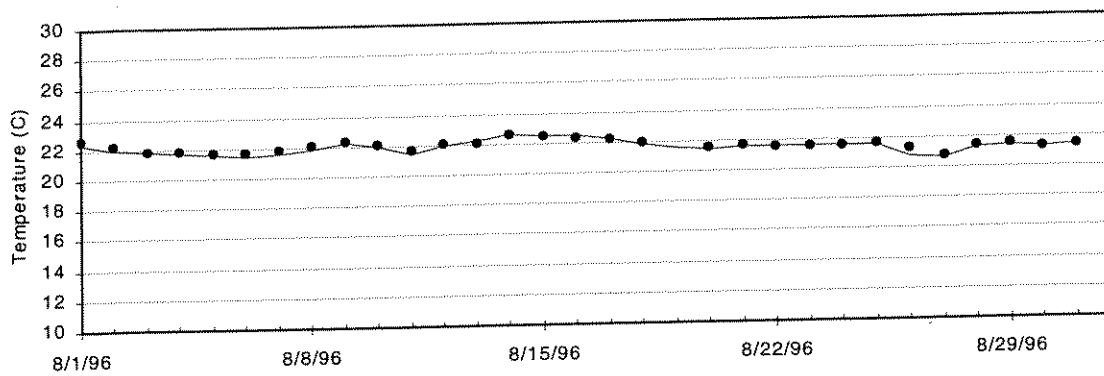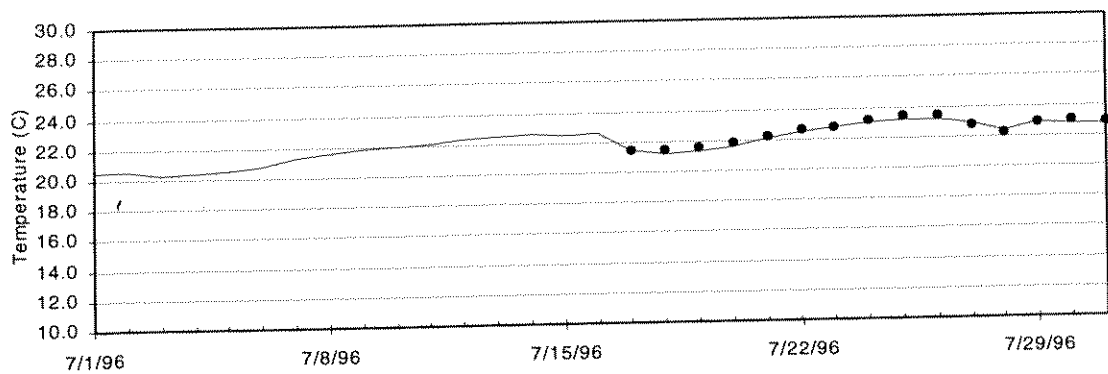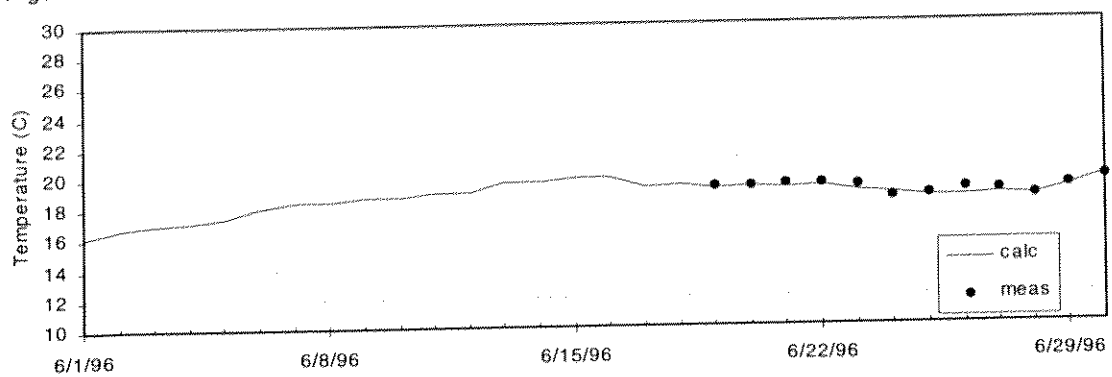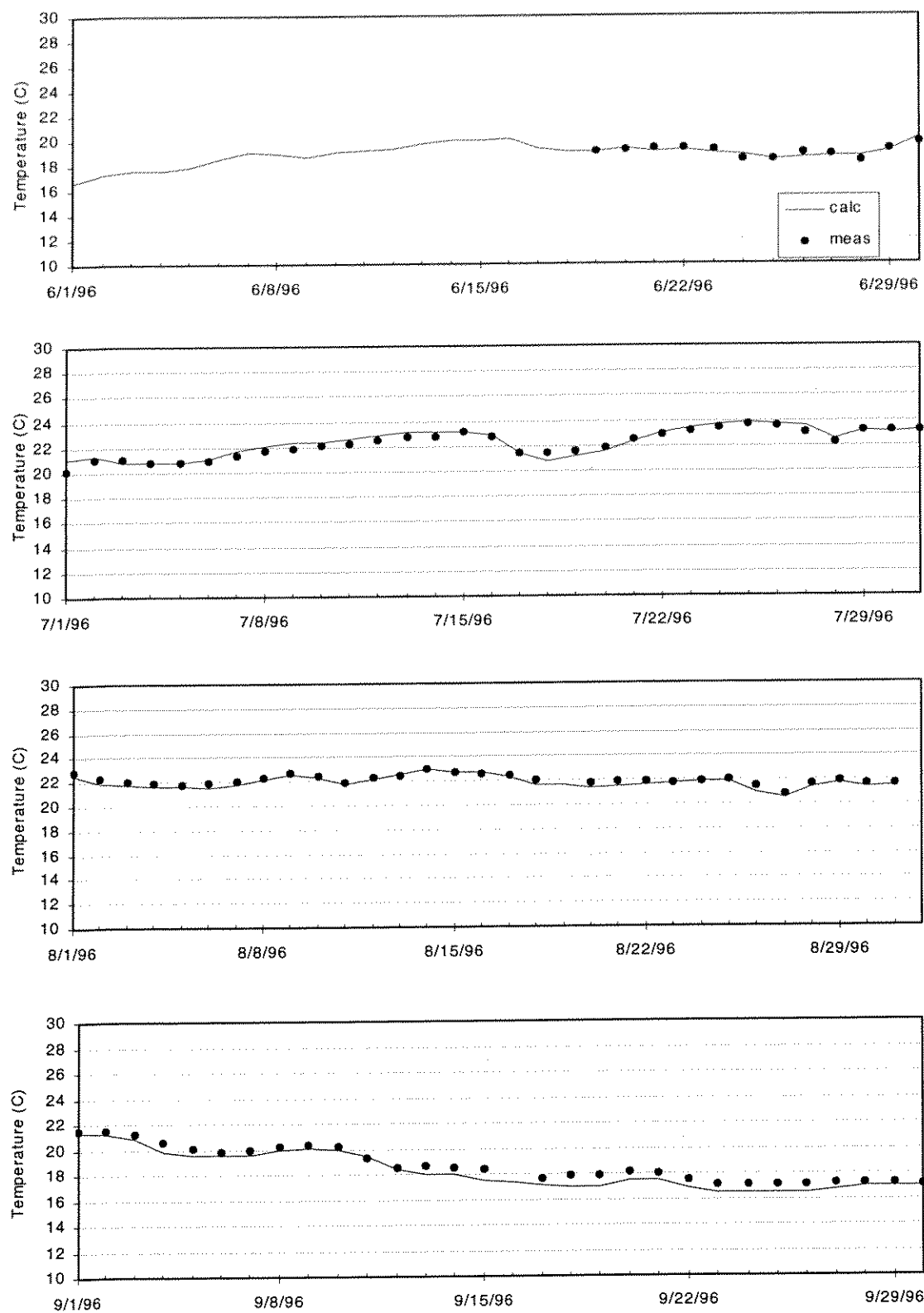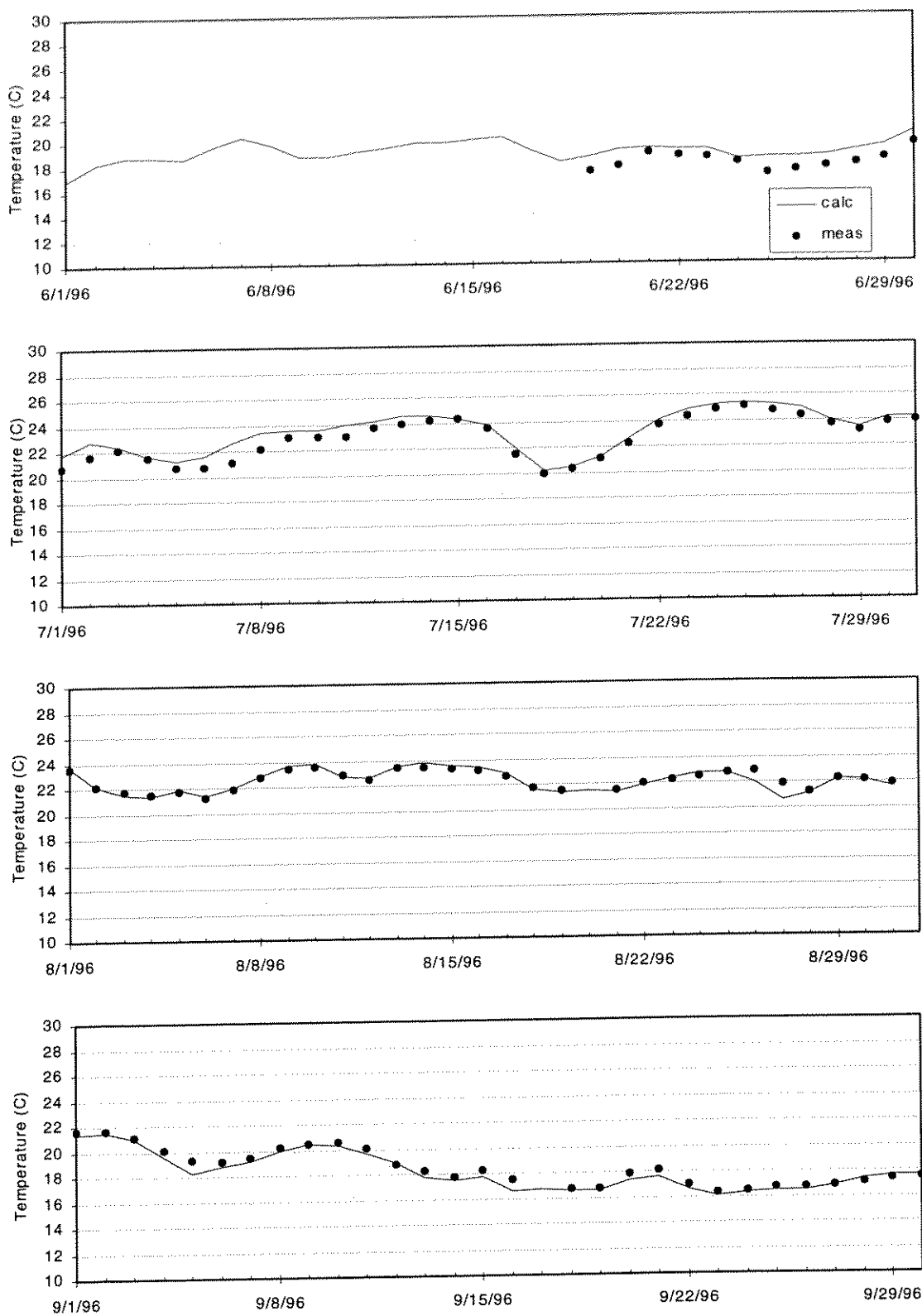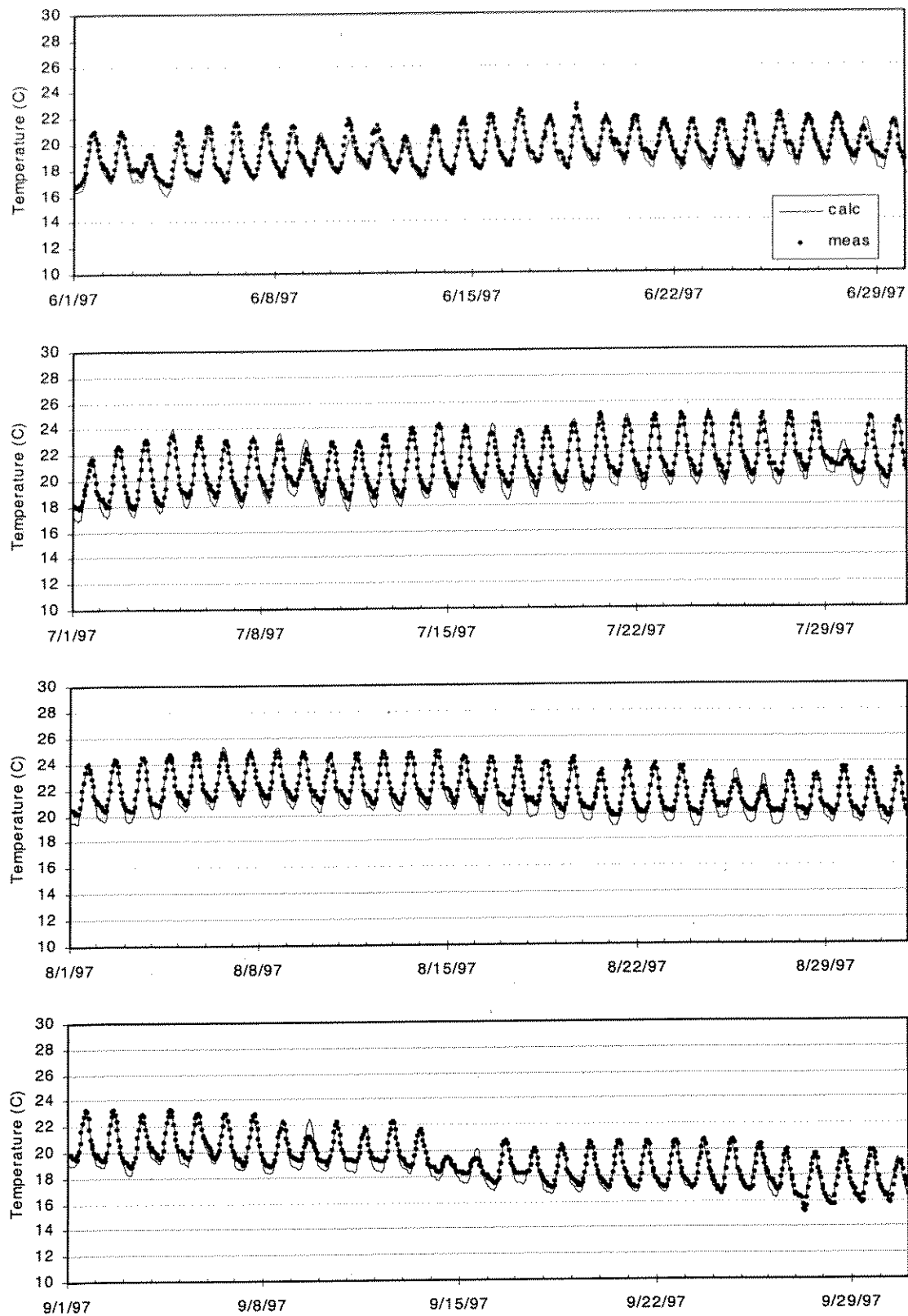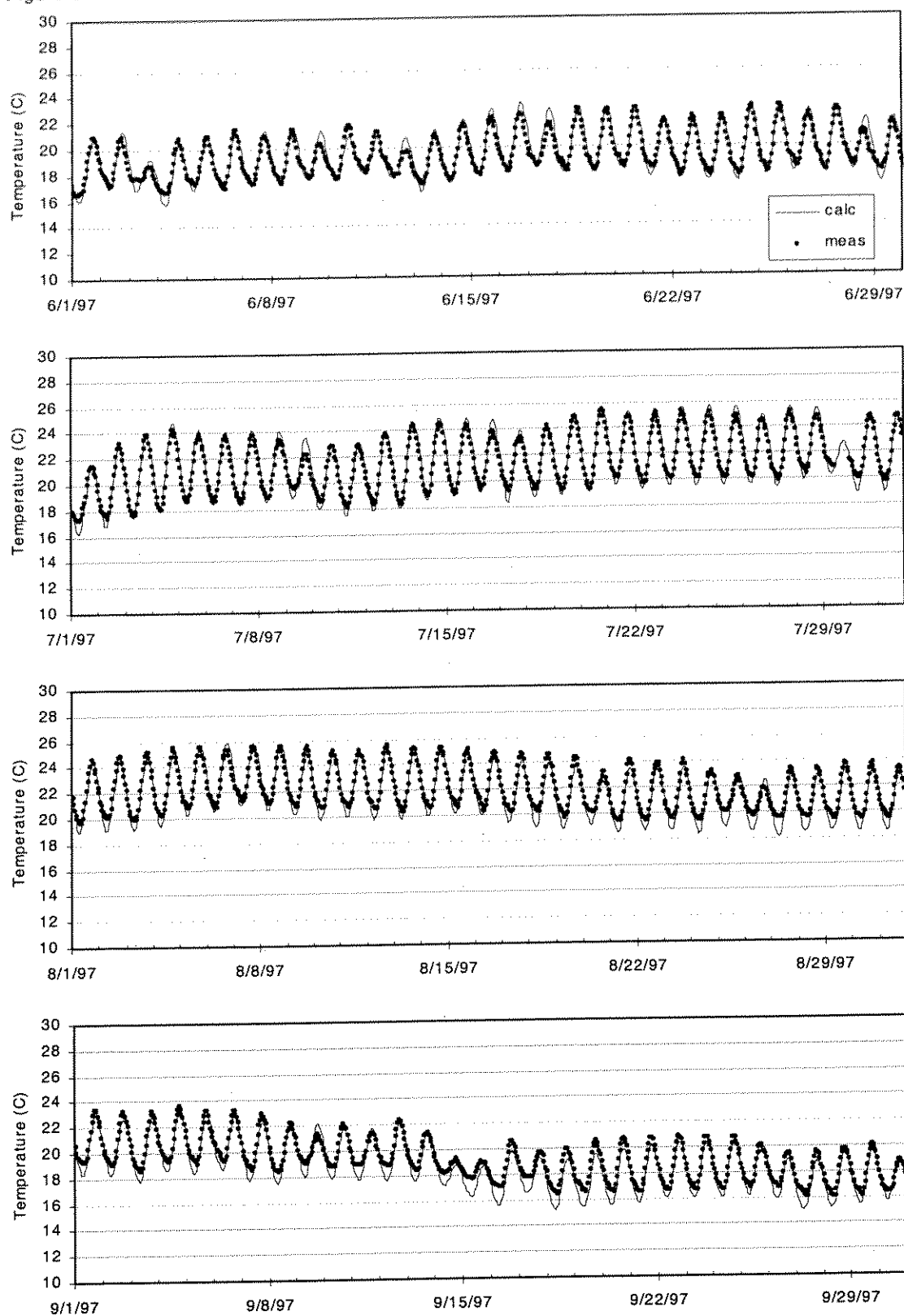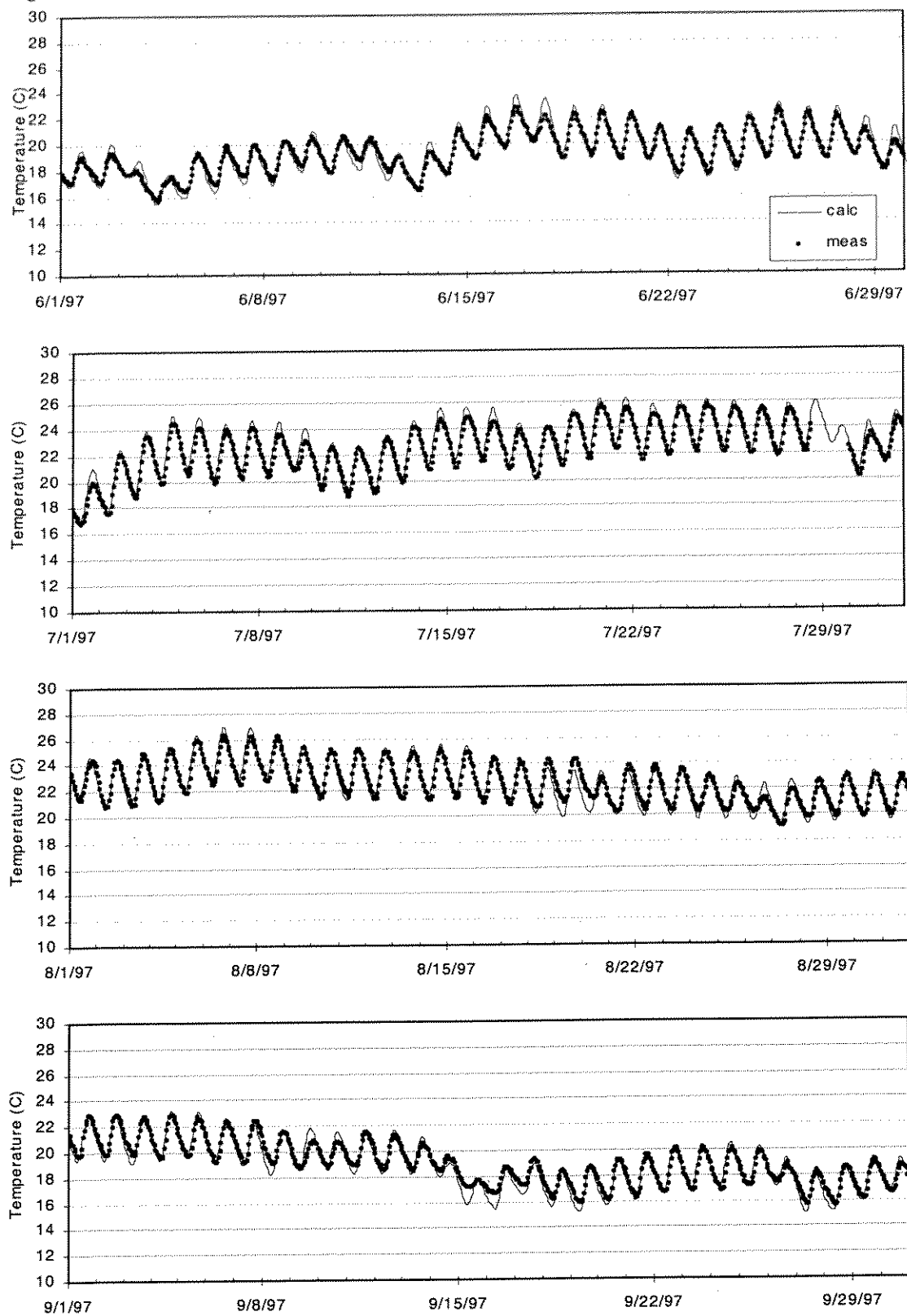Figure D.10 Klamath River near Cottonwood Creek, Daily - June-Sept. 1997
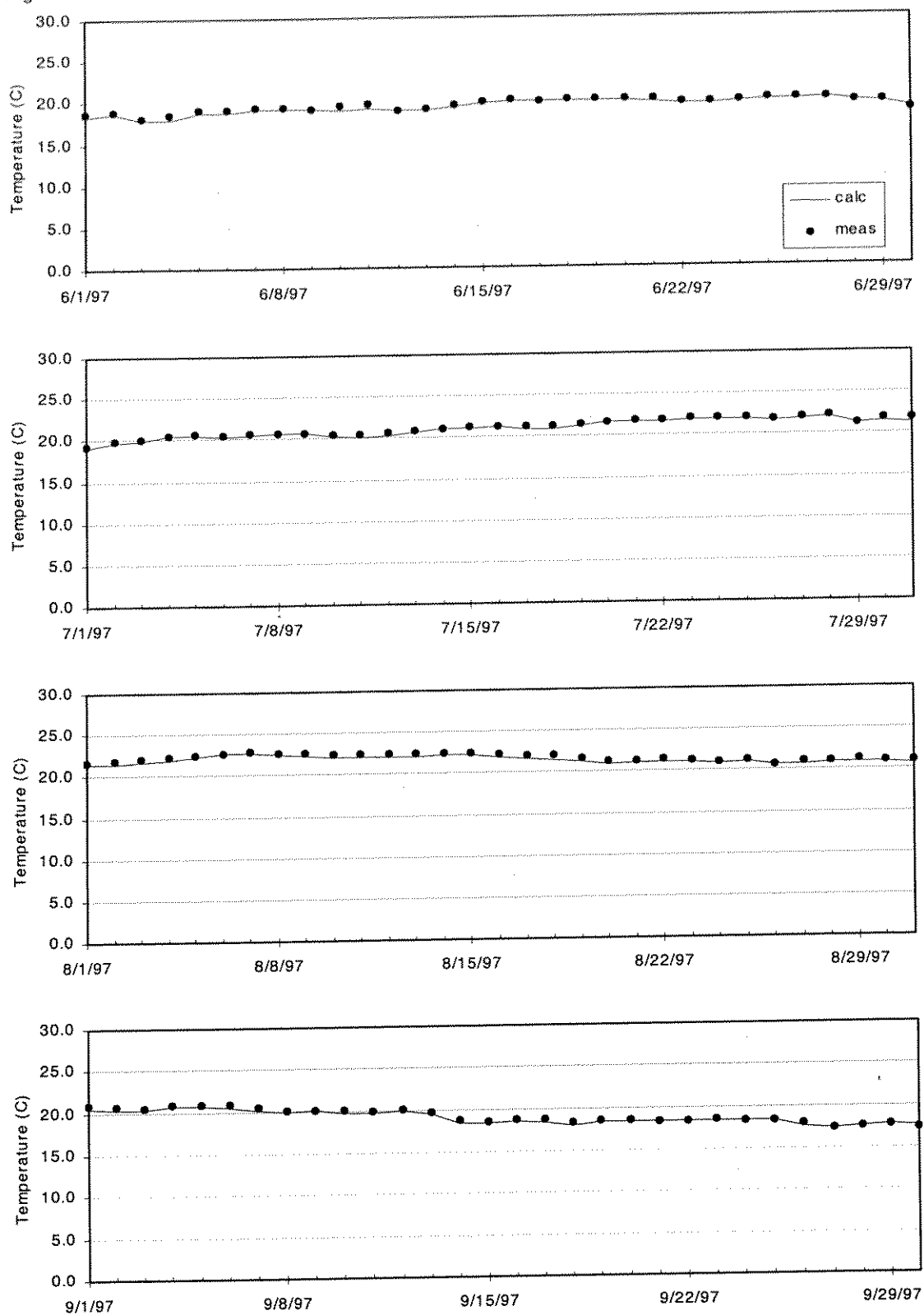
Figure D.11 Klamath River below Shasta River, Daily - June-Sept. 1997
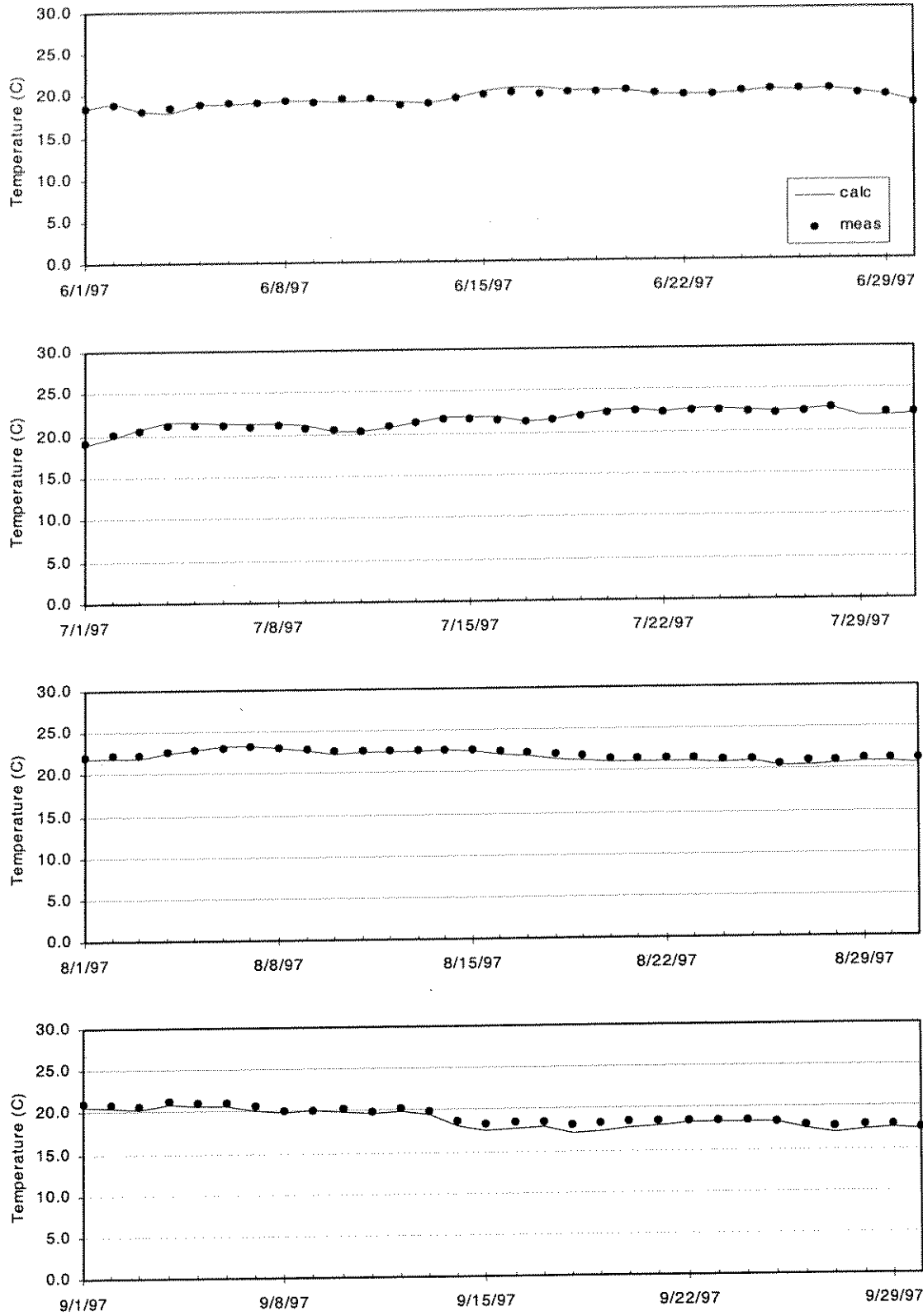
Figure D.12 Klamath River below Scott River, Daily - June-Sept. 1997
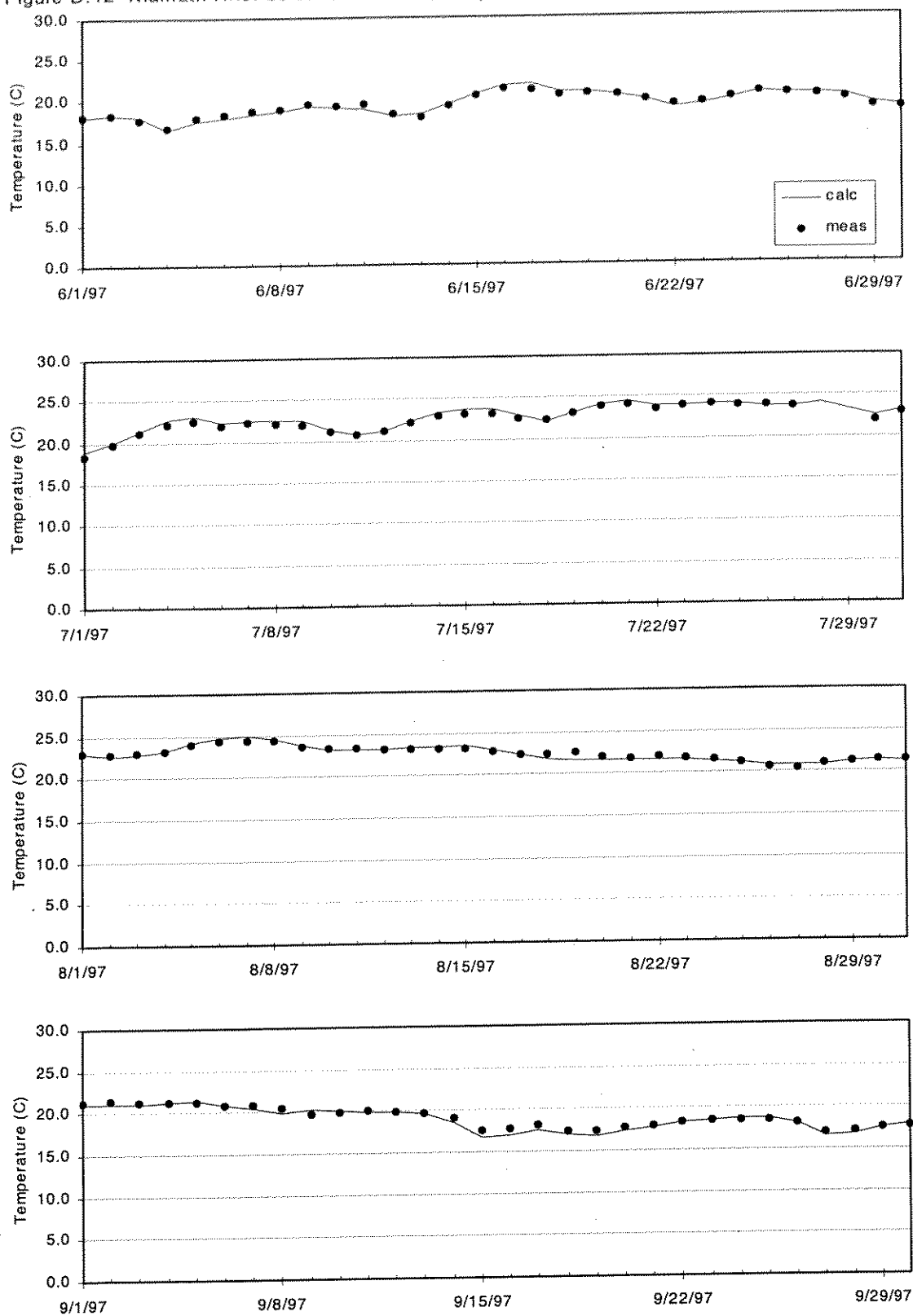
In the original formulation of RMA-11, algae was modeled as a state variable, that is, it was included in the solution scheme of the advection-diffusion equation like other dissolved constituents. This formulation proved unacceptable in the highly advective, attached algae dominated system of the Klamath River. To accommodate attached algae, the RMA-11 code was modified. The authors provided the general attached algae logic to Dr. Ian King, the creator of the code. Dr. Ian King, with minor modification implemented and tested these modifications. Further testing was carried out by the authors.

In the modified version of the code, phytoplankton remains an available option, but attached algae can be modeled as well. Attached algae are assumed to be associated with the benthos. Such a condition may not hold in systems where attached algae occupy substantial portions of the water column, but for streams with sufficient velocity, small streams, streams with forest canopy, or turbid streams, the assumption represents a valid condition. Herein, "attached algae" or "bed algae" shall refer to the loose assemblages of periphyton (films) and macrophytes (as attached submerged flora).

Bed algae interacts with water column constituents in several ways. Bed algae can uptake inorganic nutrients (ammonia, nitrate, and phosphorous) for growth. Logic is included for ammonia uptake preference. Dissolved oxygen may be produced during photosynthesis (growth) and/or consumed during respiration. Finally, reductions in bed algae concentrations due to respiration result in additions of water column nutrients to organic nutrients (organic nitrogen and organic phosphorous). The inter-relationships between bed algae and water column constituents are outlined in Figure E.1

E.1   Bed Algae Growth

Attached algae growth is a function of bed algal concentration, growth and respiration rate as expressed in equation E.1.

$$\partial BA/\partial t = BA[BAG-BAR] \qquad (E.1)$$

Where
BA   = bed algal concentration (g/m^2)
BAG = bed algal growth rate [1.0-3.0/d]
BAR = bed algal respiration rate [0.05-1.0/d]
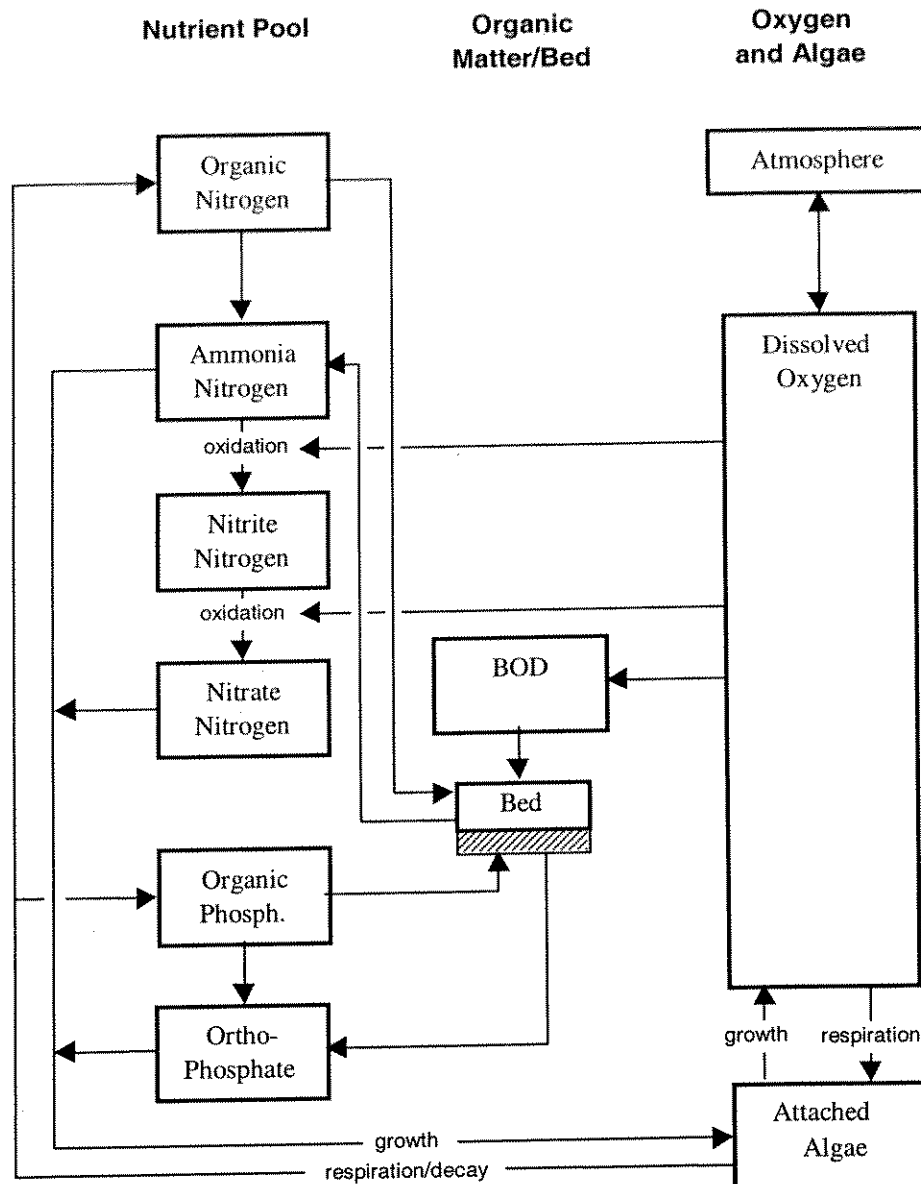
Figure E.1   Inter-relationships between attached algae and water column constituents

Growth rate can be assumed to be the product of benthal macrophyte density, local light intensity, and nutrient availability. Thus,

$$BAG = \mu_{max} \, (FL) \, \min(FN, FP) \tag{E.2}$$

Where

μ_{max} = maximum bed algae growth rate (1/d)
FL   = light limitation factor
FN   = nitrogen limitation factor
FP   = phosphorous limitation factor

110

Both algal growth and respiration are subject to temperature correction via the Van't Hoff – Arrhenius relationship as per equation 4.2, reproduced herein as equation E.3.

$$A_t = A_s(\Theta)^{(T_w - T_s)} \qquad\qquad (E.3)$$

Where
A_t = coefficient value at non-standard water temperature
A_s = coefficient value at standard water temperature of 20°C (68.0°F)
Θ = empirical constant, unique for each reaction coefficient
T_w = non-standard water temperature
T_s = standard water temperature is 20°C (68.0°F)

Further, limits on growth and respiration may be included as model input to restrict these parameters under elevated temperature conditions, i.e., when equation E.3 results in an increased rate reaction.

Attached algae occupy the bed and are measured in mass per area (g/m^2). Growth per unit length of channel is assumed uniformly distributed along an effective width equivalent to cross sectional area divided by depth. Thus, for a rectangular cross section, effective width would correspond to bottom or top width. For trapezoidal channels effective width would exceed bottom width, but be less than top width. The assumption implicit in this representation is that for wide shallow systems, channel sides present a negligible area of the system. For example, the Klamath River averages over 150 feet in width (45 m) and roughly 6 feet (2 m) in depth and is modeled with 1:1 side slopes. The difference between actual wetted perimeter and effective width is 6 feet, or slightly less than a 4 percent underestimation.

E.2   Dissolved Oxygen

Dissolved oxygen is produced by algae and consumed in plant respiration and mortality. Consumption of oxygen takes the form of gross respiration (respiration plus mortality). Gross respiration assumes that all oxygen is used immediate for energy by living organisms. Thus net production to dissolved oxygen by attached algae can be represented as

$$DO_{production} = [(\alpha_3)\,(BAG) - (\alpha_4)\,(BAR)] \qquad\qquad (E.4)$$

Where
α_3 = Stoichiometric ratio for oxygen to biomass for oxygen production by algae and macrophytes (mg-O/mg-A).

111

α_4 = Stoichiometric ratio for oxygen to biomass for oxygen production by algae and macrophytes (mg-O/mg-A).

Net production due to bed algae may be positive or negative, and is added to other sources and sinks of dissolved oxygen for numerical solution of the governing equation set.

E.3   Organic Nitrogen

The rate of organic nitrogen accumulation resulting from bed algae decay is proportional to the rate of decay of the algae. Nitrogen content of phytoplankon is roughly 7 to 10 percent by weight, whereas the nitrogen content of macrophytes is typically 2 to 4 percent (Environmental Lab 1995). All bed algal nitrogen is assumed to be released as organic nitrogen upon decay of the cell (respiration). Contribution (gain) of organic nitrogen to the water column due to bed algae respiration is

$$OrgN_{contribution} = \alpha_1*(BA)(BAR) \tag{E.5}$$

Where
α_1 = stoichiometric ratio nitrogen to biomass in bed algae: 0.02-0.04 mg-N/mg-BA

Contributions by bed algae are added to other sources and sinks of organic nitrogen for numerical solution of the governing equation set.

E.4   Ammonia (NH$_3$) and Nitrate (NO$_3^-$)

Nutrient uptake by attached aquatic can be represented in several ways. First, attached plants can be assumed to use roots for nutrient uptake from the stream bed, second roots can be assumed merely for attachment to the bed and all nutrients are derived from the water column, and finally, a combination of the two could be applied. Although different species utilize different methods, the second approach is applied herein: that attached algae draw their nutrient requirement from the water column.

Further, attached algae are assumed to follow a similar potential for ammonia preference as phytoplankton. Thus, the rate of ammonia and nitrate uptake (loss to the water column) by bed algae is

$$NH3_{uptake} = F_1*[\alpha_1 (BA)(BAG)] \tag{E.6}$$

112

Where

F_1 = fraction of algal nitrogen uptake from ammonia pool based on preference factor.

α_1 = stoichiometric ratio nitrogen to biomass in bed algae: 0.02-0.04 mg-N/mg-A

and

$$NO3_{uptake} = (1 - F_1) * [\alpha_1 (BA)(BAG)] \qquad (E.7)$$

Contributions by bed algae are added to other sources and sinks of ammonia and nitrate for numerical solution of the governing equation set. Nitrite required no modification.

E.5   Organic Phosphorous (OrgP)

The rate of organic phosphorous accumulation resulting from bed algae decay is proportional to the rate of decay of the algae. Phosphorous content of bed algae is roughly 1 percent by weight (Environmental Lab 1995). All bed algae phosphorous is assumed to be released as organic phosphrous upon decay of the cell (respiration). Contribution (gain) of organic phosphrous to the water column due to bed algae respiration is

$$OrgP_{contribution} = \alpha_2 * (BA)(BAR) \qquad (E.8)$$

Where

α_2 = stoichiometric ratio phosphorous to biomass in bed algae: 0.01mg-P/mg-BA

Contributions by bed algae are added to other sources and sinks of organic phosphorous for numerical solution of the governing equation set.

E.6   Orthophosphate (PO_4^{3-})

Similar to inorganic nitrogen species, phosphate is also utilized by bed algae. Thus, the rate of orthophosphate uptake (loss to the water column) by bed algae is

$$PO4_{uptake} = \alpha_2 (BA)(BAG) \qquad (E.9)$$

where parameters are the same as those outlined above.

Outlined herein are general model operation and temperature calibration parameters for WQRRS. Associated water quality parameters used in model calibration are included in Appendix C. Model parameters include allocation of inflow, withdrawal option, representation of effective diffusion, atmospheric turbidity, and water solar radiation fraction. Details of this discussion are summarized from the WQRRS User's Manual. For other model parameters the reader is referred to the input files and WQRRA user's manual.

F.1   General Model Operation Parameters

Though there are several parameters which control the computer program flow logic, only four of principal interest will be covered herein: allocation of inflow, withdrawal option, effective diffusion method, heat exchange method, atmospheric turbidity, and water solar radiation fraction. The reader is referred to the input files (Appendix J) and the WQRRS user's guide for additional details and details on other model parameters.

F.1.1   Allocation of Inflow

The allocation of inflow is based on the assumption that inflow water will seek a level of similar density within the reservoir ("entry level"). The switch controlling allocation of inflow is provided on card PHYS4, variable RLEN. RLEN is effective reservoir length. For stratified conditions, a positive value of RLEN distributes inflows about the entry level with a uniform velocity distribution, and a negative value distributes water in proportion to element size down to the entry level. This latter method is applicable to reservoirs where the inflow is located several miles from the deepest part of the reservoir and was selected for this application.

F.1.2   Withdrawal Option

WQRRS contains two options for allocating reservoir withdrawal through an outlet gate to individual layers; Debler-Craya and WES. Results of Tsaras (1980) indicate that for deep, well-stratified reservoirs differences of less than 1°C (1.8°F) are typical between the two methods. The WES withdrawal technique was employed for this application (JOB3, variable IWES = 0)

F.1.3   Effective Diffusion

Besides advection, effective diffusion is the other mechanism to transport heat and mass between the elements. Two methods are available to calculate effective diffusion: the stability method and wind method. Because Iron Gate Reservoir is strongly stratified and wind mixing does not dominate the reservoir, the stability method was selected (PHYS3A versus PHYS3B).

F.1.4   Water Surface Heat Exchange

Water surface heat exchange can be addressed using a heat budget or equilibrium temperature method in WQRRS. The heat budget method was used herein (JOB7, variable $IEQF = 0$)

F.1.5   Atmospheric Turbidity

Atmospheric turbidity is used in the determination of the amount of scattering of incoming short wave radiation. Data was available for estimating atmospheric turbidity and clear, unpolluted atmosphere assumed (PHYS1, variable $TURB = 2.0$). Though certain periods of the year may exhibit these conditions, other periods (e.g. summer) may exhibit increased turbidity. Currently WQRRS allows the user to enter a single value for the analysis period. Further definition of this parameter should be investigated.

F.1.6   Solar Radiation Absorption

Fraction of solar radiation absorbed with depth is addressed through two variables: XQPCT and XQDEP. XQPCT is the fraction of solar radiation absorbed in depth XQDEP. Variables XQPCT and XQDEP were set at 32.5% (0.325) and 1.0 meter, respectively (PHYS2).

F.2   Model Calibration Parameters

Calibration parameters outlined herein include secchi depth, water column stability and diffusion parameters, and evaporation coefficients. The final set of calibration parameters is included in Table F.1. For further description of model parameters the reader is referred to USACOE – HEC (1986).

F.2.1   Secchi Depth

The secchi depth is a measure of light transparency for distribution of light energy with depth in the reservoir. If algal dynamics are included in the simulation the secchi depth should be reflect non-bloom conditions since the program adjusts the light extinction coefficient to account for decreased light penetration as a function of the increased algal concentrations. Thus, during calibration, it may be necessary to adjust secchi depth to influence the location of the thermocline (USACOE-HEC 1986). Secchi depths at Iron Gate Reservoir ranged from approximately 0.8m (2.6 ft) to 2.7 meters (8.9 ft) during the 1996 and 1997 field seasons. Secchi depth varied spatially in the reservoir as well. At NCRWQCB station 5 near the reservoir inflow (below Copco Dam), secchi depths exceeded 3 meters (9.8 ft) on rare occasions. These measurements were assumed not to represent the transparency of the main body of the reservoir.

F.2.2   Water Column Stability and Diffusion Coefficients

There are two mechanisms used in WQRRS to transport heat energy vertically through the reservoir system: advection and diffusion. Advection is the physical transport fluid particles (flow) in the vertical direction. Effective diffusion consists of molecular and turbulent diffusion and convective mixing. Effective diffusion is modeled in WQRRS using water column stability considerations based on thermally driven water density gradients. This method assumes that stronger thermal stratification (more stable) results in less mixing in the vertical direction. A relationship between effective diffusion and water column stability (WRE, 1969) defines several calibration coefficients incorporated in WQRRS. Specifically,

- Critical water column stability, GSWH
- Minimum water column stability, GMIN
- Diffusion coefficient for water quality stability less than GSWH, A1
- Constant to compute density based gradient diffusion coefficients, A3

The minimum water column stability (GMIN) is the density gradient above which mixing of the water column will occur. A positive value will cause the thermocline to form more quickly and delay destratification. The value may range from zero up to 0.001 $mg/m^2/meter$ (USACOE-HEC 1986). Although the constant A3, used to compute density based gradient diffusion coefficients, was varied to determine system sensitivity, the value was ultimately set to –0.7, the suggested calibration value as per USACOE-HEC (1986). The critical water column stability (GSWH) and diffusion coefficient (A1) were varied through a wide range of

116

values prior to arriving at final values of 1.0×10^{-8} kg/m^3 m^{-1} and 1.0×10^{-3} kg/m^3 m^{-1}, respectively. During calibration it was found that there was not necessarily a unique set of parameters to achieve a particular calibration objective.

F.2.3   Evaporation Coefficients

In the model WQRRS evaporation is represented by

$$E = (a+bu)(e_s-e_a) \hspace{4cm} (F.1)$$

Where E is evaporation, a and b are coefficients, u is wind speed, and e_s and e_a are saturation and air vapor pressure, respectively. WQRRS, though supplied with data in English units, converts all data to metric units. Thus wind speed is in meters per second (m s^{-1}), vapor pressures are in millibars (mb), and coefficients a and b have units of m s^{-1} mb^{-1} and mb^{-1}, respectively.

The original format of WQRRS requires that the user specify a single annual set of values for coefficients a and b. However, seasonal differences in these parameters occur due to atmospheric boundary layer thickness and stability. To accommodate seasonal differences, the original WQRRS code was modified to accept a two sets of evaporation coefficients: one for late fall, winter and early spring (October – May), and one set for the late spring, summer, and early fall (June – September). Due to the short period of analysis (mid-May through October) a single set of evaporation coefficients were employed.

[The new evaporation parameters are included in the WQRRS input file under Physical Card 1. Fields 3 and 4, which originally represented annual coefficient values, represent October 1 through May 31 a and b values. Fields 8 and 9 have been added to this card to accept evaporation coefficient values aa and bb, representing the months June through September.]

F.2.4   Final Calibration Parameters

The final calibration parameters are summarized in Table F.1

117

Table F.1   WQRRS calibration parameters and values for Iron Gate Reservoir

Parameter	Value
Evaporation coefficient; October – May, a (m mb^{-1} s^{-1})*	2.0e-9
Evaporation coefficient; October – May, b (mb^{-1})*	2.0e-9
Evaporation coefficient; June - September, aa (m mb^{-1} s^{-1})*	2.0e-9
Evaporation coefficient; June - September, bb (mb^{-1})*	2.0e-9
Critical water column stability, GSWH (kg/m^3 m^{-1})*	1.0e-8
Minimum water column stability, GMIN (kg/m^3 m^{-1})*	0.0
Diffusion coefficient for water quality stability < GSWH, A1 (m^2 s^{-1})*	1.0e-3
Constant to compute density based gradient diffusion coeff., A3 (-)	-0.7
Secchi depth (ft)	5.0

*WQRRS converts all data to metric units

Longitudinal mixing is an important process in one-dimensional river systems. Longitudinal mixing is parameterized by a dispersion coefficient, D_x and can be estimated as

$$D_x = (0.011u^2w^2)/(du^*) \qquad (G.1)$$

Where:
D_x = longitudinal dispersion (m^2/s)
u = average velocity (m/s)
w = river width (m)
d = river depth (m)
u^* = shear velocity (m/s)
$u^* = (gR_hS)^{1/2}$
Where:
g = gravitational acceleration (m/s^2)
R_h = hydraulic radius (cross sectional area divided by wetted perimeter) (m)
S = hydraulic gradient (m/m)

The result is approximate because it is based on an estimate of transverse mixing (ε_t = 0.6du*) and does not explicitly reflect all system processes (e.g., dead zones) (Fischer et al 1979).

A longitudinal dispersion coefficient for the Klamath River, calculated based on mean hydraulic values in the study reach, was found to be 317 m^2/s (Table G.1). Table G.2 presents similar river system data, calculated, and observed longitudinal dispersion coefficients presented by Fischer et al (1979).

Table G.1   Mean hydraulic parameters used to estimate longitudinal dispersion coefficient for the Klamath River.

Velocity u (m/s)	Width w (m)	Depth d (m)	Shear Velocity u* (m/s)	Longitudinal Dispersion, D_x (m^2/s)
1.2	40	2.8	0.282	317

Shear velocity, $u^* = (gR_hS)^{0.5} = [(9.81 \ m/s^2)(3 \ m)(0.002695)]^{0.5} = 0.282$ m/s

(Bed slope used to approximate hydraulic gradient)

As illustrated in Table G.2, calculated longitudinal dispersion coefficients range significantly from observed values, but are typically smaller than observed values.

Table G.2   Hydraulic parameters, calculated and observed longitudinal dispersion coefficients for selected rivers (Fischer et al 1979).

River	Velocity u (m/s)	Width w (m)	Depth d (m)	Shear Velocity u* (m/s)	$D_{x\,(Calc)}$ (m^2/s)	$D_{x\,(obs)}$ (m^2/s)
Clinch R.	0.94	60	2.1	0.104	73	54
Clinch R.	0.83	53	2.1	0.107	28	47
Wind/Bighorn R.	0.88	59	1.1	0.12	232	42
Wind/Bighorn R.	1.55	69	2.16	0.17	340	160
John Day R.	1.01	25	0.58	0.14	20	65
John Day R.	0.82	34	2.47	0.18	88	14

For the finite element method, longitudinal dispersion for a one-dimensional element can be determined using Peclet Number ($Pe^{\#}$) criteria. The dimensionless $Pe^{\#}$ represents a ratio of the rate of advective to diffusive/dispersive transport and is used in numerical modeling to determine solution stability (positivity), and control oscillation and truncation error.

$$Pe^{\#} = Lu/D_x \tag{G.2}$$

Where;
L = length scale [L]
u = stream velocity [L/T]
D_x = diffusion/dispersion coefficient [L^2/T]

General critieria are

- $Pe^{\#} < 2$ Positivity ensured, stable solutions, but subject to oscillation

- $Pe^{\#} \approx 1$ Oscillations dampened

- $Pe^{\#} < 0.3$ Truncation error minimized

For a selected Pe# of 1.0, a longitudinal dispersion coefficient can be calculated based on a representative length scale (e.g., the length of a finite element) and local stream velocity. That is,

$$D_x = Lu/Pe^{\#} \tag{G.3a}$$

$$D_x = Lu \tag{G.3b}$$

The model RMA-11 uses this formulation with a scale factor (e.g., $D_x = (C_{SF})Lu/Pe^{\#}$, where C_{SF} is a scale factor) to calculate longitudinal dispersion for each element at each time step to ensure effective numerical representation of constituent concentrations.

Using a representative element length of 300 m, mean system velocity of 1.2 m/s, and a scale factor of 1.0, longitudinal dispersion is computed as 360 m^2/s – similar to the calculated

120

value of 317 m^2/s using equation G.1. Diffusion is reduced in the model by a scale factor of 0.1; using representative values outlined above, this results in a value of 36 m^2/s – within the range of field observations for similar size rivers presented in Table G.2.

Appendix H   Simulated River Temperature Profiles

Figure H.1   Alternative HF-1: Klamath River mean daily water temperature profiles from Iron Gate Dam to Seiad Valley, May through October

123
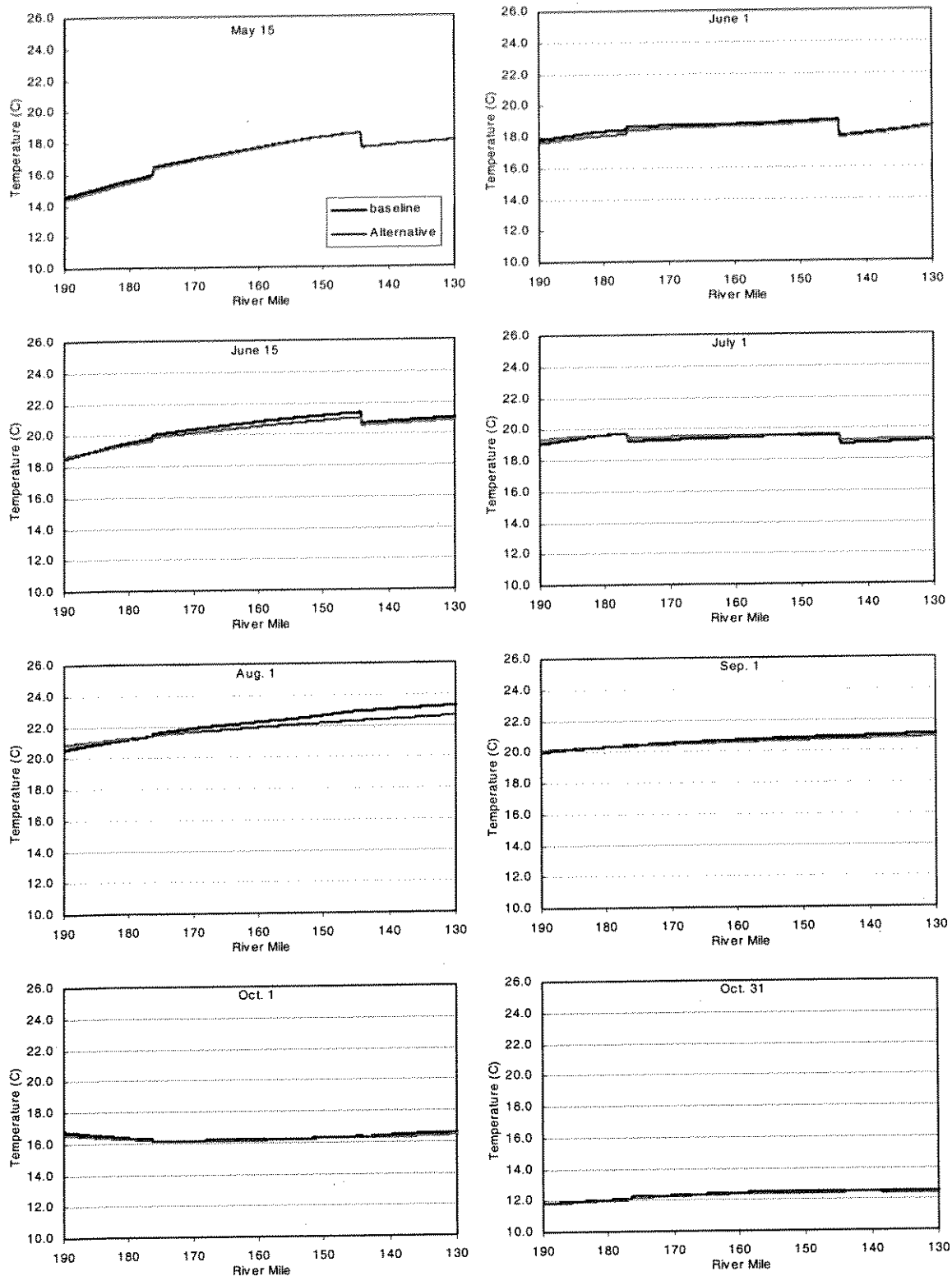
Figure H.2   Alternative HF-2: Klamath River mean daily water temperature profiles from Iron Gate Dam to Seiad Valley, May through October

124
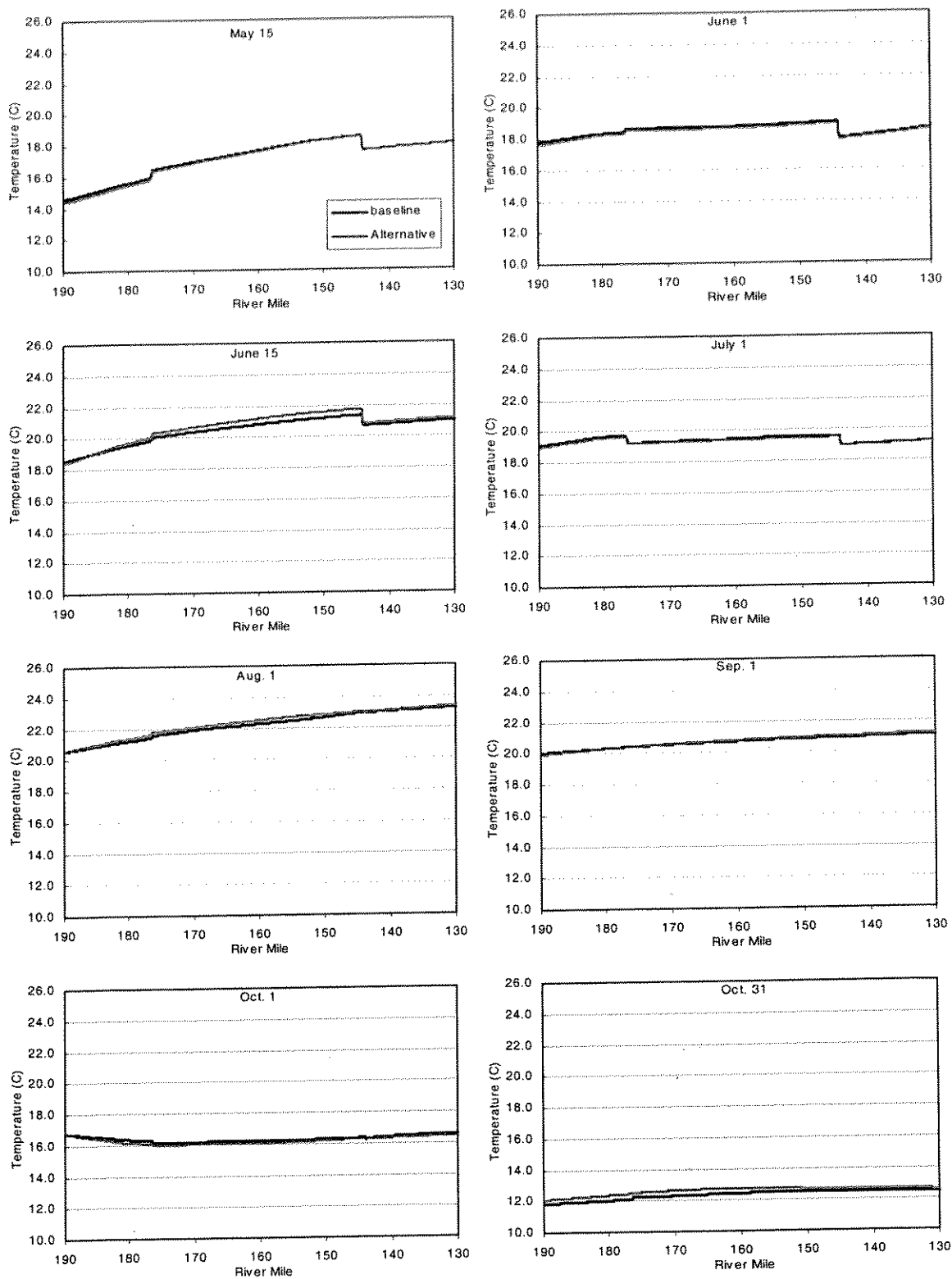
Figure H.3   Alternative LF: Klamath River mean daily water temperature profiles from Iron Gate Dam to Seiad Valley, May through October

Figure H.4   Alternative MF: Klamath River mean daily water temperature profiles from Iron Gate Dam to Seiad Valley, May through October
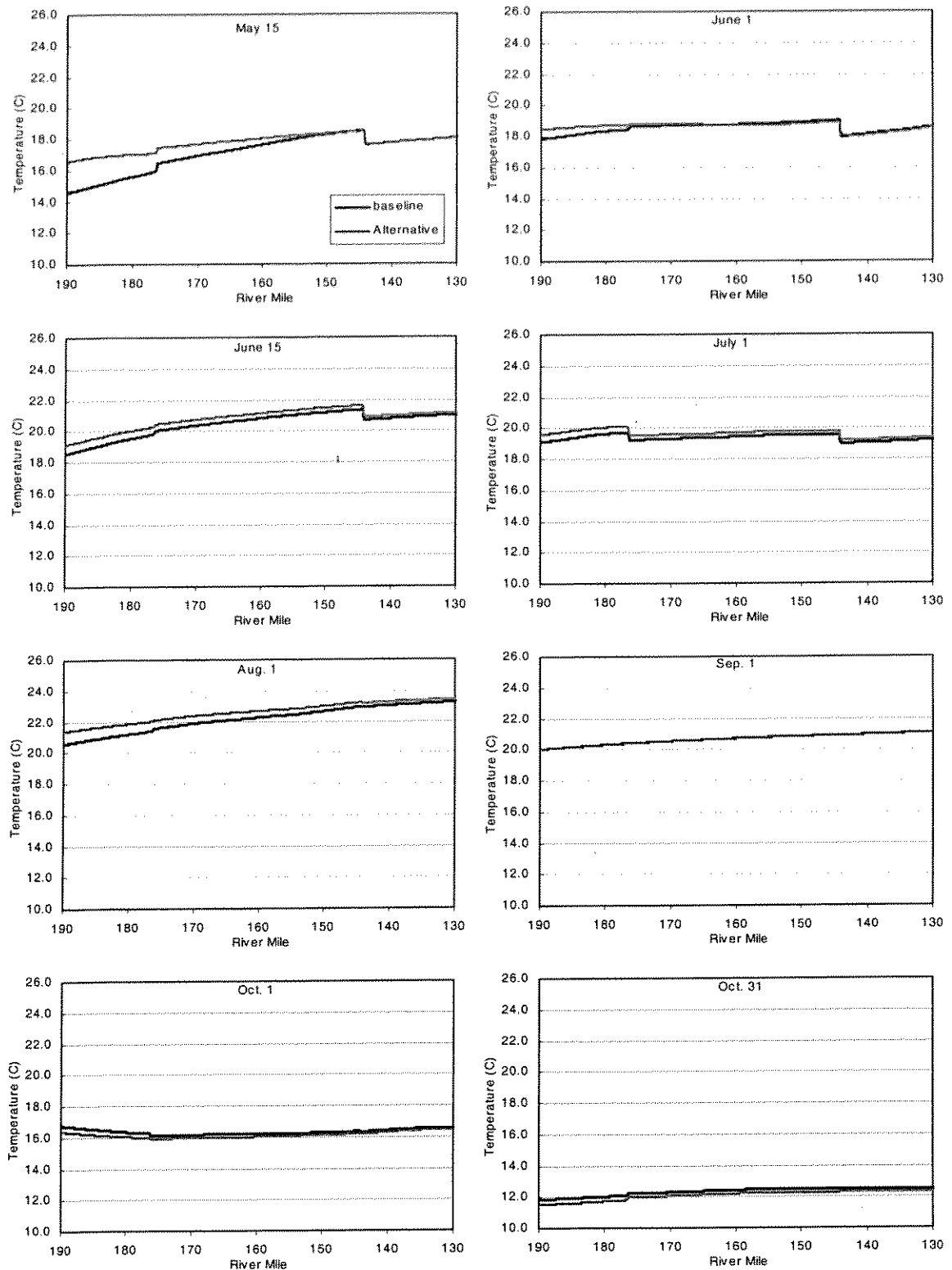
Figure H.5   Alternative RS: Klamath River mean daily water temperature profiles from Iron Gate Dam to Seiad Valley, May through October

127
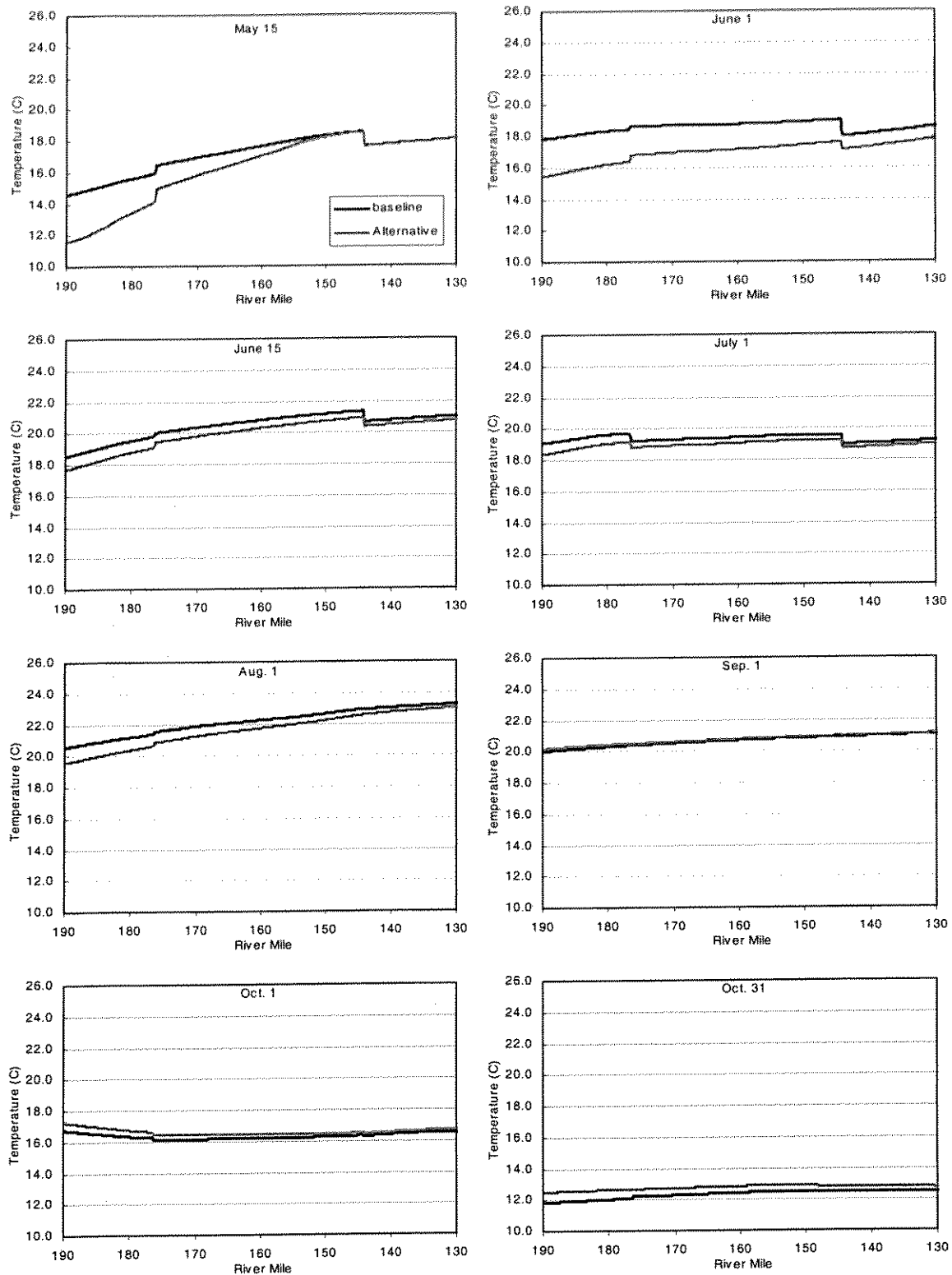
Figure H.6 Alternative IS: Klamath River mean daily water temperature profiles from Iron Gate Dam to Seiad Valley, May through October

128
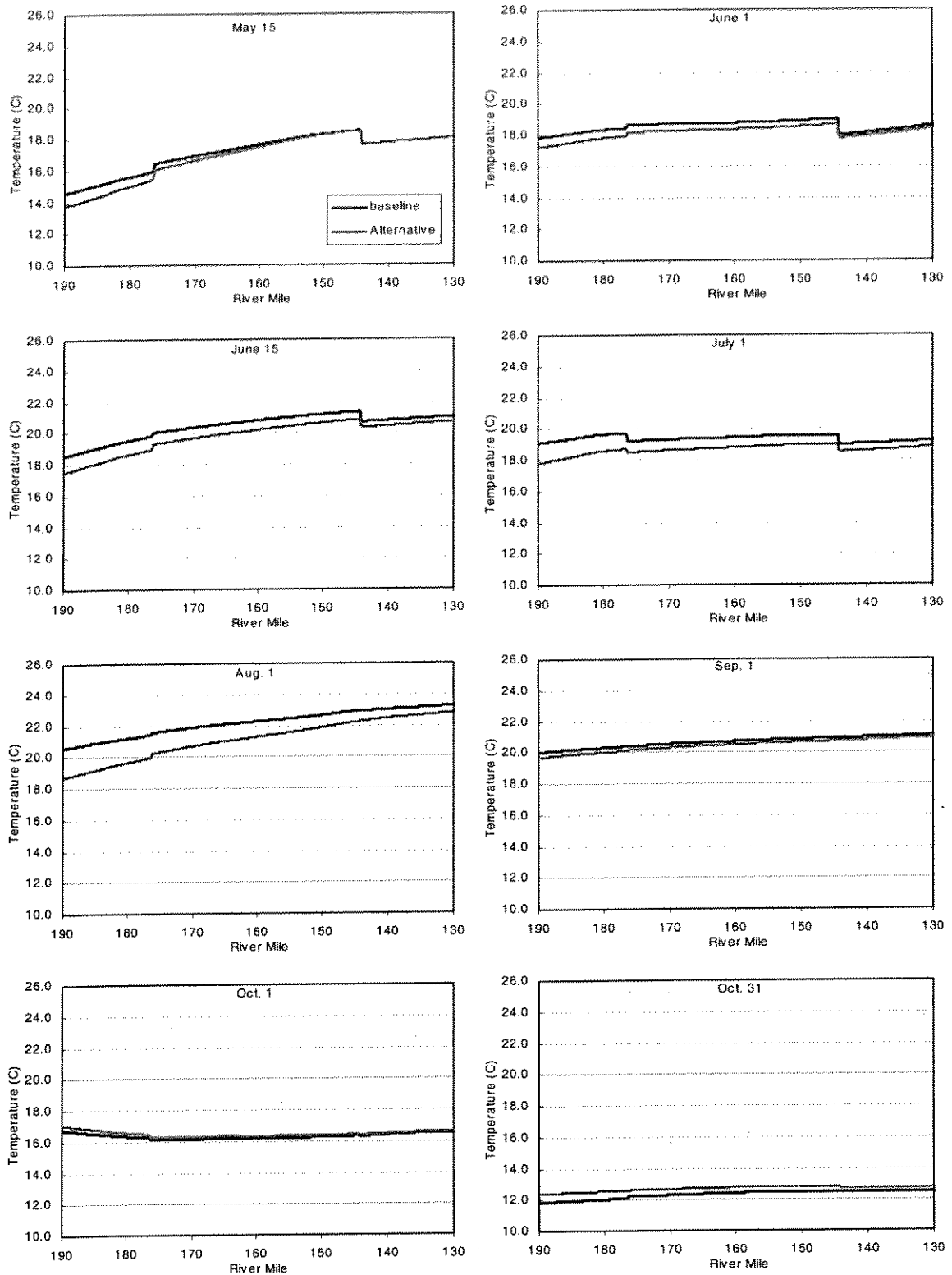
Figure H.7   Alternative SW-IS: Klamath River mean daily water temperature profiles from Iron Gate Dam to Seiad Valley, May through October
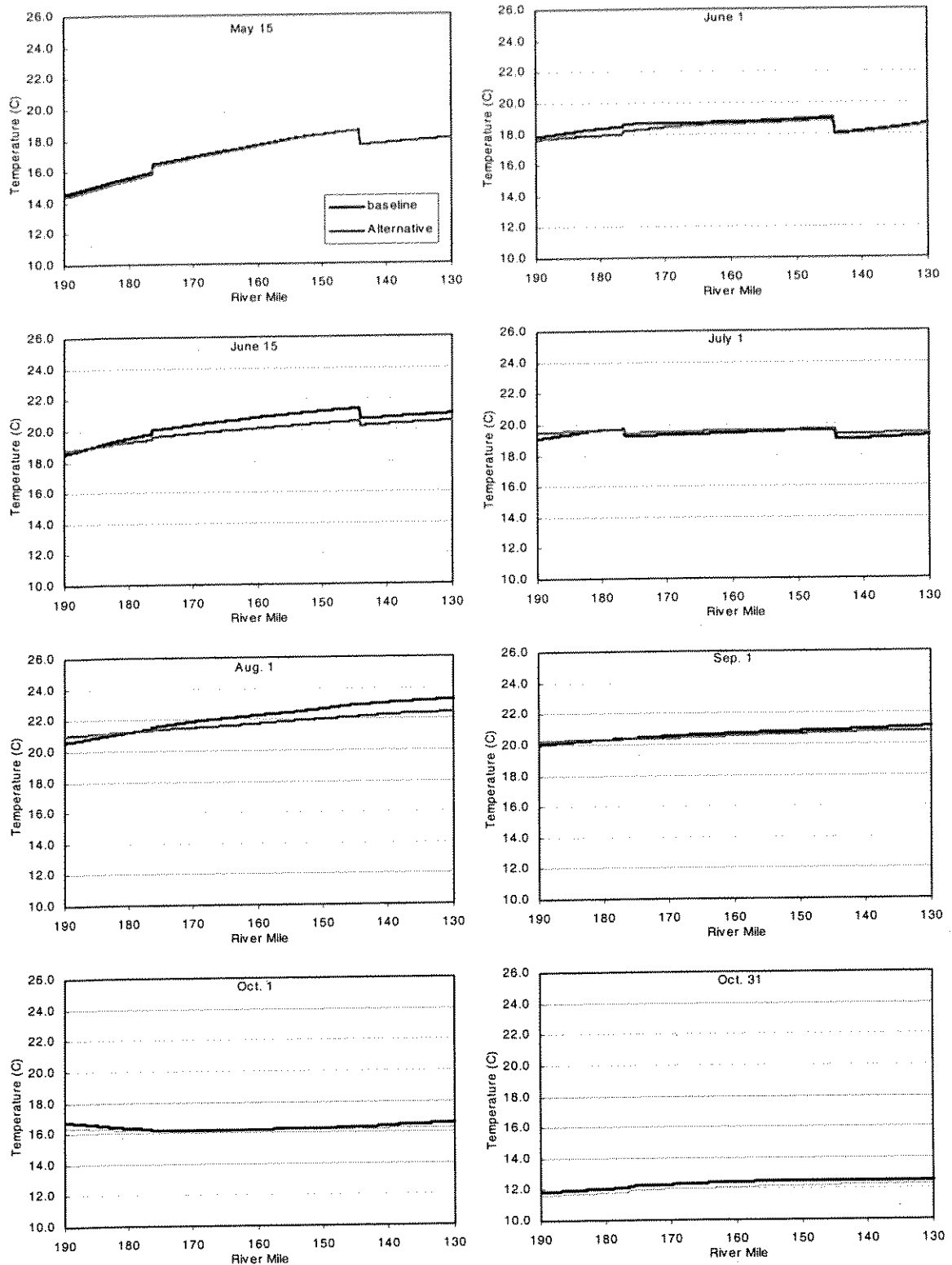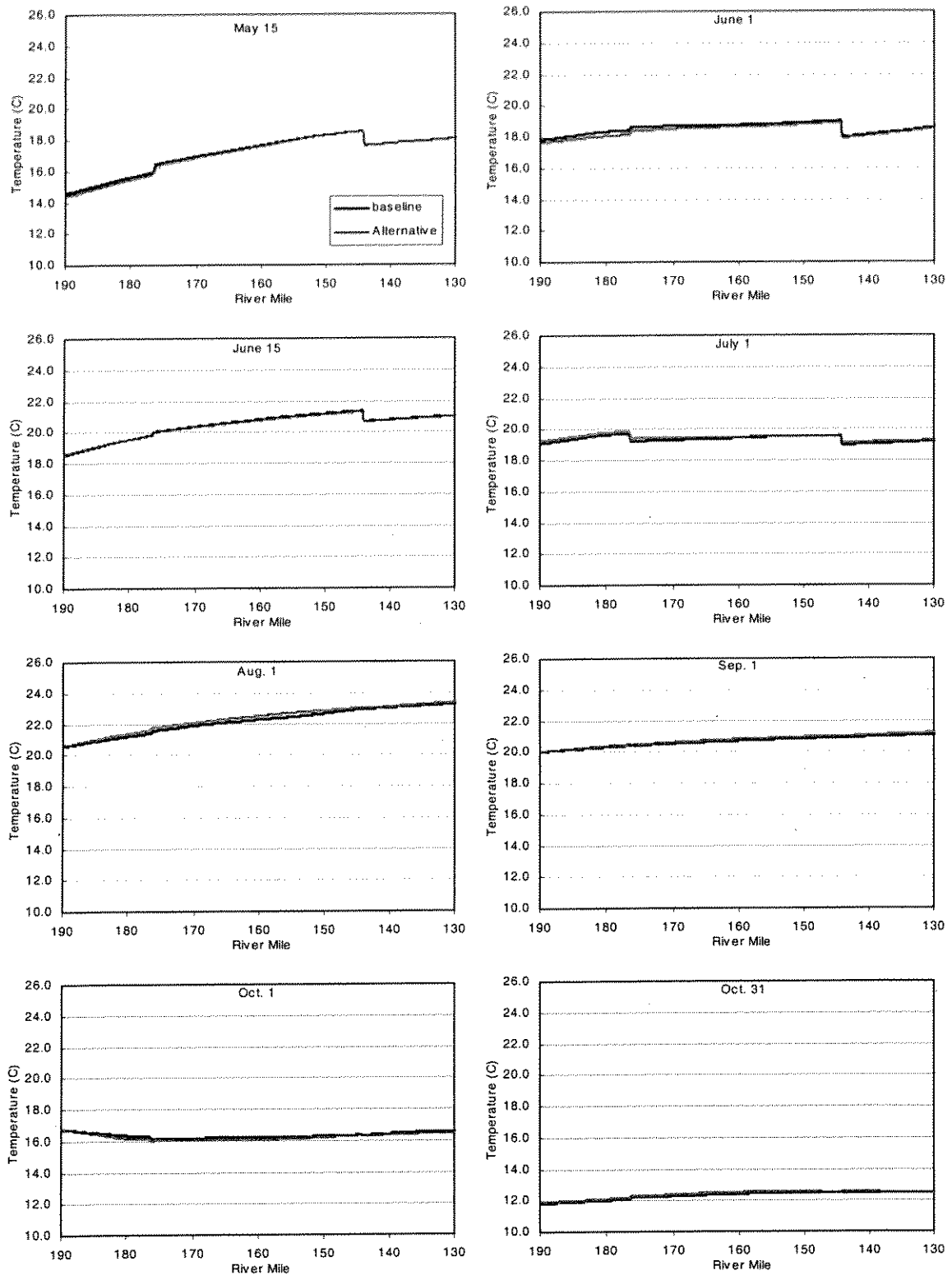
129

I.1   Introduction

A water quality index provides a system of classification for assessing surface water conditions. An index generally avoids absolute values, and is used on a comparative basis. Typical parameters include physical, chemical, and biological constituents; however, inclusion of too many parameters can result in a methodology that is overly complex and too cumbersome for application.

Horton (1965) developed one of the first water quality indices based on physical and chemical parameters, though biological indices had been formulated as early as 1908 in England (House and Ellis 1987). Other water quality indices were subsequently developed by Brown (et al 1970), Prati et al (1971), Harkins (1974), and Ross (1977). House (1980) completed a review of several water quality indices, including a comparison of several water quality index formulations used in water quality classification systems developed by the United Kingdom National Water Council and the Scottish Development Department. Recent work by Zanderbergen and Hall (1998) presents water quality indices based on attainment of water quality objectives throughout southern British Columbia. These objectives include physical and chemical parameters that vary seasonally and in some cases are modified for individual life stages of salmonids.

Water quality indices have distinct advantages and disadvantages. Advantages include reducing complexity of a variety of constituents with different units to form a single parameter, and illustrating spatial and temporal trends in conditions in comparison to a reference or baseline site/condition. Disadvantages include potential reduction in the roles of individual parameters, lack of consideration for parameter interaction, lack of transferability from one region to another, and difficulties in interpretation of results. Further, indices cannot be used to compute averages over time and space, or used for regression analysis, and interpretation must be within the limits of how the index was developed (Zandbergen and Hall 1998). Not discounting the limitations of water quality indices, and noting there is no panacea, the pursuit of representative, functional indices continues.

The purpose of development of a water quality index for the Klamath River is based on the compelling need for an objective comparative measure to assess simulation results for management alternatives. Though there are multiple parameters that play potentially important roles in ecosystem health, only temperature and dissolved oxygen have been included in this development.

Examining life stage periodicity for Klamath River fall-run chinook and coho salmon and steelhead (Table I.1) it can be seen that life stages of one or more species occur in each month of the study period. Iron Gate Hatchery operations lend further insight into the dynamics of anadromous fishes in the main stem Klamath downstream of Iron Gate Dam. Adult chinook generally enter the hatchery from early fall through early winter. Coho and salmon typically arrive during the higher flows of winter. The hatchery releases both smolts and yearling fish at various times of the year. Just under 5 million chinook smolts are released each year between May and June. Approximately a million "yearling" chinook are released in November. Roughly 75,000 yearling coho and 200,000 yearling steelhead are released in late winter. The study area and period for this project predominantly address adult migration and juvenile rearing.

Preferred thermal and dissolved oxygen ranges for each species and life stages for each species may differ, as discussed in Chapter 3. Ignoring species differentiation, a set of thermal and dissolved oxygen criteria were developed for application of a water quality index. Life stages of adult and juvenile forms were combined as (1) adult migration and spawning and (2) juvenile rearing and emigration, respectively. Egg incubation was neglected.

Using literature values, three "condition levels" were defined for the two life stages outlined above: (1) desirable range, (2) degraded range, and (3) undesirable range. These condition levels were approximately defined based on literature values and with respect to anadromous fishes roughly correspond to

- Level 1 (L1) - Desirable range: little or no effect on salmonid
- Level 2 (L2) - Degraded range: salmonids begin to exhibit signs of stress (temperature or dissolved oxygen), most effects reversible
- Level 3 (L3) - Undesirable range: a large portion of the population is affected and/or deleterious effects may be severe if conditions persist more than a few hours, (i.e., most effects irreversible)

131

Water quality indices were developed for water temperature, dissolved oxygen, and to account for parameter interaction, a combined effect index was developed for temperature and dissolved oxygen.

Table I.1   Life stage periodicities for Klamath River fall-run and coho salmon and steelhead.

Species	May	June	July	August	Sept.	Oct.
Fall-run Chinook						
Adult Migration					•	•
Adult Spawning					•	•
Egg Incubation					•	•
Juvenile Rearing and Emigration	•	•				
Coho						
Adult Migration					•	•
Adult Spawning						
Egg Incubation						
Juvenile Rearing and Emigration	•	•				
Steelhead (winter)						
Adult Migration					•	•
Adult Spawning						
Egg Incubation						
Juvenile Rearing and Emigration	•	•	•	•		

Adapted from Birk (1996)

I.2   Temperature Index

Temperature ranges for physiological response vary widely, not only from species to species, but also from study to study. Moreover, criteria have been defined for various levels of physiological response: chronic, 50 percent instantaneous mortality, 24-hour temperature for 100 percent survival, or criteria based on 24-hour or 7-day average temperatures, just to name a few. Because it was necessary to assess sub-daily simulation results, developed criteria were assumed to represent short-term exposure (e.g., hours). Table I.2 presents the selected no effect/chronic (T_{NC}) and chronic/acute (T_{CA}) thresholds for definition of desirable, degraded, and undesirable levels, levels L1, L2, and L3, respectively.

Index weighting coefficients for each level were assigned in accordance with the criteria presented in Table I.2. Several weighting coefficient values were explored, including series that increased linearly, geometrically, and exponentially. A geometric progression was

132

selected; wherein index weighting coefficients L1, L2, and L3 were assigned values of 0.0, 0.5, and 2.0, respectively.

Table I.2   Temperature criteria to define condition levels for adult and juvenile salmonids

Life stage	Temperature Criteria (°C (°F))	
	No-Effect/Chronic Threshold T_{NC}	Chronic/acute Threshold T_{CA}
Adult Migration/Spawning	18.0 (64.4)	22.0 (71.6)
Juvenile Rearing and Emigration	16.0 (60.8)	20.0 (68.0)

Temperature acclimation in juvenile fish has been noted; however, Armour (1991) reports that the most significant impacts occur between 5°C (41°F) and 10°C (50°F). Because temperatures in the Klamath River below Iron Gate Dam are typically in excess of 15°C (59°F) by May and the study reach is relatively short there is most likely limited benefit from acclimation.

Because water temperature can vary significantly diurnally, the index was constructed to utilize sub-daily system responses, thus daily maximum, minimum and mean temperatures were employed. The three daily temperature statistics were categorized and assigned weighting coefficient values according to the designated condition levels (L1, L2, and L3). The temperature index value for any particular day at any location was calculated as the average of the three assigned weighting coefficients. Figure I.1 shows a schematic of the process

$$I_T = \sum_i \omega_i / 3, \quad i = max, mean, min \qquad (I.1)$$

Where
I_T = temperature index
ω_i = index weighting coefficient for max, mean, or min daily water temperature
i = counter

At a given location, the diurnal temperature response of the system and the selected threshold values define the state of the system, or its condition level (i.e., L1, L2, and L3) for a particular day. The possible states are listed in Table I.3 and shown graphically in Figure I.2. For example, when conditions are such that the daily maximum, mean, and minimum water temperatures all fall below the "no effect/chronic threshold" (state (a)), I_T is zero, denoting no effect. At the other end of the spectrum is state (j) where even the minimum temperature exceeds the chronic/acute threshold, corresponding to I_T having a value of 2.0, i.e., the entire day experiences acute conditions. Intermediate states show varying levels of degradation. Thus, the selected linear progression of weighting coefficients results in a scale

133
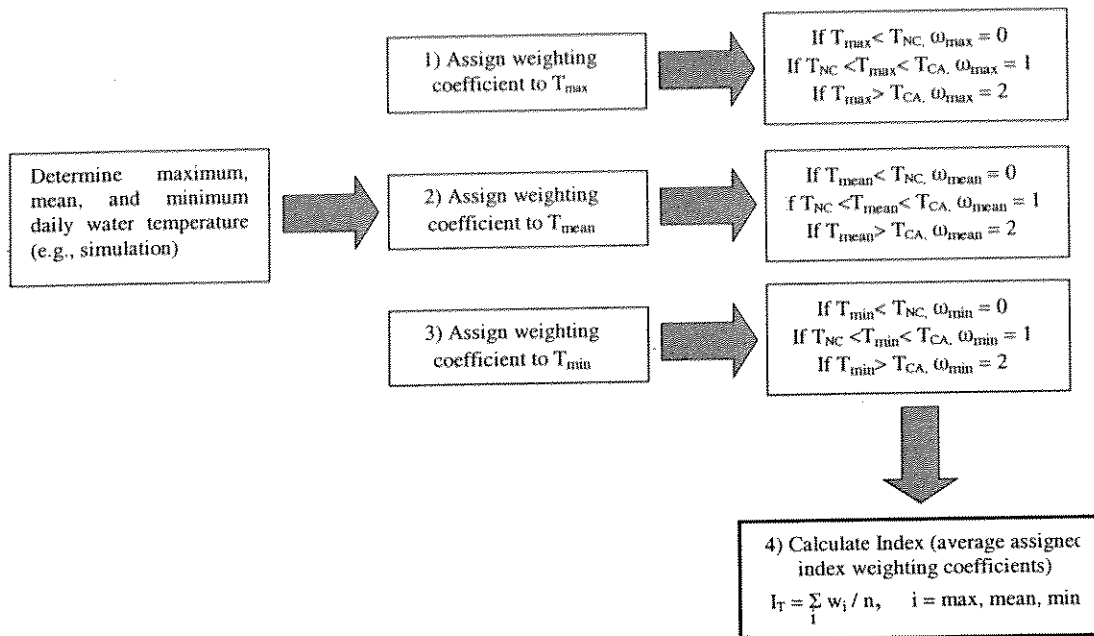
Figure I.1   Temperature index determination for L1, L2, and L3 linear weighting coefficients 0, 1, 2, respectively

from zero to 2.0. Different weighting coefficients would lead to different index values and potentially to a different scale. Further, for a given set of daily temperature statistics and selected threshold levels not all states will be feasible. For example, immediately downstream of Iron Gate Dam where daily temperature fluctuations are often less than 1°C (1.8°F) states (a), (e), and (j) will be dominant.

It is notable that several of the states have the same temperature index value, i.e., they are weighted equally (e.g., states (c) and (d), (e) and (f), and (g) and (h). Index weighting coefficients could be modified or instead of averaging the three values as per equation I.1, the values could be summed, multiplied, or aggregated in some other appropriate fashion.

Table I.3 Potential condition levels (states) for maximum, mean, and minimum water temperatures, associated index weighting coefficients, and temperature index values

State	Level			Weighting Coefficient, ω			Temperature Index, I_T
	$T_{w(MAX)}$	$T_{w(MEAN)}$	$T_{w(MIN)}$	$T_{w(MAX)}$	$T_{w(MEAN)}$	$T_{w(MIN)}$	(Scale)
(a)	L1	L1	L1	0	0	0	0.00
(b)	L2	L1	L1	1	0	0	0.33
(c)	L3	L1	L1	2	0	0	0.67
(d)	L2	L2	L1	1	1	0	0.67
(e)	L2	L2	L2	1	1	1	1.00
(f)	L3	L2	L1	2	1	0	1.00
(g)	L3	L2	L2	2	1	1	1.33
(h)	L3	L3	L1	2	2	0	1.33
(i)	L3	L3	L2	2	2	1	1.67
(j)	L3	L3	L3	2	2	2	2.00

Figure I.2 Potential condition levels (states) for daily maximum, mean, and minimum water temperatures over a representative 24-hour period (referenced to Table I.3)

135

I.3   Dissolved Oxygen

As with temperature, dissolved oxygen ranges for physiological response vary among species and life stages. Davis (1975) provides dissolved oxygen levels for freshwater salmonids including steelhead. These levels are reproduced below in Table I.4, below.

Table I.4   Response of freshwater salmonid populations to variable dissolved oxygen levels (Davis 1975)

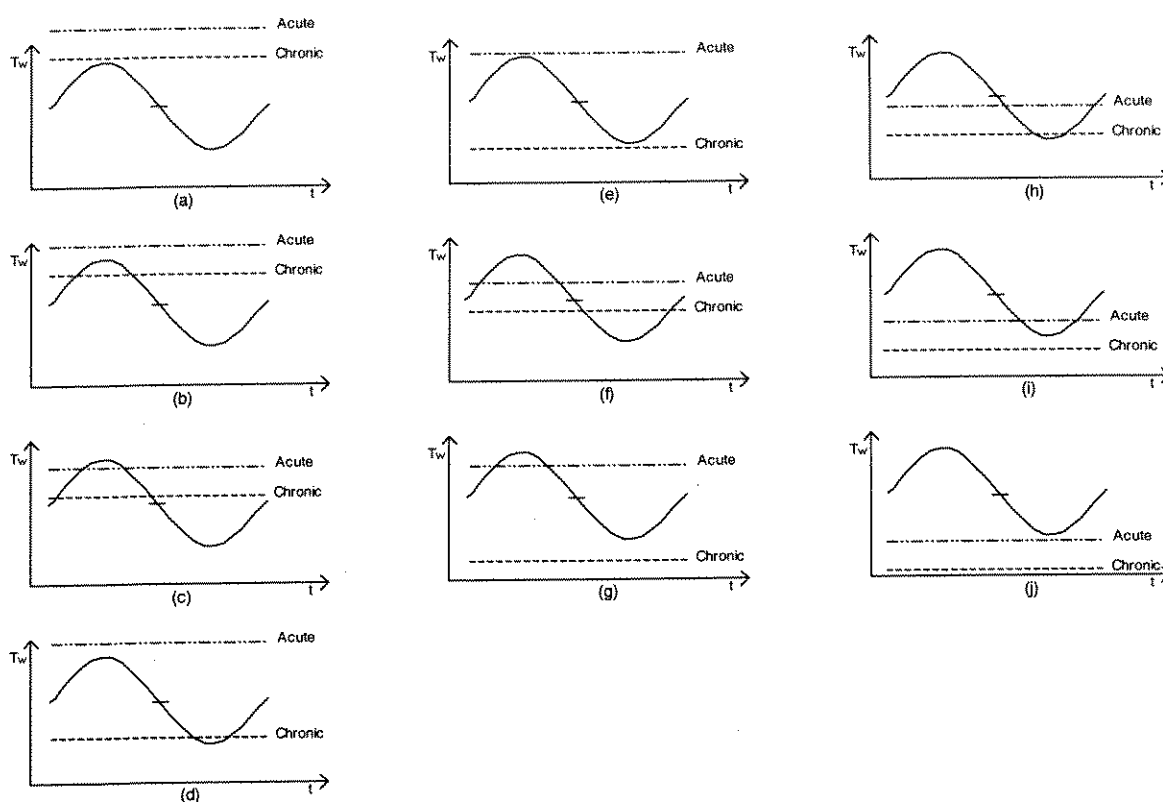| Response	Dissolved Oxygen Saturation at given temperature (°C)					
	0	5	10	15	20	25
			Percent			
Function w/o impairment	76	76	76	76	85	93
Initial oxygen distress	57	57	57	59	65	72
Widespread oxygen impairment	38	38	38	42	46	51

Davis notes that the criteria defined in Table I.4 under percent saturation provide for both sufficient oxygen gradient and adequate oxygen to fulfill metabolism requirements. Thus, index values for dissolved oxygen are based on percent saturation and water temperature rather than absolute values in mg/l. Nonetheless, dissolved oxygen concentrations in mg/l are also addressed because most regulatory requirements are based on absolute values. These dissolved oxygen criteria were applied to all species for all life stages, i.e., adult migration and spawning, and juvenile rearing and emigration. Using data from Davis (1975), saturation dissolved oxygen criteria were developed to define desirable, degraded, and undesirable ranges similar to temperature criteria. Table I.5 includes both absolute dissolved oxygen criteria (DO_{NC} = 7.0 mg/l and DO_{CA} = 5.0 mg/l), and criteria based saturation concentrations associated with a particular temperature.

The dissolved oxygen index, I_{DO}, was developed (equation I.2) in the same manner as that for water temperature. A geometric set of index weighting coefficients were selected, wherein index weighting coefficients L1, L2, and L3 were assigned values of 0.0, 0.5, and 2.0, respectively. Because dissolved oxygen has the potential to exhibit appreciable diurnal variations, the range of daily dissolved oxygen concentrations and the selected threshold values define the state of the system (i.e., L1, L2, and L3) for a particular day similar to Figure I.2. Similar to the temperature index, I_{DO} ranges from zero (no effect) to 2.0 (entire day experiences acute conditions).

Table I.5   Water quality index dissolved oxygen criteria

| Temperature | Dissolved Oxygen Criteria (%sat) | |
(°C (°F))	No-Effect/Chronic Threshold, DO_{NC}	Chronic/Acute Threshold, DO_{CA}
Absolute DO thresholds:	7.0 mg/l	5.0 mg/l
5.0 - 14.0 (41.0 - 57.2)	68	46
15.0 (59.0)	69	49
16.0 (60.8)	70	50
17.0 (62.6)	71	51
18.0	72	52
19.0	74	53
20.0	76	54
21.0	77	55
22.0	78	56
23.0	80	57
24.0	82	59
25.0	84	60
26.0	86	61
27.0	88	63
28.0	90	64
29.0	92	66
30.0	94	68

$$I_{DO} = \sum_i \alpha_i / 3, \quad i = max, mean, min \tag{I.2}$$

Where

I_{DO} = dissolved oxygen index
α_i = index weighting coefficient for max, mean, or min daily dissolved oxygen
i   = counter

Though the same representation of index weighting coefficients was selected for temperature and dissolved oxygen, this was not a requirement.

I.4   Combined Stresses: Temperature and Dissolved Oxygen

I.4.1   Introduction

Aquatic ecosystems are complex environments controlled by various physiochemcial and biological processes. The field of ecotoxicology addresses the multiple mechanisms and their actions and effects on the physiological response of organisms within such systems. Responses of organisms to environmental conditions are the integrated consequences of

direct and indirect impacts. These impacts can be associated with contaminants, hydrologic variability, water quality variability, as well as combinations of natural and anthropogenic activities, and lead to modified population characteristics and dynamics, community structure and function, and overall ecosystem function (Adams, et al 1998). Application of models to assess the fate, transport and effects of constituents is a valid and useful method to examine system response to these multiple stresses and predict undesirable conditions (Anderson 1998, Levin 1998). The theories of fate and transport are well developed compared to that of effects upon organisms, with the primary issue being the validity of extrapolation of limited laboratory data to field conditions. While data collection is critical to analysis, simulation models can provide dynamic descriptions of systems through space and time that would otherwise be unavailable to the investigator (Levin, 1998).

This study does not assess stresses at an ecosystem level. That is, the impacts of dissolved oxygen, temperature, or other direct or indirect impacts on organisms other than salmonids are ignored. During adult migration, when fish are not actively feeding and are living off body stores, the impact of this assumption is probably minimal. However, from egg incubation through juvenile rearing and emigration the impacts become progressively more profound. Issues of food availability, nutrition, feeding, habitat influences, competition, temperature, varying hydrologic regime and turbidity may play increasingly important roles (Adams et al 1998). Further, there is little specific data delineating direct and indirect affects. General responses were derived from available literature data.

I.4.2   Combined Stresses and Anadromous Fish

Few studies have addressed quantitative impacts of combined stresses of elevated water temperatures and depressed dissolved oxygen levels on anadromous fishes. General responses of salmonids to elevated temperatures and depressed dissolved oxygen have been reported by Mathews and Berg (1997), Forsberg and Bergheim (1996), Vinson and Levesque (1994), Cech et al (1990) and others. Davis (1975) states that higher temperatures are usually accompanied by increased metabolic demand for oxygen. Severe respiratory problems can result from a combination of high temperatures and reduced oxygen tension (water not fully saturated). This is a primary reason that fish kills occur at low oxygen levels most often during warm water periods. Finally, mobility, or avoidance behavior, although potentially an important issue for anadromous fish restoration, was not addressed herein.

Formulation of a water quality index to address combined stresses requires sufficient flexibility to address multiple parameters, address relative impacts of the various stressors/parameters, and account for varying levels of combined effects. Equation I.3 presents a method for combining up to n individual indices (e.g., the temperature and dissolved oxygen indices developed previously). Relative weighting of the individual parameter indices and interaction between parameters is included. The presented methodology explicitly addresses interaction between two parameters, and implicitly addresses the combined effect of multiple parameter interactions by considering the product of the combined effect weighting coefficients. The methodology can be extended to multiple parameter interactions (versus pair-wise interaction) if desired.

$$I_C = \sum_{i=1}^{n} \gamma_i \, I_i \prod_{j=1}^{n} \phi_j \, \beta_{i,j} \tag{I.3}$$

Subject to:

$$\phi_j = \left\{ \begin{array}{l} 0, \text{if } i = j \\ 1, \text{if } i \neq j \end{array} \right. \tag{I.4}$$

$$\sum_{i=1}^{n} \gamma_i = 1.0 \tag{I.5}$$

Where
I_C = combined effect index (combined stresses)
I_i = parameter index, i
γ_i = relative bias for parameter i
$\beta_{i,j}$ = combined effect factor between parameters i and j
n = number of parameters in the combined index
i,j = counters

The methodology is best described through a simple example. For three parameters equation I.3 takes on the form

$$I_C = \gamma_1 \, I_1 \, [(\beta_{1\text{-}2}) \times (\beta_{1\text{-}3})] + \gamma_2 \, I_2 \, [(\beta_{1\text{-}2}) \times (\beta_{2\text{-}3})] + \gamma_3 \, I_3 \, [(\beta_{1\text{-}3}) \times (\beta_{2\text{-}3})] \tag{I.6}$$

The relative bias values, γ_1, γ_2, and γ_3 provide a means to accommodate the impact of unequal biological responses to the individual parameters included in the combined index. Selecting equal bias values (e.g., $\gamma_1 = \gamma_2, = \gamma_3 = 0.333$) assigns equal priority to all parameters. Parameter interaction is represented through the combined effect factor, $\beta_{i,j}$. Specifically, parameter number one (I_1) can interact with I_2 ($\beta_{1\text{-}2}$) and I_3 ($\beta_{1\text{-}3}$), while I_2 can interact with I_1 ($\beta_{1\text{-}2}$) and I_3 ($\beta_{2\text{-}3}$), and I_3 can interact with I_1($\beta_{1\text{-}3}$) and I_2($\beta_{2\text{-}3}$). As noted previously, although the combined effect of any two pairs of parameters are explicitly entered (e.g., $\beta_{1\text{-}2}$ and $\beta_{1\text{-}3}$), the combined effect of a parameter interacting with several

parameters is accommodated by multiplying the coefficients (e.g., $(\beta_{1-2}) \times (\beta_{1-3})$). Combined effect factors can take on a range of values as denoted below.

Case 1: $\beta = 1.0$ No parameter interaction, i.e., no combined stress
Case 2: $\beta > 1.0$ Combined effect provides negative impact
Case 3: $\beta < 1.0$ Combined effect provides positive impact

Although indices based on combined effects are detrimental to biological health, case 3 does not actually exist. If indices are constructed to examine benefits of parameter interactions (e.g., cold water and elevated dissolved oxygen for anadromous fishes), case 3 would be applied, but case 2 would not exist. For the purposes of this report, only cases 1 and 2 are examined.

For the case of two parameters, e.g., temperature and dissolved oxygen, equation I.6 reduces to

$$I_C = \gamma \, I_T \, \beta + (1 - \gamma) \, I_{DO} \, \beta \qquad\qquad (I.7)$$

Where
I_C = combined effect index for temperature and dissolved oxygen
I_T = temperature index value
I_{DO} = dissolved oxygen index value
γ = relative parameter bias ($0 < \gamma < 1.0$)
β = combined effect factor for temperature-dissolved oxygen interaction ($\beta \geq 1.0$)

J.1   Field Data (/field)

Igtemp96.xls	Iron Gate Reservoir profile temperature data: 1996
Igtemp97.xls	Iron Gate Reservoir profile temperature data: 1997
Temp96a.xls	Klamath River water temperature data: 1996
Temp96b.xls	
Temp96c.xls	
Temp96d.xls	
Temp97a.xls	Klamath River water temperature data: 1997
Temp97b.xls	
Temp97c.xls	
Temp97d.xls	
Temp97e.xls	
Temp97f.xls	

J.2   Geometry Data Files (/geometry)

Klamathgeo.xls   river cross section geometry
reservoir stage-volume data: see Appendices B.9.3 and I.7)

J.3   Meteorological Data Files (/met)

Rmamet96.xls	1996 meteorological data for rma11: Brazie Ranch
Rmamet96.xls	1997 meteorological data for wqrrs: Brazie Ranch
Wqrrsmet96.xls	1996 meteorological data for rma11: Brazie Ranch
Wqrrsmet97.xls	1997 meteorological data for wqrrs: Brazie Ranch

J.4   Flow Data Files (/flow)

igflow96.xls	1996 water balance for Iron gate Reservoir
igflow97.xls	1997 water balance for Iron gate Reservoir
rma296.xls	Iron Gate release and tributary flows: 1996
rma297.xls	Iron Gate release and tributary flows: 1997

J.5   Water Quality Files (/quality)

Cop9697.xls   Iron Gate inflow temperature data (1996, 1997)
See also, Appendix I.1 and NCRWQCB (1997)

J.6   Calibration and Validation Data Files (/calval)

igtemp9697.xls	Iron Gate Reservoir profile temperature, 1996
igtemp97.xls	Iron Gate Reservoir profile temperature, 1997

J.7   WQRRS Calibration/Validation Input Files (/wqrrsdata)

igcal96wq   WQRRS input file 1996: calibration
igval97wq   WQRRS input file 1997: validation

J.8   RMA-2/RMA-11 Calibration/Validation Input Files

(/rma2data)
Klamath.geo   geometry file
RMA-2
1996: kr96bcs.bcs   boundary condition control file
      kr96elm.elm   tributary inflow and accretion file
      kr96elv.elv   downstream boundary condition file
      kr96hyd.hyd   Iron Gate Reservoir release file
      krm96rm2.rm2   RMA-2 input file: May
      krjn96rm2.rm2   RMA-2 input file: June
      krjl96rm2.rm2   RMA-2 input file: July
      kra96rm2.rm2   RMA-2 input file: August
      krs96rm2.rm2   RMA-2 input file: September
      kro96rm2.rm2   RMA-2 input file: October
      kr96w2rm2rst   start up file, used for May simulation

1997: kr97bcs.bcs   boundary condition control file
      kr97elm.elm   tributary inflow and accretion file
      kr97elv.elv   downstream boundary condition file
      kr97hyd.hyd   Iron Gate Reservoir release file
      krm97rm2.rm2   RMA-2 input file: May
      krjn97rm2.rm2   RMA-2 input file: June
      krjl97rm2.rm2   RMA-2 input file: July
      kra97rm2.rm2   RMA-2 input file: August
      krs97rm2.rm2   RMA-2 input file: September
      kro97rm2.rm2   RMA-2 input file: October
      kr97w2rm2rst   start up file, used for May simulation

(/rma11data)
RMA-11
1996: kr96met.met   meteorological data file
      kr96r4q.r4q   water quality control parameter file
      kr96grh.grh   boundary condition file
      krbcs.bcs   boundary condition control file
      krm96r11.r11   RMA-11 input file: May
      krjn96r11.r11   RMA-11 input file: June
      krjl96r11.r11   RMA-11 input file: July
      kra96r11.r11   RMA-11 input file: August
      krs96r11.r11   RMA-11 input file: September
      kro96r11.r11   RMA-11 input file: October
1997: kr97met.met   meteorological data file
      kr97r4q.r4q   water quality control parameter file
      kr97grh.grh   boundary condition file
      krbcs.bcs   boundary condition control file

krm97r11.r11	RMA-11 input file: May
krjn97r11.r11	RMA-11 input file: June
krjl97r11.r11	RMA-11 input file: July
kra97r11.r11	RMA-11 input file: August
krs97r11.r11	RMA-11 input file: September
kro97r11.r11	RMA-11 input file: October

J.9 WQRRS Program Files (/wqrrscode)

(See disk for file list)

J.10 RMA-2 and RMA-11 Program Files (/rmacodes)

Rma2v64c.zip	rma2 code
Rma11v24.zip	rma11 code (phytoplankton only)
Rma11v31a.zip	rma11 code (phytoplankton and attached algae)

Note: files may in many cases are compressed to save space (*.zip)